

Design Guidelines for Horizontal Drains used for Slope Stabilization

WA-RD 787.1

Greg M. Pohl
Rosemary W.H. Carroll
Donald M. Reeves
Rishi Parashar
Balasingam Muhunthan
Sutharsan Thiyagarjah
Tom Badger
Steve Lowell
Kim A. Willoughby

March 2013



Washington State
Department of Transportation
Office of Research & Library Services

WSDOT Research Report

Design Guidelines for Horizontal Drains used for Slope Stabilization



Greg M. Pohll, DRI
Rosemary W.H. Carroll, DRI
Donald M. Reeves, DRI
Rishi Parashar, DRI
Balasingam Muhunthan, WSU
Sutharsan Thiyagarjah, WSU
Tom Badger, WSDOT
Steve Lowell, WSDOT
Kim A. Willoughby, WSDOT

1. REPORT NO. WA-RD 787.1	2. GOVERNMENT ACCESSION NO.	3. RECIPIENTS CATALOG NO	
4. TITLE AND SUBTITLE Design Guidelines for Horizontal Drains used for Slope Stabilization		5. REPORT DATE March 2013	
		6. PERFORMING ORGANIZATION CODE	
7. AUTHOR(S) Greg M. Pohll, Rosemary W.H. Carroll, Donald M. Reeves, Rishi Parashar, Balasingam Muhunthan, Sutharsan Thiyagarjah, Tom Badger, Steve Lowell, Kim A. Willoughby		8. PERFORMING ORGANIZATION REPORT NO.	
9. PERFORMING ORGANIZATION NAME AND ADDRESS Desert Research Institute 2215 Raggio Parkway Reno, NV 89512		10. WORK UNIT NO.	
		11. CONTRACT OR GRANT NO. GCA6381	
12. CO-SPONSORING AGENCY NAME AND ADDRESS Washington State Department of Transportation 310 Maple Park Ave SE Olympia, WA 98504-7372 Research Manager: Kim Willoughby 360.705.7978		13. TYPE OF REPORT AND PERIOD COVERED Final Report	
		14. SPONSORING AGENCY CODE	
15. SUPPLEMENTARY NOTES This study was conducted in cooperation with the U.S. Department of Transportation, Federal Highway Administration through the pooled fund, TPF-5(151) in cooperation with the state DOT's of California, Maryland, Mississippi, Montana, New Hampshire, Ohio, Pennsylvania, Texas, Washington and Wyoming.			
16. ABSTRACT The presence of water is one of the most critical factors contributing to the instability of hillslopes. A common solution to stabilize hillslopes is installation of horizontal drains to decrease the elevation of the water table surface. Lowering the water table dries a large portion of the hillslope which increases the shear strength of the soil, thereby decreasing the probability of slope failure. The purpose of this manual is to provide a single comprehensive reference for geotechnical engineers and hydrogeologists on designing horizontal drainage systems to improve slope stability. Guidelines are provided for translational and rotational failure and consider fractured systems. Basics of hydrogeologic and geotechnical terminology, site characterization and conceptualization, groundwater modeling techniques and template projects help to guide the user with respect to identifying important parameters to drainage design. An iterative approach is presented for determining the minimum drain construction to lower water levels enough to keep the factor of safety (FOS) greater than 1.2.			
17. KEY WORDS Subsurface drainage, slope stabilization, horizontal drains		18. DISTRIBUTION STATEMENT	
19. SECURITY CLASSIF. (of this report) None	20. SECURITY CLASSIF. (of this page) None	21. NO. OF PAGES 377	22. PRICE

ACKNOWLEDGMENTS

Funding for this project was obtained from the Washington State Department of Transportation through the Transportation Pooled Fund, TPF-5(151). The partner states of TPF-5(151) included: California, Maryland, Mississippi, Montana, New Hampshire, Ohio, Pennsylvania, Texas, Washington and Wyoming. The DRI contract was 650-646-0250.

Project oversight and data transfer was facilitated by Tom Badger, Steve Lowell and Kim Willoughby with the Washington State Department of Transportation (WSDOT). Geotechnical modeling was accomplished by Dr. Balasingam Muhunthan and doctoral student Sutharsan Thiyagarjah from Washington State University (WSU). The Desert Research Institute (DRI) performed all hydrologic analysis. Dr. Greg Pohl acted as project manager, Dr. Rosemary Carroll performed all modeling and Dr. Donald Reeves and Dr. Rishi Parashar conducted all fracture analysis.

DISCLAIMER

The contents of this report reflect the views of the authors, who are responsible for the facts and the accuracy of the data presented herein. The contents do not necessarily reflect the official views or policies of the Washington State Department of Transportation or the Federal Highway Administration. This report does not constitute a standard, specification, or regulation.

Authorship of the document:

Chapter 1 – Greg Pohl
Chapter 2 – Balasingam Muhunthan
 Sutharsan Thiyagarjah
Chapter 3 – Rosemary Carroll
Chapter 4 – Rosemary Carroll
 Donald M. Reeves
 Rishi Parashar
 Balasingam Muhunthan
 Sutharsan Thiyagarjah
Chapter 5 – Rosemary Carroll
Chapter 6 – Rosemary Carroll
Chapter 7 – Rosemary Carroll
 Balasingam Muhunthan
 Sutharsan Thiyagarjah
Chapter 8 – Donald M. Reeves
 Rishi Parashar
Chapter 9 – Rosemary Carroll
Appendices A-D – Rosemary Carroll

EXECUTIVE SUMMARY

The presence of water is one of the most critical factors contributing to the instability of hillslopes. A common solution to stabilize hillslopes is installation of horizontal drains to decrease the elevation of the water table surface. Lowering the water table dries a large portion of the hillslope which increases the shear strength of the soil, thereby decreasing the probability of slope failure. The purpose of this manual is to provide a single comprehensive reference for geotechnical engineers and hydrogeologists on designing horizontal drainage systems to improve slope stability. Guidelines are provided for translational and rotational failure and consider fractured systems. Basics of hydrogeologic and geotechnical terminology, site characterization and conceptualization, groundwater modeling techniques and template projects help to guide the user with respect to identifying important parameters to drainage design. An iterative approach is presented for determining the minimum drain construction to lower water levels enough to keep the factor of safety (FOS) greater than 1.2.

Simple systems may only require an analytic approach to computing maximum water levels. Techniques are supplied for steady state conditions given a flat surface, a sloped surface less than 10° and a discussion is provided on the influence of recharge and hydraulic conductivity on drainage design. Analytic equations for transient solutions for a flat surface are given for different drain depths with respect to the impermeable barrier as well as for sloping surface with a declining water table over time. Past research has found that flow to ditches; water table elevation and the rate of water table decline were independent of slope for slopes less than 15-30%. For these relatively shallower slopes, flat-surfaced assumptions can be maintained with little error. In all cases drainage design based on analytic (and graphical) approaches is focused only on drain spacing or the location of the first interceptor drain in a sloped system. However, analytic results can be used to assess impact of system response to lowering the overall water table prior to a rapid rise caused by a large storm event.

Irregular drain networks, heterogeneous or anisotropic aquifer conditions, complex slope geometry, a rapid rise in pore pressures, as well as fractured rock network may mandate a numeric modeling approach. As a general rule, drains installed a significant distance into the hillside at the lowest possible elevation, will capture the majority of groundwater and have the largest effect on lowering the water table. Drains located in the upper region of a slope are found to have no real significance if additional deeper drains are in the lower part of a slope as the water table will eventually be reduced to the lowest drain level and any drains above the lowest-most drain will no longer be effective. The only exception to this rule might be for site conditions that have the ability to setup significant perched water table conditions.

Translational failure of thin geologic sections is found more sensitive to water level increases in the upper slope compared to groundwater seepage in the lower slope. In contrast, rotational failure in the slope toe is susceptible to rising pore pressures in the lower slope region. In both cases, toe drains should be installed, with length and density of drain network increasing with decreasing hydraulic conductivity and storage and with increasing anisotropy. Horizontal drains may be ineffectual at promoting slope stability in low conductive soils with low storage. The ability to stabilize slopes with horizontal drains declines for all soil types with increased anisotropy.

Table of Contents

Chapter 1: Introduction

1.1	Problem Statement.....	1
1.2	Background.....	2
1.3	Objective of Manual.....	5
1.4	References Cited.....	6

Chapter 2: Slope Stability Analysis

2.1	Introduction.....	10
2.2	Factor of Safety.....	11
2.3	Methods of Slope Stability Analysis.....	11
2.3.1	Slice Method	11
2.3.2	Janbu's Method.....	13
2.3.3	Morgenstern-Price Method	14
2.3.4	Infinite Slope Method.....	15
2.3.5	Wedge Method of Analysis.....	16
2.3.6	Infinite Slope: Hydraulic Gradient Effects.....	17

Chapter 3: Introduction to Groundwater Hydrology

3.1	Aquifer Types.....	22
3.2	Hydraulic Head	22
3.3	Properties of Aquifers.....	24
3.3.1	Porosity and Sorting	24
3.3.2	Specific Yield	26
3.3.3	Specific Storage and Storativity	27
3.3.4	Hydraulic Conductivity	28

3.3.5	Transmissivity.....	29
3.3.6	Homogeneity and Isotropy	29
3.3.7	Representative Elementary Volume (REV)	31
3.4	Darcy's Law	33
3.5	Groundwater Flow Equation for a Confined Aquifer	34
3.5.1	Transient Conditions	34
3.5.2	Homogenous/Isotropic.....	36
3.5.3	Steady State Conditions.....	36
3.6	Groundwater Flow Equation for an Unconfined Aquifer	37
3.6.1	Transient Conditions	37
3.6.2	Steady State Conditions.....	38
3.7	References Cited.....	39

Chapter 4: Site Characterization

4.1	Introduction.....	40
4.2	Hydrogeologic Model.....	40
4.2.1	Watershed Delineation and Topography	40
4.2.2	Hydrostratigraphy	41
4.2.3	GrounwaterData	44
4.2.4	Precipitation.....	46
4.2.5	Hydrologic Soil-Cover Complexes	47
4.2.6	Hydraulic Conductivity	48
4.2.6.1	Grain-Size Distribution.....	51
4.2.6.2	Laboratory Estimates of Hydraulic Conductivity.....	51
4.2.6.3	Slug Tests	53
4.2.6.4	Aquifer Pump Tests	57
4.3	Specific Yield.....	63
4.4	Horizontal Drain Characteristics and Drain Flow.....	64
4.5	Fractured Rock Characterization	66
4.5.1	Spacing.....	69
4.5.2	Length.....	71

4.5.3	Displacement-Length Scaling Relations.....	73
4.5.4	Hydraulic Conductivity	75
4.5.5	Density.....	76
4.6	Geotechnical Characterization	77
4.6.1	In-Situ Testing	78
4.7	References Cited.....	88

Chapter 5: Estimating Groundwater Recharge

5.1	Introduction.....	94
5.2	SCS Method for Abstractions	94
5.2.1	Example Calculation for Recharge	96
5.2.2	Modifications to the Curve Number	96
5.3	SCS 100-Year 24-Hour Storm Event	98
5.3.1	Example Problem: Recharge Calculation for 100-Year, 24-Hour Storm.....	104
5.4	Steady State Recharge	105
5.5	References Cited.....	110

Chapter 6: Introduction to Groundwater Modeling

6.1	Introduction.....	112
6.2	Conceptual Model.....	113
6.3	MODFLOW.....	114
6.3.1	Finite Difference Numerical Method.....	115
6.3.2	Grid Design.....	117
6.3.3	Boundary Conditions and Applied Stresses.....	120
6.3.3.1	Specified Head Boundary Cells.....	120
6.3.3.2	Specified Flux	120
6.3.3.3	Head Dependent Boundaries.....	122
6.3.4	Initial Conditions	123
6.3.5	MODFLOW Numeric Solvers.....	124
6.4	Calibration Strategies.....	124

6.4.1	Sensitivity Analysis	127
6.4.2	Verification.....	129
6.5	References Cited.....	129

Chapter 7: Horizontal Drain Design

7.1	Introduction.....	131
7.2	Controlling Factors of Drainage Design.....	131
7.3	Preliminary Analysis.....	136
7.4	Analytical Equations.....	137
7.4.1	Steady-State Conditions	138
7.4.1.1	Hooghoudt Equation (Flat Surface)	138
7.4.1.2	Slopes Less than 10°	142
7.4.1.3	Influence of Recharge and Hydraulic Conductivity on Drainage Design (all slopes)	147
7.4.2	Transient Solutions.....	150
7.4.2.1	Flat Surfaces	150
7.4.2.2	Sloping Surface – Maximum Water Levels and Rates of Decline	155
7.4.3	Limitations of Analytical Approaches	159
7.5	Numeric Modeling Approach to Drainage Design	160
7.5.1	Hydraulic Soil Properties	160
7.5.2	Translational Failure (Site D).....	160
7.5.2.1	Site Description	160
7.5.3	Design Storm.....	161
7.5.3.1	Model Domain and Conceptual Model.....	161
7.5.3.2	MODFLOW-NWT	163
7.5.3.3	Geotechnical Parameters and Preliminary Slope Stability Analysis	165
7.5.3.4	Drain Configurations.....	166
7.5.3.5	Analysis – No Calibration	174
7.5.3.6	Analysis - Observed Data Available (Isotropic Conditions Assumed)	194
7.5.4	Rotational Failure (Site B)	202
7.5.4.1	Site Description	202
7.5.4.2	Model Domain and Conceptual Model.....	202

7.5.4.3	Drain Configurations.....	203
7.5.4.4	Geotechnical Parameters and Initial Slope Stability Analysis	205
7.5.4.5	Analysis – No Observed Data	205
7.6	References Cited.....	217

Chapter 8: Network-Scale Flow and Drainage Design in Fractured Rock

8.1	Introduction.....	219
8.2	Network Structure and Flow	220
8.2.1	Network Structure.....	220
8.2.2	Hydraulic Conductivity Tensor	224
8.3	Hillslope Drainage Network Design for Fractured Rock.....	234
8.3.1	Differentiating Fracture Types	235
8.3.2	Fracture Intersection Analysis.....	237
8.3.2.1	Influence of Fracture Length and Transmissivity	237
8.3.2.2	Influence of Fracture Set Orientation and Density	238
8.3.2.3	Deviations between Individual Realizations and the Ensemble	240
8.3.2.4	Site-Specific Fracture Networks	241
8.3.3	Summary.....	244
8.4	References.....	245

Chapter 9: Summary

9.1	Concluding Remarks.....	248
-----	-------------------------	-----

Appendix A: Definition of Symbols Used

Geotechnical Symbols	251
Hydrologic Symbols	252

Appendix B: MODFLOW Tutorial using Groundwater Vistas Graphical User Interface

B-1	Site Description.....	256
B-2	Model Domain and Conceptual Model	257
B-3	Steady State Model (Isotropic Conditions)	258
B-3.1	Model Grid and Domain	258
B-3.2	Top and Bottom Elevations.....	263
B-3.3	Initial Heads	267
B-3.4	Hydraulic Parameters	268
B-3.5	Boundary Conditions	269
B-3.6	MODFLOW-NWT	273
B-3.7	Model Execution	276
B-3.8	Steady State Calibration	280
B-4	Transient Conditions (Isotropic Conditions, Pre-Drain)	289
B-4.1	Stress Period Set Up	289
B-4.2	Observation Wells	291
B-4.3	Recharge	293
B-4.4	Storage Parameters.....	294
B-4.5	Model Execution.	295
B-4.6	Transient Calibration	297
B-5	Design Storm (Isotropic Conditions)	303
B-6	Modeling Anisotropy	315
B-6.1	Adding Model Layers.....	315
B-6.2	Calibration of VKA.....	320

Appendix C: Groundwater Modeling Example- Site SR 101 MP 69.8

C-1	Site Description.....	323
C-2	Model Domain and Grid.....	324
C-3	Modeling Strategy.....	325
C-3.1	Steady State Conditions.....	325

C-3.2	Transient Conditions	325
C-4	Design Storm	329
C-5	Geotechnical Analysis and Drain Arrays.....	330

Appendix D: Major Soils and Associated Soil Groups in the United States

D-1	NRCS Interactive Website	333
D-2	Tabulated Hydrologic Soil Groups for the United States	336
D-3	References Cited	377

Chapter 1

Introduction

1.1 Problem Statement

The presence of water is one of the most critical factors contributing to the instability of hillslopes. A common solution to improve the stability of hillslopes is the installation of horizontal drains to decrease the elevation of the water table surface and reduce pore pressures within the effected soil/rock units. Reduction of water pressures results in a corresponding increase in the shear strength of soil or decrease in hydrostatic pressures within discontinuities in a fractured rock mass, thereby improving slope stability.

Due to the complex geometry of slopes and subsurface conditions, the heterogeneity and anisotropic nature of hydraulic conductivity, and the transient nature of the groundwater, the design of such drains for hillslope drainage can be a difficult task. Aquifer characterization and groundwater modeling techniques common to hydrogeologic practice are generally not well known or routinely employed in the geotechnical practice of stabilizing slopes with subsurface drainage by governmental transportation, public works, and resource agencies. The reasons for this might be attributed to the higher investigation costs for adequate hydrogeologic characterization, as compared to a more standard geotechnical investigation, and the necessary knowledge or experience in this discipline that many geotechnical specialists lack. Furthermore, while a wealth of literature exists for the design of drainage systems in relatively flat irrigated areas (e.g., Maasland, 1940; Donnan, 1946; Israelsen, 1950; Talsma & Haskew, 1959; Kirkham, 1958; U.S. Department of the Interior, 1978), robust design approaches for hillslope drainage are not readily available. As a result, subsurface drains for hillslopes have often been installed in a makeshift manner with varying degrees of success.

The purpose of this manual is to consolidate information related to, and provide guidance for, the design of horizontal drains for slope stability. The design guidance provides the necessary information and techniques to better characterize the hydrogeology and then estimate water levels under drained conditions, applying a clear methodology. The approach taken is to provide options for the geotechnical designer such that the hydrogeologic analysis can be tailored for site-specific conditions. For example, a straightforward approach to drainage design using currently available analytic/graphical methods may be appropriate for hillslopes with simple geologic and hydrogeologic regimes. In other instances, subsurface conditions may be sufficiently complex to require additional characterization and numerical modeling of the groundwater system. Ultimately, geotechnical designers will be able to use this guidance to better assess hydrogeologic conditions and develop a drainage design to improve slope stability with more predictable results and optimal efficiencies.

1.2 Background

As the intended audience for this manual is primarily the geotechnical specialist, only a brief overview of slope stability analysis involving common failure modes in soil and rock and the associated contribution of groundwater are provided in Chapter 2.

Numerous textbooks, peer-reviewed journal articles, and agency reports (e.g. U.S. Geological Survey, U.S. Bureau of Reclamation, etc.) exist that describe how to collect and analyze hydrogeologic data. Some of the more popular hydrogeology textbooks include Freeze & Cherry (1979), Fetter (1996; 2001), Domenico & Schwartz (1990), and Driscoll (1986). Although there are a number of similarities amongst these textbooks, each one has a slightly different focus. The critical elements of hydrogeologic science are summarized in Chapter 3 of this manual. Topics such as hydraulic head, fluid potential, Darcy's Law, hydraulic conductivity, permeability, anisotropy and heterogeneity are summarized for those less familiar with these concepts. These textbooks, along with other references, such as, Jacob (1940), Cooper & Jacob (1946), and Papadopoulos, et al. (1973), and Bennett (1976), provide excellent sources for the measurement of hydrogeologic parameters (i.e. hydraulic conductivity, and storage parameters) using slug and pumping tests, with only rudimentary discussion provided here.

Another important component to characterizing a site is the construction of a conceptual hydrogeologic model. Anderson & Woessner (1991) provide an excellent overview of this process. Regardless of the complexity of site conditions, a conceptual model provides a simplification of the field conditions and organization of the associated field data so the system can be analyzed more readily. Typical data sources for a hydrogeologic assessment include:

- Geologic maps and cross sections
- Topographic maps and digital terrain models
- Maps of surface water features such as streams and springs
- Water table and potentiometric maps
- Generalized maps of hydraulic conductivity distributions
- A groundwater budget including rates of groundwater recharge, evapotranspiration, and any natural groundwater inflows and outflows

This information is detailed in Chapter 4 of the manual to provide a basis for the groundwater characterization effort.

The need for a design method for drains has been noted by several researchers and various charts and diagrams were initially developed to aid in the analysis and design of drains (Choi, 1974; Kenney et al., 1978; Prellwitz, 1978; Nonveiller, 1981). Typically, they describe effectiveness in terms of increased factor of safety (ratio of shear strength to shear stress) once horizontal drains are installed. In addition, some early studies on drainage design for slope stability employed physical and centrifuge modeling techniques on idealized slopes (Kennedy et al. 1977; Resnick and Znidarcic 1991), but these tools have yet to be calibrated against field data.

There have been a few studies (Royster, 1980; Lau & Kenney, 1984; Martin et al., 1994, Pathmanathan, 2009), which attempted to describe in part the many parameters controlling the horizontal drainage design or evaluate the feasibility of using a system of horizontal drains to lower groundwater levels in hillsides (e.g., Craig and Gray, 1985). For example, Martin et al., 1994 suggested that a small number of drains installed at appropriate locations in accordance with a well-conceived conceptual groundwater model may be more effective than a large number of drains installed at uniform spacing over the slope. Presently, there isn't a single comprehensive reference within the geotechnical literature that provides practical guidelines for the design of subsurface drainage for improving slope stability.

Existing drainage design guidelines fall into two distinct categories: steady-state, and transient-based methods. Since slope stability problems commonly occur during or shortly following intense precipitation events, over relatively short periods, the steady-state design equations may not be appropriate for drainage design for slope stability. The transient design equations rely on analytic solutions to the groundwater flow equation and require a number of simplifying assumptions such as parallel and regularly spaced subsurface drains, and homogeneous hydraulic conductivity. Although these conditions may not be met in real field situations, the analytic design equations may still prove useful for preliminary design purposes.

Research developed over the last seven decades provides numerous analytic solutions for a variety of field conditions and assumptions. Hooghoudt (1940) presented one of the first design equations for subsurface drainage conditions and this method falls into the steady-state category. U.S. Department of Interior (1978) provides useful transient design equations to determine appropriate drain spacing and depth. The U.S. Department of Interior (1978) method was developed for flat conditions, but other researchers have found that it is applicable for steep slopes (Ram & Chauhan, 1987). The equations require an estimate of the hydraulic conductivity (K), specific yield (S_y), and the depth to an impermeable barrier. The design manual also provides a relationship between rainfall and the amount of rainfall and infiltration that becomes groundwater recharge. The trial-and-error solution begins with a measured pre-drainage water table elevation, and then curves are provided that relate maximum water table height to hydrogeologic parameters (K and S_y), groundwater recharge, and drain spacing and depth. Drain spacing and depth are adjusted until the maximum water table height is lower than a pre-defined design condition.

Drainage of sloping lands has been discussed by many writers (Bouwer, 1955; Schmid & Luthin, 1964; Wooding & Chapman, 1966; Childs, 1971; Towner, 1975; Lesaffre, 1987; Lesaffre & Zimmer, 1988; Ram & Chauhan, 1987; Fipps & Skaggs, 1989), but it has seldom been studied in transient conditions with variable recharge. Furthermore, limited in situ investigations and model validations have been carried out. Most of the validation has been achieved by use of Hele-Shaw viscous flow models, such as the one developed by Luthin & Guitjens (1967) and Marei & Towner (1975). Results indicated that slopes up to 30% have little effect on the designed drain spacing, and this result was confirmed by Chauhan et al. (1968) and Childs (1971). Benoit & Bornstein (1972) focused on the hydrologic drainage functioning of a transverse sloping system. Lesaffre (1987) demonstrated that under steady-state conditions, the influence of slope depends on the ratio between the net recharge rate and the saturated hydraulic conductivity. More importantly, these papers provide analytic, semi-analytic, or graphical solutions to

aid in the design of drainage systems on sloping land. Hartani et al. (2003) incorporated these drainage solutions into the drainage model SIDRA, which simulates hourly values of water table elevations and drain flow rates.

In many situations, the complexity of the field site requires the use of a numerical model to develop accurate estimates of water table position under drainage conditions. Highly heterogeneous hydraulic conductivity fields (e.g. fractured systems) and/or complex drainage geometries are examples of conditions that require a more robust modeling approach. Cai, et al. (1998) simulated the effect of horizontal drains on the water table position using a three-dimensional finite element model. They extended the modeling effort by integrating a three-dimensional, elasto-plastic shear strength, finite element model to calculate a global safety factor. The model was used to investigate the influence of drain spacing, orientation, and length; rainfall intensity; and hydraulic conductivity on the increase in the safety factor. Their research found the safety factor is linearly dependent on pressure heads near the slope surface.

Rahardjo et al. (2003) performed a rigorous measurement campaign combined with numerical modeling to determine the effectiveness of horizontal drains for slope stability. One of the key findings is that shallow drains are ineffective in improving the stability of a slope and drains are most effective when placed at the lowest elevation possible. The basic tenet is to lower the main water table, with less emphasis placed on direct capture of infiltration. If installed a significant distance into the hillside at the lowest possible elevation, drains will capture the majority of groundwater and have the largest effect on lowering the water table. These results are also consistent with the research findings of Lau & Kenney (1984) and Martin et al. (1994).

There are a variety of numerical groundwater models that can be used to analyze the impact of drainage systems on water table behavior. In general there are two main categories of groundwater models: fully saturated and saturated/unsaturated models. MODFLOW (Harbaugh, et al., 2000) is, by far, the most popular saturated groundwater flow model used by hydrogeologists. One reason for its popularity is its modular structure, which allows developers to easily incorporate packages to simulate a variety of subsurface processes. Two such packages that are useful for drainage analysis include the “drain package” and the “unsaturated-zone flow package”. The drain package has been used for over two decades to simulate subsurface drainage (e.g. Pohl & Guitjens, 1994). The recent addition of the unsaturated-zone flow package allows one to simulate the vadose zone in an efficient manner (Niswonger et al., 2006). Given the results of Rahardjo, et al. (2003), unsaturated zone analysis may not be necessary for most sites. The use of the unsaturated zone package may prove useful for cases where the exact timing of flow through the vadose zone to the saturated groundwater system becomes important. Most recently, the U.S. Geological Survey released the GSFLOW model which is a fully coupled ground-water and surface-water flow model based on PRMS and MODFLOW (Markstrom et al., 2008). Although this model would provide the most rigorous analysis for drainage design by linking surface and groundwater processes, site-specific models require numerous input parameters, significant pre-processing, and calibration before they can be used effectively. As such, it is unlikely that complex models such as GSFLOW would be used for regular analysis of slope stability problems.

1.3 Objective of Manual

The primary focus of the design manual is to provide hydrogeologic assistance to geotechnical engineers. Specific objectives include:

1. To review all applicable literature related to the design of subsurface drainage systems.
2. To develop a standard protocol for proper hydrogeologic site characterization using standard and accepted methodologies common to geotechnical and hydrogeological practice.
3. Select design guidelines that utilize both analytic and numerical models to cover a wide range of field conditions.
4. Validate selected design methodologies against field data.
5. Provide charts, equations, and useful numerical models for the optimal design of a subsurface drainage system.

Benefits to users of this manual include:

- A single comprehensive reference that can be used by geotechnical engineers and hydrogeologists to design horizontal drainage systems to increase slope stability.
- Safety of unstable slopes and landslides should increase significantly as designs mitigating subsurface drainage are better understood.
- As drainage systems become better understood, they will most likely be used more extensively for slope stabilization which will significantly reduce expenditures for slope stabilization, improve performance, and provide for more rapid installation.
- Drainage designs should become more efficient and cost-effective.
- Construction projects using these designs should have more predictable results.

The manual is organized into nine chapters and four appendices:

Chapter 1: Provides an overview of the problem and a review of previous research relevant to objectives of this work.

Chapter 2: Briefly presents slope stability analysis involving common failure modes in soil and rock and the associated contribution of groundwater.

Chapter 3: Includes a presentation of critical hydrologic parameters that are required to properly parameterize a groundwater system. This includes an explanation of aquifer types, aquifer properties, Darcy's Law, the groundwater flow equation and groundwater recharge.

Chapter 4: Details are provided on how to characterize a field site for hydrologic parameters necessary for drain design. Data collection techniques are discussed, along with how these data define hydrologic parameters, the pragmatic use of these parameters for groundwater modeling and how to estimate these parameters if data are not collected.

Chapter 5: Recharge calculations based on the SCS curve number are detailed with step-by-step guidelines. Calculations for steady state, 100-year precipitation events, as well as observed precipitation time series data are outlined.

Chapter 6: Groundwater modeling basics are provided to familiarize one with a standard and defensible approach to numeric modeling. This includes the development of a conceptual model, defining boundary conditions, typical calibration procedures and the verification of model results.

Chapter 7: Drain design is catalogued with analytical solutions and numeric techniques. For numeric techniques, generic sites for translational and rotational failure. Proper communication between groundwater modeling and geotechnical analysis is outlined for efficient drain design. Results point to sensitive hydrologic parameters and threshold processes important to drain design guidelines.

Chapter 8: Techniques to characterize the hydraulic conductivity tensor for fractured rock are discussed in the context of data collected on fracture spacing, orientation and length.

Chapter 9: Summarizes design considerations and modeling results.

Appendix A: Contains a comprehensive list of symbols used in the manual with units and definitions.

Appendix B: Is a step-by-step guide to creating a groundwater model for a translational failure surface using the GUI Groundwater Vistas. The guide includes developing a conceptual model, how to build a finite difference grid, add boundary conditions and stresses, integration with geotechnical analysis, importing/exporting data, visual analysis. Analysis is done with and without calibration.

Appendix C: Provides a demonstration site for groundwater modeling is presented that contains long term data. The site is a single layer of disrupted claystone. The site is complex but affords a discussion of modeling techniques as well as the advantages and limitations of the approach.

Appendix D: Contains a listing of major soils and associated hydrologic soil groups to aid in curve number calculation necessary for the SCS approach used to calculate recharge.

1.4 References Cited

- Anderson, M. P., and W. W. Woessner, 1991. Applied Groundwater Modeling – Simulation of Flow and Advective Transport, Academic Press, San Diego, 381p.
- Bazaraa, A. S., M. S. Abdel-Dayem, A. Amer, and L. S. Willardson, 1986. Artesian and anisotropic effects on drain spacing, Journal of Irrigation and Drainage Engineering, 112(1), 55-64.
- Bennett, G. D., 1976. Introduction to Ground-Water Hydraulics, Techniques of Water-Resources Investigations of the U.S. Geological Survey, Chapter B2, Book 3, Washington, D.C., 172p.
- Benoit, G. R., and J. Bornstein, J., 1972. Considerations for effective sloping land drainage systems. Proceedings of the Soil Science Society of America, 36, 819– 823.
- Bouwer, H, 1955. Tile drainage of sloping fields, Agricultural Engineering, 36, 400–403.

- Cai, F., K. Ugai, A. Wakai, and Q. Li, 1998. Effects of horizontal drains on slope stability by three-dimensional finite element analysis, *Computers and Geotechnics*, 23(4), 255-275.
- Chauhan, H. S., G. O. Schwab, and M. Y. Hamdy, 1968. Analytical and computer solutions of transient water tables of drainage of sloping lands." *Water Resources Research*, 4, 453-479.
- Childs, E. C., 1971. Drainage of groundwater resting on a sloping bed, *Water Resources Research*, 7(5), 1256-1263.
- Choi, Y. L., 1974. Design of horizontal drains, *Journal of Engineering Society, Hong Kong*, December, 37-49.
- Cooper, H. H., and C. E. Jacob, 1946. A generalized graphical method for evaluating formation constants and summarizing well field history, *Transactions of the American Geophysical Union*, 27, 526-534.
- Craig, D.J., and I. Gray, 1985. Groundwater Lowering by Horizontal Drains, Geotechnical Control Office Publication No. 2/85, Engineering Development Department, Hong Kong, 123p.
- Domenico, P. A., and F. W. Schwartz, 1990. *Physical and Chemical Hydrogeology*, John Wiley and Sons, New York, 824p.
- Donnan, W. W., 1946. Model tests of a tile-spacing formula, *Proceedings of the Soil Science Society of America*, 11, 131-136.
- Driscoll, F. G., 1986. *Groundwater and Wells*, Johnson Screens, Minnesota, 1089p.
- Fetter, C.W., 2001. *Applied Hydrogeology*, 4th Edition, Prentice-Hall, Inc., New Jersey, 598p.
- Fetter, C.W. 1994. *Applied Hydrology*. Third Edition. Prentice-Hall, Inc., New Jersey. 691 p.
- Fipps, G., and W. Skaggs, 1989. Influence of slope on subsurface drainage of hillsides, *Water Resources Research*, 25(7), 1717-1726.
- Freeze, R. A., and J. A. Cherry, 1979. *Groundwater*, Prentice-Hall, Inc., New Jersey, 604p.
- Harbaugh, A. W., E.R. Banta, M.C. Hill, and M.G. McDonald, 2000. MODFLOW-2000, The U.S. Geological Survey Modular Ground-Water Model – User Guide to Modularization Concepts and the Ground-Water Flow Process, U.S. Geological Survey Open File Report 00-92, Reston, Virginia.
- Hartani, T., D. Zimmer, and B. Lesaffre, 2003. Drainage of sloping lands with variable recharge model – Validation and Applications, *Journal of Irrigation and Drainage Engineering*, 129(4), 284-290.
- Hooghoudt, S.B. 1940. General consideration of the problem of field drainage by parallel drains, ditches, watercourses, and channels. Publ. No.7 in the series Contribution to the knowledge of some physical parameters of the soil (titles translated from Dutch). Bodemkundig Instituut, Groningen, The Netherlands.
- Israelsen, O. W., 1950. *Irrigation Principles and Practices*, John Wiley and Sons, New York.
- Jacob, C. E., 1940. On the flow of water in an elastic artesian aquifer, *Transactions of the American Geophysical Union*, 2, 574-586.

- Kenney, T. C., M. Pazin, and W. W. Choi, 1977. Design of horizontal drains for soil slopes. *Journal of Geotechnical Engineering*, ASCE, 103(11), 1311-1323.
- Kirkham, D. 1958. Seepage of steady rainfall through soil into drains, *Transactions of the American Geophysical Union*, 39, 892-908.
- Kuichling, E., 1889. The relation between the rainfall and the discharge of sewers in populous districts, *Transactions of the American Society of Civil Engineers*, 20.
- Lau, K.C., Kenney, T.C., 1984. Horizontal drains to stabilize clay slopes. *Canadian Geotechnical Journal* 21 (2), 241–249.
- Lesaffre, B., 1987. Analytical formulae for traverse drainage of sloping lands with constant rainfall, *Irrigation Drainage Systems*, 1, 105–121.
- Lesaffre, B., and D. Zimmer, 1988. Subsurface drainage peak flows in shallow soils, *Journal of Irrigation and Drainage Engineering*, 114(3), 266–277.
- Luthin, J. N., and J. C. Guitjens, 1967. Transient solutions for drainage of sloping lands, *Journal of Irrigation and Drainage Engineering*, 43–51.
- Martin, R.P., Siu, K.L., Premchitt, J., 1994. Review of the performance of horizontal drains in Hong Kong. Special Project Report, SPR 11/94, Geotechnical Engineering Office, Civil Engineering Department, Hong Kong, p. 106.
- Maasland, M., 1956. The relationship between permeability and the discharge, depth, and spacing of tile drains, Bulletin No. 1, Groundwater and Drainage Series, Water Conservation and Irrigation Commission, New South Wales, Australia.
- Marei, S. A., and G. D. Towner, 1975. A Hele-Shaw analog study of the seepage of groundwater resting on a sloping bed, *Water Resources Research*, 11(4), 589–594.
- Markstrom, S.L., Niswonger, R.G., Regan, R.S., Prudic, D.E., and Barlow, P.M., 2008, GSFLOW-Coupled Ground-water and Surface-water FLOW model based on the integration of the Precipitation-Runoff Modeling System (PRMS) and the Modular Ground-Water Flow Model (MODFLOW-2005): U.S. Geological Survey Techniques and Methods 6-D1, 240 p.
- Martin, R.P., Siu, K.L., Premchitt, J., 1994. Review of the performance of horizontal drains in Hong Kong. Special Project Report, SPR 11/94, Geotechnical Engineering Office, Civil Engineering Department, Hong Kong, p. 106.
- Miller, J. F., R. H. Frederick, and R. J. Tracey, 1973. *Precipitation-Frequency Atlas of the Western United States*, NOAA Atlas 2, 50p.
- Niswonger, R.G., Prudic, D.E., and Regan, R.S., 2006, Documentation of the Unsaturated-Zone Flow (UZF1) Package for modeling unsaturated flow between the land surface and the water table with MODFLOW-2005: U.S. Geological Techniques and Methods Book 6, Chapter A19, 62 p.

- Nonveiller, E., 1981. Efficiency of horizontal drains on slope stability, Proceedings of the 10th International Conference on Soil Mechanics and Foundation Engineering, Stockholm, Sweden, 3, 495-500.
- Papadopoulos, S. S., J. D. Bredehoeft, and H. H. Cooper, 1973. On the analysis of 'slug test' data, Water Resources Research, 9(4), 1087-1089.
- Pathmanathan, M. L., 2009. Numerical Simulation of the Performance of Horizontal Drains for Subsurface Slope Stabilization, M.S. Thesis, Washington State University, 95p.
- Pohll G. and J. Guitjens, 1994. Modelling regional flow and flow to drains, Journal of Irrigation Drainage Engineering, 20(5), 71–82.
- Prellwitz, R. W., 1978. Analysis of parallel drains for highway cut-slope stabilization, Proceedings of the 16th Annual Idaho Engineering Geology and Soils Engineering Symposium, Boise, Idaho: 153-180.
- Rahardjo, H., K. J. Hritzuk, E. C. Leong, and R. B. Rezaur, 2003. Effectiveness of horizontal drains for slope stability, Engineering Geology, 69, 295-308.
- Ram, S., and H. S. Chauhan, 1987. Drainage of sloping lands with constant replenishment. Journal of Irrigation and Drainage Engineering, 113(2), 213–223.
- Resnick, G. S., and D. Znidarcic, D., 1990, Centrifugal modeling of drains for slope stabilization. Journal of Geotechnical Engineering, ASCE, 116(11), 1607-1624.
- Royster, D.L., 1980. Horizontal drains and horizontal drilling: an overview. Transportation Research Record 783, 16– 25.
- Schmid, P., and N. J. Luthin, N. J. 1964. The drainage of sloping lands, Journal of Geophysical Research, 69(8), 1525–1529.
- Talsma, T., and H. C. Haskew, 1959. Investigation of water-table response to tile drains in comparison with theory, Journal of Geophysical Research, 64(11), 1933-1944.
- Towner, G. D. 1975. Drainage of groundwater resting on a sloping bed with uniform rainfall, Water Resources Research, 11(1), 144–147.
- U.S. Department of the Interior, 1978. Drainage Manual, Water Resources Technical Publication, Washington, D.C., 286p.
- Wooding, R. A., and T. J. Chapman, 1966. Groundwater flow over a sloping impermeable layer. 1: Application of the Dupuit-Forchheimer assumption, Journal of Geophysical Research, 71(12), 2895–2902.

Chapter 2

Slope Stability Analysis

2.1 Introduction

Gravitational and seepage forces contribute to slope instability. The most important types of slope failure are illustrated in their generalized form in Figure 2.1. They are the circular rotational slip; non-circular rotational slip; translational slip and compound slip.

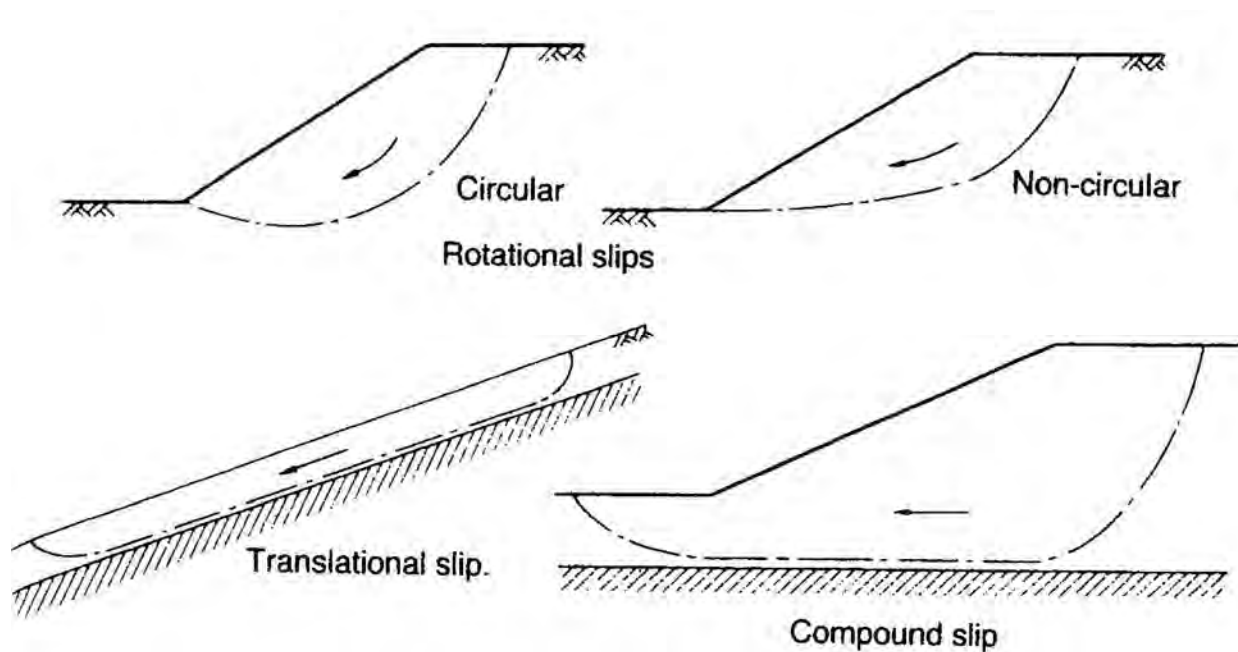


Figure 2.1: Types of slope failures (Craig 1997)

In practice, limit-equilibrium methods are used in the analysis of slope stability. It is considered that failure is incipient along an assumed or a known failure surface. The shear strength required to maintain a condition of limit equilibrium is compared with the available shear strength of the soils giving the average (lumped) factor of safety along the failure surface.

The critical role ground water plays in the stability of slopes was recognized by Terzaghi (1923) in his principle of effective stress; $\sigma' = \sigma - u$, where σ' is the effective normal stress, σ the total normal stress, and u the pore water pressure. It is evident that a slope stability analysis carried out in terms of effective stress requires an understanding of the distribution of pore water pressures in the slope, and this understanding implies knowledge of the groundwater flow system. When sufficient funding is

available and a slope failure or potential failure surface has been identified, piezometers can be installed and pore pressures can be measured directly. However, even with such measurements, extrapolations must often be made over large distances to approximate pore pressure distribution between known points (Hodge and Freeze 1977).

The mathematical simulation of groundwater systems similar to the one reported here using the MODFLOW would prove to be useful as an independent check on field measured pore pressures, and when anomalies arise, they may point to unanticipated field conditions that can lead to a modification of the subsurface model used for analysis. It is also important to note that serious errors may result in the factor-of-safety evaluation using limit-equilibrium stability analyses if groundwater data are inadequate or incorrectly interpreted.

This chapter first presents a summary of the widely used limit-equilibrium-based slope stability analysis. It is concluded with an analysis (Iverson 1991) that highlights the importance of the groundwater flow field, especially the direction of pore pressure gradients, in influencing the stability of infinite slopes. The insights drawn from this and other such studies would apply to other more complex limit-equilibrium analyses.

2.2 Factor of Safety

Factor of safety (FOS) is defined as the ratio of available shear strength (τ_f) to shear strength (τ_m) which must be mobilized to maintain a condition of limiting equilibrium. This is illustrated by equation 2.1,

$$FOS = \frac{\tau_f}{\tau_m} \quad (2.1)$$

An $FOS \leq 1$ indicates an unstable slope. The acceptable minimum value of factor of safety is variable. FOS on the order of 1.2 to 1.3 are considered stable. For slopes where critical structures are sited, a higher minimum of 1.5 is commonly adopted as the consequences of failure are severe.

2.3 Methods of Slope Stability Analysis

Slope stability analysis can be carried out by using different methods with the primary ones being the slice method and the plane translational slip method.

2.3.1 Slice Method

The potential failure surface is assumed to be a circular arc with center O and radius r as shown in Figure 2.2. Width of each slice is b , u is the pore water pressure at the center of the base, and l is the length of the base. For any slice the inclination of the base to the horizontal is α , and the height, measured on the center-line, is h . Factor of safety is taken as being same for each slice. The forces acting on the slices are the total weight of the slice (W); total normal forces on the base (N); the shear force on the base (T); total normal forces on the sides (E_1 and E_2); and shear forces on sides (X_1 and X_2).

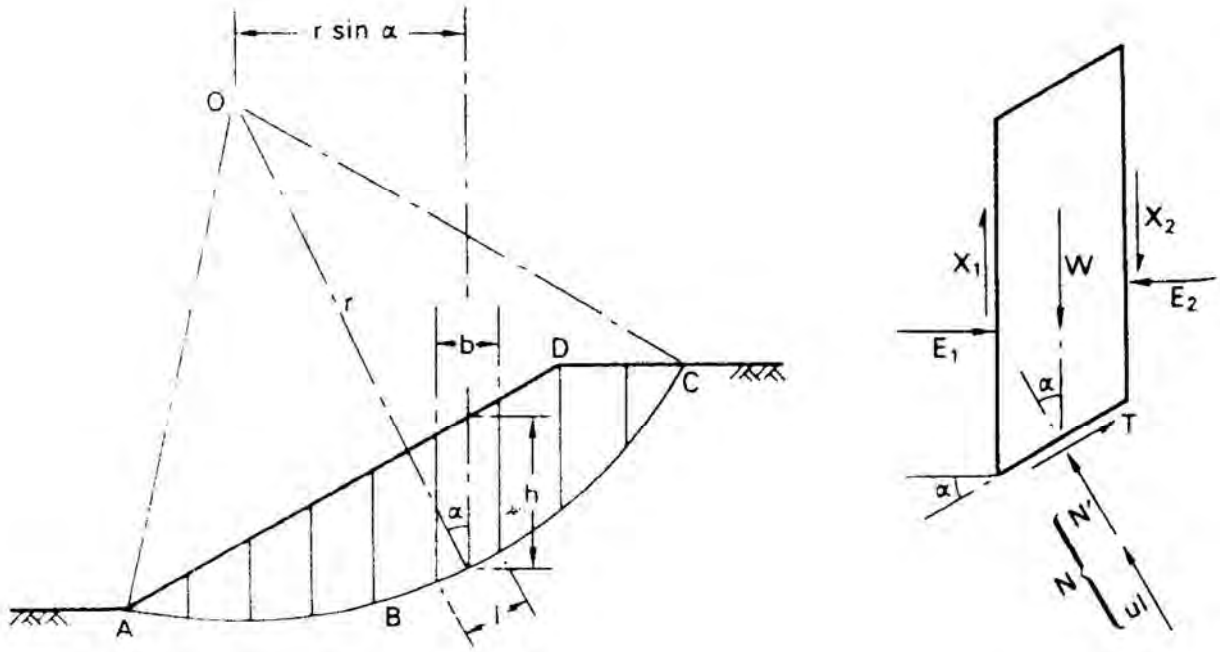


Figure 2.2: The method of slices (Adapted from Craig, 1997)

Considering momentum about O , the sum of the moments of the shear forces T on the failure arc AC must equal the moment of the weight of the soil mass $ABCD$. For any slice the level arm of W is $r \sin \alpha$, and therefore

$$\sum Tr = \sum Wr \sin \alpha \quad (2.2)$$

Shear force (T) on the base is calculated by using:

$$T = \tau_m l \quad (2.3)$$

Equation (2.1) can be rewritten as:

$$\tau_m = \frac{\tau_f}{FOS} \quad (2.4)$$

Substituting Eq. (2.4) into Eq. (2.3)

$$T = \frac{\tau_f}{FOS} l \quad (2.5)$$

Substituting Eq. (2.5) to Eq. (2.2)

$$\sum \frac{\tau_f}{FOS} l = \sum W \sin \alpha \quad (2.6)$$

$$FOS = \frac{\sum \tau_f l}{\sum W \sin \alpha} \quad (2.7)$$

For analysis in terms of effective stress, according to Mohr-Coulomb failure criterion available shear strength is calculated by using:

$$\tau_f = c' + \sigma' \tan \phi' \quad (2.8)$$

Here, c' is cohesion; ϕ' is friction angle and σ' is effective normal stress.

Substituting Eq. (2.9) to Eq. (2.7) results in:

$$FOS = \frac{\sum (c' + \sigma' \tan \phi') l}{\sum W \sin \alpha} \quad (2.9)$$

$$N' = \sigma' l \quad (2.10)$$

Where N' is the effective normal force.

If arc length AC is L_a ,

$$\sum l = L_a \quad (2.11)$$

Substituting Eqs. (2.10) and (2.11) into Eq.(2.9)

$$FOS = \frac{c' L_a + \tan \phi' \sum N'}{\sum W \sin \alpha} \quad (2.12)$$

Since the problem is statically indeterminate, assumptions need to be made in order to estimate N' in Eq. (2.9). The methods of slices differ in the manner in which these assumptions are made. We present a summary of the methods that are used in this report. Detailed accounts of these and other methods are available in soil mechanics texts. Computer software that uses most of these methods are widely available. This study uses the XSTABL program and the student version of SLOPE/W.

2.3.2 Janbu's Method

Janbu (1954) developed a general method of slices on the basis of limit equilibrium of blocks. It allows for an arbitrary shaped, slope failure surface. Forces and moments acting on individual blocks must satisfy the equilibrium except the uppermost block. The blocks are created by dividing the soil above the slip surface with dividing planes. Forces acting on individual blocks are showed in the Figure 2.3.

Forces and moment are calculated on individual blocks by taking the following assumptions (www.finesoftware.eu):

- the dividing planes between blocks are always vertical,
- the line of action of the block weight W_i passes through the center of the i^{th} segment of slip surface represented by point M,
- the normal force N_i is acting in the center of the i^{th} segment of slip surface, at point M,

position Z_i of the forces E_i acting between blocks is assumed at the slip surface end points where $z=0$.

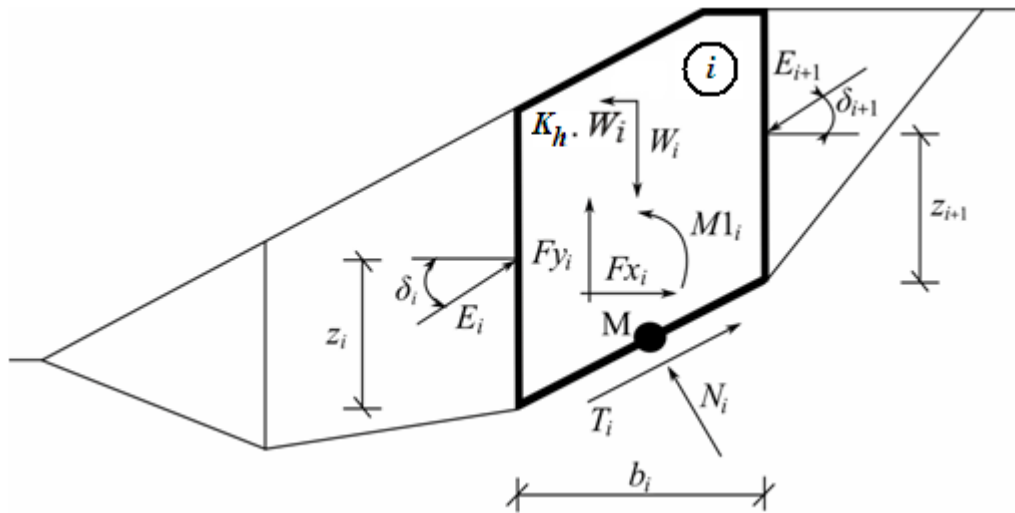


Figure 2.3: Forces acting on an individual block (adapted from www.finesoftware.eu)

The following relationships are used to find the factor of safety:

- relationship between effective and total value of the normal force acting on the slip surface,
- Mohr-Coulomb condition representing the relation between the normal and shear forces on a given segment of the slip surface (N_i a T_i),
- force equation of equilibrium in the direction normal to the i^{th} segment of the slip surface,
- force equation of equilibrium along the i^{th} segment of the slip surface, and
- moment equation of equilibrium about point M .

2.3.3 Morgenstern-Price Method

Morgenstern and Price (1965 and 1967) developed a general method of slices on the basis of limit equilibrium. Forces and moments acting on individual blocks must satisfy the equilibrium. The blocks are created by dividing the soil above the slip surface with dividing planes. Forces acting on individual blocks are showed in the Figure 2.3.

Forces and moments are calculated on individual blocks by taking the following assumptions (www.finesoftware.eu):

- dividing planes between blocks are always vertical,
- the line of action of the block weight W_i passes through the center of the i^{th} segment of slip surface represented by point M ,
- the normal force N_i is acting in the center of the i^{th} segment of slip surface at point M , and

- the inclination of forces E_i acting between blocks is different on each block (δ_i) at slip surface end point $\delta=0$.

The relationships similar to those used in Janbu's method are used to calculate the factor of safety (section 2.3.2).

2.3.4 Infinite Slope Method

The infinite slope or plane translational slip surface model is shown in Figure 2.4. The angle β indicates inclination of the slope with the horizontal, and z indicates depth of the failure plane. Location of the water table is taken at a height of mz above the failure plane. The m value lies between 0 and 1.

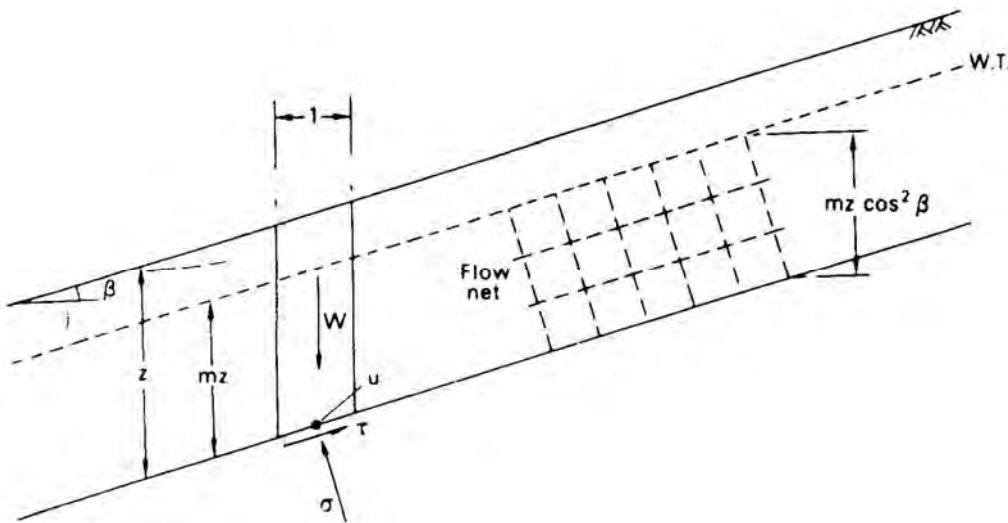


Figure 2.4: Plane translational slip (Craig, 1997)

There are five assumptions considered in the plane translational failure analysis:

- potential failure surface is parallel to the surface of the slope;
- potential failure surface is at a depth that is small compared with the length of the slope;
- length of the slope is infinite;
- water table is *parallel* to the failure surface; and
- water table is between failure surface and top soil surface.

The shear strength (τ_f) of the soil along the failure plane according to Mohr-Columb criterion is given in terms of effective stress as:

$$\tau_f = c' + (\sigma - u)\tan\phi \quad (2.13)$$

Here, c' is cohesion ϕ is the friction angle; u is the pore water pressure; and σ is the total normal stress. τ is shear strength which must be mobilized to maintain a condition of limiting equilibrium as shown in Figure 2.4.

$$\tau_m = \tau \quad (2.14)$$

Substituting Eqs. (2.13) and (2.14) into Eq. (2.1), results in the factor of safety (FOS) as:

$$\text{FOS} = \frac{c' + (\sigma - u)\tan\phi'}{\tau} \quad (2.15)$$

Expressions for σ , τ , and u are given respectively by:

$$\sigma = [(1 - m)\gamma + m\gamma_{sat}]z \cos^2 \beta \quad (2.16)$$

$$\tau = [(1 - m)\gamma + m\gamma_{sat}]z \sin \beta \cos \beta \quad (2.17)$$

$$u = mz\gamma_w \cos^2 \beta \quad (2.18)$$

where γ and γ_{sat} are the dry and saturated unit weights of the soil, respectively.

2.3.5 Wedge Method of Analysis

The wedge slip surface is shown in the Figure 2.5. The angle β indicates inclination of the slope with the horizontal, and θ indicates the angle of the failure plane with the horizontal.

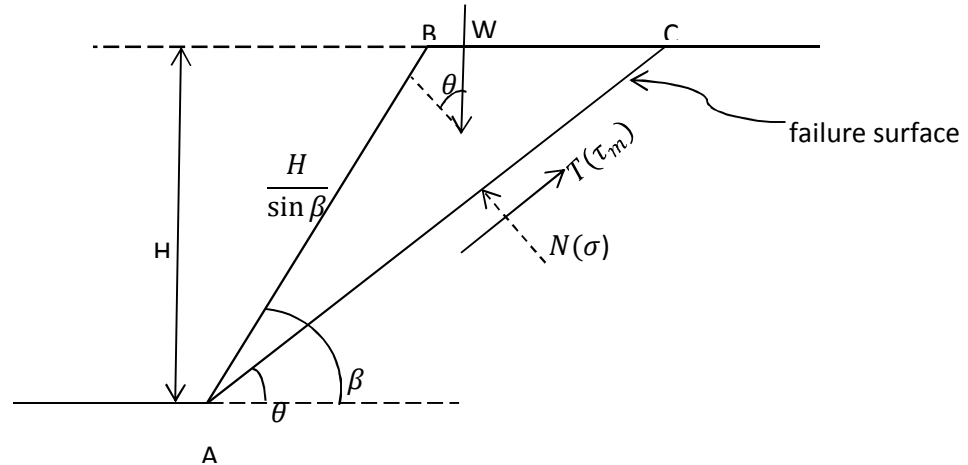


Figure 2.5: Wedge slip surface

Multiplying Eq. (2.1) by the area of AC results in:

$$F = \frac{\tau_f}{\tau_m} = \frac{\tau_f \times (\text{area of AC})}{\tau_m \times (\text{area of AC})} \quad (2.19)$$

$$\tau_m \times (\text{area of AC}) = T = W \sin \theta \quad (2.20)$$

$$\text{area of AC} = \frac{H}{\sin \theta} \quad (2.21)$$

Substituting Eqs (2.20), (2.21) and (2.8) into Eq. (2.19) results in:

$$F = \frac{\frac{H}{\sin \theta} (c' + \sigma' \tan \phi')}{W \sin \theta} \quad (2.22)$$

The above expression can be simplified as:

$$F = \frac{\frac{c'H}{\sin \theta} + (W \cos \phi' \tan \phi')}{W \sin \theta} \quad (2.23)$$

Weight (W) of the soil wedge is given by:

$$W = \gamma \times (\text{area of ABC}) = \frac{1}{2} \frac{\gamma H^2}{\sin \beta \sin \theta} \sin(\beta - \theta) \quad (2.24)$$

Substituting (2.24) into (2.23) results in the factor of safety (F) as:

$$F = \frac{\tan \phi'}{\tan \theta} + \frac{2 c'}{\gamma H} \frac{\sin \beta}{(\sin(\beta - \theta) \sin \theta)} \quad (2.25)$$

The limit-equilibrium-based method of slope stability analysis uses the pore pressure information along an assumed failure surface with little consideration of the gradient of the seepage vector or the complex ground water flow pattern that is contributed by hydraulic anisotropy, presence of impermeable strata, heterogeneity, and other such factors. In addition, while the assumption that the slope-parallel flow assumed in most infinite slope stability models (Fig. 2.4) allows for simplicity, the actual directionality of the hydraulic gradients (contributed by flow fields) involved require careful evaluation of the resultant stability as shown below.

2.3.6 Infinite slope: Hydraulic gradient effects

Iverson (1991) considered the state of static equilibrium in an infinite slope shown in Fig. 2.6 with hydraulic head gradients in X and Y directions and developed a method to calculate the factor of safety.

The hydraulic head (h) is given (in infinite slope) as:

$$h = \frac{p}{\gamma_w} - y \cos \theta - x \sin \theta \quad (2.26)$$

where, p is the pore water pressure and $-y \cos\theta$ and $x \sin\theta$ is the vertical elevation with respect to horizontal datum that passes through the origin (Fig. 2.6).

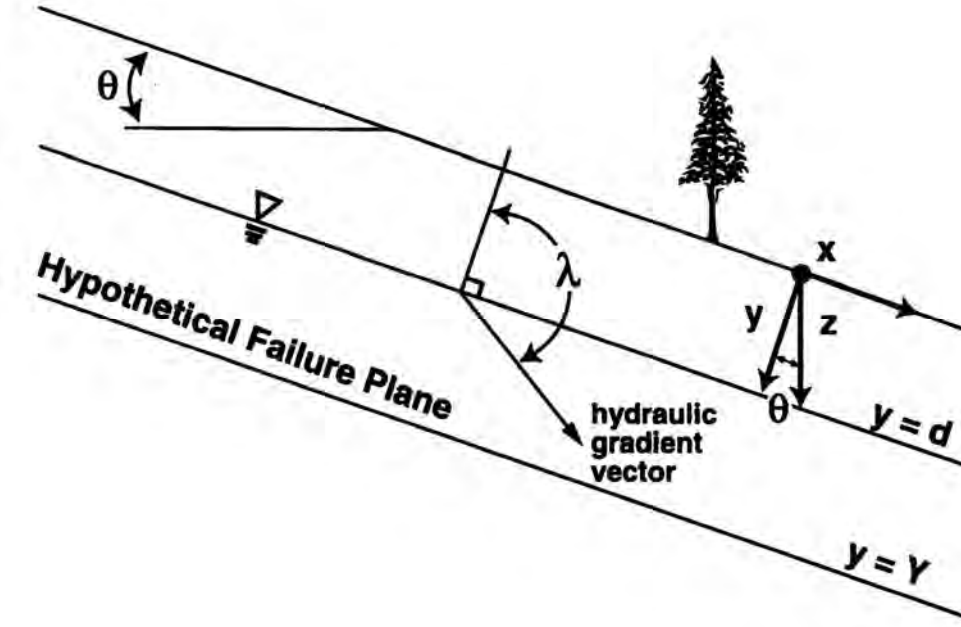


Figure 2.6: Schematic profile and definition on geometric parameters for an infinite slope with groundwater head gradient in an arbitrary direction λ . Note that water table necessarily parallels the ground surfaces as do all surfaces with constant p in infinite slopes (Iverson et al. 1997).

The hydraulic gradient in X and Y direction is obtained by from Eq. (2.26) respectively:

$$\overline{\partial h / \partial x} = -\sin \theta \quad (2.27)$$

$$\overline{\partial h / \partial y} = \frac{1}{\gamma_w} \frac{\partial p}{\partial y} - \cos \theta \quad (2.28)$$

Where, $\frac{\partial p}{\partial y}$ is the mean gradient of p between the water table and depth $y=Y$.

Along the hypothetical failure surface, the effective normal $((\sigma - u))$ and shear stress (τ) are, respectively:

$$(\sigma - u) = [\gamma_t Y - \gamma_w (Y - d)] \cos \theta - \gamma_w (\overline{\partial h / \partial y}) (Y - d) \quad (2.29)$$

$$\tau = [\gamma_t Y - \gamma_w (Y - d)] \sin \theta - \gamma_w (\overline{\partial h / \partial x}) (Y - d) \quad (2.30)$$

where, γ_t is total unit weight of the soil.

Substituting Eqs (2.27), (2.28), (2.29), (2.30) and (2.31) into Eq. (2.15) results in the factor of safety (F) as:

$$F = \frac{\left[\cos \theta + \left(\frac{d}{Y} - 1 \right) \frac{1}{\gamma_t} \frac{\partial p}{\partial y} \right] \tan \varphi + \frac{c}{\gamma_t Y}}{\sin \theta} \quad (2.31)$$

For the special case, $\frac{\partial p}{\partial y} = \gamma_w \cos \theta$, which implies the hydraulic head gradient parallels the slopes, Eq. (2.31) reduces to the factor of safety (Eq. 2.15) derived earlier. In general cases, however (Iverson 1991),

$$\frac{\partial p}{\partial y} = \gamma_w \left(\frac{\sin \theta}{\tan \lambda} + \cos \theta \right) \quad (2.32)$$

In which λ is the angular direction of hydraulic gradient measured with respect to an outward-directed surface-normal vector (Figure 2.6).

In order to compare the above equation with conventional derivation, it is convenient to express Eq. (2.31) as the sum of a friction term (T_f), ground water term (T_w), and a cohesion term (T_c) (Iverson 1992; Iverson et al. 1997):

$$F = T_f + T_w + T_c \quad (2.33a)$$

In which,

$$T_f = \frac{\tan \varphi}{\tan \theta}$$

$$T_w = \frac{[(d/Y) - 1](\partial p / \partial y) \tan \varphi}{\gamma_t \sin \theta}$$

$$\text{Cohesion term} = T_c = \frac{c}{\gamma_t Y \sin \theta}.$$

A quantitative understanding of ground water effects can be gained by examining Eqs. (2.33) and analyzing the influence of T_w , T_f and T_c on the factor of safety. Figure 2.7 shows the variation of $\frac{\partial p}{\partial y}$ as a function of several values of the slope angle θ . It can be seen that the condition $\frac{\partial p}{\partial y} > 0$ results for all cases in which $\theta < 180^\circ$, that is, for all values of θ smaller than that which specifies a vertically downward ∇h . Thus, unless ∇h is vertically downward or directed more normally into the slope, $\frac{\partial p}{\partial y}$ is positive, T_w is negative, and groundwater tends to destabilize the slope. Figure 2.7 also shows that this destabilizing groundwater effect varies systematically as a function of the slope angle. Moreover, the destabilizing effect is most pronounced for small values of θ , because (2.32) requires that $\frac{\partial p}{\partial y} \rightarrow \infty$ as $\theta \rightarrow 0$.

The ratio T_w/T_f measures the relative contribution of ground water and friction to the factor of safety. This ratio can be obtained by combining Eqs. (2.33 b, c) and (2.32) (Iverson 1992):

$$\frac{T_w}{T_f} = \frac{[(d/Y)-1](\partial p/\partial y)}{\gamma_t \cos \theta} \quad \text{or as} \quad (2.33b)$$

$$\frac{T_w}{T_f} = \frac{\gamma_w}{\gamma_t} \left[\frac{d}{Y} - 1 \right] \left[\frac{\tan \theta}{\tan \lambda} + 1 \right] \quad (2.33c)$$

Figure 2.7 also shows the variation of T_w/T_f (multiplied by γ_t/γ_w which typically has a value of 2) for various slope angles. The stabilizing and destabilizing effect of this term on slope stability is evident.

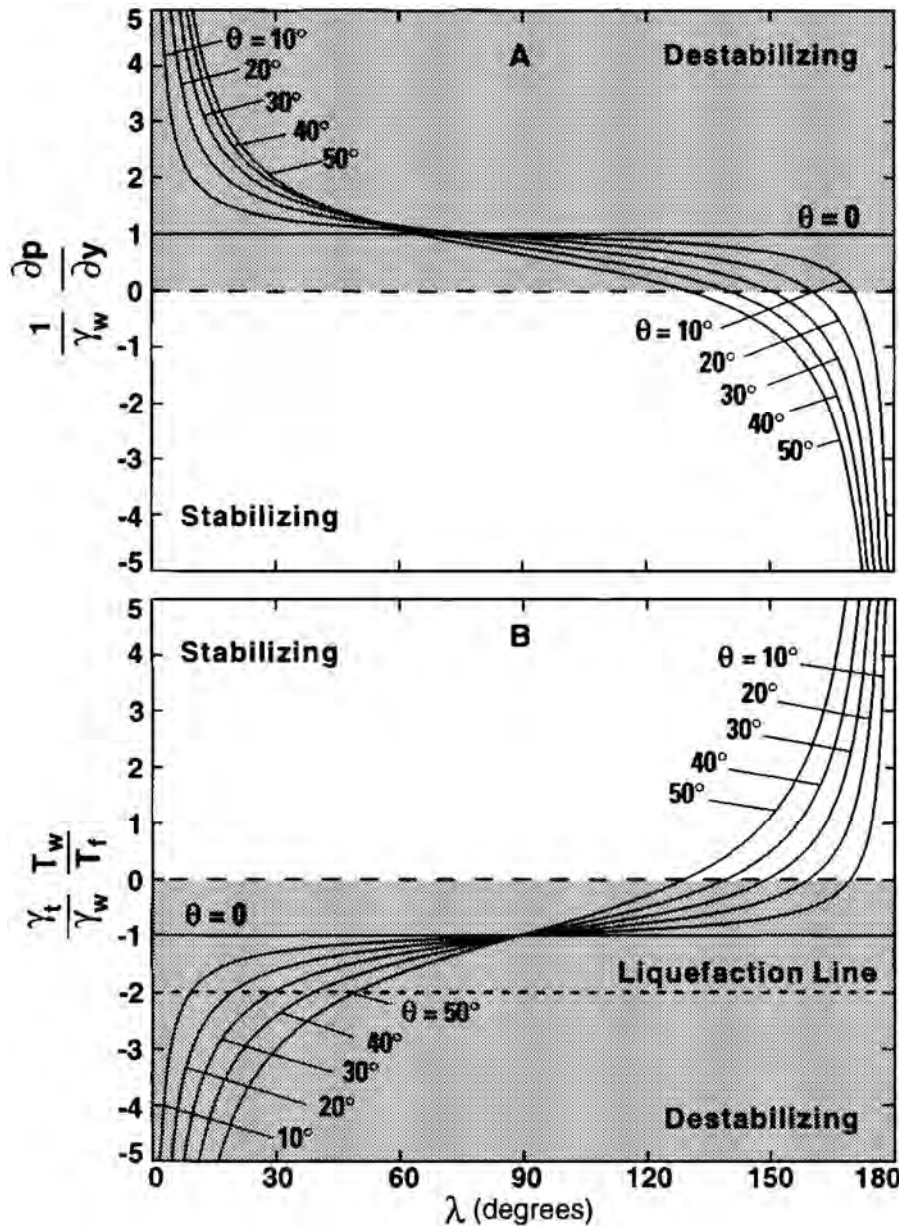


Figure 2.7 Graphs illustrating the influence of the hydraulic gradient direction on (A) the pore-pressure gradient magnitude and (B) the size of the groundwater term (T_w) normalized by the friction term (T_f) for infinite slopes inclined at various angles. Shaded zones denote the parts of the parameter space in which groundwater effects reduce the stability of the slope. (Iverson et al. 1997).

References Cited

- Craig, N. R. 1997. *Soil Mechanics*. pp. 386-387.
- Hodge, R.A. and R. Allan Freeze, 1977. "Groundwater flow systems and slope stability." *Canadian Geotechnical Journal* 14.4: pp. 477-476.
- Iverson, R. M. 1991. Sensitivity of stability analyses to ground water data. *Landslides*, Bell(ed.), Balkema, Rotterdam.
- Iverson, R.M., 1992. Sensitivity of stability analyses to groundwater data: *Landslides* (Proceedings of the Sixth International Symposium on Landslides, vol. 1) D.H. Bell, ed., Balkema, Rotterdam, pp. 451-457.
- Iverson, R. M., M. E. Reid, and R. G. LaHusen, 1997. Debris flow mobilization from landslides, *Annu. Rev. Earth Planet. Sci.*, 25, pp. 85–138.
- Janbu, N. 1954. Application of Composite Slip Surface for Stability Analysis. European Conference on Stability Analysis, Stockholm, Sweden.
- Lau, K. C and T. C. Kenney, 1984. Horizontal drains to stabilize clay slopes. *Canadian Geotechnical Journal*, Vol. 21, No 2, pp. 241-249.
- Morgenstern, N.R., and V.E. Price, 1967. A numerical method for solving the equations of stability of general slip surfaces. *Computer Journal*, 9: pp. 388–393.
- Morgenstern, N.R., and V.E. Price, 1965. The analysis of the stability of general slip surfaces. *Géotechnique*, 15(1): pp. 79–93.
- Reid, M. E., and R.M. Iverson, 1991. Gravity-driven groundwater and slope failure potential:2. Effects of material properties, slope morphology, and hydraulic heterogeneity. *Water Resources Research*.
- [www.Finesoftware.edu:http://www.finesoftware.eu/geotechnical-software/help/slope-stability/morgenstern-price-01/](http://www.finesoftware.eu/geotechnical-software/help/slope-stability/morgenstern-price-01/)

Chapter 3

Introduction to Groundwater Hydrology

One of the foremost texts on basic hydrogeologic principals is given by Fetter (1994), and most of the concepts presented here can be referenced to this text. Aquifer characteristics and the principals of groundwater flow are presented to provide an understanding of these parameters that are necessary to predict groundwater elevations.

3.1 Aquifer Types

Aquifers are classified as *unconfined*, *confined* or *perched*. Slope stability analysis in this manual is primarily limited to unconfined systems, but it is necessary to define all three aquifer types for greater context. Unconfined aquifers exhibit a water table, or a surface at which pore water pressures are equal to atmospheric pressure. Since the water table surface is not under pressure, water table levels in an observation well placed in an unconfined aquifer will rise to the elevation of the water table (Figure 3.1). Recharge to the aquifer principally occurs from the downward seepage of infiltrated water through the unsaturated zone above the water table. Horizontal movement of groundwater in unconfined aquifers tends to exhibit the following properties: (1) if the water table is flat, then groundwater movement does not occur, (2) groundwater movement occurs if the water table is sloping, with movement from higher water table elevations to lower water table elevations, (3) groundwater discharge may occur in topographic lows, (4) the water table surface has the same general shape as surface topography and (5) groundwater generally flows from topographic highs to topographic lows.

Confined aquifers (refer to Figure 3.1) are overlain by a geologic layer with low ability to transmit water. This low-transmitting unit is termed a *confining unit*. The pressurized water level, or potentiometric surface, in a confined aquifer will rise above the top of the aquifer. If water levels drop below the top of the aquifer, then the system reverts to unconfined status. Recharge will occur in recharge zones where the aquifer outcrops, or via slow downward movement of infiltrated precipitation through the confining unit.

Lastly, perched aquifers (Figure 3.2) occur where groundwater mounds upon a geologic layer of relatively impermeable sediments. Unsaturated conditions exist below these impermeable sediments, and seepage of water can occur where the impermeable layer intersects with land surface to create a spring.

3.2 Hydraulic Head

The total mechanical energy of water is expressed as hydraulic head (h). Head is in units of energy per unit weight, or ML^2/T^2 divided by ML/T^2 (M =mass, L =length, and T =time), which equals length units (e.g. feet, meters). The Bernoulli equation (Eq. 3.1) for head considers three types of energy: kinetic, gravitational potential, and fluid pressure.

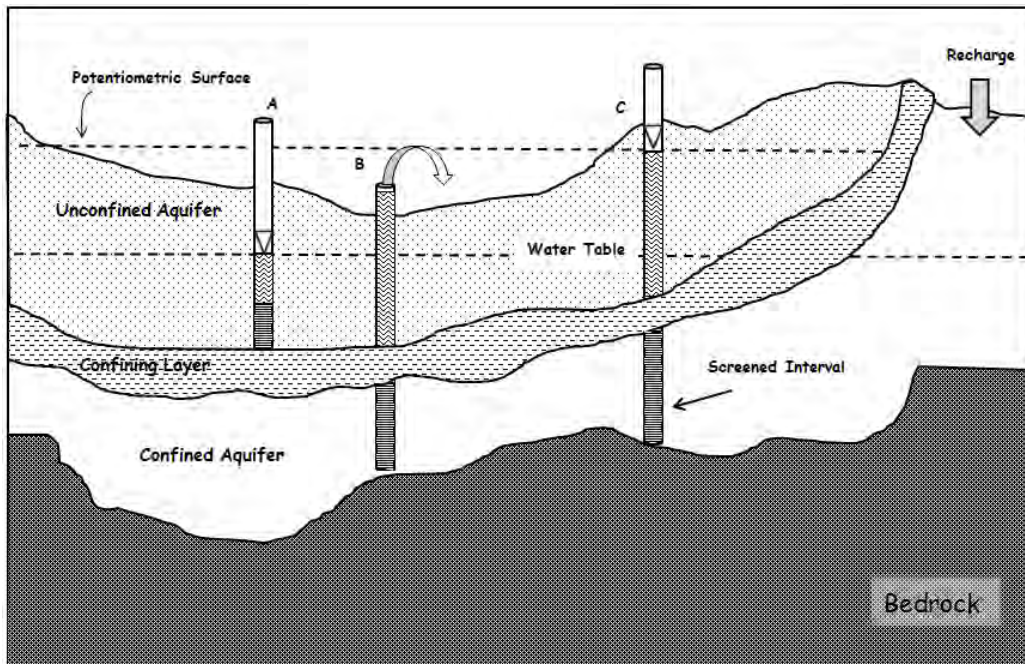


Figure 3.1: A schematic of unconfined and confined aquifers depicting water level rise (white triangle) in wells screened in each aquifer type, (A) unconfined aquifer, (B) flowing well in the confined aquifer, and (C) non-flowing well in the confined aquifer. Screened intervals are marked.

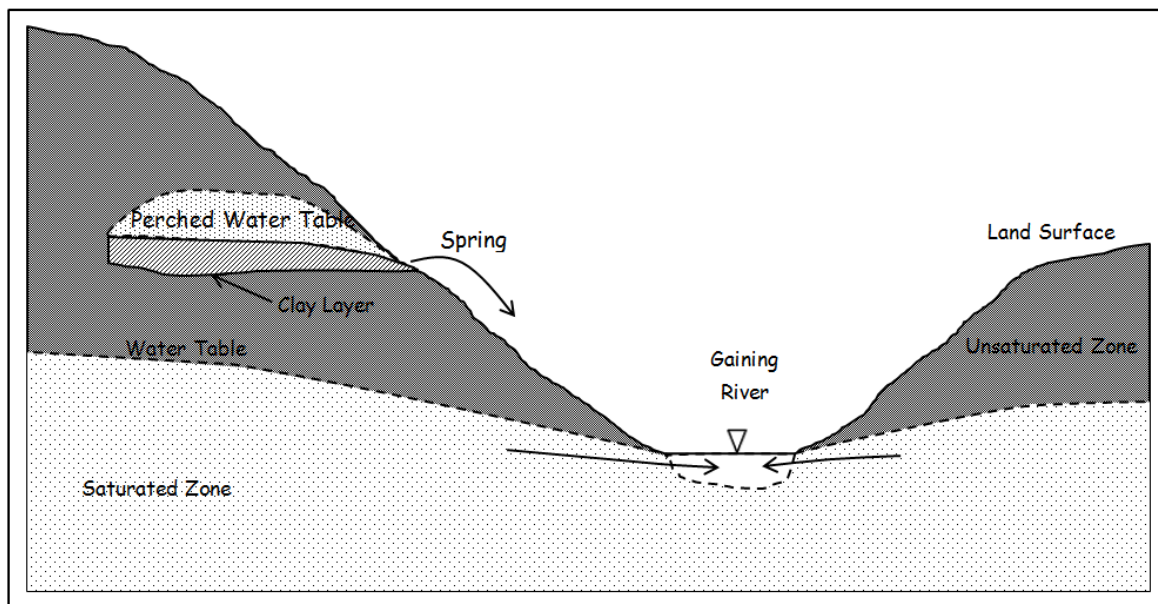


Figure 3.2: A schematic diagram of unconfined and perched aquifers.

$$h = \frac{1}{2} \frac{v^2}{g} + z + \frac{p^*}{\rho_w g} \quad (3.1)$$

Where v is velocity (L/T), g is gravitational acceleration (L/T²), z is elevation (L), p^* is pressure (M/LT²), and ρ_w is water density (M/L³). Kinetic energy is very small for groundwater systems, with karst aquifer systems being the exception, and is safely discarded in laminar-dominated groundwater flow systems, resulting in a simplified equation (3.2).

$$h = z + \frac{p^*}{\rho_w g} \quad (3.2)$$

3.3 Properties of Aquifers

The hydrologic properties of aquifers most important to estimating water levels are those that define the abilities of the soil and rock to transfer and store water. Several techniques to estimate parameter values are discussed in Chapter 6. Focus in this chapter is on the physical meaning of important parameters and to give a numeric context of these parameters in the governing equations of groundwater flow.

3.3.1 Porosity and Sorting

Porosity is the fraction of earth material that is void of material. It is the void space that fluid may occupy. Porosity can be a function of depositional environment (water, wind, ice or gravity), or secondary processes of dissolution (e.g. karst) or fracturing. Mathematically, porosity (n) is defined as,

$$n = \frac{V_v}{V_T}, \quad (3.3)$$

Where V_v is the volume of voids (L³), and V_T is the total volume of the earth material, including voids (L³). If the mineral grains in a sedimentary setting are uniform spheres and packed directly above one-another, which is known as cubic packing (Figure 3.3a), then the associated porosity is 47.65% (Meinzer 1923a). If the spheres stack in the hollow spaces, or rhombohedral packing (Figure 3.3b), the resulting porosity is reduced to 25.95% (Meinzer 1923a). The end members of porosity for well-sorted, rounded sediment grains are independent of the diameter of the grains. If the sediment is a mixture of grain sizes, then smaller grains will fill in the spaces and significantly reduce its porosity (Figure 3.3c). The wider the range of sediment sizes, then the smaller the porosity. Geologic processes that can result in large particle-size variability include glaciation (e.g. glacial tills) and mass wasting.

The *uniformity coefficient* (C_u) is a measure of sorting and is defined as the ratio of the grain size that is 60% finer by weight (d_{60}) to the grain size that is 10% finer by weight (d_{10}).

$$C_u = \frac{d_{60}}{d_{10}} \quad (3.4)$$

A sample is well sorted if C_u is less than 4, and poorly sorted if C_u is greater than 6. Figure 3.4 is an example taken from Fetter (1994). Two materials have similar average grain sizes (0.15 – 0.2 mm). The

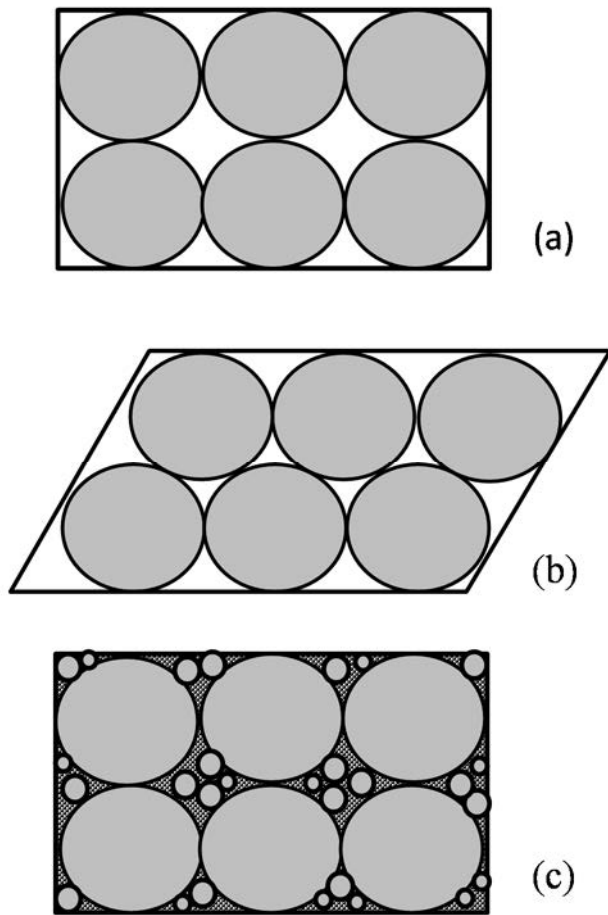


Figure 3.3: Different packing arrangements for spherical grains (a) cubic packing with porosity = 47.65%, (b) rhombohedral packing with porosity = 25.95% and (c) cubic packing with pore spaces occupied with grains of smaller diameter. Resulting porosity is significantly lowered. (Adopted from Fetter C.W., Applied Hydrogeology, 3rd Edition © 1994, pp 82-83, Reprinted by permission of Pearson Education, Inc., Upper Saddle River, NJ).

silty fine to medium sand $C_u = 0.15 \text{ mm} / 0.018 \text{ mm} = 8.3$ is poorly sorted (Fig. 3.4a), while the fine sand $C_u = 0.21 / .15 = 1.4$ and is well sorted (Fig. 3.4b). Correspondingly, the fine sand will have a larger porosity compared to the poorly sorted silty fine to medium sand, despite having similar median grain size.

The percent porosity in sedimentary rocks can vary tremendously. Clastic rocks can range from 3% to 30%, while limestones and dolomites can have porosities as low as 1% and high as 30%. Clays can have very large porosities based on irregular shapes that reduce packing and the dispersive effect of electrostatic charge, which causes some clays to repel each other.

Although porosity is an important parameter, and is often measured in geotechnical studies, it is only used directly in quantitative assessment of groundwater transport and not in the analysis of head. Porosity is discussed primarily to compare with specific yield and specific storage, which are the parameters used for quantitative assessment of groundwater levels.

3.3.2 Specific Yield

Specific yield (S_y) is the ratio of the volume of water that drains from a saturated rock due to gravity to the total volume of rock (Meinzer 1923b). Surface tension will hold some water to the

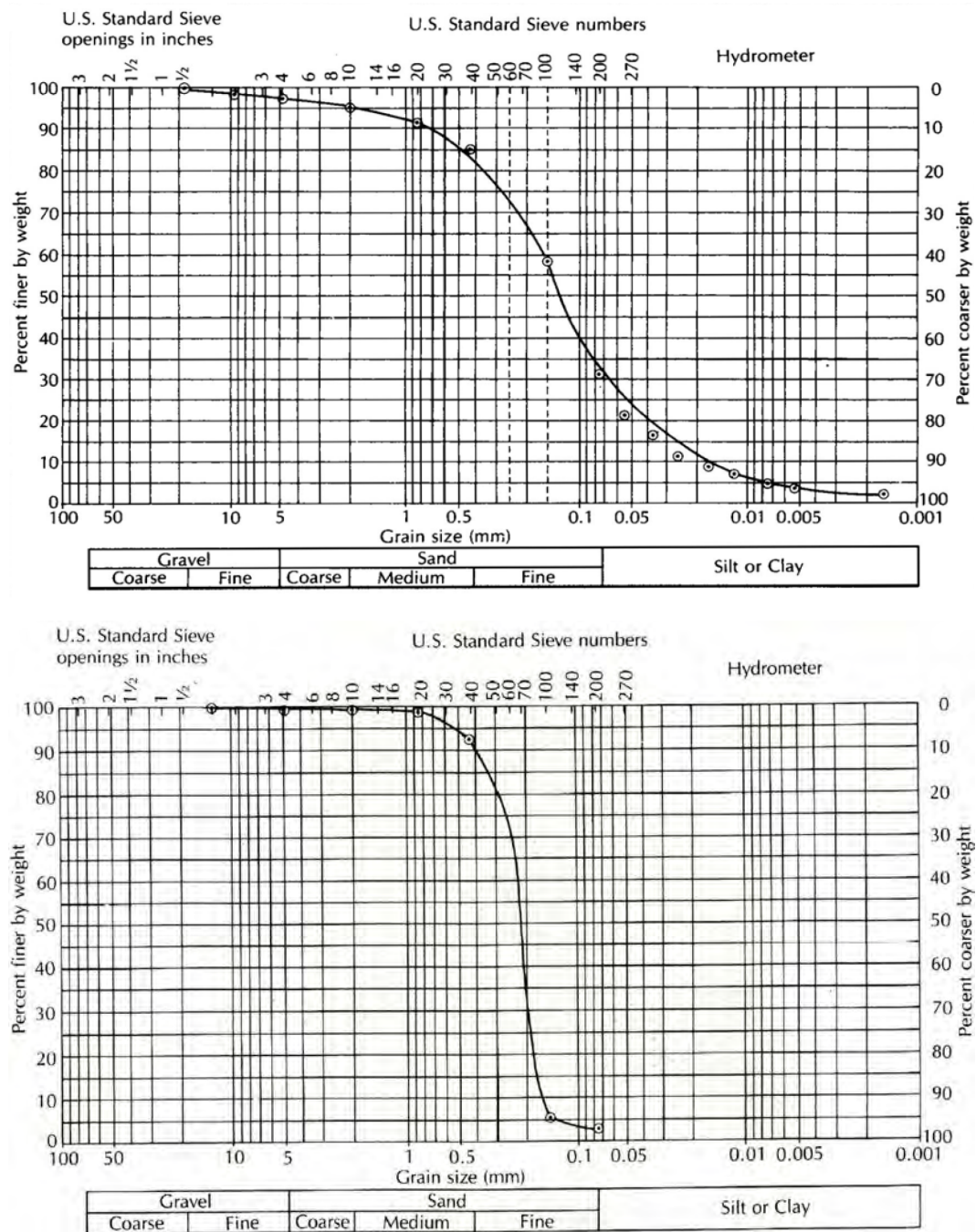


Figure 3.4: Grain size distributions curve for (a) a silty fine to medium sand with $C_u=8.3$ and (b) fine sand with $C_u=1.4$ (Adopted from Fetter C.W., Applied Hydrogeology, 3rd Edition © 1994, pp 85-86, Reprinted by permission of Pearson Education, Inc., Upper Saddle River, NJ).

Material	Specific Yield (Percent)		
	Minimum	Maximum	Average
Clay	0	5	2
Sandy Clay	3	12	7
Silt	3	19	18
Fine Sand	10	28	21
Medium Sand	15	32	26
Coarse Sand	20	35	27
Gravelly Sand	20	35	25
Fine Gravel	21	35	25
Medium Gravel	13	26	23
Coarse Gravel	12	26	22

Table 3.1: Specific yield ranges for various sediment textures. Table obtained from Fetter (1994), page 91 with original source Johnson (1967). (Adopted from Fetter C.W., Applied Hydrogeology, 3rd Edition © 1994, Reprinted by permission of Pearson Education, Inc., Upper Saddle River, NJ).

surface of mineral grains. Finer grains will retain more water through surface tension, under gravity, than coarser grains. Therefore, clays may have a porosity of 50%, but retain 48% of water and have a specific yield of only 2%. In all cases, S_y will be less than porosity. Table 3.1 provides characteristic values of S_y for various sediment textures. The highest S_y values occur in medium to coarse sands (0.5 to 1.0 mm diameter), and decrease rapidly with increased percentages of silt and clay.

3.3.3 Specific Storage and Storativity

In a confined aquifer, water is released from storage but the aquifer remains saturated. This is the result of the expansion of mineral grains and water as pressure is reduced. *Specific storage* (S_s) is the amount of water per unit volume of saturated material that is stored (or expelled) as a function of compressibility of the mineral skeleton and pore water per unit decrease in water level (1/L). This is sometimes referred to as the elastic storage coefficient. Jacob (1940, 1960) and Cooper (1966) define specific storage as,

$$S_s = \rho_w g (\alpha + n\beta), \quad (3.5)$$

where ρ_w is the density of water (M/L^3), g is acceleration of gravity (L/T^2), α is the compressibility of the aquifer's skeleton ($1/M/LT^2$), n is porosity, and β is the compressibility of water ($1/M/LT^2$). The value of S_s is very small (generally less than 0.0001/ft).

For a confined aquifer, *storativity* (S) is the specific storage multiplied by the aquifer thickness B and accounts for the release of water across the entire thickness of the aquifer. Storativity is dimensionless.

$$S = BS_s \quad (3.6)$$

For an unconfined aquifer,

$$S = S_y + hS_s \quad (3.7)$$

With the head (h) equal to the saturated thickness of the unconfined aquifer. The second term on the right hand side of equation 3.7 generally ranges from 5×10^{-3} to 5×10^{-5} and is several orders of magnitude smaller than S_y (refer to Table 3.1) and is often ignored for unconfined systems.

3.3.4 Hydraulic Conductivity

Hydraulic conductivity in horizontal direction (x-direction) is a function of the material's ability to transmit water (e.g. size and shape of grains, sorting, fracturing) as well as the fluid's properties (e.g. density and dynamic viscosity). Material properties of size and sorting are defined by the intrinsic permeability (K_i) given by,

$$K_i = Cd^2 \quad (3.8)$$

where C is a dimensionless shape factor with ranges for common soil types provided in Table 3.2, and d is pore size diameter. The shape coefficient decreases with decreasing grain size. This reflects an increase in sediment surface area and the potential for increased contact between water and sediment when grain sizes are small. The result is greater frictional resistance to flow, and a decline in intrinsic permeability. Intrinsic permeability is in units of area (L^2), but in petroleum engineering literature is often expressed in units of darcy, with 1 darcy equal to $9.87 \times 10^{-9} \text{ cm}^2$.

Hydraulic conductivity combines intrinsic permeability with the properties of the fluid,

$$K_x = K_i \left(\frac{\rho_w g}{\mu} \right) \quad (3.9)$$

where ρ_w is the fluid density (M/L^3), g is acceleration of gravity (L/T^2), and μ is dynamic viscosity ($F T/L^2$). For fresh water at 20°C , $\rho_w = 0.998 \text{ g/cm}^3$, $\mu = 0.010 \text{ g/s}\cdot\text{cm}$. Ranges of intrinsic permeability and hydraulic conductivity are given in Table 3.3. Groundwater movement is sensitive to the value of hydraulic conductivity, but ranges in K_x span several orders of magnitude for any given material. Therefore these ranges should act only as a guide. More accurate methods to estimate K_x based on grain size distribution, laboratory techniques and aquifer tests are given in Chapter 4 on site characterization.

Table 3.2: Ranges of the dimensionless shape coefficient hydraulic conductivity of soils (Adopted from Fetter C.W., Applied Hydrogeology, 3rd Edition © 1994, page 99, Reprinted by permission of Pearson Education, Inc., Upper Saddle River, NJ).

Material	C
Very fine sand, poorly sorted	40-80
Fine sand with appreciable fines	40-80
Medium sand, well sorted	80-120
Coarse sand, poorly sorted	80-120
Coarse sand, well sorted, clean	120-150

Table 3.3: Ranges of intrinsic permeability and hydraulic conductivity for unconsolidated sediments

(Adopted from Fetter C.W., Applied Hydrogeology, 3rd Edition © 1994, page 98, Reprinted by permission of Pearson Education, Inc., Upper Saddle River, NJ).

Material	Intrinsic Permeability (darcys)	Hydraulic Conductivity	
		(cm/s)	(ft/d)
Clay	10^{-6} to 10^{-3}	10^{-9} to 10^{-6}	2.8×10^{-6} to 0.0028
Silt, sandy silts, clayey sands, till	10^{-3} to 10^{-1}	10^{-6} to 10^{-4}	0.0028 to 0.28
Silty sands, fine sands	10^{-2} to 1	10^{-5} to 10^{-3}	0.028 to 2.8
Well-sorted sands, glacial outwash	1 to 10^2	10^{-3} to 10^{-1}	2.8 to 283
well-sorted gravel	10 to 10^3	10^{-2} to 1	28.3 to 2834

3.3.5 Transmissivity

Transmissivity (T) is analogous to storativity, in that it provides an overall response of the system based on aquifer thickness. Transmissivity (L^2/T) is used to describe the amount of water an aquifer can transmit through a unit width of aquifer material,

$$T = BK_x \quad (3.10)$$

The primary assumption is that water is flowing horizontally. For unconfined aquifers, saturated thickness is less than aquifer thickness and head (h) is substituted into equation 3.10 for aquifer thickness (B).

3.3.6 Homogeneity and Isotropy

An aquifer is considered homogenous if hydraulic properties (K_x, S_y, S_x, T) are the same at all locations. The system is heterogeneous if these properties change spatially. Heterogeneity can be as simple as a thickening wedge of sandstone, such that T and S increase, despite K_x and S_y remaining the same. Stratigraphic layering in the vertical direction (Figure 3.5a) or facies changes in the horizontal direction (Figure 3.5b) are common examples of heterogeneity. To compute an effective hydraulic conductivity for each case, respectively, use equations 3.11 and 3.12, where m = the number of layers, and b is the individual layer thickness (L).

$$K_x^1 = \frac{B}{\sum_{i=1}^m b_i / K_{x,i}} \quad (3.11)$$

$$K_x^2 = \sum_{i=1}^m \frac{K_{x,i}}{B} \quad (3.12)$$

For equation 3.11 and Figure 3.5a, the drop in head is equal for each layer, but the flow through individual layers are different. With respect to equation 3.12 and Figure 3.5b, flow across each layer is the same, but the drops in head across individual layers are different.

An isotropic condition is a property that is constant in all directions, while anisotropic means an aquifer property is dependent on direction. Figure 3.6 shows an example of each, with anisotropy caused by

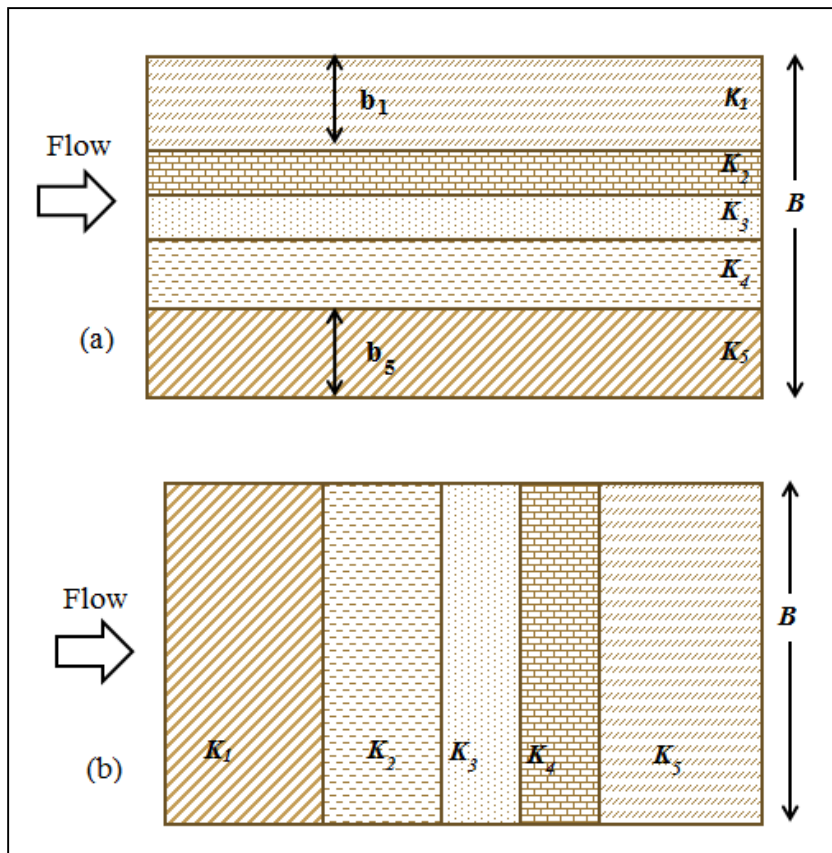


Figure 3.5: Heterogeneous formations (a) horizontal layering (b) vertical layering.

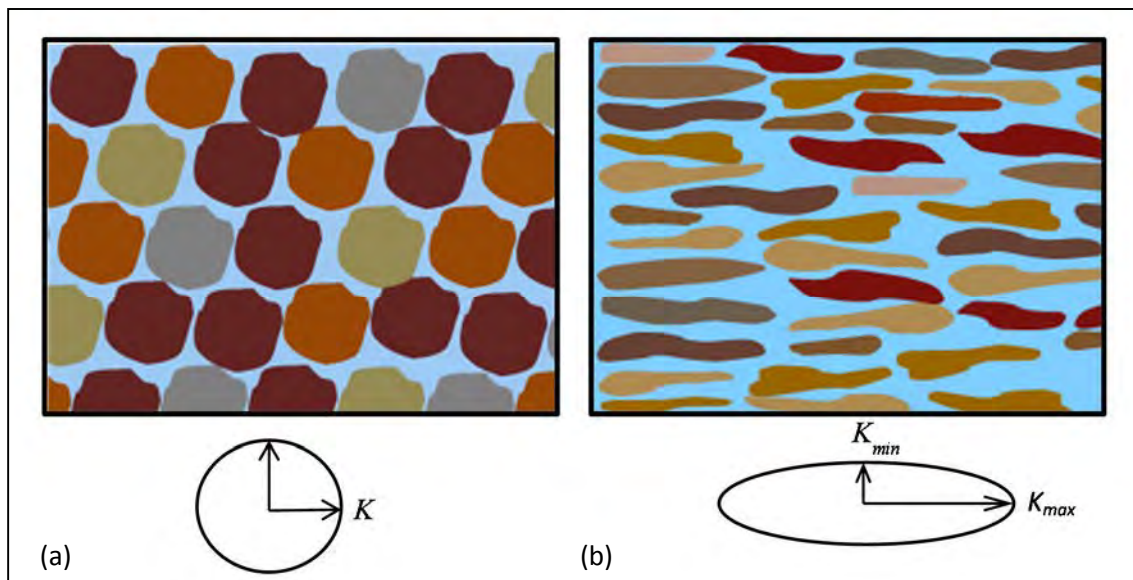


Figure 3.6 Examples of (a) isotropic conditions and (b) anisotropic conditions due to grain shape and arrangement (Adopted from Fetter C.W., Applied Hydrogeology, 3rd Edition © 1994, page 122, Reprinted by permission of Pearson Education, Inc., Upper Saddle River, NJ).

flattened grains. Hydraulic conductivity is at a minimum orthogonal to maximum K_x . Figure 3.7 shows anisotropy in a fractured system, with groundwater flow constrained by the orientation of fractures.

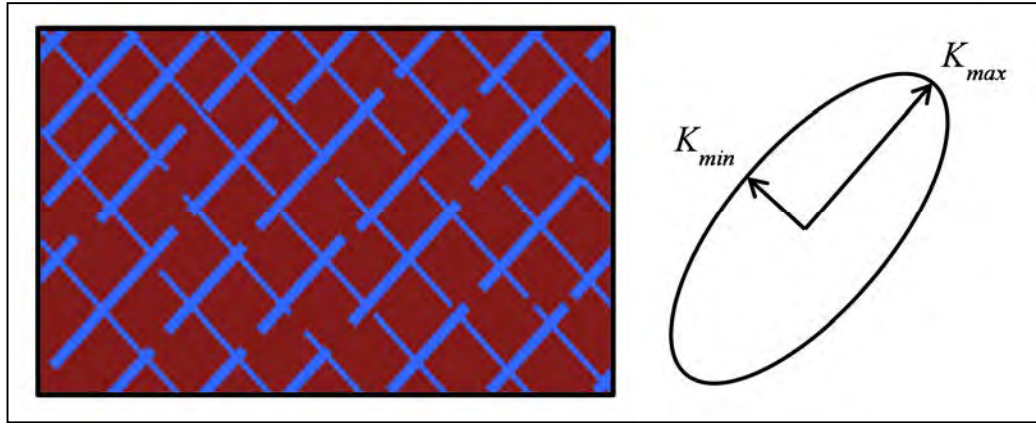


Figure 3.7 Fracture network and associated anisotropy.

Flow paths in homogenous and isotropic systems will be perpendicular to lines of constant head. Figure 3.8a shows a cross section with a recharge and discharge zone in homogeneous and isotropic sediments. Lines of equal head are color coded with flow moving right to left. In anisotropic conditions, flow direction is a function of gradient (change in head over distance) and the resultant hydraulic conductivity vector. If the two vectors are not parallel, then flow paths adjust based on the angular difference.

With respect to Figure 3.8b, K_x is 10 times greater than K_y . The bias toward the x-direction is witnessed with flow paths that do not align with modeled equipotential lines at 90 degrees. Instead, flow bends toward the horizontal. For Figure 3.8c, the opposite is true, with flow paths bending toward the vertical in the recharge and discharge zones. The no-flow boundary condition at the bottom of the modeled cross section, however, forces flow in the horizontal in the center of the domain.

Flow paths in heterogeneous materials follow the law of refraction, where groundwater flow bends away from the normal in less conductive materials. As an example, in Figure 3.8d, groundwater moves around the low conductivity lens, but moves toward and through the more conductive lens in Figure 3.8e. In the case of subsurface drains that have a higher conductivity than the surrounding material, the drainage pipes will consequently act as conduits for flow with gradients bending toward them.

3.3.7 Representative Elementary Volume (REV)

A representative elementary volume, or REV, refers to the scale at which a cube of porous material is large enough to represent the properties of that porous material, but small enough that a change in head in that volume is relatively small. Within the REV groundwater flow is treated as a continuum and one needs to define effective hydraulic properties of hydraulic conductivity and storage for the size of

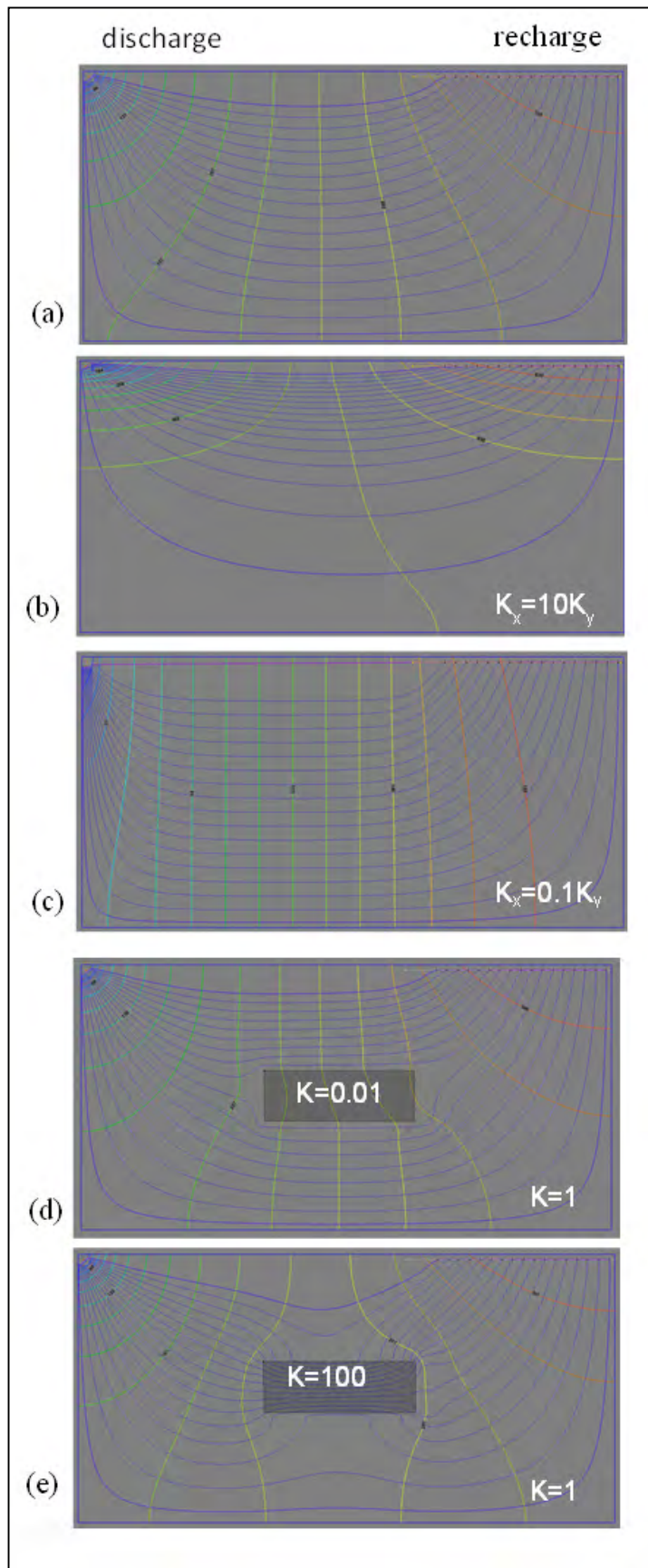


Figure 3.8: Cross section of flow paths (blue lines) in sediments that are (a) homogeneous and isotropic, (b) homogeneous and anisotropic ($K_x = 10K_y$), (c) homogeneous and anisotropic ($K_x = 0.1K_y$), (d) heterogeneous and isotropic with lens 100 times less conductive than surrounding rock and (e) heterogeneous and isotropic with lens 100 times more conductive than surrounding rock. Lines of equal head are color lines (red = high head, blue = lower head)

the REV (e.g aquifer testing, water balances, model calibration, or literature cited properties). The REV approach is a means of smoothing small scale heterogeneity to a macroscopic scale that is homogenous.

3.4 Darcy's Law

Darcy's law defines the steady state rate of fluid flow through porous media (flow in = flow out) as,

$$Q = -K_x A \frac{(h_1 - h_2)}{(x_1 - x_2)}, \quad (3.13)$$

with parameters displayed in Figure 3.9. Q is the flow rate through the porous material (L^3/T), A is the cross sectional area perpendicular to flow, h_1 is the head (L) (i.e. water level elevation) at location x_1 (L), and h_2 is the head at location x_2 . The proportionality constant K_x (L/T) is the hydraulic conductivity of the porous medium in the x-direction (horizontal). Flow rate will increase if the head difference increases, length is shortened, pipe diameter is increased and/or K_x is increased.

As an example, a medium-grained sand with a $K_x = 0.017$ cm/s (48 ft/d), a cross sectional area of 30 cm^2 , length of 20 cm and a change in head of 10 cm results in a discharge $Q = -0.017(30)(-10/20) = 0.255 \text{ cm}^3/\text{s}$.

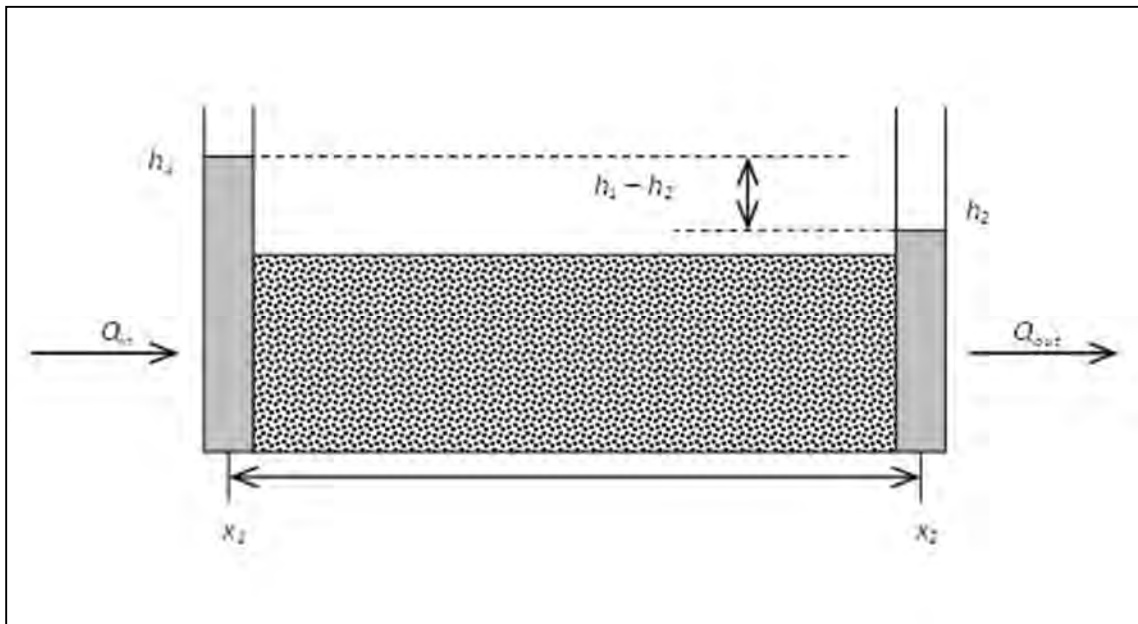


Figure 3.9: Horizontal pipe filled with unconsolidated porous medium to demonstrate Darcy's Law.

3.5 Groundwater Flow Equation for a Confined Aquifer

3.5.1 Transient Conditions

The groundwater flow equation is the governing equation for groundwater hydrology to describe groundwater movement. It combines Darcy's Law with the conservation of mass. The conservation of mass states that the mass into a unit volume minus the mass out of the unit volume is equal to a change in storage.

$$\text{Mass In} - \text{Mass Out} = \text{Change of Storage} \quad (3.14)$$

Figure 3.10 focuses on the conservation of mass in the x-direction for a fully saturated control volume.

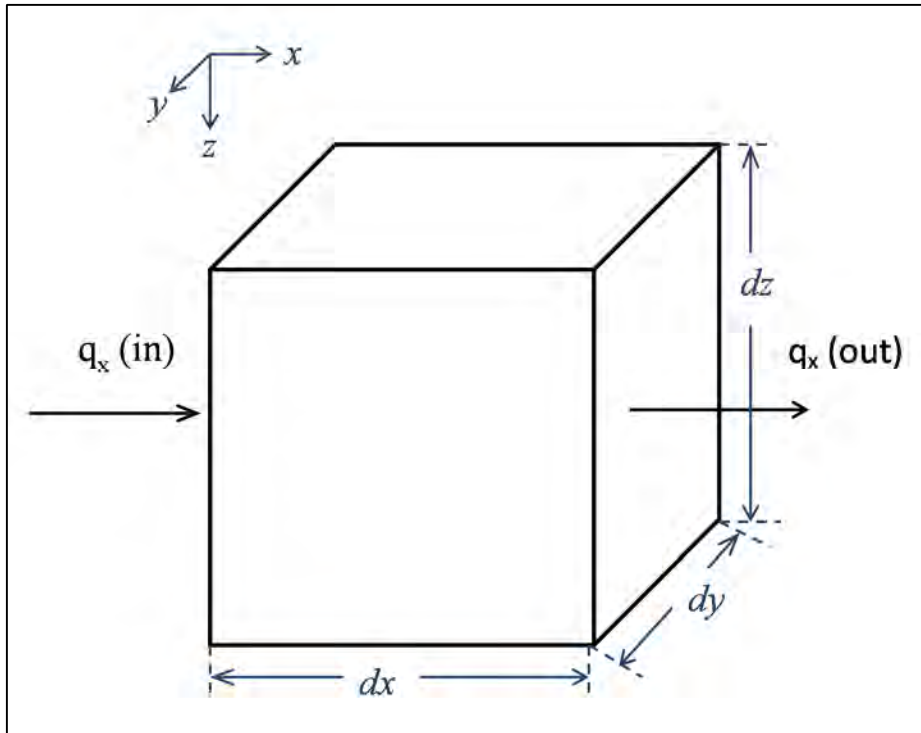


Figure 3.10: Control volume for flow through a confined aquifer with flow per unit cross sectional area in the x-direction (q_x) shown.

The assumption is that no internal sources or sinks exist in the control volume. The net change in the control volume due to fluid movement parallel to the x-direction (left hand side of equation 3.14) is,

$$\rho_w q_x \Delta y \Delta z - \left[q_x \Delta y \Delta z + \frac{\delta}{\delta x} (\rho_w q_x) \Delta x \Delta y \Delta z \right] \quad (3.15)$$

And results in, $-\frac{\delta}{\delta x} (\rho_w q_x) \Delta x \Delta y \Delta z$, with similar terms derived for the other two directions - $\frac{\delta}{\delta y} (\rho_w q_y) \Delta x \Delta y \Delta z$ and $-\frac{\delta}{\delta z} (\rho_w q_z) \Delta x \Delta y \Delta z$.

The mass in the control volume,

$$M = n\rho_w\Delta x\Delta y\Delta z \quad (3.16)$$

Where n is porosity. The change in mass of water (right hand side of equation 3.14) with respect to time requires one to take the derivative of equation 3.16. The vertical dimension (Δz) is allowed to compress/expand with time while the other dimensions are assumed fixed.

$$\frac{\delta M}{\delta t} = \Delta x\Delta y \frac{\delta}{\delta t} (\rho_w n \Delta z) \quad (3.17)$$

In order to get terms as a function of head, it is necessary to convert n and ρ_w into functions of pressure and time. From the product rule

$$\frac{\delta}{\delta t} (\rho_w n) = n \Delta z \frac{\delta \rho_w}{\delta t} + \rho_w \Delta z \frac{\delta n}{\delta t} + \rho_w n \frac{\delta \Delta z}{\delta t} \quad (3.18)$$

And the chain rule and P = pressure (M/LT^2),

$$\frac{\delta \rho_w}{\delta t} = \frac{\delta \rho_w}{\delta P} \frac{\delta P}{\delta t} \quad (3.19)$$

$$\frac{\delta n}{\delta t} = \frac{\delta n}{\delta P} \frac{\delta P}{\delta t} \quad (3.20)$$

$$\frac{\delta \Delta z}{\delta t} = \frac{\delta \Delta z}{\delta P} \frac{\delta P}{\delta t} \quad (3.21)$$

Equations 3.19, 3.20 and 3.21 are substituted into 3.18 and rearranged to produce,

$$\Delta x\Delta y \frac{\delta}{\delta t} (\rho_w n \Delta z) = \Delta x\Delta y \left(n \Delta z \frac{\delta \rho_w}{\delta P} + \rho_w \Delta z \frac{\delta n}{\delta P} + \rho_w n \frac{\delta \Delta z}{\delta P} \right) \frac{\delta P}{\delta t} \quad (3.22)$$

Where $\frac{\delta \rho_w}{\delta P}$ is the compressibility of water () with respect to pressure and is assumed constant.

$$\beta = \frac{1}{\rho_w} \frac{\delta \rho_w}{\delta P} = 4.4 \times 10^{-10} \text{ m}^2/N \quad (3.23)$$

If one assumes that the aquifer matrix is elastic, then the coefficient of compressibility of solids () is defined as either a function of Δz or n as,

$$\alpha = \frac{1}{\Delta z} \frac{\delta(\Delta z)}{\delta P} = \frac{1}{(1-n)} \frac{\delta n}{\delta P} \quad (3.24)$$

Equation 3.22 becomes,

$$\Delta x\Delta y \frac{\delta}{\delta t} (\rho_w n) = \Delta x\Delta y \Delta z (\rho_w (n\beta - \alpha)) \frac{\delta P}{\delta t} \quad (3.25)$$

The right hand and left hand sides of equation 3.14 are equated,

$$\frac{\delta(\rho_w q_x)}{\delta x} + \frac{\delta(\rho_w q_y)}{\delta y} + \frac{\delta(\rho_w q_z)}{\delta z} = -\rho_w (n\beta - \alpha) \frac{\delta P}{\delta t} \quad (3.26)$$

Rearranging equation 3.2,

$$P = (h - z)\rho_w g \quad (3.27)$$

Taking the time derivative of equation 3.27 and assuming ρ_w is constant,

$$\frac{\delta P}{\delta t} = \rho_w g \frac{\delta h}{\delta t} \quad (3.28)$$

And substituting equation 3.26 results in,

$$\frac{\delta q_x}{\delta x} + \frac{\delta q_y}{\delta y} + \frac{\delta q_z}{\delta z} = -\rho_w g (n\beta - \alpha) \frac{\delta h}{\delta t} \quad (3.29)$$

Specific storage (S_s) is the constant that controls the amount of fluid volume that the aquifer matrix can hold and does not differentiate between compressibility due to water and the compressibility of aquifer matrix. S_s is defined in equation 3.5. Substituting equation 3.5 and Darcy's Law for flow per unit cross sectional area into equation 3.29 results in the groundwater flow equation for a confined aquifer that is both heterogeneous and anisotropic and for transient conditions becomes,

$$\frac{\delta}{\delta x} \left(K_x \frac{\delta h}{\delta x} \right) + \frac{\delta}{\delta y} \left(K_y \frac{\delta h}{\delta y} \right) + \frac{\delta}{\delta z} \left(K_z \frac{\delta h}{\delta z} \right) = S_s \frac{\delta h}{\delta t} \quad (3.30)$$

3.5.2 Homogenous/Isotropic

If the confined aquifer is considered homogenous, then hydraulic conductivity does not change with location and can be pulled from the space-derivative. Equation 3.30 simplifies to,

$$K_x \frac{\delta^2 h}{\delta x^2} + K_y \frac{\delta^2 h}{\delta y^2} + K_z \frac{\delta^2 h}{\delta z^2} = S_s \frac{\delta h}{\delta t} \quad (3.31)$$

If the aquifer is isotropic, then $K = K_x = K_y = K_z$. If the aquifer is homogenous and isotropic, the groundwater flow equation further reduces to,

$$\frac{\delta^2 h}{\delta x^2} + \frac{\delta^2 h}{\delta y^2} + \frac{\delta^2 h}{\delta z^2} = \frac{S_s}{K} \frac{\delta h}{\delta t} = \frac{S}{T} \frac{\delta h}{\delta t} \quad (3.32)$$

3.5.3 Steady State Conditions

Steady state means that head does not change over time and $\frac{\delta h}{\delta t} = 0$, and storage terms are no longer required for the solution. The simplest groundwater flow equation is for 1-dimensional flow given steady state conditions in a confined aquifer. The groundwater flow equation reduces to,

$$\frac{\delta^2 h}{\delta x^2} = 0. \quad (3.33)$$

Equation 3.33 is relatively easy to solve analytically by integrating once (indefinitely), then substituting in Darcy's Law, separating the variables and integrating to produce,

$$h_2 = h_1 - \frac{q_x}{K_x} x. \quad (3.34)$$

For flow per unit width (Q') is equated to flow per unit area (q_x) as,

$$Q' = q_x B \quad (3.35)$$

For an example, refer to Figure 3.11. Given $h_1 = 100$ ft, $K = 1$ ft/d, $B = 100$ ft, $x = 1000$ ft and $Q' = 1$ ft²/d then $q_x = 1/100$ ft/d, and $h_2 = 100 - (1)(1000)/(1)(100) = 90$ ft

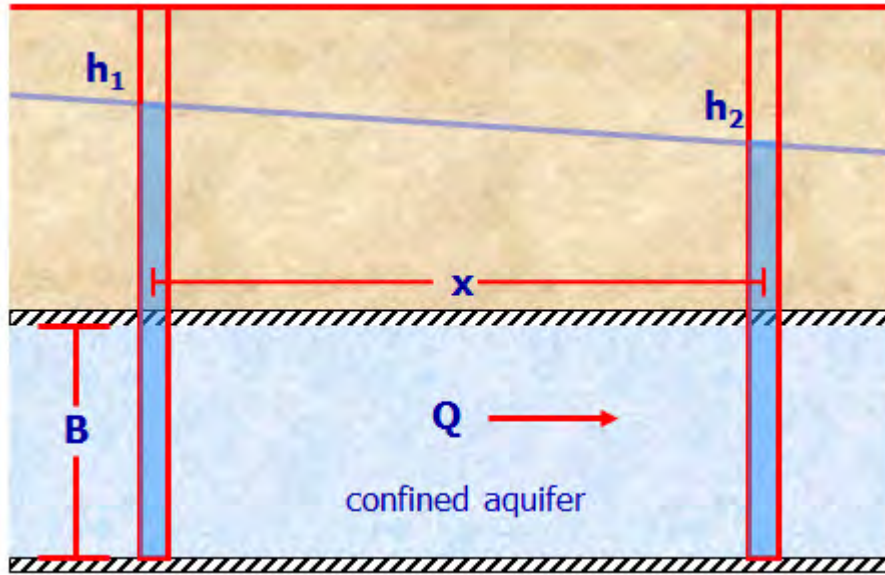


Figure 3.11: Schematic diagram for a confined aquifer in one dimension.

3.6 Groundwater Flow Equation for an Unconfined Aquifer

3.6.1 Transient Conditions

Refer to Figure 3.12 for the head profile in a 1-dimensional, unconfined aquifer with the water table surface defined by equation 3.2. The water table (point A) is at atmospheric pressure and $P/P_w = 0$. Therefore, all mechanical energy at point A is from potential energy, such that $h = z$, and hydraulic head is equal to the saturated thickness of the aquifer.

The area (A) term in Darcy's law (Equation 3.13) is impacted by replacing aquifer thickness (B) with saturated thickness. Flow is defined as,

$$Q = -Kh w \frac{dh}{dx} , \quad (3.35)$$

Where w = unit aquifer width (L). Use of Darcy's law assumes that flow is horizontal. For unconfined flow, the hydraulic gradient ($\frac{dh}{dx}$) must be small compared to the overall saturated thickness for this assumption to be valid (also referred to as Dupuit assumption). To be valid, the hydraulic gradient (or $\tan \theta$) should closely match the slope of the water table ($\sin \theta$), where θ is the angle from horizontal. This assumption is valid for $\theta < 15^\circ$.

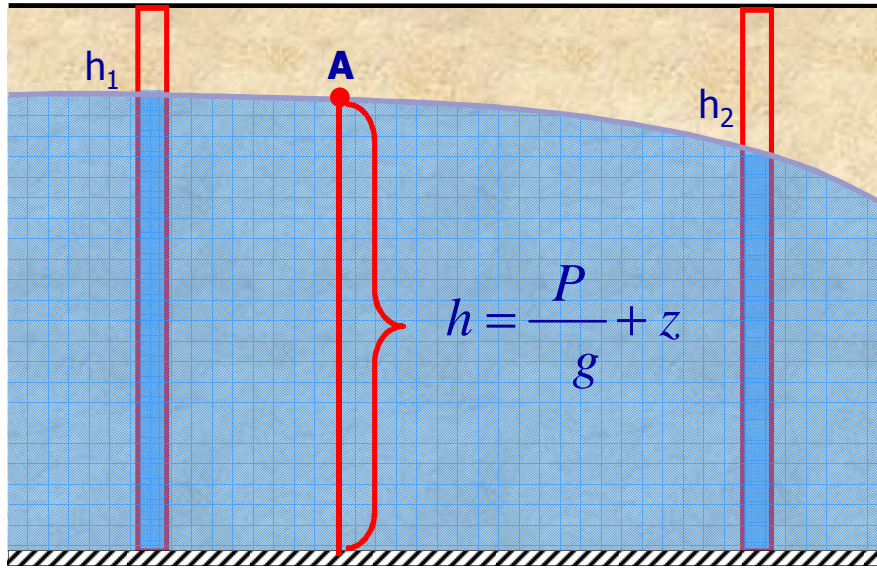


Figure 3.12: Schematic diagram for an unconfined aquifer in one dimension.

Drainage in an unconfined aquifer results in a lowering of the water table and the saturated thickness is reduced, as is the ability of the aquifer to transmit water ($T = Kh$). The resulting non-linear, groundwater flow equation becomes,

$$\frac{\delta}{\delta x} \left(K_x h \frac{\delta h}{\delta x} \right) + \frac{\delta}{\delta y} \left(K_y h \frac{\delta h}{\delta y} \right) + \frac{\delta}{\delta z} \left(K_z h \frac{\delta h}{\delta z} \right) = S_y \frac{\delta h}{\delta t} \quad (3.36)$$

For homogenous and isotropic conditions,

$$\frac{\delta^2 h^2}{\delta x^2} + \frac{\delta^2 h^2}{\delta y^2} + \frac{\delta^2 h^2}{\delta z^2} = \frac{S_y}{K} \frac{\delta h}{\delta t} \quad (3.37)$$

3.6.2 Steady State Conditions

Using equation 3.35 for flow per unit width,

$$Q' = -Kh \frac{dh}{dx} \quad (3.38)$$

and integrate,

$$Q' = -\frac{K}{2x} (h_2^2 - h_1^2) \quad (3.39)$$

To compare with the example provided in a confined aquifer (section 3.5.2). Given $h_1 = 100$ ft, $K = 1$ ft/d, $B = 100$ ft, $x = 1000$ ft and $Q' = 1$ ft²/d then $h_2 = (100^2 - (2)(1)(1000)/(1))^{0.5} = 89.4$ ft. For the same flow rate in an unconfined aquifer, head drop is more than 0.5 ft greater than for a confined aquifer over the same distance.

3.7 References Cited

Fetter, C.W. 1994. Applied Hydrology. Third Edition. Prentice-Hall, Inc., New Jersey. 691 p.

Johnson, A.I. 1967. Specific Yield – Compilation of Specific Yields for Various Materials. U.S. Geological Survey Water-Supply Paper 1662-D.

Meinzer, O.E. 1923a. The Occurrence of Groundwater in the United States, with a Discussion on Principles. U.S. Geological Survey Water-Supply Paper 489.

Meinzer, O.E. 1923b. Outline of Groundwater Hydrology with Definitions. U.S. Geological Survey Water-Supply Paper 494.

Chapter 4

Site Characterization

4.1 Introduction

Site characterization is focused on defining the parameters necessary to construct and parameterize a hydrogeologic model (refer to Chapter 6), as well as defining the geotechnical aspects for subsequent slope stability analyses. For the purposes of this report, the hydrogeologic model includes

1. the topography and watershed boundaries,
2. the stratigraphy with associated hydrogeologic characteristics, and
3. the precipitation and surface runoff characteristics that influence groundwater recharge.

4.2 Hydrogeologic Model

Details are provided on how to characterize a field site for hydrogeologic parameters necessary for drain design. Data collection techniques are discussed, along with how these data define hydrogeologic parameters, the pragmatic use of these parameters for groundwater modeling, and how to estimate these parameters if field data are not collected.

4.2.1 Watershed Delineation and Topography

Watershed delineation is an important initial step in establishing hydrologic divides and will define the extent of the hydrogeologic model domain. The watershed boundary is recognized as a no-flow boundary condition, which greatly simplifies water budget components and characterization of numeric model boundary conditions.

Several documents (e.g. <http://www.nh.nrcs.usda.gov/technical/Publications/Topowatershed.pdf>) and computer programs (e.g. ArcGIS) exist to aid in reading or generating topographic maps and how to delineate a watershed boundary. Using the example provided in Figure 4.1, the first step of establishing the watershed boundary is to define the outlet, or downstream location of the study site. This topographic low spot is highlighted with a circle in Figure 4.1a. Second, it is necessary to find the high points, or ridges, along both sides of the drainage system beginning from the watershed outlet, and extending uphill to the watershed's headwaters. In the case of a uniform slope with no distinct surface drainage pattern or with no surrounding hydrologic divides, establishment of the watershed boundary should be made by extending the study site well beyond the region of concern and assuming lateral inflow is minimal. In this circumstance, the upgradient boundary condition is monitored with an observation well to track water level response to precipitation events.

Surface water falling anywhere in the watershed's area will flow through the basin and eventually exit the basin via the system's outlet. Regional groundwater flows can occur across watershed domains, but

the necessity of quantifying groundwater flux across the watershed boundary is minimized by including the entire watershed in the analysis.

Topographic data is often available as a digital elevation model (DEM) from U.S. Geological Survey topographic mapping, generated from conventional land surveying or use of a Light Detection and Ranging (LiDAR) survey. Graphical user interfaces (GUI) developed specifically for groundwater models allow importation of topographic data as well as several interpolation algorithms to assign elevations across the model domain. Appendix B provides a step-by-step guide on how to import topographic data into a groundwater model platform. Scale of the topographic survey will depend on the level of heterogeneity, the water level change in space and time (i.e. perturbed by recharge) and should be indicative of the REV discussed in chapter 3.3.7. Those systems experiencing a large change in water level over small spatial or temporal scales will need a smaller resolution in their survey. Topographic surveys on the order of 1 m intervals or the use of USGS 30 m DEM grids should be adequate for most circumstances. Surveys of well locations, and piezometer elevations should be accurate (tenths to hundredths of a meter) to properly quantify water level (or pore pressure) changes in the system.

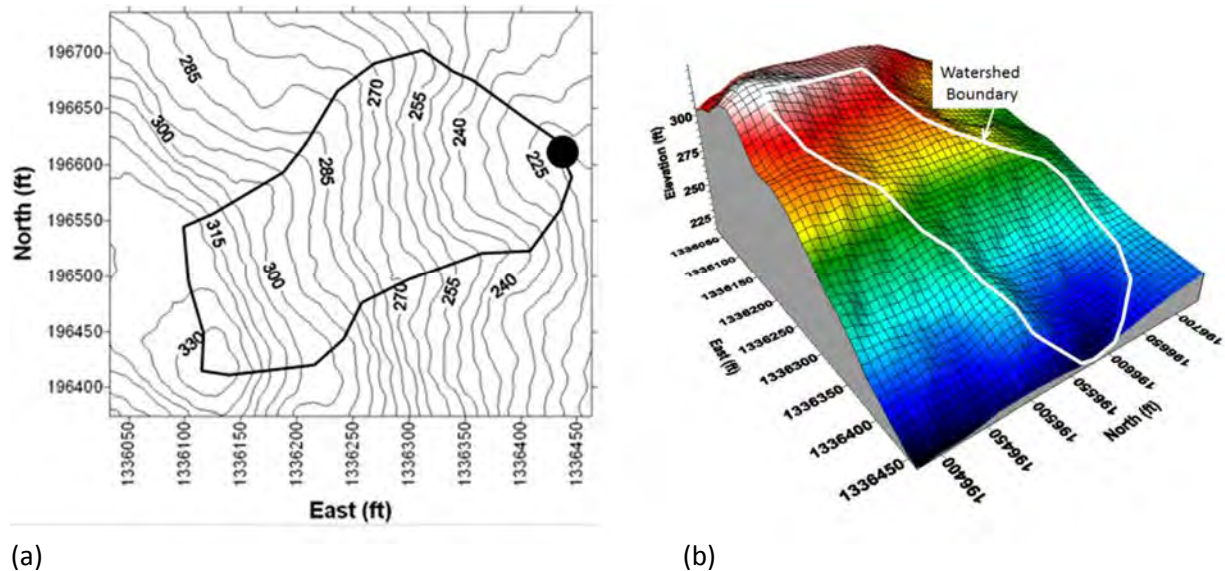


Figure 4.1: (a) Topographic map showing land surface elevation at 5 ft intervals. The black circle (right edge) represents watershed outlet and thick black line delineates the watershed. (b) A surface map showing elevation in color scale and the watershed boundary given as a white line.

4.2.2 Hydrostratigraphy

The next site characterization step is to define the hydrostratigraphy within the watershed boundary. Stratigraphy refers to the composition, thickness, and distribution/position/orientation of the

hydrogeologic units that underlie the site. Hydrostratigraphy controls how and where groundwater is recharged, moves through the watershed, and is discharged.

Distinct geologic units can have similar hydrogeologic properties and can be combined into a single water bearing unit. In contrast, facies changes within a single geologic unit, or highly heterogeneous strata may result in highly variable hydrogeologic properties, requiring a single geologic unit to be subdivided into distinct hydrogeologic units. The decision to combine or subdivide geologic units into a single or multiple hydrogeologic units is based on measured values for hydraulic conductivity, porosity, storage and ability of groundwater models to replicate observed water levels.

The development of the stratigraphy of a site is common practice for geotechnical design. Typical resources and methods employed include published/unpublished geologic mapping and other geotechnical/geologic/hydrogeologic references, airphotos and remotely sensed data, geologic site reconnaissance and mapping, subsurface exploration, and geophysical methods.

The review of regional-scale geologic maps and remotely sensed data are usually insufficient for detailed site characterization and generally need to be augmented with site-specific data collection. Geologic site reconnaissance and mapping is highly valuable for identifying local surface drainage patterns, geomorphic processes, and surficial distribution of geologic units, and informs the scope of further site investigation.

Subsurface explorations are typically necessary to develop the stratigraphy underlying the site and to provide needed hydrogeologic data. Most often, these would include test borings and/or test pits and trenches. A boring/well log is prepared summarizing the composition, depth and thickness of the geologic units encountered, as well as any water-bearing zones. If possible, subsurface conditions encountered in the explorations should be correlated with regional geologic conditions. Land surface elevation, coordinates of the boring/well, and boring construction details are also required. If practical, borings should penetrate the full depth of the geologic unit of interest and be screened in that unit for which analysis is pertinent. Typically, a minimum of two to three borings is needed to define subsurface conditions for a simple slope. These can be placed down the central axis of the slope. More complex slope geometry and/or stratigraphy will require a greater number of borings.

Surface geophysical methods can be extremely useful and a cost-effective means to gain additional subsurface data between widely spaced borings and outcrops. According to Fetter (1994), the most common surficial geophysical techniques for hydrogeologic characterization include:

- Direct current resistivity: This technique has large application to hydrologic studies. Current is introduced into the ground between two metal electrodes. Knowing the current flowing through the ground, and the potential difference between the electrodes, it is possible to compute the resistivity of earth materials, which can vary widely. Gravel has a higher resistance than does silt or clay under similar moisture conditions because of the greater number of charged surfaces associated with finer materials. As moisture increases so does the material's ability to conduct electricity. Therefore, dry materials have a higher resistance compared to those that are wet.

- Electromagnetic conductivity: This is the inverse technique to resistivity. A magnetic field is generated by passing an alternating current through a transmitter coil. The magnetic field induces an electric current through the ground at different strengths depending on the material's conductivity, with field strength measured via a passive receiver coil. Changes in phase, amplitude and orientation can be measured in space or time and are related to electrical properties of the earth. There are several electromagnetic methods, with all being relatively rapid to conduct. Similar results are attainable with resistivity and electromagnetic conductivity surveys.
- Seismic refraction: Seismic methods are often used to determine the depth to bedrock, slope of bedrock, or depth to water table and often used in hydrogeologic mapping. Seismic refraction is most common for determining thickness of unconsolidated sediment overlying bedrock. An artificial seismic wave underground will travel more slowly through unconsolidated material in comparison to solid bedrock. The travel time of seismic waves over varying distances will allow mapping of the bedrock-unconsolidated material interface.
- Ground-penetrating radar (GPR): This technique is based on the transmission of repetitive pulses of electromagnetic waves into the ground. These pulses are reflected back to the surface when they encounter the interface between materials with differing dielectric properties, and show variations in strata. Lower frequency waves (down to 10 MHz) will travel to greater depth, while higher frequencies (1000 MHz) are limited to shallower depths but provide greater resolution. Ranges in GPR signal depths are about 20 ft in fine-grained glaciolacustrine sediments and may be up to 70 ft in coarse-grained sands and gravels. GPR, in conjunction with borehole data, can distinguish fine-grained and coarse-grained sediments, bedrock, as well as the water table in coarse grained material. The depth to the water table in fine-grained material (with a substantial capillary fringe) is not easily identified with GPR.
- Magnetic surveys: Magnetic anomalies indicate the types of rocks in a very general way, and can be used to track those types of rocks that exhibit magnetic behavior. Most unconsolidated sediments are not magnetic and cannot be delineated with a magnetic survey.
- Gravity anomalies: The mass of rock in the subsurface will affect the local value of the acceleration of gravity. Using a reference value and several corrections for elevation, latitude, terrain and tidal effects, it is possible to map buried bedrock.

Geophysical techniques used within a test boring are common in the petroleum industry, research projects and with large municipal wells. They are less common with small production wells and small projects. However, several of these techniques are helpful in estimating porosity, permeability and changes in lithology, and are noted (Fetter, 1994).

- Single-Point Resistance: Several resistive techniques are available with the simplest being the single-point technique. A single electrode is lowered down the borehole while the second electrode is kept at land surface. The single point approach measures resistance of all the rocks between the electrodes. If the fluid in the borehole is homogenous, then changes in resistance are due to changes in lithology. Sand, gravel, sandstone and lignite have high resistance. Clay

and shale have the lowest resistance. Fractures will exhibit lower resistance, as will increased salinity.

- Resistivity: Resistivity is different than resistance. The former is measured in ohm-meters, while the latter is given in ohms. Two current electrodes are lowered down the borehole with resistance measured between two additional electrodes. Resistivity traces are similar to the single-point resistance technique, but this technique allows for different electrode configurations (e.g. short normal and long normal) to provide resistivity at varying radial distances from the borehole. All resistivity configurations will provide data at greater distances compared to the single-point resistance technique.
- Natural Gamma Radiation: This technique measures the natural radiation of gamma from potassium-40, part of the uranium-238 and thorium-232 decay series. Increased gamma activity will occur from sedimentary rocks that contain potassium-rich shale, clays or rocks containing phosphate. Therefore, lithologic differences in the rock can be distinguished. For example, a shaley sandstone will have much higher radiation than a clean, quartz-rich sandstone.
- Neutron Logging: A probe containing a radioactive substance, such as PbBe , is lowered down the borehole. Neutrons emitted from the probe collide with the nuclei of hydrogen atoms, and detectors measure the resulting gamma radiation produced by these interactions or the energy levels of the neutrons that are captured or moderated by the hydrogen atom. Water in the pore spaces is the dominant source of hydrogen. Therefore, saturated rocks with high porosity will capture/moderate more neutrons than rocks with low porosity. Along with porosity, it is possible to measure specific yield in unconfined aquifers. Above the water table, moisture content can be measured but not porosity.
- Gamma-Gamma Radiation: This technique allows an estimate of porosity based on a material's bulk density (weight of rock divided by the total volume). Cobalt-60 is lowered down the borehole which emits gamma radiation. Gamma protons are absorbed or scattered by all material it comes into contact with, with absorption proportional to bulk density.

The reader is referred to Wightman et al. (2004) for more in depth treatment of geophysical methods and their suitability for characterizing a variety of site conditions.

4.2.3 Groundwater Data

Initial water level (or pore pressure) data should be collected at the time of drilling, and piezometers should be installed in suspected water-bearing zones to monitor water levels over time. Accurate characterization of the stratigraphy and proper piezometer construction and development are vital to ensure accurate characterization of groundwater levels. For standpipe-type piezometers, screened/sanded intervals within suspected water-bearing zones must be sufficiently isolated from overlying water-bearing zones to avoid cross communication of aquifers and inaccurate groundwater measurements. Driscoll (1986) provides a thorough treatment of well construction. Alternatively, vibrating wire piezometers can be sanded or grouted in place within the desired geologic unit of interest. Piezometer construction should be well detailed on the boring log to document the source zone and to be able to assess the quality of the groundwater data.

Consideration should be given to monitoring frequency of piezometers. Infrequent manual measurements may be sufficient for aquifers that do not respond rapidly to precipitation (or drainage) and fluctuate slowly through wet and dry seasons. For aquifers that exhibit flashy response, continuous monitoring with the use of a datalogger should be considered. Often, the degree of responsiveness is not known or is misjudged at the beginning of an investigation (Fig 4.2). Higher initial equipment costs

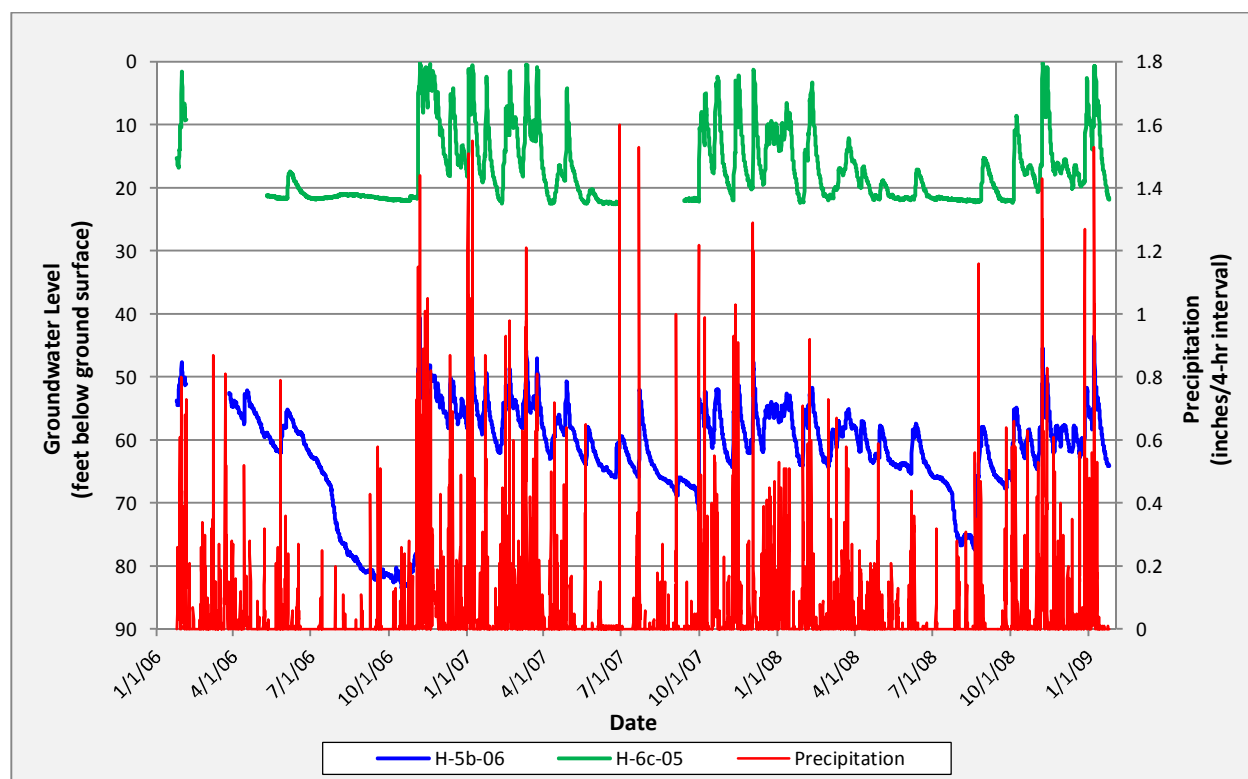


Figure 4.2 Graph depicts groundwater response to rainfall (data collected on 4-hour intervals with dataloggers) in a large landslide complex on the western Olympic Peninsula, Washington that receives about 120 inches of precipitation annually. Piezometer H-6c-05 is constructed in a glacially over-consolidated outwash consisting of very dense silty gravel with sand; note large flashy response to storm events. Piezometer H-5b-06 is constructed within intensely sheared siltstone; note comparable responsiveness.

for continuous monitoring are offset by increased labor costs for frequent manual readings and more complete and useful data.

As mentioned in section 4.2.2, a minimum of two to three borings are required for fairly simple slope configurations, with a greater number of borings necessary for more complex slopes and subsurface conditions. If possible, one boring should be placed at/near the upper edge of the site domain to measure the groundwater conditions entering the system. A minimum of three wells are also required

to determine the shape of the potentiometric surface and horizontal movement of groundwater flow. If vertical head differences are important, then piezometer nests are needed, with piezometers placed in conjunction with different screened intervals. If the well is fully screened, then piezometer nests are not informative. Nested piezometers should be installed if anisotropy is expected to be important. Such examples occur if there exist extensive silt/clay lenses, confining layers and/or thick units of glacial till.

4.2.4 Precipitation

Precipitation can vary significantly by geographic location based on elevation and slope aspect. Therefore, it is highly recommended that on-site precipitation data is collected. Rain depths at six hour intervals, or less, are used to compute groundwater recharge and are useful when evaluating aquifer responsiveness (refer to Chapter 5). The standard rain gauge consists of an 8-inch open cylinder with a funnel and a smaller measuring tube inside. The measuring tube is constructed with a cross sectional area 1/10 that of the larger collecting cylinder. Therefore, one-tenth of an inch of rain will rise one inch in the measuring tube and make measuring rain depth more precise. The tipping bucket gauge is an alternative to the standard gauge. Collection buckets tip when they sense the weight of 0.1 inches of precipitation, which an electronic signal sent to the recorder each time a bucket tips. The tipping bucket is good at measuring light rain, but can fail to keep up during large events. Lastly, weighing-rain gauges are available, in which the depth of water is tracked based on the weight of water in the collection container. Automated gages for weighing and tipping are available.

If on-site precipitation collection is not possible, or not coordinated with observed water level data, then agency data should be used. Agency data are typically archived at the daily level and easily downloadable. Data at a finer temporal resolution can be available, but may require special inquiry and a fee to obtain.

The primary data archive site is with NOAA's regional climate centers (<http://www.ncdc.noaa.gov/oa/climate/regionalclimatecenters.html>). These are federal-state cooperatives and managed by NOAA's National Climate Data Center (NCDC). There are six regional centers with Figure 4.3 showing centers by region/state. As an example, follow links to the Western Regional Climate Center (WRCC). Listed are two programs with readily available data

- Remote Automatic Weather Service (RAWs) under WRCC Projects (<http://www.raws.dri.edu/index.html>)
- Historic Climate Information (<http://www.wrcc.dri.edu/CLIMATEDATA.html>)

RAWs data provides historic daily data, while historic stations (e.g. COOP stations) provide averaged daily values, with minimum and maximum observed, for specified periods of record. If necessary, scaling of weather station data with study site data is recommended to fill in data gaps. However, variability between weather stations and the study site are not consistent and can introduce significant error.

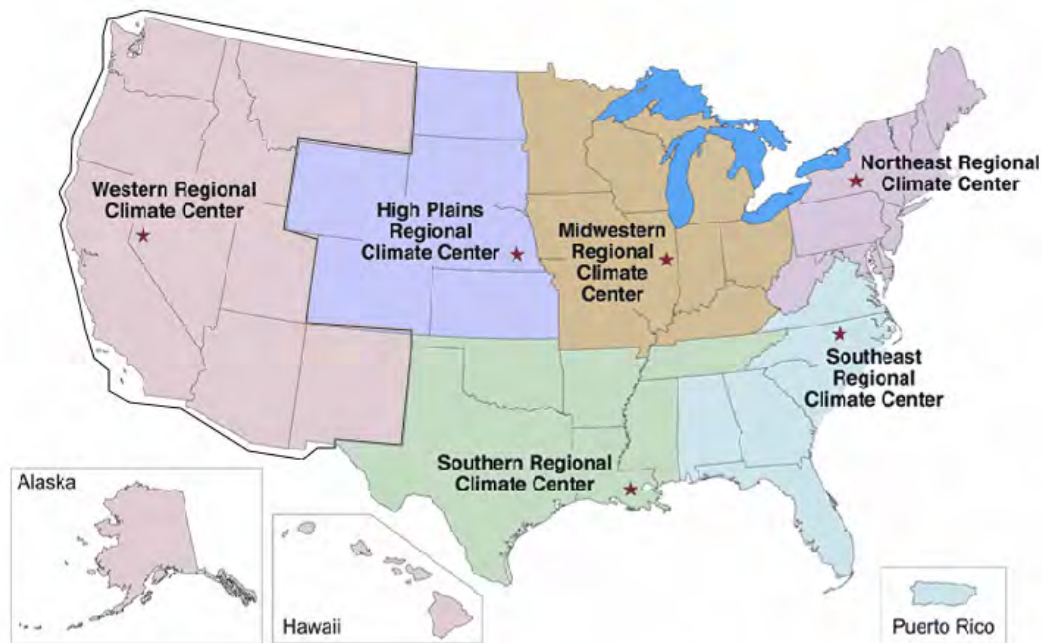


Figure 4.3: Regional climate centers by state (figure obtained from <http://www.ncdc.noaa.gov/oa/climate/regionalclimatecenters.html>)

4.2.5 Hydrologic Soil-Cover Complexes

Soil type and vegetation status, as well as land use, are used to predict the amount of precipitation that is partitioned into groundwater recharge. While rigorous approaches to soil infiltration are available, such as Horton (1933, 1939), Philip (1957, 1969) or Green-Ampt (1911), a relatively simple approach developed by the USDA Natural Resources Conservation Service (NRCS), formally called the Soil Conservation Service (SCS), is recommended. A full description of the SCS approach is discussed in Chapter 5 of this manual with hydrologic soil groups provided in Appendix D.

Hydrologic characteristics of soils are defined in terms of a dimensionless curve number (CN). The curve number ranges between 0 and 100, with 100 representing an impervious surface (e.g. concrete). Natural systems have $CN < 100$. Examples of CNs for “other” agricultural lands are provided in Table 4.1, while arid and semi-arid rangelands are given in Table 4.2. The National Hydrology Engineering Handbook (630), Chapter 7 (USDA, 2009) discusses hydrologic soil groups, while Chapter 8 classifies land use treatments in the field (USDA, 2002). Chapter 9 of the National Hydrology Engineering Handbook (USDA, 2004) provides curve number estimates for forest ranges in the western United States, with CN modified by ground cover density and soil group. The Handbook is found online at www.nrcs.usda.gov/wps/portal/nrcs/detailfull/national/wntsc/?&cid=stelprdb1043063. Hydrologic soil groups are affected by subsurface permeability and soil-intake rates. Soils are classified into one of four

groups (A, B, C and D) according to their minimum infiltration rate on bare soil and after prolonged wetting. Soil groups are defined as follows (NRCS, 1986,).

- Group A: low runoff potential and high infiltration rates even when thoroughly wetted. Generally consist of deep, well to excessively drained sands or gravel and have a high transmission rate of water (> 0.30 inches per hour)
- Group B: Moderate infiltration rates when thoroughly wetted. Generally consists of deep, moderately well to well drained soils with moderately fine to moderately coarse textures. Water transmission rates are on the order of 0.15 to 0.30 inches per hour.
- Group C: Soils have low infiltration rates when thoroughly wetted. Soils generally contain a layer that impedes downward movement of water, with soils of moderate to moderately-fine texture. Transmission rates are on the order of 0.05 to 0.15 inches per hour.
- Group D: Soils have a high runoff potential. Infiltration rates are very low when thoroughly wetted. Soils consist primarily of clays with a high swelling potential, permanently high water table, claypan or clay layer at or near the land surface and/or shallow soils over an impervious material. Transmission rates are 0 to 0.05 inches per hour.

TR-55 (USDA, 1986) lists many of the major soils and associated soil groups in the United States and is provided in Appendix D. Soils in a specific area of interest are obtained by soil reports conducted by local SCS offices or water conservation districts. The USDA also offers archived papers discussing local sources of runoff CN, past and present procedures of the SCS approach, etc.

<http://www.nrcs.usda.gov/wps/portal/nrcs/detailfull/national/water/manage/?&cid=stelprdb1043053>.

Cover type (bare soil, vegetation type and density) are determined by a field reconnaissance, aerial photographs and/or land use maps, while hydrologic condition refers to the effect of cover type and condition on runoff potential. Hydrologic condition can be assessed by density of vegetation, amount of year round cover, amount of grass, or degree of surface roughness. Good hydrologic condition denotes a soil with low runoff potential for a specific hydrologic soil group, cover type and treatment.

Modifications of the CN, based on antecedent moisture conditions or slope, are discussed in Chapter 6 of this manual, along with sensitivity of estimated recharge to uncertainty in CN. Chapter 7 examines the impacts on drain design based on uncertainty in CN for a site susceptible to translational failure.

4.2.6 Hydraulic Conductivity

Hydraulic conductivity (K_x) ranges over 12 orders-of-magnitude, depending on the water-transmitting characteristics of the aquifer materials (refer to Figure 4.4). Hydraulic conductivity of similar materials can vary over several orders-of-magnitude based on heterogeneity, anisotropy, sorting, as well as post-diagenetic circumstances (e.g. solution cavities, fracturing). It is therefore not recommended to use material type of an aquifer as the sole basis of estimating hydraulic conductivity. Instead, material type should be used as a means to check measured values for consistency.

Most common practices for estimating hydraulic conductivity include correlation with sediment grain-size distribution, lab-scale permeameters, field-scale slug or pump tests, and numeric model calibration.

The latter is discussed in Chapter 6 – Introduction to Groundwater Modeling, while a step-by-step guide to calibrating hydraulic conductivity is given in Appendix B.

Table 4.1: Runoff curve numbers (CN) for other agricultural lands

Cover description		Curve numbers for hydrologic soil group			
Cover type	Hydrologic condition	A	B	C	D
Pasture, grassland, or range—continuous forage for grazing. ^{2/}	Poor	68	79	86	89
	Fair	49	69	79	84
	Good	39	61	74	80
Meadow—continuous grass, protected from grazing and generally mowed for hay.	—	30	58	71	78
Brush—brush-weed-grass mixture with brush the major element. ^{3/}	Poor	48	67	77	83
	Fair	35	56	70	77
	Good	30 ^{4/}	48	65	73
Woods—grass combination (orchard or tree farm). ^{5/}	Poor	57	73	82	86
	Fair	43	65	76	82
	Good	32	58	72	79
Woods. ^{6/}	Poor	45	66	77	83
	Fair	36	60	73	79
	Good	30 ^{4/}	55	70	77
Farmsteads—buildings, lanes, driveways, and surrounding lots.	—	59	74	82	86

¹ Average runoff condition, and $I_a = 0.2S$.

² *Poor:* <50% ground cover or heavily grazed with no mulch.

Fair: 50 to 75% ground cover and not heavily grazed.

Good: > 75% ground cover and lightly or only occasionally grazed.

³ *Poor:* <50% ground cover.

Fair: 50 to 75% ground cover.

Good: >75% ground cover.

⁴ Actual curve number is less than 30; use CN = 30 for runoff computations.

⁵ CN's shown were computed for areas with 50% woods and 50% grass (pasture) cover. Other combinations of conditions may be computed from the CN's for woods and pasture.

⁶ *Poor:* Forest litter, small trees, and brush are destroyed by heavy grazing or regular burning.

Fair: Woods are grazed but not burned, and some forest litter covers the soil.

Good: Woods are protected from grazing, and litter and brush adequately cover the soil.

Table 4.2: Runoff curve numbers (CN) for arid and semi-arid rangelands.

Cover description		Curve numbers for hydrologic soil group			
Cover type	Hydrologic condition ^{2/}	A ^{3/}	B	C	D
Herbaceous—mixture of grass, weeds, and low-growing brush, with brush the minor element.	Poor		80	87	93
	Fair		71	81	89
	Good		62	74	85
Oak-aspen—mountain brush mixture of oak brush, aspen, mountain mahogany, bitter brush, maple, and other brush.	Poor		66	74	79
	Fair		48	57	63
	Good		30	41	48
Pinyon-juniper—pinyon, juniper, or both; grass understory.	Poor		75	85	89
	Fair		58	73	80
	Good		41	61	71
Sagebrush with grass understory.	Poor		67	80	85
	Fair		51	63	70
	Good		35	47	55
Desert shrub—major plants include saltbush, greasewood, creosotebush, blackbrush, bursage, palo verde, mesquite, and cactus.	Poor	63	77	85	88
	Fair	55	72	81	86
	Good	49	68	79	84

¹ Average runoff condition, and $I_a = 0.2S$. For range in humid regions, use table 2-2c.

² Poor: <30% ground cover (litter, grass, and brush overstory).

Fair: 30 to 70% ground cover.

Good: > 70% ground cover.

³ Curve numbers for group A have been developed only for desert shrub.

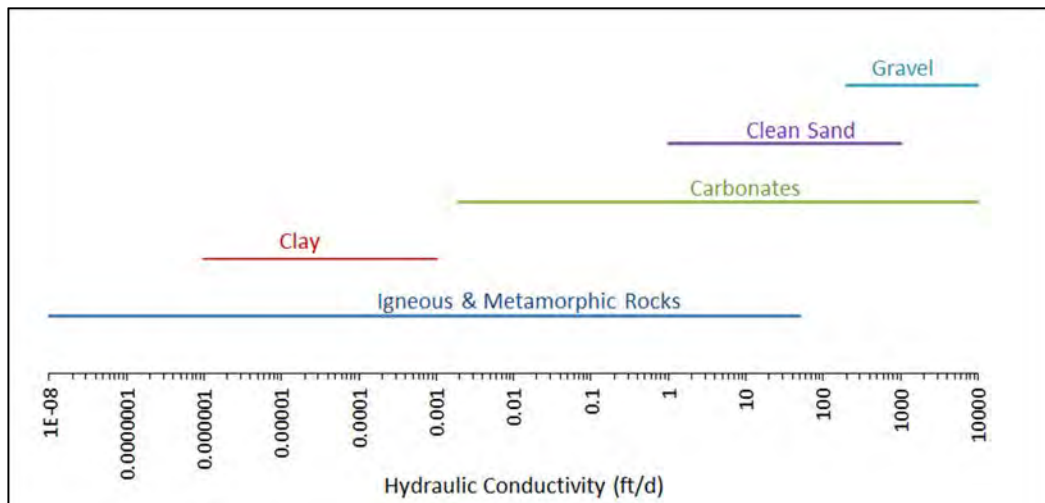


Figure 4.4: Ranges of hydraulic conductivity (ft/d) for many aquifer materials (modified from Fetter, 1994).

4.2.6.1 Grain-Size Distribution

The first, and simplest, method for estimating hydraulic conductivity is to assume a correlation with grain-size distribution. As the medium grain size increases, so does hydraulic conductivity due to larger pore openings. However, if a sample is poorly sorted (i.e. well graded) then the standard deviation of particle sizes increases and permeability will decrease. The Hazen method gives large weight to grain-size variability with the following relationship,

$$K_x = Cd_{10}^2 \quad (4.1)$$

Where K_x is in units of cm/s, C is the dimensionless shape coefficient provided in the discussion of aquifer properties (Table 3.2), and d_{10} is the effective grain size (cm) defined by the grain size that is 10% finer by weight. To help illustrate the importance of sorting on estimates of hydraulic conductivity computed with the Hazen method, refer to Figure 3.4. The median grain size in both distributions are nearly equal (0.15-0.2 mm) but variance in grain size for the silty fine to medium sand is much larger than for the fine sand. For the poorly sorted, silty fine to medium sand, $d_{10} = 0.018$ mm, C is estimated at 80 and the resulting $K_x = 2.6 \times 10^{-4}$ cm/s (0.74 ft/d). In contrast, a well sorted (poorly graded) fine sand with $d_{10} = 0.15$ mm and C estimated at 80 will produce $K_x = 1.8 \times 10^{-2}$ cm/s (1555 ft/d), or an increase in hydraulic conductivity by over three orders-of-magnitude.

4.2.6.2 Laboratory Estimates of Hydraulic Conductivity

Hydraulic conductivity can also be measured in the laboratory with a permeameter. These devices are typically cylindrical chambers that hold a sample of rock or sediment. Two types of permeameters are widely used. The constant-head permeameter (Figure 4.5) works well for non-cohesive materials, such as sands, gravels, or rock. It contains an inflow reservoir of constant water level and steady state outflow rates. Hydraulic conductivity is computed using Darcy's Law such that $h = h_1 - h_2$ and L = length of the sample or $x_1 - x_2$,

$$K_x = -\frac{QL}{Ah} \quad (4.2)$$

Fetter (1994) warns that hydraulic gradients should approximate those seen in the field and that the change in head (h) should never be more than 0.5 times the sample length L . If the head is too large, then flow velocities can become large enough to produce turbulent flow and negate Darcy's law (quick sand conditions can arise).

A falling-head permeameter is used for cohesive materials with potentially low hydraulic conductivities and a relatively low volume of water moving through the sample, (Figure 4.6). The initial water level (h_0) compared to the outflow height at initial time t_0 , and the water level (h_1) at a later time $t_1 = t$ are tabulated. It is also necessary to know the inside area of the falling tube (A_t), the length of the sample (L) and the cross sectional area of the sample (A_c).

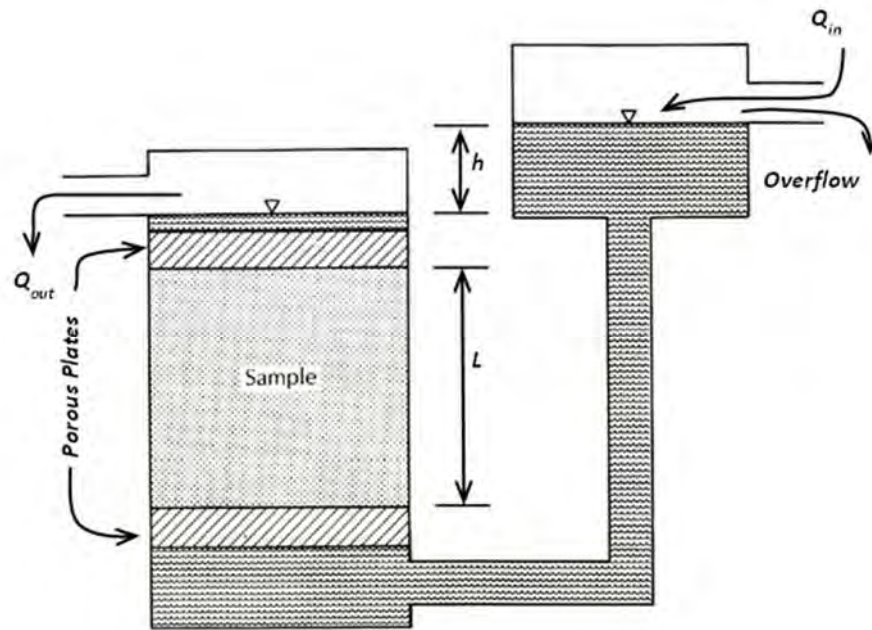


Figure 4.5: Schematic of a constant-head permeameter.

(Adopted from Fetter C.W., Applied Hydrogeology, 3rd Edition © 1994, page 105, Reprinted by permission of Pearson Education, Inc., Upper Saddle River, NJ).

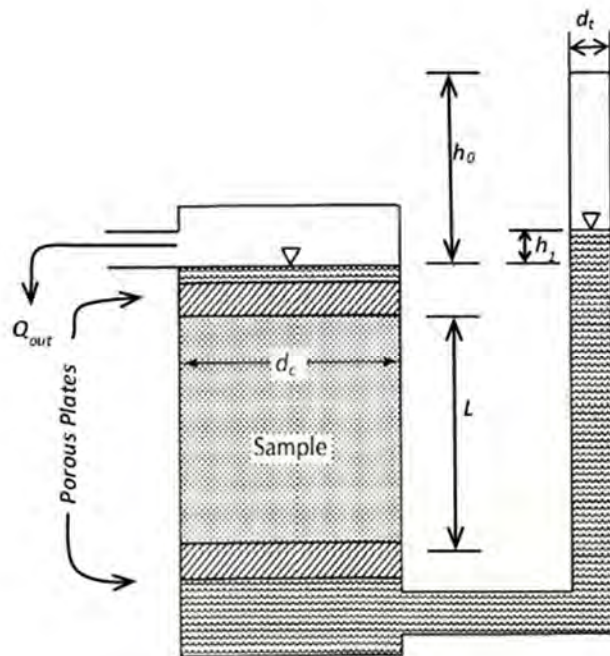


Figure 4.6: Schematic of a falling-head permeameter.

(Adopted from Fetter C.W., Applied Hydrogeology, 3rd Edition © 1994, page 105, Reprinted by permission of Pearson Education, Inc., Upper Saddle River, NJ).

Using Darcy's law and the principal of continuity that states $Q_{in} = Q_{out}$,

$$-A_t \frac{dh}{dt} = K_x A_c \frac{h}{L} \quad (4.3)$$

Solving for hydraulic conductivity in the x direction,

$$K_x = -\frac{A_t L}{A_c h} \frac{dh}{dt} \quad (4.4)$$

and integrating from $t_0 = 0$ to $t_1 = t$, given $h = h_0$ at $t=0$ and $h = h_1$ at t_1 produces,

$$K_x = \frac{A_t L}{A_c t} \ln \left(\frac{h_0}{h_1} \right) \quad (4.5)$$

4.2.6.3 Slug Tests

Slug tests allow relatively quick and inexpensive point-estimates of hydraulic conductivity at the field scale to account for system heterogeneity at a larger scale than measured in the laboratory. Slug test estimates of hydraulic conductivity can be conducted across the site, or combined with laboratory or grain-size distribution estimates for more complete site characterization. In addition, slug tests can be used at contaminated sites to limit the discharge of contaminated water and can be used as a precursor to larger multi-well pump test as a means for design.

Data collected for a slug tests includes an initial measurement of water level in a monitoring well prior to any disturbance. This is followed by a rapid removal, or addition, of a known quantity of water to closely approximate instantaneous change in head (Figure 4.7). The rate at which the water level rises or falls to its original state is used to compute hydraulic conductivity in the immediate vicinity of the well. For analytical considerations, head displacement is assumed positive regardless of whether water is removed or added to the well.

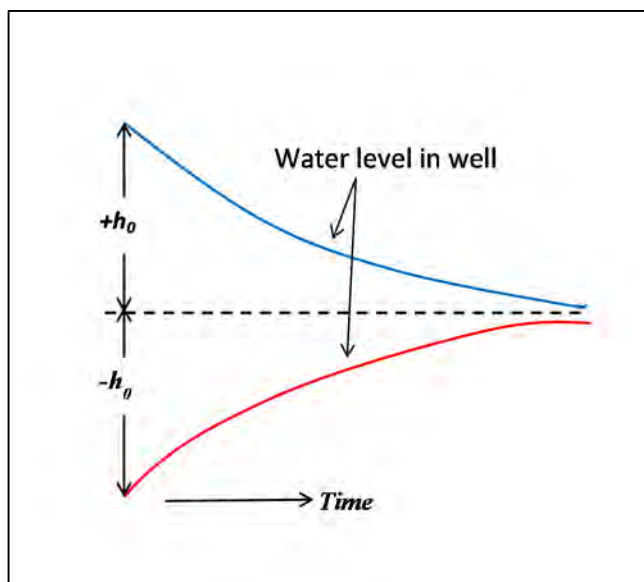


Figure 4.7: Schematic of a slug test in which the dashed line is the water original water level in the well prior to any disturbance. Displacement due to an addition of water ($+h_0$), or rapid removal of water ($-h_0$), is recorded, as are water levels over time as the well returns to its original state.

Several methods for solving for K_x given slug-test data exist (e.g. Cooper et al., 1967; van der Kamp, 1976). This manual will focus on the Bouwer-Rice method (Bouwer and Rice, 1976; Bouwer, 1989) for its general applicability. The Bouwer-Rice approach can be performed in open boreholes or screened wells and is applicable to fully or partially penetrating wells. The method was originally designed for unconfined systems, but it can also be used in confined aquifers if the bottom of the confining layer is far above the top of screened interval in the well (Fetter, 1994). For higher hydraulic conductivity materials (1-100 ft/d), it is recommended to repeat the slug test two or three times (rising and falling scenarios) with consistent hydraulic conductivity values asserting proper well development and proper recording of well response to pulse input.

The Bouwer-Rice slug test analysis is given below with important well design parameters noted in Figure 4.8.

$$K_x = \frac{r_c^2 \ln\left(\frac{R_e}{r_w}\right)}{2L_e} \frac{1}{t} \ln\left(\frac{h_0}{h_t}\right) \quad (4.6)$$

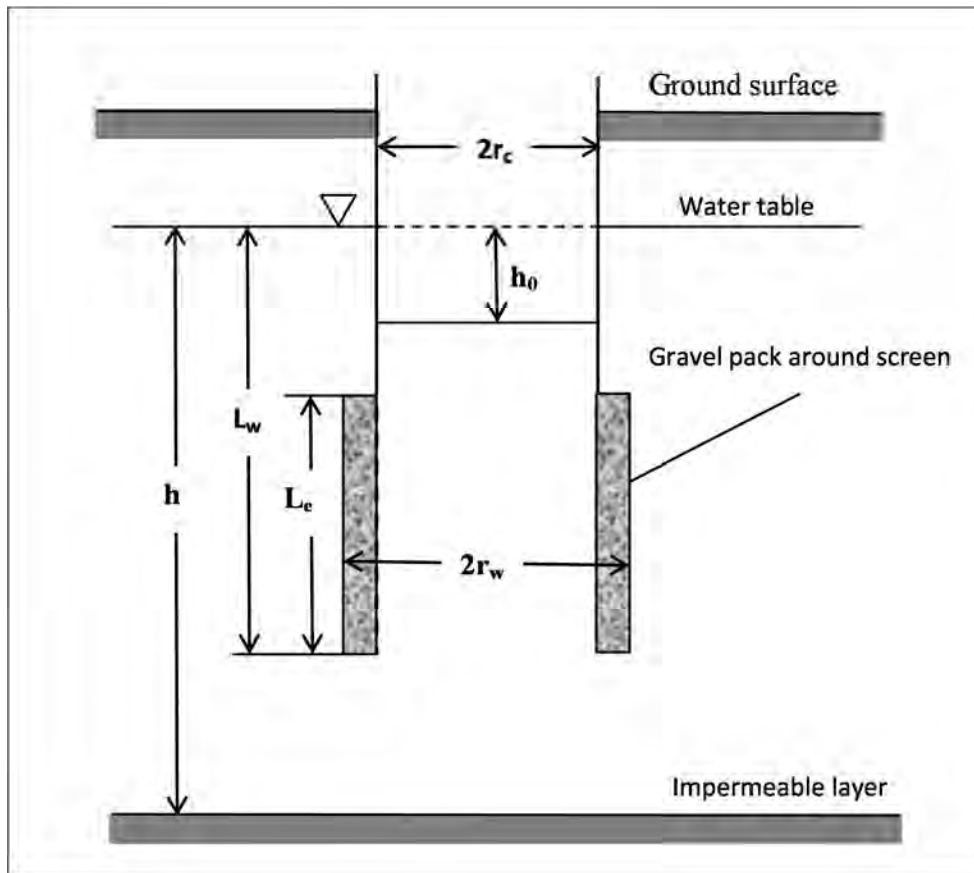


Figure 4.8: Well parameters defined for the Bouwer-Rice slug test analysis given in equations 4.7, 4.8 and 4.9.

where h_0 is the drawdown/rise at time $t=0$, while h_t is drawdown at time $t=t$; R_e is the effective radial distance at which head is dissipated, and can be thought of as the distance away from the well for which hydraulic conductivity is being measured. It is not possible to measure R_e . Therefore it is necessary to estimate its value and then test the validity of the choice of R_e using theoretical considerations. If the monitoring well is partially penetrating such that L_w is less than the saturated thickness of the aquifer (h), the R_e is calculated as,

$$R_e = r_w \left(\exp \left[\frac{1.1}{\ln(L_w/r_w)} + \frac{A+B\ln[h-L_w]/r_w}{L_e/r_w} \right]^{-1} \right) \quad (4.7)$$

If the well is fully penetrating ($L_w=h$), then the relationship simplifies to,

$$R_e = r_w \left(\exp \left[\frac{1.1}{\ln(L_w/r_w)} + \frac{C}{L_e/r_w} \right]^{-1} \right) \quad (4.8)$$

The coefficients A , B and C are graphically derived from Figure 4.9 or gotten from Table 4.4. It is also common to assume that $R_e = r_c$ or $R_e = r_w$, using the latter relationship if the filter pack surrounding the well is more than twice as permeable as the formation (Butler, 1997).

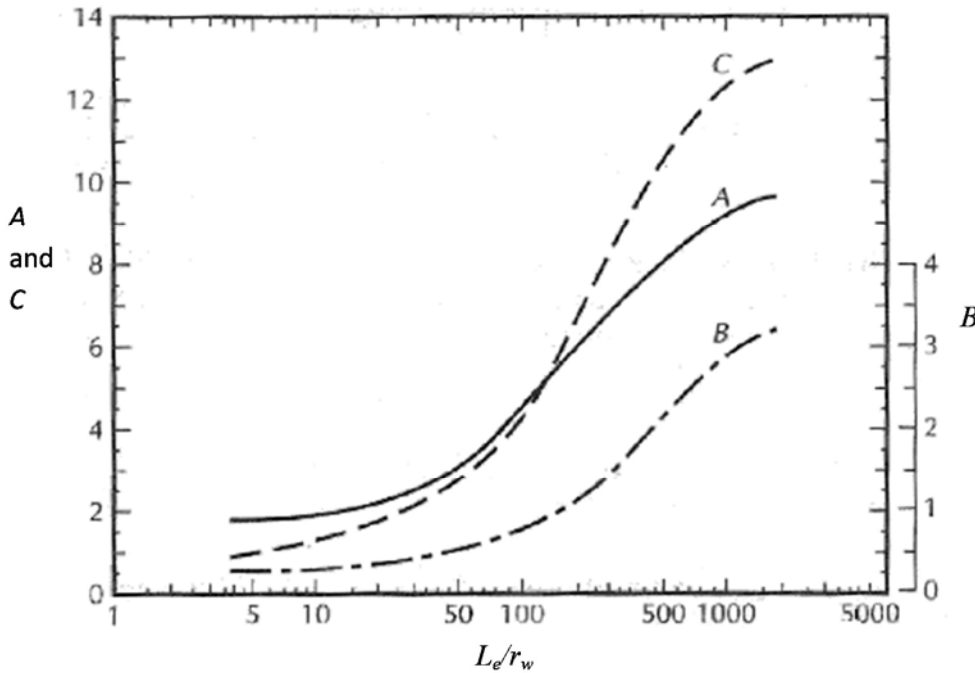


Figure 4.9: Dimensionless parameters A , B and C plotted as a function of L_e and r_w , and used in equations 4.7 or 4.8 based on L_w with respect to h .

(Reprinted from Ground Water, 27(3), Bouwer, H., The Bouwer and Rice Slug Test – An Update, pp 304-309, 1989, with permission from John Wiley and Sons).

Table 4.4: Empirical look up table for Bouwer-Rice method for slug test analysis

(Credit: U.S. Geological Survey, Department of the Interior/USGS, taken from Halford and Kuniansky, 2002).

$\log(L_e/r_w)$	A	B	C
0.5000	1.738	0.229	0.835
0.6891	1.738	0.229	0.835
0.8911	1.802	0.269	1.09
0.9893	1.87	0.265	1.192
1.2849	2.175	0.339	1.696
1.4578	2.464	0.407	2.023
1.6855	3.057	0.49	2.698
1.8274	3.604	0.585	3.283
1.9870	4.397	0.738	4.183
2.2708	6.022	1.103	6.732
2.4581	7.069	1.51	8.675
2.6754	8.062	2.1275	10.58
2.9806	9.156	2.8485	12.32
3.2772	9.767	3.3175	13.126

To solve K_x in equation 4.6, it is necessary to plot the value of h_t versus time on a semi-logarithmic plot with h_t on the log axis. Data will fall on a straight line from small values of time and large displacements. As time progresses, points will begin diverting from a straight line. Figure 4.10 shows that at very short times a straight line (A-B) may form with a steeper slope than for slightly later times (A-C). This initial steep slope reflects rapid movement of water into or out of the gravel pack encasing the well. In contrast, the second straight line (B-C) represents movement of water into the geologic material and should be the line which one does the following analysis for hydraulic conductivity.

Any two points are picked along the straight line portion of the graph (B-C) to solve K_x , in which h_1 and h_2 are the head displacements at time t_1 and t_2 respectfully.

$$K_x = \frac{r_c^2 \ln\left(\frac{R_e}{r_w}\right)}{2L_e} \frac{1}{(t_2 - t_1)} \ln\left(\frac{h_1}{h_2}\right) \quad (4.9)$$

A warning is given to possible “skin effects” as a consequence of well development. This is the result of low hydraulic conductivity materials, such as clays and drilling muds, being smeared along the screen of the well. If the material is not removed during well development via pumping or surging the well to stir up the fines, then slug tests will produce incorrectly low K_x values.

The USGS has developed excel spread sheets to aid practitioners in the calculation of hydraulic conductivity using the Bouwer-Rice analysis for slug tests (Halford and Kuniansky, 2002). These tools are available to the public for download at <http://pubs.usgs.gov/of/2002/ofr02197/>.

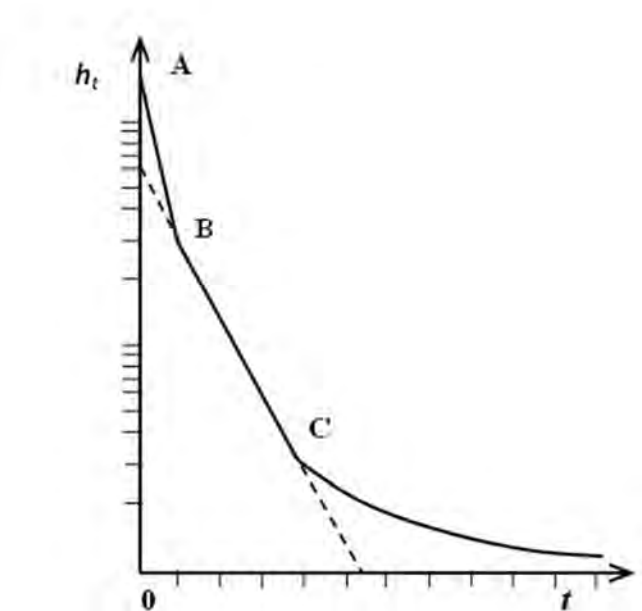


Figure 4.10: Head in a borehole as a function of time during a slug test. The line-segment B-C is used in the analysis for Bouwer- Rice to calculate hydraulic conductivity.

(Reprinted from Ground Water, 27(3), Bouwer, H., The Bouwer and Rice Slug Test – An Update, pp 304-309, 1989, with permission from John Wiley and Sons).

4.2.6.4 Aquifer Pump Tests

Aquifer pump tests are based on drawdown response in a well based on pumping. In contrast to slug tests, the imposed stress of pumping for greater time durations should provide estimates of hydraulic properties over a greater region than the immediate vicinity of the well. Pump tests, however, take significantly more planning and are considerably more expensive to carry out than slug tests. Pump test planning will require the following:

- An estimate of maximum drawdown at the pumped well.
- Estimate of maximum pumping rate.
- Evaluation of the best method to measure the pumped volume.
- Plan discharge of pumped volumes away from the well.
- Estimate drawdowns at observation wells.
- Ensure the system is at steady state before initiating the pump test.
- Ability to maintain a constant pumping rate.

- Construct at least two observation wells
- Establish how drawdown and/or recovery will be measured.
- Determine time interval(s) for water level measurement.

Driscoll (1986) is an excellent reference for all aspects of well design, drilling and testing, while Kruseman and de Ridder (1994) provide detailed guidance on aquifer tests. The USGS has software programs for analysis of pump tests, including WTAQ (Barlow and Moench, 1999) for radial axisymmetric flow to a well under confined and unconfined conditions. TENSOR2D (Sepulveda, 1992) will solve the transmissivity tensor using multi-well tests under anisotropic conditions, while Halford and Kuniansky (2002) have created user-friendly spreadsheet applications for several pump test methods (<http://pubs.usgs.gov/of/2002/ofr02197/>).

Pump test analysis is done using analytic solutions to well equations. A full derivation of these approaches is beyond the scope of this manual. Instead, the following discussion focuses on governing assumptions and application for the different approaches presented. Well equations can be divided into various classes based on confined or unconfined conditions, as well as steady state or transient pumping scenarios. Additional modifications for leaky aquifers (Huntush-Jacob, 1955), storage in an aquitard (Huntush-Jacob, 1955), fracture flow via double porosity (Warren Root, 1963), and wellbore storage (Cooper et al, 1967) are available but not discussed.

The performance of pump tests and the analysis of the results may be beyond internal technical capabilities of some State DOT geotechnical groups and may warrant external contracting for the hydrogeological expertise.

4.2.6.4.1 Confined/Steady State (Theis and Thiem)

The Theis (1935) is a method that predicts drawdown in a fully confined aquifer given knowledge of transmissivity ($T = K_s B$) and the storage coefficient (S). A pumping well and single observation well are required. The Theis method is useful for estimating water level response to pumping, pump capacity and well spacing, all necessary for designing a successful pump test. The Theis solution assumes the aquifer is (1) infinite in extent, (2) homogenous, (3) isotropic, and that (4) well discharge is constant, (5) the well fully penetrates a confined aquifer resulting in horizontal flow to the well, (6) flow to the well is laminar, the aquifer has uniform thickness and is horizontal and (7) the potentiometric surface is initially horizontal. The Theis equation solves for drawdown,

$$h_0 - h = \frac{Q}{4\pi T} \int_u^\infty \frac{e^{-a}}{a} da \quad (4.10)$$

Where h_0 is the initial head prior to pumping (L), and h is the steady-state head (L). Therefore, $s = h_0 - h$ is drawdown. T is transmissivity (L^2/T) and the well integral, $W(u) = \int_u^\infty \frac{e^{-a}}{a} da$, where

$$u = \frac{r^2 S}{4Tt} \quad (4.11)$$

And r is the radial distance from the pumping well that an observation occurs. The well integral can be approximated by truncating the infinite sum in equation (4.12). Tabulated values for the well integral are also readily available on the web or in Fetter (1994).

$$W(u) = -0.577216 - \ln(u) + u - \frac{u^2}{2 \cdot 2!} + \frac{u^3}{3 \cdot 3!} - \frac{u^4}{4 \cdot 4!} + \dots \quad (4.12)$$

Assuming a value for S and T , one can solve for u in equation (4.11), then solve for $W(u)$ using equation (4.12) and solve for estimated drawdown for a given pumping rate (Q) in equation (4.10).

The Thiem (1906) equation for steady radial flow in a confined aquifer is used to estimate transmissivity. This approach integrates Darcy's Law in radial coordinates and solves for transmissivity given two monitoring wells at a distance from the pumping well at r_1 (L) and r_2 (L), with pumped steady-state water levels of h_1 and h_2 , respectfully.

$$T = \frac{Q}{2\pi(h_2 - h_1)} \ln\left(\frac{r_2}{r_1}\right) \quad (4.13)$$

Q , h , r and T only need to be in consistent units of length and time. Given steady-state conditions, it is not possible to solve for the storage coefficient (S), however, the estimate of T (or K_x) is likely more accurate than subsequent transient methods.

4.2.6.4.2 Unconfined/Steady (Thiem)

A variation of the Thiem equation is used to solve for hydraulic conductivity in an unconfined aquifer knowing the drawdown in two observation wells located at a distance from a pumping well.

$$T = \frac{Q}{\pi(h_2^2 - h_1^2)} \ln\left(\frac{r_2}{r_1}\right) \quad (4.14)$$

4.2.6.4.3 Confined/Transient (Cooper-Jacob)

The Cooper-Jacob (1946) analysis is the simplest approach for analysis given confined, transient conditions. More complex graphical methods for the Theis equation are available but not discussed. The Cooper-Jacob approach is best utilized given a minimum of a single observation well and assumes that when

$$u = \frac{r^2 S}{4Tt} < 0.05, \quad (4.15)$$

then $W(u)$ is solved using only the first two terms on the right hand side of equation (4.12). The limiting condition is met at either large times or small radial distances from the pumping well (r), and reduces the Theis equation to,

$$\sigma(r, t) = \frac{2.3Q}{4\pi T} \log\left(\frac{2.25Tt}{r^2 S}\right) \quad (4.16)$$

Analysis is then a two-step process. First, the drawdown over one log-cycle of time (e.g. 1 minute and 10 minutes) will reduce to $\left(\frac{2.25Tt}{r^2 S}\right) = 1$; then, it is possible to solve for T . Second, at $t = t_0$, it is assumed there is no drawdown and $\log\left(\frac{2.25Tt}{r^2 S}\right) = 0$, meaning $\left(\frac{2.25Tt}{r^2 S}\right) = 1$. It then is possible to solve for S . As

an example taken from Fetter (1994), refer to Figure (4.11) in which drawdown in an observation well is plotted over time. $Q = 42,000 \text{ ft}^3/\text{d}$, and $r = 824 \text{ ft}$.

$$T = \frac{2.3Q}{4\pi\Delta h} = \frac{2.3(42,000)}{4\pi(5.5)} = 1,400 \text{ ft}^2/\text{d} \quad (4.17)$$

$$S = \frac{2.25Tt_0}{r^2} = \frac{2.25(1400)(3.6 \times 10^{-3})}{(824)^2} = 1.7 \times 10^{-5} \quad (4.18)$$

Now it is necessary to see if the limiting criterion is met (equation 4.15). If it is not, then data at greater times is necessary (and was hopefully collected).

$$u = \frac{r^2 S}{4Tt} = \frac{(824)^2(1.7 \times 10^{-5})}{4\pi(1400)} = 6.6 \times 10^{-4} < 0.05 \quad (4.19)$$

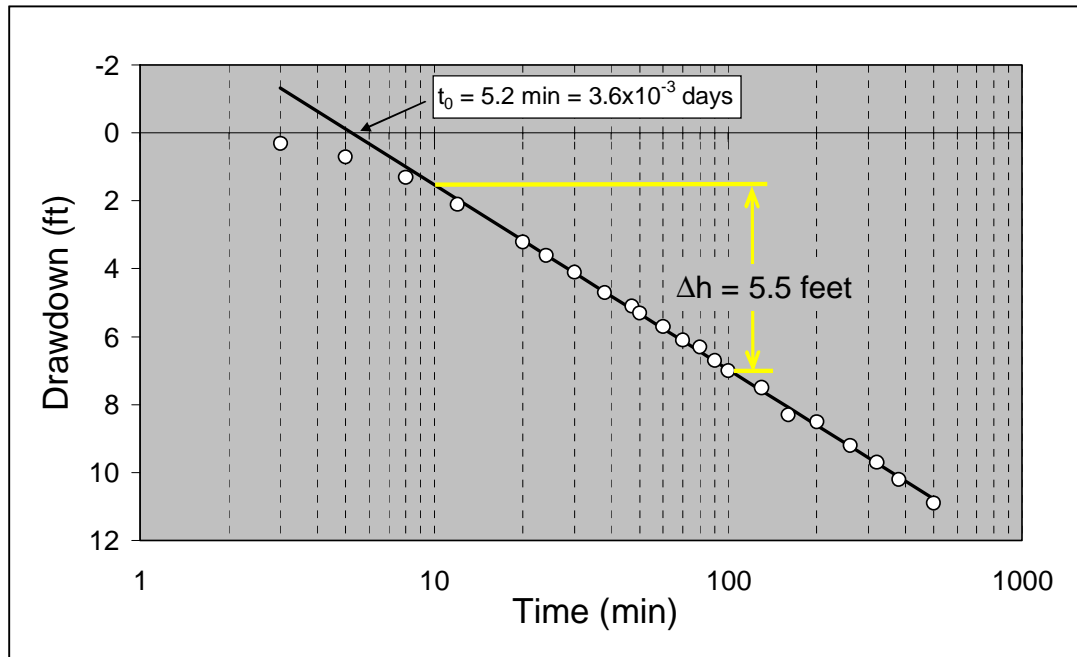


Figure 4.11: An example of the Cooper-Jacob method for a fully confined aquifer. Drawdown data (white circles) are plotted as a function of logarithmic time. t_0 is the time when a straight line intersects the zero drawdown (3.6×10^{-3} days), while Δh (L) is drawdown over one log-cycle of time.

Halford and Kuniansky (2002) provide a spreadsheet application of the Cooper-Jacob method given no observation well (<http://pubs.usgs.gov/of/2002/ofr02197/>). The single-well test allows estimates of transmissivity, but not storage. Examples are given for a pumping and recovery scenario.

4.2.6.4.4 Unconfined/Transient (Graphical Theis)

The Theis graphical solution for unconfined, unsteady aquifer pump test is relatively complicated, but several private graphical user interfaces are available to aid the practitioner (e.g. Aquifer Test). The

USGS program WTAQ (Barlow and Moench, 1999) can also be used to help solve more complex pump test problems with included uncertainty in estimated hydraulic parameter values. For guidance, the basics are presented here.

The solution to the flow equation is,

$$\sigma = \frac{Q}{4\pi T} W(u_a, u_b, \Gamma). \quad (4.20)$$

With tabulated $W(u_a, \Gamma)$ and $W(u_b, \Gamma)$ tabulated by Fetter (1994). Early-time drawdown when water is released from storage uses,

$$u_a = \frac{r^2 S}{4Tt}. \quad (4.21)$$

While at later times gravity drainage is more important, such that,

$$u_b = \frac{r^2 S_y}{4Tt} \quad (4.22)$$

where S_y is specific yield. The gamma function is defined as,

$$\Gamma = \frac{r^2 K_v}{B^2 K_x} \quad (4.23)$$

where K_v is the vertical hydraulic conductivity in the aquifer, and B is the initial saturated thickness of the aquifer. It important that drawdown () is small compared to B ; if this is not true, then modifications to the approach are recommended (Neuman, 1974).

The graphical method requires both Theis Type A and Type B curves to be plotted as $W(u_a)$ and $W(u_b)$ versus $1/u_a$ or $1/u_b$, respectfully, in log-log scale. Type curves are presented in Figure 4.12. Using the same log-log scale, drawdown is plotted on the y-axis and time (minutes) plotted on the x-axis. The data should have a similar form to the Type curves. The Type curves are laid over the observed data until they are lined up. Refer to Figure 4.13. Once the curves are aligned, Γ can be determined. Next, two match points are chosen. They do not need to be on the curve. The easiest match points to pick are represented by $W(u_a) = 1$ and $1/u_a = 1$, as well as $W(u_b) = 1$ and $1/u_b$. From these match points, one reads drawdown and t , units are converted to be consistent, and finally equations 4.20, 4.21, 4.22 and 4.23 are rearranged to solve for T , S , S_y , and K_x , the latter is solved since K_x equal to T/B .

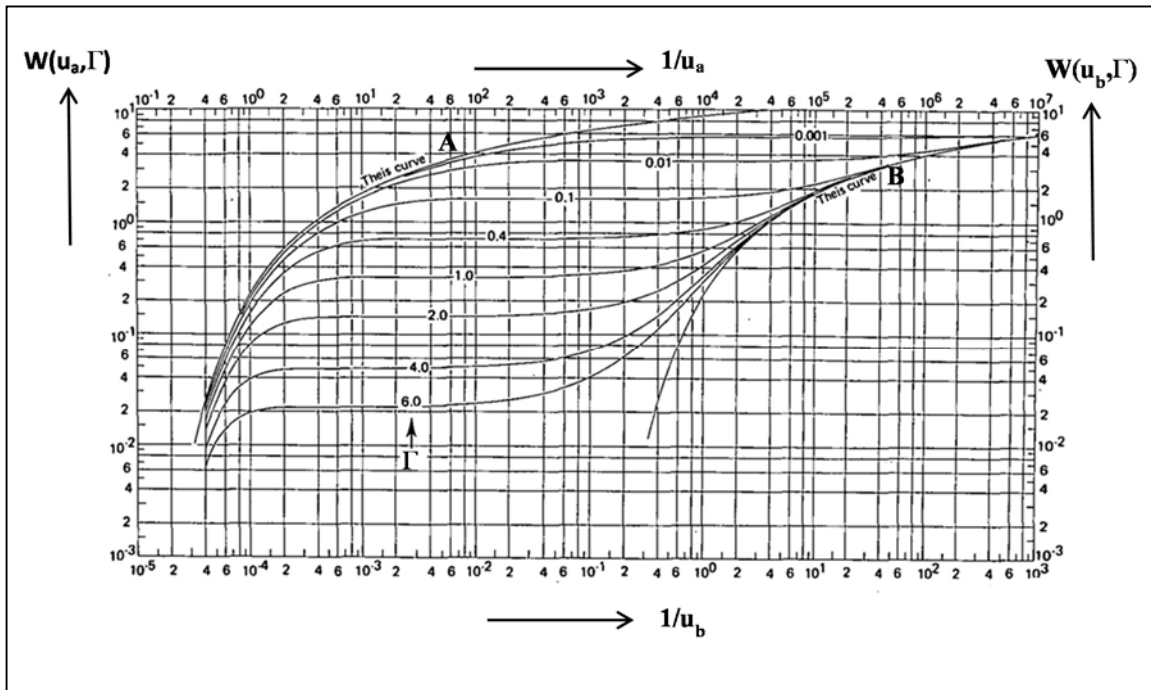


Figure 4.12: Theis Type A (early time) and B (later time) curves for drawdown data in an unconfined aquifer. Deviation from curves due to leakage is included with Γ (adopted from Fetter, 1994, Source Neuman, 1975).

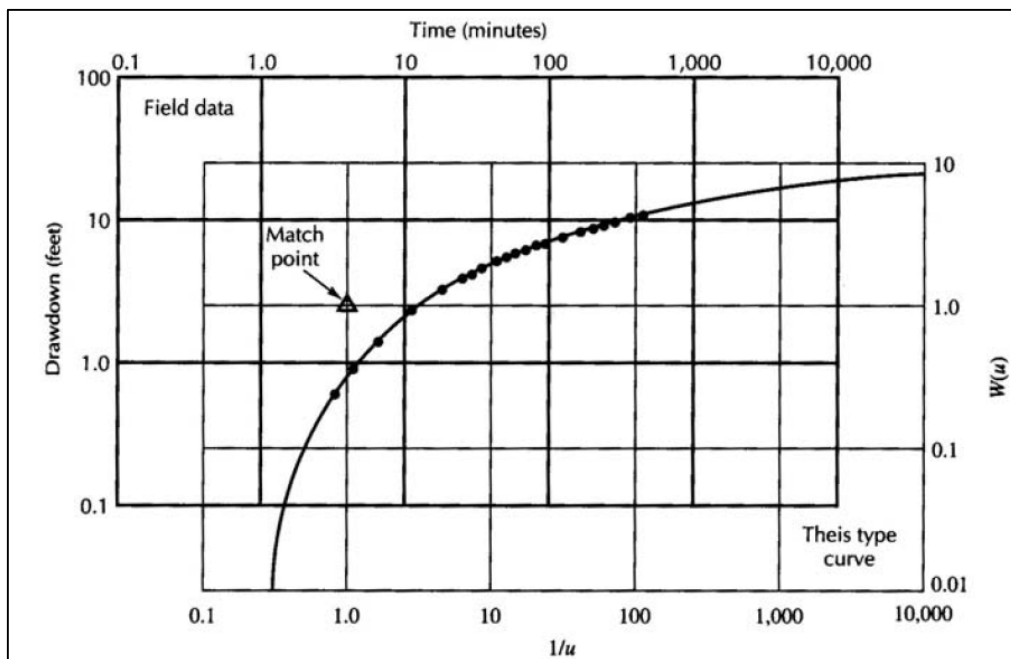


Figure 4.13: Schematic of lining data (black circles) along a Type Curve (black line) and picking a match point. (Adopted from Fetter C.W., Applied Hydrogeology, 3rd Edition © 1994, page 105, Reprinted by permission of Pearson Education, Inc., Upper Saddle River, NJ).

4.3 Specific Yield

Laboratory and field tests for specific yield, S_y , are expensive and time consuming. A large number of tests must be conducted to get an average for the study site. Undisturbed soil samples can be collected and carefully packaged in an air tight container to prevent drying or cracking in transport. In addition, the samples should not be subjected to vibration to maintain soil structure. In the lab, tension tables are used for soils with little swelling clay, while pressure cookers are used for samples containing swelling clay to prevent excessive cracking. Whether a tension table or pressure cooker, these devices should be able to maintain a constant tension from 0 to 160 cm of water. Field tests rely on mercury manometers placed at each significant change in soil texture. Most field offices are not equipped to measure S_y .

Alternatively, Figure 4.14 provides a recommended correlation method to estimate specific yield from the hydraulic conductivity (U.S. Department of the Interior, 1978). This correlation is derived from 2,000 laboratory tests on a wide variety of soil samples, and is within 10% of the best attainable value.

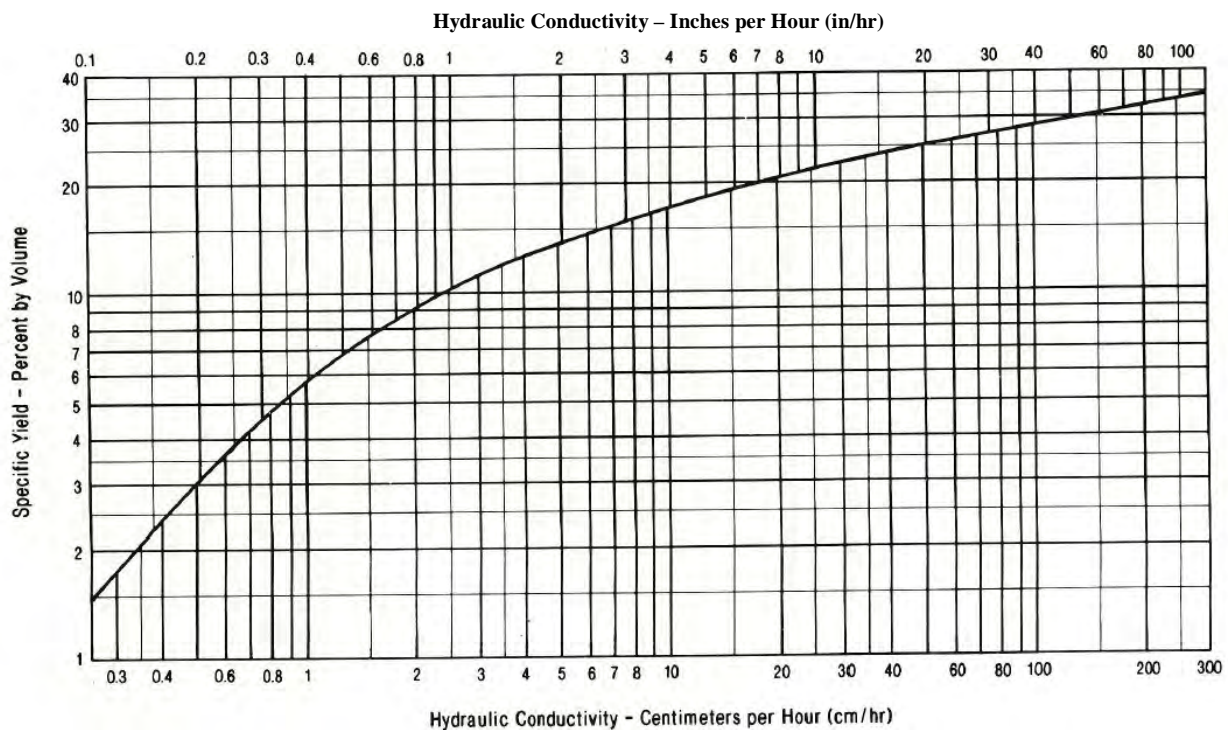


Figure 4.14: Curve showing general relationship between specific yield and hydraulic conductivity (adopted from the U.S. Department of the Interior, 1978)

4.4 Horizontal Drain Characteristics and Drain Flow

When horizontal drains are installed to reduce water levels, drain location, drain dimensions (length, diameter), drain elevations, angle of drilling, construction details should be noted. Water level data in observation wells should be collected prior to drain installation and after, along with drain flow from individual drain clusters.

An example of mapped drains is provided in Figure 4.15 for site SR101 MP321. Knowledge of drain elevations is critical to properly assessing impact of drains on water levels in the system. Drilling logs should note the subsurface conditions encountered for correlation with the hydrogeologic model.

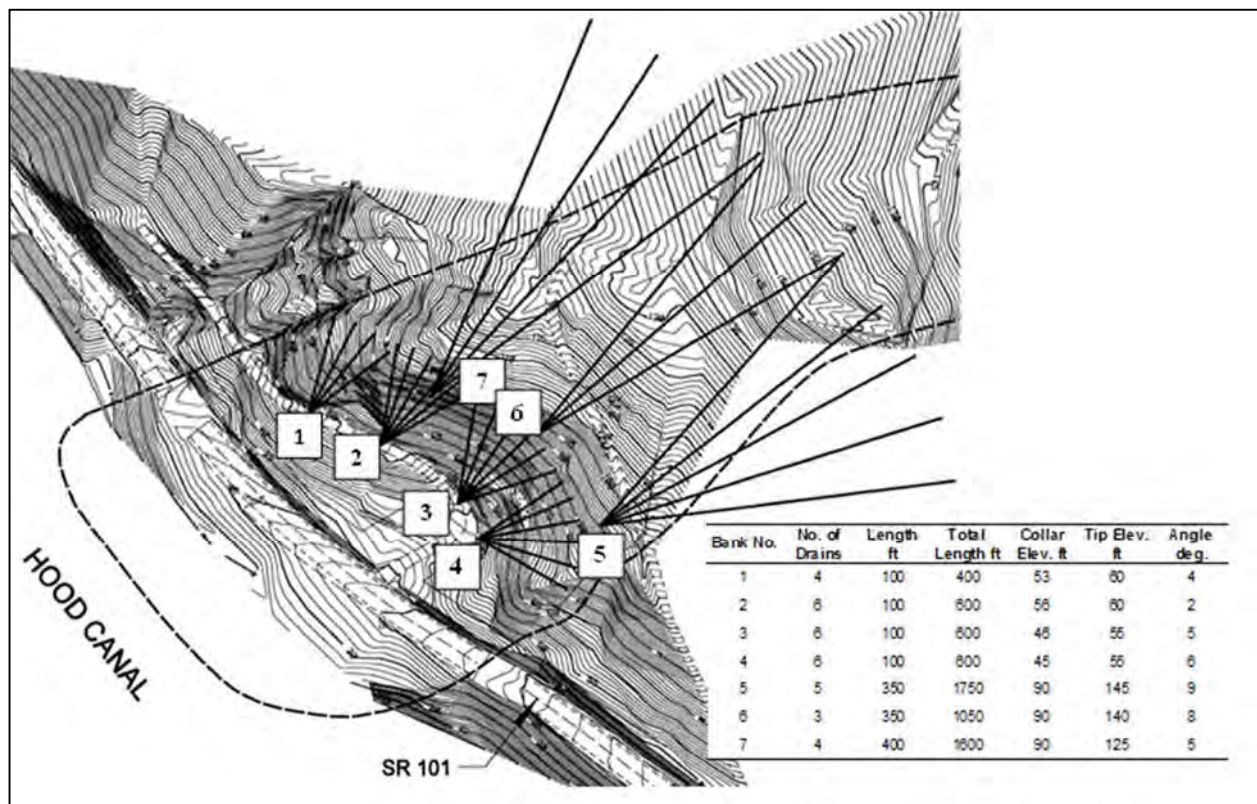


Figure 4.15: Horizontal drain placement for slide site SR101 MP321 with topographic contour lines at 1 ft intervals. Road is identified as is the Hood Canal. Drain lengths, collar and tip elevations and estimated angle for each drain bank, or cluster, provided (Lowell, 2001).

Various texts provide guidelines on drain installation (e.g., U.S. Department of the Interior, 1978; Forrester, 2001) with respect to grade and alignment issues, envelope materials, stability considerations and are not discussed here. However, understanding drain efficiency is very important to properly predicting water level response to drain placement. In groundwater studies, drain efficiency is defined via drain conductance ($C_d L^2/T$) and is discussed in Chapter 6. Drain conductance represents all head

losses between the aquifer and the drain, including convergent flow toward the drain (Figure 4.16), flow through the envelope material, and flow through the wall of the drain. The last is dependent on the degree that slots in the drain are blocked by chemical precipitates, plant roots or other obstructions. Each of these processes can be assumed proportional to drain discharge and added in series. However, in practice this is very difficult to quantify. Head loss across the envelope and drain can be approximated by assuming the hydraulic conductivity of the envelope materials represent the drain as a whole and are the major cause of head loss in the system,

$$C_d = K_d A / B' \quad (4.24)$$

Where A is the surface area (L^2) of the drain, B' is the thickness of the drain material (L) and K_d is the hydraulic conductivity of the drain and its envelope material (L/T). Diameter of the drain and thickness of the envelope material surrounding the drain are needed for the calculation. The hydraulic conductivity of the drain, K_d is dominated by the permeability of the envelope material.

Envelope material surrounding the drain provides a permeable path for water to move from the base material to the drain. Base material refers to the geologic unit being drained. The U.S. Bureau of Reclamation (BOR) (1993) provides design considerations for envelope material with respect to base material in Table 4.5, but is limited to low-head conditions in agricultural settings for which design is based. However, knowledge of envelope grain-size distribution can aid in a quick calculation of K_d using equation 4.1. In addition, constant-head permeameters using envelope material can offer guidance on the value of K_d . As a general guideline, hydraulic conductivity of the envelope material that is ten-times the base material will adequately move water from the aquifer into the drain system (BOR, 1993).

Using equation 4.24 to calculate C_d is only an estimate and likely underestimates head loss, since it fails to acknowledge convergent flow toward the drain, which forces progressively steeper head gradients in the vicinity of the drain. In practice, the way to capture all three components impacting head loss is to measure values of drain flow versus head in the drain and head in the surrounding aquifer. But if the change in head is not accurately known, then C_d is most often adjusted to match drain flow (equation 6.4), with K_d estimates from equation 4.24 used as an upper guide of drain conductance

Flow meters should be set at drain outlets, with manual spot-checks done to verify flow meter output. Long-term data collection will allow assessment of efficiency response to large rain events, and ascertain if efficiency is declining over time (i.e. clogging).

Table 4.5: Relationships between base materials and envelope materials for low head conditions (BOR, 1993)

Base Material 40% retained Particle Diameter (mm)	Envelope Material Size Limits - Particle Diameter (mm)									
	Lower Limit - % Retained						Upper Limit - % Retained			
	0	40	70	90	95	100	0	40	70	100
0.02-0.05	9.52	2	0.81	0.33	0.3	0.074	38.1	10	8.7	2.5
0.05-0.10	9.52	3	1.07	0.38	0.3	0.074	38.1	12	10.4	3
0.10-0.25	9.52	4	1.3	0.4	0.3	0.074	38.1	15	13.1	3.8
0.25-1.0	9.52	5	1.45	0.42	0.3	0.074	38.1	20	17.3	5

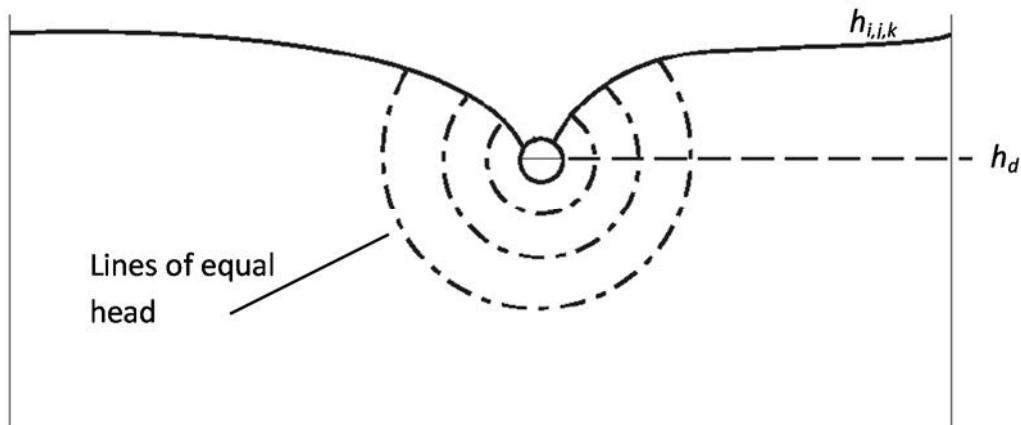


Figure 4.16: Cross section through cell i,j,k illustrating head loss in convergent flow to a drain (modified from McDonald and Harbaugh, 1988)

4.5 Fractured Rock Characterization

This section, with the exception of the displacement-length scaling relations, is a slightly altered version of Section 2: Fractured Rock Characterization in: Reeves et al. (2011).

Bedrock typically has little or no primary porosity and permeability, and networks of fractures serve as primary conduits for fluid flow. These networks are spatially discontinuous and highly irregular in geometry and hydraulic properties. Full characterization of fractured rock masses is not possible since known fracture locations and their attributes consist of an extremely small sample of the overall fracture network, i.e., any fracture characterization effort grossly undersamples a field site due to limited accessibility to the fractures themselves. Fractured rock masses are typically characterized during field campaigns that measure fracture attributes from a number of sources including boreholes, rock outcrops, road cuts, tunnel complexes, seismic images and hydraulic tests. This fracture data can then be used to generate representative, site-specific fracture networks through the derivation of probabilistic descriptions of fracture location, orientation, spacing, length, aperture, hydraulic conductivity/transmissivity and values of network density (Figure 4.17). This theoretical treatment of fracture networks is necessary to guide drainage network design for successful hillslope dewatering. Statistical analysis of the fracture attributes collected from field data is extensively covered in this section.

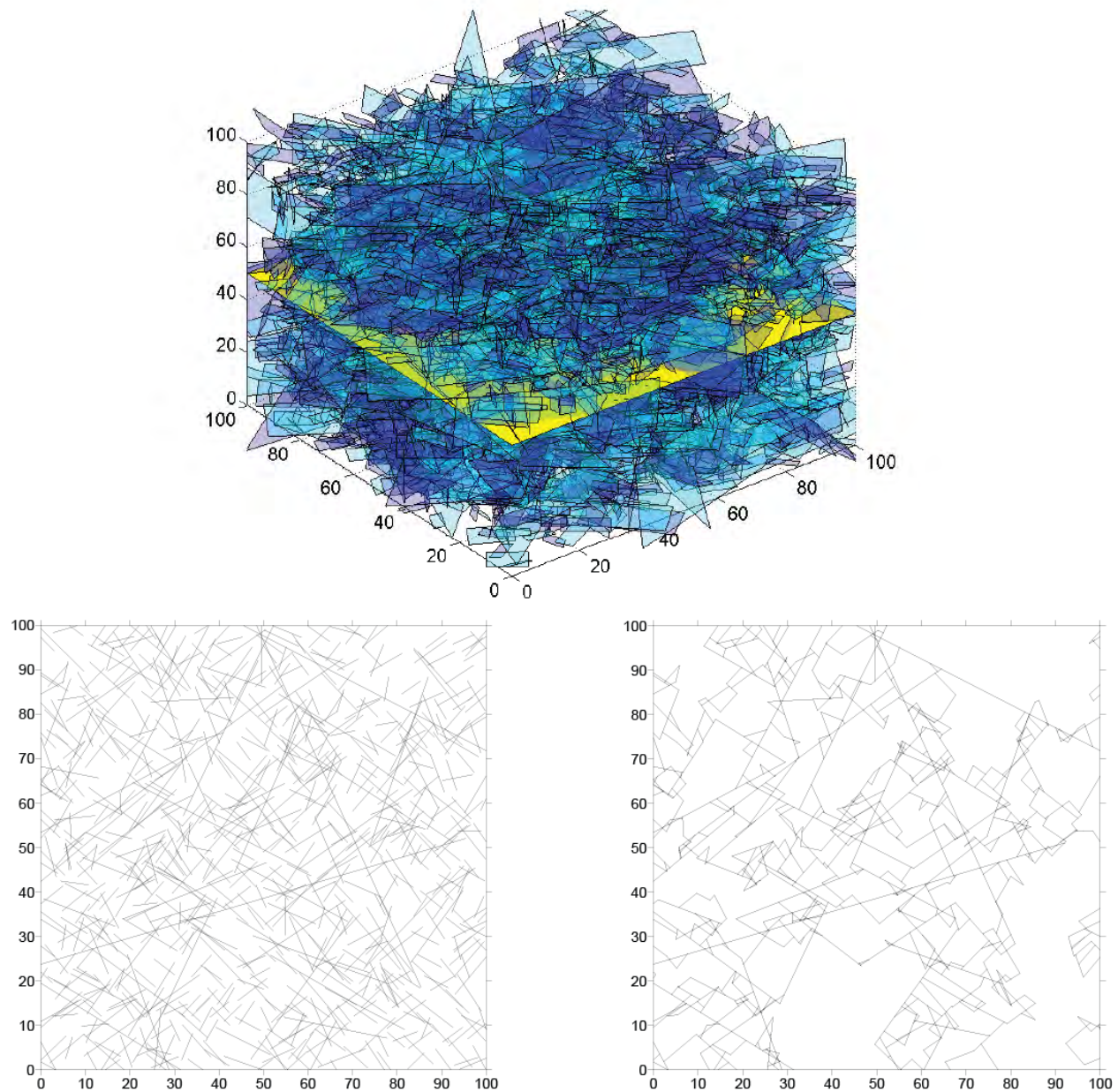


Figure 4.17: Illustration showing the correspondence between two- and three-dimensional fracture networks. The three-dimensional network (top) is generated according to two fracture sets with significant variability about mean fracture orientations, a power-law length distribution exponent of $a = 2$, and a relatively sparse density. The two-dimensional network at the bottom left is computed by projecting all fractures onto the yellow horizontal slice located in the center of the three-dimensional network. The two-dimensional network on the bottom right is the result of identifying the hydraulic backbone by eliminating all dead-end fracture segments and non-connected clusters. Once the hydraulic backbone is identified, flow can then be computed for the network. (Reprinted with permission from Reeves, D.M. et al., Radioactive Waste, 2012, InTech Publishing.)

Fracture networks commonly have two or more fracture sets characterized by similar fracture orientation (e.g., Barton, 1995; Bour, 1999; Bonnet et al., 2001; Pohlmann et al., 2004; Reeves et al., 2010). The presence of at least two intersecting sets of fractures reflects the physics of rock fracture propagation, where two sets of fractures can arise from a single, stationary stress field (Jaeger et al., 2007; Twiss and Moores, 2007). Unless fractures are very long, such as regional-scale faults, it is important from a groundwater flow perspective to have at least two intersecting fracture sets to promote connectivity through a rock mass.

The orientation of fracture planes is generally denoted by either strike and dip or dip and dip direction conventions. Analysis of fracture orientation begins with projecting the poles of measured fracture planes onto a stereonet plot and using contours of pole density to identify fracture sets (Figure 4.18). Upon identification of fracture sets, mean orientation and the variability of fracture poles for each fracture set can be determined.

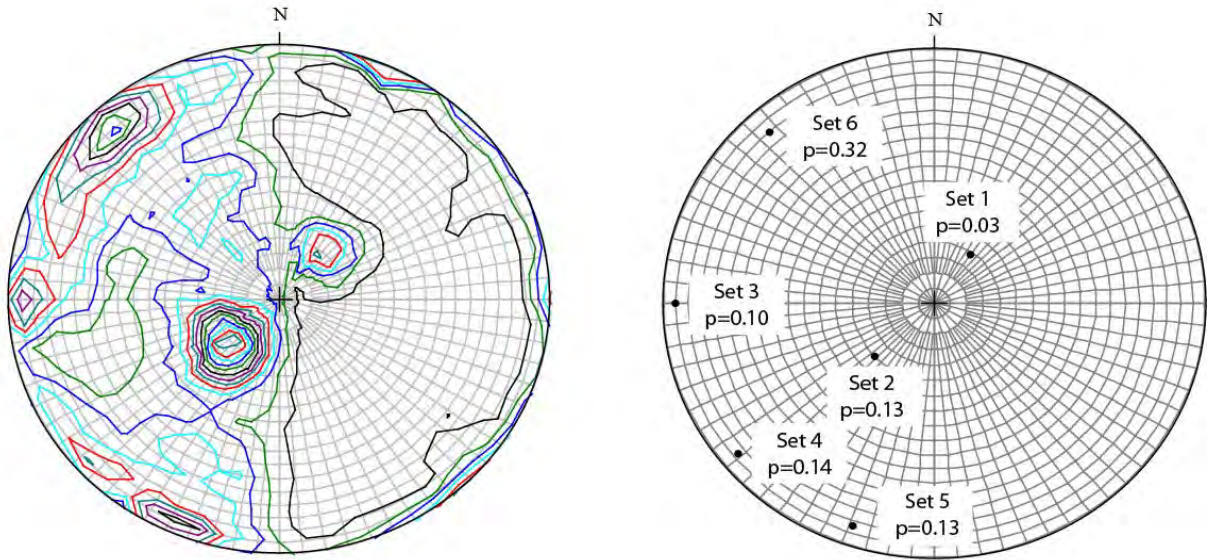


Figure 4.18: Stereonet plots of poles to fracture planes with contour plots of all poles (left) and identified fracture sets along with prior probability (right). (Reprinted with permission from Reeves, D.M. et al., *Radioactive Waste*, 2012, InTech Publishing.)

The distribution of fracture orientation is usually modeled using a Fisher distribution (Fisher, 1953):

$$f(x) = \frac{K \cdot \sin x \cdot e^{K \cos x}}{e^K - e^{-K}} \quad (4.25)$$

where the divergence, x (degrees), from a mean orientation vector is symmetrically distributed

$\left(-\frac{\pi}{2} \leq x \leq \frac{\pi}{2}\right)$ according to a constant dispersion coefficient, K . The Fisher distribution is a special case of the Von Mises distribution, and is similar to a normal distribution for spherical data (Mardia and Jupp, 2000). The extent to which individual fractures cluster around the mean orientation is described by K where higher values of K describe higher degrees of clustering. It is our experience that values of K are commonly in the range of $10 \leq K \leq 50$ for natural fracture networks. Stochastic simulation of Fisher random deviates in the discrete fracture networks in the Chapter 8 on Fractured Media Flow is based on the method proposed by Wood (1994).

The Bingham distribution provides an alternative to the Fisher distribution for cases in which fracture strike and dip are asymmetrically clustered around mean fracture orientations (Bingham, 1964):

$$f(x) = \frac{\exp\left[K_1(M_1x)^2 + K_2(M_2x)^2 + K_3(M_3x)^2\right]}{4 \cdot F(1/2, 3/2; E)} \quad (4.26)$$

where K_1 , K_2 , and K_3 are dispersion coefficients that satisfy the condition: $K_1 \leq K_2 \leq K_3 = 0$; M_1 , M_2 , and M_3 are the column vectors of matrix \mathbf{M} , \mathbf{E} is the eigenvector matrix, and $F(1/2, 3/2; \mathbf{E})$ is a hypergeometric function of the matrix argument. The probability distribution function described by (4.26) can occur for faults that exhibit a greater range in deviations in strike than dip. A shortcoming of the Bingham distribution, however, is that it is not mathematically possible to use (4.26) for the stochastic generation of asymmetric deviates.

4.5.1 Spacing

Fracture spacing refers to the linear distance between fractures. This distance also provides a length scale for unfractured matrix blocks. Fracture spacings from a data set require a correction (Terzaghi, 1965):

$$D = D' \sin(\theta) \quad (4.27)$$

to convert the apparent spacing D' measured along a transect to true fracture spacing D . Values of θ denote the angle of the transect relative to the mean fracture orientation or a pre-determined reference direction (Figure 4.19). Apparent spacing is equal to true spacing, if the transect is perpendicular to the mean fracture orientation or reference direction. If $\theta = 90^\circ$, the Terzaghi correction factor $f = \sin(\theta)$ reduces to 1.

Once the spacing between fractures is corrected, values of fracture frequency and average fracture spacing can be computed. Fracture frequency [units of inverse length, L^{-1}] is defined as the total number of fractures along the distance of a transect. Average fracture spacing [units of length, L] is simply the inverse of fracture frequency, and defines the size of the unfractured matrix block.

Spacing in natural fracture networks is most commonly an exponentially distributed, random variable. This can be tested by plotting the inverse empirical cumulative distribution function of fracture spacing,

also known as a survival function (Ross, 1985). If spacing is exponential, the probability decay of the tail of the empirical fracture spacing distribution will exhibit a straight line on a semi-log plot (Figure 4.20). A Poisson-point process, defined by independent and identically distributed uniform deviates, provides easy generation of exponential spacing (Ross, 1985).

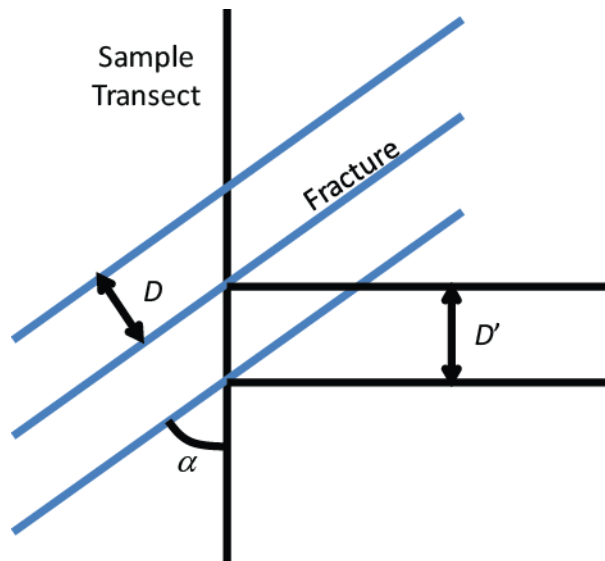


Figure 4.19: Illustration showing how the Terzaghi correction accounts for the bias between apparent spacing D' and true spacing D based on the orientation of the sample transect in relation to mean fracture orientation. After http://www.rocscience.com/downloads/dips/WebHelp/dips/Terzaghi_Weighting.htm. (Reprinted with permission from Reeves, D.M. et al., Radioactive Waste, 2012, InTech Publishing.)

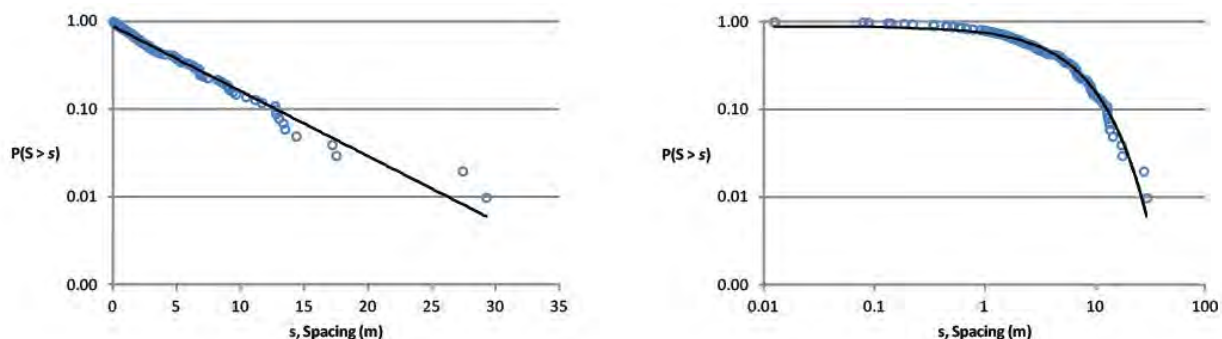


Figure 4.20: Survival plots of 100 synthetic fracture spacings generated according to a Poisson-point process along a 500 m transect. Exponential trends are linear on a semi-log plot (left) and steeply decay in log-log plots (right). Note that this transect has a 0.5 m^{-1} fracture frequency, which corresponds to an average spacing of 5 m.

Other possible distributions of fracture spacing include uniform (Rivers et al., 1992) and fractal clustering (Barton, 1995; Darcel et al., 2003), both of which are considered extreme end members. Uniform spacing may occur in thin geologic layers, which restrict fracture growth in the vertical direction and promote long horizontal fracture growth with nearly constant spacing (Rives et al., 1992). Exact causes of fractal clustering are less known and may be related to the role of mechanical fracture interaction during propagation, which likely controls fracture length and spacing (Segall and Pollard, 1983; Olson, 1993; Ackermann and Schische, 1997; Darcel et al., 2003). Networks with fractal clustering can be generated via a multiplicative cascade process (Mandelbrot, 1974; Schertzer and Lovejoy, 1987).

4.5.2 Length

Fracture length denotes the trace length of a fracture. There is a consensus in recent literature that fracture lengths above a lower length cutoff, l_{min} , are power-law:

$$P(L > l) = Cl^{-\alpha} \quad (4.28)$$

with a power law exponent, α , that ranges between 1 and 3 in natural fracture networks

(Bonnet et al., 2001; Bour and Davy, 1997, 1999; Renshaw, 1999). C is a constant based on l_{min} and α . Though log-normal distributions of fracture length have been reported in the literature, they are a result of improper sampling of the largest fractures within a sampling window. Log-normal distributions easily arise in data sets with power-law tails, if the largest values are censored (e.g., Figure 4.21).

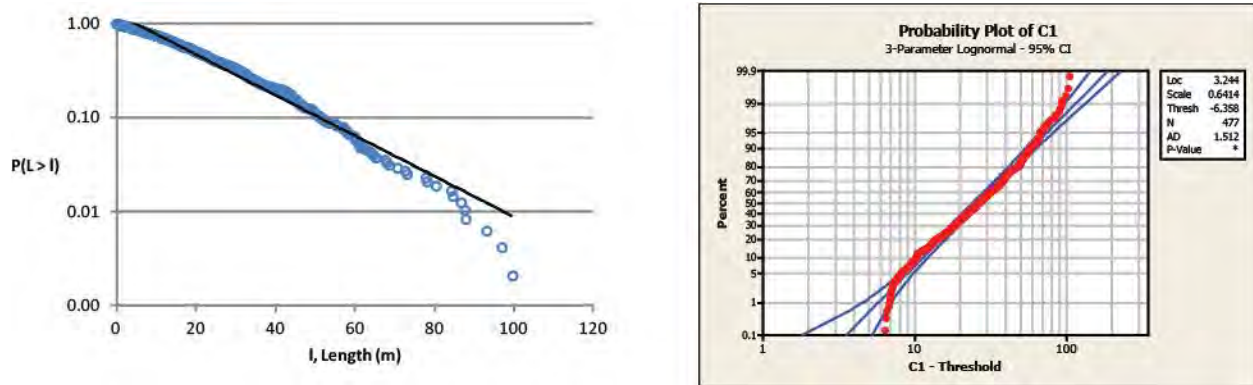


Figure 4.21: Censored data from Figure 4.20 intended to simulate an outcrop exposure where the longest fracture is constrained by the size of the sampling window (100 m). Note that the censoring of the 23 fracture lengths greater than 100 m causes the power-law trend observed in Figure 4.20 to become an exponential (left). A probability plot indicates that the censored data fits a log-normal distribution (right).

Determination of the distribution of fracture length is similar to that of fracture spacing and involves the analysis of an inverse empirical cumulative distribution function. Fracture lengths that are power-law

will exhibit linear trends on a log-log plot for the tail of the distribution (Figure 4.22). In this example, the tail of the distribution refers to the greatest 5-10% of length values. The slope of the power-law trend of the data is equal to $-\alpha$.

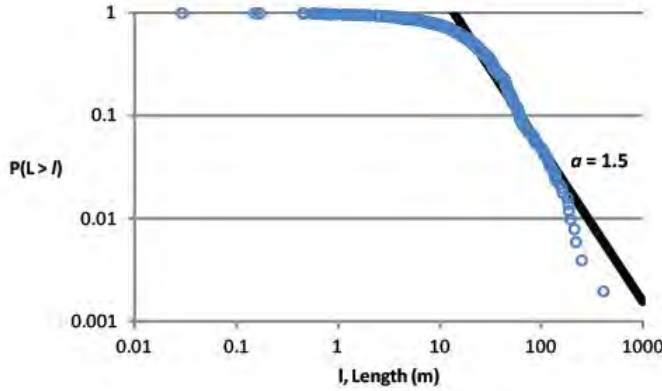


Figure 4.22: Survival plot of 500 synthetic fracture lengths generated according to an alpha-stable, heavy-tailed distribution with $\alpha = 1.5$. Best-fit line (black) depicts trend of power-law decay for largest fracture lengths. Deviations from the trend line for the largest 5-8 values are attributed to numerical oscillations. Power-law distributions exhibit linear trends in log-log plots. Random deviates generated using the program STABLE written by J.P. Nolan, are available at <http://www.academic2.american.edu/~jpnolan>.

Truncations can frequently occur in fracture length data, due to constraints imposed by the finite scale of the sampling window. For example in Reeves et al. (2010), the longest fracture measured in a tunnel drift was parallel to the drift and was approximately two-thirds of the total drift length. Instead of choosing between a traditional power-law or log-normal distribution, an upper truncated Pareto (power law) model (Aban et al., 2006):

$$P(L > l) = \frac{\Gamma^a \left(\Gamma^{-a} - l^{-a} \right)}{1 - \left(\frac{\Gamma}{l} \right)^a} \quad (4.29)$$

was used to compute the power-law trend in the data, where $L_{(1)}, L_{(2)}, \dots, L_{(n)}$ are fracture lengths in descending order, and $L_{(1)}$ and $L_{(n)}$ represent the largest and smallest fracture lengths, Γ and l are lower and upper fracture length cutoff values, and a describes the tail of the distribution. Truncated power-law models like (4.29) can also be useful for imposing an upper length scale to the generation of stochastic networks at the regional scale. Lacking evidence of domain-spanning faults (with the

exception of bounding faults of the stock itself) for a 5 km wide granitic stock, Reeves et al. (2010) assigned an upper limit of 1 km in the stochastic generation of fault networks.

4.5.3 Displacement-Length Scaling Relations

There are many situations where fracture characterization efforts produce little or no data on fracture lengths. This is unfortunate as fracture length is a critical parameter that controls connectivity of fractures within a network (e.g., de Dreuzy, 2001; Reeves et al. 2008b; Klimczak et al., 2010). This typically occurs when data on fracture length is limited to only very small outcrops or road cuts, or fracture data is exclusively collected from boreholes. In these situations, displacement-length scaling relations allow for estimation of fracture dimensions based on displacement (Scholz, 1997; Olson, 2003; Schultz et al., 2006, 2008; Klimczak et al., 2010; Schultz et al, in review). Displacement-scaling relations are based on the mechanics of rock fracture propagation, and their formulation is unique to fracture displacement mode, i.e., shear-mode fractures (e.g., faults) exhibit different displacement-scaling relations than opening-mode fractures (e.g., joints).

Displacement-scaling relations for faults can be described by (Scholz, 1997, Schultz et al., 2006, 2008):

$$\frac{D_{\max}}{L} = \frac{2(1-\nu^2)}{E} N(\sigma_d - C_y) \quad \text{change } C \text{ to } C^* \quad (4.30)$$

where D_{\max} is the maximum shearing displacement located at the fault midpoint, L is the horizontal fault trace length, σ_d is the shear driving stress, C_y is the yield strength of the rock at the fault tip, E and ν are Young's modulus and Poisson's ratio of the rock mass, respectively, N is the ratio of geologic offset to short-term slip, and C^* is a variable that relates to how the stress singularity at the fault tip is removed [e.g., Schultz et al. (1996)]. These parameters can be either measured in the field or inferred from literature values. However, direct field measurement of fault lengths and displacement reduces (4.30) to the form:

$$D_{\max} = \Gamma L \quad (4.31)$$

where $\Gamma = \frac{2(1-\nu^2)}{E} N(\sigma_d - C_y)$. Compilation of displacement-length scaling for a variety of fault types

across a broad scale consisting of 9 orders of magnitude in length show that values of Γ are in a surprisingly narrow range of $0.001 \leq \Gamma \leq 0.1$, with a central tendency of 0.01 (Figure 4.23). This implies that, on average, horizontal fault trace length can be related to maximum displacement according to $D_{\max} = 0.01L$. On a final note, the dimensions of faults tend to be asymmetric with regards to length and height. A review paper on this subject by Nicol et al. (1996) suggests that normal fault length is typically 2.2 times greater than height.

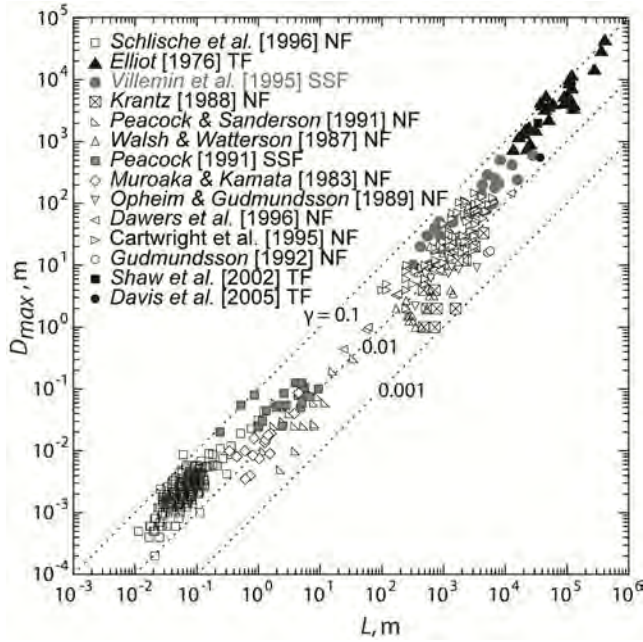


Figure 4.23: Compilation of displacement-length scaling of faults from Schultz et al. (2008). Normal faults (NF) open symbols; strike-slip faults (SSF), gray symbols; thrust faults (TF), filled symbols. Lines of constant slope (dotted) are shown for different values of Γ . (Reprinted from Journal of Structural Geology, 30, Schultz, R.A., R. Soliva, H. Fossen, C. Okubo, and D.M. Reeves, Dependence of Displacement-Length Scaling Relations for Fractures and Deformation Bands on the Volumetric Changes Across Them, pp 1405-1411, 2008, with Permission from Elsevier.)

Displacement-length scaling relationships for joints can be described by (Olson, 1993; Schultz et al., 2008; Klimczak et al, 2010):

$$D_{\max} = \frac{K_c (1 - \nu^2)^{1/2} \sqrt{8}}{E} \sqrt{L} \quad (4.32)$$

where D_{\max} is maximum distance (or width of void opening) between fracture walls located at the midpoint of a joint (also referred to as aperture), K_c is fracture toughness which describes the critical stress intensity at which a fracture propagates in an elastic medium, and E and ν are Young's modulus and Poisson's ratio of the rock mass, respectively. Similar to (4.30) for faults, parameters in (4.32) can be measured in the field or inferred from literature values. Direct field measurement of joint lengths and displacement (aperture) reduces (4.32) to:

$$D_{\max} = L^{0.5} \quad (4.33)$$

where $\Gamma = \frac{K_c (1 - \nu^2)^{1/2} \sqrt{8}}{E}$. Unlike fault data, compilation of displacement-length scaling for a variety of opening-mode (tensile) fractures across a broad scale consisting of 7 orders of magnitude in length show that values of Γ are within a relatively wide range of $0.0001 \leq \Gamma \leq 1.0$ (Klimczak et al., 2010). However, restricting the analysis to data sets for joints and veins in Klimczak et al. (2010) yields a more realistic range of $0.01 \leq \Gamma \leq 0.0001$. A central tendency is not present within this range. Displacement-length scaling relations assume that joints are 'penny-shaped' and have symmetric length to height ratios.

4.5.4 Hydraulic Conductivity

Boreholes are commonly used to characterize fractured rock masses. Borehole geophysics can provide useful information about fractures within the rock, including fracture frequency, orientation, aperture and presence of mineral infilling. Fracture aperture, defined as the width of the void space normal to fracture walls, can be used to infer hydraulic properties of fractures. Fracture apertures at land surface have low confining stresses that are not representative of subsurface confining stresses within a rock mass. We therefore recommend that fracture aperture values used to compute flow are measured in boreholes where in-situ stress is preserved.

The cubic law, a solution to the Navier-Stokes equation for laminar, incompressible flow between two parallel plates, describes a general relationship between fluid flow and fracture aperture (Snow, 1965):

$$Q = \frac{g}{12} b^3 \nabla h \quad (4.34)$$

where fluid discharge per unit width, Q [L^2/t], is proportional to the cube of the hydraulic aperture, b . Similar to Darcy's Law, the cubic law (10) assigns discharge through a fracture as a linear function of the hydraulic gradient, ∇h . The relationship between hydraulic aperture and transmissivity (T), hydraulic conductivity (K) and permeability (k) is described by: $T = \frac{g}{12} b^3$, $K = \frac{g}{12} b^2$, and $k = b^2$, respectively.

Fluid-specific properties density, ρ , and viscosity, μ , allow for conversions between permeability and hydraulic conductivity/transmissivity. As a note of caution, the relationship between mechanical aperture, the physical distance between fracture walls, and hydraulic aperture, the equivalent aperture for a given flow rate, is unclear. As a general rule, hydraulic aperture is typically smaller than mechanical aperture (Cook et al., 1990; Renshaw, 1995; Zimmerman and Bodvarsson, 1996; Chen et al., 2000). Discrepancies between mechanical aperture and hydraulic aperture are attributed to surface roughness, flow-path tortuosity, and stress normal to the fracture. Though empirical correction factors have been used to correlate mechanical and fracture apertures (Bandis et al., 1985; Cook et al., 1990; Renshaw, 1995), no method is reliable for a wide range of aperture values.

Hydraulic testing of boreholes yields reliable estimates of fracture T and K . While there are many different hydraulic testing techniques, the isolation of specific intervals during testing with the use of dual-packer systems provides the best data to characterize the distribution of hydraulic conductivity/transmissivity. These tests yield flow rate information for applied fluid pressures, which also allows for the inverse computation of hydraulic aperture using (4.34). These aperture values, in addition to T and K estimates, are useful for parameterizing flow models.

Studies in well characterized rock masses have shown that fracture K is extremely heterogeneous and may encompass 5 to 8 orders of magnitude (Paillet, 1998; Guimera and Carrera, 2000; Andersson et al., 2002a,b). Often the distribution of K (and T) is considered log-normal:

$$p(x) = \frac{1}{x\sqrt{2\sigma^2}} \exp\left[-\frac{(\log x - \mu)^2}{2\sigma^2}\right] \quad (4.35)$$

where x is the mean and σ is the standard deviation. Values of $\log(\sigma)$ are typically around 1 for fractured media (Stigsson et al., 2001; Andersson et al., 2002a,b). However, other studies suggest power-law distributions (Gustafson and Fransson, 2005; Kozubowski et al., 2008), and that these log-normal distributions, similar to length, could be caused by censoring flow data, possibly due to instrument limitations. Additionally, flow through rough-walled fractures can be non-Darcian (Cardenas et al., 2007; Qian et al., 2011; Quinn et al., 2011). This may further complicate the estimation of hydraulic conductivity in field hydraulic tests, as flow is no longer linearly proportional to a pressure gradient as described by (4.34).

4.5.5 Density

Fracture networks consist of two-dimensional planes embedded within a rock matrix (Figure 4.17). The lack of access to the total rock volume makes it impossible to directly measure the three-dimensional fracture density of a rock mass. Instead, three-dimensional density for discrete fracture networks is estimated from density measurements of lower dimensions, i.e., one-dimensional fracture frequency from boreholes and/or tunnel drifts or two-dimensional fracture density from outcrops and fracture trace maps. Definitions of fracture density according to dimension are: one-dimensional density (also known as fracture frequency), ρ_{1D} [L^{-1}], is expressed as the ratio of total number of fractures, f_i , to

transect length, L : $\rho_{1D} = \sum_{i=1}^n f_i / L$; two-dimensional fracture density, ρ_{2D} [L/L^2], is expressed as the ratio of

the sum of fracture lengths, l , to area, A : $\rho_{2D} = \sum_{i=1}^n l_i / A$; and three-dimensional fracture density, ρ_{3D}

[L^2/L^3], is expressed as the ratio of the sum of fracture plane area, A_i , to rock volume, V : $\rho_{3D} = \sum_{i=1}^n A_i / V$.

Numerical techniques can be used to upscale one-dimensional fracture frequency [L^{-1}] estimates to a three-dimensional spatial density [L^2/L^3] (Holmén and Outters, 2002; Munier, 2004). For example, one-dimensional transects can be used to upscale two-dimensional networks by adding fractures until the one-dimensional transect density is satisfied along several transects placed along the two-dimensional network. Three-dimensional networks can be generated in a similar fashion by either generating fractures until the frequency along one-dimensional boreholes is satisfied or by projecting fractures onto sampling planes (e.g., Figure 4.17) until a two-dimensional density criterion is satisfied.

Fracture density is highly dependent on the distribution of fracture lengths in a model domain, where the density at the percolation threshold increases with increasing values of α (Renshaw, 1999; Darcel et al., 2003; Reeves et al., 2008b; Klimczak et al., 2010). This will become apparent in the fracture network examples shown in Chapter 8 on flow in fractured rock.

4.6 Geotechnical Characterization

The purpose of this manual is for geotechnical specialists and only generalized information is provided for completeness. One is referred to Mayne et al. (2002) and Sabatini et al. (2002) for detailed descriptions pertaining to geotechnical site characterization.

Geological information for slope characterization can be obtained from different sources. Widely used sources of geological information are listed Table 4.6.

Geotechnical parameters of the subsurface layers can be obtained either by laboratory testing or by in-situ testing. Laboratory testing is conducted on soils sample from a location. Soil sampling are divided into two categories; disturbed and undisturbed sampling. If soil experiences large structural disturbance during sampling then it is termed disturbed sample. If soil experiences absolute minimum structural disturbance, then it is termed undisturbed sample.

The popular disturbed sampling method is the split barrel sampler. There are some other methods also available those are Retractable Plug method; Auger method (Continuous Helical Flight, Disc, Bucket and Hollow Stem) and Diamond Core Barrels (single tube, double tube and triple tube). Sampling method can be used to explore undisturbed samples are Shelby Tube; Stationary Piston; Hydraulic Piston (Osterberg); Denison; and Pitcher Sampler and Hand cut block or cylindrical sample. Suitable sampler can be obtained to get disturbed and undisturbed samples by using Tables 4.7 and 4.8 respectively.

There are several types of test boring can be used. Those are Auger boring; Hollow-stem flight auger; Wash-type boring for undisturbed or dry sample; rotary drilling; Percussion drilling (Churn drilling); rock core drilling and wire-line drilling. Suitable test boring type can be selected by using Table 4.9.

Requirements for Boring Layout vary with investigation area. Suitable boring layout can be selected by using Table 4.10.

4.6.1 In-Situ Testing

Soil properties can also be found from in-situ testing. Over the years, several in-situ testing devices have emerged to characterize soil and to measure strength and deformation properties. The most popular devices are Standard penetration test (SPT) Vane shear test (VST) Cone Penetration Test (CPT) Pressuremeter test (PMT) and Flat plate dilatometer test (DMT). Any of these in-situ methods can be used for site investigation. Most in-situ device data rely on empirical or semi-theoretical correlations.

For example if we use standard penetration test, the corrected penetration resistance can be correlated to soil strength properties as shown in Tables 4.11 and 4.12.

Table 4.6: Sources of geological information NAVFAC (1982).

Publications	Description of Material
U.S. Geological Survey (USGS)	Consult USGS Index of Publications from Superintendent of Documents, Washington, D.C. Order publications from Superintendent of Documents. Order maps from USGS, Washington, D.C. Contact regional distribution offices for information.
Geological index map	Individuals maps of each state showing coverage and sources of all published geological maps.
Folios of the Geological Atlas of the United States	Contains maps of bedrock and surface materials for many important urban and seacoast areas. When out of print, obtain folios through suppliers of used technical literature.
Geological Quadrangle Maps of United States	This series supplants the older geological folios including areal or bedrock geology maps with brief descriptive text. Series is being extended to cover areas not previously investigated.
Bulletins, professional papers, circulars, annual reports, monographs	General physical geology emphasizing all aspects of earth sciences, including mineral and petroleum resources, hydrology and seismicity. Areal and bedrock geology maps for specific locations included in many publications.

Table 4.6 continued:

Publications	Description of Material
Water supply papers	Series includes papers on groundwater resources in specific localities and are generally accompanied by description of subsurface conditions affecting groundwater plus observations of groundwater levels.
Topographic maps	Topographic contour maps in all states, widespread coverage being continually expanded.
Libraries	Regional office libraries contain geological and seismological information from many sources. Data on foreign countries are often suitable.
State Geological Surveys/State Geologist's Office	Most states provide excellent detailed local geological maps and reports covering specific areas or features in the publications of the state geologists. Some offices are excellent sources of information on foreign countries.
U.S. Department of Agriculture (USDA), Soil Conservation Service	Consult "List of Published Soil Surveys," USDA, Soil Conservation Service, January 1980 (published annually). Listing by states and countries.
Soil maps and reports	Surveys of surface soils described in agricultural terms. Physical geology summarized. Excellent for highway or airfield investigations. Coverage mainly in midwest, east, and southern United States.
National Oceanic and Atmospheric Administration (NOAA), National Ocean Survey (NOS)	Consult Catalog 1, Atlantic and Gulf Coasts; 2, Pacific Coast; 3, Alaska; 4, Great Lakes; and 5, Bathymetric Maps and Special Charts. Order from Distribution Service, National Ocean Survey, Riverdale, Maryland 20840.
Nautical Charts	Charts of coastal and inland waterways showing available soundings of bottom plus topographic and cultural features adjacent to the coast or waterways.
Geological Society of America (GSA)	Write for index to GSA, P.O. Box 9140, 3300 Penrose Place, Boulder, Colorado 80302.
Monthly bulletins, special papers, and memoirs.	Texts cover specialized geological subjects and intensive investigations of local geology. Detailed geological maps are frequently included in the individual articles.
Geological maps	Publications include general geological maps of North and South America, maps of glacial deposits, and Pleistocene aeolian deposits.

Table 4.6 continued:

Publications	Description of Material
Association of Engineering Geologists (AEG)	Their journal covers topics in engineering geology, geological engineering and geotechnical engineering. Occasionally extensive articles concerning the engineering geology aspects of a city will be published.
Trautmann & Kulhawy (1983)	paper that summarizes many data sources: Data Sources for Engineering Geologic Studies, Bulletin of the Association of Engineering Geologists, Vol. XX, No. 4, 1983, pp. 439 – 454.
Library of Congress	Maintains extensive library of U.S. and foreign geologic reports by geographical area. Inquiry to Library of Congress, 10 First Street, Washington, D. C. 20540.
Worldwide National Earth-Science Agencies	For addresses consult “Worldwide Directory of National Earth-Science Agencies,” USGS Circular 716, 1975.
World Wide Web (WWW)	You can (almost) find just about everything, if you have time, patience!

Table 4.7: Common Samplers for Disturbed Soil Samples and Rock Cores

Sampler	Dimensions	Best Results in Soil or Rock Types	Methods of Penetration	Causes of Disturbance or Low Recovery	Remarks
Split Barrel	2: OD – 1.375" ID is standard. Penetrometer sizes up to 4" OD – 3.5" ID available.	All fine-grained soils in which sampler can be driven. Gravels invalidate drive data.	Hammer driven	Vibration	SPT is made using standard penetrometer with 140# hammer falling 30". Undisturbed samples often taken with liners. Some sample disturbance is likely.
Retractable Plug	1" OD tubes 6" long. Maximum of 6 tubes can be filled in single penetration.	For silts, clays, fine and loose sands.	Hammer driven	Improper soil types for sampler. Vibration.	Light weight, highly portable units can be hand carried to job. Sample disturbance is likely.
Augers: Continuous Helical Flight	3" to 16" dia. Can penetrate to depths in excess of 50 feet.	For most soils above water table. Will not penetrate hard soils or those containing cobbles or boulders.	Rotation	Hard soils, cobbles, boulders.	Rapid method of determining soil profile. Bag samples can be obtained. Log and sample depths must account for lag between penetration of bit and arrival of sample at surface.
Disc	Up to 42" dia. Usually has maximum penetration of 25 feet.	Same as flight auger.	Rotation	Same as flight auger.	Rapid method of determining soil profile. Bag samples can be obtained.
Bucket	Up to 48" dia. common. Larger available. With extensions, depths greater than 80 feet are possible	For most soils above water table. Can dig harder soil than above types, and can penetrate soils with cobbles and small boulders when equipped with a rock bucket	Rotation	Soil too hard to dig	Several type buckets available including those with ripper teeth and chopping buckets. Progress is slow when extensions are used.

Table 4.7 continued:

Sampler	Dimensions	Best Results in Soil or Rock Types	Methods of Penetration	Causes of Disturbance or Low Recovery	Remarks
Augers: Hollow Stem	Generally 6" to 8" OD with 3" to 4" ID hollow stem.	Same as Bucket.	Same	Same	A special type of flight auger with hollow center through which undisturbed samples or SPT can be taken.
Diamond Core Barrels	Standard sizes 1-1/2" to 3" OD, 7/8" to 2-1/8" core. Barrel lengths 5 to 10 feet for exploration.	Hard rock. All barrels can be fitted with insert bits for coring soft rock or hard soils.			
Single Tube		Primarily for strong, sound and uniform rock		Fractured rock.	Drill fluid must circulate around core – rock must not be subject to erosion. Single tube not often used for exploration.
Double Tube		Non-uniform, fractured, friable and soft rock.		Rock too soft Improper rotation or feed rate in fractured or soft rock.	Has inner barrel or swivel which does not rotate with outer tube. For soft, erodible rock. Best with bottom discharge bit.
Triple Tube		Same as Double Tube.		Same as Double Tube.	Differs from Double Tube by having an additional inner split tube liner. Intensely fractured rock core best preserved in this barrel.

Table 4.8: Common Samplers for Undisturbed Samples

Sampler	Dimensions	Best Results in Soil Types	Methods of Penetration	Causes of Disturbance	Remarks
Shelby Tube	3" OD - 2.875" ID most common. Available from 2" to 5" OD. 30" sampler length is standard.	For cohesive fine-grained or soft soils. Gravelly soils will crimp the tube.	Pressing with fast, smooth stroke. Can be carefully hammered.	Erratic pressure applied during sampling, hammering, gravel particles, crimping tube edge, improper soil types for sampler.	Simplest sampler for undisturbed samples. Boring should be clean before lowering sampler. Little waste area in sampler. Not suitable for hard, dense or gravelly soils.
Stationary Piston	3" OD most common. Available from 2" to 5" OD. 30" sample length is standard.	For soft to medium clays and fine silts. Not for sandy soils.	Pressing with continuous, steady stroke.	Erratic pressure during sampling, allowing piston rod to move during press. Improper soil types for sampler.	Piston at end of sampler prevents entry of fluid and contaminating material. Requires heavy drill rig with hydraulic drill head. Generally less disturbed samples than Shelby. Not suitable for hard, dense or gravelly soil. No positive control of specific recovery ratio.
Hydraulic Piston (Osterberg)	3" OD most common – available from 2" to 4" OD, 36" sample length.	For silts-clays and some sandy soils.	Hydraulic or compressed air pressure.	Inadequate clamping of drill rods, erratic pressure.	Needs only standard drill rods. Requires adequate hydraulic or air capacity to activate sampler. Generally less disturbed samples than Shelby. Not suitable for hard, dense or gravelly soil. Not possible to limit length of push or amounts of sample penetration.

Table 4.8 Continued:

Sampler	Dimensions	Best Results in Soil Types	Methods of Penetration	Causes of Disturbance	Remarks
Denison	Samplers from 3.5" OD to 7-3/4" OD. (2.375" to 6.3" size samples). 24" sample length is standard.	Can be used for stiff to hard clay, silt and sands with some cementation, soft rock.	Rotation and hydraulic pressure.	Improperly operating sampler. Poor drilling procedures.	Inner tube face projects beyond outer tube which rotates. Amount of projection can be adjusted. Generally takes good samples. Not suitable for loose sands and soft clays.
Pitcher Sampler	Sampler 4.125" OD used 3" Shelby Tubes. 24" sample length.	Same as Denison.	Same as Denison.	Same as Denison.	Differs from Denison in that inner tube projection is spring controlled. Often ineffective in cohesionless soils.
Hand cut block or cylindrical sample	Sample cut by hand.	Highest quality undisturbed sampling in cohesive soils, cohesionless soil, residual soil, weathered rock, soft rock.		Change of state of stress by excavation.	Requires accessible excavation. Requires dewatering if sampling below groundwater.

Table 4.9: Types of Test Boring

Boring	Procedure Utilized	Applicability
Auger boring	Hand or power operated augering with periodic removal of material. In some cases continuous auger may be used requiring only one withdrawal. Changes indicated by examination of material removed. Casing generally not used.	Ordinarily used for shallow explorations above water Table in partly saturated sands and silts, and soft to stiff cohesive soils. May be used to clean out hole between drive samples. Very fast when power-driven. Large diameter bucket auger permits examination of hole. Hole collapses in soft soils and soils below groundwater Table.
Denison	Samplers from 3.5" OD to 7-3/4" OD. (2.375" to 6.3" size samples). 24" sample length is standard.	Can be used for stiff to hard clay, silt and sands with some cementation, soft rock.
Pitcher Sampler	Sampler 4.125" OD used 3" Shelby Tubes. 24" sample length.	Same as Denison.
Hand cut block or cylindrical sample	Sample cut by hand.	Highest quality undisturbed sampling in cohesive soils, cohesionless soil, residual soil, weathered rock, soft rock.
Hollow-stem flight auger	Power operated, hollow stem serves as a casing.	Access for sampling (disturbed or undisturbed) or coring through hollow stem. Should not be used with plug in granular soil. Not suitable for undisturbed sampling in sand and silt.
Wash-type boring for undisturbed or dry sample	Chopping, twisting, and jetting action of a light bit as circulating drilling fluid removes cuttings from holes. Changes indicated by rate of progress, action of rods, and examination of cuttings in drilling fluid. Casing used as required to prevent caving.	Used in sands, sand and gravel without boulders, and soft to hard cohesive soils. Most common method of subsoil exploration. Usually can be adapted for inaccessible locations, such as on water, in swamps, on slopes, or within buildings. Difficult to obtain undisturbed samples.

Table 4.9 Continued:

Boring	Procedure Utilized	Applicability
Percussion drilling (Churn	Power chopping with limited amount of water at bottom of hole. Water becomes slurry that is periodically removed with bailer or sand pump. Changes indicated by rate of progress,	Not preferred for ordinary exploration or where undisturbed determining strata changes, disturbance caused below chopping bit, difficulty of access, and usually higher cost. Sometimes used in combination with auger or wash borings for penetration of coarse gravel, boulders, and rock formations. Could be useful to probe cavities and weakness in rock by changes in drill rate.
Rock core drilling	Power rotation of a core barrel as circulating water removes ground-up materials from hole. Water also acts as coolant for core barrel bit. Generally hole is cased to rock.	Used alone and in combination with boring types to drill weathered rocks, bedrock, and boulder formations.
Wire-line drilling	Rotary type drilling method where the coring device is an integral part of the drill rod string which also serves as a casing. Core samples obtained by removing inner barrel assembly from the core barrel portion of the drill rod. The inner barrel is released by a retriever lowered by a wire-line through drilling rod.	Efficient for deep hole coring over 100 feet on land and offshore coring and sampling.

Table 4.10: Requirements for Boring Layout (NAVFAC, 1982)

Areas of Investigation	Boring Layout
Slope stability, deep cuts, high embankments.	Provide three to five borings on line in the critical direction to provide geological section for analysis. Number of geological sections depends on extent of stability problem. For an active slide, place at least one boring upslope of sliding area.

Table 4.11: Correlations and Approximations for Cohesive Soils.

Consistency	Very Soft	Soft	Medium	Stiff	Very Stiff	Hard
Compressive strength, q_u (kPa)	< 25	25 – 50	50 – 100	100 – 200	200 – 400	> 400
Compressive strength, q_u (tsf)	< 0.25	0.25 – 0.5	0.5 – 1.0	1.0 – 2.0	2.0 – 4.0	> 4.0
Corrected Standard Penetration Resistance, N_1	0 – 2	3 – 5	6 – 9	10 – 16	17 – 30	> 30
Approx. range of moist unit weight, g , (kN/m ³)	16 – 18	16 – 19	17 – 20	18 – 21	19 – 22	19 – 22
NOTE: The undrained strength is $\frac{1}{2}$ of the unconfined compressive strength						

Table 4.12: Correlations and Approximations for Granular Soils.

Description	Very Loose	Loose	Medium	Dense	Very Dense
Relative Density, D_r (%)	0 – 15	15 – 35	35 – 65	65 – 85	> 85
Corrected Standard Penetration Resistance, N_1	0 – 4	5 – 10	11 – 30	31 – 50	> 50
Approx. Angle of Internal Friction, f	25° – 30°	27° – 32°	30° – 35°	35° – 40°	38° – 43°
Approx. range of moist unit weight, g (kN/m ³)	11.0 – 16	14 – 18	17 – 20	18 – 22	20 – 24

4.7 References Cited

- Aban, I.B.; Meerschaert, M.M. and A.K. Panorska, 2006. Parameter estimation methods for the truncated Pareto distribution, *J. Amer. Stat. Assoc.*, Vol. 101, 270--277.
- Ackermann, R.V. and R.W. Schlische, 1997. Anticlustering of small normal faults around larger faults, *Geol.*, Vol. 25, No. 12, 1127--1130.
- Andersson, P.; Byegård, J.; Dershowitz, B.; Doe, T.; Hermanson, J.; Meier, P.; Tullborg, E.-L.; and A. Winberg, 2002a. Final Report on the TRUE Block Scale Project: 1. Characterization and Model Development, Swedish Nuclear Fuel and Waste Management Company SKB, Technical Report TR-02-13, Stockholm, Sweden.
- Andersson, P.; Byegård, J.; and A. Winberg, 2002b. Final Report on the TRUE Block Scale Project: 2. Tracer Tests in the Block Scale, Technical Report TR-02-14, Swedish Nuclear Fuel and Waste Management Co. SKB, Stockholm, Sweden.
- Bandis, S.C.; Makurat A. and G. Vik, 1985. Predicted and measured hydraulic conductivity of rock joints, *Proceedings of the International Symposium on Fundamentals of Rock Joints*, Björckliden, Norway, September 15-20.
- Barton, C.C. 1995. Fractal analysis of scaling and spatial clustering of fractures, *Fractals in the Earth Science*, Barton, C.C. and P.R. LaPointe, eds., pp. 141--178, Plenum, New York.
- Bingham, C. 1964. Distributions on the sphere and the projective plane, Ph.D. Dissertation, Yale University.
- Bonnet, E.O.; Bour, O.; Odling, N.; Davy, P.; Main, I.; Cowie, P. and B. Berkowitz, 2001. Scaling of fracture systems in geologic media, *Rev. Geophys.*, Vol. 39, No. 3, 347--383.
- Bour, O. and P. Davy, 1997. Connectivity of random fault networks following a power law fault length distribution, *Water Resour. Res.*, Vol. 33, 1567--1583.
- Bour, O. and P. Davy, 1999. Clustering and size distributions of fault patterns: Theory and measurements, *Geophys. Res. Lett.*, Vol. 26, No. 13, 2001--2004.
- Bouwer, Herman and R.C. Rice, 1976, A slug test for determining hydraulic conductivity of unconfined aquifers with completely or partially penetrating wells, *Water Resources Research* 12(3) 423--428.
- Butler, J.J., Jr., 1997, *The design, performance, and analysis of slug tests*: Lewis Publishers, Washington, D.C., 252 p.
- Cardenas, M.B.; Slottke, D.T.; Ketcham, R.A. and J.M. Sharp, 2007. Navier-Stokes flow and transport simulations using real fractures shows heavy tailing due to eddies, *Geophys. Res. Lett.*, Vol. 34, No. L14404, doi:10.29/2007/GL030554.

- Chen, Z.; Neuman, S.P.; Yang, Z. and S.S. Rahman, 2000. An experimental investigation of hydraulic behavior of fractures and joints in granitic rock, *Int. J. Rock. Mech. Min. Sci.*, Vol. 37, 267--273.
- Cook, A.M.; Myer, L.R.; Cook, N.G.W. and F.M. Doyle, 1990. The effect of tortuosity on flow through a natural fracture, In: *Rock Mechanics Contributions and Challenges, Proceedings of the 31st U.S. Symposium on Rock Mechanics*, W.A. Hustrulid and G.A. Johnson, eds., A.A. Balkema, Rotterdam.
- Cooper, H.H. and C.E. Jacob, 1946, A generalized graphical method for evaluating formation constants and summarizing well field history, *American Geophysical Union Transactions*, v. 27, 526--534.
- Cooper, H.H., Jr., Bredehoeft, J.D., and I.S. Papadopoulos, 1967, Response of a finite-diameter well to an instantaneous charge of water. *Water Resources Research* v. 3, 263--269.
- Darcel, C.; Davy, P.; Bour, O and J.R. de Dreuzy, 2003. Connectivity properties of two-dimensional fracture networks with stochastic fractal correlation, *Water Resour. Res.*, Vol. 39, No. 10, doi:10.1029/2002WR001628.
- de Dreuzy, J.R.; Davy, P. and O. Bour, 2001. Hydraulic properties of two-dimensional random fracture networks following a power-law length distribution: 1. Effective connectivity, *Water Resour. Res.*, Vol. 37, No. 8, 2065--2078.
- Fetter, C.W. 1994. *Applied Hydrology*. Third Edition. Prentice-Hall, Inc., New Jersey. 691 p.
- Fisher, R. 1953. Dispersion on a sphere, *Proc. R. Soc. Lond. Ser. A.*, 217, 295--305.
- Forrester, K. 2001. *Subsurface Drainage for Slope Stabilization*, ASCE Press, 208 p.
- Green, W.H. and G.A. Ampt, 1911. Studies on soil physics, part I, the flow of air and water through soils. *Journal of Agricultural Science*. 4(1): 1-24.
- Guimerá, J. and J. Carrera, 2000. A comparison of hydraulic and transport parameters measured in low-permeability fractured media, *J. Contam. Hydrol.*, Vol. 41, 261-281.
- Gustafson, G. and A. Fransson, 2005. The use of the Pareto distribution for fracture transmissivity assessment, *Hydrogeol. J.*, Vol. 14, 15-20, doi:10.1007/s10040-005-0440-y.
- Halford, K.J. and E.L. Kuniansky, 2002. Documentation of Spreadsheets for the Analysis of Aquifer-Test and Slug-Test Data. U.S. Geological Survey Open File Report 02-197. 51 pp.
- Hantush, M.S. and C.E. Jacob, 1955, Non-steady flow in an infinite leaky aquifer: *Transactions of the American Geophysical Union*, vl. 36, 95--100.
- Holmén, J.G. and N. Outters, 2002. Theoretical study of rock mass investigation efficiency, TR-02-21, Swedish Nuclear Fuel and Waste Management Company SKB, Stockholm, Sweden.

- Horton, R.E. 1939. Analysis of runoff plat experiments with varying infiltration capacity. Transaction of the American Geophysical Union. 20:693711.
- Horton, R.E. 1933. The role of infiltration in the hydrologic cycle. Transactions, American Geophysical Union. 14:446-60.
- Jaeger, J.C.; Cook, N.G.W. and R.W. Zimmerman, 2007. Fundamentals of Rock Mechanics, 4th Ed., Blackwell, Malden, MA.
- Klimczak, C.; Schultz R.A.; Parashar, R. and D.M. Reeves, 2010. Cubic law with correlated aperture to length and implications for network scale fluid flow, Hydrol. J., doi:10.1017/s10040-009-0572-0.
- Kleinfelder, Inc. 2006. SR 101 MP 69.8 Landslide Aberdeen, Washington. Project 65017.
- Kozubowski, T.J.; Meerschaert, M.M. and G. Gustafson, 2008. A new stochastic model for fracture transmissivity assessment, Water Resour. Res., Vol. 44, No. W02435, doi:10.1029/2007WR006053.
- Lowel, S.M. 2001. Eldon Landslide: geotechnical student of the Eldon vicinity landslide adjacent to the Hood Canal, SR 101, MP 321, C.S. 2302, Washington Department of Transportation, Field Operation Support Service Center. Materials Laboratory – Geotechnical Branch, Olympia, Washington.
- Mandelbrot, B. 1974. Intermittent turbulence in self-similar cascades: Divergence of high moments and dimension of the carrier, J. Fluid Mech., Vol. 62, 331--350.
- Mardia, K.V. and P.E. Jupp, 2000. Directional Statistics, Wiley, New York.
- Mayne et al, 2002 – Subsurface Investigations-Geotechnical Site Characterization, FHWA
- Munier, R. 2004. Statistical analysis of fracture data adopted for modeling discrete fracture networks -- Version 2., Rep. R. 04-66, Swedish Nuclear Fuel and Waste Management Company SKB, Stockholm, Sweden.
- Neuman, S.P. 1975. Analysis of pumping test data from anisotropic unconfined aquifers considering delayed gravity response. Water Resources Research. 11: 329-42.
- Nicol, A.; Watterson, J.; Walsh, J.J. and C. Childs, 1996. The shapes, major axis orientations and displacement patterns of fault surfaces, J. Struct. Geol., Vol. 18, no. 2/3, 235--248.
- NRCS. 1986. Urban Hydrology for Small Watersheds, TR-55. United States Department of Agriculture Conservation Engineering Division. 164 pp.
- Olson, J.E. 1993. Joint pattern development: Effects of subcritical fracture growth and mechanical crack interaction, J. Geophys. Res., Vol. 98, No. B9, 12,225--12,265.

- Olson, J.E. 2003. Sublinear scaling of fracture aperture versus length: an exception or the rule? *J. Geophys. Res.*, Vol. 108, doi:10.1029/2001JB0000419.
- Paillet, F.L. 1998. Flow modeling and permeability estimation using borehole flow logs in heterogeneous fractured formation, *Water Resour. Res.*, Vol. 34, No. 5, 997--1010.
- Philip, J.R. 1957. The theory of infiltration. 1. The infiltration equation and its solution. *Soil Science*. 83(5): 345-357.
- Philip, J.R. 1969. Theory of infiltration. In *Advances in Hydrosience*. Vol. 5. Ed V.T. Chow. 215-96. New York, Academic Press.
- Pohlmann, K.; Pohll, G.; Chapman, J.; Hassan, A.E.; Carroll, R; and C. Shirley, 2004. Modeling to support groundwater contaminant boundaries for the Shoal underground nuclear test, Desert Research Institute Report No. 45184.
- Qian, J.; Chen, Z.; Zhan, H. and H. Guan, 2011. Experimental study of the effect of roughness and Reynolds number on fluid flow in rough-walled single fractures: a check of the local cubic law, *Hydrol. Process.*, Vol. 25, No. 4, 614--622, doi:10.1002/hyp.7849.
- Quinn, P.M.; Cheery, J.A.; and B.L. Parker, 2011. Quantification of non-Darcian flow observed during packer testing in fractured sedimentary rock, *Water Resour. Res.*, Vol 47, No. W09533, doi:10.1029/2010WR009681.
- Reeves, D.M.; Benson, D.A.; Meerschaert, M.M. and H.-P. Scheffler, 2008b. Transport of conservative solutions in simulated fracture networks: 2. Ensemble solute transport and the correspondence to operator-stable limit distributions, *Water Resour. Res.*, Vol. 44, No. W05410, doi:10.1029/2008WR006858.
- Reeves, D.M.; Pohlmann, K.; Pohll, G.; Ye, M. and J.Chapman, 2010. Incorporation of conceptual and parametric uncertainty into radionuclide flux estimates from a fractured granite rock mass, *Stoch. Environ. Res. Risk Assess.*, doi:10.1007/s00477-010-0385-0.
- Reeves, D.M., R. Parashar, and Y. Zhang. 2011. Hydrogeological Characterization of Fractured Rock Masses Intended for Disposal of Radioactive Waste, In: *Radioactive Waste*, Ed. R.O.A. Rahman, InTech Publishing, ISBN 979-953-307-274-5, accepted.
- Renshaw, C.E. 1995. On the relationship between mechanical and hydraulic apertures in rough walled fractures, *J. Geophys. Res.*, Vol. 100, No. B12, 24,629--24,363.
- Renshaw, C.E. 1999. Connectivity of joint networks with power law length distributions, *Water Resour. Res.*, Vol. 35, No. 9, 2661--2670.
- Rives, T.M.; Razack, M.; Petit, J.-P. and K.D. Rawnsley, 1992. Joint spacing: Analogue and numerical simulations, *J. Struct. Geol.*, Vol. 14, 925--937.

Ross, S.M. 1985. Introduction to Probability Models, 3rd Ed., Academic Press, Orlando, FL.

Sabatini et al., 2002 – Geotechnical Engineering Circular No. 5 – Evaluation of Soil and Rock Properties, FHWA

Schertzer, D. and S.Lovejoy, 1987. Physical modeling and analysis of rain and clouds by anisotropic scaling multiplicative processes, J. Geophys. Res., Vol. 85, No. D8, 9693–9714.

Schultz, R.A.; Okubo, C.H.; and S.J. Wilkins, 2006 Displacement-length scaling relations for faults on the terrestrial planets, J. Struct. Geol., Vol. 28, 2181--2193.

Schultz, R.A.; Soliva, R.; Fossen, H.; Okubo, C.; and D.M. Reeves, 2008. Dependence of displacement-length scaling relations for fractures and deformation bands on the volumetric changes across them, J. Struct. Geol., Vol. 30, 1405--1411, doi:10.1016/j.jsg.2008.08.001.

Schultz, R.A., Klimczak, C.; Fossen, H.; Olson, F.E.; Exner, U. and D.M. Reeves, in review.Statistical tests of scaling relations for geologic structures, J. Struct. Geol.

Schulz, C.H. 1997. Earthquake and fault populations and the calculation of brittle strain, Geowissenschaften, Vol. 15, 124--130.

Segall, P. and D.D. Pollard, 1983. Joint formation in granitic rock in the Sierra Nevada, Geol. Soc. Am. Bull., Vol. 94, 563--575.

Snow, D.T. 1965. A parallel plate model of fractured permeability media, Ph.D. Dissertation, University of California, Berkeley.

Stigsson, M.; Outters, N. and Hermanson, J. 2001. \{"A\}sp\{"o\} Hard Rock Laboratory, Prototype Repository Hydraulic DFN Model no. 2, IPR-01-39, Swedish Nuclear Fuel and Waste Management Company SKB, Stockholm, Sweden.

Terzaghi, R. 1965. Sources of error in joint surveys, Geotechnique, Vol. 15, No. 3, 287--304.

Thiem, G., 1906, Hydrologische Methodern: Leipzig, Geghardt, 56 p.

Theis, C.V., 1935, The relation between the lowering of the piezometric surface and the rate and duration of discharge of a well using ground water storage: Transaction of American Geophysical Union, v. 16, 519–524 p.

Twiss, R.J. and E.M. Moores, 2007. Structural Geology, 2nd Ed., W.H. Freeman, New York.

USDA. 1986. Urban Hydrology for Small Watersheds. Technical Release 55. United States Department of Agriculture, Conservation Engineering Division. 164 pp.

USDA. 2002. Chapter 8: Land Use and Treatment Classes. Part 630 Hydrology National Engineering Handbook. Natural Resources Conservation Service. 210-VI-NEH.

- USDA. 2004. Chapter 9: Hydrologic Soil-Cover Complexes. Part 630 Hydrology National Engineering Handbook. Natural Resources Conservation Service. 210-VI-NEH.
- USDA. 2009. Chapter 7: Hydrologic Soil Groups. Part 630 Hydrology National Engineering Handbook. Natural Resources Conservation Service. 210-VI-NEH.
- U.S. Department of the Interior, 1978. Drainage Manual, Water Resources Technical Publication, Washington, D.C., 286 p.
- van der Kamp, Garth, 1976, Determining aquifer transmissivity by means of well response tests: the underdamped case: Water Resources Research, v. 12(1), pp. 71–77.
- Warren, J.E. and P.J. Root, 1963. The behavior of naturally fractured reservoirs. Journal of the Society of Petroleum Engineering. 245-255.
- Wightman, W.E., Jalinoos, F, Sirles, P., and K. Hanaan, 2004. Application of Geophysical Methods to Highway Related Problems. Federal Highway Administration, FHWA-IF-04-021, 716 p.
- Wood, A.T.A. 1994. Simulation of the Von Mises distribution, Commun. Stat.-Sim., Vol. 21, No. 1, 157--164.
- Zimmermann, R.W. and G.S. Bodvarsson, 1996. Hydraulic conductivity of rock fractures, Trans. Porous Media, Vol. 23, 1--30.

Chapter 5

Estimating Groundwater Recharge

5.1 Introduction

Recharge is defined as that proportion of precipitation that reaches the water table. An estimation of recharge is needed for the design of subsurface drainage. A very simplified approach is provided to estimate the amount and timing of precipitation that becomes groundwater recharge. Specifically, the method employed is that developed by the United States Department of Agriculture Soil Conservation Service (USDA-SCS, 1972) to estimate abstractions, or the depth of precipitation that does not become overland flow or is lost to evapotranspiration. Abstraction is analogous to infiltration. Estimating both steady state recharge, or long term average conditions (e.g. annual rate), as well as transient recharge of 100 year 24-hour precipitation event, are discussed.

5.2 SCS Method for Abstractions

The SCS methodology is based on the assumption that direct runoff, after some initial abstraction (e.g. loss to storage depressions, interception, and plant uptake) will depend on land surface cover, land use, soil type and antecedent moisture conditions. The approach is widely accepted and used in a variety of hydrologic, erosion and water quality models (e.g. Foster et al., 1980; Williams et al., 1984a; 1984b; Young et al., 1987; Arnold et al., 1990; Meinardus et al., 1998). The approach uses one parameter – the curve number (CN), which has been defined over a wide range of geographic, soil and land management conditions. Chapter 4 on Site Characterization provides literature sources for estimating the curve number based on hydrologic soil cover complexes.

One of the earliest equations for infiltration was developed by Horton (1933, 1939) in which infiltration begins at some initial rate (f_0) and decreases exponentially over time until it reaches a constant rate (f_c), where k is the decay constant ($1/T$).

$$f(t) = f_0 + (f_0 - f_c)e^{-kt} \quad (5.1)$$

A plot of $f(t)$ is superimposed on precipitation rates in Figure 5.1. Using Figure 5.1 for reference, the SCS approach to estimating storm precipitation assumes that

- The depth (amount measured in length, i.e., inches) of cumulative excess precipitation (P_e) for runoff is always less than cumulative total precipitation (P).
- The depth of precipitation that recharges the system (F_a) is less than some potential maximum retention (S').
- There is some amount of rainfall (I_a) that occurs before any runoff can occur such that the maximum runoff is $P - I_a$.
- The ratio of actual-to-potential (maximum) for infiltration and runoff are equal.

The resulting ratios become,

$$\frac{\text{Actual}}{\text{Maximum}} = \frac{F_a}{S'} = \frac{P_e}{P - I_a} \quad (5.2)$$

From continuity, runoff P_e equals,

$$P_e = P - I_a - F_a \quad (5.3)$$

Combining equations 5.2 and 5.3 and solving for cumulative recharge, F_a ,

$$F_a = \frac{S'(P - I_a)}{P - I_a + S'}. \quad (5.4)$$

It is assumed that initial losses are equal to 20% of total storage potential,

$$I_a = 0.2S', \quad (5.5)$$

with storage (inches) assumed to be a function of the soil's curve number such that,

$$S' = \frac{1000}{CN} - 10. \quad (5.6)$$

Assigning a CN and knowing the cumulative precipitation (P), one can then solve for cumulative recharge, F_a . For modeling purposes it is assumed that I_a does not recharge the groundwater system. Instead, it is assumed to be lost to soil storage, plant interception and evapotranspiration.

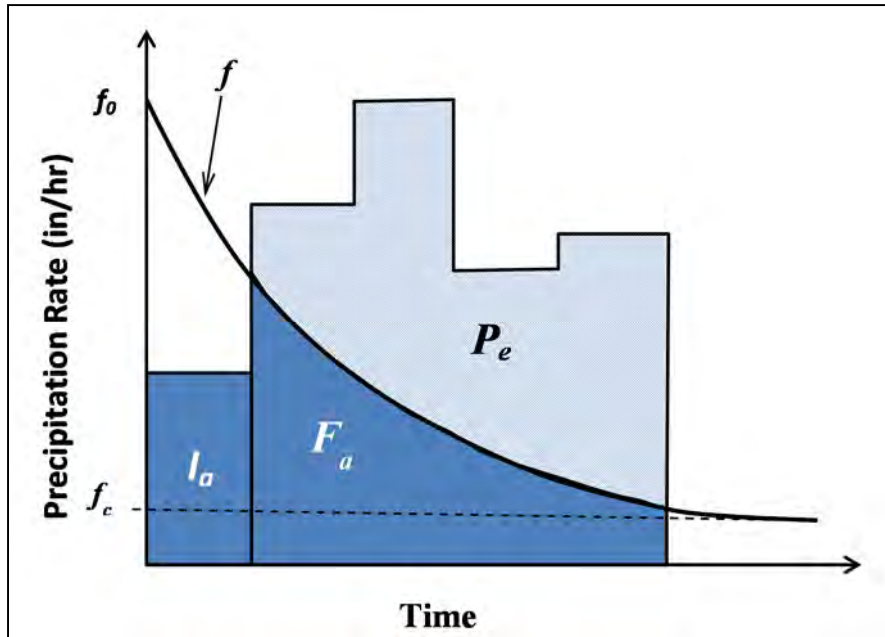


Figure 5.1: Graphical representation of the SCS method of rainfall abstractions where I_a = initial abstractions, P_e = rainfall excess and F_a = continuing abstractions (modified from Chow et al., 1988)

5.2.1 Example Calculation for Recharge

To illustrate the calculation of recharge, Table 5.1 lists hourly precipitation for a single storm event lasting seven hours. For a CN = 80, the the basin's storage potential is computed as $S' = (1000/80) - 10 = 2.5$ inches, and the initial abstraction $I_a = 0.2S' = 0.2(2.5 \text{ inches}) = 0.5$ inches. This means that 0.5 inches of rain must fall before any runoff or recharge is generated. From Table 5.1, only 0.2 inches of rain falls in the first hour and no recharge occurs. In the second hour, 0.7 inches falls, and the cumulative precipitation (P) of 0.9 inches surpasses the initial abstraction. From equation 5.4, $F_a = 2.5(0.9 - 0.5)/(0.9 - 0.5 + 2.5) = 0.34$ inches of recharge. Note that $0.5 + 0.34 = 0.84$ inches. Given 0.9 inches of rain has fallen, the balance of 0.06 inches of rain becomes runoff (P_e). During the second hour, an additional 0.37 inches of rain falls. $P = 1.27$. From equation 5.4, $F_e = 0.59$ inches. This is cumulative, and the incremental recharge for the third hour, $F_{a,inc} = 0.59 - 0.34 = 0.24$ inches of recharge. Over the 7-hour storm, SCS calculations given a CN = 80 produce 1.65 inches of recharge. For comparison, a CN = 65 will produce 70% more recharge (2.39 inches) while a CN = 95 will generate a lot of runoff and very little recharge (0.48 inches).

For individual storms it is necessary to reinitialize the sequence such that the initial abstraction is met prior to any recharge. It is recommended that individual storms are separated by at least 24 hours with no rain. However, site specific expert judgment should be used as to what lag between rainfall constitutes an individual storm event.

Table 5.1: Example calculations for a 7-hour rain event given CN = 80. P_{inc} = incremental precipitation, P = cumulative precipitation, I_a = initial abstraction, F_a = cumulative recharge, $F_{a,inc}$ = incremental recharge and P_e = cumulative runoff.

time hr	P_{inc} inches	P inches	I_a inches	F_a inches	$F_{a,inc}$ inches	P_e inches
1	0.20	0.20	0.20	0.00	0.00	0.00
2	0.70	0.90	0.50	0.34	0.34	0.06
3	0.37	1.27	0.50	0.59	0.24	0.18
4	1.04	2.31	0.50	1.05	0.46	0.76
5	2.25	4.56	0.50	1.55	0.50	2.51
6	0.73	5.29	0.50	1.64	0.10	3.15
7	0.07	5.36	0.50	1.65	0.01	3.21

5.2.2 Modifications to the Curve Number

The curve number designated to various soil hydrologic groups may need to be modified based on antecedent moisture conditions (USDA-SCS, 1972). The designated CN are based on normal antecedent moisture class (AMC II). If soil conditions are dry (AMC I) or wet (AMC III), then empirical evidence suggests equivalent curve numbers are computed as,

$$CN(I) = \frac{4.2CN(II)}{10-0.058CN(II)} \quad (5.7)$$

$$CN(III) = \frac{23CN(II)}{10+0.13CN(II)} \quad (5.8)$$

Classification of antecedent moisture classes are provided in Table 5.2. The curves for dry and moist antecedent moisture conditions are non-linear. Curves deviate most from AMC II conditions at low CN values and converge toward AMC II conditions at high CN values. Therefore, characterizing soil moisture conditions becomes more critical for systems with relatively large infiltration capabilities. In addition, Table 5. 1 is not site specific. For example, two inches of rain over a five day period on the Olympic Peninsula, WA may not require one to consider the system AMC III, but for an arid system in eastern Washington, it would. Under these circumstances, it is best to use the lower CN in the calculations as it will produce the most groundwater recharge and force a conservative approach to horizontal drainage design.

Table 5.2: Classification of antecedent moisture classes (AMC) for SCS method of rainfall abstractions (modified from USDA-SCS, 1972).

AMC Group	total 5 day antecedent rainfall (inches)	
	Dormant Season	Growing Season
I	< 0.5	< 1.4
II	0.5 to 1.1	1.4 to 2.1
III	> 1.1	> 2.1

The CN approach is based in agricultural sciences where slopes are generally less than 5°. If surface runoff increases with increased slope, then adjustment to the CN may be required. Huang et al. (2006) empirically derived an expression for gradients on the order of 0.14 to 1.4 (8°-54°)

$$CN(II)_\alpha = CN(II) \frac{322.79+15.63\alpha}{\alpha+323.52}, \quad (5.9)$$

where α is the slope gradient (L/L).

Figure 5.2 shows the impact on estimated recharge (expressed as a cumulative depth over time) when a CN of 75 is modified for dry, wet or steep slope conditions. For dry AMC the CN(I) falls to 56 (equation 5.7), while for moist AMC the CN(III) increases to 87 (equation 5.8). A larger CN correspond to greater runoff and less groundwater recharge. A steep slope of 40° increases the CN(II) for flat surfaces only slightly from 75 to 77.6. Impacts to cumulative recharge (F_a) as a result of wet AMC or steep slope are not large compared to changes in recharge as a function of dry moisture conditions. A reduction in CN from 75 to 56 causes a delay in the onset of recharge based on a larger initial abstraction (I_a , soil

storage, plant interception and evapotranspiration), but after 5 hours the amount of cumulative recharge surpasses wet conditions and steep slope conditions.

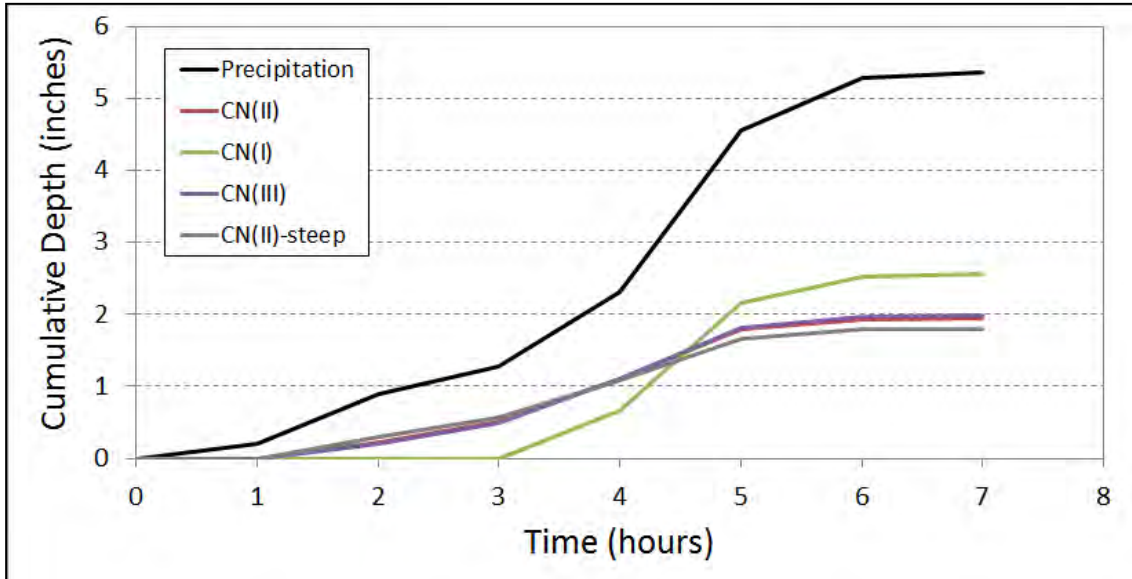


Figure 5.2: Impact on cumulative recharge (F_o) by modifying the $CN(II) = 75$ based on AMC and slope ($\theta = 40^\circ$) for a given precipitation event over 7 hours.

5.3 SCS 100-Year 24-Hour Storm Event

For horizontal drain design a large event is simulated to see if the drains can lower water levels quickly. The extreme event chosen for design considerations is the 100-year 24 hour event, though less extreme events could also be considered depending upon the criticality of the application.

The U.S. Department of Agriculture, SCS (1986) developed synthetic storm hyetographs for storms given a 24-hour duration. Four storm types in the United States are identified, Type IA, I, II and III. Figure 5.3 gives the geographic locations for each storm type. Rainfall distributions are tabulated in Table 5.3 and plotted in Figure 5.4. Types IA and I define the Pacific maritime climates with wet winters and dry summers. Type III is for the Gulf of Mexico and Atlantic coastal regions where tropical storms result in large 24-hour rainfall amounts. Type II storms are for the remainder of the nation. Type II and III storms have the largest intensity, in that a greater proportion of rain for these storms falls over a relatively short period of time. Type IA distributes its precipitation more gradually across the 24-hour period. Rainfall in a 24-hour period is obtained from the National Weather Service (NWS) for different parts of the country. NWS Technical Paper 40, or TP-40 (Hershfield, 1961) gives 24-hour isopluvial maps for the areas east of the 105^{th} meridian, with the map of the 100-year return period provided in Figure 5.5. For regions west of the 105^{th} meridian, TP-40 has been superseded by NOAA Atlas 2 (1972). NOAA (1972)

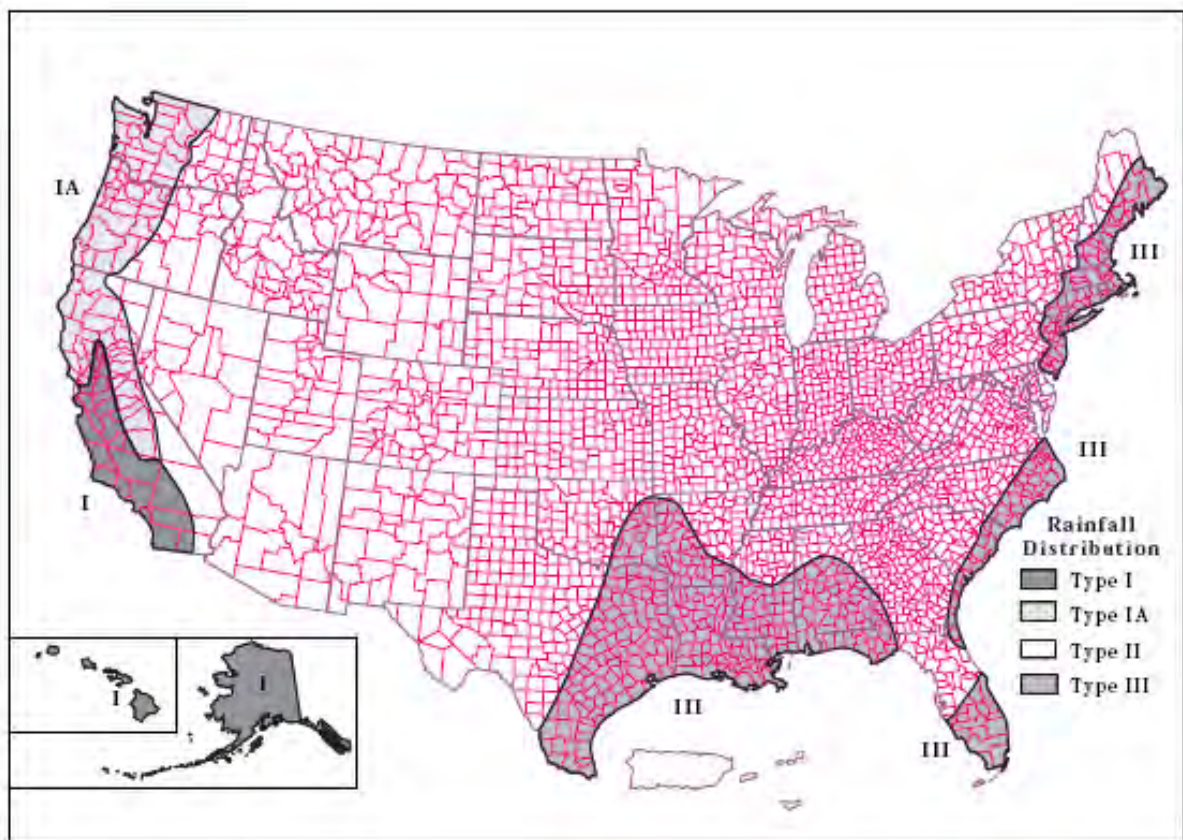


Figure 5.3: Location with in the US the 24-hour storm hyetographs for each of the four SCS storm types (USDA-SCS, 1986).

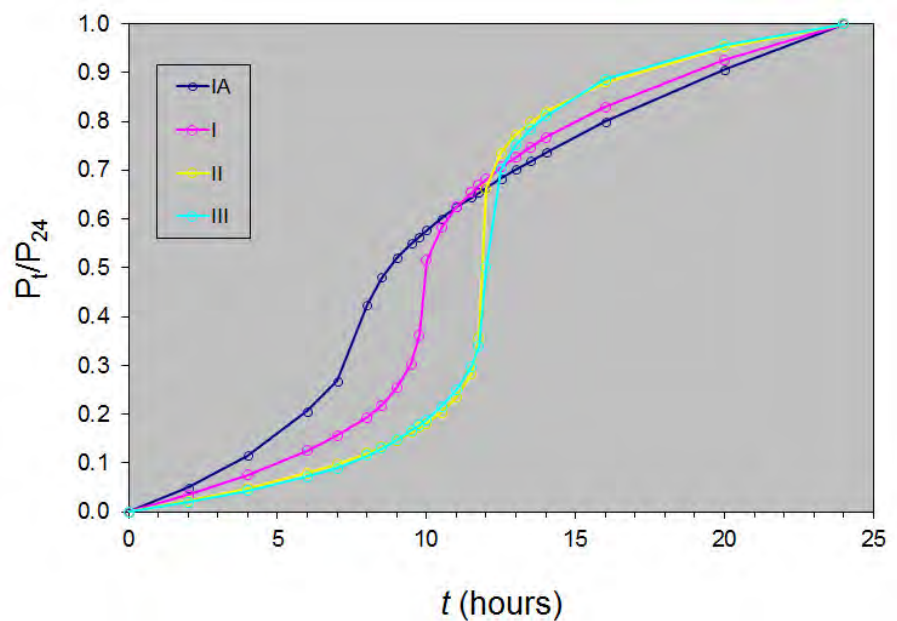


Figure 5.4: SCS 24-hour storm hyetographs (USDA-SCS, 1986)

hours	Fraction of Storm Total			
	1A	I	II	III
0	0	0	0	0
2	0.05	0.035	0.022	0.02
4	0.116	0.076	0.048	0.043
6	0.206	0.125	0.08	0.072
7	0.268	0.156	0.098	0.089
8	0.425	0.194	0.12	0.115
8.5	0.48	0.219	0.133	0.13
9	0.52	0.254	0.147	0.148
9.5	0.55	0.303	0.163	0.167
9.75	0.564	0.362	0.172	0.178
10	0.577	0.515	0.181	0.189
10.5	0.601	0.583	0.204	0.216
11	0.624	0.624	0.235	0.25
11.5	0.645	0.654	0.283	0.298
11.75	0.655	0.669	0.357	0.339
12	0.664	0.682	0.663	0.5
12.5	0.683	0.706	0.735	0.702
13	0.701	0.727	0.772	0.751
13.5	0.719	0.748	0.799	0.785
14	0.736	0.767	0.82	0.811
16	0.8	0.83	0.88	0.886
20	0.906	0.926	0.952	0.957
24	1	1	1	1

Table 5.3: USDA-SCS (1986) 24-hour rainfall distributions for different storm types.

isopluvial maps for 6-mo, 2-, 5-10-, 25-, 50- and 100-year return periods for individual states in the western US are archived by WRCC (<http://www.wrcc.dri.edu/pcpnfreq.html>). The 100-year return period for Washington State is given in Figure 5.6.

Recharge as a function of CN and total precipitation in a 100-year, 24-hour storm event (for a type IA storm distribution) is plotted in Figure 5.7. Recharge depth increases with total precipitation for all values of CN. For low total precipitation depths, low CNs will have lower total recharge than higher CN values, based on losses to the initial abstraction. As an example, total precipitation must be greater than 3.2 inches for a CN of 55 to produce more recharge than a CN equal to 80 (marked in Figure 5.7a). For larger precipitation totals ($P > 5$ inches), raising the CN will always cause a decrease in estimated recharge. Focusing on the percentage of precipitation that becomes recharge (Figure 5.7b) shows that for $CN < 80$, the percentage of recharge decreases with increased total precipitation. For CN values equal to or less than 80, maximum recharge occurs between 3 and 5 inches. Lower total precipitation loses water to initial abstraction, while larger precipitation forces more water to run off. Maximum recharge is always less than 50% the total precipitation when I_a is assumed not to recharge the groundwater system.

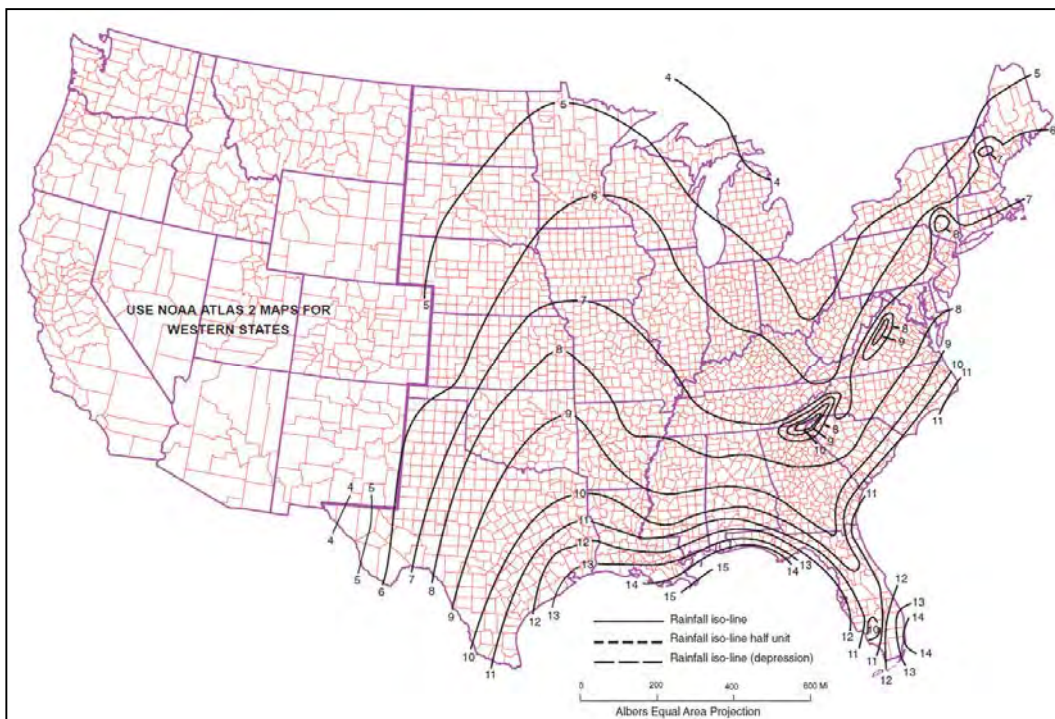


Figure 5.5: 100-year, 24-hour rainfall depth (inches) for regions east of the 105th meridian. Map published by Hershfield (1961) and TR-55 (USDA-SCS, 1986). Isopluvial contours at one inch.

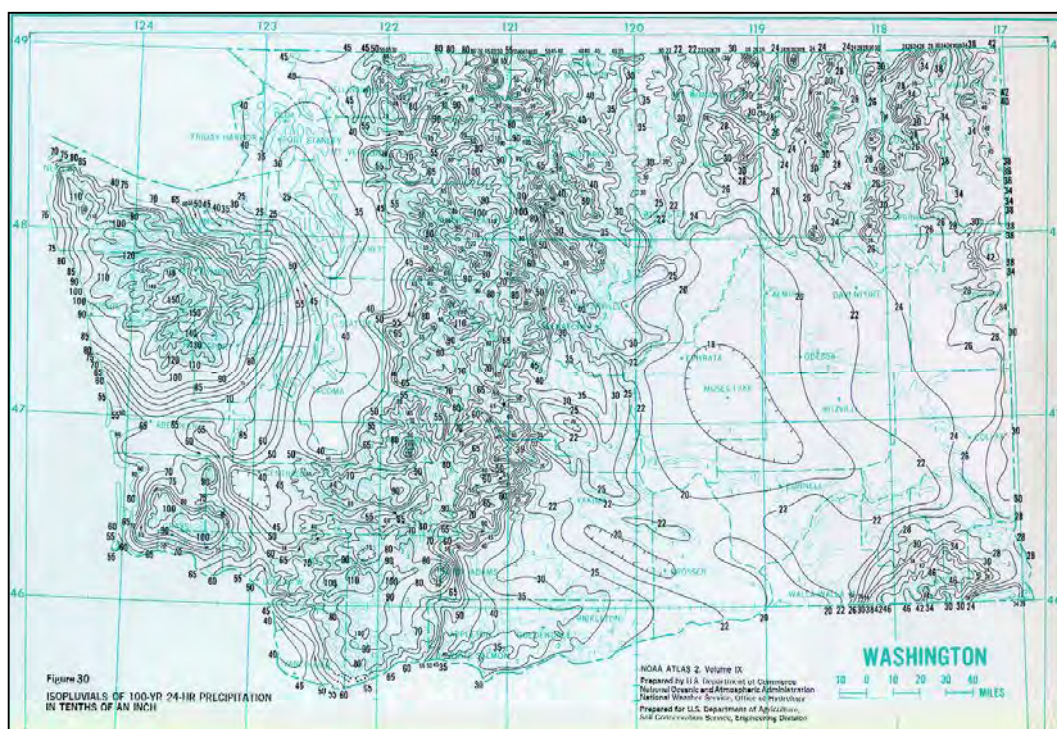
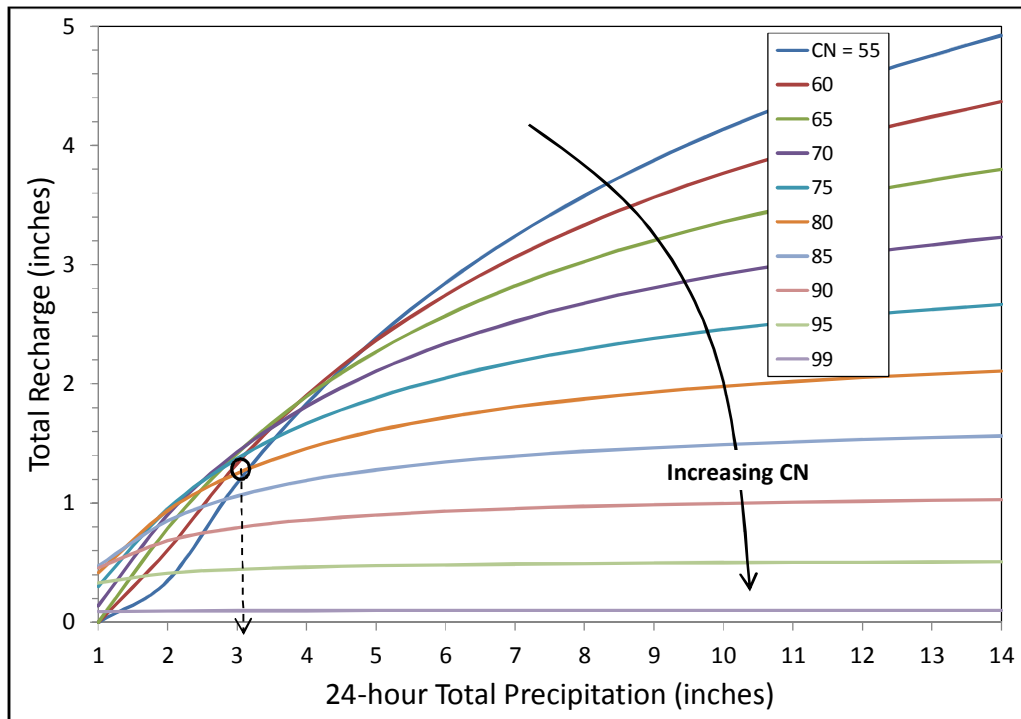


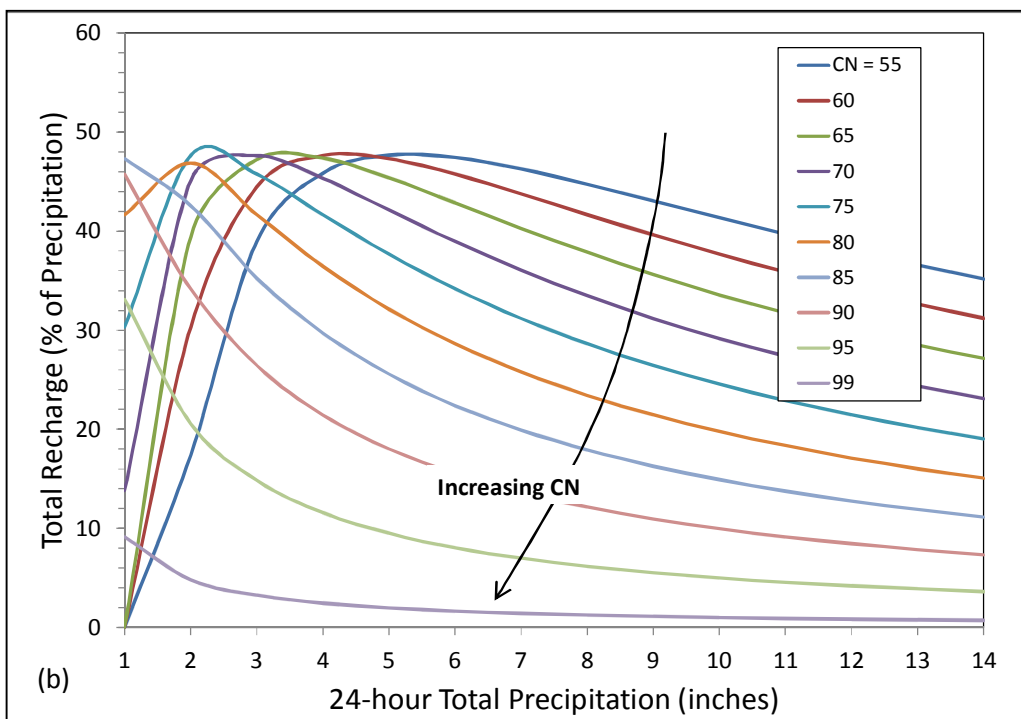
Figure 5.6: 100-year, 24-hour isopluvial map for Washington State (NOAA, 1972). Depths in 10th of an inch.

Table 5.4: Computed recharge (R , ft/d) for site MP 321 for a 100-year, 24-hour storm event, assuming a CN = 80.

hours	day	Storm Dist.	P	Computed Recharge	
		IA	inches	F_a inches	R ft/d
0	0.000	0	0	0.0000	0.0000
2	0.083	0.05	0.45	0.0000	0.0000
4	0.167	0.116	1.044	0.4468	0.4468
6	0.250	0.206	1.854	0.8783	0.4315
7	0.292	0.268	2.412	1.0834	0.4102
8	0.333	0.425	3.825	1.4270	0.6873
8.5	0.354	0.48	4.32	1.5111	0.3361
9	0.375	0.52	4.68	1.5644	0.2132
9.5	0.396	0.55	4.95	1.6007	0.1454
9.75	0.406	0.564	5.076	1.6167	0.1281
10	0.417	0.577	5.193	1.6311	0.1149
10.5	0.438	0.601	5.409	1.6564	0.1013
11	0.458	0.624	5.616	1.6794	0.0917
11.5	0.479	0.645	5.805	1.6992	0.0795
11.75	0.490	0.655	5.895	1.7084	0.0730
12	0.500	0.664	5.976	1.7164	0.0643
12.5	0.521	0.683	6.147	1.7328	0.0658
13	0.542	0.701	6.309	1.7478	0.0598
13.5	0.563	0.719	6.471	1.7622	0.0575
14	0.583	0.736	6.624	1.7753	0.0524
16	0.667	0.8	7.2	1.8207	0.0454
20	0.833	0.906	8.154	1.8845	0.0319
24	1.000	1	9	1.9318	0.0237



(a)



(b)

Figure 5.7: Cumulative recharge as a function of CN and total 24-hour precipitation given a SCS type IA storm distribution in (a) inches, (b) percentage of total precipitation.

5.3.1 Example Problem: Recharge Calculation for 100-Year, 24-Hour Storm.

For the example site, SR 101 MP 321 is located in western WA with a type IA 24-hour storm pattern. Figure 5.8 is an enlargement the NOAA (1972) Atlas 2 of Washington State with MP 321 location identified. Contours are given at the 10th of an inch for total storm precipitation. Storm total for MP 321 is approximately 9 inches.

For the 8th hour in the storm, the cumulative fraction of storm total is 0.425, or $P = 3.83$ inches given a storm total of 9 inches. Initial abstraction for a $CN = 80$ is 0.5. Since $P > I_a$, then F_a from equation 5.4 equals 1.43 inches. F_a for the previous time step ($t = 7$ hours) is 1.0834 inches, therefore the incremental recharge is 0.34 inches in one hour, or 0.69 ft/day. Table 5.4 gives computed recharge estimates for all storm stress periods.

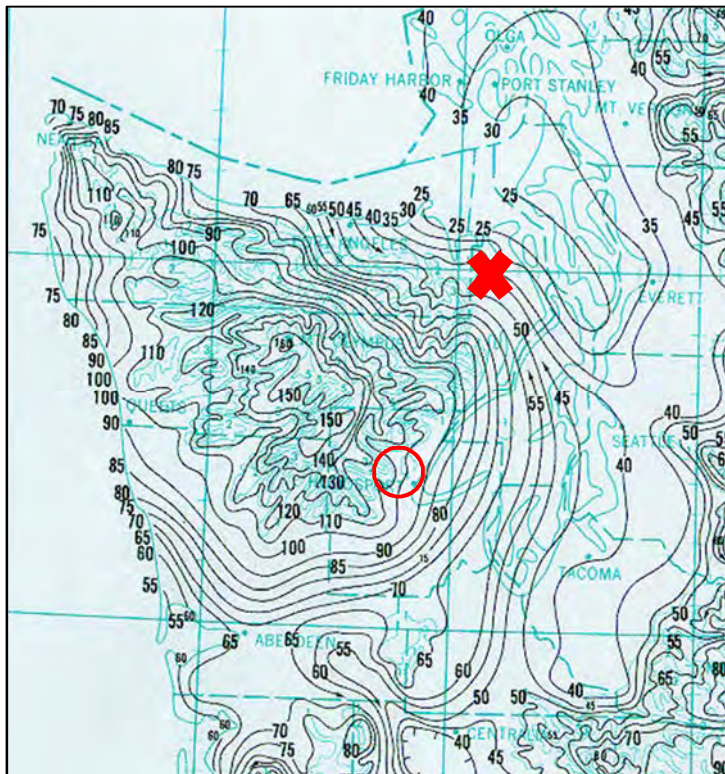


Figure 5.8: NOAA Atlas 2 (1972) for

Table 5.4: Computed recharge (R , ft/d) for site MP 321 for a 100-year, 24-hour storm event, assuming a CN = 80.

hours	day	Storm Dist.	P	Computed Recharge	
		IA	inches	F _a inches	R ft/d
0	0.000	0	0	0.0000	0.0000
2	0.083	0.05	0.45	0.0000	0.0000
4	0.167	0.116	1.044	0.4468	0.4468
6	0.250	0.206	1.854	0.8783	0.4315
7	0.292	0.268	2.412	1.0834	0.4102
8	0.333	0.425	3.825	1.4270	0.6873
8.5	0.354	0.48	4.32	1.5111	0.3361
9	0.375	0.52	4.68	1.5644	0.2132
9.5	0.396	0.55	4.95	1.6007	0.1454
9.75	0.406	0.564	5.076	1.6167	0.1281
10	0.417	0.577	5.193	1.6311	0.1149
10.5	0.438	0.601	5.409	1.6564	0.1013
11	0.458	0.624	5.616	1.6794	0.0917
11.5	0.479	0.645	5.805	1.6992	0.0795
11.75	0.490	0.655	5.895	1.7084	0.0730
12	0.500	0.664	5.976	1.7164	0.0643
12.5	0.521	0.683	6.147	1.7328	0.0658
13	0.542	0.701	6.309	1.7478	0.0598
13.5	0.563	0.719	6.471	1.7622	0.0575
14	0.583	0.736	6.624	1.7753	0.0524
16	0.667	0.8	7.2	1.8207	0.0454
20	0.833	0.906	8.154	1.8845	0.0319
24	1.000	1	9	1.9318	0.0237

5.4 Steady State Recharge

Steady state recharge represents the long-term, or average, recharge. It does not include episodic events such as the 100-year storm event discussed in the previous section. Instead, steady state recharge and resultant steady state groundwater levels (or pore pressures) indicate a system in equilibrium. Quantifying steady state conditions is necessary to understanding baseline conditions prior to a large and/or sudden perturbation in system stress (such as a 100 year storm).

Two different methods for assigning steady state recharge are provided, depending on availability of site-specific precipitation data. If site-specific data is available and collected over a significant period of

time to reflect wet and dry seasons (e.g. one or more years), then recharge is computed and averaged over the period of record. For example, using the 2010 water year precipitation record of site MP 321, F_a is calculated at approximately 10 inches/year. Given 365 days, the steady state recharge rate is estimated at 0.0023 ft/d.

If data are not readily available, or only available for a short period of record, then steady state recharge can be approximated by using the average annual total precipitation for the site based on precipitation records tabulated by regional climate centers (refer to Chapter 4.2.4) and using historic data. For site MP 321, and assuming Quilcene 2SW (COOP) historic data most closely represents MP 321 (refer to Figure 5.8), average depth of precipitation is 51 inches per year (between years 1920 and 2010). For this site, the 100-year 24-hour event is 9 inches and a CN = 80 will produce 1.93 inches of recharge, or 21% (refer to Figure 5.7 or Table 5.5). If one assumes the same percentage of recharge between the 100-year storm and the long-term average, then 51 inches multiplied by 0.21 will equal 10.7 inches, or a recharge rate of 0.0024 ft/d.

Table 5.5 Recharge and maximum infiltration rates as a function of CN, storm total precipitation and storm type.

CN	24 hr Total P (inches)	Recharge (inches) All Storms Types	% recharge all types	Storm Max Recharge Rate (ft/d)			
				IA	I	II	III
55	1	0.00	0	0.00	0.00	0.00	0.00
55	2	0.35	17	0.09	0.09	0.12	0.13
55	3	1.17	39	0.33	0.47	2.70	1.78
55	4	1.83	46	0.84	3.22	7.23	2.79
55	5	2.38	48	0.95	5.38	9.98	5.78
55	6	2.85	47	1.64	5.85	10.76	6.32
55	7	3.24	46	1.84	6.22	11.34	6.74
55	8	3.58	45	1.95	6.51	11.77	7.07
55	9	3.88	43	2.04	6.73	12.08	7.32
55	10	4.14	41	2.11	6.89	12.30	7.52
55	11	4.37	40	2.17	7.01	12.44	7.66
55	12	4.57	38	2.22	7.10	12.52	7.77
55	13	4.76	37	2.26	7.15	12.56	7.84
55	14	4.92	35	2.29	7.18	12.56	7.89

Table 5.5 Continued:

CN	24 hr Total P (inches)	Recharge (inches) All Storms	% recharge	Storm Max Recharge Rate (ft/d)			
		Types	all types	IA	I	II	III
60	1	0.00	0	0.00	0.00	0.00	0.00
60	2	0.61	30	0.14	0.21	0.54	0.38
60	3	1.33	44	0.46	1.64	4.78	2.12
60	4	1.90	48	0.77	4.34	8.06	4.67
60	5	2.37	47	1.40	4.81	8.84	5.20
60	6	2.75	46	1.53	5.16	9.38	5.59
60	7	3.06	44	1.63	5.42	9.75	5.89
60	8	3.33	42	1.71	5.59	9.99	6.10
60	9	3.57	40	1.77	5.72	10.14	6.25
60	10	3.77	38	1.82	5.80	10.21	6.35
60	11	3.95	36	1.85	5.84	10.24	6.41
60	12	4.10	34	1.88	5.86	10.22	6.45
60	13	4.24	33	1.89	5.86	10.16	6.46
60	14	4.37	31	1.91	5.84	10.09	6.45
65	1	0.00	0	0.00	0.00	0.00	0.00
65	2	0.79	39	0.22	0.35	1.90	1.23
65	3	1.42	47	0.60	3.37	6.24	3.14
65	4	1.89	47	1.12	3.87	7.11	4.18
65	5	2.27	45	1.25	4.21	7.64	4.57
65	6	2.57	43	1.35	4.44	7.97	4.83
65	7	2.82	40	1.42	4.59	8.16	5.01
65	8	3.03	38	1.46	4.68	8.25	5.12
65	9	3.21	36	1.50	4.72	8.27	5.19
65	10	3.36	34	1.52	4.73	8.24	5.21
65	11	3.49	32	1.54	4.72	8.17	5.21
65	12	3.61	30	1.54	4.69	8.08	5.19
65	13	3.71	29	1.54	4.65	7.98	5.15
65	14	3.80	27	1.54	4.60	7.86	5.11
70	1	0.14	14	0.05	0.04	0.04	0.03
70	2	0.90	45	0.40	1.33	3.38	1.39
70	3	1.43	48	0.76	3.00	5.53	3.24
70	4	1.81	45	1.00	3.36	6.09	3.64
70	5	2.11	42	1.09	3.57	6.39	3.89
70	6	2.34	39	1.15	3.69	6.54	4.04
70	7	2.52	36	1.19	3.75	6.58	4.12
70	8	2.68	33	1.21	3.77	6.55	4.15
70	9	2.81	31	1.23	3.75	6.49	4.14
70	10	2.92	29	1.23	3.72	6.39	4.12
70	11	3.01	27	1.23	3.67	6.27	4.07
70	12	3.10	26	1.22	3.61	6.15	4.02
70	13	3.17	24	1.21	3.55	6.01	3.95
70	14	3.23	23	1.20	3.48	5.88	3.89

Table 5.5 Continued:

CN	24 hr Total P (inches)	Recharge (inches) All Storms	% recharge	Storm Max Recharge Rate (ft/d)			
		Types	all types	IA	I	II	III
75	1	0.30	30	0.07	0.10	0.27	0.19
75	2	0.95	48	0.38	2.17	4.03	2.33
75	3	1.37	46	0.77	2.58	4.69	2.80
75	4	1.67	42	0.85	2.80	5.00	3.05
75	5	1.88	38	0.91	2.90	5.11	3.18
75	6	2.05	34	0.94	2.93	5.11	3.22
75	7	2.18	31	0.95	2.92	5.04	3.22
75	8	2.29	29	0.96	2.88	4.94	3.19
75	9	2.38	26	0.95	2.83	4.82	3.14
75	10	2.46	25	0.94	2.77	4.69	3.08
75	11	2.52	23	0.93	2.70	4.56	3.01
75	12	2.58	21	0.92	2.63	4.42	2.94
75	13	2.62	20	1.00	2.56	4.29	2.87
75	14	2.67	19	1.05	2.49	4.16	2.80
80	1	0.42	42	0.12	0.26	1.22	0.75
80	2	0.94	47	0.54	1.85	3.39	2.00
80	3	1.25	42	0.64	2.10	3.75	2.29
80	4	1.46	36	0.69	2.19	3.84	2.40
80	5	1.61	32	0.71	2.19	3.80	2.42
80	6	1.72	29	0.72	2.16	3.71	2.39
80	7	1.81	26	0.71	2.11	3.58	2.34
80	8	1.88	23	0.70	2.04	3.45	2.28
80	9	1.93	21	0.69	1.97	3.32	2.21
80	10	1.98	20	0.77	1.90	3.18	2.13
80	11	2.02	18	0.80	1.84	3.06	2.06
80	12	2.05	17	0.82	1.77	2.93	1.99
80	13	2.08	16	0.83	1.71	2.82	1.92
80	14	2.11	15	0.85	1.65	2.71	1.86
85	1	0.47	47	0.20	1.12	2.08	1.09
85	2	0.85	43	0.44	1.46	2.62	1.59
85	3	1.06	35	0.49	1.55	2.71	1.70
85	4	1.19	30	0.51	1.54	2.64	1.70
85	5	1.28	26	0.50	1.48	2.52	1.65
85	6	1.34	22	0.49	1.42	2.39	1.58
85	7	1.39	20	0.54	1.35	2.25	1.51
85	8	1.43	18	0.57	1.28	2.13	1.44
85	9	1.47	16	0.59	1.21	2.01	1.37
85	10	1.49	15	0.60	1.15	1.90	1.30
85	11	1.51	14	0.61	1.10	1.80	1.24
85	12	1.53	13	0.62	1.05	1.71	1.19
85	13	1.55	12	0.62	1.00	1.63	1.13
85	14	1.56	11	0.63	0.96	1.56	1.08

Table 5.5 Continued:

CN	24 hr Total P (inches)	Recharge (inches) All Storms	% recharge	Storm Max Recharge Rate (ft/d)			
		Types	all types	IA	I	II	III
90	1	0.46	46	0.26	0.86	1.56	0.93
90	2	0.68	34	0.31	0.98	1.70	1.07
90	3	0.79	26	0.32	0.94	1.61	1.05
90	4	0.86	21	0.31	0.88	1.47	0.98
90	5	0.90	18	0.36	0.81	1.34	0.91
90	6	0.93	16	0.37	0.74	1.23	0.84
90	7	0.95	14	0.39	0.69	1.13	0.78
90	8	0.97	12	0.39	0.64	1.04	0.72
90	9	0.99	11	0.40	0.59	0.97	0.67
90	10	1.00	10	0.40	0.56	0.90	0.63
90	11	1.01	9	0.40	0.52	0.84	0.59
90	12	1.02	8	0.39	0.49	0.79	0.56
90	13	1.02	8	0.39	0.46	0.75	0.53
90	14	1.03	7	0.39	0.44	0.71	0.50
95	1	0.33	33	0.15	0.46	0.80	0.51
95	2	0.41	21	0.15	0.41	0.68	0.46
95	3	0.45	15	0.18	0.34	0.57	0.39
95	4	0.46	12	0.19	0.29	0.48	0.33
95	5	0.48	10	0.19	0.25	0.41	0.29
95	6	0.48	8	0.19	0.22	0.36	0.25
95	7	0.49	7	0.18	0.20	0.32	0.23
95	8	0.49	6	0.19	0.18	0.29	0.21
95	9	0.50	6	0.21	0.16	0.26	0.19
95	10	0.50	5	0.23	0.17	0.24	0.17
95	11	0.50	5	0.24	0.18	0.22	0.16
95	12	0.50	4	0.26	0.20	0.21	0.15
95	13	0.51	4	0.27	0.21	0.19	0.14
95	14	0.51	4	0.28	0.22	0.18	0.13
99	1	0.09	9	0.04	0.05	0.08	0.05
99	2	0.10	5	0.04	0.03	0.04	0.03
99	3	0.10	3	0.06	0.05	0.03	0.03
99	4	0.10	2	0.06	0.05	0.04	0.04
99	5	0.10	2	0.07	0.06	0.05	0.04
99	6	0.10	2	0.07	0.07	0.05	0.05
99	7	0.10	1	0.08	0.07	0.06	0.05
99	8	0.10	1	0.08	0.07	0.06	0.06
99	9	0.10	1	0.08	0.08	0.06	0.06
99	10	0.10	1	0.08	0.08	0.07	0.06
99	11	0.10	1	0.08	0.08	0.07	0.07
99	12	0.10	1	0.09	0.08	0.07	0.07
99	13	0.10	1	0.09	0.08	0.07	0.07
99	14	0.10	1	0.09	0.08	0.07	0.07

5.5 References Cited

- Arnold, J.G., J.R. Williams, R.H. Griggs, and N. B. Sammons. 1990. Simulator for Water Resources in Rural Basins (SWRRB) - A Basin Scale Simulation Model for Soil and Water Resources Management. Texas A & M Press
- Chow, V.T., Maidment, D.R., and L.W. Mays, 1988. Applied Hydrology. McGraw-Hill, Inc. New York. 572 p.
- Foster, G. R., L. J. Lane, J. D. Nowlin, J. M. Laflen and R. A. Young, Smith, S. J., D. E. Kissel and J. R. Williams. 1980. Chemicals, Runoff and Erosion from Agricultural Management Systems (CREAMS). United States Department of Agriculture (USDA) in conjunction with the Science and Education Administration-Agriculture Research (SEA-AR)
- Hershfield, D.M. 1961. Rainfall Frequency Atlas of the United States: for Durations from 30 minutes to 24 Hours and Return Periods from 1 to 100 years. United States Department of Agriculture National Weather Service Technical Paper No. 40.
- Horton, R.E. 1939. Analysis of runoff-plot experiments with varying infiltration capacity. Transactions American Geophysical Union. 20: 693-711.
- Horton, R.E. 1933. The Role of Infiltration in the Hydrologic Cycle. Transactions American Geophysical Union. 14: 446-460.
- Huang, M., Gallichand, J., Wang, Z., and M. Goulet, 2006. A Modification to the Soil Conservation Service Curve Number Method for Steep Slopes in the Loess Plateau of China. Hydrological Processes. 20: 579-589.
- Maxey, G. B., and T. E. Eakin. 1949. Ground water in White River Valley, White Pine, Nye, and Lincoln Counties, Nevada. No. 8, State of Nevada Office of the State Engineer prepared in cooperation with the United State Department of the Interior Geological Survey, Carson City, Nevada.
- Meinardus, A., Griggs, R. H., Benson, V., and J. Williams, 1998. "EPIC on-line documentation and downloads." (<http://www.brc.tamus.edu/epic>)
- NOAA. 1972. Atlas 2, Precipitation Frequency Atlas of the Western United States, Volume IX Washington.
- United States Department of Agriculture, Soil Conservation Service (USDA-SCS). 1972. National Engineering Handbook, section 4, Hydrology.
- Washington State Department of Ecology Water Quality Program (WSDE). 2005. Storm Water Management in Western Washington: Volume III, Hydrologic Analysis and Flow Control Design/BMPs. Publication No. 05-10-31. 181 p.
- Williams, J. R., Jones, C. A., and P. T. Dyke, 1984a. "A modeling approach to determining the relationship between erosion and soil productivity." *Trans. ASAE*, 27, 129–144.

Williams, J. R., Jones, C. A., and P. T. Dyke, 1984b. "The EPIC model and its application." *Proc., ICRISAT-IBSNAT-SYSS Symp. on Minimum Data Sets for Agrotechnology Transfer*, Hyderabad, India, 111–121.

USDA-SCS, Technical Release No. 55: Urban Hydrology for Small Watersheds, 1986.

Young, R. A., C. A. Onstad, D. D. Bosch, and W. P. Anderson. 1987. AGNPS, Agricultural Non-Point Source Pollution Model - A watershed analysis tool. United States Department of Agriculture, Conservation Research Report 35: 1-80. Washington, D.C.: USDA.

Chapter 6

Introduction to Groundwater Modeling

6.1 Introduction

The purpose of chapter 6 is to familiarize the reader with basic groundwater modeling terminology and approaches. Appendix C provides a tutorial for MODFLOW, with the purpose of walking individuals through an example of model creation, model calibration and verification. Chapter 6 provides the basics of groundwater modeling in an abridged format. Refer to the text *Applied Groundwater Modeling: Simulation of Flow and Advective Transport* (Anderson and Woessner, 1992) for greater depth on the topic as well as many examples.

What is a model, and how can groundwater modeling help a practitioner evaluate slope stability? First, a model is a simplified approximation of the natural system. Physical groundwater models would include, as an example, sand tanks in the laboratory to investigate groundwater flow. In contrast, mathematical models solve for flow using a governing equation believed to represent important physical processes. The groundwater flow equation is the governing equation for groundwater hydrology, and is presented in Chapter 3. The groundwater flow equation is constrained by equations that represent flow and/or water levels at the boundaries of the model domain (called boundary conditions), and if time dependent, will also incorporate equations defining the beginning water levels at the start of the simulation (called initial conditions). Analytic solutions for drainage problems are presented in Chapter 7, but these approaches impose many simplifying assumptions and may not be appropriate for many complex, real-world situations. For example, analytic solutions cannot account for complex geology, horizontal drains in a fan array, or boundary conditions. For these more complex groundwater flow problems, a numeric model is needed. A numeric model is a powerful tool that allows practitioners to relax assumptions on system homogeneity, as well as allow complex geometry and/or superimpose multiple boundary conditions and stresses, by approximating solutions to the groundwater flow equation through numeric techniques.

Numeric models are generally used for prediction purposes. For example, what horizontal drain configurations will suffice in lowering water levels below some critical point to prevent slope failure during a 100-year 24-hour storm event? How will drain configuration change based on geologic materials and storm pattern? And what data are most important to determine drain design? In this sense, models not only help one predict system response, but can be used to gain insight on controlling parameters and possible threshold responses to stresses on the system. To create an effective and verifiable numeric model necessitates a full understanding of the assumptions applied, can require significant amounts of data, and be expensive to build. However, numeric models can more fully incorporate data into a unified conceptual rendering of the site so more informed decisions can be made on designing, constructing, and managing the drainage system.

The purpose of the model must be defined first, followed by the degree of certainty required and funds available for the project. The general rule of thumb is to use the simplest model available to achieve the stated purpose or goal of the project. In some situations, analytic solutions are appropriate if data and money are limited. However, numeric models should be used if simpler approaches fail to account for processes considered.

6.2 Conceptual Model

Building a conceptual model is fundamental to creating a worthwhile numeric model. Without proper conceptualization of the site, the model may be inadequately defined and fail to capture important components of the physical system. Subsequently, the resultant solutions are likely incorrect. All conceptual models are simplified versions of the actual system. However, simplifying assumptions must be valid, and enough detail must be maintained to capture observed system response.

Prior to collecting data, an initial conceptual model should be established. This will dictate what data and where sampling will occur. With data collection, and preliminary modeling, one may need to revisit the conceptual model and revise it based on an inability to correctly capture system response. In these circumstances, it may be necessary to collect more data and revise the modeling approach.

Four steps are required to construct a conceptual mode: (1) define the model boundary, (2) define hydrostratigraphic units, (3) delineate important water budget components and (4) define the flow system (Anderson and Woessner , 1992).

The first step is to establish the model boundaries. Ideally, model boundaries should be placed along natural hydrologic boundaries. For example, flow divides, water bodies, or impermeable bedrock. In Chapter 4, Figure 4.1 shows an example of assigning the model domain to the watershed boundary. Flow divides occur at the watershed boundaries with all flow exiting the site at the topographic low. By placing model boundaries at natural groundwater divides, one greatly simplifies the conceptual rendering of the site and limits the amount of data needed to define the model . When the model domain is restricted to an area less than the natural boundaries, then data collection needs to include water levels and/or groundwater flux estimates at the edges of the model domain to properly capture all water budget aspects of the site.

The second step to developing a valid conceptual model is to map the important hydrogeologic units at the site. Chapter 4 discusses hydrogeologic mapping in some detail. Locations, thicknesses and hydraulic properties for each unit are required to parameterize a groundwater model.

At the conceptual model development phase, water budget components need to be identified. Figure 6.1 shows possible water sources and sinks related to site SR101 MP321. Block arrows depict boundary condition fluxes that must be quantified before model execution can occur. Measuring seepage from the basalt basement is difficult and simplifying the conceptual model may be warranted to avoid this quantification. If one assumes that glacio-lacustine silts and clays (Unit 2) are relatively impermeable, then the no flow boundary is assigned to the top of this unit. If the assumption is not valid, then model results will fail to capture water level response to precipitation events and the assumption will need to

be discarded. If silts and clays (Unit 2) as well as the underlying glacial tills (Unit 3) are included in the model domain, then water level information specific to these units must be collected (piezometers isolated only in these units). To further simplify the conceptual model, it may be possible to assume that up-gradient fluxes are small compared to water entering the system via recharge. This may be valid if the domain extends to the ridge defining the watershed boundary. However, inter-basin groundwater flow can occur and the assumption may not be valid. Placing a piezometer at the model boundary and tracking observed heads with respect to precipitation events will aid in defining this component of the water budget.

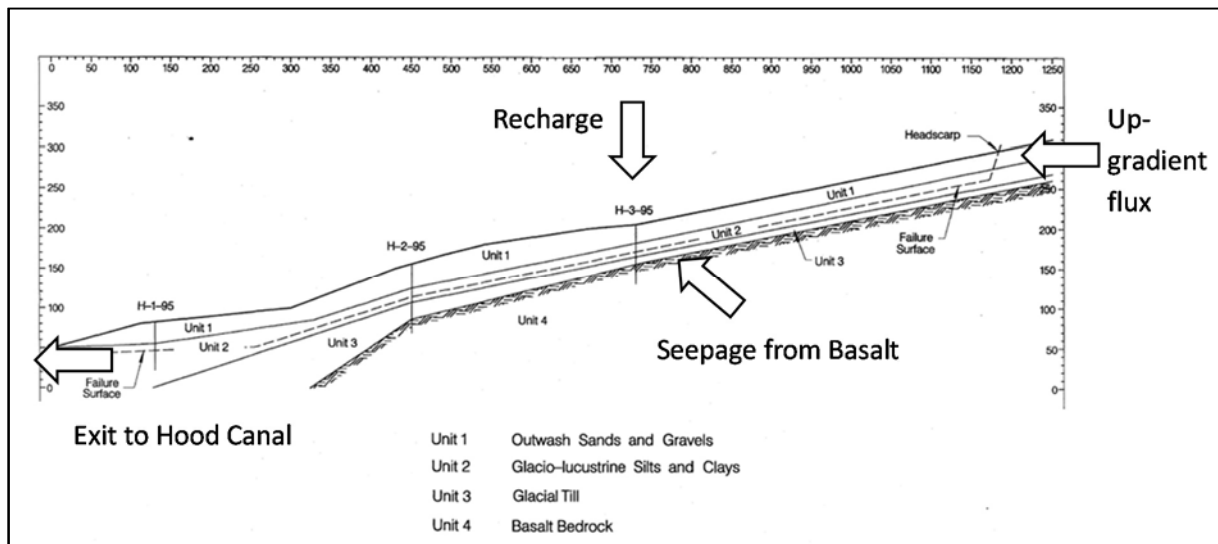


Figure 6.1: Water budget components for a conceptual model of SR101 MP321. (Figure modified from WSDOT, 2000)

Lastly, one needs to understand the flow system. For many natural slopes, flow systems are relatively simple with unconfined water table surfaces mimicing topography. However, if faulting, complex stratigraphy, fracturing and/or pressurized aquifers are located within the model domain, it is necessary to use observed water levels to help define flow paths.

6.3 MODFLOW

MODFLOW (McDonald and Harbaugh, 1988; Harbaugh and McDonald, 1996; Harbaugh et al., 2000; Harbaugh, 2005; Niswonger et al., 2011) is a widely accepted, finite-difference, public domain groundwater flow model produced by the United States Geologic Survey (USGS). MODFLOW uses the groundwater flow equation (refer to equation 3.36 for unconfined aquifers) as its governing equation. Head is solved by MODFLOW in both space and time such that the solution to the groundwater flow equation satisfies initial conditions and all boundary conditions.

6.3.1 Finite Difference Numerical Method

Finite difference is a numerical method used to obtain approximate solutions to the governing equation, in which a continuous system is broken into discrete points in both space and time and partial derivatives are replaced by the differences in head between these discrete points. MODFLOW uses a block-centered approach with the groundwater flow equation solved for the center of each cell (refer to Figure 6.2). An example of converting a conceptual model into a finite difference grid is provided in Figure 6.3. Cells are defined by their row, column (and by layer in three dimensions). Using the continuity equation all flow into the cell less the flow out of the cell is the change in water stored in the cell. The change in storage is represented as,

$$S_s(\Delta r_j \Delta C_i \Delta V_k) \frac{h_{i,j,k} - h_{i,j,k}^{m-1}}{\Delta t} = S_s(\Delta r_j \Delta C_i \Delta V_k) \left(\frac{h_{i,j,k}^m - h_{i,j,k}^{m-1}}{t^m - t^{m-1}} \right) \quad (6.1)$$

Where S_s is specific storage (1/L); $\Delta r_j \Delta C_i \Delta V_k$ is the cell volume $h_{i,j,k}$ is the head at node i,j,k and Δt is change in time (T). As an approximation of the time derivative at time t^m the head difference is divided by the time interval. Since the head at time t^m is estimated by going backwards in time and using the head preceding it, or head at t^{m-1} , the analysis is termed backward-difference. Flow across all six faces of the cell are accounted for, as are external sources of water (i.e. boundary conditions). As an example of flow across a cell face, refer to Figure 6.4. Flow is calculated entering the cell i,j,k from cell $i,j-1,k$ (along a row), with positive flow assigned to water entering the cell,

$$q_{i,j-\frac{1}{2},k} = K_{x_{i,j-\frac{1}{2},k}} \Delta C_i \Delta V_k \frac{(h_{i,j-1,k} - h_{i,j,k})}{\Delta r_{j-\frac{1}{2}}} \quad (6.2)$$

Where $q_{i,j-\frac{1}{2},k}$ is the volumetric flow rate through the cell face between $i,j-1,k$ and i,j,k (L³/T); $K_{x_{i,j-\frac{1}{2},k}}$ is the hydraulic conductivity along the row between the nodes $i,j-1,k$ and i,j,k (L/T); $\Delta C_i \Delta V_k$ is the area of cell face perpendicular to flow; $h_{i,j-1,k} - h_{i,j,k}$ is the difference in heads between nodes $i,j-1,k$; and i,j,k and $\Delta r_{j-\frac{1}{2}}$ is the distance between nodes $i,j-1,k$ and i,j,k (L). The notation of $\frac{1}{2}$ indicates an effective property for the region between the cell nodes considered, and not a specific point. It is noted, that the default for computing effective hydraulic conductivity between two nodes (in this case $i,j-1,k$ and i,j,k) in MODFLOW is via the harmonic mean (Collins, 1961).

Sources/sinks of water external to the cell are applied as either head dependent, such as through a river bed ($P_{i,j,k} h_{i,j,k}$), or independent of head ($Q_{i,j,k}$), such as recharge.

All flow into and out of the model cell is represented by a set of linear, algebraic difference equations given below,

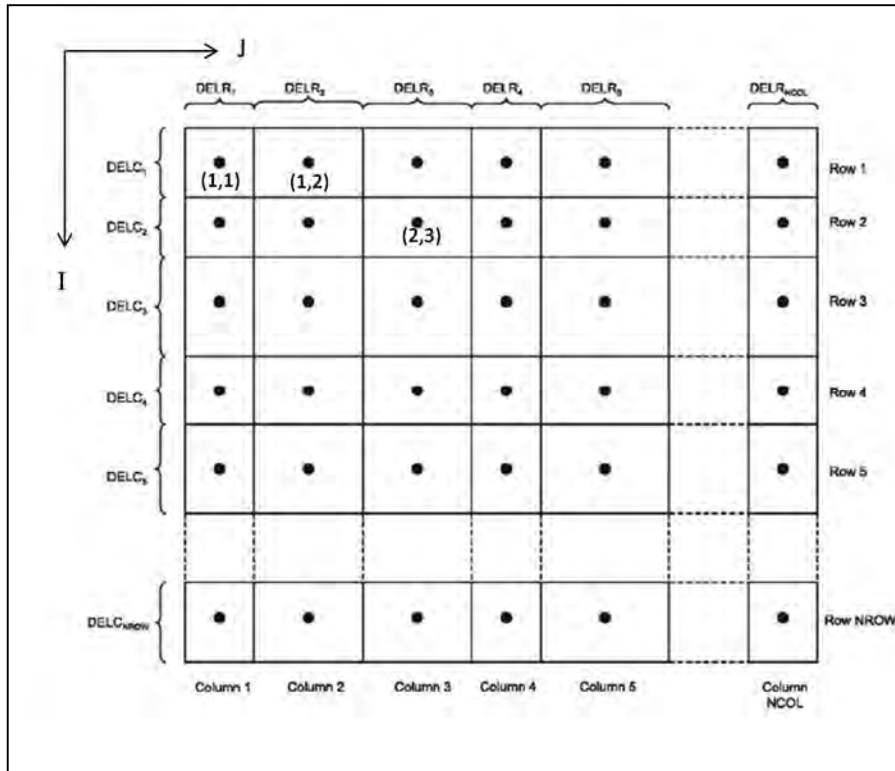


Figure 6.2: A center-blocked grid used in MODFLOW. Discrete points, or nodes, for which the groundwater flow equation is solved are located at the center of user defined cells. Cells are located by position in the grid in terms of row (i) and column (j), with i and j representing indices of cell location (k is the index for the layer if modeling in three dimensions). For reference, a few cells are identified by (i,j) . Cell dimensions are given by $DELR_j$, which is the length of a cell along a row, and $DELC_i$, the length of cell along columns (modified from Harbaugh, 2005).

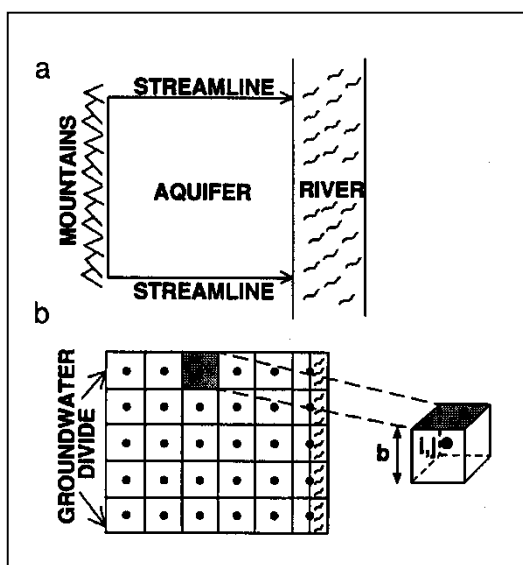


Figure 6.3: (a) A conceptual model and (b) the finite difference grid describing it. The center of each cell represents the location that the groundwater flow equation is approximated (modified from McDonald and Harbaugh, 1988).

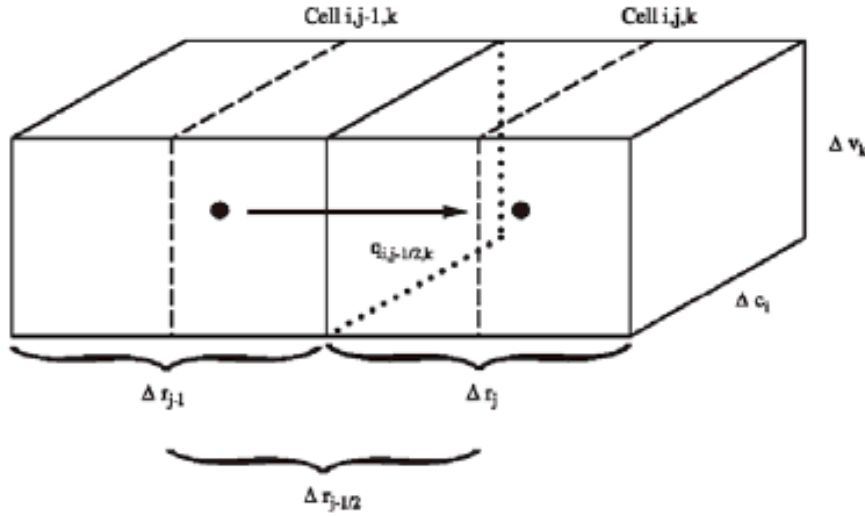


Figure 6.4: Flow into cell i,j,k from cell $i,j-1,k$ (modified from McDonald and Harbaugh, 1988).

$$\begin{aligned}
 & K_{x_{i,j-\frac{1}{2},k}} \Delta c_i \Delta v_k \frac{(h_{i,j-1,k}^m - h_{i,j,k}^m)}{\Delta r_{j-\frac{1}{2}}} + K_{x_{i,j+\frac{1}{2},k}} \Delta c_i \Delta v_k \frac{(h_{i,j+1,k}^m - h_{i,j,k}^m)}{\Delta r_{j+\frac{1}{2}}} + K_{y_{i-\frac{1}{2},j,k}} \Delta r_j \Delta v_k \frac{(h_{i-1,j,k}^m - h_{i,j,k}^m)}{\Delta c_{i-\frac{1}{2}}} + \\
 & K_{y_{i+\frac{1}{2},j,k}} \Delta r_j \Delta v_k \frac{(h_{i+1,j,k}^m - h_{i,j,k}^m)}{\Delta c_{i+\frac{1}{2}}} + K_{z_{i,j,k-\frac{1}{2}}} \Delta r_j \Delta c_i \frac{(h_{i,j,k-1}^m - h_{i,j,k}^m)}{\Delta v_{k-\frac{1}{2}}} + K_{z_{i,j,k+\frac{1}{2}}} \Delta r_j \Delta c_i \frac{(h_{i,j,k+1}^m - h_{i,j,k}^m)}{\Delta v_{k+\frac{1}{2}}} + \\
 & P_{i,j,k} h_{i,j,k}^m + Q_{i,j,k} = S_s (\Delta r_j \Delta c_i \Delta v_k) \left(\frac{h_{i,j,k}^m - h_{i,j,k}^{m-1}}{t^m - t^{m-1}} \right) \quad (6.3)
 \end{aligned}$$

All seven heads at time t^m are unknown making it impossible to solve the single equation 6.3 independently. Unknown heads are highlighted in gray (duplicates of $h_{i,j,k}^m$ are not highlighted). However, if this equation is written for each active cell in the model domain, and there is only one unknown for each cell, then there are n -equations with n -unknowns, and the system of equations can be solved simultaneously.

6.3.2 Grid Design

Grid design is focused on grid orientation, scale and linking the grid to the real-world site. For anisotropic conditions (e.g. fracture flow), grids should be orientated such that axis are collinear with the diagonal terms of the hydraulic conductivity tensor. Figure 6.5 shows grid rotation with respect to the hydraulic conductivity tensor.

If flow is isotropic ($K_x = K_y$), then the grid should be aligned to decrease the number of active cells and to coincide with natural boundaries, such as topographic flow divides, and in the primary direction of flow.

Grid scale is based on the expected change in water level over the model domain. Large change in water levels will require more nodes (more cells). Similarly, the greater the spatial heterogeneity the greater

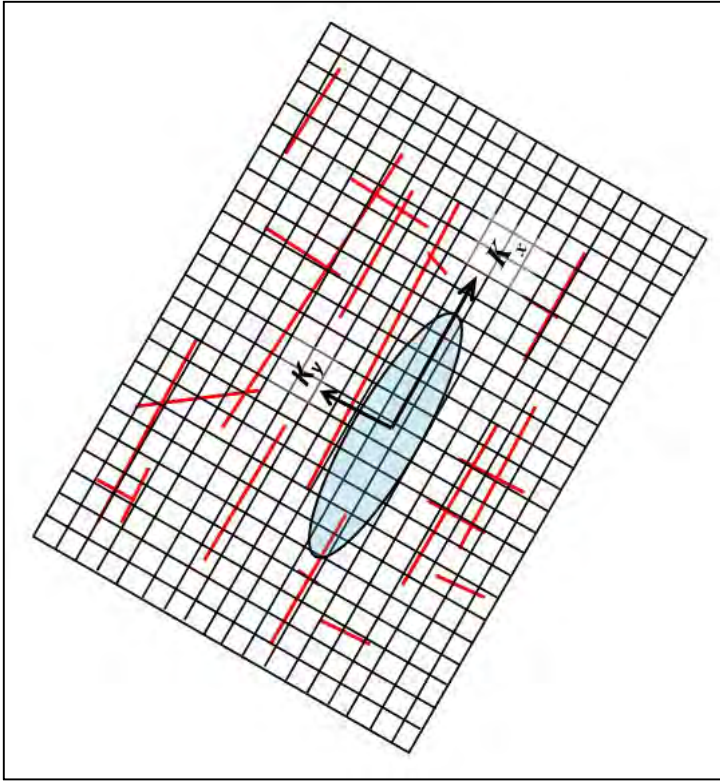
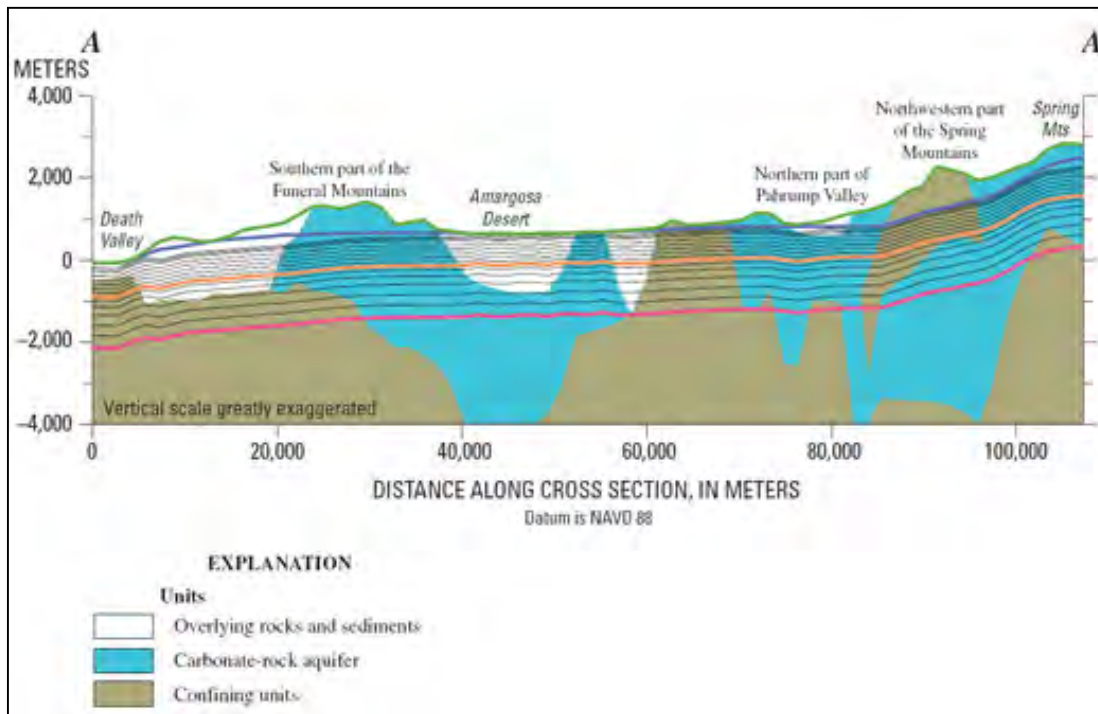


Figure 6.5: Grid orientation based on fracture traces (red lines).

number of nodes needed. It is important to maintain a grid scale that allows proper representation of hydrologic features, including wells, surface water bodies, spatially variable recharge, as well as fault length and thickness. And it is important that the size of the cell adequately portray the representative elementary volume (REV) described in Chapter 3.

Computational efficiency is linked to the number of nodes, with large heterogeneity decreasing efficiency. As a general rule of thumb, less than 10,000 nodes is very efficient, but it's possible to model over 1,000,000 nodes. Only very large and fast computers can handle large numbers of nodes on the order of 20,000,000. Techniques are available to provide a finer resolution but limit the number of cells. This includes finite element modeling and telescopic mesh refinement. However, these techniques are beyond the scope of this manual. In addition, modeling with a single layer is recommended for most slope stability as complexity in model greatly increases with increased model layers. However, it is noted, that vertical discretization can be accomplished independent of geology or can depend on geology (Figure 6.6). If model layering is independent of hydrogeologic units, then it is necessary to define cell parameters with an average, or effective value, for the region of the cell. MODFLOW offers the HUF package to help the user convert hydrogeologic units into effective properties for model execution.



(a) Credit: USGS Geological Survey, Department of the Interior/USGS

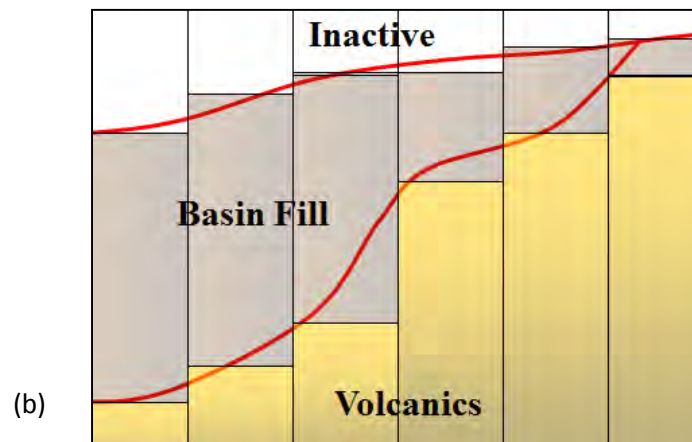


Figure 6.6: Vertical discretization for MODFLOW (a) independent of geology (modified from Belcher et al., 2004) and (b) dependent on geology.

6.3.3 Boundary Conditions and Applied Stresses.

Boundary conditions can be applied at the edges of the model domain, or internal to the domain. Three types of boundary conditions are considered, (1) specified head, (2) specified flux, and (3) head-dependent flux. Specified fluxes and head-dependent fluxes are often termed applied stress.

6.3.3.1 Specified Head Boundary Cells

For most slope stability problems, the specified head boundary conditions is likely assigned to the up- and down-gradient model boundary locations. Specified head boundary conditions are applied to those cells for which MODFLOW does not need to solve heads. Specified head cells are assigned a head value for a specified time for which head does not change. For steady state simulations, or transient simulations for which the specified head does not change in time, these cells are termed constant-head. Specified/constant head cells are often used to describe lakes, rivers, streams, or to observed heads at a significant distance from the region of interest in the model domain. The specified head anchors the solution in space. Without some sort of specified head boundary, the model will not know where to begin the solution. Caution is noted when using a specified head boundary condition, since its value does not change despite possible stresses to the system (e.g. a well pumping large volumes) and can inadvertently represent a nearly inexhaustible source of water. Nor can a specified head change its value, if a large amount of areal flux is applied (i.e. recharge). For these situations, it is recommended to extend specified head boundary conditions well away the region investigated in the model. In this way, boundary condition influence on the model objective is limited.

6.3.3.2 Specified Flux

Specified flux boundary conditions are used when discharge is known and MODFLOW will still solve for head where this flux is specified. There are several types of specified flux conditions, including: no flow, inter-basin flow, pumping/injection wells, and groundwater recharge. In equation 6.3 specified fluxes are denoted by $Q_{i,j,k}$, with positive values indicating water into the cell and negative values indicating water removed from the well.

No-flow cells are those cells for which no water is allowed to enter or exit the cell. In essence, no-flow cells are excluded from the model domain and heads are not estimated with MODFLOW. No flow cells are placed along hydrogeologic divides and bedrock contacts. Delineating model boundaries at the edges of a watershed allows confident use of the no-flow boundary condition and greatly simplifies the number of water budget components necessary to quantify with data. MODFLOW automatically assigns a no-flow boundary if no other boundary type is specified.

The MODFLOW WEL package is used to simulate both wells that are used to withdraw or inject water to the aquifer, as well as simulate inter-basin groundwater fluxes at the margins of the model domain (refer to Figure 6.7 for an example). Water is added (or removed) at a constant rate (L^3/T) for a given stress period in which the rate is independent of the cell's head or the dimensions of the cell. MODFLOW's recharge (RCH) package is used to simulate areally distributed recharge to the

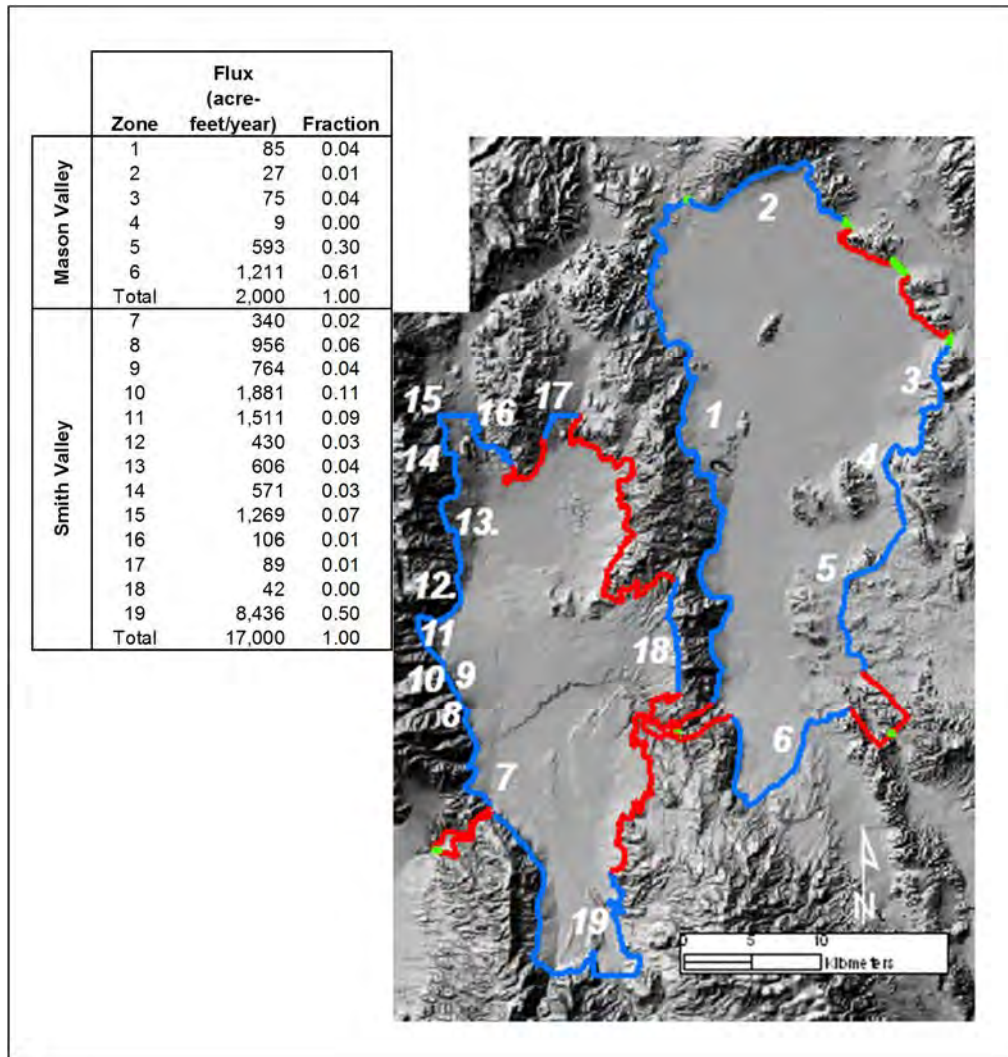


Figure 6.7: Example of boundary conditions applied around the Smith and Mason Valleys, Nevada (Collopy and Thomas, 2009) with red = no-flow, blue = specified flux, and green regions = general head boundaries. Specified fluxes defined using Maxey Eakin (1949) approach to mountain block recharge with computed values provided in the inset by marked zone.

groundwater system. This includes precipitation that percolates to the potentiometric surface. Recharge is applied to the cell as,

$$Q_{r_{i,j}} = R_{i,j} \Delta r_j \Delta c_i \quad (6.4)$$

Given $Q_{r_{i,j,k}}$ is the recharge flow rate applied to cell i,j (L^3/T), and R_{ij} is the recharge flux (L/T) applicable to the mapped area (L^2) of cell ($\Delta r_j \Delta c_i$). Values of R_{ij} are defined by the user for each stress period and applied to one cell in a vertical column of cells. The user can specify recharge to a specific model layer or

allow MODFLOW to apply R_{ij} to the upper most active layer. As a word of caution, if a cell goes dry and if dry cells are forced to be inactive, then the first option will negate any recharge entering the model cell. Therefore, if there is a potential for a model cell to go dry due to changing water levels over time, then the second option is desired to ensure recharge is added to the model. Recharge will only be added to variable-head cells. Recharge is not assigned to cells designated as a constant/specified head or as a no-flow cell.

6.3.3.3 Head Dependent Boundaries

These boundary conditions calculate flux as a function of head difference between the cell and some point inside (or outside) the model domain. Darcy's law (equation 3.13) computes the flux. Several MODFLOW packages exist that support head-dependent boundaries, and a sum of these fluxes into a single MODFLOW cell are represented by $P_{i,j,k} h_{i,j,k}^m$ in equation 6.3. Listed below are those MODFLOW packages that might be useful for modeling water levels in a slope environment susceptible to slope failure.

6.3.3.3.1 Drains

Drains (DRN) in MODFLOW are designed to remove water from the aquifer based on the difference between head in the aquifer and the drain's elevation. Flow into the drain (and out of the aquifer) occurs only when water levels in the aquifer are higher than the drain, and drop to zero when heads drop below the drain elevation (Figure 6.8). The relationship is expressed as

$$Q_d = -C_d(h_{i,j,k} - h_d) \quad \text{when } h_{ijk} > h_d \quad (6.5)$$

$$Q_d = 0 \quad \text{when } h_{ijk} \leq 0 \quad (6.6)$$

Given Q_d is flow out of the aquifer and into the drain, $h_{i,j,k}$ is the head in the aquifer, h_d is the drain elevation and C_d is drain conductance. To understand drain conductance in a physical sense, refer to section 4.2.7: Horizontal Drain Flow Characteristics and Drain Flow.

6.3.3.3.2 General Head Boundary

The general head boundary (GHB) package in MODFLOW simulates flow into/out of a cell based on a proportion of the head difference between the GHB cell and a MODFLOW-computed head. The representative equation is,

$$Q_b = C_b(h_b - h_{d,i,j,k}) \quad (6.7)$$

Where Q_b is the flow into cell i,j,k from the boundary (L^3/T), C_b is the boundary conductance (L^2/T), h_b is the user-defined head in the GHB cell, and $h_{i,j,k}$ is the MODFLOW-computed head (L).

High values of C_b , or large differences in head, will force the GHB cell to act like a specified/constant head cell with no limit on into/out of the model and should be monitored to ensure that fluxes are reasonable. Figure 6.9 illustrates that the relationship between $h_{i,j,k}$, h_b and Q_b . A positive Q_b refers to flow into the aquifer and negative Q_b is flow out of the aquifer.

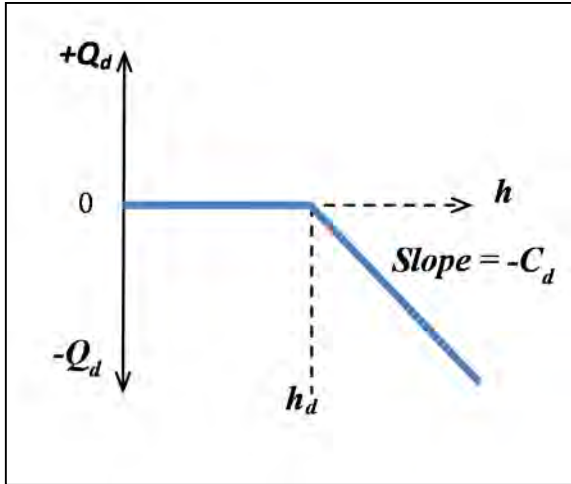


Figure 6.8: Plot of flow to a drain (Q_d) as a function of head in the cell (h), where elevation of the drain is h_d , and the slope of drain flow is $-C_d$ (Modified from McDonald and Harbaugh, 1988).

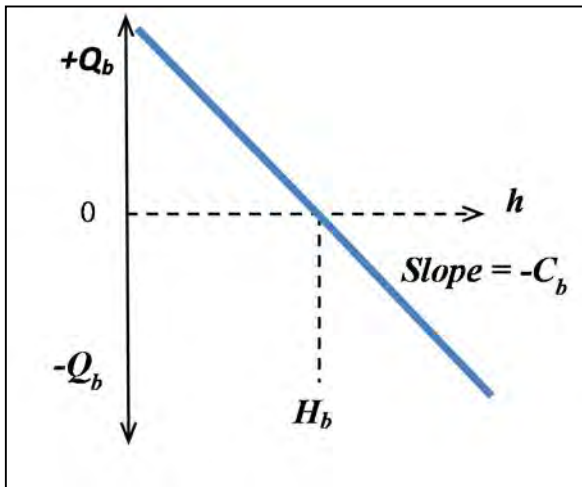


Figure 6.9: Plot of flow into/out of a GHB cell (Q_b) as a function of head in the cell (h), and assigned GHB head h_b , and GHB conductance C_b (Modified from McDonald and Harbaugh, 1988).

6.3.4 Initial Conditions

The initial head distribution across the modeled domain is required for all simulations. For steady state simulations, the choice of initial heads is not critical except the closer the initial head distribution is to the steady state solution, then the quicker the model will converge on a solution. It is also important to make sure the initial heads are all above the bottom of the cell to remove instability issues associated with wetting and drying of model cells. For steady state solutions, it is recommended to set initial heads at the top elevation of the modeled cells.

For transient simulations the choice of initial head is very important. Figure 6.10 shows a simulation in which initial heads are not well defined (Model 1), and more accurately defined (Model 2). Initial heads are determined by either interpolating observed water level data across the modeled domain for the time period representing the start of the model, or using modeled steady state head distributions. Steady state conditions are generally assumed to represent average conditions; such as mean water level for a long period of record, mean annual water level or mean water level for a specific period of

time. The latter is really a quasi-steady state condition and can be assumed to occur during the relatively dry periods in the year when little precipitation occurs, or when very consistent precipitation occurs over a significant period of time and observed hydrographs are fairly stable. It's analogous to baseflow conditions in a stream.

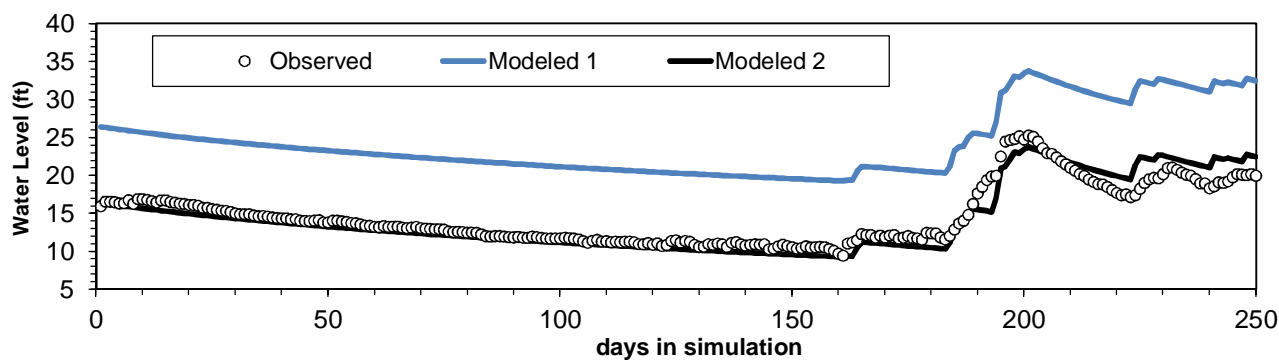


Figure 6.10: An example of transient water levels in an observation well and model results. Model 1 initial conditions are too high. Model 2, initial conditions are more realistic.

6.3.5 MODFLOW Numeric Solvers

MODFLOW provides several solvers, and which solver to use is problem dependent. For most non-linear problems, such as unconfined conditions, the geometric multi-grid (GMG) solver is appropriate (Wilson and Naff, 2004). For unconfined situations where fluctuation of the water table results in wetting and drying of model cells, the newly created Newton-formulation of MODFLOW, or MODFLOW-NWT is required (Niswonger et al., 2011). Refer to the cited documents for a full description of the approaches used by either solver. Example problems in Chapter 7 highlight the solver used and parameter choices.

6.4 Calibration Strategies

Calibration refers to adjusting model parameters to best match observed data. Calibration strategies can range from fairly simple to very complex and generally improve with modeling experience. Hydraulic properties, as well as boundary conditions and stresses can be altered to reproduce simulated heads and fluxes that best match field measured values. Measured parameters, as well as expected ranges in parameter values, constrain how much adjustment in a calibration parameter is acceptable. Calibration is sometimes referred to as the “inverse problem”, in which observed heads are used to obtain parameter values, versus known parameter values used to predict groundwater heads.

Calibration can be done in either steady state or transient simulations. In general, steady state model calibration focuses on adjusting hydraulic conductivity to best match steady state head distributions. Likewise, the basic conceptual model can be evaluated. For example, if model calibration is only possible with unrealistic parameter values, then the conceptual model must be revisited. It may be

necessary to modify existing boundary conditions, include additional water sources or sinks, reconsider system heterogeneity, or incorporate a geologic feature that was left out of the original model.

Transient calibration generally focuses on storage parameters to match water level response to change in stress. Decreasing storage will increase water level response, while increasing storage will mute the response. Figure 6.11 provides an example of how specific yield impacts observed water level response to a precipitation event. In addition, it is not uncommon that the steady state calibrated hydraulic conductivity needs further adjustment in the transient simulation. In this circumstance, the steady state calibrated hydraulic conductivity value acts as an initial guess. Drain conductance (C_d) is likewise adjusted to match drain outflow. If necessary, drain elevations (h_d) can also be tweaked given the uncertainty in elevation with drilling practice. A difference of only a few feet can significantly impact drain response.

Model calibration is qualitatively assessed by matching observed and predicted contour maps of groundwater head. It is important that flow paths observed are reproduced in the model. Quantitative assessment of calibration success is accomplished when the calibration target is simulated within an acceptable level of error. A calibration target is a measured, observed, calculated or estimated hydraulic head or groundwater flow rate that the model must reproduce (within a range of acceptable error) for the model to be considered calibrated (ASTM D5981, 1996). Uncertainty in the calibration target

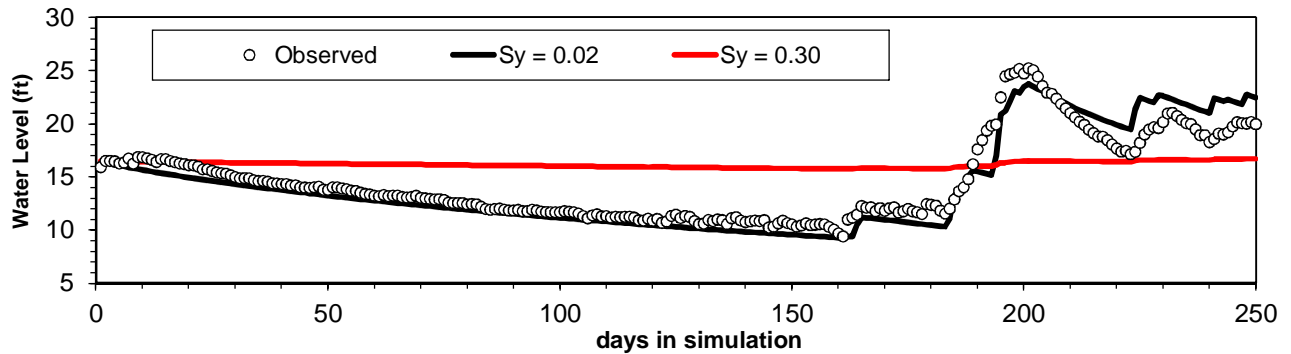


Figure 6.11: An example of changing specific yield (S_y) in transient calibration. Observed water levels are better replicated with $S_y = 0.02$ compared to $S_y = 0.30$.

should also be considered, so that excessive effort is not expended in trying to perfectly match a target that is highly uncertain. Error is often measured using the root mean-squared error (*rmse*),

$$rmse = \left[\frac{1}{n} \sum_{i=1}^n (h_p - h_o)^2 \right]^{0.5} \quad (6.8)$$

Where h_p and h_o are the predicted and observed heads, and n is the number of observed data. Error assessment is subjective to project objectives; however, error greater than 10% is often indicative of a

poor model, 5-10% is acceptable, while less than 5% is a very good model. An example of error assessment is provided using Figure 6.11, the *rmse* for S_y equal 0.02 and 0.30 is 1.3 ft and 3.9 ft, respectively. Normalized by the difference in observed minimum and maximum head (15.8 ft), this equates to 8% and 24% error, respectively. Model results for $S_y = 0.02$ more accurately represents observed water levels by reducing error compared to $S_y = 0.30$.

The *rmse* criterion for successful model calibration is limited to the average error in the model and can hide portions of the model that are poorly predicted. It is important for model error to be randomly distributed across the domain and not show any specific trend. Figure 6.12 provides an example of unbiased and biased error. Figure 6.12 demonstrates a one-to-one plot of observed versus predicted water and a plot of residuals (observed – predicted). For the un-biased results, error is randomly distributed about the 1:1 line (or residual = 0). For the biased example, error increases with increased observed water level, with the model increasingly under-predicting water levels at larger and larger observed values. If heads are consistently too high or too low in a particular region of the model, then boundary conditions may need to be adjusted, or eliminated, to remove the bias. If the source of error cannot be isolated, then additional field data should be collected to improve conceptual understanding of the system being modeled.

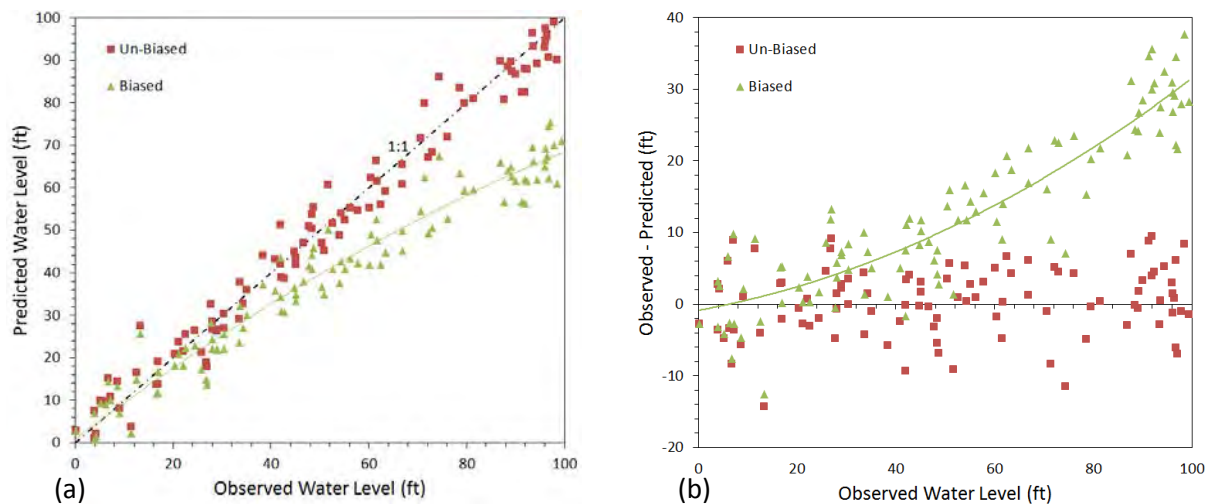


Figure 6.12: An example of biased an un-biased model error represented in a (a) one-to-one plot (b) plot of residuals.

Calibration can be achieved using manual trial and error by adjusting one parameter at a time, or using sophisticated auto-calibration techniques that are available. Both are discussed within the context of an application in the Appendix B – Groundwater Modeling Tutorials. Caution is noted that just because calibration targets are met, that the model is valid. This is because groundwater model calibration rarely produces a unique solution. Instead, many different combinations of parameter values may result in an equal solution. Uncertainty is exacerbated if little data exists to constrain parameters values, little

observed water level or flux data exist, or water level data are poorly distributed across the model domain. If calibration error is clearly defined, then at least interpretation is possible of uncertainty distribution in the model and of predicted water level values. In the end, a calibrated model clearly demonstrates the ability to reproduce observed data. Verification will test the model's ability to predict future behavior.

6.4.1 Sensitivity Analysis

A sensitivity analysis is the process of changing one parameter in the model at a time and re-computing the error function. The purpose is two-fold. First, it can determine the best parameters to use in the calibration process. Parameters that have the greatest impact on model output make better calibration parameters than those parameters less sensitive. Secondly, a sensitivity analysis is the most rudimentary uncertainty analysis one can perform. It allows some quantification of uncertainty in modeled response if parameters are adjusted over expected ranges. Figure 6.13 gives an example of a typical graph displaying sensitivity of recharge, specific yield and hydraulic conductivity. Each parameter is adjusted independently between -50% and +50% of their calibrated value (calibrated value is 0% change in input parameter). The calibrated value should fall at the global minimum for all parameters (minimum *rmse*). In this example, model output is more sensitive to recharge than specific yield. Hydraulic conductivity is non-unique with two minimum *rmse*. One *rmse* minimum occurs at a lower hydraulic conductivity than the chosen calibrated value. Final choice of the hydraulic conductivity value is decided with field and/or laboratory data, or using expert judgment. It is also notable, that the system is insensitive to hydraulic conductivity at larger values, such that K_x values 10% larger than the calibrated value produce no appreciable increase or decrease in the error function.

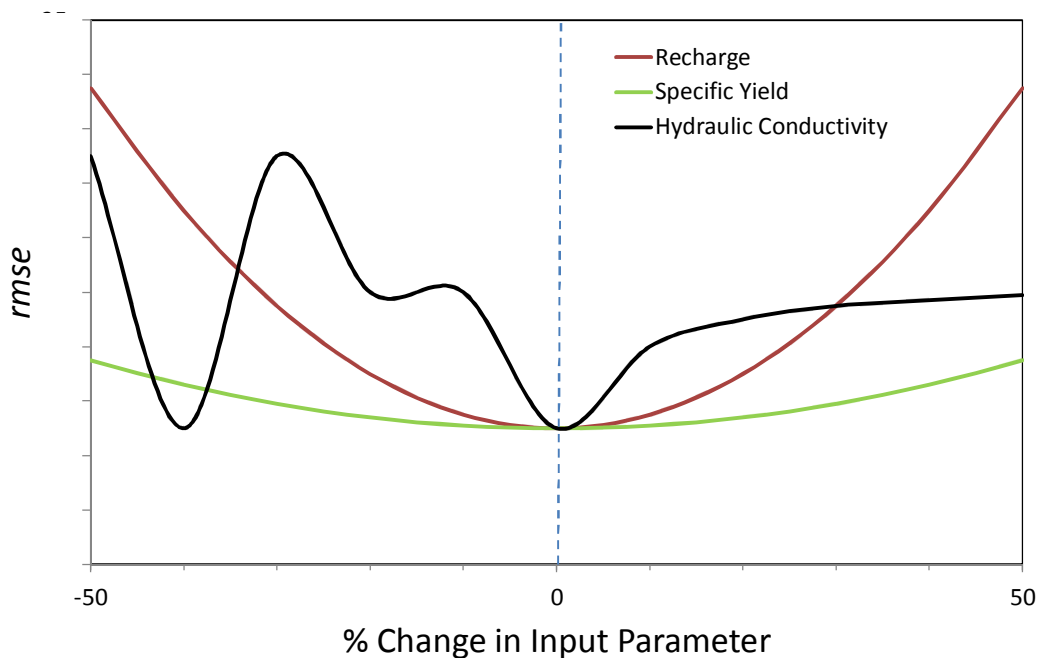


Figure 6.13: An example of a sensitivity analysis looking at influence of independent adjustment of recharge, specific yield and hydraulic conductivity on *rmse*.

Independent adjustment of parameters will likely fail to capture covariance between parameters. Figure 6.14 provides a contour map where two normalized, hypothetical parameters, X_1 and X_2 , are adjusted simultaneously. Error is represented as 1-unit contour lines. The solution space is convoluted with a dip in error occurring near the one-to-one negative correspondence for X_1 and X_2 . The resulting global minimum for the parameter ranges (space) evaluated occurs at 0.6 the range for X_2 and 0.3 for the range modeled for X_1 . Complexity arises in that a ridge of high error occurs for low values of X_2 that is relatively insensitive to low values of X_1 , while a local minimum also occurs at high X_1 and high X_2 . Negotiating a complex solution space becomes increasingly complex with more and more parameters included in the calibration strategy. Sensitivity analysis is one way to decipher what level of complexity arises, what parameters can be disregarded in the calibration process, and if a parameter needs to be

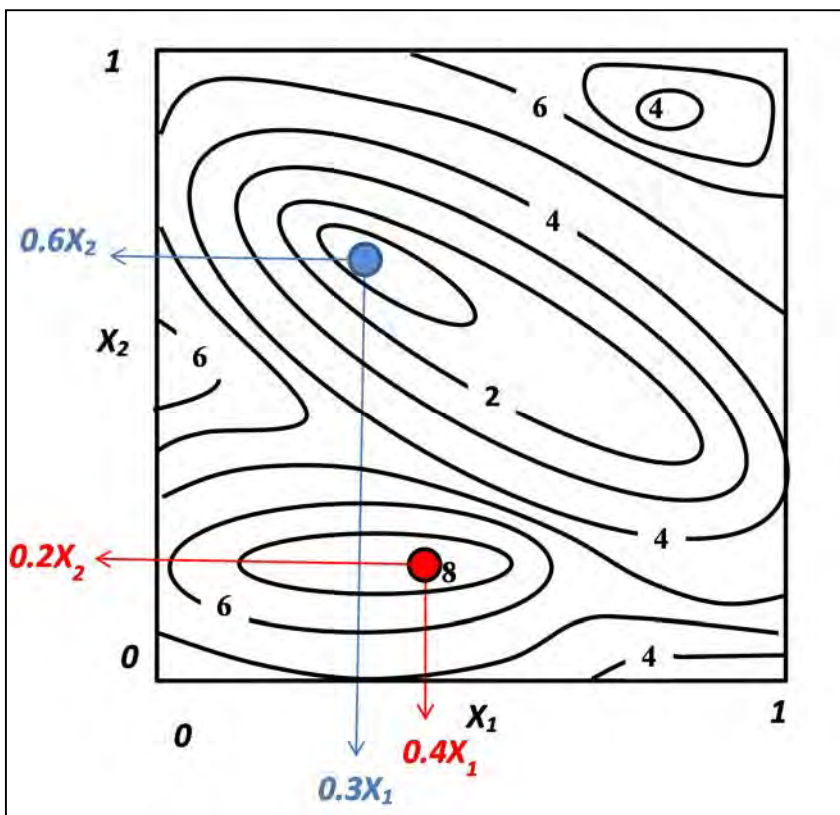


Figure 6.14: Error (e.g. *rmse*) in model prediction given simultaneous adjustment of hypothetical parameters X_1 and X_2 . Range in parameter values are normalized (0 to 1), while contours are given in 1-unit intervals. The blue-circle represents the global minimum value in error for the parameter spaces considered. The red-circle is the global maximum.

included, then how to quantify this uncertainty. Complex solutions spaces, and/or multiple calibration parameters are very difficult to assess through trial-and-error approaches. Instead, sophisticated optimization algorithms can negotiate complex solution spaces fairly efficiently. Implementation of one of these algorithms is discussed in the tutorial section of the manual on auto-calibration (refer to Appendix C).

6.4.2 Verification

A well calibrated model will reproduce observed behavior for which the model is calibrated. However, the other purpose of a model typically is to predict future behavior in which boundary conditions and applied stresses are different than those used in the calibration process. Verification is a test of the model's robustness over different scenarios, and if verification is successful, will provide confidence in the calibration and the ability of the model to replicate system behavior over a range of applied stresses. In order to perform a verification of the model, a subset of available data that was not used in the calibration process is used. Ideally, this second set of data corresponds to very different hydrologic conditions. For instance, if the calibration data corresponds to water levels for an average water year, then water level data for a drought year can serve as a verification data set. If water level data is limited, then one can use a secondary set of data for the same calibration time period. For instance, if drain conductance is adjusted to help match observed water level response, then correlation of observed and modeled drain flow can serve as an independent verification. If the model fails to reproduce the second set of data, then the modeler may need to revisit the conceptual model and revise calibration strategies

6.5 References Cited

- ASTM-D5981-96. 1996. Standard Guide for Calibrating a Ground-Water Flow Model Application. American Society for Testing and Materials. ASTM Committee D-18 on Soil and Rock, Subcommittee D18.21 on Ground Water and Vadose Zone Applications. 100 Barr Harbor Dr., West Conshohocken, PA 19428. Annual Book of ASTM Standards.
- Anderson, M.P., and W.W. Woessner, 1992. Applied Groundwater Modeling: Simulation of Flow and Advective Transport. Academic Press, San Diego, CA. ISBN 0-12-059485-4. 381 p.
- Belcher, W, R., D'Agnese, F.A., and G.M. O'Brian, 2004. Introduction. Chapter D of Death Valley Regional Groundwater Flow System, Nevada and California – Hydrogeologic Framework and Transient Groundwater Flow Model. U.S. Geological Survey Scientific Investigations Report 2004-5205. Pp. 3-20.
- Collins, R.E., 1961. Flow of fluids through porous materials. New York, Reinhold Publishing Corp., 270 p.
- Callopy, M.W. and J.M. Thomas, 2009. Restoration of a Desert Lake in an Agriculturally Dominated Watershed: The Walker Lake Basin. Bureau of Reclamation Report. 1092 p.
- Harbaugh, A.W. 2005. MODFLOW-2005: The U.S. Geological Survey modular ground-water model—the Ground-Water Flow Process: U.S. Geological Survey Techniques and Methods 6-A16, variously p.
- Harbaugh, A.W., and M.G. McDonald, 1996. User's documentation for MODFLOW-96, an update to the U.S. Geological Survey modular finite-difference ground-water flow model: U.S. Geological Survey Open-File Report 96-485, 56.

- Harbaugh, A.W., Banta, E.R., Hill, M.C., and M.G. McDonald, 2000. MODFLOW-2000, The U.S. Geological Survey modular ground-water model -- User guide to modularization concepts and the Ground-Water Flow Process: U.S. Geological Survey Open-File Report 00-92, 121 p.
- Maxey, G. B. and T. E. Elkin, 1949. Ground water in White River Valley, White Pine, Nye, and Lincoln Counties, Nevada. No. 8, State of Nevada Office of the State Engineer prepared in cooperation with the United State Department of the Interior Geological Survey, Carson City, Nevada.
- McDonald, M.G. and A.W.Harbaugh, 1988. A modular three-dimensional finite-difference ground-water flow model: U.S. Geological Survey Techniques of Water-Resources Investigations, book 6, chap. A1, 586 p.
- Niswonger, R.G., Panday, S., and M. Ibaraki, 2011. MODFLOW-NWT, A Newton Formulation for MODFLOW-2005. Groundwater Resources Program. Techniques and Methods 6-A37. 44p.
- Washington State Department of Transportation (WSDOT). 2000. Eldon Landslide: Geotechnical Study of the Eldon Vicinity Landslide Adjustment to Hood Canal. SR-101, MP 321, C.S. 2303. Reviewed by T. M. Allen, State Engineer, and S.M. Lowell, Chief Engineering Geologist. 9 pp.

Chapter 7

Horizontal Drain Design

7.1 Introduction

While significant research has occurred with respect to the characterization and function of drainage systems, most of this work has focused on irrigation systems with relatively shallow slopes and been fairly qualitative in its assessment. Often drainage design is based on experience from past installations, rather than on hydraulic conductivity and quantitative assessment using drainage equations or numeric analysis. Merva (1984) stated that drainage design is often a trial-and-error procedure, while Willardson (1982) recognized that adequate estimates for hydraulic conductivity and drainage coefficients are difficult to obtain and largely selected based on tradition and local experience. Forrester (2001) provided very useful guidance to geotechnical designers on the use of horizontal drains for slope stability, but did not offer methodology on evaluating the efficacy of drains for a particular site or a quantitative design method to determine the location, type or number of drains. In fact, little to no quantitative procedural guidelines are published on drain placement with the goal of increasing slope stability during rapid rises in pore pressures. Every drainage problem is unique, in which experience and expert opinion cannot be superseded. However, a more quantitative framework for drain design can aid practitioners to improve drainage performance and to reduce ad hoc decision making.

The proposed methodology for drain design is given in Figure 7.1, and shows a preliminary analysis followed by an iterative procedure between hydrogeologic and geotechnical analysis for slope stability. Prior to hydrogeologic analysis, it is necessary to characterize the site (described in Chapter 4) and develop a design storm to test system response to a large event (described in Chapter 5). The technical aspects of groundwater influences on slope stability are given in Chapter 2. The basics of groundwater hydrology and groundwater modeling are provided in Chapters 3 and 6, respectively. Important factors controlling success or failure of drain design, the initial feasibility study as well as quantitative analyses using analytical, graphical and numerical techniques, are provided in this chapter.

7.2 Controlling Factors of Drainage Design

Many factors can influence the effectiveness of a drainage system, which can be grouped into the following categories:

- aquifer characterization,
- aquifer recharge/response to precipitation,
- drainage system design,
- construction methods, and
- maintenance

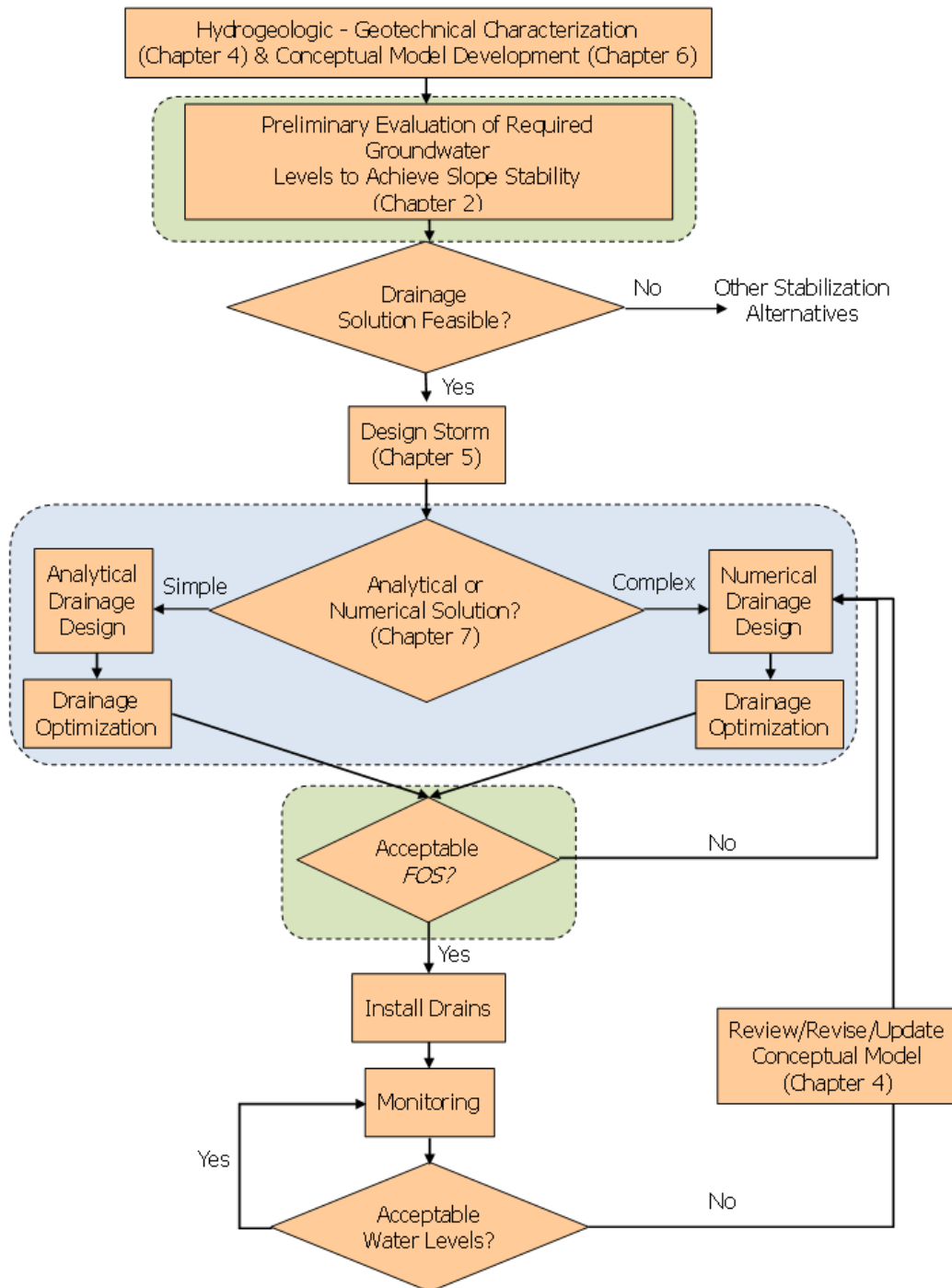


Figure 7.1: Methodology for drain design to promote slope stability that iterates between hydrogeologic analysis (blue region) and slope stability analysis (green region).

This chapter focuses on effectiveness of drainage system design, primarily considering drain length, elevation, spacing and efficiency, as a function of aquifer characteristics and storm events. To demonstrate the importance of each of these variables, an idealized cross section is presented with a linearly sloping ground surface that drops in elevation from 300 ft to 75 ft over a distance of 1000 ft distance (slope of 12.7°). Figures 7.2, 7.3, and 7.4 show the impact of drain length, elevation and spacing, respectively, on water table elevations under steady state recharge using MODFLOW. Site parameters are assigned isotropic with $K = 1 \text{ ft/d}$, $R = 0.01 \text{ ft/d}$ and drain hydraulic conductivity equal to that of the geologic material (i.e. 1 ft/d).

In Figure 7.2, all drains are installed at the toe of slope, and are installed at the toe of slope. As drain length increases, water table elevations drop.

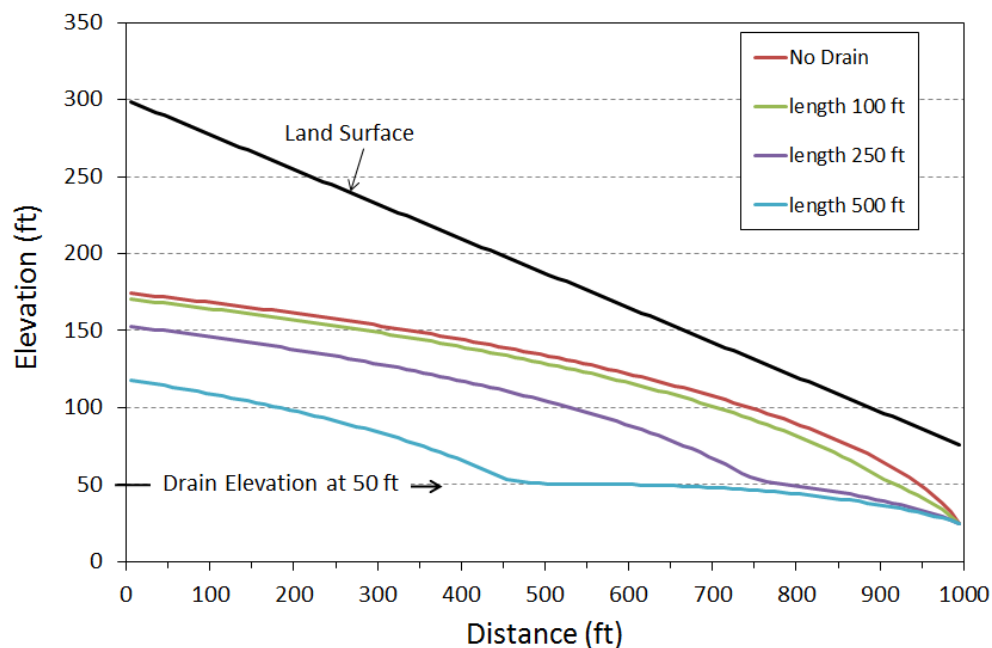


Figure 7.2: Water table elevations in an idealized cross section as a function of drains with different lengths. All drains are installed at the toe of slope at an elevation of 50 ft, with the bottom of the geologic unit at an elevation of 0 ft. Water levels results obtained using MODFLOW.

In contrast, Figure 7.3 shows that increasing the elevation of a drain will reduce the maximum drop in water table. Drains are installed at an elevation of 50 ft, 100 ft and 150 ft and extend 500 ft into the slope. Drains located at the lowest elevation facilitate the greatest lowering of water table elevations. For the example provided, the drain installed at an elevation of 50 ft, or the toe of the slope, is more effective at lowering water levels compared to a drain installed upslope at an elevation of 150 ft.

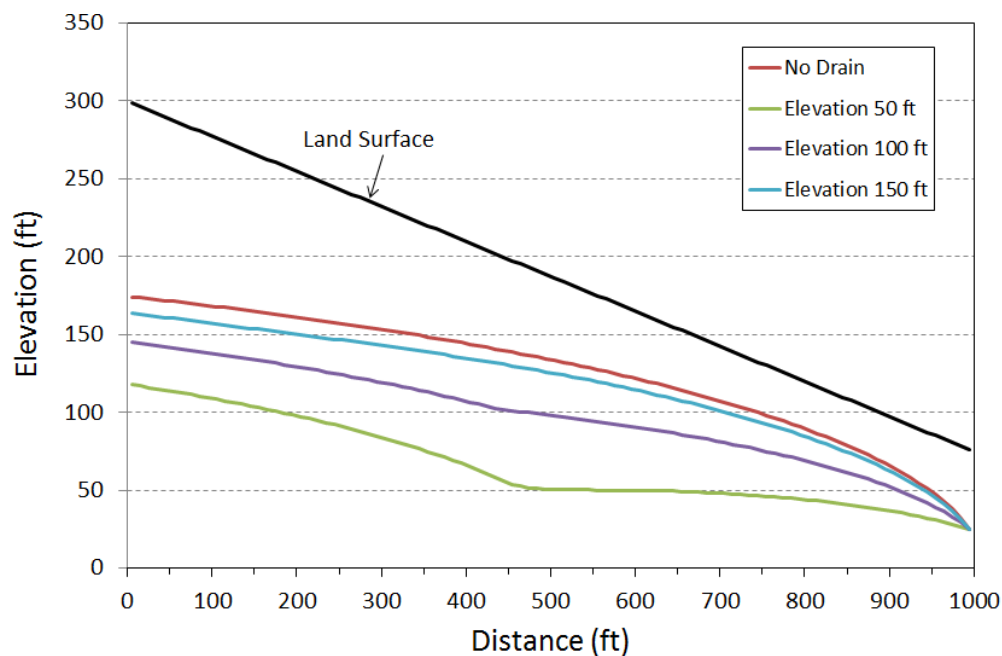


Figure 7.3: Water table elevations in an idealized cross section given drain elevations of 50 ft, 100 ft and 150 ft and extending 500 ft into the slope.

Rahardjo et al., 2003 performed a rigorous measurement campaign combined with numerical modeling to determine the effectiveness of horizontal drains for slope stability. One of the key findings is that shallow drains, or drains running parallel and near the ground surface, are ineffective in improving the stability of a slope. In other words, drains installed in the vadose zone are generally ineffective at capturing recharge from precipitation events. Instead, drains are most effective when placed at the lowest elevation possible. The basic tenet is to lower the main water table, with less emphasis placed on direct capture of infiltration. If installed a significant distance into the slope at the lowest possible elevation, drains will capture the majority of groundwater and have the largest effect on lowering the water table. These results are also consistent with the research findings of Lau and Kenney (1984) and Martin et al., 1994. Parametric studies have also shown that drains located in the upper region of a slope are of no real significance if additional deeper drains are in the lower part of a slope. The water table will eventually be reduced to the lowest drain level and any drains above the bottom drain will no longer be effective. With the overall lowering of the water table, the upper drains serve only as

interceptor drains during large events, and Rahardjo et al. (2003) found these drains ineffectual. The only exception to this rule might be for site conditions where significant perched water table conditions can develop. If a low permeability layer exists at depth, precipitation events may induce a perched water table, which may cause the slope to fail.

The findings of Rahardjo, et al. (2003) are important when considering which type of model is best for drainage design. If water table position is the most important aspect of slope stability and the physical processes and matric pressures within the vadose are judged to be less significant, then one can rely on saturated models for use in drainage design. This significantly reduces the complexity of the analysis and may allow for the use of analytical solutions for many field conditions. One still has to determine the net infiltration that contributes to groundwater recharge following a precipitation event, but this analysis can most likely be de-coupled from the groundwater analysis.

Figure 7.4 tests drain spacing, with drains drilled parallel to the slope strike. Drain direction is dictated by the one-dimensional aspect of MODFLOW simulation. In other words, the model consists of a single cross section with no aerial considerations. The drain layout, however, is typical of all analytical approaches. For an example of drain layout, refer to Figure 7.5 for drains installed at 250 ft intervals. As expected, given equal recharge and hydraulic characteristics of the site, decreasing the drain spacing will lower water table elevations.

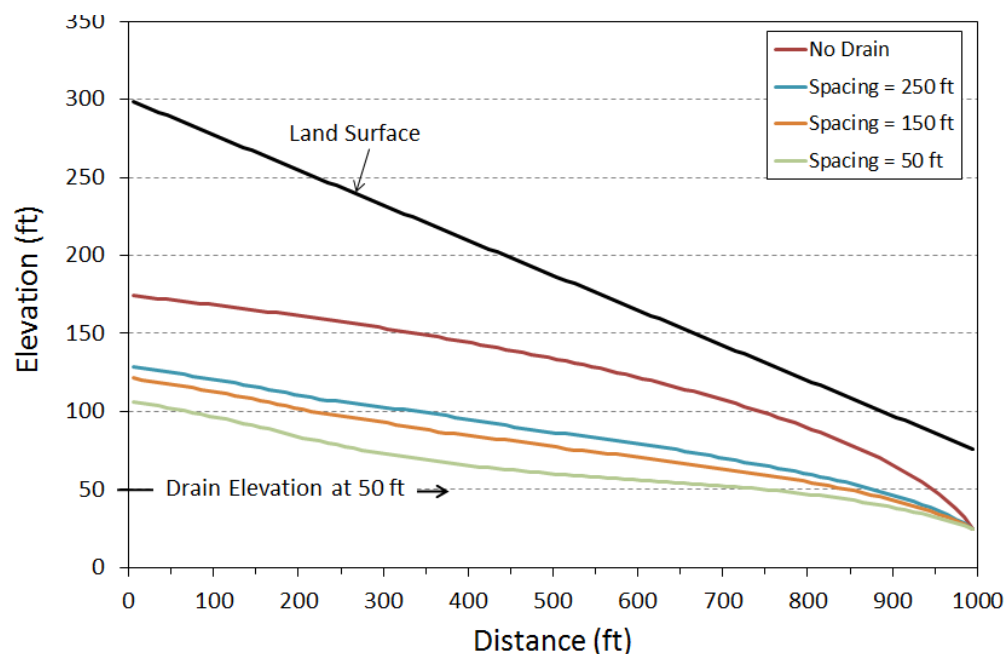


Figure 7.4: Water table elevations in an idealized cross section with for different drain spacing. Drains are parallel to the slope strike (into the page) and all are located at an elevation of 50 ft.

Water level response to drain placement is also a function of site characteristics. Specifically, hydraulic conductivity, specific yield (for transient simulations) and recharge rates are important to drainage design, and need to be considered. Figure 7.5 shows water table profiles for a range of hydraulic conductivity and recharge rates given a drain spacing of 250 ft. Water table elevations will rise with increased recharge and/or decreased hydraulic conductivity. Drain design will need to adjust to accommodate for variable hydraulic properties. Similarly, Figure 7.6 provides water table elevations as a function of K and R, but given a single drain extending from the toe of the slope and into the geologic material. Properly quantifying K and R become important to understanding aquifer response to drain design.

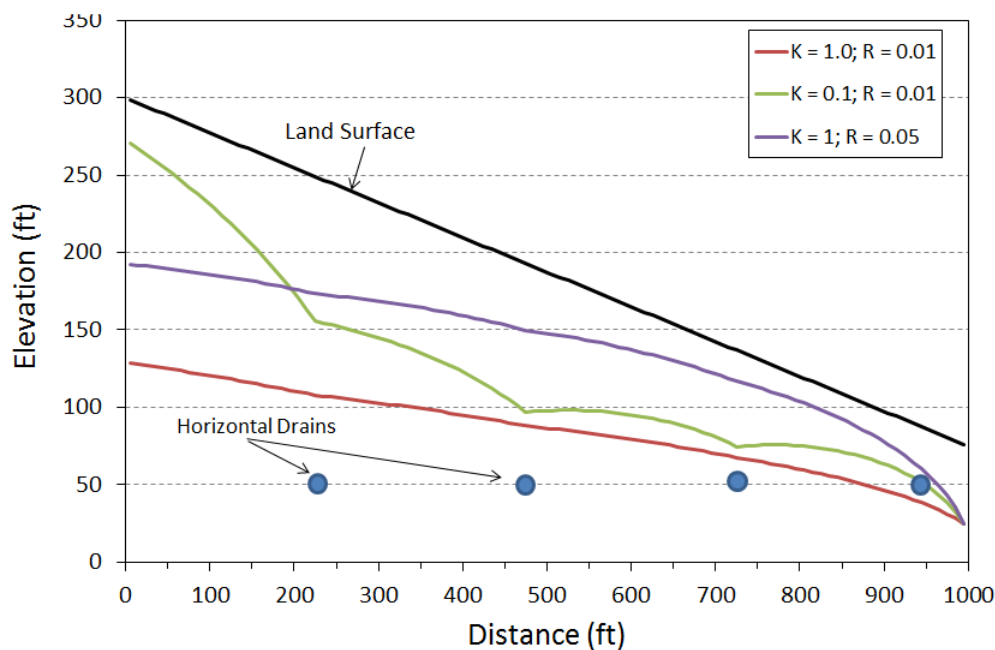


Figure 7.5: Water table profiles as a function of hydraulic conductivity (K) and recharge rate (R). Units are in feet per day. Drain spacing is 250 ft at an elevation of 50 ft and into-the-page. Drains are shown as blue circles.

7.3 Preliminary Analysis

The preliminary analysis requires an estimate of the critical water level for which FOS = 1.0. This is done along the primary of the slope. Data requirements include a pre-defined failure surface, the friction angle, cohesion, unit soil weight, unit saturated soil weight and layer thickness for each hydrostratigraphic unit. Choice of analysis methods are provided in chapter 2, and it is recommended one compare several methods to ensure a convergence on the estimated critical water level for which slope failure is eminent.

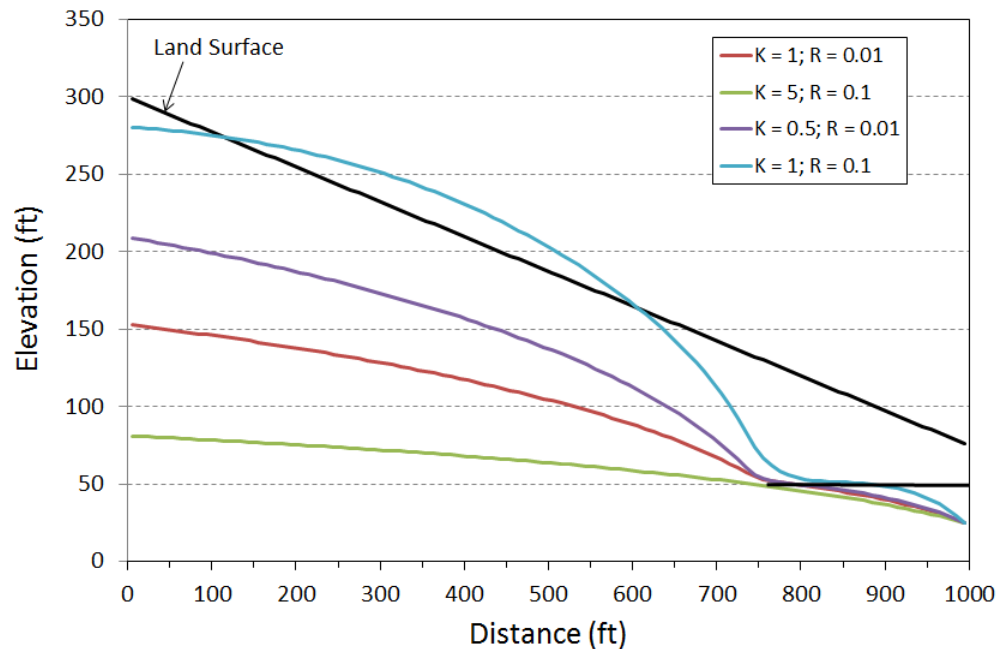


Figure 7.6: Water table profiles as a function of hydraulic conductivity (K) and recharge rate (R). Units are in feet per day. Drain length is 250 ft at an elevation of 50 ft. Drain is shown as a thick black line originating at the toe of slope.

Once the critical water level is defined, the question posed in the Figure 7.1 flow chart, “Is a drainage solution feasible”? At this juncture, one must assess the conductance of materials, storage potential and recharge rate of the site. As displayed in Figure 7.5 and 7.6, feasibility of horizontal drains to stabilize systems is significantly reduced with a combination of low K, large R, and an estimated critical water level at significant depth. If the system also has a low storage potential (low S_y) and is highly anisotropic, the feasibility of a drainage solution further diminishes. However, if ambiguity in feasibility arises, then one should proceed forward in the analysis with either an analytical or numerical approach to drainage design.

7.4 Analytical Equations

Analytic equations represent mathematical models with a closed form solution. In order to maintain a closed form solution, these equations are limited by many simplifying assumptions. For example, these equations require simple geometry, homogeneous and isotropic conditions, and simple boundary conditions. A numeric model is also a mathematical model, but can relax some of the simplifying assumptions necessary to solve an analytic equation. This can be done because numeric models compute an approximation to the solution through a time-stepping procedure that attempts find successively better approximations to the roots of the real-valued function (e.g. Newton-Raphson method). In other words, the solution to an analytic model is exact while the solution to a numeric model is an approximation. .

Site complexity will determine if one chooses an analytical or numerical approach to modeling hydrogeologic response to storm events and impact on horizontal drain design. Conditions that mandate a numerical approach include an irregular drain network, heterogeneous aquifer properties and fractured systems. Analytical solutions assume that drains are installed perpendicular to the hillslope. This assumption is immediately invalidated by practical installation procedures that often situate horizontal drains into steep slopes as fan-networks. Analytical solutions, however, can provide the designer a first-cut at quantitatively assessing possible drainage configurations and should not be discounted as a viable means for design.

7.4.1 Steady-State Conditions

Steady-state conditions are those that represent a system in equilibrium. These conditions are not indicative of episodic events but greatly simplify the approach. The applicability is that steady-state recharge can represent a baseline boundary condition and resulting water levels, while storm calculated recharge can provide worst-case scenario for storm related water levels. The latter is not realistic because large precipitation events do not last long and the slope system never reaches a steady-state condition. Assuming steady-state for a storm event will over-estimate water level elevations. However, such estimates can provide insight to system response as long as the practitioner is cognizant of these limitations.

Steady-state analytical approaches are provided for both flat and sloped surfaces.

7.4.1.1 Hooghoudt Equation (Flat Surface)

Hooghoudt (1940) developed the first design equations for subsurface drainage conditions and this approach is still used today. The Hooghoudt methodology calculates steady state drawdown for a given recharge rate per unit area, R (L/T). Recharge and drainage are assumed to occur simultaneously and do not change with time. Drains are installed in a flat system, at equal depth and are assumed parallel. The approach is dependent on horizontal groundwater flow and the existence of an impermeable layer at relatively shallow depths. Parallel drain spacing (L_d) is calculated using Wesseling (1973) formulation in SI units,

$$L_d = \sqrt{\frac{8H_m}{R} (K_2 d_e + K_1 H_a)} \quad (7.1)$$

Parameters in Equation (7.1) are shown in Figure 7.7. K_1 is hydraulic conductivity above the drains and K_2 is hydraulic conductivity below the drains. Homogenous systems assume $K = K_1 = K_2$. H_m is the height of the water table midway between the drains (m), and H_a is $H_m/2$ or the average height of the water table above the drain (m). The equivalent depth, d_e (m), accounts for convergent flow toward the drain (refer to Figure 4.17). As flow converges toward a drain, flow is no longer horizontal but acquires a longer flow path with greater head loss required for the same volume of water flowing into the drain.

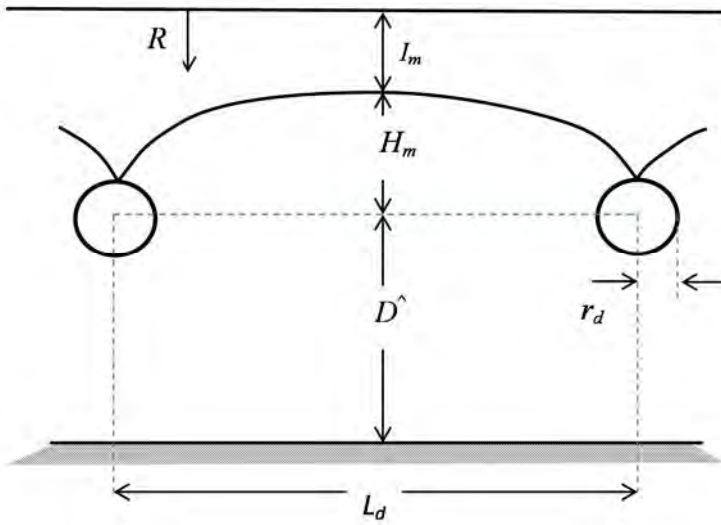


Figure 7.7: Hooghoudt (1940) parameters for estimating drain spacing in steady state, flat surfaced systems with a parallel drain network.

The greater head loss results in a higher water table elevation. In addition, greater head loss occurs with a smaller wetted perimeter of the drain. To maintain the Dupuit's assumption of horizontal flow, Hooghoudt (1940) replaced the actual thickness to the impervious layer ($D^$) below the drain, with a smaller equivalent depth (d_e), through which flow will travel to reach the drain. The higher flow per unit area introduces additional head loss, which is equivalent to losses caused by converging flow lines.

The equivalent depth is dependent on the depth ($D^$) of the impermeable layer below the drains and the radius of the drain (or drain and envelope material, r_d). Hooghoudt (1940) published several tables for common-sized pipes. As an example, Table 7.1 gives d_e for $r_d = 0.1$ m and incremental values of $D^$ and L_d , using graphs provided in Figures 7.8 and Figure 7.9, or to use the following approximations.

$$d_e = \frac{D^}{1 + \frac{D^}{L_d} (2.55 \ln \left(\frac{D^}{r_d} \right) - c)}; \quad \text{for } D^/L_d \leq 0.31 \quad (7.2a)$$

$$d_e = \frac{L_d}{(2.55 \ln \left(\frac{L_d}{r_d} \right) - 1.15)}; \quad \text{for } D^/L_d > 0.31 \quad (7.2a)$$

Where

$$c = 3.55 - 1.6 \frac{D^}{L_d} + 2 \left(\frac{D^}{L_d} \right)^2 \quad (7.3)$$

The value of d_e increases with $D^$ until $D^$ is approximately $1/4 L_d$, after which d_e remains relatively constant. For depths greater than $1/4 L_d$, little additional impact occurs on drain spacing as a result of convergent flow toward drains.

Since drain spacing (L_d) is a function of equivalent depth, which is a function of drain spacing, the only way to solve Hooghoudt's equation is either use nomographs Van Beers (1979), to iterate manually via trial and error, or to set up a solver in a spreadsheet application.

Table 7.1: Effective depths (d_e) for various drain spacings (L_d) and depths of impermeable layer below drain (D) for a drain with an effective radius of $r_d = 0.1$ m. Table adopted from the U.S. Department of the Interior (1978) and uses $D = D^*$ and $L = L_d$.

L →	5 m	7.5	10	15	20	25	30	35	40	45	50	L →	50	75	80	85	90	100	150	200	250
D												D									
0.5 m	0.47	0.48	0.49	0.49	0.49	0.50	0.50	0.50	0.50	0.50	0.50	0.5	0.50	0.50	0.50	0.50	0.50	0.50	0.50	0.50	0.50
0.75	0.60	0.65	0.69	0.71	0.73	0.74	0.75	0.75	0.75	0.76	0.76	1	0.96	0.97	0.97	0.97	0.98	0.98	0.99	0.99	0.99
1.00	0.67	0.75	0.80	0.86	0.89	0.91	0.93	0.94	0.96	0.96	0.96	2	1.72	1.80	1.82	1.82	1.83	1.85	1.90	1.92	1.94
1.25	0.70	0.82	0.89	1.00	1.05	1.09	1.12	1.13	1.14	1.14	1.15	3	2.29	2.49	2.52	2.54	2.56	2.60	2.72	2.70	2.83
1.50	0.70	0.88	0.97	1.11	1.19	1.25	1.28	1.31	1.34	1.35	1.36	4	2.71	3.04	3.08	3.12	3.16	3.24	3.46	3.58	3.66
1.75	0.70	0.91	1.02	1.20	1.30	1.39	1.45	1.49	1.52	1.55	1.57	5	3.02	3.49	3.55	3.61	3.67	3.78	4.12	4.31	4.43
2.00	0.70	0.91	1.08	1.28	1.41	1.5	1.57	1.62	1.66	1.70	1.72	6	3.23	3.85	3.93	4.00	4.08	4.23	4.70	4.97	5.15
2.25	0.70	0.91	1.13	1.34	1.50	1.69	1.69	1.76	1.81	1.84	1.86	7	3.43	4.14	4.23	4.33	4.42	4.62	5.22	5.57	5.81
2.50	0.70	0.91	1.13	1.38	1.57	1.69	1.79	1.87	1.94	1.99	2.02	8	3.56	4.38	4.49	4.61	4.72	4.95	5.68	6.13	6.43
2.75	0.70	0.91	1.13	1.42	1.63	1.76	1.88	1.98	2.05	2.12	2.18	9	3.66	4.57	4.70	4.82	4.95	5.23	6.09	6.63	7.00
3.00	0.70	0.91	1.13	1.45	1.67	1.83	1.97	2.08	2.16	2.23	2.29	10	3.74	4.74	4.89	5.04	5.18	5.47	6.45	7.09	7.53
3.25	0.70	0.91	1.13	1.48	1.71	1.88	2.04	2.16	2.26	2.35	2.42	12.5	3.74	5.02	5.20	5.38	5.56	5.92	7.20	8.06	8.68
3.50	0.70	0.91	1.13	1.50	1.75	1.93	2.11	2.24	2.35	2.45	2.54	15	3.74	5.20	5.40	5.60	5.80	6.25	7.77	8.84	9.64
3.75	0.70	0.91	1.13	1.52	1.78	1.97	2.17	2.31	2.44	2.54	2.64	17.5	3.74	5.30	5.53	5.76	5.99	6.44	8.20	9.47	10.4
4.00	0.70	0.91	1.13	1.52	1.81	2.02	2.22	2.37	2.51	2.62	2.71	20	3.74	5.30	5.62	5.87	6.12	6.60	8.54	9.97	11.1
4.50	0.70	0.91	1.13	1.52	1.85	2.08	2.31	2.50	2.63	2.76	2.87	25	3.74	5.30	5.74	5.96	6.20	6.79	8.99	10.7	12.1
5.00	0.70	0.91	1.13	1.52	1.88	2.15	2.38	2.58	2.75	2.89	3.02	30	3.74	5.30	5.74	5.96	6.20	6.79	9.27	11.3	12.9
5.50	0.70	0.91	1.13	1.52	1.88	2.20	2.43	2.65	2.84	3.00	3.15	35	3.74	5.30	5.74	5.96	6.20	6.79	9.44	11.6	13.4
6.00	0.70	0.91	1.13	1.52	1.88	2.20	2.48	2.70	2.92	3.09	3.26	40	3.74	5.30	5.74	5.96	6.20	6.79	9.44	11.8	13.8
7.00	0.70	0.91	1.13	1.52	1.88	2.20	2.54	2.81	3.03	3.24	3.43	45	3.74	5.30	5.74	5.96	6.20	6.79	9.44	12.0	13.8
8.00	0.70	0.91	1.13	1.52	1.88	2.20	2.57	2.85	3.13	3.35	3.56	50	3.74	5.30	5.74	5.96	6.20	6.79	9.44	12.1	14.3
9.00	0.70	0.91	1.13	1.52	1.88	2.20	2.57	2.89	3.18	3.43	3.66	60	3.74	5.30	5.74	5.96	6.20	6.79	9.44	12.1	14.6
10.00	0.70	0.91	1.13	1.52	1.88	2.20	2.57	2.89	3.23	3.48	3.74	∞	3.88	5.38	5.76	6.00	6.26	6.82	9.55	12.2	14.7
∞	0.71	0.93	1.14	1.53	1.89	2.24	2.58	2.91	3.24	3.56	3.88										

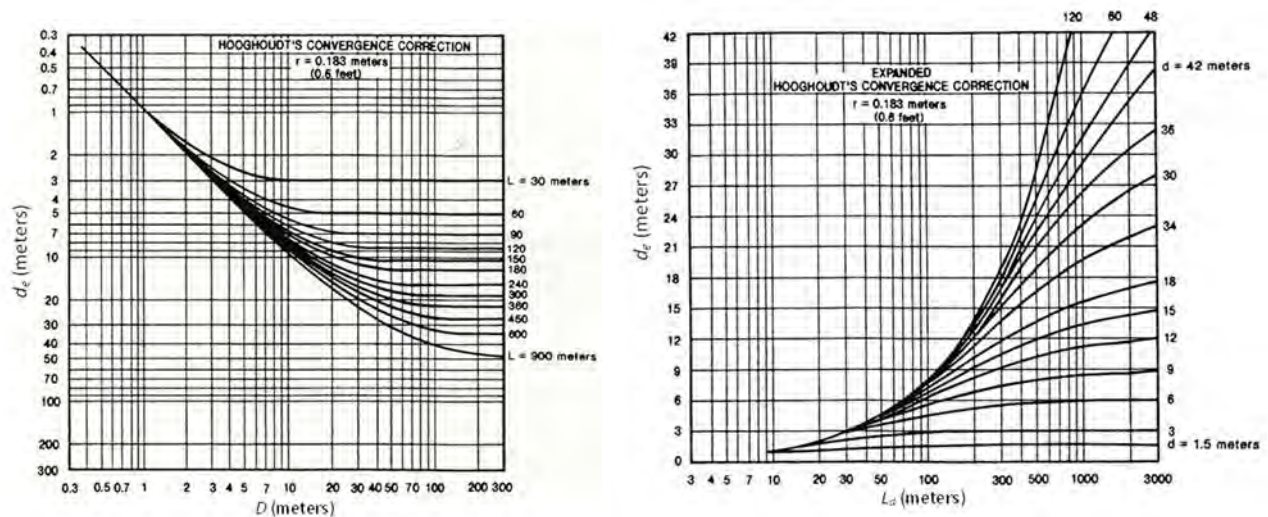


Figure 7.8: Curves for determining Hooghoudt's convergence correction for a drain radius of 0.6 ft, metric units (Adopted from U.S. Department of the Interior, 1978).

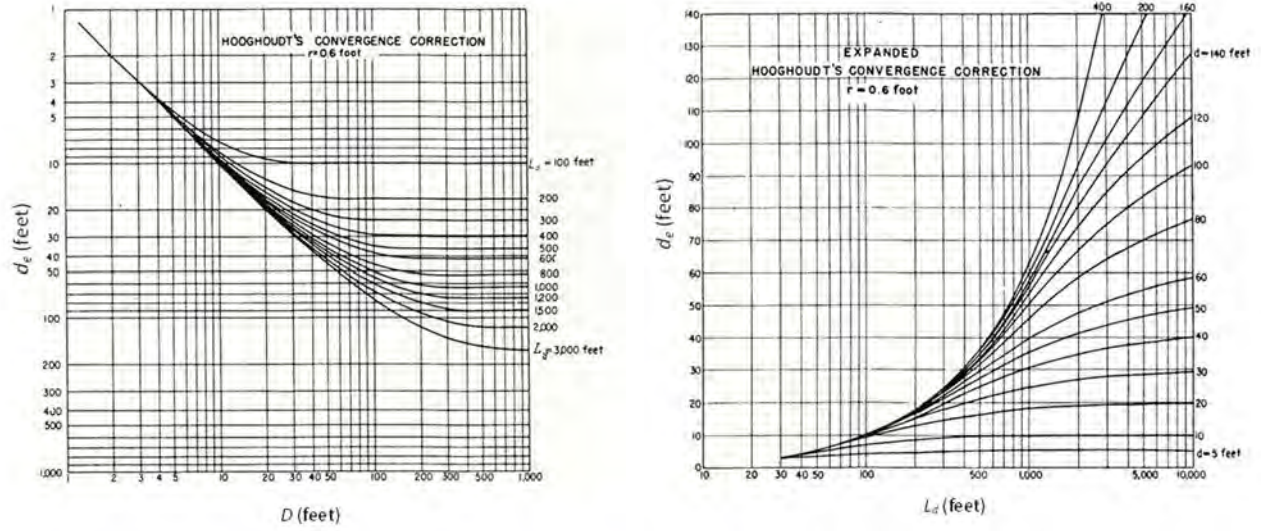


Figure 7.9: Curves for determining Hooghoudt's convergence correction for a drain radius of 0.6 ft, English units. (Adopted from U.S Department of the Interior, 1978)

As an example, to find the depth to water table (I_m) based on $D^* = 5$ m, $L_d = 30$ m, $r_d = 0.1$ m,

$$d_e = (30/8) / \{ [(30-8*1.41)^2 / (8*30*5)] + (1/3.14) * \ln(30/(0.1*1.41)) \} = 2.38$$

The effective depth is more than 50% less than the actual depth, and agrees with Table 7.1.

Rearranging equation 7.2 to produce a quadratic equation using H_m

$$\frac{K_1}{2} (H_m)^2 + K_2 d_e H_m - \frac{R(L_d)^2}{8} = 0 \quad (7.3)$$

And the solution roots become,

$$H_m = \frac{-K_2 d_e + \sqrt{(K_2 d_e)^2 + 4 \left(\frac{K_1}{2} \right) \left(\frac{R(L_d)^2}{8} \right)}}{K_1} \quad (7.4)$$

With depth to maximum water table surface calculated as,

$$I_m = B - H_m - D^* \quad (7.5)$$

Where B is the total thickness of the sediment.

Since the equivalent depth d_e and the drain spacing L_d are functions of each other, the problem is iterative. However, one can and solve with the steps given below.

1. Determine/estimate hydraulic conductivity (K).

2. Determine/estimate design storm recharge (R).
3. Set the elevation of the drain above the impermeable layer (D^{\wedge})
4. Assume a drain spacing (L_d) and drain radius (r_d)
5. Calculate d_e as a function of r_d , D^{\wedge} and L_d .
6. Solve H_m via a quadratic root
7. Solve for $I_m = B - H - D^{\wedge}$
8. Is the drain spacing reasonable to keep I_m below the critical water surface as determined in the preliminary analysis (section 7.3)?

Note that the solution is steady state and is not dependent on the initial water level. In addition, the assumption of steady state, in essence, is very conservative as it assumes that the system is in equilibrium with the design storm recharge.

Figure 7.10 illustrates Hooghoudt output using an iterative approach. For the example, the geologic layer susceptible to failure is 20 ft thick and the critical water surface determined in the preliminary analysis is land surface ($I_m = 0.0$ ft). In Figure 7.10a, drain location is at an intermediate depth (20 ft) and hydraulic conductivity is allowed to vary. For equal drain depth, lowering K decreases drain spacing considerably such that silty materials and till require drains of approximately 20 ft to maintain a water table elevation below the critical water surface ($I_m > 0$). Such a tight drain configuration is likely not feasible. In contrast, well sorted sands may not require drains. Figure 7.10b assumes a silty, fine sand hydraulic conductivity and varies drain depth. Drain spacing decreases dramatically as drains become increasingly shallow. Drains located at a depth of 18 ft may require drains at 100 ft increments, while drains placed only 2 ft below land surface may require spacing on the order of 25 ft. Changes toward a thinner geologic layer and/or higher recharge rate will reduce drain spacing more.

7.4.1.2 Slopes Less than 10°

Dupuit-Forchheimer (DF) assumptions state that groundwater movement is (1) parallel to the slope and (2) horizontal. While the first DF assumption holds under most slope conditions, the second DF assumption is only maintained for gentle slopes. Guitjens and Luthin (1965) conducted a complete set of experiments to test solutions and determine under what conditions the DF assumptions break down given steady state infiltration. Chauhan et al. (1968) and Childs (1971) suggest DF assumption 2 is invalidated at slopes in the range of 8-10%. Luthin and Guitjens (1967) repeated their experiments for transient conditions and found that flow to ditches, water table elevation, and the rate of water table decline were independent of slope for slopes less than 30%. Likewise, Fipps and Skaggs (1989) investigated steady-state drainage of hillslopes up to 40% and found that slopes less than 15% had little effect on drain flow rates and water table depths in the center location between drains. For these relatively shallower slopes, flat-surfaced assumptions can be maintained with little error

The U.S Department of the Interior (1978) defines a methodology for drain spacing valid for slopes less than 10%. While drain spacing is assumed to not change for these slopes in comparison to horizontal surfaces, the location of the first transverse drain can be computed by mapping the water table surface

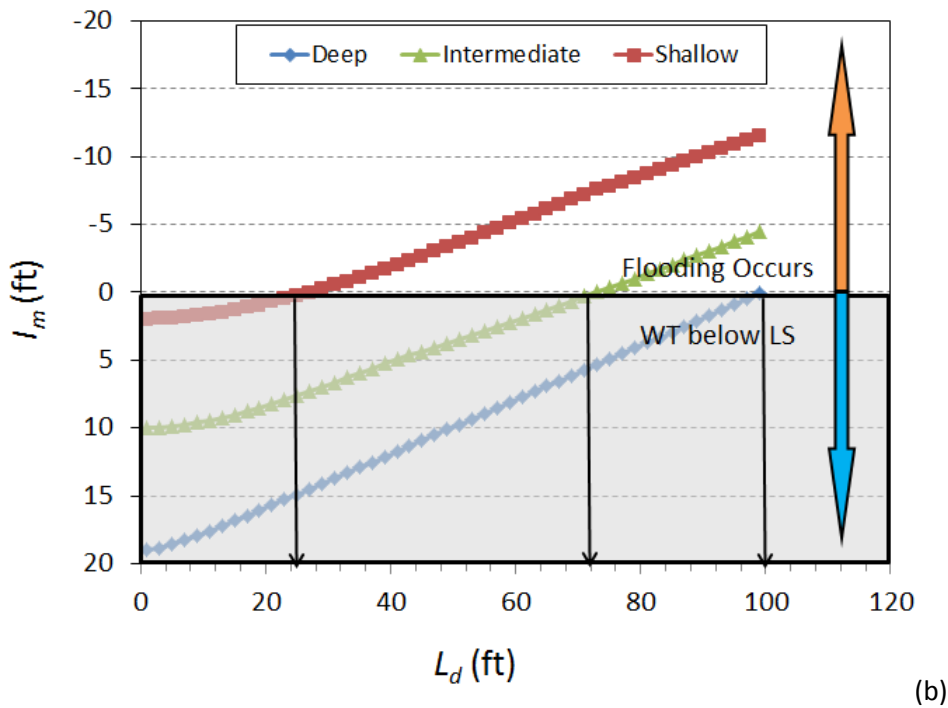
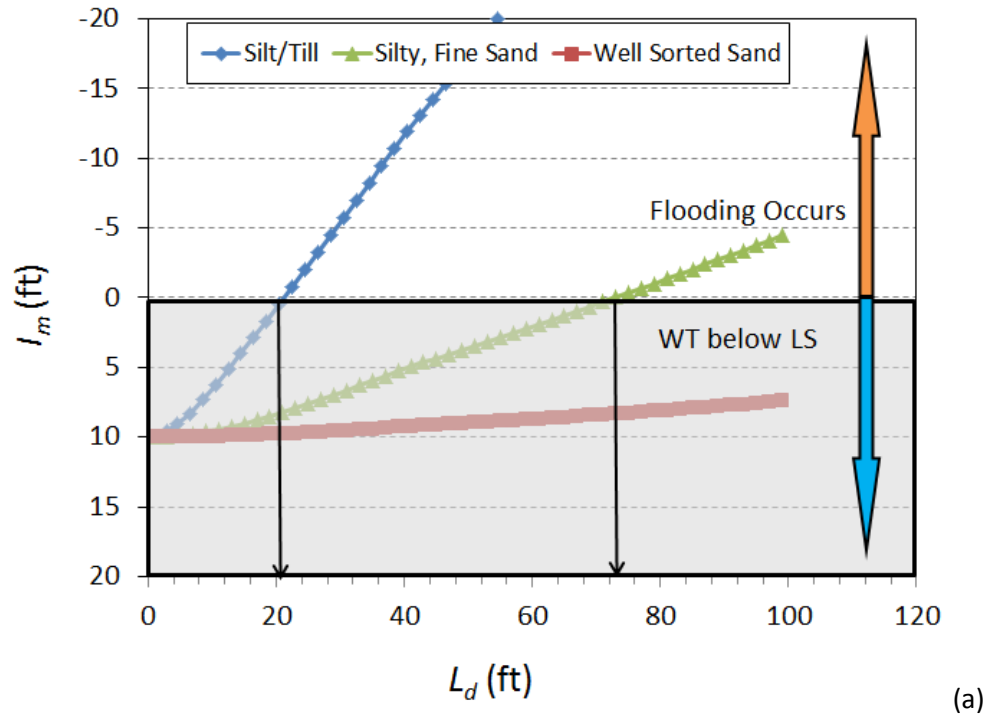


Figure 7.10: Examples of Hooghoudt calculated minimum depth to water table (I_m) assuming a recharge rate of 0.161 ft/d, and drain diameter $r_d = 0.3$ ft, (a) drain depth set to 10 ft below land surface and hydraulic conductivity is varied (b) hydraulic conductivity set to equal a silty, fine sand and drain depth varied. Water table elevations rise above land surface when $I_m \leq 0$ m, and surpasses the estimated critical surface.

with graphical techniques. To illustrate the graphical procedure, Figure 7.11 gives profiles based on i/KS_b^2 , h/S_bL and X/L , where S_b is the slope of the impermeable barrier, X is distance along the slope (L), L is the total length of the slope (L), i = deep infiltration from irrigation (synonymous with recharge, R) and h is the height above the barrier.

A design question could be asked as to where should the first drain be placed if drains are installed 2.44 m below ground surface and depth to maximum water table (l_m) is not to exceed 1.22 m? To demonstrate, an example is provided with parameters defined as $K = 1.22$ m/d, $L = 457$ m, $i = R = 0.00068$ m/d (stead state), $S^* = 0.03$ (land surface slope), $S_b = 0.27$, aquifer depth at the top of the slope is 7.32 m and at the bottom of the slope is 5.94 m (refer to Figure 7.12). Therefore,

$$\frac{i}{KS_b^2} = \frac{R}{KS_b^2} = \frac{0.00068}{(1.22)(0.027)^2} = 0.76 \quad (7.6)$$

From Figure 7.11, the water table surface for $\frac{R}{KS_b^2} = 0.76$ lies just above the line depicting 0.75. Table 7.2 provides values for $\frac{h}{S_bL}$ for increasing values of X/L . From these normalized values, one can solve for X and h knowing S_b and L . For example, water levels at $X/L = 0$, and $\frac{R}{KS_b^2} = 0.76$ produces an $\frac{h}{S_bL} = 0.335$. Solving, $h = 4.13$ m above the barrier. Given a barrier depth of 7.32 m at $X = 0$, the depth from land surface of the water table is $7.32 - 4.13 = 3.2$ m. At $X=0$, land surface is at 0 m and the depth to the barrier is given as 7.32 m. Therefore, the depth from land surface to the water table surface is $(0 + 7.32) - 4.13 = 3.2$ m. This falls below the established 2.44 m for drain depth.

A follow-up question might be, at what distance from the up-gradient edge ($X=0$) does natural groundwater flow force the water table to reach 2.44 m below ground surface? Referring to Table 7.2, at $X/L = 0.058$, $\frac{h}{S_bL} = 0.3885$. Using $X = 0.058 * L = 0.058 * 457 = 26.5$, and $h = (0.027)(457)(0.3885) = 4.77$ m, and the depth to the barrier at $X_{26.5m} = 7.32 + S_b(26.5) = 8.03$ m, the depth to the water table is close to 2.44 m. Therefore, no water will enter a drain placed between $X = 0$ and 26.5 m at a depth of 2.44 m below land surface. When the water table reaches 2.44 m depth at $X=26.5$ m, it is the same effect as placing a drain at this location, and is treated as a virtual drain.

To maintain a minimum depth to land surface of 1.22 m, which corresponds to a maximum height above the drain elevation (H_m) of 1.22 m, the steady-state Hooghoudt method for flat surfaces will suffice for slopes up to 10%. Again, the approach is iterative, since drain spacing L_d depends on the effective depth d_e , and d_e is dependent on drain spacing. The steps are as follows:

1. Assume a drain spacing (L_d) of 300 m as an initial guess.
2. Drain spacing begins where the water table reaches 2.44 m depth, or $X=26.5$ m.
3. Since the slopes for land surface and barrier are not equal, it is necessary to calculate an average thickness (B_{avg}) of the aquifer between $X = 0$ m and $X = L_d + 26.5$ m = 326.5 m: $B_0 = 7.32 - 0 = 7.32$ m and $B_{326.5} = (7.32 + S_b(326.5)) - (0 + S_a(326.5)) = 6.38$ m. Therefore $B_{avg} = 6.85$ m.
4. The average depth below the drains is the average thickness of the aquifer less the depth that drains are placed (2.44 m). $D_{avg}^{\wedge} = 6.85 - 2.44 = 4.41$ m.

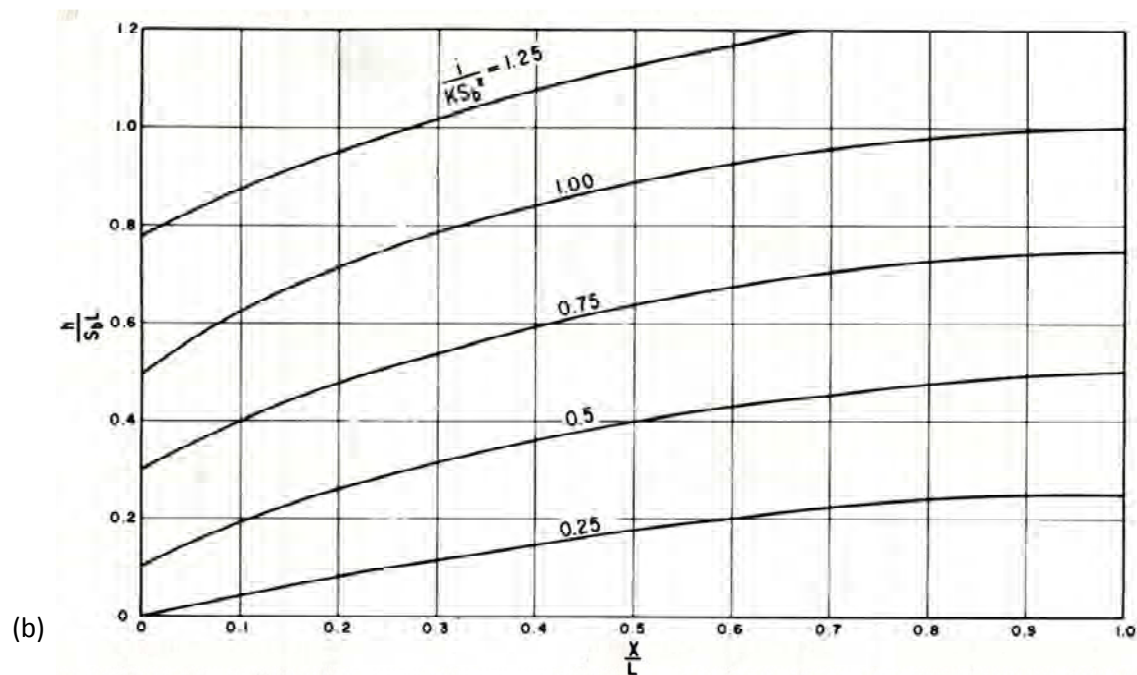
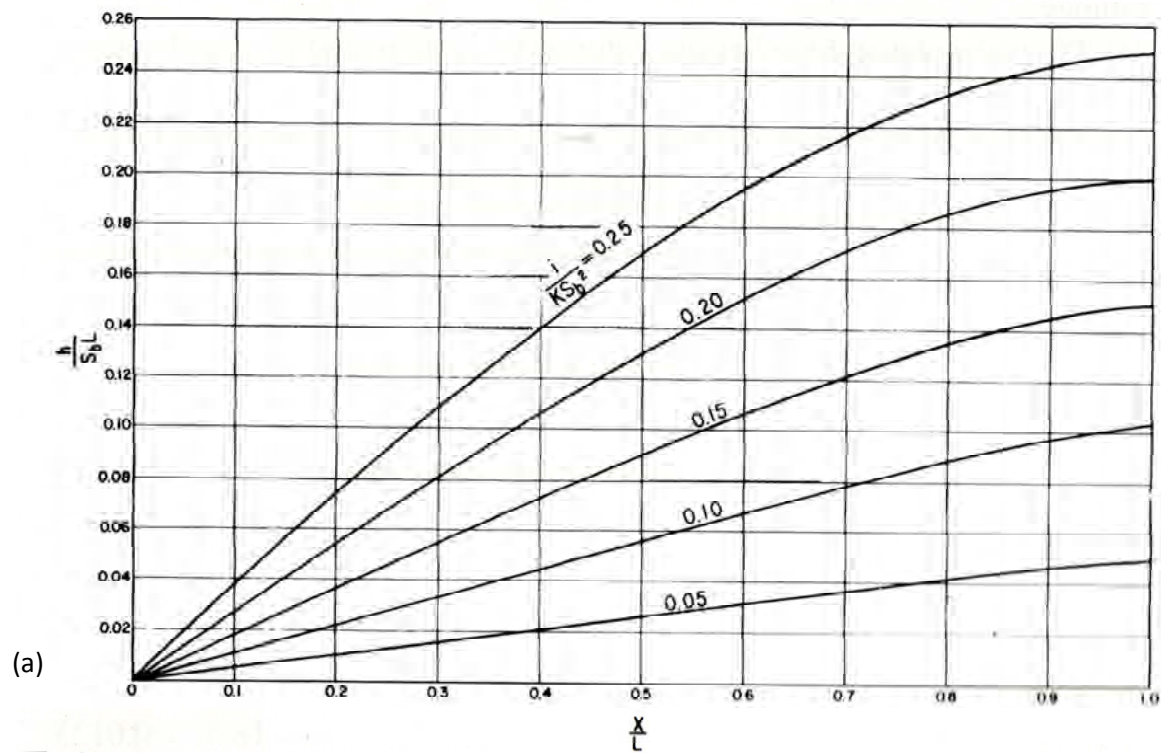


Figure 7.11: Water table profiles on sloping barriers for (a) $\frac{R}{KS_b^2} \leq 0.25$ and (b) $0.25 \leq \frac{R}{KS_b^2} \leq 1.25$.

(adopted from U.S. Department of the Interior, 1978). Deep infiltration (i) is synonymous with recharge R .

Table 7.2: Water Table Surface for $\frac{R}{KS_b^2}=0.76$ obtained from Figure 7.11b and parameter values for given example ($L = 457$ m, $S_b = 0.27$)

<u>Graphical</u>		<u>Actual</u>	
X/L	h/S _b L	X	h
0	0.335	0	4.13
0.05	0.38	22.85	4.69
0.058	0.3885	26.506	4.79
0.1	0.425	45.7	5.24
0.15	0.46	68.55	5.68
0.2	0.496	91.4	6.12
0.25	0.528	114.25	6.51
0.3	0.555	137.1	6.85
0.31	0.56	141.67	6.91
1	0.78	457	9.62

5. The effective depth d_e is calculated using equation 7.2a since $D^{\wedge}/L_d < 0.31$. For this example, assume a drain radius of 0.183 m, and d_e computes as 4.14 m.
6. Iterate until L_d defining d_e (equation 7.2) produces an equal L_d in equation 7.1.
7. The final $L_d = 287.5$ m. Since slopes are less than 10%, it is assumed that $L_d = L_d \cos(S_b)$, or the that drain spacing is essentially the horizontal distance of the drain. Drain length begins where the water table first reaches 2.44 m below land surface, or $X = 26.5$ m. Therefore the drain is placed at 314 m from $X=0$.

For another example, a surface water body at the end of the slope has an elevation of 13.7 m at $X = 457$ m which is a distance of 143 m from the drain. The maximum water level between the drain and the water body is estimated to occur at the mid-point, or $X = 314 + (143/2) = 385.5$ m. The height of the water table at this location is estimated with the following procedure,

1. Ground surface elevation at the mid-point between the drain and water body is $(385.5 \times 0.03) = 11.6$ m.
2. The depth below land surface for the barrier mid-point between the drain and surface water body is $7.32 + (314 + 71.5)(0.03) = 17.7$ m
3. The drain elevation at $X=314$ m is $(314 \times 0.03) + 2.44 = 11.9$ m
4. Average elevation between the drain and surface water body = $(13.7 + 11.9)/2 = 12.8$ m
5. $D^{\wedge} = 17.7 - 12.8 = 3.9$ m
6. $d_e = 3.5$ m
7. Using equation 7.1 solve for H_m such that $L_d = 143$ m.
8. $H_m = 0.39$ m and the water table is located at $12.8 - 0.39 = 12.4$ m

9. Depth to water table surface is $12.4 - 11.6 = 0.81$ m, which is less than the design minimum of 1.22 m.

Results are plotted in Figure 7.12. Graphically one can see that a single drain cannot maintain water levels 1.22 m below ground surface past $X = 370$ m based on the surface water boundary condition. However, the single drain, under steady-state conditions, can reduce seepage along much of the slope compared to the no-drain scenario. The inundation of water in the lower slope may be too little to cause slope failure, but if not, then an additional drain may be installed. It should be noted, that in all situations, the constant head boundary condition at the toe of slope will not allow the water table to be lowered to 1.22 m in its immediate vicinity.

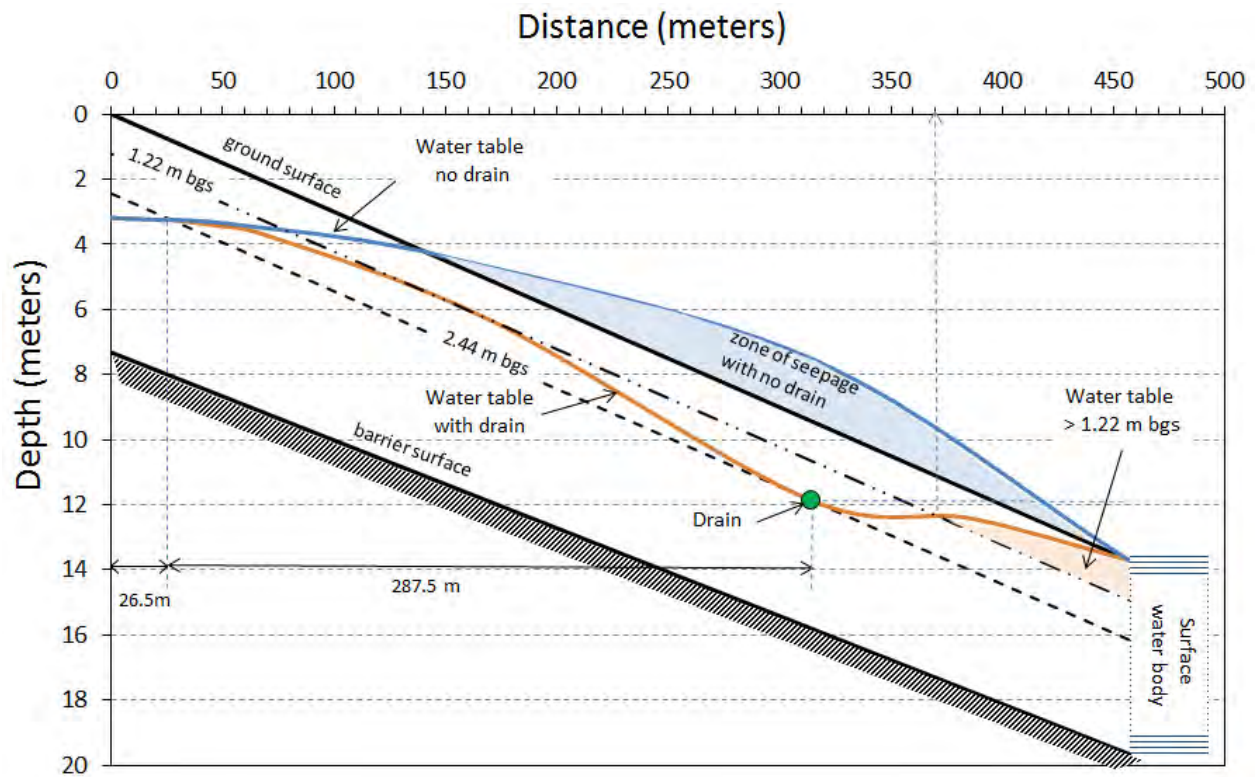


Figure 7.12: Analytically derived water table profiles under steady state conditions with and without a transverse drain.

7.4.1.3 Influence of Recharge and Hydraulic Conductivity on Drainage Design (all slopes)

Lesaffre (1987) demonstrated that under steady-state infiltration the influence of slope on drainage is determined by a single factor (σ),

$$\sigma = \frac{S_b(1 - \frac{R}{K})}{2\sqrt{R/K}} \quad (7.7)$$

Where S_b is the barrier slope (L/L), R is the recharge rate (L/T) and K the saturated hydraulic conductivity (L/T). The shape of the water table surface is related to σ , with shape changing at the critical value of $\sigma = 1$. For $\sigma < 1$, part of the flow to the drain is upslope. For $\sigma \geq 1$, flow to the drain is only downslope. Lesaffre (1987) demonstrated that the ratio between steady-state drain spacing in a sloped surface (L_d^*) and a horizontal surface (L_d) is directly related to σ . For values of $\sigma < 1$, L_d^*/L_d is nearly 1, and the effect of slope is negligible. For $\sigma > 1$, L_d^*/L_d increases such that slope and the ratio of R/K become important on drain spacing (Figure 7.13).

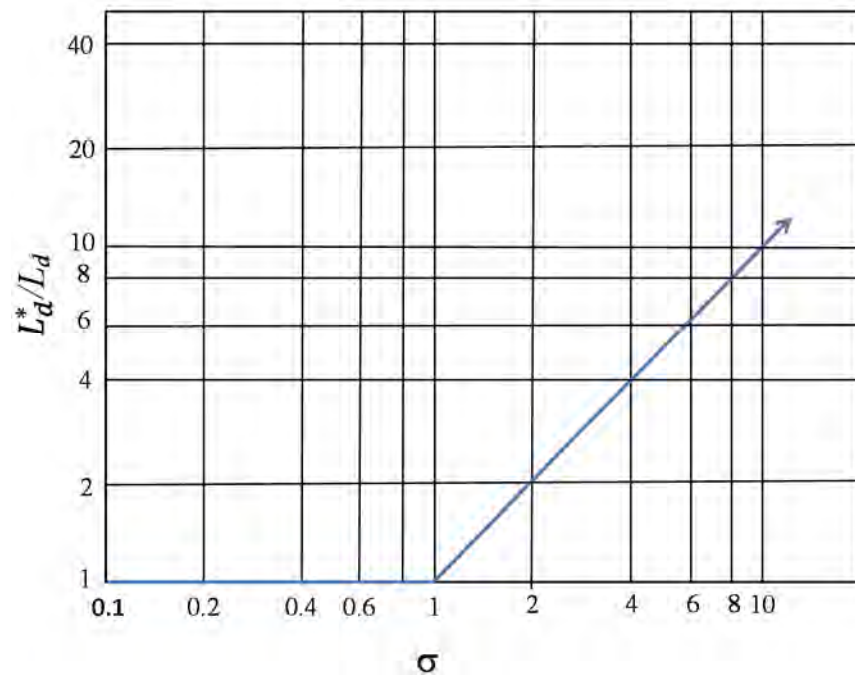


Figure 7.13: Impact of slope on drain spacing as described by Lesaffre (1987).

The functional relationship of equation 7.7 is plotted in Figure 7.14. L_d^* increases with increased slope, and also increases with a decreased ratio of recharge to hydraulic conductivity (R/K). The ratio of recharge to hydraulic conductivity is a means to assess the ability of the system to transmit available water to mitigate large fluctuations in water level. For example, systems with low recharge and conductive geologic materials will produce a very low ratio indicating system capable mitigating large water table fluctuations and the spacing between drains will increase. In contrast, systems with large recharge volumes and low conductive materials produce a large R/K ratio to indicate a system are more susceptible to increased water table elevations. Figure 7.14 shows that for a given slope, L_d^* increases only minimally as the ratio of R/K decreases. Only at very low ratios of recharge and hydraulic conductivity at which L_d^* increases at a substantially faster rate, with steeper slopes showing producing larger increases in L_d^* than shallower slopes.

For example, Figure 7.145 shows that a slope as low as 5% and an $R/K = 0.0001$ will produce $L_d^*/L_d = 2.5$. Figure 7.13, this equates to a $L_d^*/L_d = 2.5$. Therefore, at a slope of 5% drain spacing can be 2.5 times greater than for a flat sloped surface. In contrast, a slope of 20% and a system with either much larger recharge or much less ability to transmit recharge (e.g. $R/K = 0.01$) will produce $L_d^*/L_d < 1.0$ and drain spacing is not impacted by the steep slope.

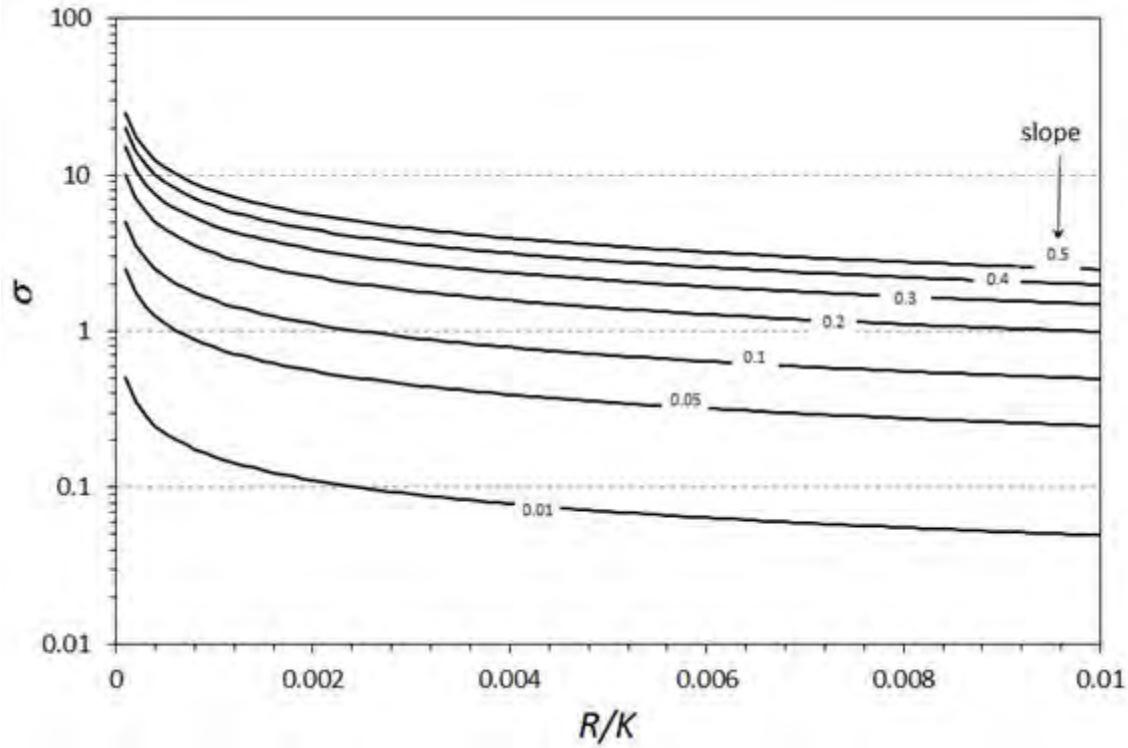


Figure 7.14: Influence of R/K and slope on L_d^*/L_d , as defined by equation 7.7.

Lesaffre (1987) presents the following estimate of drain spacing dependent on slope given steady-state infiltration,

$$L_d^* = H_m \sqrt{4 \frac{K}{R} + \frac{8Kd_e}{RH_m} + \left(\frac{K}{R} - 1\right)^2 (S_b)^2} \quad (7.8)$$

Where d_e is the equivalent depth calculated by equation 7.2. Equation 7.8 reverts to Hooghoudt equation 7.1 when $S_b = 0$. As an example, Figure 7.15 plots L_d vs L_d^* given $K = 1.0$ m/hr, $R = 0.002$ m/hr. For $S_b = 0.01$, $L_d^*/L_d = 0.11$ and consequently L_d^* is approximately equal to L_d . Drain spacing then increases with increased slope for $S_b \geq 0.1$.

The implications of Lesaffre's (1987) work, is that flatter surfaces require drains to be closer together, and in this essence, represent the most conservative approach to drain design.

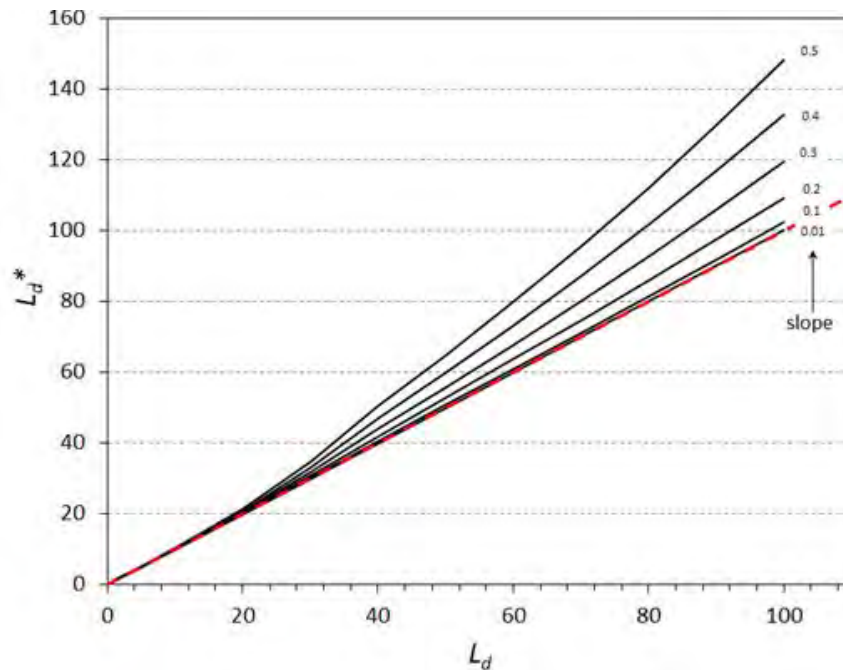


Figure 7.15: Drain spacing on a sloped surface (L_d^*) compared to a flat surface (L_d) for different slopes. Red dashed line represents 1:1 line.

7.4.2 Transient Solutions

Slope failure is generally caused by rapid increase in water levels (pore pressures) that cause instability, and are typically not a function of steady-state recharge conditions. Graphical methods for flat surfaces (U.S. Department of the Interior, 1978) and semi-analytical methods for sloping surfaces (Skukla et al., 1990) are presented. In all cases, drain design is limited to parallel, equally spaced, transverse drain layouts.

7.4.2.1 Flat Surfaces

The U.S. Department of the Interior (1978) method for computing drain spacing is based on maintaining dynamic equilibrium in water levels below a specified water level. The approach was developed for irrigation systems, not for maintaining slope stability. Figure 7.16 shows curves for estimating drain spacing based on if the drain is situated directly on the impervious surface or some height above this surface. Axes represent normalized dimensionless parameters with parameters defined within the figure.

To illustrate the use of Figure 7.16, an example is modified from U.S. Department of the Interior (1978) given a drain situated above the impermeable layer, and assuming $\hat{D} = 6.7$ m (22 ft), the depth of the drain is 2.4 m (8 ft), and drain spacing $L_d = 442$ m (1,450 ft). As an example, if one wishes to keep the maximum water table surface 1.2 m (4 ft) below ground surface, then $H_0 = 2.4$ m – 1.2 m = 1.2 m (4 ft). Hydraulic conductivity is 3.05 m/d (10 ft/d) and assumed uniform with depth. Use Figure 4.16 to

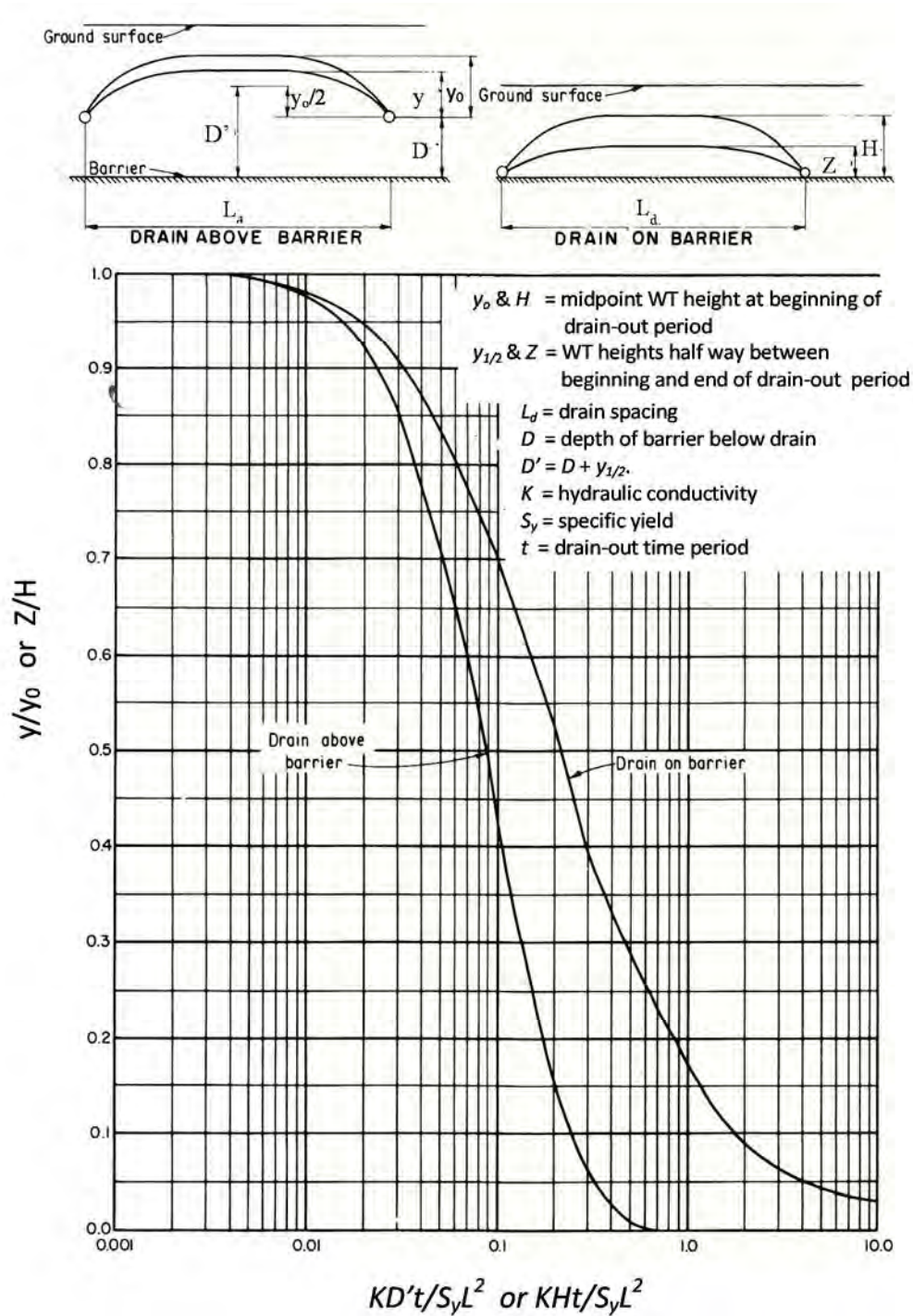


Figure 7.16: Curves showing relationship of parameters needed for drain spacing calculations using the transient flow theory presented by U.S. Department of the Interior (1978) for flat surfaces.

estimate S_y from hydraulic conductivity, $S_y = 0.18$. The effective depth d_e is then found using equation 7.2, which equals 6.1 m. The approach will use the effective depth in place of actual depth (D^{\wedge}) in the calculation of D' , such that $D_e' = d_e + y_0/2$.

The problem is initiated by assuming that initial water level (y_0) begins at the maximum allowable height, or 1.2 m above the drains and the system is first modeled through its dry period. Recharge events are then added throughout the wet period to test if the system rebounds over the maximum allowable height. Table 7.3 provides calculations.

1. Assume maximum allowable water table elevation at the beginning, $y_0 = 1.2$ m
2. The dry period is 233 days with no recharge. This is divided into two periods of 117 days and 116 days, respectfully.
3. First stress period: $D_e' = y_0/2 + 6.1$ m = 7.3 m; $KD_e'/S_yL_d^2 = (3.05)(7.3)*117/(0.18)(442)^2 = 0.0742$. From Figure 7.16, this corresponds to a $y_0/y = 0.575$. Knowing y_0 , y is calculated as 0.69 m.
4. Second stress period: this stress period occurs during the dry period and there is no recharge. The initial water table height (y_0) equals the water table height at the end of the last stress period. $Y = 0.69$. $D_e' = 6.1 + 0.69/2 = 6.45$ m, $KD_e'/S_yL_d^2 = 0.0695$ and from Figure 7.16, $y/y_0 = 0.59$ such that the water level at the end of the dry season is 0.407 m above the drains.
5. Third stress period: First recharge event occurs with 0.0252 m assumed to occur instantaneously. The water table build up is 0.0252 m/ $0.18 = 0.14$ m, and the initial water table height is the water table height at the end of stress period 2 plus the recharge, or $0.407 + 0.14 = 0.547$ m. Computation of D' , $KD_e'/S_yL_d^2$, y/y_0 and y are done similar to step 3 and 4.

Table 7.3: Calculation of water table fluctuation (in meters) with a drain above the barrier layer. (Example modified from U.S. Department of the Interior, 1978).

Stress period (d)	recharge (m)	time (d)	cumul. time (d)	WT build up (m)	Y_0 (m)	D_e' (m)	$KD't/S_yL^2$	Y/y_0	y (m)
1	0	117	0		1.200	6.71	0.0730	0.575	0.690
2	0	116	117		0.690	6.45	0.0695	0.590	0.407
3	0.0252	45	233	0.14	0.547	6.37	0.0267	0.870	0.476
4	0.0252	25	278	0.14	0.616	6.41	0.1490	0.958	0.590
5	0.0252	20	303	0.14	0.730	6.47	0.0120	0.978	0.714
6	0.0252	14	323	0.14	0.854	6.53	0.0085	0.985	0.841
7	0.0252	14	337	0.14	0.981	6.59	0.0086	0.985	0.967
8	0.0252	14	351	0.14	1.107	6.65	0.0087	0.985	1.090
9	0.0252		365	0.14	1.230				

Successive stress periods are treated in the same manner. At the conclusion of the last recharge event, the water table surface is at 1.23 m above the drains, or approximately the maximum allowable height. Therefore, a drain spacing of 442 m maintains water levels in dynamic equilibrium. Figure 7.17 displays calculated water levels over time using the U.S. Department of the Interior (1978) transient-step approach, assuming a flat surface. As mentioned above, this approach was developed for agricultural systems, not slope stability problems. In this light, it is recommended to use these equations only as a first cut of maximum drain spacing at the end of a fan array.

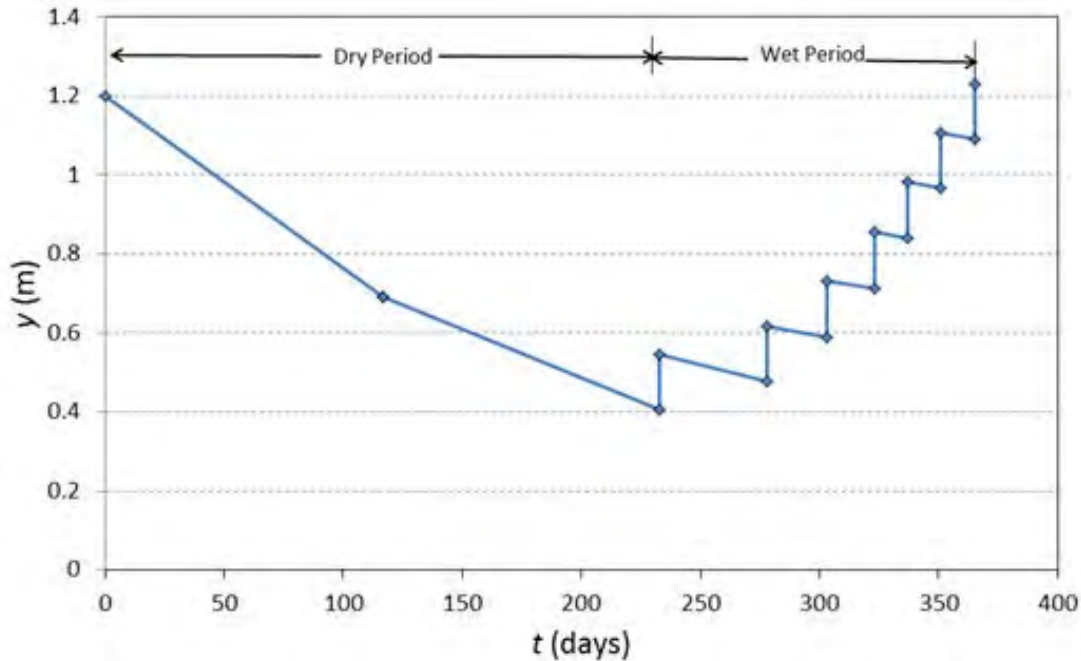


Figure 7.17 Height of the water table above drains (y) over time for the example problem provided in Table 7.3. (modified from U.S. Department of the Interior, 1978)

The equations presented also allow the designer to compute the time to drop the water table a certain amount for a given drain spacing, or the drain spacing to drop the water table a given amount over a specified period of time.

To demonstrate, the example is $K = 3.05$ m/d, $D = 6.1$ m, depth to the drain $y_0 = 2.7$ m, $S_y = 0.07$ and existing drains are 91 m apart. Assume drain radius is 0.183 m. If the water table is at land surface at $t = 0$, how many days will it take for the water table to drop 1.2 m below ground surface?

To solve, the effective depth $d_e = 4.4$ m is computed from equation 7.2. Therefore $D_e' = 4.4 + 2.7/2 = 5.75$ m. The ratio of $y/y_0 = 1.2/2.7 = 0.44$, which gives 0.096 for $KD_e'/S_yL_d^2$ from Figure 7.16. Now it is possible to solve for t .

$$t = \frac{0.096 S_y L_d^2}{K D_e'} = \frac{0.096(0.07)(91)^2}{(0.305)(5.75)} = 31.8 \text{ days} \quad (7.9)$$

It takes nearly 32 days for the water level to recede from land surface to a depth of 1.2 m given a drain spacing of 91 m. If one wants to drop the water table the same amount, but in only 10 days, then one solves for L_d . However, as with steady state solutions, d_e and D_e' are dependent on L_d and iteration must be done to solve for L_d . To solve,

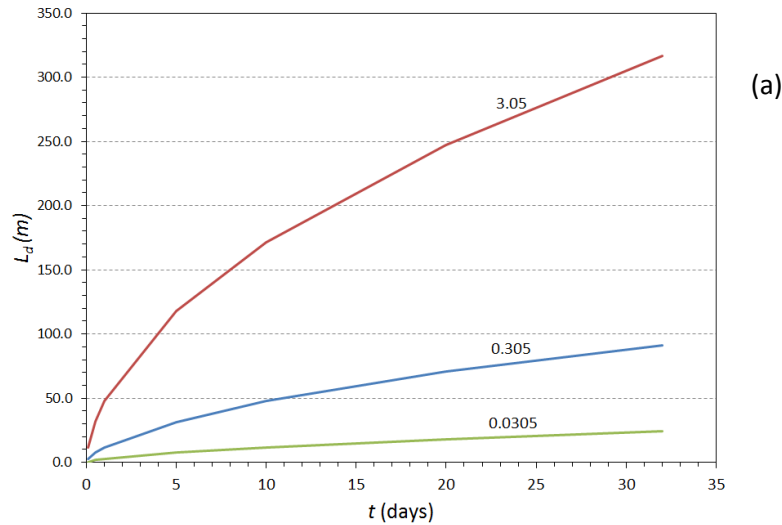
1. Initial guess of $L_d = 70$ m
2. $D_e'/L_d = 6.1/70 = 0.08$, therefore use equation 7.2a and $d_e = 4.18$ m.
3. Calculate $D_e' = 4.18 + (2.7/2) = 5.53$ m
4. Compute $\frac{K D_e' t}{S_y L_d}$ using $t = 10$ days. For $L_d = 70$ m, $\frac{K D_e' t}{S_y L_d} = 0.049$
5. Compare with graphical value of $\frac{K D_e' t}{S_y L_d} = 0.096$ given $y_0/y = 0.44$. $0.049 < 0.096$, therefore L_d must be lowered.
6. Final iteration, $L_d = 47.6$ m.¹

To decrease the time of drainage by 1/3, it is necessary to decrease spacing of drains by over 47% given $K = 0.305$ m and $S_y = 0.07$. Drain spacing required to lower the water table 1.2 m for different time intervals and for changes in K and S_y are plotted in Figure 7.18, and tabulated in Table 7.4. With decreases in K , drain spacing must be significantly reduced to lower the water table for equivalent periods of time compared to systems with large hydraulic conductivity. Likewise, increasing S_y will force L_d to significantly smaller values.

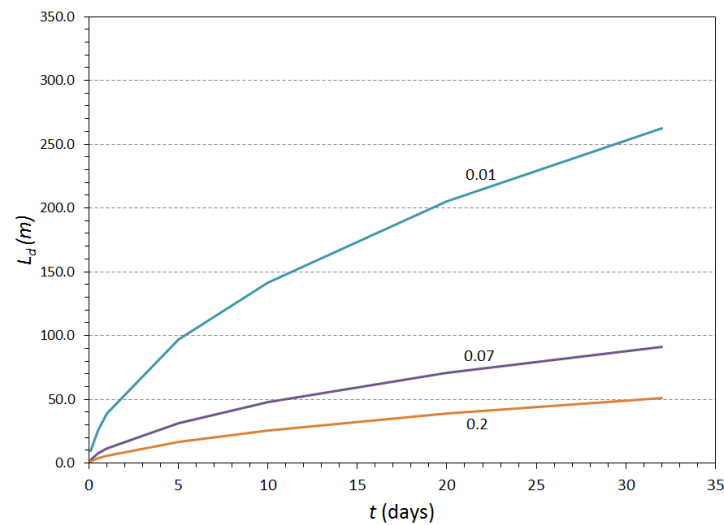
Table 7.4: Drain spacing, L_d (meters) required to lower water table elevations 1.2 m in time t for various values of S_y and K .

S_y	0.07	0.07	0.07	0.01	0.2
$K, \text{ m/d}$	0.305	3.05	0.035	0.305	0.305
$t, \text{ d}$	$L_d, \text{ m}$	$L_d, \text{ m}$	$L_d, \text{ m}$	$L_d, \text{ m}$	$L_d, \text{ m}$
32	91.0	316.4	24.1	262.4	50.9
20	71.0	247.3	18.1	205.0	38.7
10	47.6	171.4	11.7	141.6	25.5
5	31.6	118.0	7.5	97.0	16.6
1	11.7	47.7	2.7	38.7	5.9
0.5	7.5	31.6	1.8	25.5	3.8
0.1	2.7	11.7	-	9.3	1.5

¹ Iteration can be either manual, or use solver capabilities in many spread sheet application. For example, the Excel add-in Solver allows one to set up an objective function (e.g. error between graphical value and computed value) in which L_d is changed until objective function is minimized.



(a)



(b)

Figure 7.18: Drain spacing, L_d , required to lower water table elevation 1.2 m in time t given (a) $S_y = 0.07$ and changing K , (b) $K = 0.305$ m/d and changing S_y . Table 7.4 provides actual values.

7.4.2.2 Sloping Surface – Maximum Water Levels and Rates of Decline

Analytical, numerical and experimental solutions for drainage given unsteady-state conditions abound for flow regimes where parallel ditches penetrate to an impermeable layer, or a covered drain lies on the impermeable layer. Luthin and Guitjens (1967) obtained a transient solution for drainage on sloping surfaces using a Hele-Shaw model and concluded that slopes less than 30% can be treated as a flat surface. Chauhan et al. (1968) used an analytic solution to a linearized Boussinesq equation, an analogue computer solution as well as experimental solutions from a Hele-Shaw model to solve several solutions for unsteady drainage in sloping lands with a variety of boundary conditions, but slopes were limited to less than 8% and limited to the rate of fall (no recharge) of the water table surface. Ram and Chauhan (1987a) also used a linearized form of the Boussinesq equation to solve for a transient solution but allowed steady rate of recharge, and then added an exponential recharge function over time (Ram and Chauhan 1987b).

Shukla et al. (1999) uses a combination of explicit and implicit difference methods to numerically solve a nonlinear Boussinesq equation for slopes 0-70% to investigate the rate of water table fall after a rain event. Results compared well to experimental solutions provided by Luthin and Guitjens (1967), Chauhan et al. (1968), and the finite difference solutions of Moody (1966) for partially penetrating drains in a horizontal aquifer. Shukla et al. (1999) assumes that boundary conditions are defined by antecedent vertical recharge, in which the water table rises uniformly to a vertical height of H_m^0 (parallel to the impermeable layer), and then solves for transient head based on drawdown over time between two drains ($h(x,t)$). Numerical solutions are presented graphically using dimensionless parameters similar to the flat-surface solution in section 7.4.2.1. With parameters defined in Figure 7.19. Figure 7.20 provides a dimensionless form of maximum water table height (h_m/H_m^0) versus a dimensionless time function incorporating S_y , K and drain spacing (L_d) for slopes equal to 10%, 30%, 50% and 70% and different depths of the impermeable layer ($m = 1.0, 0.8, 0.4, 0.2$ and 0.1), where h_m is the maximum water table height at time t .

Note that Skuka et al. (1999) assumes a rise in water level has already occurred to some known height and calculated the time and location of the maximum water level over time between two drains. Necessary parameters include, (1) the time required to lower the water table elevation to maintain stability, t , (2) a measured or assumed value for hydraulic conductivity and specific yield, K & S_y , (3) the water table elevation prior to a design storm, and (4) the water table elevation following a design storm (D^*).

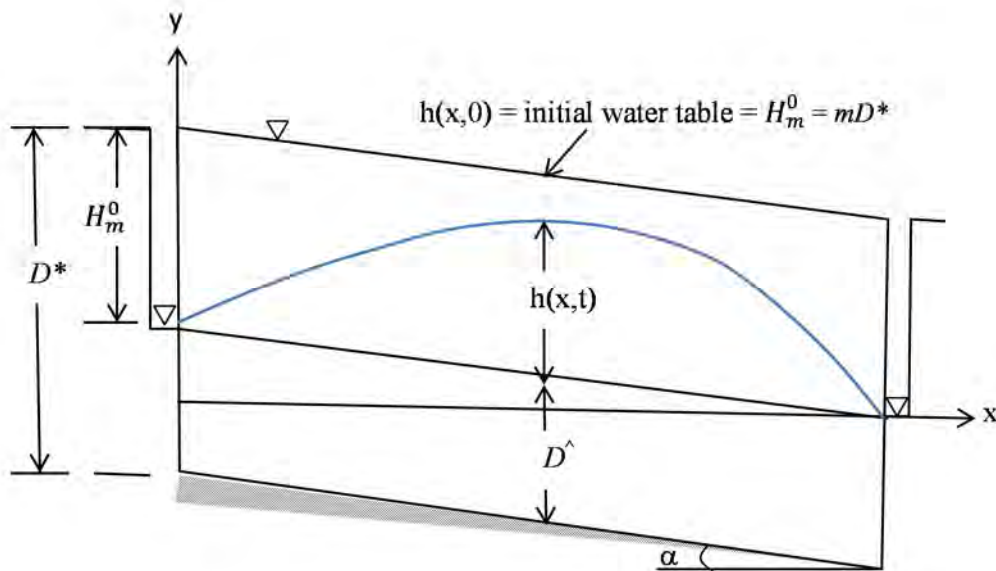


Figure 7.19: Parameters for sloping surface given transient drawdown and drains lying above an impermeable layer. (Reprinted from Journal of Irrigation and Drainage Engineering, 116(1), Shukla, K.N., H.S. Chauhan, and V.K. Srivastava, Finite Difference Solution of Boussinesq Unsteady-State Equation for Highly Sloping Lands, pp 107–113, 1990, with permission from American Society of Civil Engineers.)

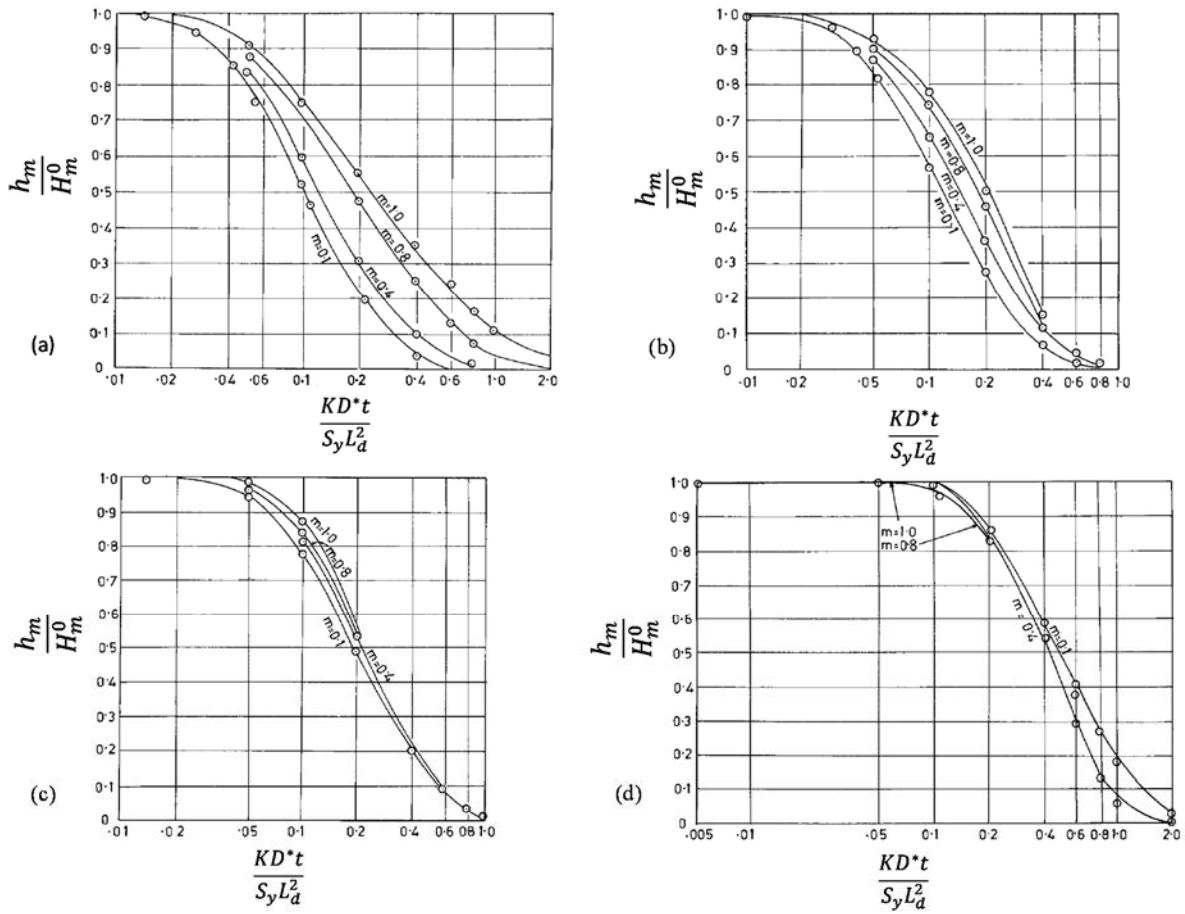


Figure 7.20: Dimensionless curves of maximum water table height with respect to time for slopes of (a) 10%, (b) 30%, (c) 50% and (d) 70%. (Reprinted from Journal of Irrigation and Drainage Engineering, 116(1), Shukla, K.N., H.S. Chauhan, and V.K. Srivastava, Finite Difference Solution of Boussinesq Unsteady-State Equation for Highly Sloping Lands, pp 107–113, 1990, with permission from American Society of Civil Engineers.)

To solve drain spacing (L_d) perform the following steps:

1. Assume a drain depth with respect to peak water level H_m^0
2. Calculate the ratio $m = H_m^0/D^*$, where D^* is height of maximum water table elevation above the impermeable surface.
3. Calculate the y-axis in Figure 7.20, h_m/H_m^0 , such that h_m is the maximum height of the water table for which stability of the slope is maintained.
4. Find the intersection of the calculated h_m/H_m^0 and curve choice m , and trace back to the x-axis.
5. Solve for drain spacing L_d for given value of x-axis, $\frac{KBt}{S_y L_d^2}$

To illustrate, an example similar to that presented in section 7.4.11 and Figure 7.10 is provided in which the thickness of the geologic layer is 20 ft, but now has a slope of 30%.

- It is assumed that the time required to sufficiently lower the water table during a large storm is 0.5 days.
- Hydraulic conductivity and specific yield are set to 1.0 ft/d (silty, fine sand) and 0.1, respectively.
- It is assumed that a design storm will force the water table to flood the system such that water rises above land surface. For convenience, let's assume the water table rises 1 foot above land surface, or $D^* = 21$ ft.
- Assume $m = 1.0$, then this signifies the drains are located on the impermeable layer.
- The drains must lower the water table below land surface. Therefore the y-axis $h_m/H_m^0 = 20/21 = 0.95$.
- Trace the y-axis to the $m = 1.0$ curve and follow the x-axis. The x-axis is in a log-scale. $\frac{KBt}{S_y L_d^2}$ is approximately 0.04.
- Solve for $L_d = \sqrt{KD^*t/0.04S_y} = 51$ ft

These results indicate a reduction in drain spacing by approximately half compared to the Hooghoudt example given in Figure 7.10b.

Figure 7.20a shows curves for a 10% slope. As the value of m increases (depth below drains to barrier decreases), then the water table declines at a slower rate with time. The rate of water table decline is slowest when the drain is placed directly on the barrier ($m = 1.0$). When slope is increased to 30% (Figure 7.20b), decline is slowest when $m = 1.0$, and no water table decline is seen beyond $\frac{KBt}{S_y L_d^2} = 0.4$. At 50% slope, no further water table decline is seen for $m = 0.1$ at the dimensionless time parameter equaling 0.2. For a 70% slope, water table fluctuations of $h_m/H_m^0 = 0.8-0.9$ are seen for time parameters less than 0.1 given $m = 0.8$ to 1.0.

For flat surfaces, the water divide, or the location of the highest water level surface, is located at the midpoint between drains and does not change with time. In the case of sloping systems, the water divide is a function of time, moving from its initial location near the upper drain and toward the lower drain. With increased slope, the movement of the divide toward the lower drain occurs more rapidly (Figure 7.21a). The values of maximum height of the water table are given in Figure 7.21b. The value of the highest water table elevation varies at a faster rate for lower slopes, moving toward a maximum distance of 0.65 of the drain span. For higher slopes, the value of the highest point of the water table varies more slowly, and its location shifts closer to the lower drain to a distance of 0.9 L_d .

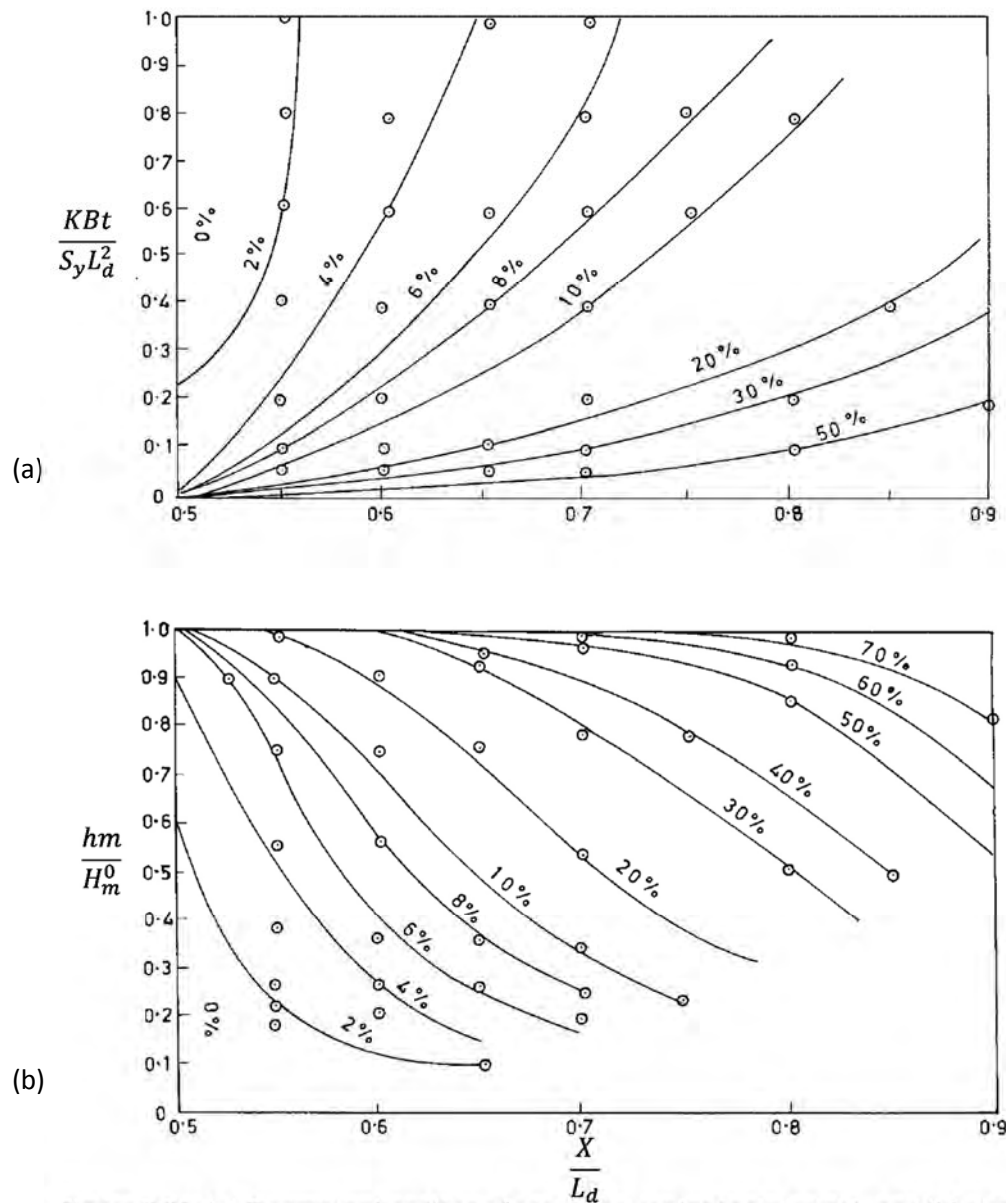


Figure 7.21: (a) Dimensionless time of maximum water table height, and (b) dimensionless height of maximum water table of at various distances for different slopes. (Reprinted from Journal of Irrigation and Drainage Engineering, 116(1), Shukla, K.N., H.S. Chauhan, and V.K. Srivastava, Finite Difference Solution of Boussinesq Unsteady-State Equation for Highly Sloping Lands, pp 107–113, 1990, with permission from American Society of Civil Engineers.)

7.4.3 Limitations of Analytical Approaches

Analytical solutions require several limiting assumptions that are not applicable to most slope stability problems. While simplified geology and steady-state conditions are readily solved via analytical approaches, spatial and temporal distributions of water levels as a function of variable recharge are not explicitly calculated. Transient approaches for flat systems are presented that can give estimates of drain spacing as a function of variable recharge. Transient solutions for sloping surfaces are more

difficult to apply and in general, slopes less than 30% can be treated as flat. In addition, the transient approaches presented only track the receding water table after peak water levels are obtained. No recharge is modeled.

Perhaps the most serious limitation to analytical approaches is that drain design is limited to drain placement orthogonal to the slope. This is suitable for irrigation practices, but is not practical for slope stability problems in which fan-drain arrays are more commonly applied. No analytical approach is available to deal with fan arrays. Instead, numerical techniques are needed to test spatially complex drain arrays, complex geology, and highly variable recharge.

7.5 Numeric Modeling Approach to Drainage Design

Recognizing the limitations of analytical approaches discussed above, numerical modeling with MODFLOW is necessary to evaluate the complex hydrogeologic conditions associated with many typical applications for horizontal drains. The following approach considers two generalized types of slope failure mechanisms - translational and rotational failures. Generic, or idealized, sites are presented for each failure scenario to serve as templates for site-specific modeling or to directly guide drainage design. Modeling results will look at important controlling features of drainage design, with emphasis on drain length, spacing, and elevation, as well as sensitivity of design to site characteristics of recharge, hydraulic conductivity, specific yield and drain efficiency. Proper communication between groundwater model results and geotechnical analysis are outlined for the most efficient drainage design. For an introduction to slope stability analysis or groundwater modeling, refer to chapters 2 and 6, respectively.

7.5.1 Hydraulic Soil Properties

Hydraulic soil properties are adjusted over applicable ranges to ascertain what types of soils are most influenced by specific drain configurations. Table 7.5 outlines the 12 soil types investigated.

7.5.2 Translational Failure (Site D)

7.5.2.1 Site Description

Site D is modeled using the topography shown in Figure 7.23. The slope is relatively uniform from the ridge crest to the base of the slope at approximately 28% (16°). The hypothetical subsurface conditions have been assumed to be a simple two-layer system, with the contact between these layers being coincident with slope. Layer 2 is a 20-ft-thick permeable layer that overlies a low permeability unit (layer 1). For modeling purposes, the lower unit is assumed to be impermeable.

Table 7.5: Twelve soil types considered based on hydraulic properties of horizontal hydraulic conductivity (K_x , ft/d), specific yield (S_y , dimensionless) and the ratio of horizontal to vertical hydraulic conductivity (VKA, dimensionless).

Soil	Hydraulic Parameter			General Soil Description
	K_x	S_y	VKA	
1	0.1	0.01	1	silt, sandy silt, clayey sand or till with very low storage (1%) and isotropic conditions
2	1	0.01	1	silty sands and fine sands with very low storage (1%) and isotropic conditions
3	10	0.01	1	well sorted sands, glacial outwash with very low storage (1%) and isotropic conditions
4	0.1	0.1	1	silt, sandy silt, clayey sand or till with average storage (10%) and isotropic conditions
5	1	0.1	1	silty sands and fine sands with average storage (10%) and isotropic conditions
6	10	0.1	1	well sorted sands, glacial outwash with average storage (10%) and isotropic conditions
7	0.1	0.01	10	silt, sandy silt, clayey sand or till with very low storage (1%) and anisotropic conditions
8	1	0.01	10	silty sands and fine sands with very low storage (1%) and anisotropic conditions
9	10	0.01	10	well sorted sands, glacial outwash with very low storage (1%) and anisotropic conditions
10	0.1	0.1	10	silt, sandy silt, clayey sand or till with average storage (10%) and anisotropic conditions
11	1	0.1	10	silty sands and fine sands with average storage (10%) and anisotropic conditions
12	10	0.1	10	well sorted sands, glacial outwash with average storage (10%) and anisotropic conditions

7.5.3 Design Storm

The design storm is defined as a 100-year, 24-hour rain event. For a generalized version of site D, the assumptions made include: CN = 80, total precipitation = 9 inches and storm distribution is type IA. The resulting recharge during a 24-hour event is shown in Figure 7.22. Sensitivity of drain design to the CN, total precipitation and storm type are discussed in the section 7.4.3.6.4 for translational failure.

7.5.3.1 Model Domain and Conceptual Model

The model domain encompasses the entire watershed to eliminate the need to designate water flux across boundary conditions (Figure 7.24). Water entering the system is assumed to only occur from precipitation, with all water flowing toward the watershed outlet at the lowest elevation. Figure 7.25 shows the MODFLOW grid placement in plan-view and a cross section of the model along d-d'. Cell size is 5 ft by 5 ft and a single homogenous unit is modeled at 20 ft thick. The model grid is orientated 27° so that modeled rows run parallel to the slope.

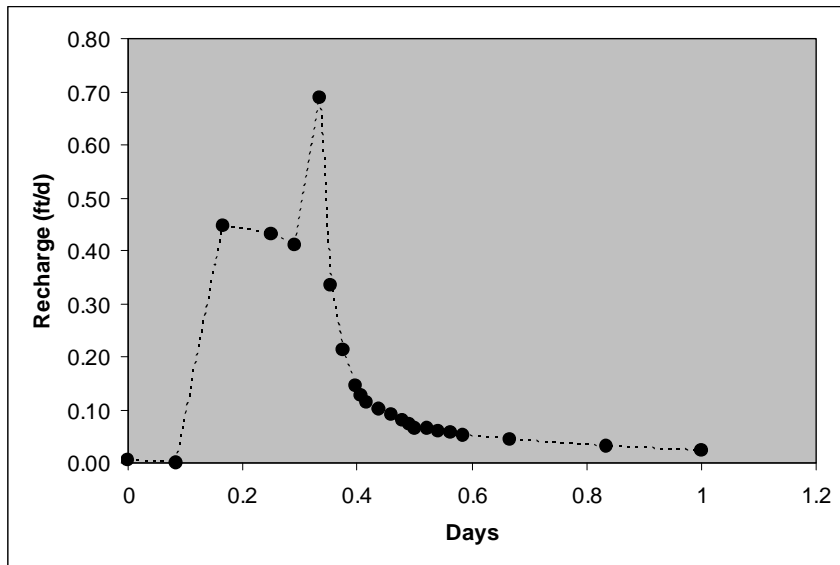


Figure 7.22: 24-hour 100 year recharge for CN = 80, total precipitation = 9 inches and type IA storm.

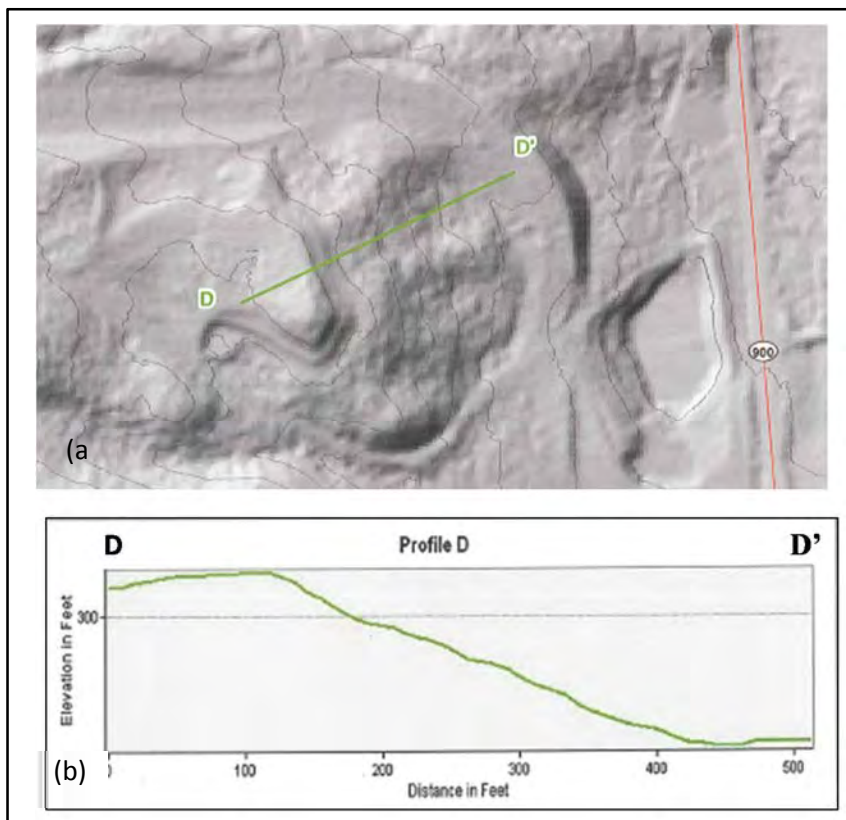


Figure 7.23 Site D topography for translational failure (a) hill shade, (b) cross sectional profile of land surface from D-D'.

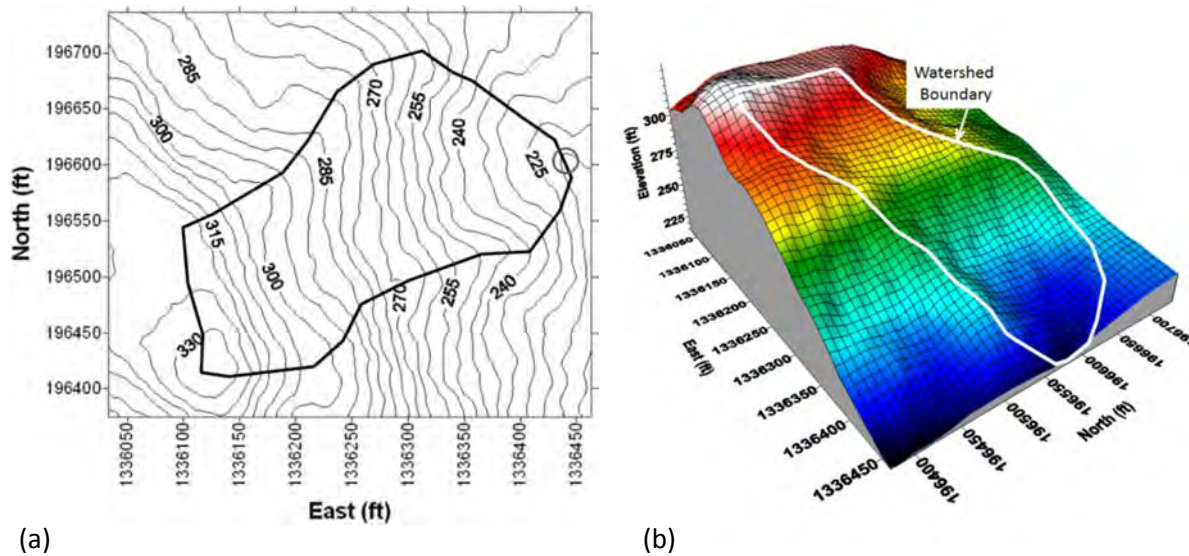


Figure 7.24: (a) Site D topographic map showing land surface elevation at 5 ft intervals. Gray circle represents watershed outlet, while thick black line delineates the watershed. (b) A surface map showing elevation in color scale and the watershed boundary given as a white line.

7.5.3.2 MODFLOW-NWT

In order to model water levels for the thin geologic layer for translational failure it is necessary to use MODFLOW-NWT. MODFLOW-NWT contains the newest USGS numeric solver (Niswonger et al., 2011) and maintains numeric stability during the wetting and drying of model cells. MODFLOW-NWT contains two input files not previously used by MODFLOW. The GUI interface, Groundwater Vista (GWV), will automatically convert the MODFLOW LPF package into the UPW package and no changes are explicitly required by the user. The NWT solver package, however, must be designated by the user with only a few NWT input parameters changed from their default status. Parameter changes are listed below, and a tutorial is provided in Appendix B on how to assign these parameters in the GWV platform.

- **OPTION = COMPLEX** replaces **OPTION = MODERATE**: This changes default parameters to those best describing very non-linear models. While “moderate” may describe steady state scenarios, large recharge rates over short stress periods during the design storm will require the complex default parameters.
- **IBOTAV** = a flag that indicates whether corrections will be made to groundwater heads relative to the cell-bottom elevation if the cell is surrounded by dewatered cells. A value of 1 means a correction will be made, while a value of 0 means no correction is made. The designation is problem specific. Tests for this problem found that a value of 1 is desirable.
- **FLXTOL** = this is the maximum root-mean-squared flux difference between outer iterations for the solution of the nonlinear problem. Units are in length cubed per time. This value is lowered from 100 to 1 ft³/d. If mass balance errors still occur, then FLXTOT needs to be lowered further.

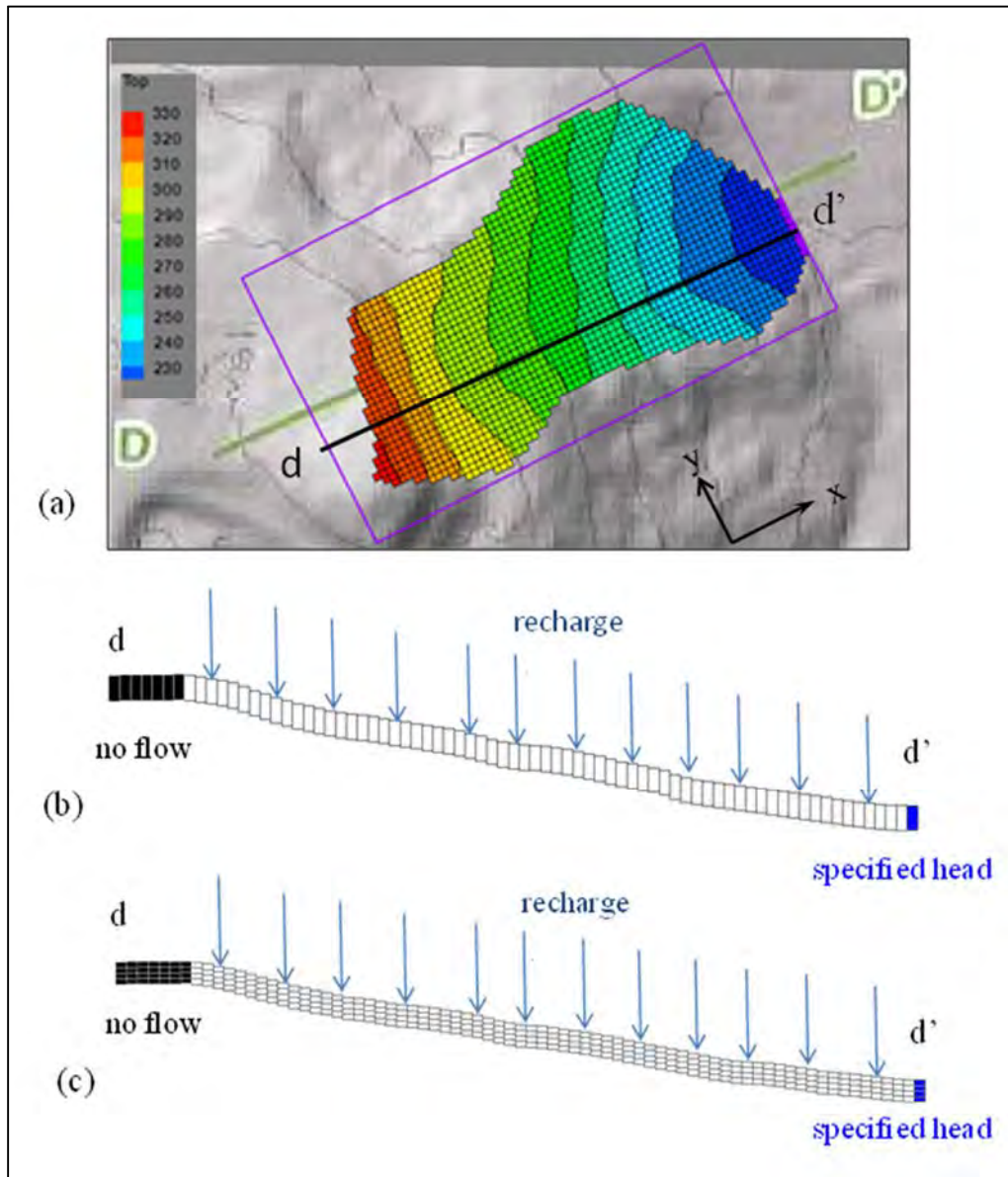


Figure 7.25: Model grid Site D with (a) plan view showing modeled grid (purple box), active cells in color scale of assigned land surface elevations, rotated x-y axis and cross section d-d'. Cell dimension is 5 ft by 5 ft. (b) Cross section d-d' depicting single layer model (thickness of layer is 20 ft) as well as no flow cells and specified head cells. Recharge is applied evenly across modeled domain. (c) Four-layer model used to test anisotropy (VKA) on drain design where $VKA = K_x/K_z$.

- MAXITEROUT = is the maximum number of iterations to be allowed for solution of the outer (nonlinear) problem. This is increased to 3000, so that a solution has adequate time to converge.
- BACKFLAG = is a flag used to specify whether residual control will be used. A value of 1 indicates that residual control is active. A value of 0 indicates it is inactive. Experimentation found that solution convergence is best achieved if set to a value of 1.

7.5.3.3 Geotechnical Parameters and Preliminary Slope Stability Analysis

Slope stability analysis was carried out using XTABL slope stability analysis software, using limit-equilibrium methods. In order to accommodate the translational failure mode, Janbu's method was used in analyses. The results of the factor of safety calculations were confirmed using Spencer's method for a few cases. Both methods provided near identical results as expected.

Figure 7.26 indicates cross section d-d'. Layer 1 and 2 are two soil layers. Layer 2 soil properties are, friction angle is 35° ; cohesion is zero; unit weight is 120 pcf and saturated unit weight is 125 pcf. Higher strength parameters were assumed for Layer 1 to ensure the translational failure of soil along Layer 1. Its properties are, friction angle is 55° ; cohesion is 4000 pcf; unit weight is 140 pcf and saturated unit weight is 145 pcf. The defined translational failure surface is shown in Figure 7.26.

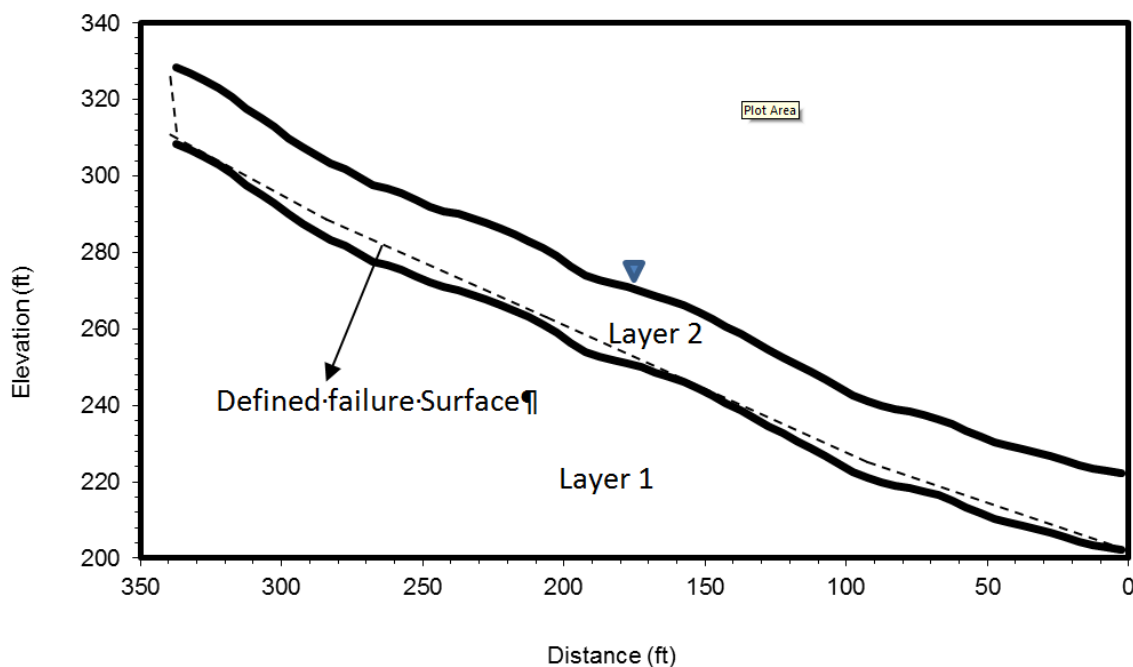


Figure 7.26: Location of translational failure surface for a typical cross section of site D when the water table surface is located at ground surface (fully saturated) and no drains are installed.

The initial analysis was carried out when the water table is on the top surface of Layer 2 as shown in Figure 7.26. The factor of safety (FOS) was calculated using three methods: simplified Janbu, Spencer and Plane translational slip. Resulting FOS are provided in Table 7.6 and show that calculations are similar. The critical water level surface is defined as that water table elevation for which slope failure is likely to occur (FOS = 1.0). For site D, the critical water level for slope failure given a soil unit 20 feet thick is approximately ground surface.

Table 7.6: FOS using different analysis methods for site D, translational failure and no drains installed.

Analysis Method	FOS
Simplified Janbu	0.972
Spencer	0.972
Plane translational slip (by using equations)	1.031

7.5.3.4 Drain Configurations

Thirteen separate drain arrays test design strategies on effectively lowering water levels below a critical water level to promote slope stability. Short length drains extend over the lower slope toe, medium length drains extend the entire slope toe, while long length drains extend from the base of the toe to the upper slope reaches. Short drains are assumed to have an angle (from the horizontal) of 5 degrees. Medium and long drain angles are adjusted so that the entire drain falls within the upper and lower elevations of the soil unit. On average, medium length drains require a 10 degree angle. Long length drains require a 16 degree angle from horizontal to avoid intersecting the underlying bedrock (or confining unit). Figure 7.27 shows a cross section with an example of a long, medium and short- length drains. Drain spacing is designated as wide (fan angle is approximately 24°), medium (fan angle = 12°) and narrow (fan angle = 6°). Each spacing category represents a near doubling in the number of drains. Four drain configurations are also investigated that combine different length drains. Drain specifications for site D are provided in Table 7.7 and illustrated in Figures 7.28 to 7.40.

Drain conductance is calculated by defining drain length, surface area and hydraulic conductivity. Drain hydraulic conductivity (K_d , ft/d) is assumed equal to surrounding geologic material. A test of model output sensitivity to K_d is discussed in the section on sensitivity analysis (section 7.5.3.6.4)

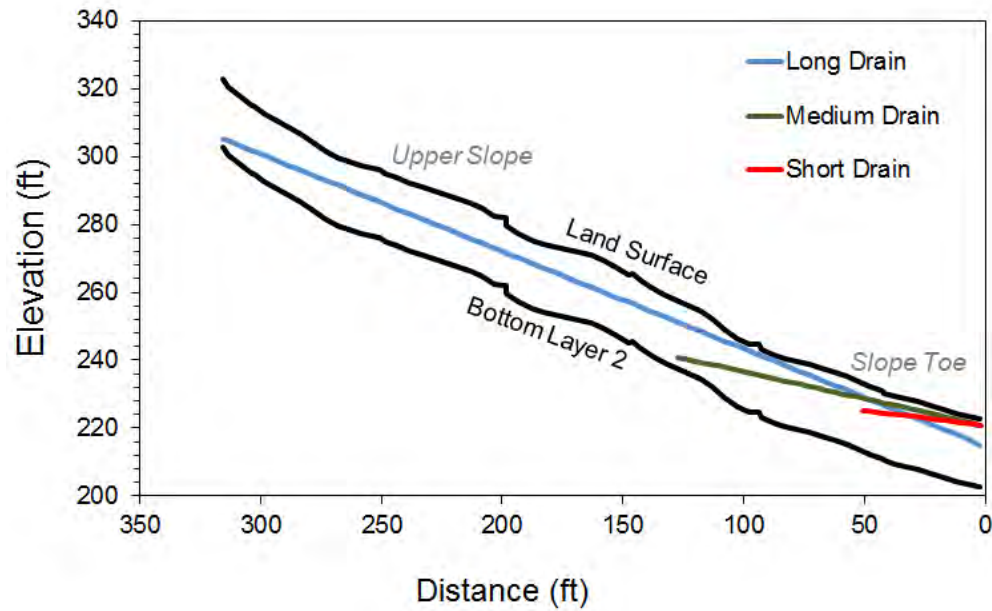


Figure 7.27: A cross section show examples of long, medium and short length drains for site D. The upper slope and the slope toe are marked for reference.

Table 7.7: Drain specifications for site D.

Drain Array	General Description		Num of Drains	Approx. Len.	Tot. Len. ft	Angle	
	Length	Spacing		ft per drain		Fan, deg.	Horiz., deg
1	short	wide	4	50	220	24	5
2	short	medium	9	50	497	12	5
3	short	narrow	18	50	987	6	5
4	medium	wide	4	130	487	24	10
5	medium	medium	9	130	1,042	12	10
6	medium	narrow	18	130	2,047	6	10
7	long	wide	4	90-325	902	24	16
8	long	medium	9	60-325	1,757	12	16
9	long	narrow	18	50-327	3,492	6	16
10	med/short	wide	9	50-130	764.99	12	5/10
11	med/short	medium	19	50-130	1583.3	6	5/10
12	long/short	wide	9	50-325	1177.32	12	5/16
13	long/short	medium	19	50-325	2304.34	6	5/16

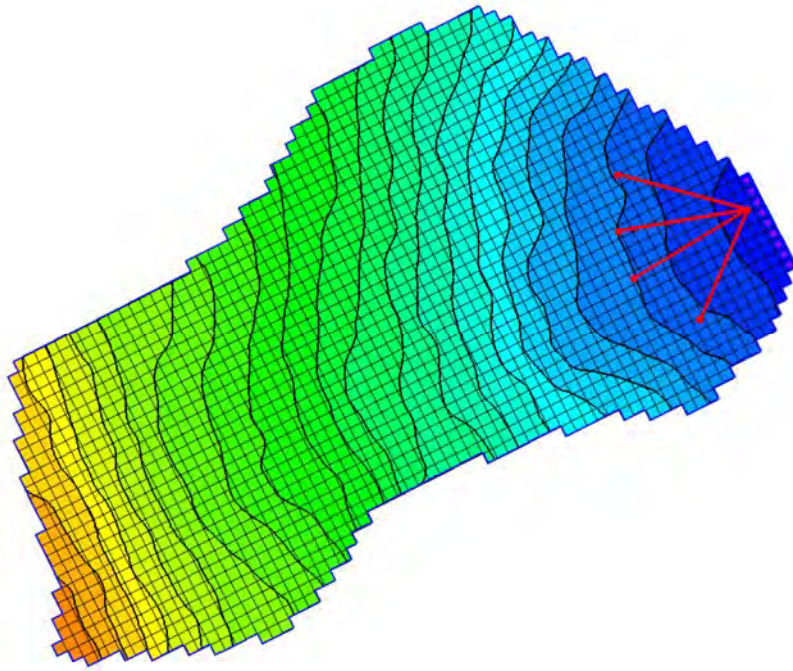


Figure 7.28: Drain array 1 in plan view. Contours represent land surface elevation and red lines represent drain placement. Model cells are 5ft by 5ft.

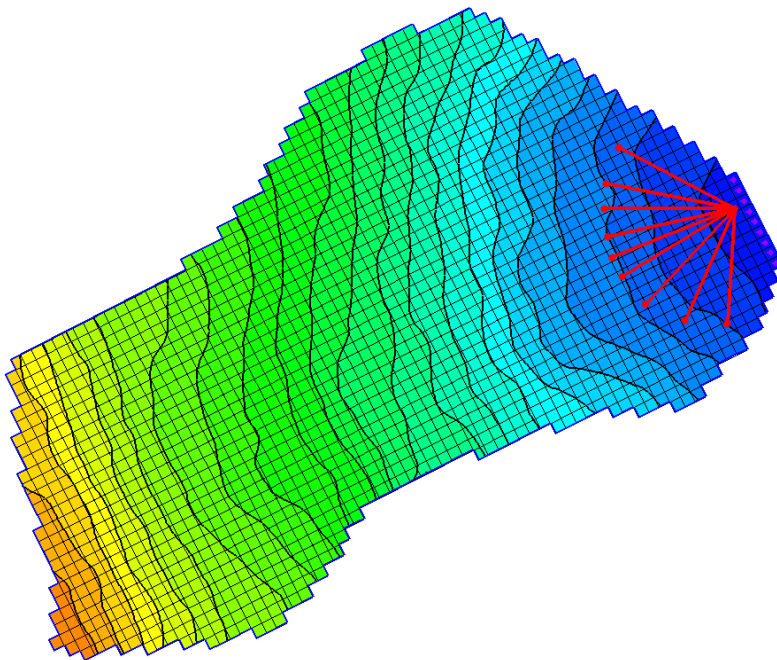


Figure 7.29: Drain array 2 in plan view. Contours represent land surface elevation and red lines represent drain placement. Model cells are 5ft by 5ft.

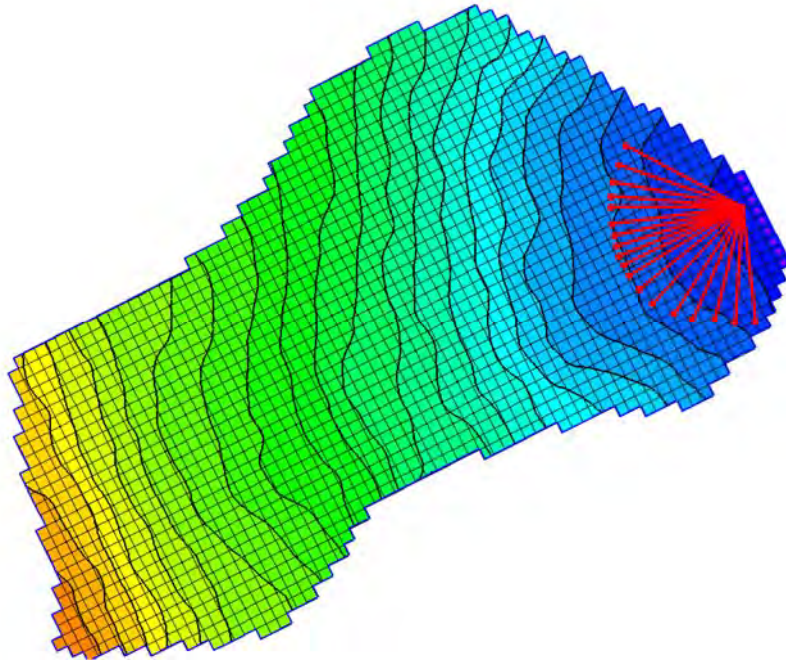


Figure 7.30: Drain array 3 in plan view. Contours represent land surface elevation and red lines represent drain placement. Model cells are 5ft by 5ft.

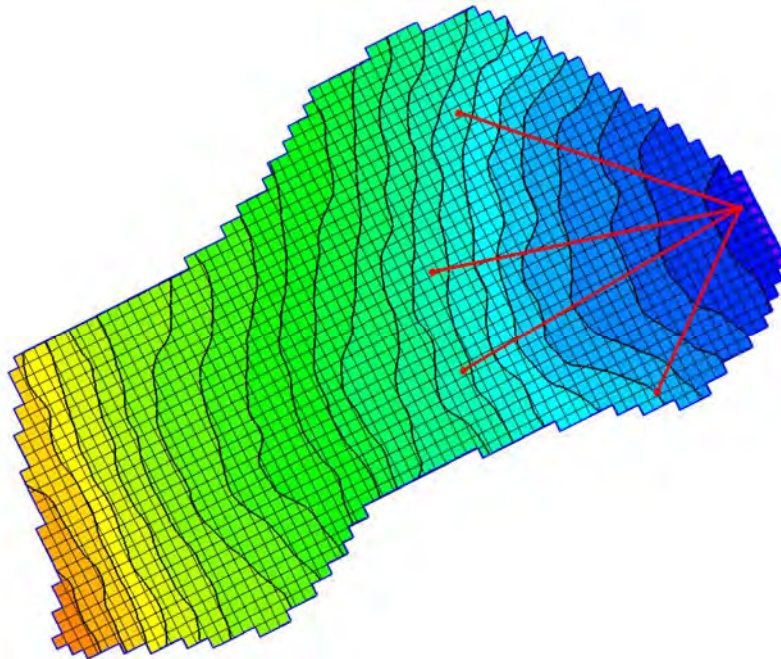


Figure 7.31: Drain array 4 in plan view. Contours represent land surface elevation and red lines represent drain placement. Model cells are 5ft by 5ft.

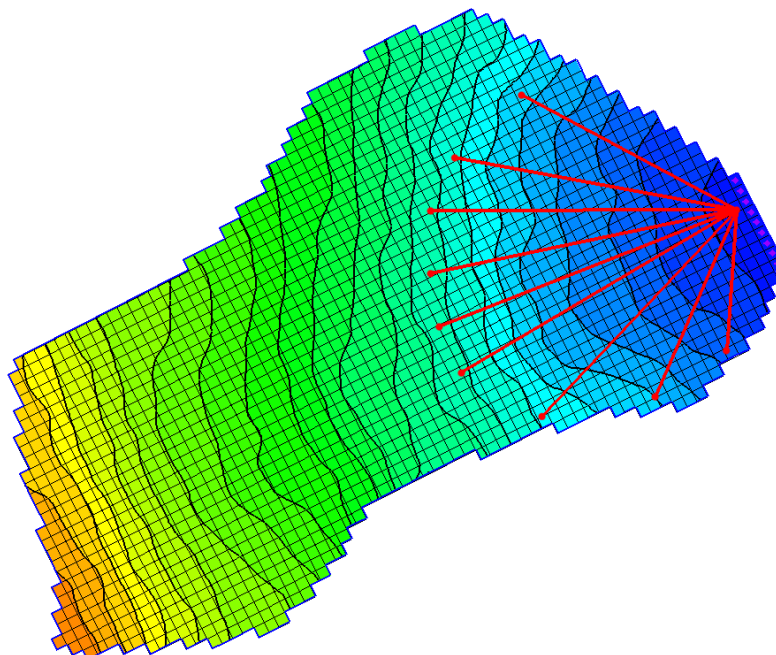


Figure 7.32: Drain array 5 in plan view. Contours represent land surface elevation and red lines represent drain placement. Model cells are 5ft by 5ft.

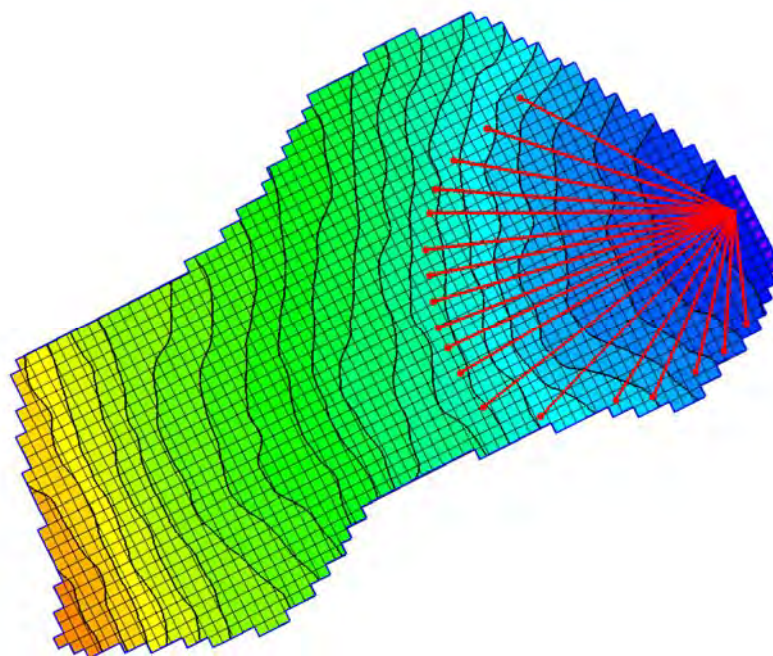


Figure 7.33: Drain array 6 in plan view. Contours represent land surface elevation and red lines represent drain placement. Model cells are 5ft by 5ft.

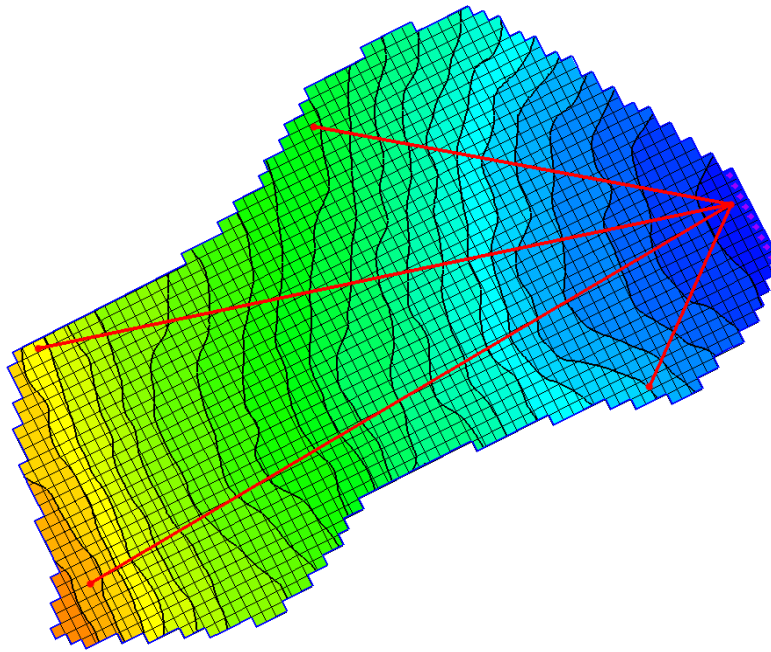


Figure 7.34: Drain array 7 in plan view. Contours represent land surface elevation and red lines represent drain placement. Model cells are 5ft by 5ft.

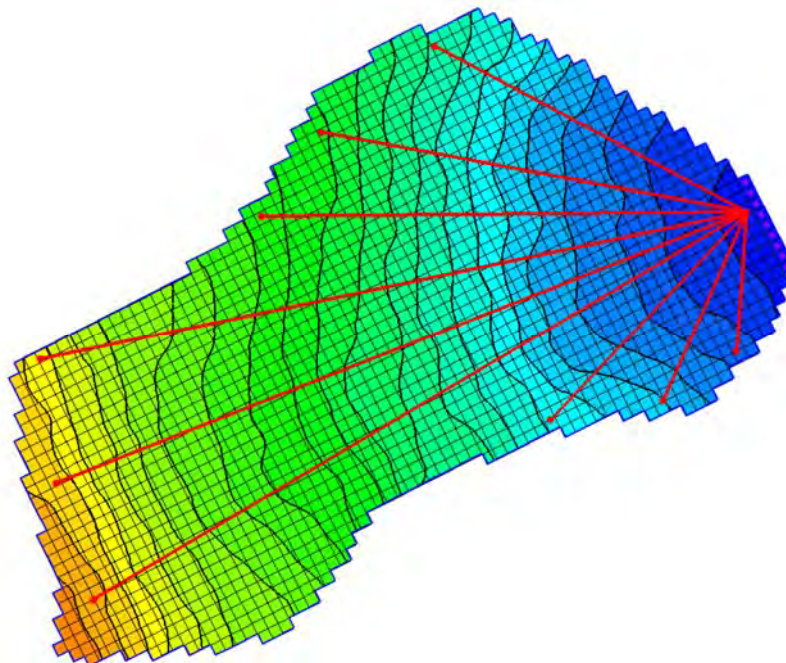


Figure 7.35: Drain array 8 in plan view. Contours represent land surface elevation and red lines represent drain placement. Model cells are 5ft by 5ft.

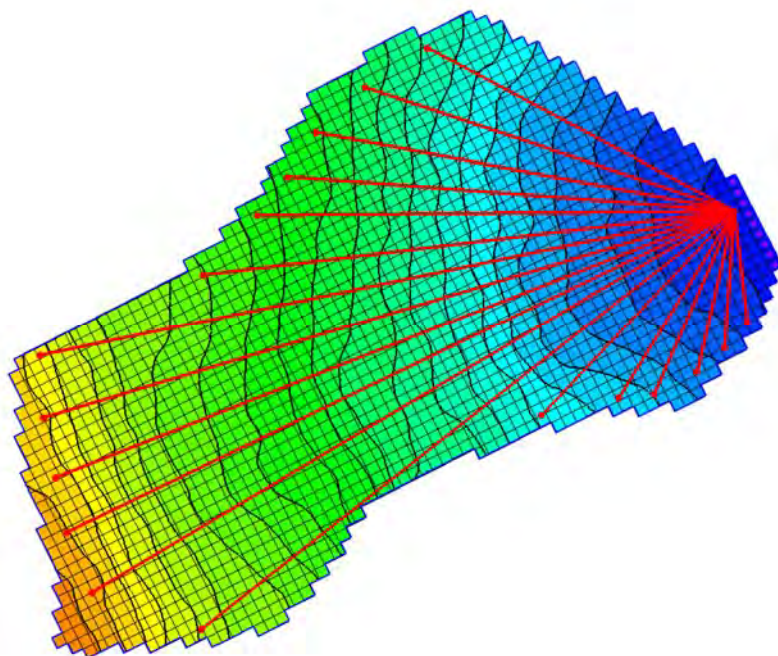


Figure 7.36: Drain array 9 in plan view. Contours represent land surface elevation and red lines represent drain placement. Model cells are 5ft by 5ft.

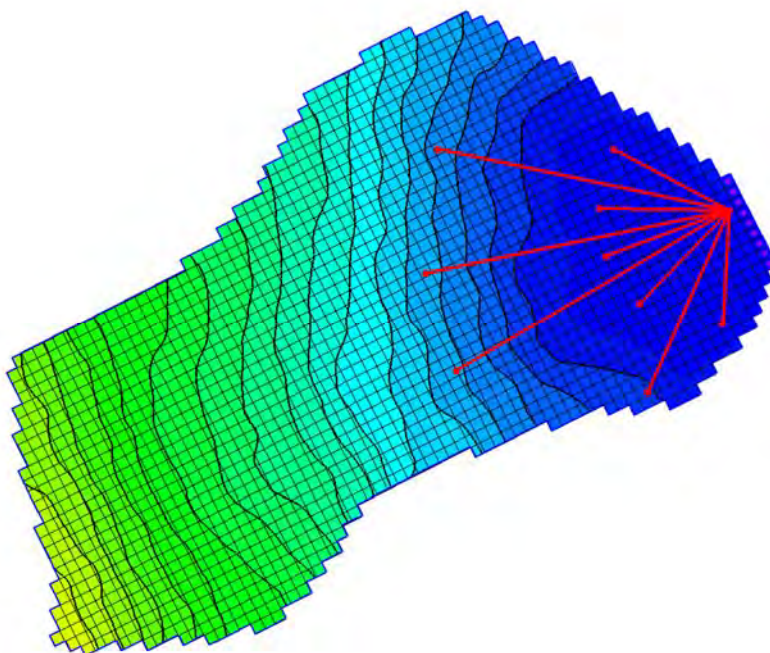


Figure 7.37: Drain array 10 in plan view. Contours represent land surface elevation and red lines represent drain placement. Model cells are 5ft by 5ft.

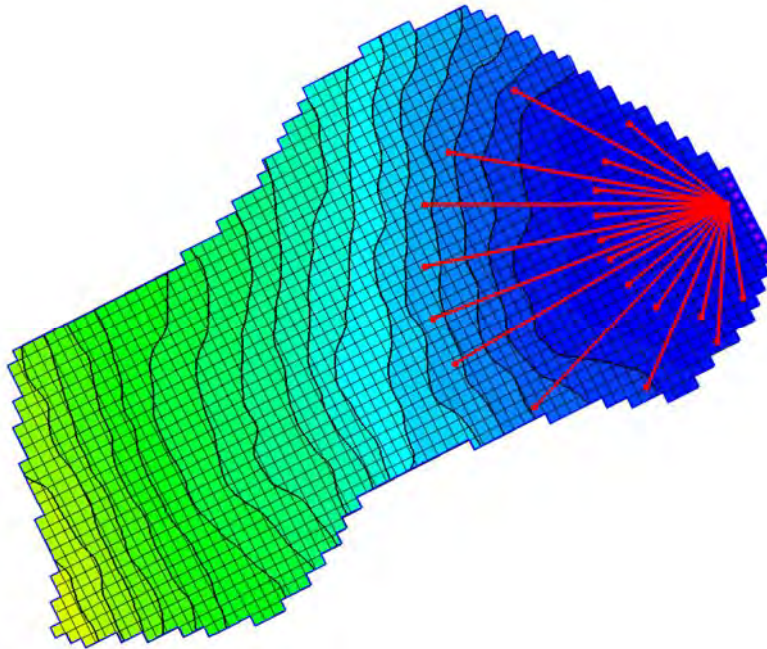


Figure 7.38: Drain array 11 in plan view. Contours represent land surface elevation and red lines represent drain placement. Model cells are 5ft by 5ft.

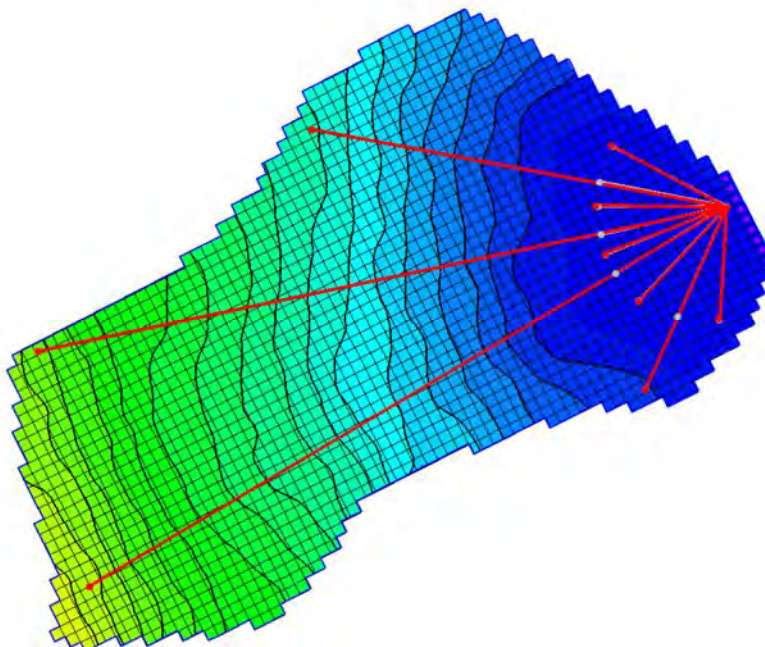


Figure 7.39: Drain array 12 in plan view. Contours represent land surface elevation and red lines represent drain placement. Model cells are 5ft by 5ft.

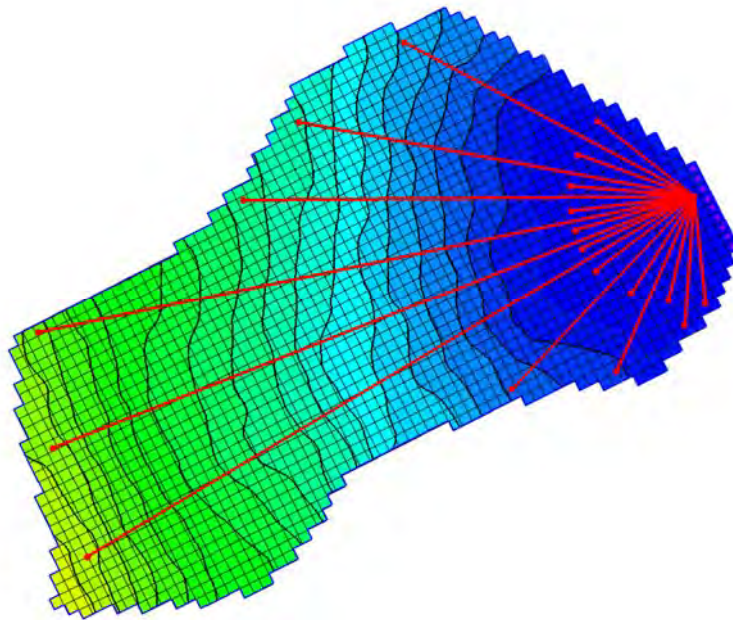


Figure 7.40: Drain array 13 in plan view. Contours represent land surface elevation and red lines represent drain placement. Model cells are 5ft by 5ft.

7.5.3.5 Analysis – No Calibration

A generalized model is constructed with no calibration or verification. All hydraulic parameters are assumed, with no need to adjust hydraulic parameters to match water levels. This is an appropriate approach if no observed water level data are available and allows one to make decisions based on relative response to drainage design. If observed water level exists, however, then calibration methods are recommended (see Appendix B for an example). Results look at the impact of different drain arrays on lowering water table elevations for a range of hydraulic parameters. Reduced water table elevations along cross section d-d' are then used in the geotechnical analysis to evaluate if slope stability requirements are met.

7.5.3.5.1 Steady State

Steady state conditions are run prior to transient simulations to establish possible thresholds of system response based on hydraulic properties given no drains. Steady-state recharge is assigned a value of 0.005 ft/d. Water table profiles are provided in Figure 7.41 given a range of $K_x = 0.2$ ft/d to 5 ft/d. $K_x = 0.1$ ft/d is not shown, since the slope would be massively flooded. K_x larger than 5 ft/d produce water table elevations similar to $K_x = 5$ ft/d. Even under steady-state recharge conditions, the system is flooded for $K_x < 0.5$ ft/d, with flooding limited to the slope toe region for values of $K_x = 0.5$ ft/d. FOS values for each scenario are given in Table 7.8 and show that $K_x \geq 0.5$ ft/d are stable under steady-state conditions with no drains, but failure may occur for lower K_x .

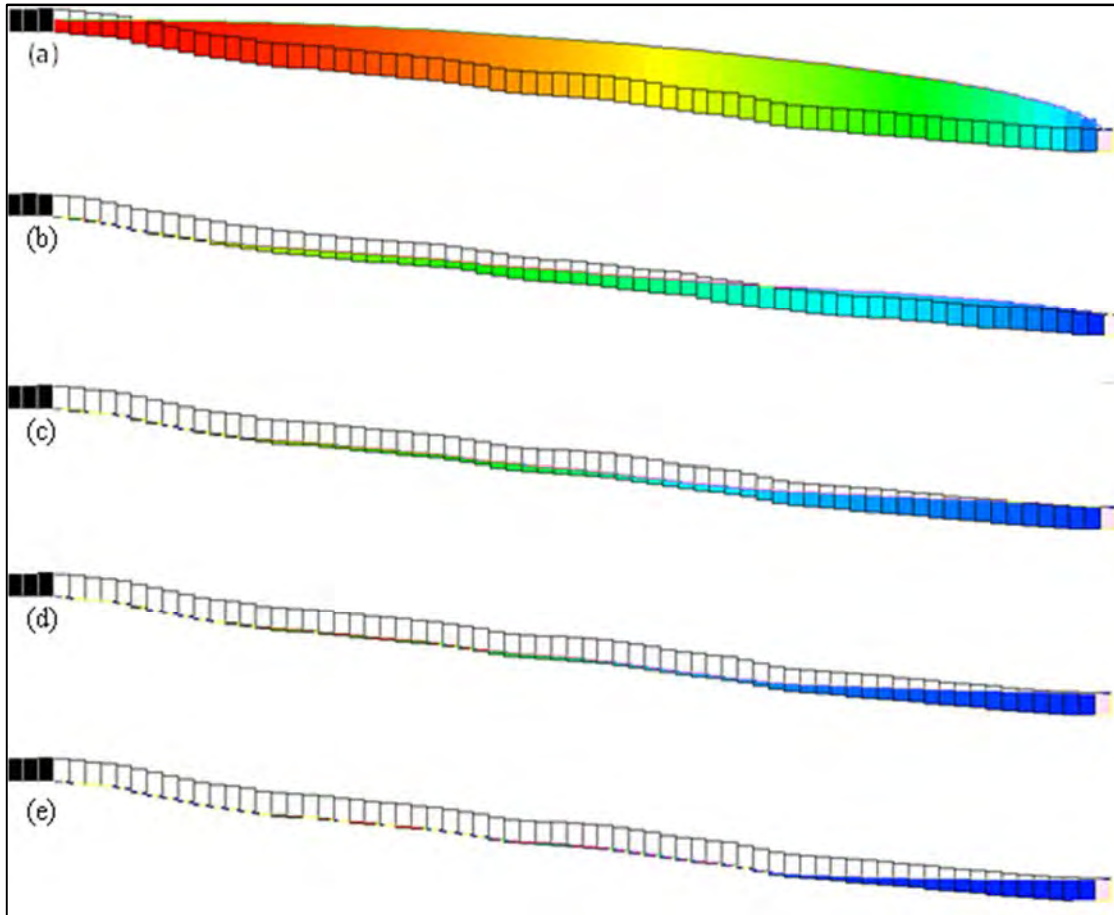


Figure 7.41: Water table profiles for cross section d-d' given steady state recharge and no drains. (a) $K_x = 0.2$ ft/d, (b) $= 0.5$ ft/d, (c) 1.0 ft/d, (d) 2.0 ft/d and (e) 5 ft/d

K_x (ft/day)	FOS
0.1	<1
0.2	<1
0.5	1.31
1	1.50
2	1.71
5	1.80

Table 7.8 FOS of site D given steady-state conditions with no drains for various hydraulic conductivity (K_x) values.

7.5.3.5.2 Maximum Water Levels during 100-Year Event

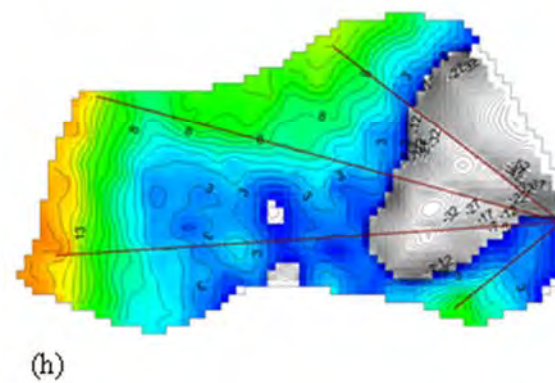
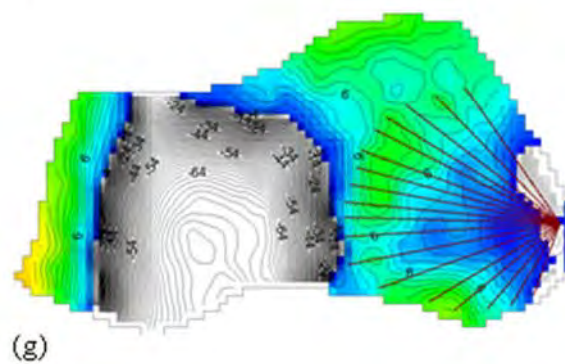
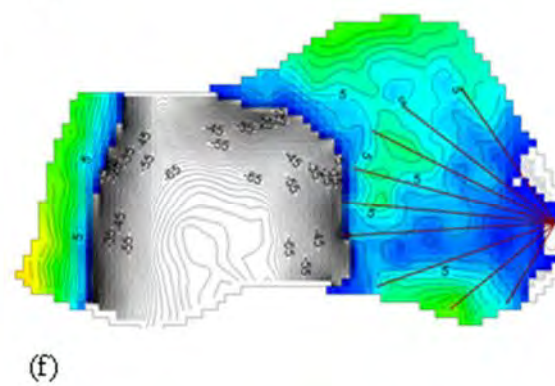
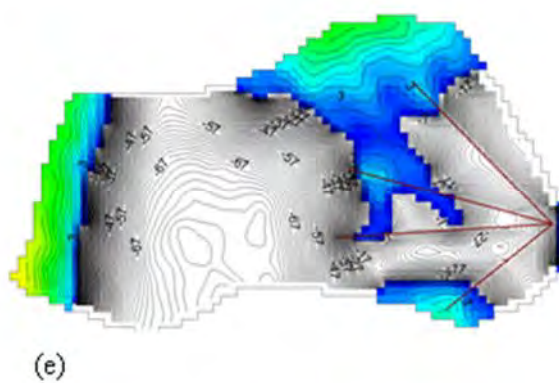
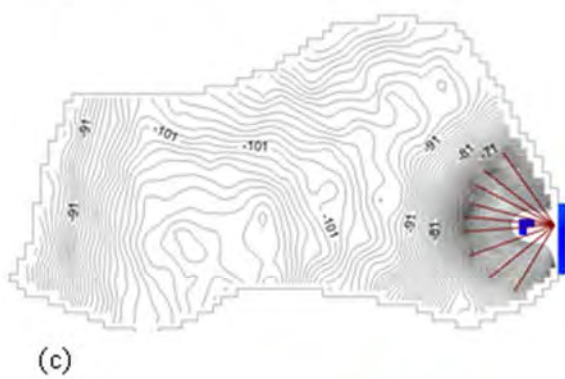
Maximum water levels occur at different times within the basin as water moves down slope. To simplify, the maximum water level is assumed to occur after maximum recharge intensity. This occurs 0.33 days into the 1-day storm event (recharge = 0.70 ft/d). Water level response to drains is discussed in terms of soil type.

Silt, Sandy Silt, Clayey Sand ($K_x = 0.1$ ft/d)

None of the horizontal drain arrays are efficient at reducing water levels below ground surface for soils with low hydraulic conductivity (0.1 ft/d). Soils with isotropic conditions ($VKA = 1$) and a storage of 1% are not drained quickly enough during large precipitation events for any of the drain arrays. Increasing drain density, drain length or both cannot lower the water table below ground surface during very large storm events. Horizontal drains placed in silt, sandy silt and clayey sand or till soils with larger storage (10%) can lower water levels below land surface for much of the basin but the required number of drains is large. Figure 7.42 shows depth to water level for $S_y=10\%$ given all drainage scenarios tested (no drains, drain arrays 1-13). Medium length drains at medium spacing (drain array 6) can effectively lower water levels at the slope toe, but water levels remain above ground surface in the upper reaches of the slope. Long drains of medium spacing can reduce water levels in the upper slope but fail to reduce water levels in the slope toe (drain array 8). Drain array 13, which combines medium spaced long and short drains, fails to reduce water levels completely below ground surface. One combining long and medium drains can lower water levels completely below ground surface (not shown). Horizontal drains in fine-grained materials, even with relatively large storage, are inefficient at lowering water levels, and given the number and length of drains required, may not be economically feasible. Therefore for soils with this range of hydraulic conductivity, horizontal drains would likely need to be used in conjunction with other geotechnical techniques to improve slope stability. Assuming anisotropic conditions reduces the ability of horizontal drains to lower the water table.

Silty Sands and Fine Sands ($K_x = 1.0$ ft/d)

Soils with hydraulic conductivity on the order of 1 ft/d experience seepage (water levels above ground surface) in the toe region of the slope. Seepage increases into the upper reaches of the slope if the system is anisotropic. Water table depths below ground surface for isotropic conditions for all drainage scenarios tested are provided in Figure 7.43 for $S_y = 10\%$ and Figure 7.44 for $S_y = 1\%$. Silty or fine sand soils with specific yield on the order of 10% are successfully drained with minimal drain placement. While most drain configurations effectively maintain water levels below ground surface, it is drain array 1 (short length drains with wide spacing) found the most cost-effective given a total drain length of only 220 ft. Model results suggest that drain array 1 is effective to specific yields as low as 5%, below which significant flooding at the slope toe can only be mitigated by increasing drain length and density. For soils with very low storage, horizontal drains may not completely drain the basin to maintain water



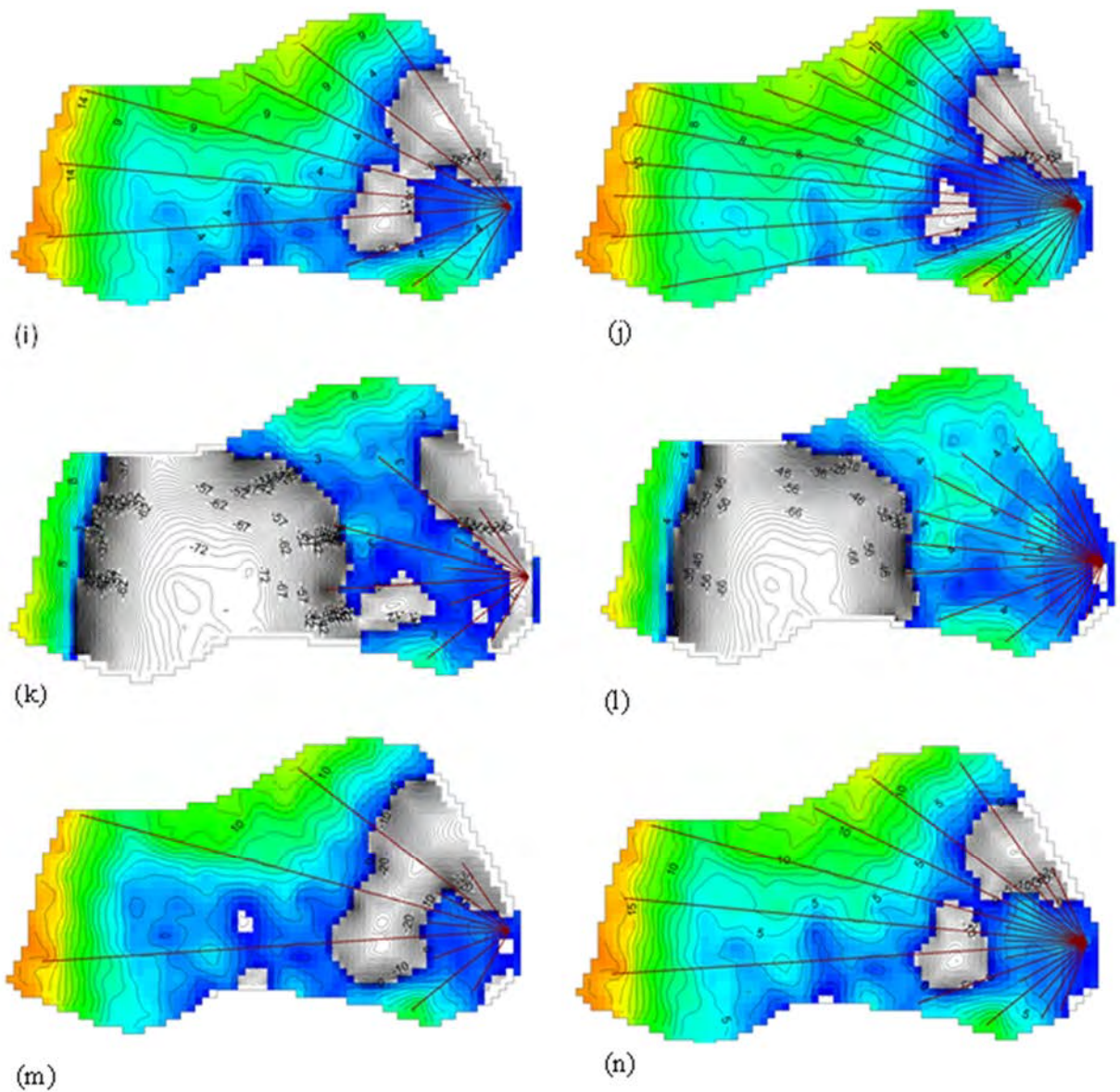
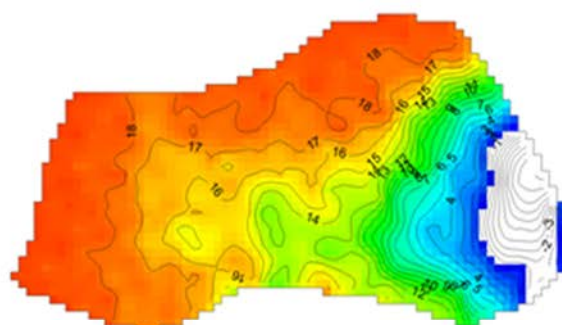
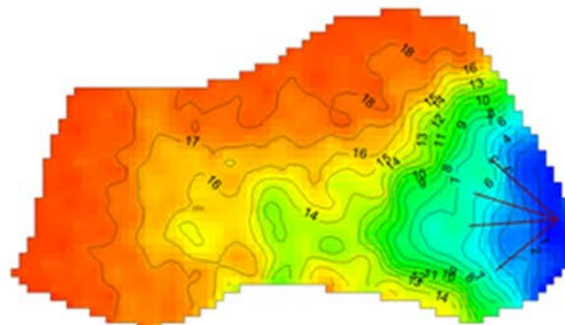


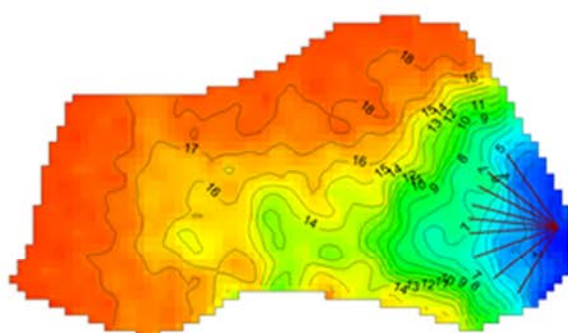
Figure 7.42: Water table depth below ground surface (ft) on day 0.35 (stress period 8) of the 100-year 24-hour precipitation event given hydraulic parameters $K_x = 0.1$ ft/d, $S_y = 0.1$ and $VKA = 1$, and (a) no drains, (b) drain array 1, (c) drain array 2, (d) drain array 3, (e) drain array 4, (f) drain array 5 (g) drain array 6, (h) drain array 7, (i) drain array 8, (j) drain array 9, (k) drain array 10, (l) drain array 11, (m) drain array 12 and (n) drain array 13. Drains are represented as brown lines and contours are at 1 ft intervals. Colored portions indicate water table is below ground surface, while white regions indicate seepage caused by the water table rising above ground surface. Water table elevations predicted above ground surface indicate groundwater seepage. Height above ground is correlated to seepage flux.



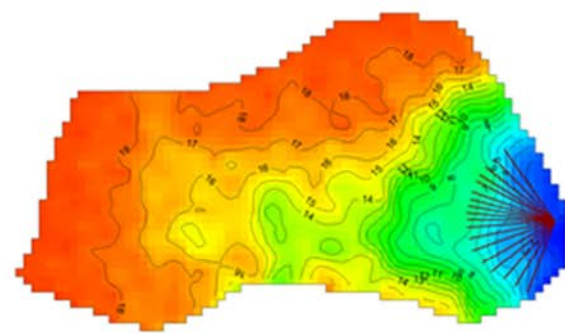
(a)



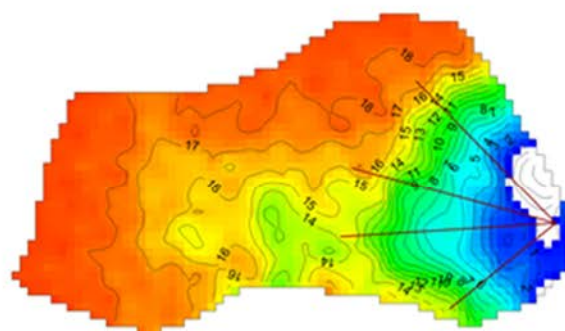
(b)



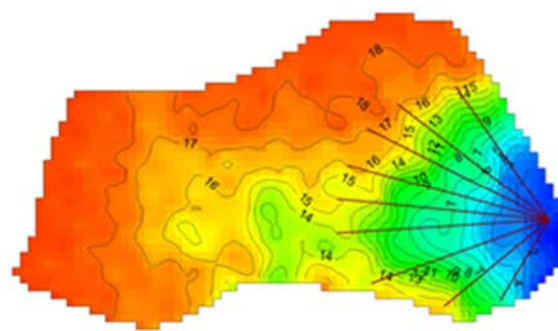
(c)



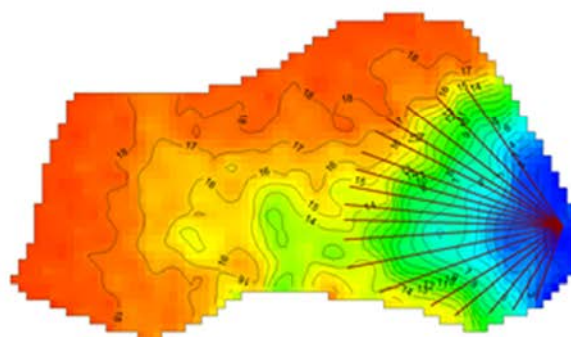
(d)



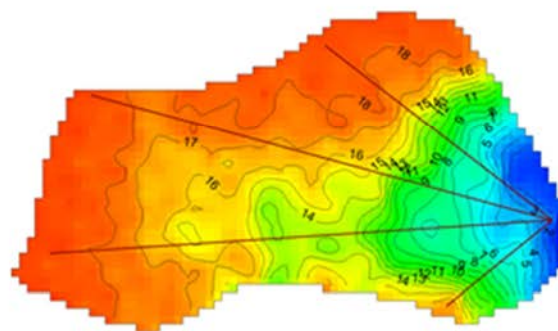
(e)



(f)



(g)



(h)

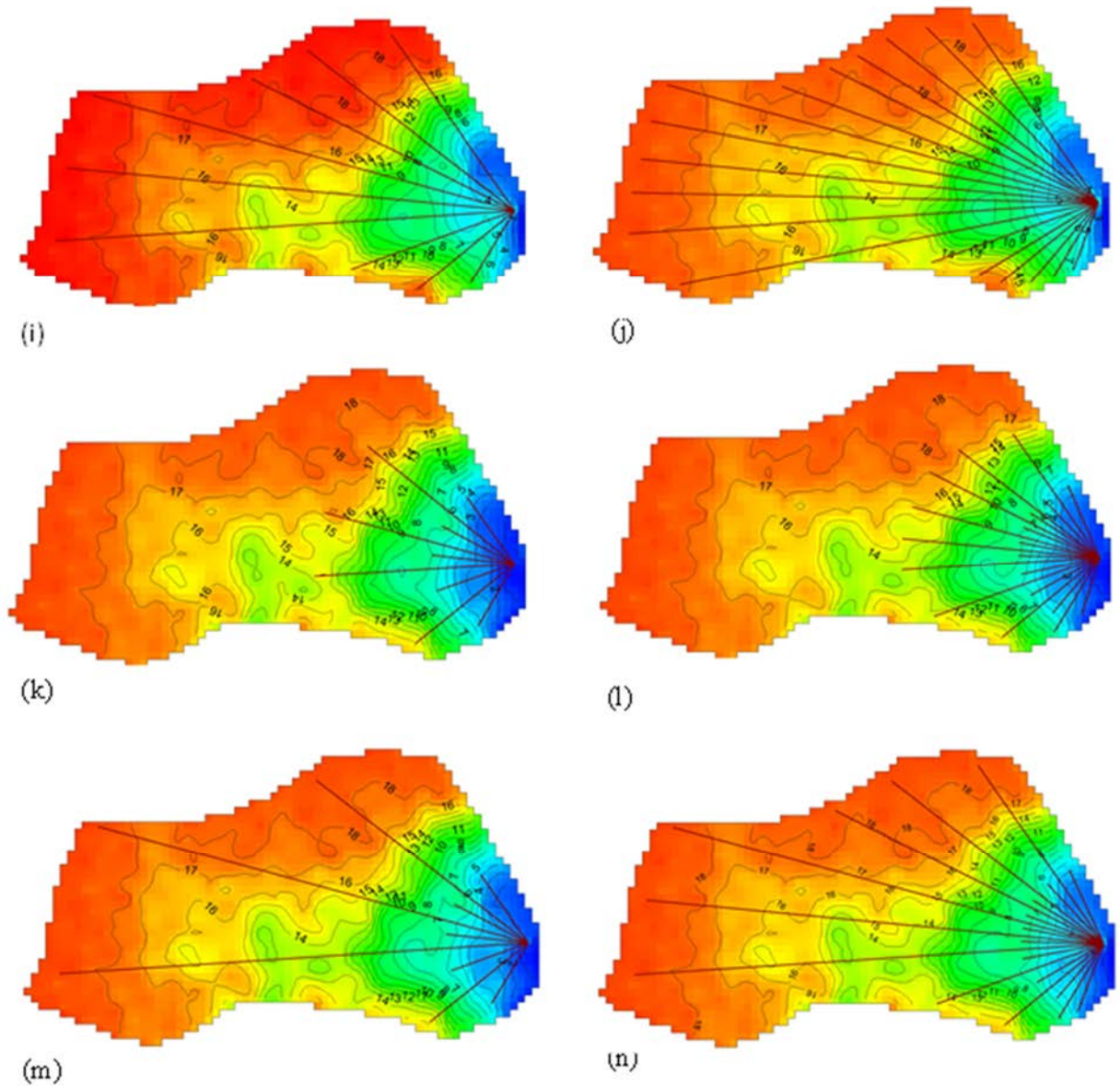
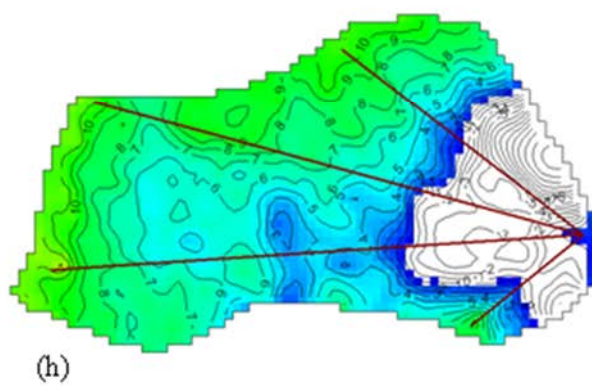
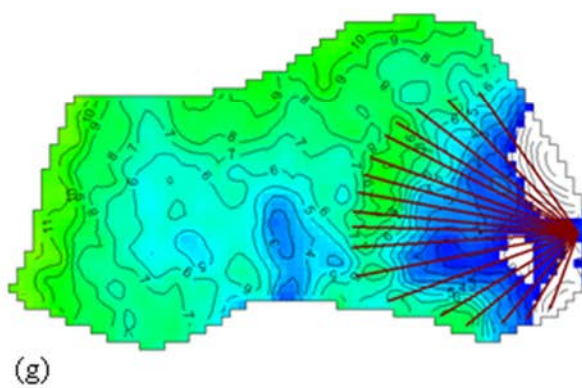
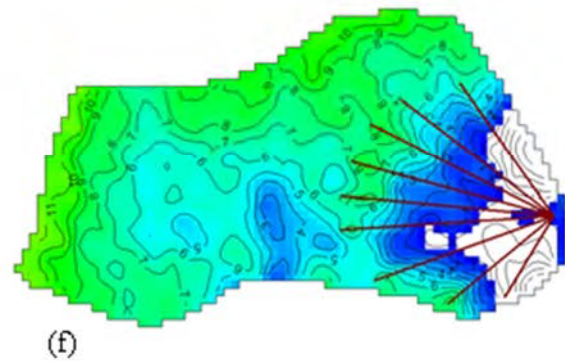
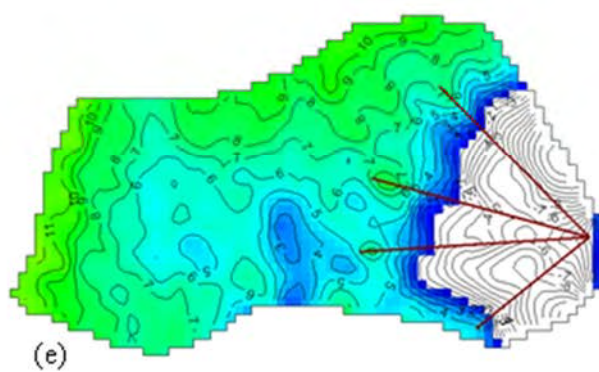
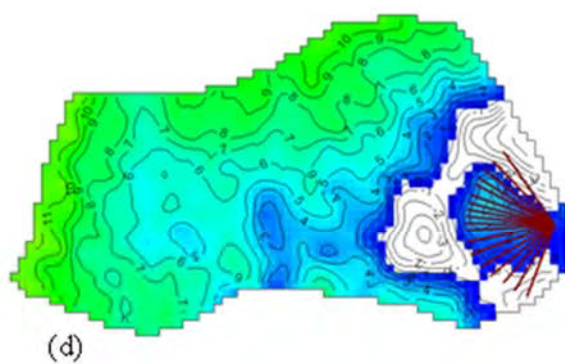
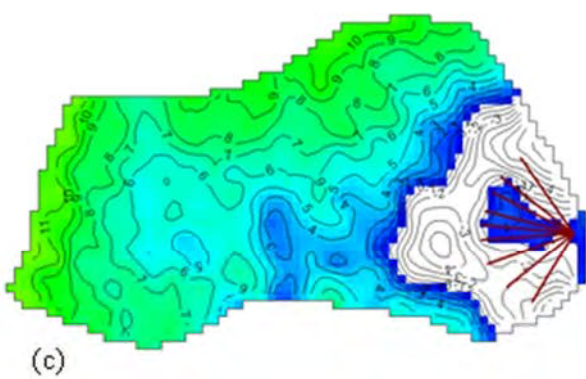
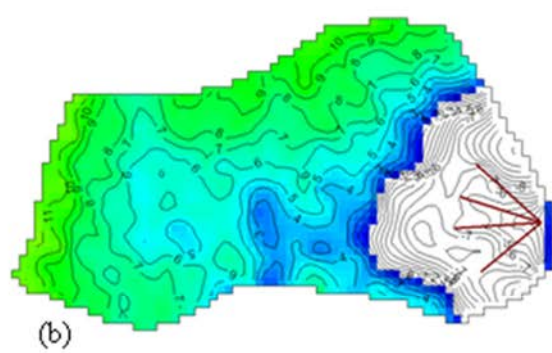
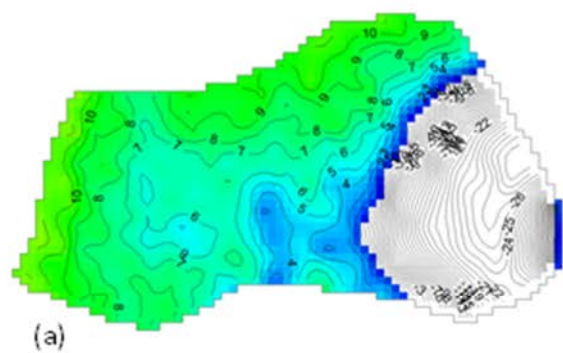


Figure 7.43: Water table depth below ground surface (ft) on day 0.35 (stress period 8) of the 100-year 24-hour precipitation event given hydraulic parameters $K_x = 1$ ft/d, $S_y = 0.1$ and $VKA = 1$, and (a) no drains, (b) drain array 1, (c) drain array 2, (d) drain array 3, (e) drain array 4, (f) drain array 5 (g) drain array 6, (h) drain array 7, (i) drain array 8, (j) drain array 9, (k) drain array 10, (l) drain array 11, (m) drain array 12 and (n) drain array 13. Drains are represented as brown lines and contours are at 1 ft intervals. Colored portions indicate water table is below ground surface, while white regions indicate seepage caused by the water table rising above ground surface. Water table elevations predicted above ground surface indicate groundwater seepage. Height above ground is correlated to seepage flux.



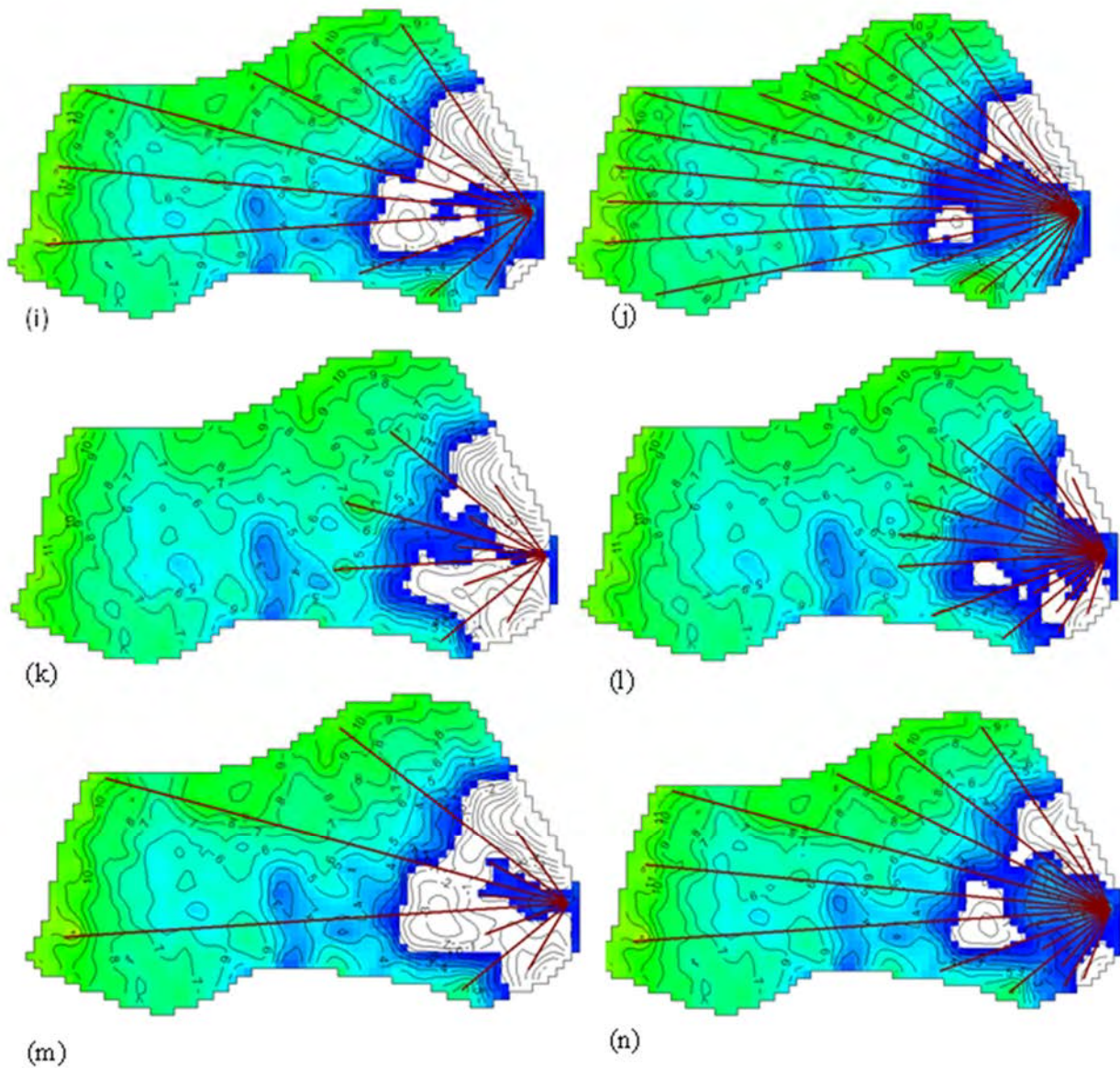


Figure 7.44: Water table depth below ground surface (ft) on day 0.35 (stress period 8) of the 100year 24-hour precipitation event given hydraulic parameters $K_x = 1 \text{ ft/d}$, $S_y = 0.01$ and $VKA = 1$, and (a) no drains, (b) drain array 1, (c) drain array 2, (d) drain array 3, (e) drain array 4, (f) drain array 5 (g) drain array 6, (h) drain array 7, (i) drain array 8, (j) drain array 9, (k) drain array 10, (l) drain array 11, (m) drain array 12 and (n) drain array 13. Drains are represented as brown lines and contours are at 1 ft intervals. Colored portions indicate water table is below ground surface, while white regions indicate seepage caused by the water table rising above ground surface. Water table elevations predicted above ground surface indicate groundwater seepage. Height above ground is correlated to seepage flux.

levels below land surface. However, a combination of medium and short length drains with medium spacing (drain array 11) lowers the water table the most of all drain arrays tested.

Anisotropy ($VKA = 10$) needs only be considered for soils with $S_y < 5\%$. For soils with larger storage, drainage design remains the same as for isotropic conditions. As an example, Figure 7.45 shows that water levels for $S_y = 0.05$ can be held below land surface for a mixture of medium and short length drains (drain array 11), but will experience appreciable flooding if $S_y = 0.01$.

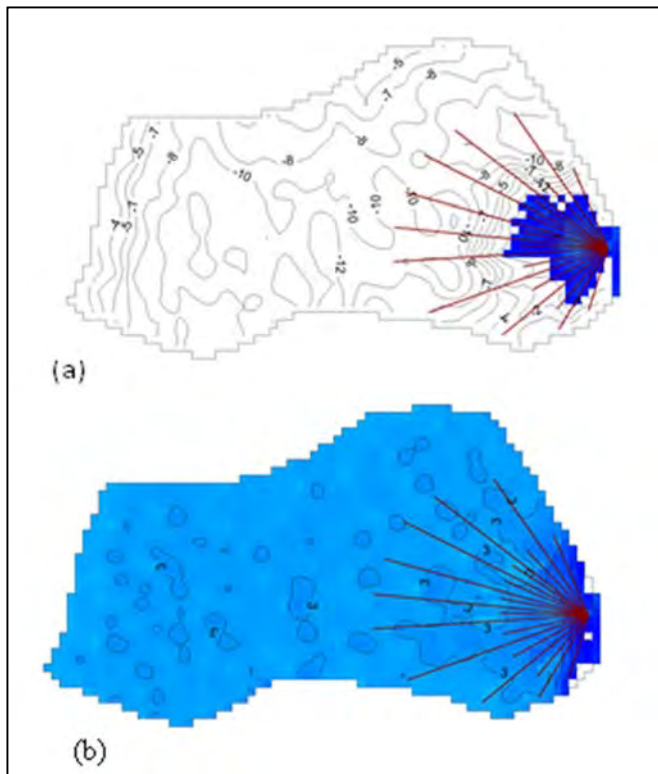


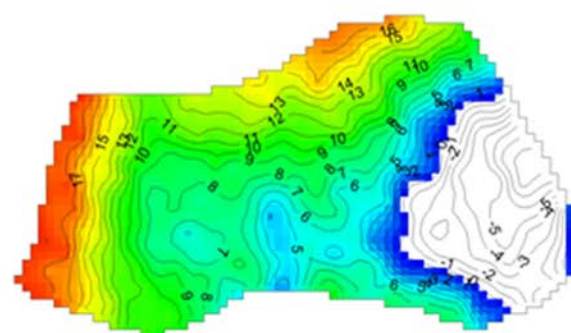
Figure 7.45: Water table depth below ground surface (ft) on day 0.35 (stress period 8) of the 100-year 24-hour precipitation event given hydraulic parameters $K_x = 1$ ft/d, $VKA = 10$ and drain array 11. (a) $S_y = 0.01$ and (b) $S_y = 0.05$. Contours are 1 ft intervals. Colored portions indicate water table is below ground surface, while white regions indicate seepage caused by the water table rising above ground surface. Water table elevations predicted above ground surface indicate groundwater seepage. Height above ground is correlated to seepage flux.

Well Sorted Sands ($K_x = 10 \text{ ft/d}$)

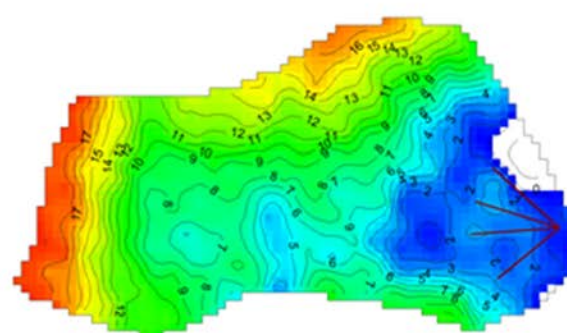
Soils with hydraulic conductivity on the order of 10 ft/d and 10% specific yield can transmit water quickly and mute large recharge events such that water levels do not exceed ground surface. Therefore drains are not needed to lower water table elevations. With decreased storage, groundwater seepage occurs in the toe region of the slope (Figure 7.46) and all drain arrays successfully maintain water levels below ground surface in the region of cross section d-d'. However, drain array 2 (short length and medium spacing) removes all seepage potential for the least linear foot of drain. Drainage design for well sorted sands and gravels are not sensitive to anisotropy given $VKA \leq 25$ (Figure 7.47). Water table elevations are increased, but drain array 2 is sufficient in lowering water levels below ground surface for much of the basin. For larger VKA it is necessary to increase length and density of drains, with no drain array tested able to lower water tables below ground surface given $VKA \geq 50$.

7.5.3.5.3 Slope Stability Analysis

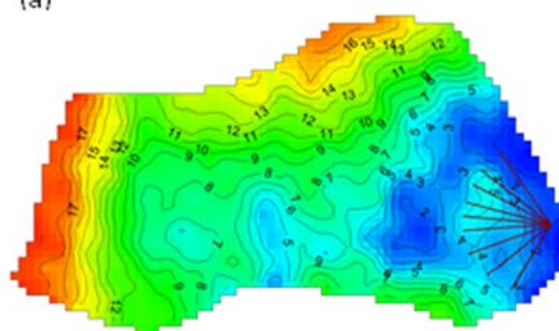
FOS calculations were conducted using the simplified Janbu method for all model scenarios along cross section d-d' (refer to Figure 7.24). Water levels predicted above ground surface (i.e. groundwater seepage) were assigned water table elevations at ground surface (Figure 7.48). FOS calculations for all modeled scenarios are provided in Table 7.9. FOS calculations do not explicitly use water levels across the entire modeled domain, but consider groundwater levels along a critical 2-dimensional section generally taken through the steepest portion of the slope. This simplification from three dimensions used in the groundwater modeling down to 2 dimensions used for the slope stability analyses may not capture portions of the slope where groundwater levels remain elevated after drain placement or other heterogeneities of the groundwater system. For this reason, multiple critical sections of varied orientations might be warranted for further iterative slope stability analyses and groundwater modeling to help ensure stability conditions are met for the entire slope area of interest. For site D, the slope is fairly uniform is modeled as homogeneous, such that hydraulic properties are the same across the basin. Therefore, a single cross section along d-d' is assumed representative of the entire slope area. FOS calculations are most sensitive to elevated water levels in the upper slope and much less sensitive to groundwater seepage in the toe of slope.



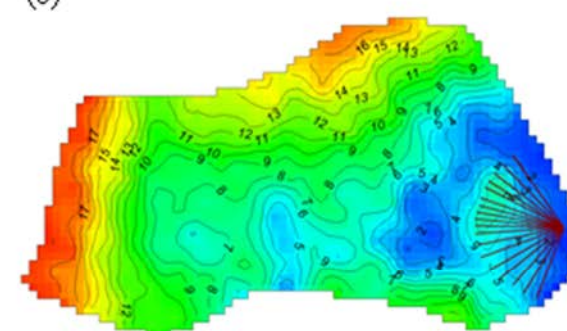
(a)



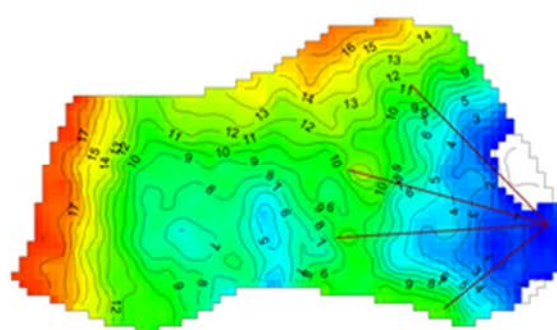
(b)



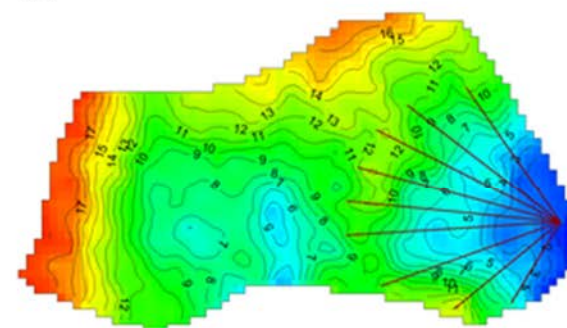
(c)



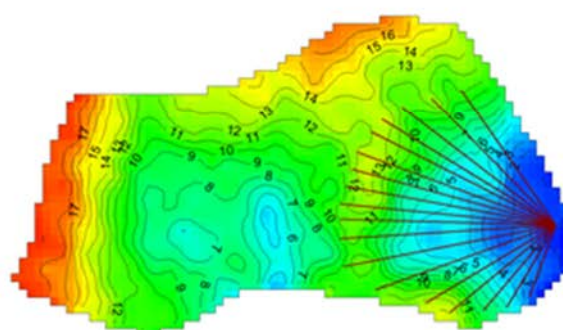
(d)



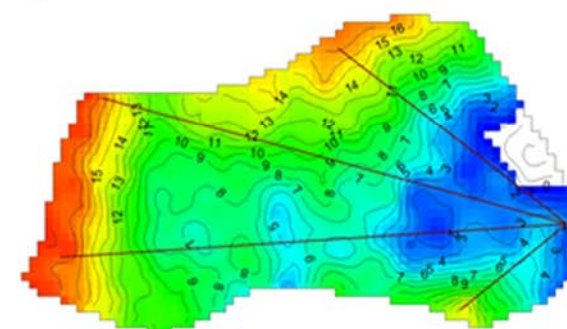
(e)



(f)



(g)



(h)

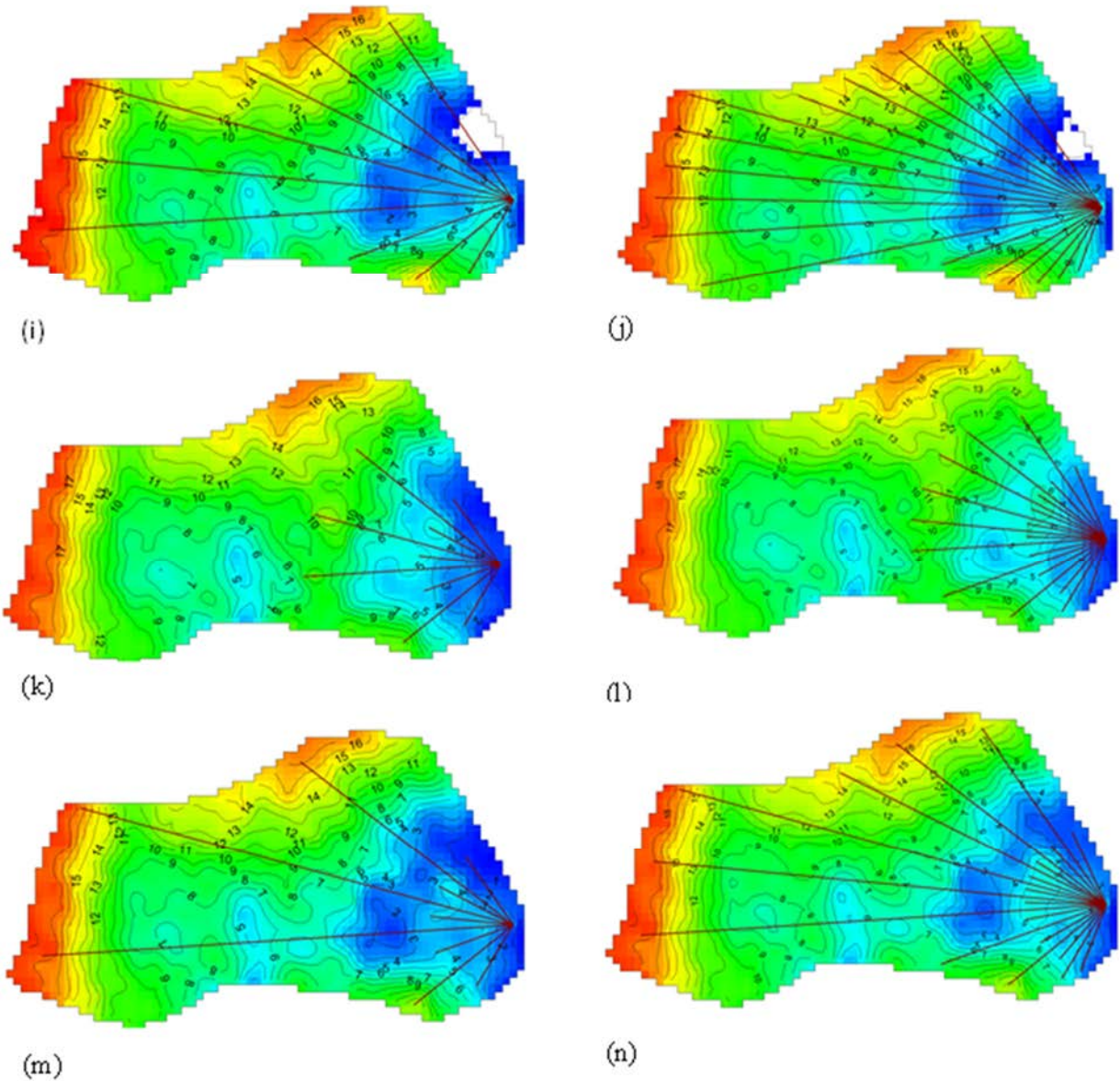


Figure 7.46: Water table depth below ground surface (ft) on day 0.35 (stress period 8) of the 100-year 24-hour precipitation event given hydraulic parameters $K_x = 10 \text{ ft/d}$, $S_y = 0.01$ and $VKA = 1$, given (a) no drains, (b) drain array 1, (c) drain array 2, (d) drain array 3, (e) drain array 4, (f) drain array 5 (g) drain array 6, (h) drain array 7, (i) drain array 8, (j) drain array 9, (k) drain array 10, (l) drain array 11, (m) drain array 12 and (n) drain array 13. Drains are represented as brown lines and contours are at 1 ft intervals. Colored portions indicate water table is below ground surface, while white regions indicate seepage caused by the water table rising above ground surface. Water table elevations predicted above ground surface indicate groundwater seepage. Height above ground is correlated to seepage flux.

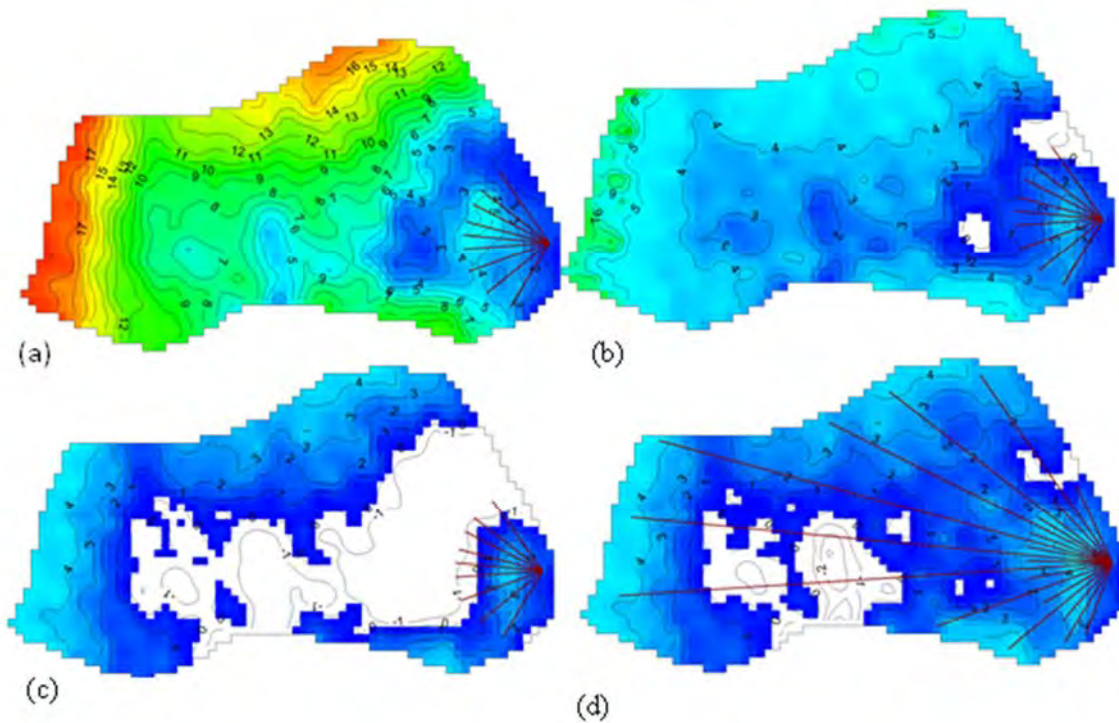


Figure 7.47: Water table depth below ground surface (ft) on day 0.35 (stress period 8) of the 100-year 24-hour precipitation event given hydraulic parameters $K_x = 10$ ft/d, $S_y = -.01$ and (a) $VKA = 1$ and drain array 2, (b) $VKA = 25$ and drain array 2, (c) $VKA = 50$ and drain array 2, and (d) $VKA = 50$ and drain array 13. Contours are 1 ft intervals. Colored portions indicate water table is below ground surface, while white regions indicate seepage caused by the water table rising above ground surface. Water table elevations predicted above ground surface indicate groundwater seepage. Height above ground is correlated to seepage flux.

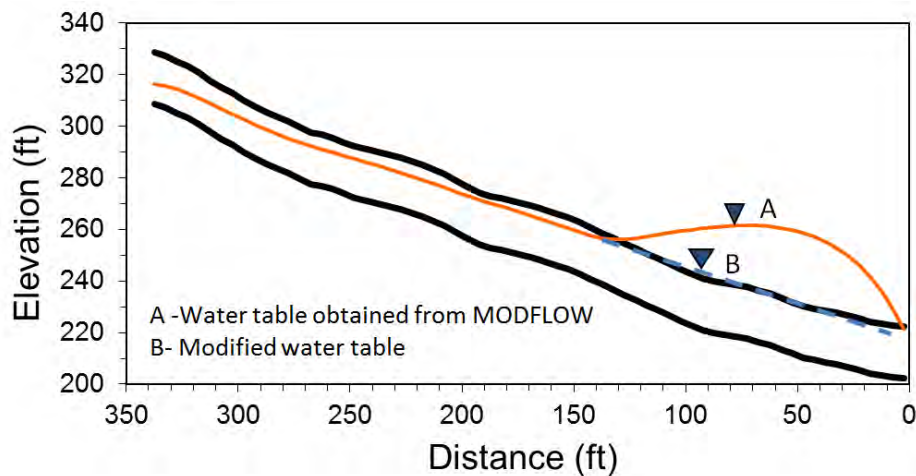


Figure 7.48: An example of modifying the water table surface with drains to be used for FOS calculation. Water table elevations predicted by MODFLOW to be above the ground surface represent an area of seepage at the surface.

Table 7.9: FOS for different hydraulic properties and drain arrays. FOS pertains to failure along the entire surface and does not consider localized instability (i.e. the toe of the slope). K_x is in units of ft/d. Shaded highlights signify stable slope conditions (FOS \geq 1.2) for the least linear feet of drains. Several soil types fail to achieve stability for all drain arrays tested.

Soil Type	Silt, Sandy Silt, Clayey Sand or Till				Silty Sands and Fine Sands				Well Sorted Sands, Glacial Outwash			
Soil ID	1	7	4	10	2	8	5	11	3	9	6	12
K_x	0.1	0.1	0.1	0.1	1	1	1	1	10	10	10	10
S_y	0.01	0.01	0.1	0.1	0.01	0.01	0.1	0.1	0.01	0.01	0.1	0.1
VKA	1	10	1	10	1	10	1	10	1	10	1	10
no drain	<1	<1	<1	<1	1.113	<1	1.426	1.153	1.273	1.268	1.647	1.343
drain 1	<1	<1	<1	<1	1.148	<1	1.462	1.158	1.449	1.366	1.647	1.343
drain 2	<1	<1	<1	<1	1.216	<1	1.462	1.158	1.449	1.366	1.647	1.343
drain 3	<1	<1	<1	<1	1.216	<1	1.462	1.158	1.449	1.336	1.647	1.343
drain 4	<1	<1	<1	<1	1.148	<1	1.462	1.158	1.462	1.336	1.647	1.343
drain 5	<1	<1	<1	<1	1.216	<1	1.462	1.158	1.462	1.166	1.647	1.343
drain 6	<1	<1	<1	<1	1.216	<1	1.462	1.158	1.462	1.166	1.647	1.343
drain 7	<1	<1	1.239	<1	1.124	<1	1.462	1.158	1.449	1.218	1.647	1.343
drain 8	<1	<1	1.239	1.026	1.216	<1	1.462	1.158	1.449	1.366	1.647	1.343
drain 9	<1	<1	1.239	1.154	1.216	<1	1.462	1.158	1.449	1.166	1.647	1.343
drain 10	<1	<1	<1	<1	1.216	<1	1.462	1.158	1.462	1.166	1.647	1.343
drain 11	<1	<1	<1	<1	1.216	<1	1.462	1.158	1.462	1.166	1.647	1.343
drain 12	<1	<1	1.239	<1	1.216	<1	1.462	1.158	1.449	1.384	1.647	1.343
drain 13	<1	<1	1.239	1.026	1.216	<1	1.462	1.158	1.449	1.166	1.647	1.343

Silt, Sandy Silt, Clayey Sand or Till ($K_x = 0.1$ ft/d)

For the example Site D having aquifers with very low hydraulic conductivity and low storage, no horizontal drain configuration examined is able to increase FOS above 1.2. In contrast, low K_x soils with higher storage capabilities and isotropic conditions can be stabilized with drain arrays 7, 8, 9, 12 and 13 despite significant ground water seepage in the toe region of the slope. FOS calculations suggest that slope stability is achieved with long drains extending to the upper reaches of the slope. Tighter drain spacing for the long drain arrays appears to have little influence on slope stability. Drain spacing becomes more important for anisotropic soils. For instance, the FOS calculation shows that long drains with narrow spacing (drain array 9) is 1.154 and is the highest FOS in the VKA = 10 analysis. In contrast, long drains with narrow spacing (drain array 7) cannot mitigate slope failure (FOS<1) while long drains with medium spacing (drain array 8) produce an FOS only slightly above 1.0.

Silty Sands and Fine Sands ($K_x = 1.0 \text{ ft/d}$)

For the example Site D having aquifers with isotropic conditions and low storage it was necessary to have short length drains of medium spacing (drain array 2) to reduce water levels enough such that FOS exceeded 1.2. Drain array 2 still worked for anisotropic soils up to $VKA = 2$, but failed to increase FOS above 1.2 for $VKA \geq 5$. For $VKA = 5$ increasing drain length and spacing helped prevent water from inundating the entire slope. For $VKA = 10$, no drain array could reduce water levels sufficiently to increase FOS to reasonable levels.

For sands with large storage, drains were not necessary. For isotropic conditions, FOS was greater than 1.2, and for anisotropic conditions ($VKA = 10$), drain installation did not improve upon $FOS = 1.15$.

Well Sorted Sands ($K_x = 10 \text{ ft/d}$)

Well sorted sands and gravels appeared not need any horizontal drains to improve stability. Short toe drains were needed to reduce groundwater seepage potential, but FOS calculations were not sensitive to elevated water levels in the toe of slope. Increased water levels in the upper slopes only occurred with very high VKA (e.g. $VKA > 25$, refer to Figure 7.47) and for these situations, drains should extend to the upper reaches of the slope. For $VKA \geq 50$, no drain array sufficed in promoting slope stability.

7.5.3.5.4 Sensitivity Analysis

Drain design sensitivity to recharge parameters and drain conductance are investigated given the level of uncertainty in these parameter groups.

Recharge

Calculation of recharge is dictated by three parameters. These include the curve number (CN), the total precipitation in a 24-hour period, and the shape of the SCS rainfall distribution curve. Sensitivity to each of these parameters is tested on isotropic well sorted sands and gravels ($K_x = 10 \text{ ft/d}$) as well as silty or fine sands ($K_x = 1 \text{ ft/d}$). The primary question posed; will drain design need to change if recharge characteristics are changed?

Decreasing the CN from 80 to 70 will increase total recharge by 50% and water table elevations will rise significantly in silty or fine sands given low storage (Figure 7.49) and to a lesser degree for higher storage (Figure 7.50). Groundwater seepage moves up slope and lowers slope stability. Drain length and density must be increased for lower storage situations, while drain array 1 (short drains of wide spacing) are all required for conditions of higher storage. In contrast, water table elevations are not sensitive to recharge parameters in well sorted sands and gravels and change to drainage design is expected (Figure 7.51 and 7.52).

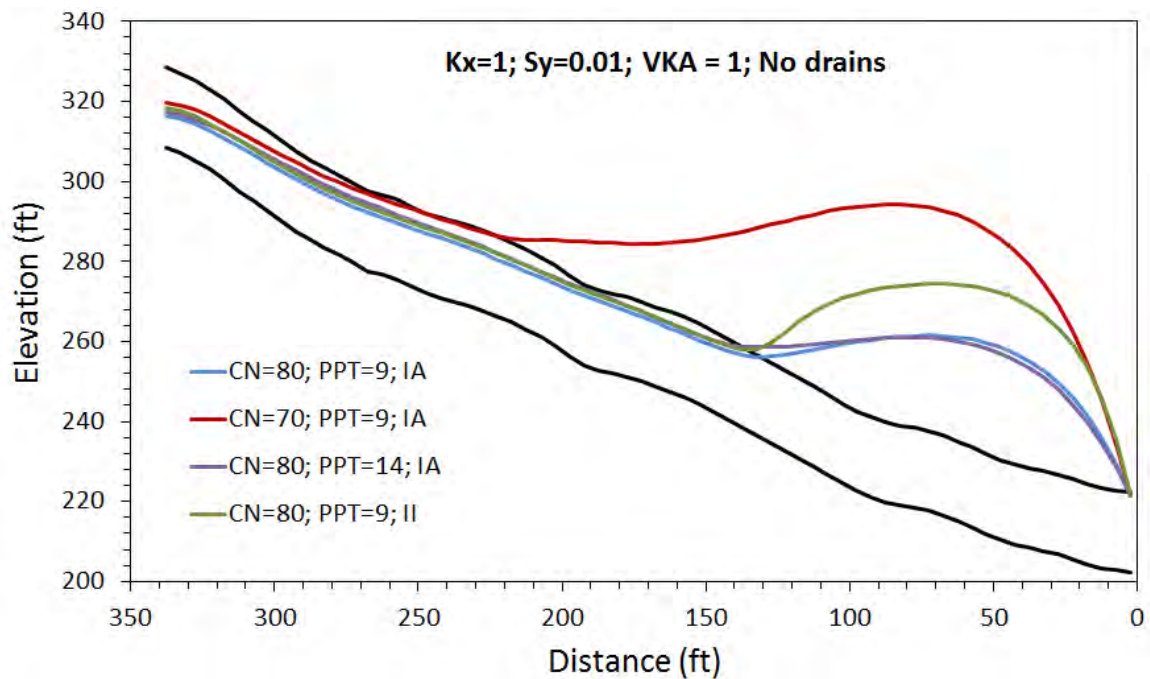


Figure 7.49: Sensitivity of water table elevations to recharge parameters for cross section d-d' given isotropic silty or fine sands of low storage. PPT = total precipitation (inches) during 24-hour event.

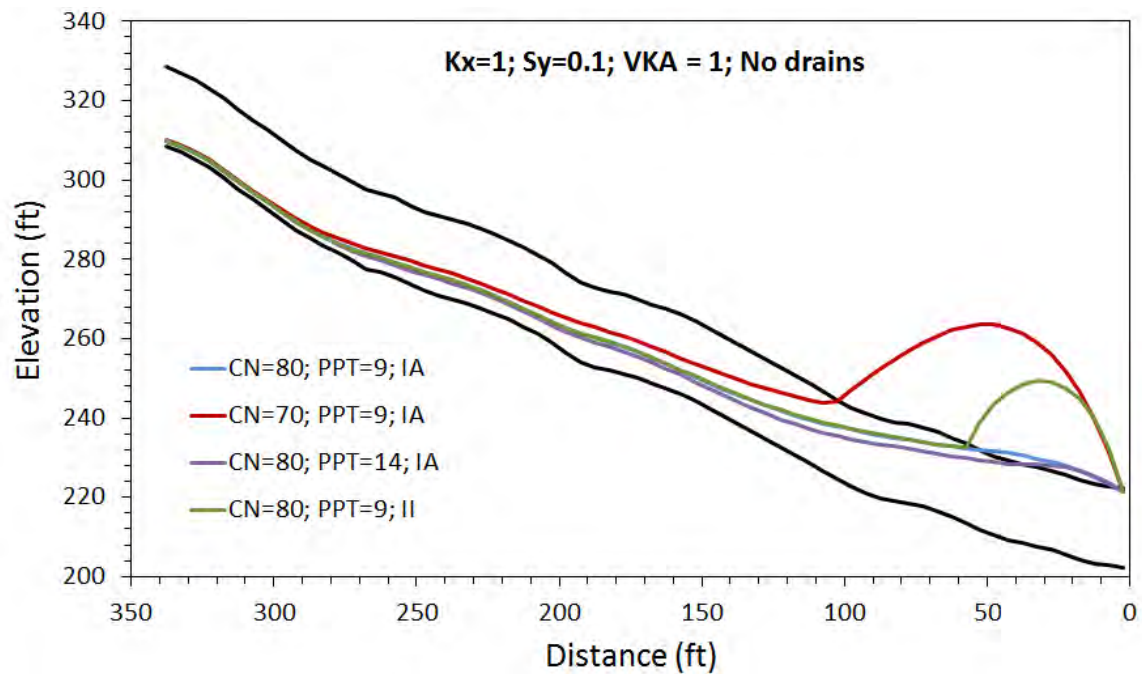


Figure 7.50: Sensitivity of water table elevations to recharge parameters for cross section d-d' given isotropic silty or fine sands of higher storage. PPT = total precipitation (inches) during 24-hour event.

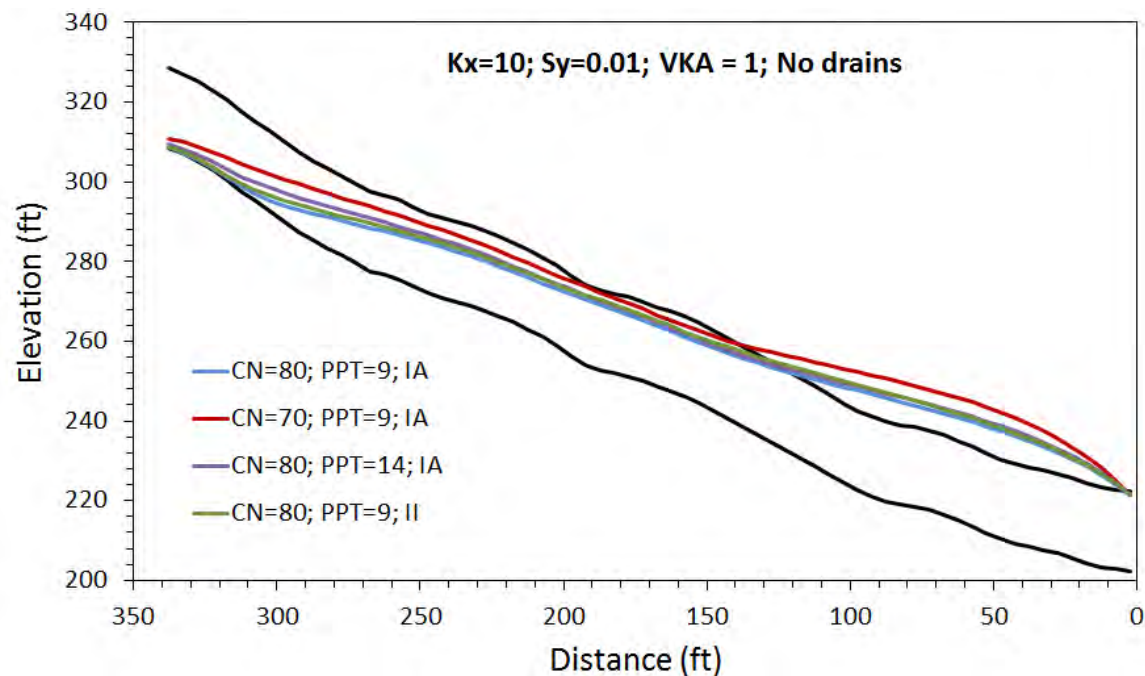


Figure 7.51: Sensitivity of water table elevations to recharge parameters for cross section d-d' given isotropic well sorted sands or gravels of low storage. PPT = total precipitation (inches) during 24-hour event.

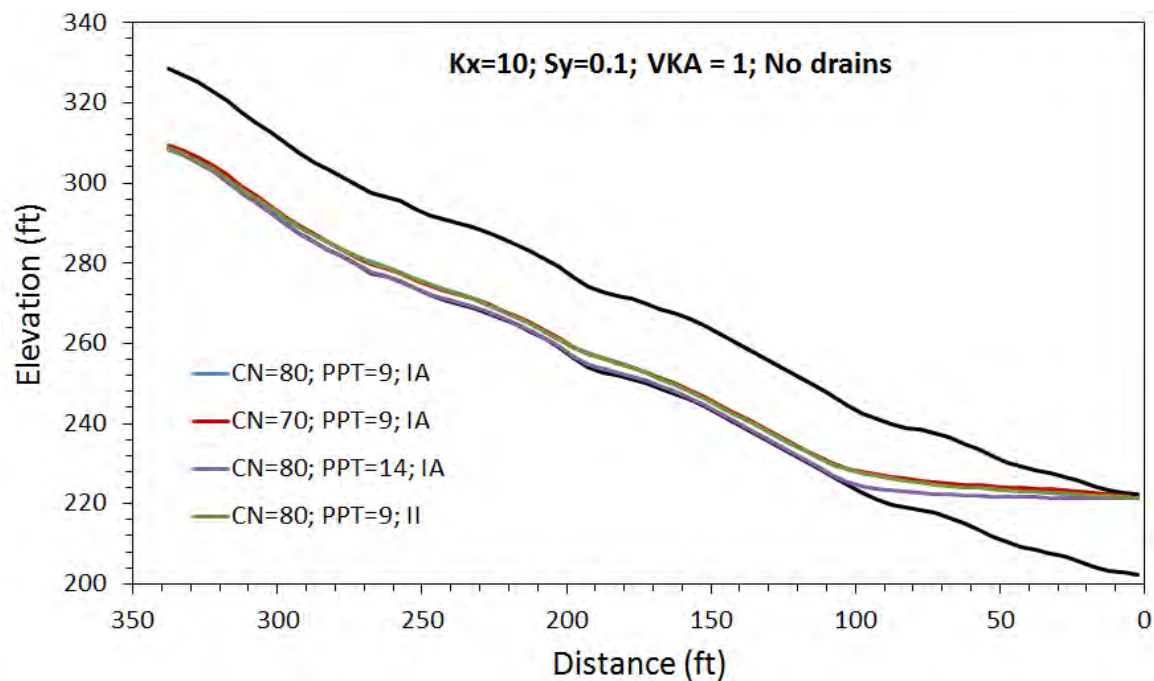


Figure 7.52: Sensitivity of water table elevations to recharge parameters for cross section d-d' given isotropic well sorted sands or gravels of higher storage. PPT = total precipitation (inches) during 24-hour event.

Maintaining a CN of 80, but increasing the precipitation for a 24-hour event from 9 inches to 14 inches (maximum tabulated 24-hour event total in the USA) will increase the amount of recharge to the site, but decreases the estimated percentage of precipitation that becomes recharge from 21% to 15% (greater percentage of precipitation becomes runoff). In addition, the maximum recharge rate for the storm decreases slightly. No change in drain design is needed for soils with storage on the order of 10%. A decrease in storage to 1%, however, will require some change in drain design in finer grained soils. For less conductive fine sands, drain array 11 will effectively reduce groundwater seepage (short and medium length drains of medium spacing).

Changing the SCS rainfall distribution curve from type IA to type II effectively increases the maximum recharge rate during a 24-hour storm event from 0.69 ft/d to 3.31 ft/d, while maintaining the same depth of recharge for the entire storm at 1.93 ft, given a CN = 80 and total precipitation of 9 inches in 24-hours. No change in drain design is anticipated in well sorted sands and gravels. For finer sands with a storage of 10%, medium length drains are required to remove groundwater seepage, while for lower storage, no drain array tested can completely remove seepage in the toe of slope.

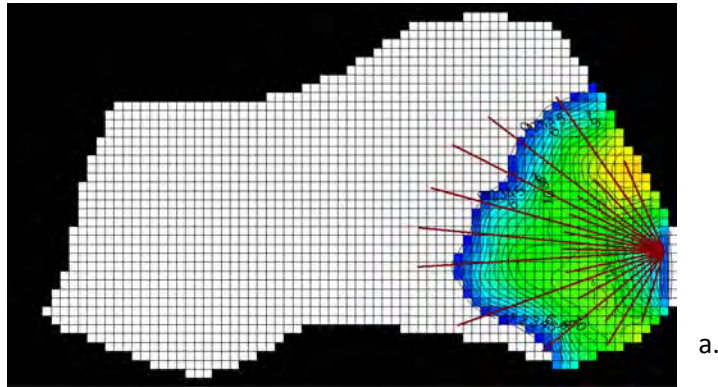
Drain Efficiency

Drain efficiency is described by the drain conductance (C_d) and is described in section 4.2.7 on Horizontal Drain Flow Characteristics and Drain Flow. The coefficient C_d is a lumped conductance term describing all the head loss between the drain and the region of the cell in which it resides. It is a function of the convergent flow toward the drain, as well as the physical characteristics of the drain itself.

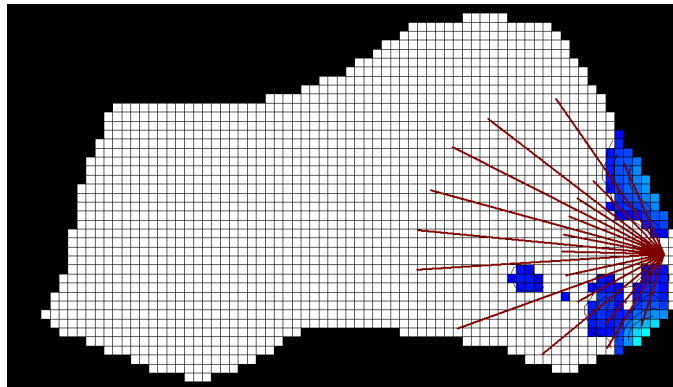
The impact of C_d on drain flow is often characterized with a threshold response. For relatively small values of C_d , a slight change in C_d will have significant changes on drain flow. In contrast, when C_d is raised above some threshold value, any further increase in drain conductance will not contribute to significant increases in drain flow. This threshold will occur when C_d equals or is greater to K_x .

To test drain efficiency, Figure 7.53 shows an example of $K_x = 1$ (silty or fine sands) with a $S_y = 0.01$ with drain array 11 installed. Results show that $K_d = 5$ ft/d reduces water levels below land surface, while $K_d = 0.1$ ft/d maintains significant flooding in the toe region of the slope. Figure 7.54 shows that the rate of increased drain flow decreases with increased K_d , such that drain flow no longer increases for K_d values greater than 10 ft/d, or a conductance of 10 times the geologic material.

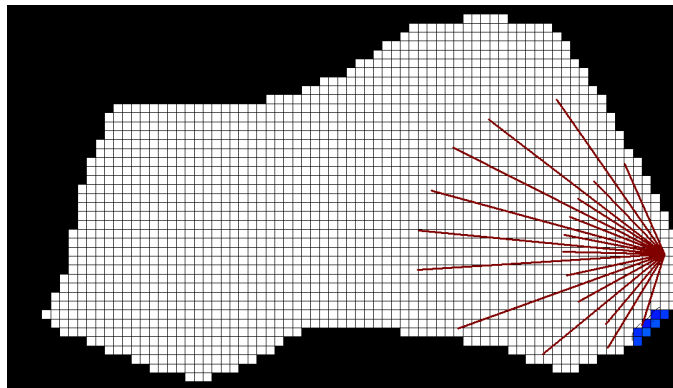
The question of drain design sensitivity to drain efficiency is an important question. If drains have a conductance 10 times lower than the geologic material of fine sands, then drains may not reduce water levels below the critical water level needed for slope stability. On the other hand, if K_d is 10 times K_x , then the number of drains can be halved (i.e. drain spacing doubled) and still maintain slope stability.



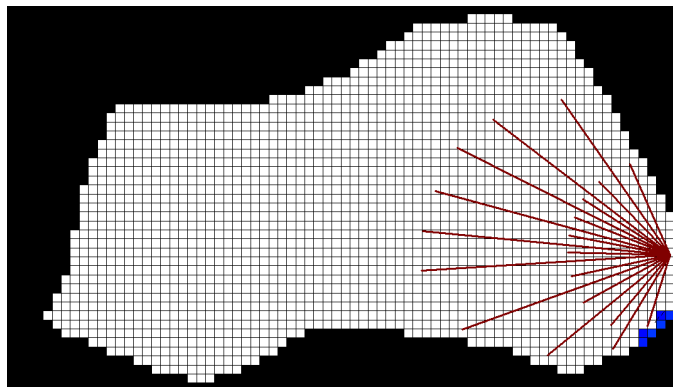
a.



b.



c.



d.

Figure 7.53: Colored regions represent depth of water above land surface as a function of drain hydraulic conductivity. The example uses soil type 2 ($K_x = 1$ ft/d, $S_y = 0.01$ and $VKA = 1$). Drain array 11 has K_d equal to (a) 0.1 ft/d, (b) 1 ft/d, (c) 5 ft/d and (d) 10 ft/d.

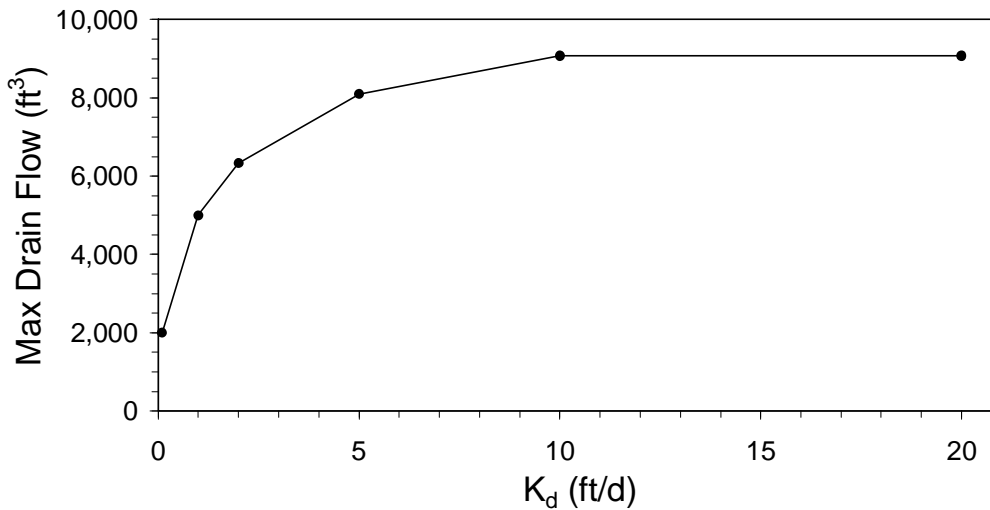


Figure 7.54: Maximum drain flow for different drain hydraulic conductivities (K_d) installed in silty or fine sands with a storage of 10% and drain array 11.

7.5.3.6 Analysis - Observed Data Available (Isotropic Conditions Assumed)

Data allows one to calibrate the numerical model. Typical calibration strategies are shown. Data for site D include:

- Precipitation data collected at the site.
- Annual average precipitation
- 24-hour total precipitation for a 100-year precipitation event.
- An estimate of CN
- Groundwater levels collected at the end of the dry period. This data serves to calibrate a steady state version of the model.
- Groundwater levels and precipitation data collected concurrently.

All data is collected prior to drain installment. Figure 7.55 Indicates observation well locations for site D. The CN is estimated to equal 80 and annual average precipitation is 35 inches, while the 100-year event produces a total of 11 inches in a 24-hour period. Calibration is done by adjusting hydraulic conductivity (K_x) and specific yield (S_y) to best match observed water levels.

7.5.3.6.1 Steady State Conditions

Steady state is modeled to establish a first estimate of hydraulic conductivity and to ensure that water levels for recharge estimate are reasonable. Two methods are presented in section 5.5 to estimate steady state recharge. Assuming limited precipitation data collected as the site, the first method in section 5.5 is used. Given a CN = 80 and 11 inches of rain in a 24-hour period will produce 18% recharge

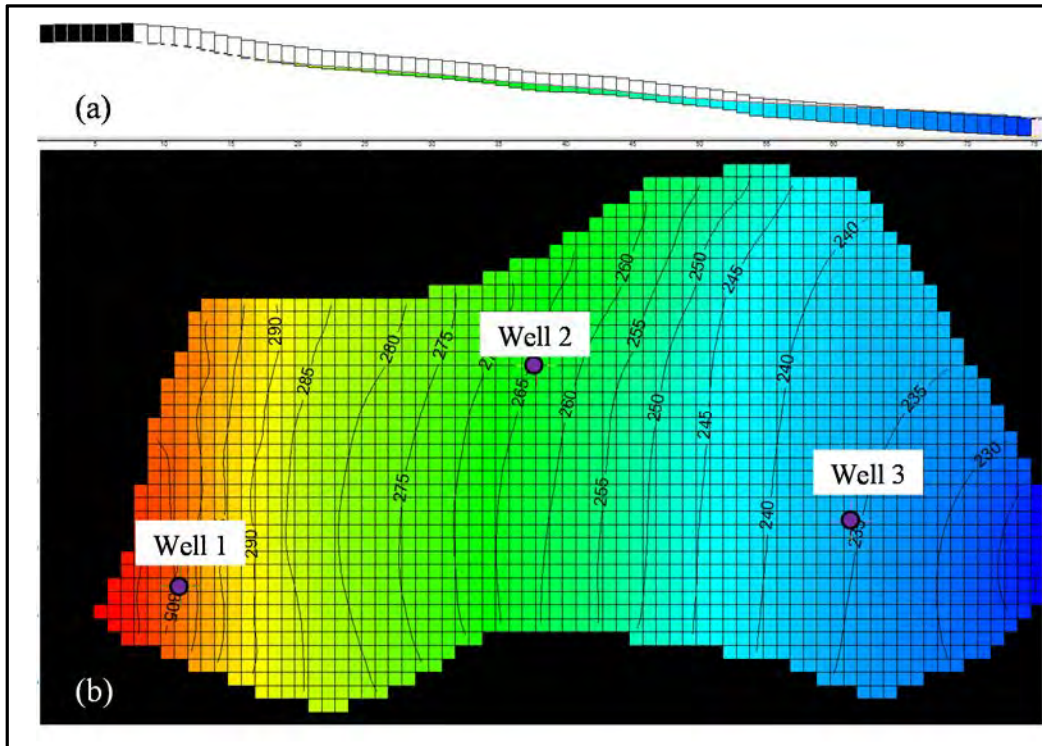


Figure 7.55: Site D (a) cross section and modeled steady state water levels for cross section d-d', (b) plan view with steady state water levels contoured at 5 ft intervals. Observation well locations shown.

(refer to Table 5.5). Given an average annual precipitation total of 35 inches, then 18% is assumed to become groundwater recharge, or 6.3 inches/yr. This equals 0.0014 ft/d and is the assumed steady state recharge.

The soil is identified as a silty sand, but no analysis has been done to refine the value of hydraulic conductivity. An initial guess of 1 ft/d replicates water levels at observation wells 1 and 2, but under predicts the dry-season water level at well 3 (Figure 7.56). A sensitivity analysis (Figure 7.57) shows that the root-mean-square error (*rmse*) is significantly reduced if $K_x = 0.2$ ft/d. While this may appear low for a silty sand, heterogeneity and anisotropy effectively lower hydraulic conductivity through averaging procedures discussed in section 3.36. Decreasing K_x from 1 ft/d to 0.2 ft/d more accurately replicates well 3 while not forcing an over prediction in water levels at wells 1 and 2.

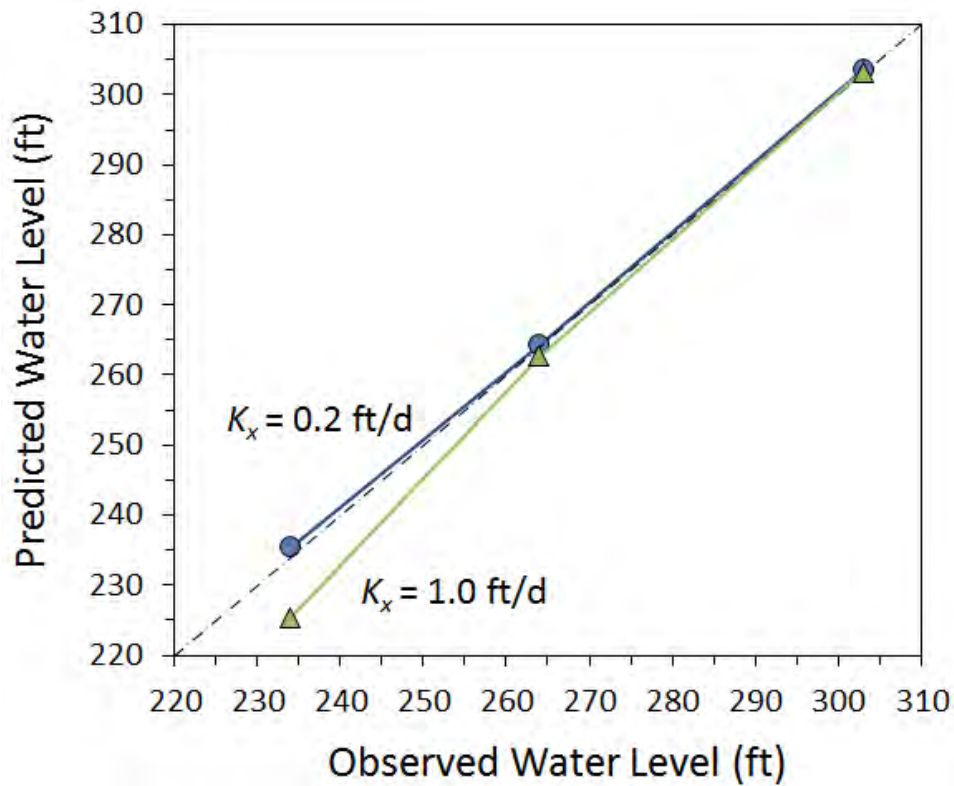


Figure 7.56: A one-to-one plot showing observed and predicted water levels under steady state recharge conditions.

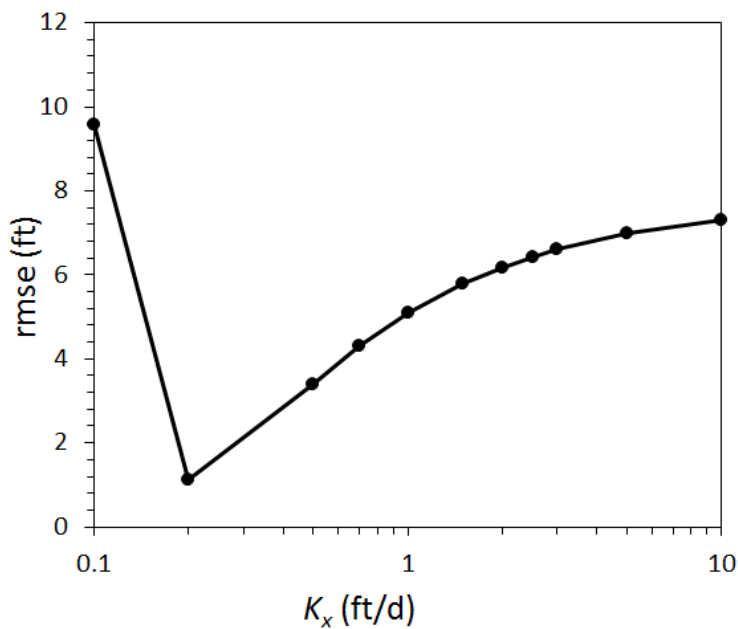


Figure 7.57: Sensitivity analysis of steady state conditions using *rmse* as the objective function.

7.5.3.6.2 Transient Conditions (pre-drain)

Observed transient water levels allow one to fine-tune the initial steady state estimate of K_x and determine an effective value of specific yield. Observed two-hour precipitation and calculated recharge are provided in Figure 7.58, with the modeled transient period specified.

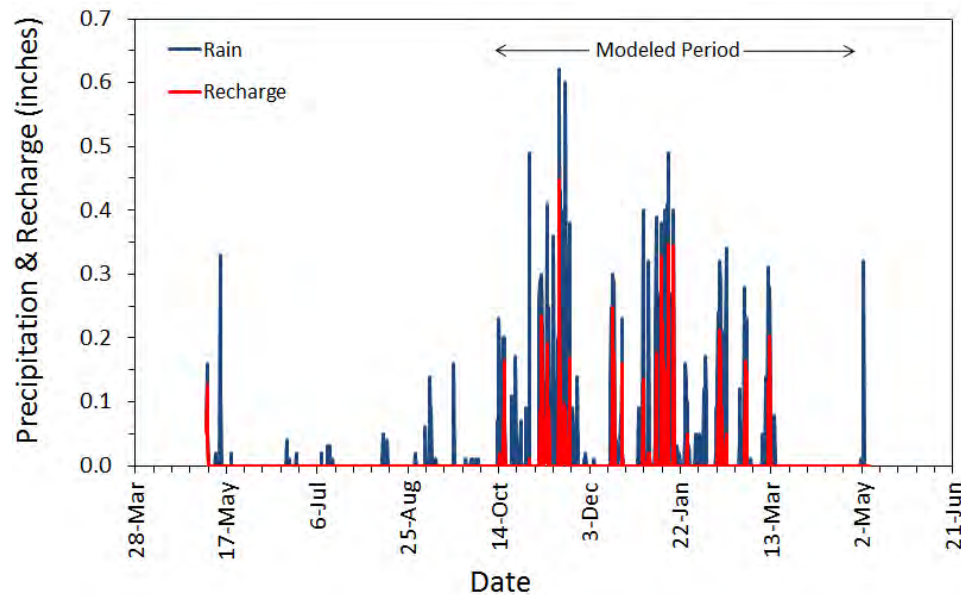


Figure 7.58: Two-hour precipitation data collected on site, and calculated recharge assuming $CN = 80$. Transient modeling period is marked.

The simulation assumes steady-state conditions prior to initiating the transient scenario. This removes the need to explicitly characterize initial heads. Steady-state recharge is assumed 0.0014 ft/d as determined in the steady-state modeling scenario. Three model simulations are provided to highlight calibration strategies. First, steady-state value of $K_x = 0.2$ ft/d is used, while $S_y = 0.1$ is assumed. Second, a sensitivity analysis is done in which K_x and S_y are adjusted independently over a range of specified values. This analysis shows that $K_x = 0.2$ and $S_y = 0.02$ produce the lowest *rmse* (Figure 7.59). Finally, auto-calibration of K_x and S_y are done simultaneously (program used Parameter Estimation, PEST, (Doherty, 2005)). Results from the sensitivity analysis are used as initial guesses to encourage a rapid convergence on a solution. Calibrated values are 0.2475 ft/d and 0.01957 for K_x and S_y , respectively. Simulated water levels for each observation well are compared to observed data in Figure 7.60. Using the steady-state calibrated $K_x = 0.2$ ft/d, and assuming an $S_y = 0.1$ (SS), produces water levels with a muted response to recharge and water levels in the middle portion of the slope and the lower portion of the slope are predicted too low, despite using a K_x nearly equal to the calibrated value. Reducing S_y to 0.02 from the transient sensitivity analysis improves predicted results appreciably, but water levels are over predicted at all observation locations. Auto-calibration shows that small changes in K_x and S_y can dramatically improve prediction.

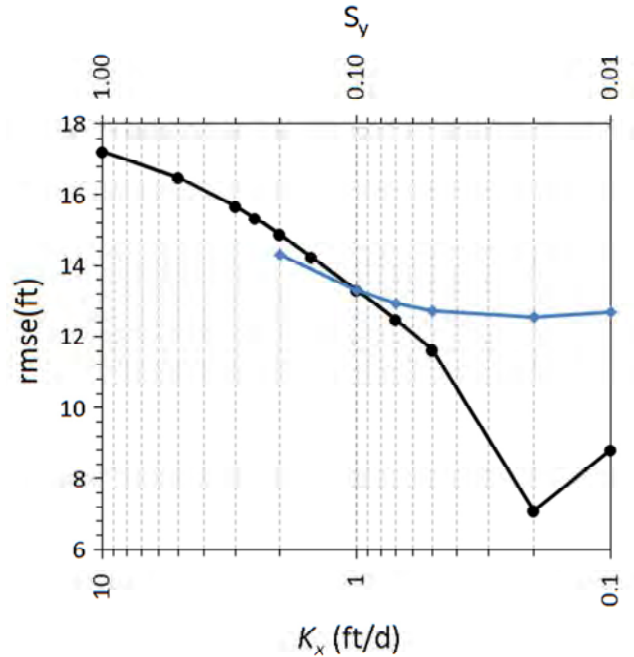


Figure 7.59: Sensitivity analysis results for K_x and S_y using $rmse$ as the objective function.

7.5.3.6.3 Transient Conditions (Design Storm)

With a calibrated model, the design storm is applied to the model using a CN = 80 and a total of 11 inches of rain in a 24-hour period and assuming a type IA storm distribution. The model is run with no drains as well as drain array 1 through 5. Plan view results for depth of water table below ground surface are given for each scenario in Figure 7.61. Cross sectional profiles of the water table for d-d' are provided in Figure 7.62

Table 7.10 Provides FOS values for the cross section d-d' indicate that short drains with wide spacing (drain array 1) can lower water table elevations appreciably to promote slope stability (FOS = 1.21), while slightly longer drains (drain array 4) can ensure no translational failure (FOS 1.34). Drain spacing must be decreased (drain array 5), however, to remove any potential for groundwater seepage in the toe region (refer to Figure 7.61)

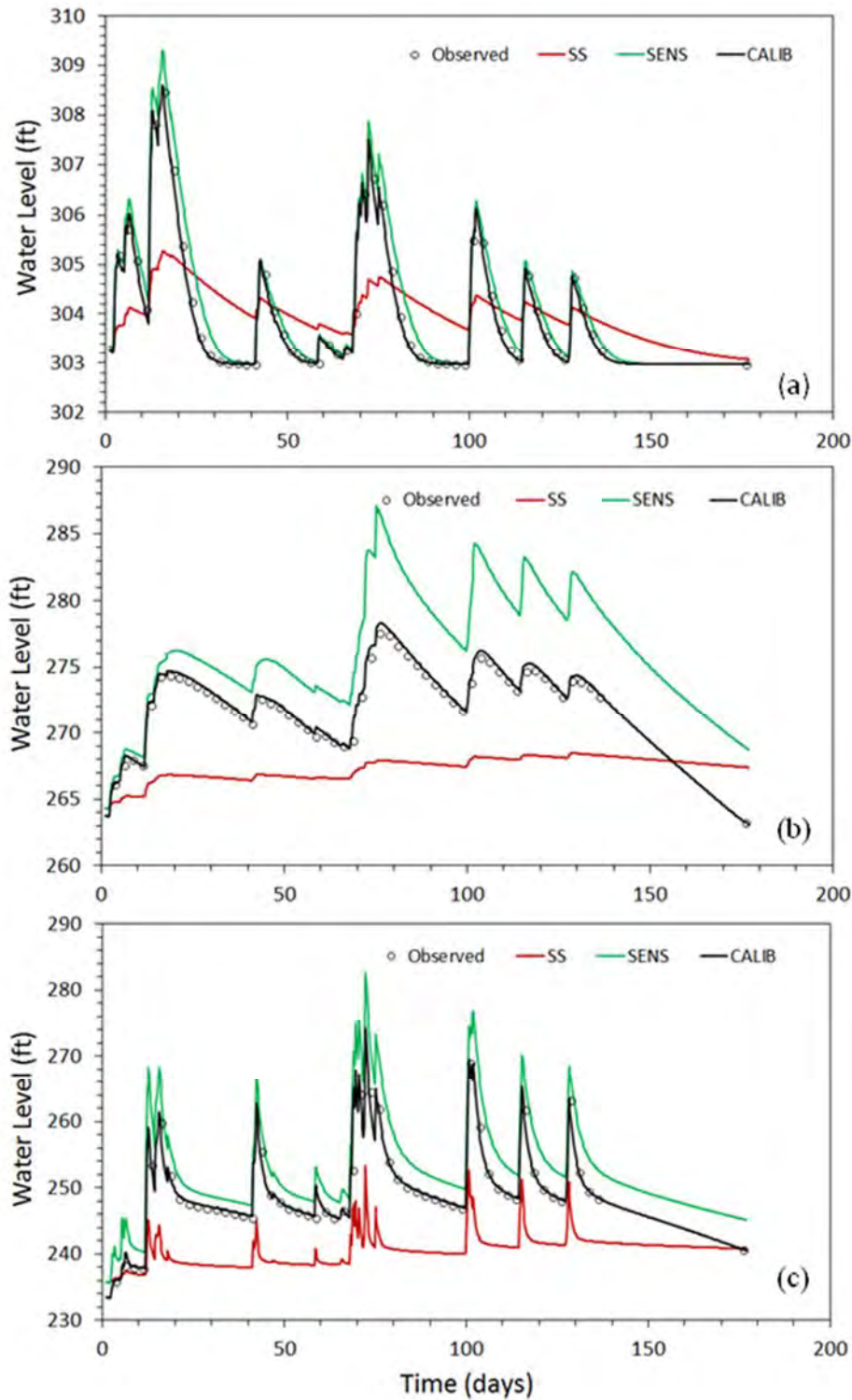


Figure 7.60: Observed and predicted water levels for (a) Well 1, (b) Well 2 and (c) Well 3. Locations identified in Figure 7.2. SS indicates steady state $K_x = 0.2$ and assumed $S_y = 0.1$. SENS indicates $K_x = 0.2$ and $S_y = 0.02$ as obtained from transient sensitivity analysis. CALIB = results from auto-calibration using PEST with a resulting $K_x = 0.2475$ ft/d and $S_y = 0.01957$.

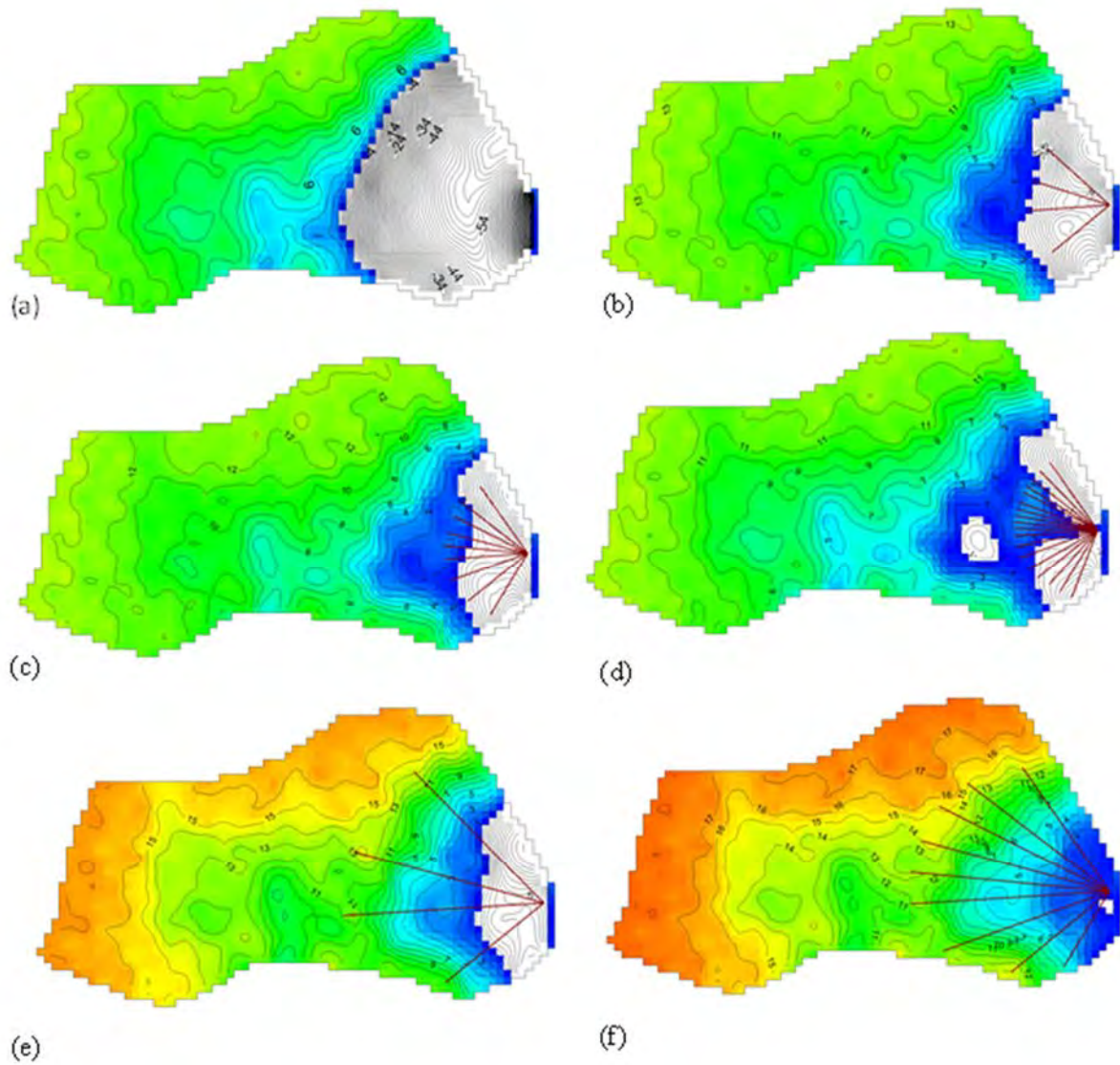


Figure 7.61: Water table depth below ground surface (ft) on day 0.35 (stress period 8) of the 100-year 24-hour precipitation event given hydraulic parameters $K_x = 0.2475$ ft/d, $S_y = 0.01957$ and $VKA = 1$, given (a) no drains, (b) drain array 1, (c) drain array 2, (d) drain array 3, (e) drain array 4, (f) drain array 5. Contour interval is 1 ft. Colored portions indicate water table is below ground surface, while white regions indicate seepage caused by the water table rising above ground surface. Height above ground is correlated to seepage flux.

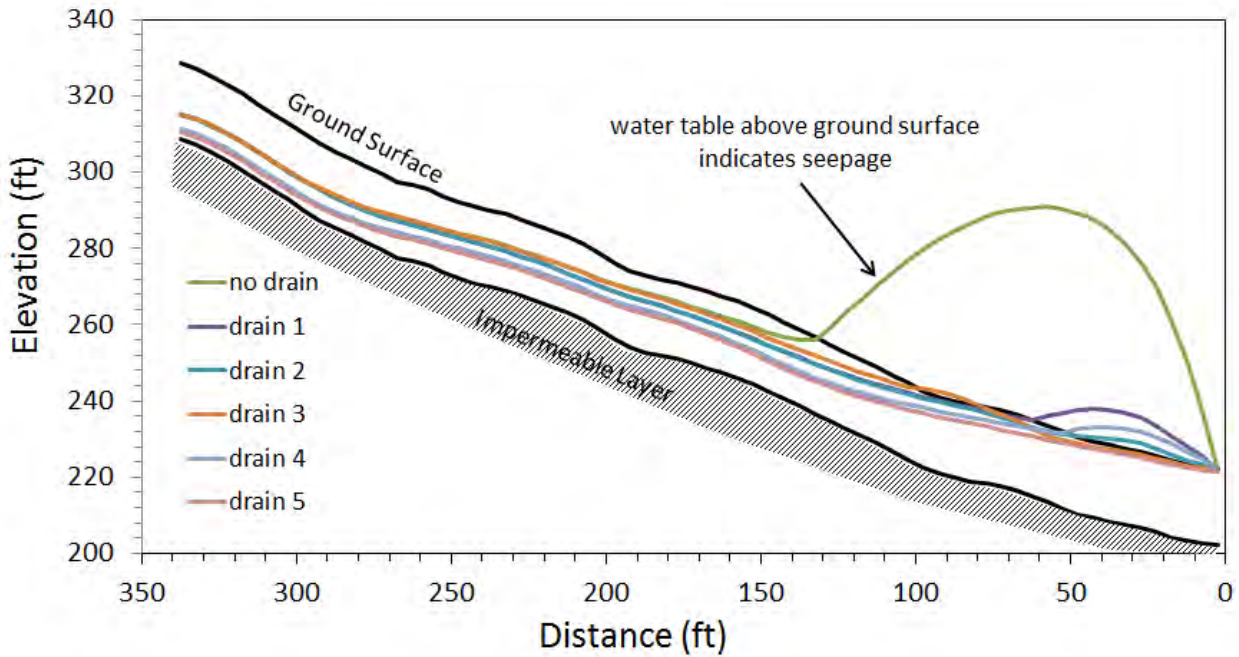


Figure 7.62: Water table profiles for cross section d-d' for different drain arrays. Water table elevations predicted above ground surface indicate groundwater seepage. Height above ground is correlated to seepage flux.

Table 7.10: FOS values for site D given K_x = are 0.2475 ft/d, S_y = 0.01957 and VKA = 1 and different drain arrays.

Drain	FOS
nodrain	1.195
1	1.21
2	1.21
3	1.21
4	1.338
5	1.338

7.5.4 Rotational Failure (Site B)

7.5.4.1 Site Description

Rotational failure is modeled using the topography shown in Figure 7.63. The slope is relatively uniform from the slope crest to the base of the slope at approximately 40% (23°). The subsurface conditions are assumed to consist of a single geologic layer reaching up to 300 feet in thickness.

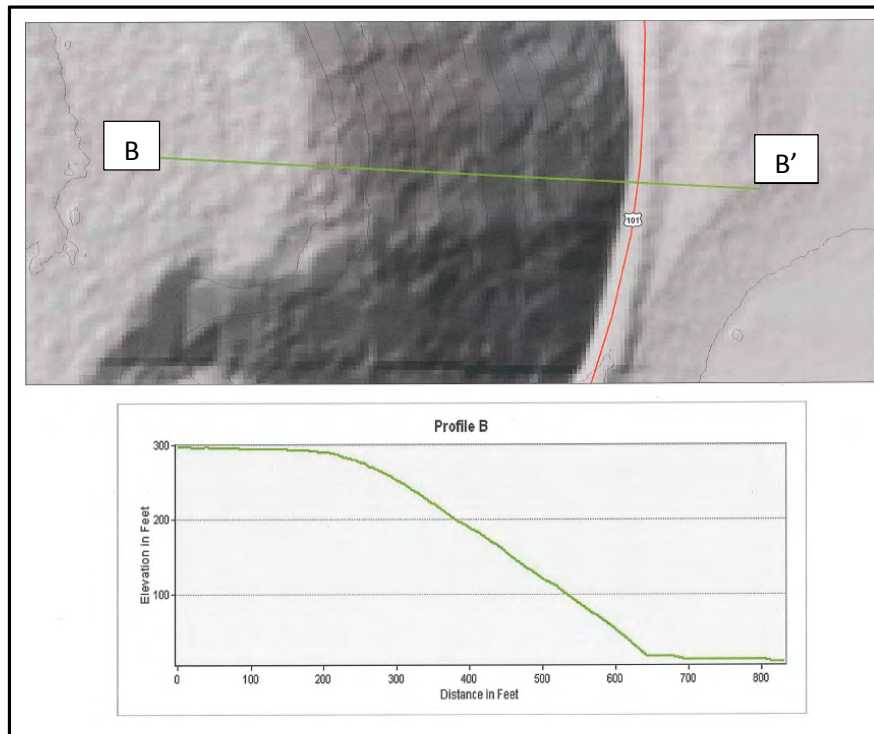


Figure 7.63 Site B topography for rotational failure (a) hill shade, (b) slope profile of ground surface from B-B'.

7.5.4.2 Model Domain and Conceptual Model

The model domain is defined in Figure 7.64 with MODFLOW cells 5 ft by 5 ft in the x-y direction, which is rotated 2 degrees so that the grid is parallel to the slope. Maximum thickness is 300 ft at location B and minimum thickness is 20 ft at location B'. The bottom of the modeled layer is at zero ft elevation. Specified head boundary conditions are assigned at the slope toe (16.9 ft) and the upslope divide (195 ft). The upslope boundary is far from the slope toe and assigned a value below the critical surface as determined by slope stability analysis, and numerical modeling found drain design not sensitive to this boundary condition. For isotropic conditions, a single layer is modeled, and for anisotropic conditions, a two layer model is used with similar thickness of layers.

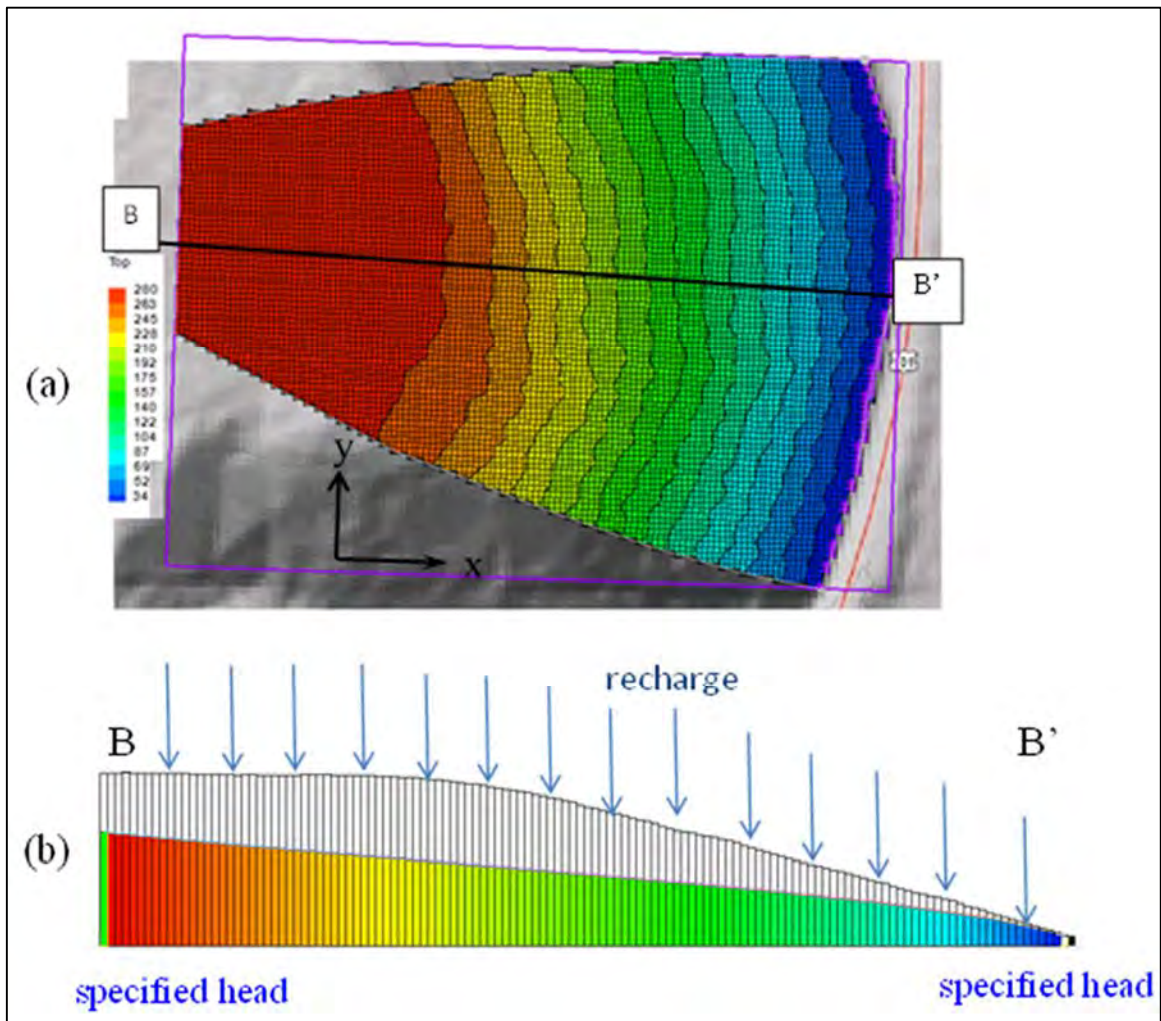


Figure 7.64: Model grid for rotational failure site. (a) Plan view showing modeled grid (purple box), active cells in color scale of assigned land surface elevations, rotated x-y axis and cross section B-B'. Cell dimension is 5 ft by 5 ft. (b) Cross section B-B' depicting single layer model (maximum thickness is 300 ft and minimum thickness is 20 ft), as well as specified head boundary conditions and recharge, are applied uniformly across the domain. Water levels are steady state for $K_x = 1$ ft/d and $S_y = 0.01$ and recharge = 0.005 ft/d.

7.5.4.3 Drain Configurations

Two drain arrays are tested for rotational failure. These are shown in Figure 7.65 and 7.66, respectively. Each horizontal drain is approximately 150 ft in length with a 5° angle from the horizontal (tip elevation at 15 ft and drain end at 30 ft). The drains are drilled at approximately 6° angles from each other. Drain

array 1 is a total of 1350 linear feet, while array 2 is approximately 2250 linear feet. Drain hydraulic conductivity is assumed equal to the hydraulic conductivity of the geologic material it is placed in.

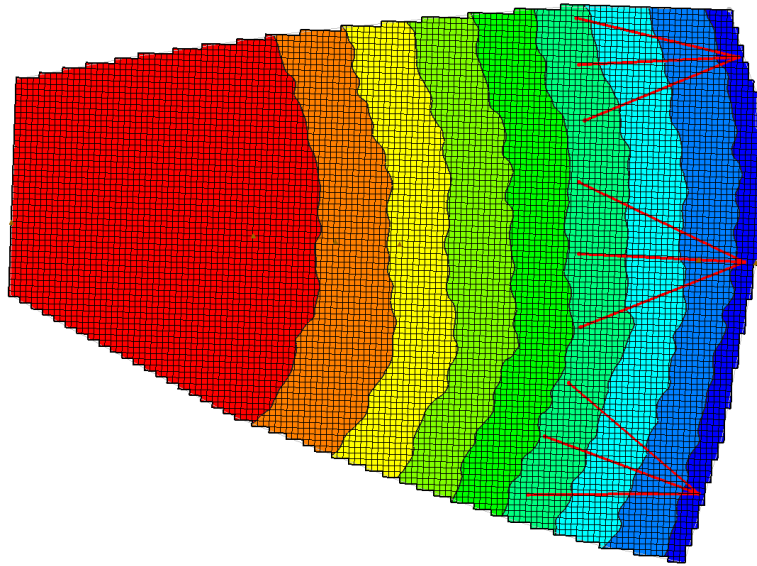


Figure 7.65: Site B drain array 1 in plan view. Contours represent ground surface elevation and red lines represent drain placement. Model cells are 5ft by 5ft.

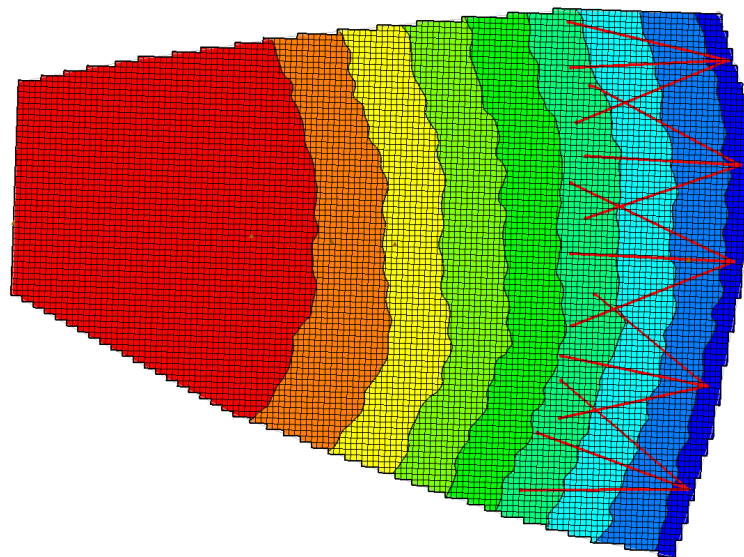


Figure 7.66: Site B drain array 2 in plan view. Contours represent ground surface elevation and red lines represent drain placement. Model cells are 5ft by 5ft.

7.5.4.4 Geotechnical Parameters and Initial Slope Stability Analysis

Soil type in site B is assumed as silty sand /gravel with high friction angle and low cohesion values. It is assumed that the friction angle is 40° and cohesion is 10 psf. Furthermore, soil density is assumed to be medium dense to dense with a unit weight of 125 pcf.

Slope stability analysis was carried out by using the SLOPE/W slope stability analysis software from GEOSTUDIO. In order to accommodate the rotational failure mode, Morgenstern-Price method was used in analyses. The results of the FOS calculations were confirmed with the simplified Janbu method for a few cases. Both methods provided near identical results. The first analysis was carried out to find the critical water surface level when FOS = 1. Figure 7.67 indicates the critical rotational failure surface and water surface level for this condition.

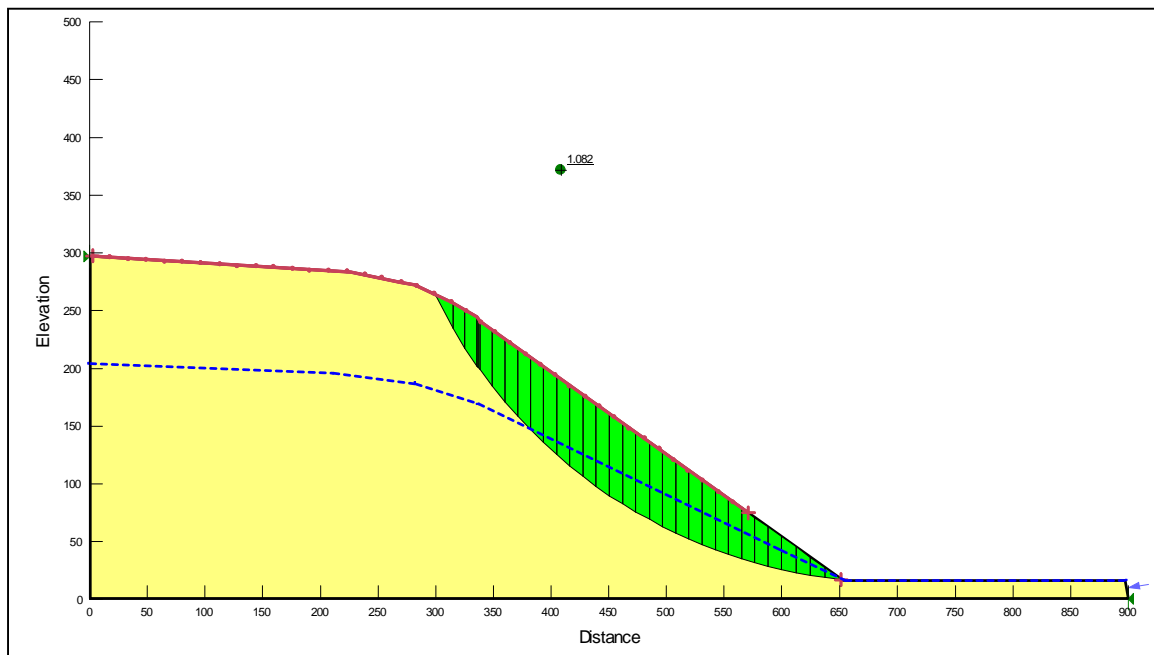


Figure 7.67: Critical water surface and critical rotational failure surface for site B

7.5.4.5 Analysis – No Observed Data

Hydraulic soil properties are provided in Table 7.5, and the design storm defined in section 7.5.2 is used.

7.5.4.5.1 Steady State

Steady-state conditions are run prior to any transient simulation. This allows the user to forego prior knowledge of the initial starting heads. Steady-state conditions are meant to mimic the “dry” season in the system, which is assumed to last long enough for steady-state conditions to occur. Steady-state recharge is assumed to be the long term average, with water levels stabilized prior to the design storm. Much of the water level lowering of site B is the result of allowing the overall water table to drain prior

to the 100-year storm event. For example, steady-state water levels are shown in Figure 7.68 for $K_x=0.1$ ft/d, $S_y=0.01$, $VKA=1$ and $R=0.005$ ft/d, given no drains and drain array 1. Without drains, the toe of slope floods, but with drains added, flooding in the toe region is significantly reduced.

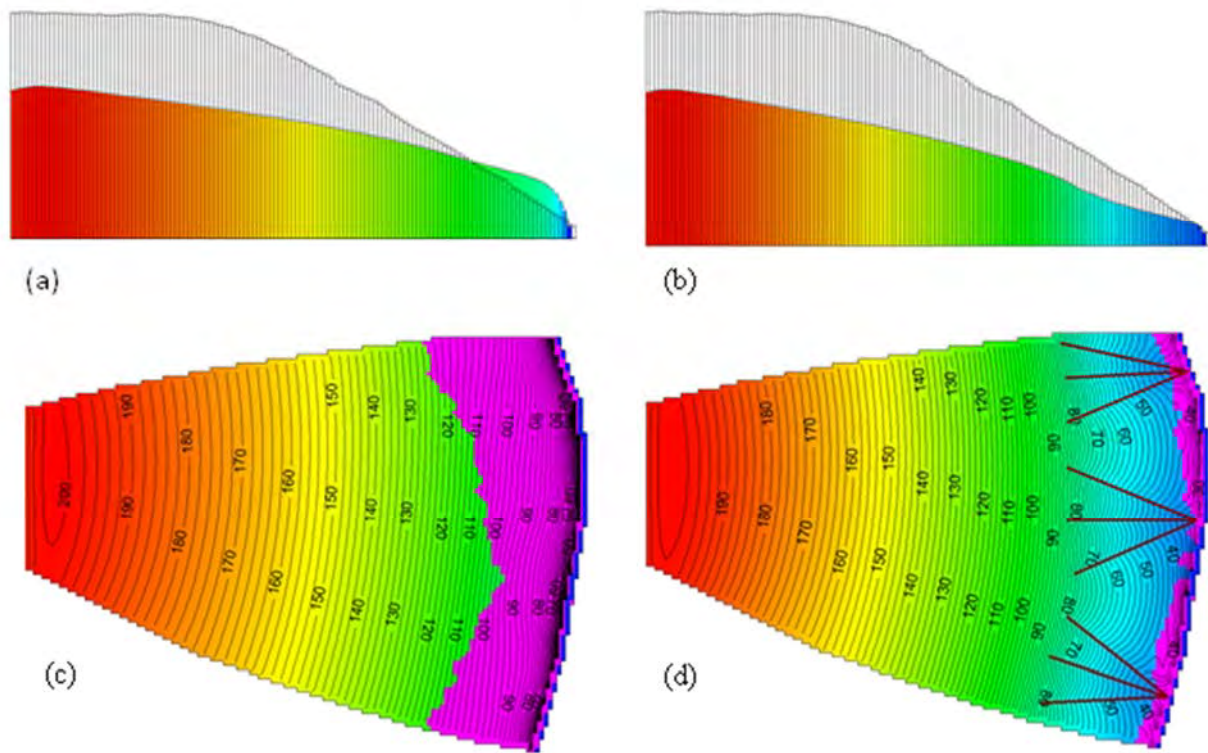


Figure 7.68: Site B steady state water levels for $K_x=0.1$ ft/d, $S_y=0.01$, $VKA=1$ and $R=0.005$ ft/d, given (a) cross section B-B' and no drains, (b) cross section B-B' and drain array 1, (c) plan view with no drains, and (d) plan view with drain array1. Contour intervals are 2 ft. Pink overlay in plain view represents regions where the water table is above ground surface (i.e. groundwater seepage).

7.5.4.5.2 Maximum Water Levels during 100-Year Event

Maximum water levels occur at different times as water moves down slope. To simplify, the maximum water level is assumed to occur after maximum recharge intensity. This occurs 0.33 days into the 1-day storm event (recharge = 0.70 ft/d). Water level response to drains is discussed in terms of soil type.

Silt, Sandy Silt, Clayey Sand or Till ($K_x = 0.1$ ft/d)

Water table elevations are provided in Figure 7.69. White regions in each diagram represent regions in

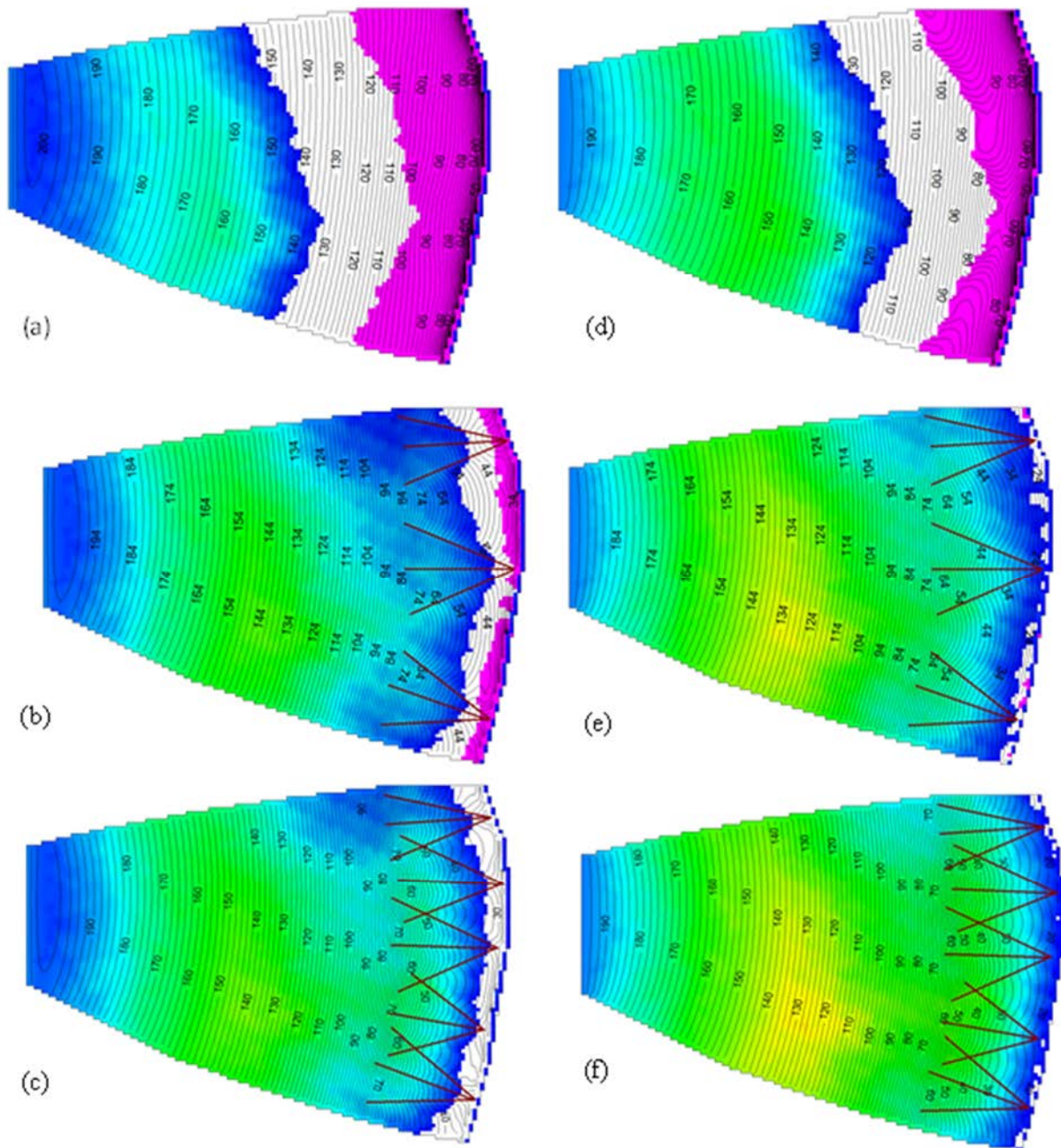


Figure 7.69: Water levels on day 0.35 (stress period 8) and isotropic, silt, sandy silt, and clayey sand (hydraulic parameters $K_x = 0.1$ ft/d, and $VKA = 1$), given (a) $S_y = 0.01$ and no drains, (b) $S_y = 0.1$ and no drains, (c) $S_y = 0.01$ and drain array 1, (d) $S_y = 0.1$ and drain array 1, (e) $S_y = 0.01$ and drain array 2, (f) $S_y = 0.1$ and drain array 2. Drains are represented as brown lines and contours are at 2 ft intervals. Colored portions are scaled by water level depth below the critical water surface (scale 0-72 ft), while white areas indicate water levels above the failure surface. Pink overlay indicates water level is above ground surface.

site B that have water levels above the critical water surface (where slope instability occurs) shown in Figure 7.67. The pink overlay shows regions where the water table is predicted above ground surface. With no drains, water levels surpass the critical water level for much of the slope, and groundwater seepage occurs along the toe of the slope. Greater seepage occurs in the corner regions of the toe as a result of slightly convex topography. Water levels are greatly lowered with the addition of drain array 1 for low and high storage scenarios, though water levels in the toe region of the slope still rise above the critical water level and seepage does occur for $S_y = 0.01$. For low storage, drain array 2 reduces all groundwater seepage.

For anisotropic soils, water table elevations increase above the critical water level for much of the slope. This was true for low anisotropy ($VKA = 2$) and higher anisotropy ($VKA = 10$). However, drain array 1 successfully lowers water levels below the critical water level for much of the slope up to $VKA = 5$ and is the same for all isotropic soils. For $VKA = 10$ (Figure 7.70) and $S_y = 10\%$, the number of drains must increase in order to lower water levels below the critical water surface. For $S_y = 0.01$ and $VKA = 10$, drain array 2 is unable to lower water levels below the critical water surface for the entire toe region of the slope.

Silty Sands and Fine Sands ($K_x = 1.0 \text{ ft/d}$)

With increased hydraulic conductivity, water table elevations still rise above the critical water level surface in the toe region if no horizontal drains are used (Figure 7.71). Groundwater seepage will occur for low and high storage, with seepage greatest at the edges of the slope toe due to convex topography. Drain array 1 sufficiently lowers water level elevations for isotropic conditions. Drain array 1 sufficiently lowers water levels for anisotropic systems up to approximately $VKA = 30$, above which additional drains may be required.

Well Sorted Sands ($K_x = 10 \text{ ft/d}$)

Figure 7.72 shows that with no drains, highly conductive soils may produce water table elevations above the critical water surface in the toe region of the slope, with groundwater seepage expected for low storage systems. Drain array 1 is sufficient in lowering water levels below the critical water surface and anisotropy does not impact drainage design.

7.5.4.5.3 Slope Stability Analysis

Maximum water table elevations along the cross section B-B' for isotropic conditions are provided in Figure 7.73, and for anisotropic conditions for silt, sandy silt, and clayey sand given in Figure 7.74. As with the translational failure, the slope stability analyses may not capture portions of the slope where groundwater levels remain elevated after drain placement or other heterogeneities of the groundwater system. For this reason, multiple critical sections of varied orientations might be warranted for further

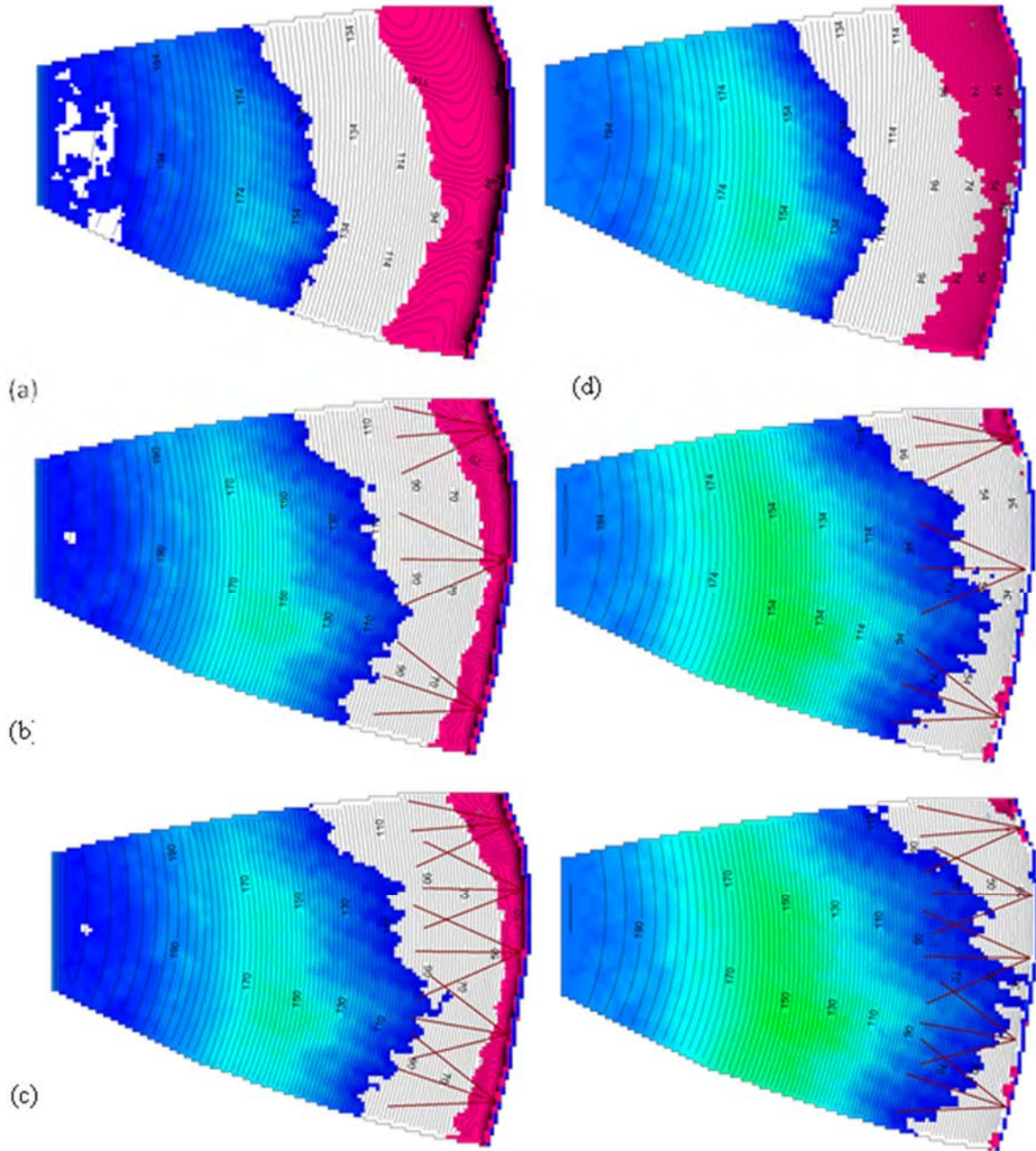


Figure 7.70: Water levels on day 0.35 (stress period 8) and anisotropic silt, sandy silt, or clayey sand (hydraulic parameters $K_x = 0.1$ ft/d, and $VKA = 10$), given (a) $S_y = 0.01$ and no drains, (b) $S_y = 0.1$ and no drains, (c) $S_y = 0.01$ and drain array 1, (d) $S_y = 0.1$ and drain array 1, (e) $S_y = 0.01$ and drain array 2, (f) $S_y = 0.1$ and drain array 2. Drains are represented as brown lines and contours are at 2 ft intervals. Colored portions are scaled by water level depth below the critical water surface (scale 0-72 ft), while white areas indicate water levels above the failure surface. Pink overlay indicates water level is above ground surface.

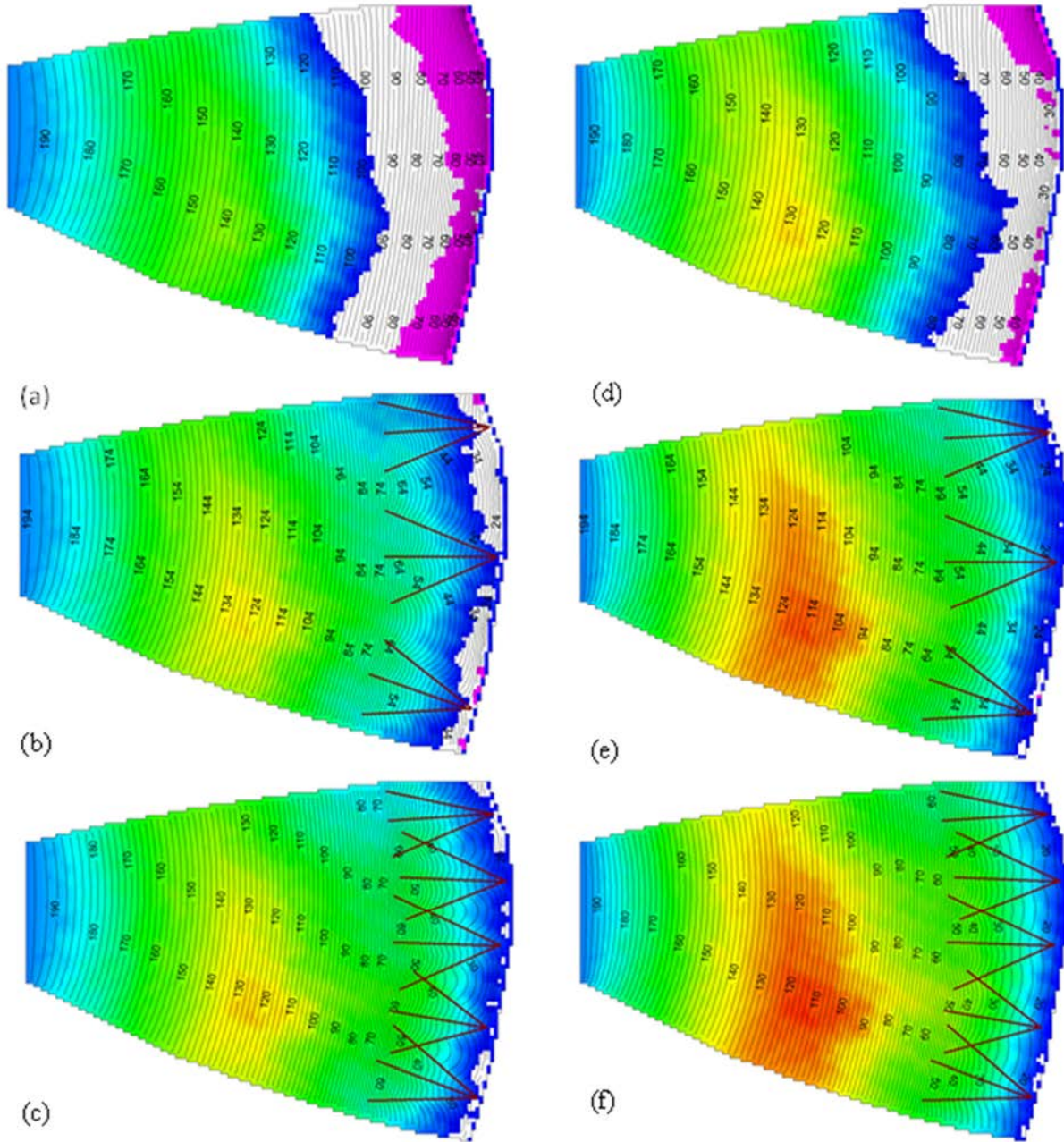


Figure 7.71: Water levels on day 0.35 (stress period 8) and isotropic silty to fine grained sands (hydraulic parameters $K_x = 1$ ft/d, and $VKA = 1$), given (a) $S_y = 0.01$ and no drains, (b) $S_y = 0.1$ and no drains, (c) $S_y = 0.01$ and drain array 1, (d) $S_y = 0.1$ and drain array 1, (e) $S_y = 0.01$ and drain array 2, (f) $S_y = 0.1$ and drain array 2. Drains are represented as brown lines and contours are at 2 ft intervals. Colored portions are scaled by water level depth below the failure surface (scale 0-60 ft), while white areas indicate water levels above the failure surface. Pink overlay indicates water level is above ground surface.

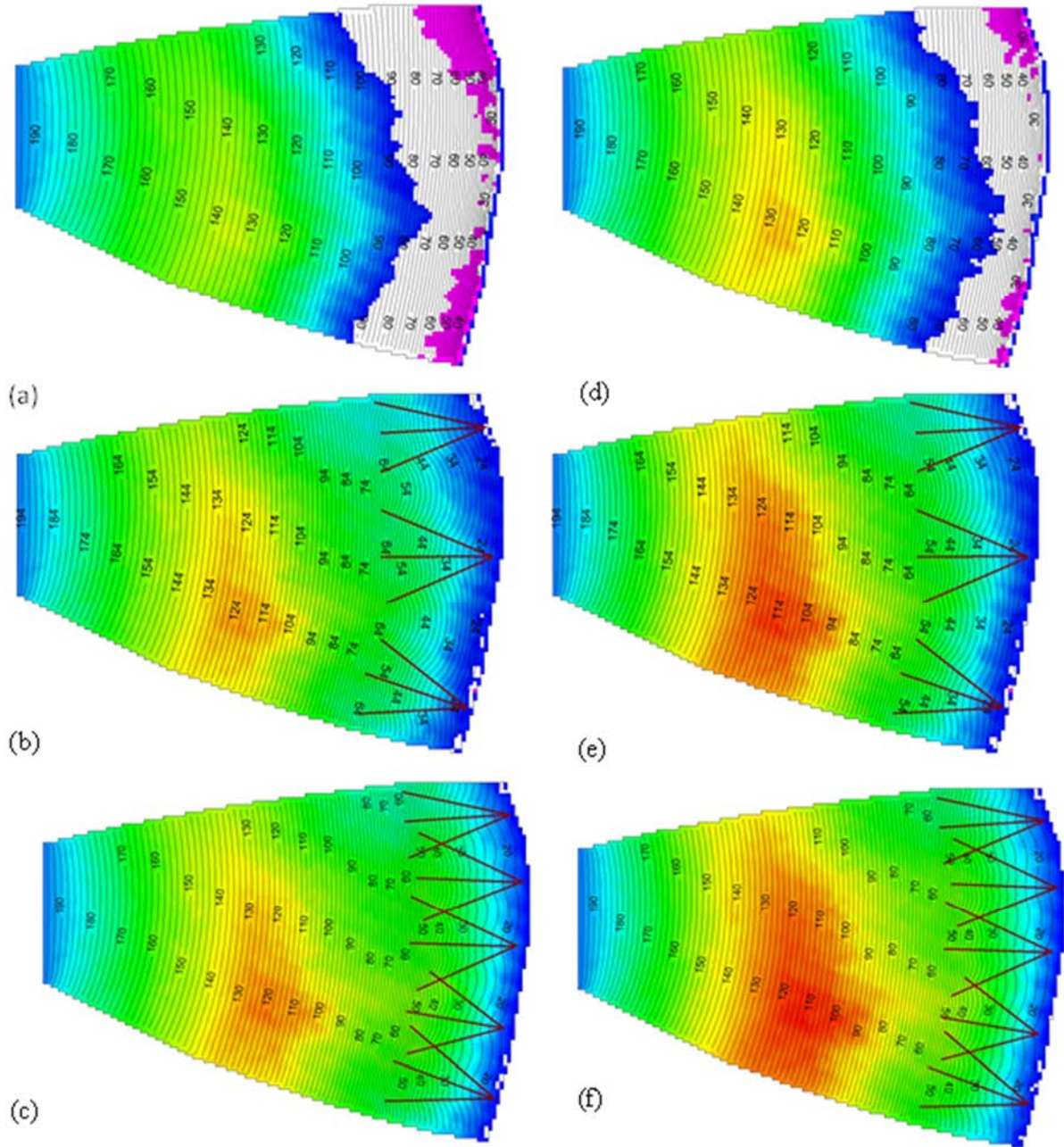


Figure 7.72: Water levels on day 0.35 (stress period 8) and isotropic well sorted sands and gravels (hydraulic parameters $K_x = 10$ ft/d, and $VKA = 1$), given (a) $S_y = 0.01$ and no drains, (b) $S_y = 0.1$ and no drains, (c) $S_y = 0.01$ and drain array 1, (d) $S_y = 0.1$ and drain array 1, (e) $S_y = 0.01$ and drain array 2, (f) $S_y = 0.1$ and drain array 2. Drains are represented as brown lines and contours are at 2 ft intervals. Colored portions are scaled by water level depth below the failure surface (scale 0-60 ft), while white areas indicate water levels above the failure surface. Pink overlay indicates water level is above ground surface.

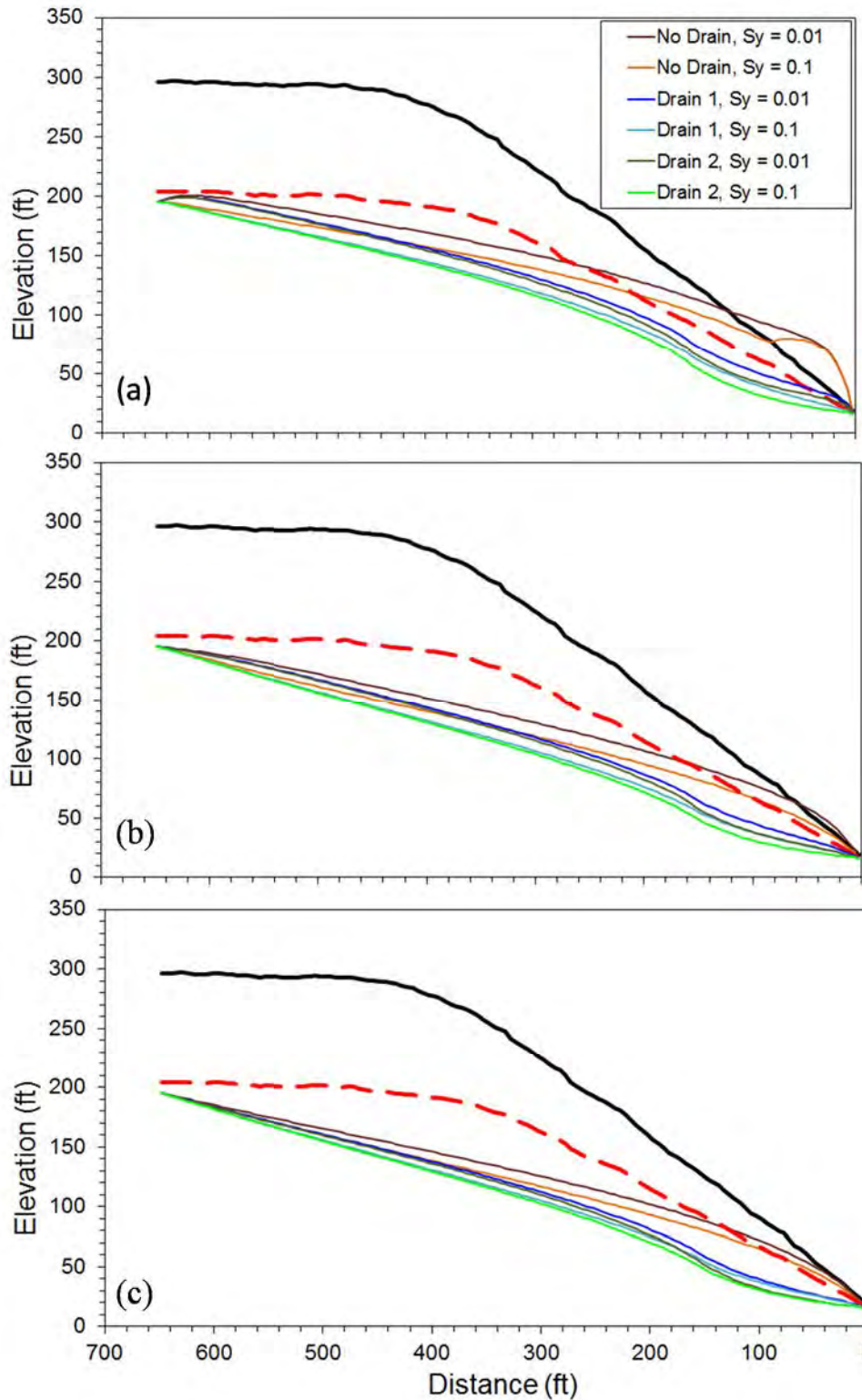


Figure 7.73: Water table elevations for site B along cross section B-B' for isotropic conditions, VKA = 1 (a) $K_x = 0.1$ ft/d, (b) $K_x = 1$ ft/d and (c) $K_x = 10$ ft/d. The red dashed line is the critical water surface for which FOS = 1.0. The black line is ground surface.

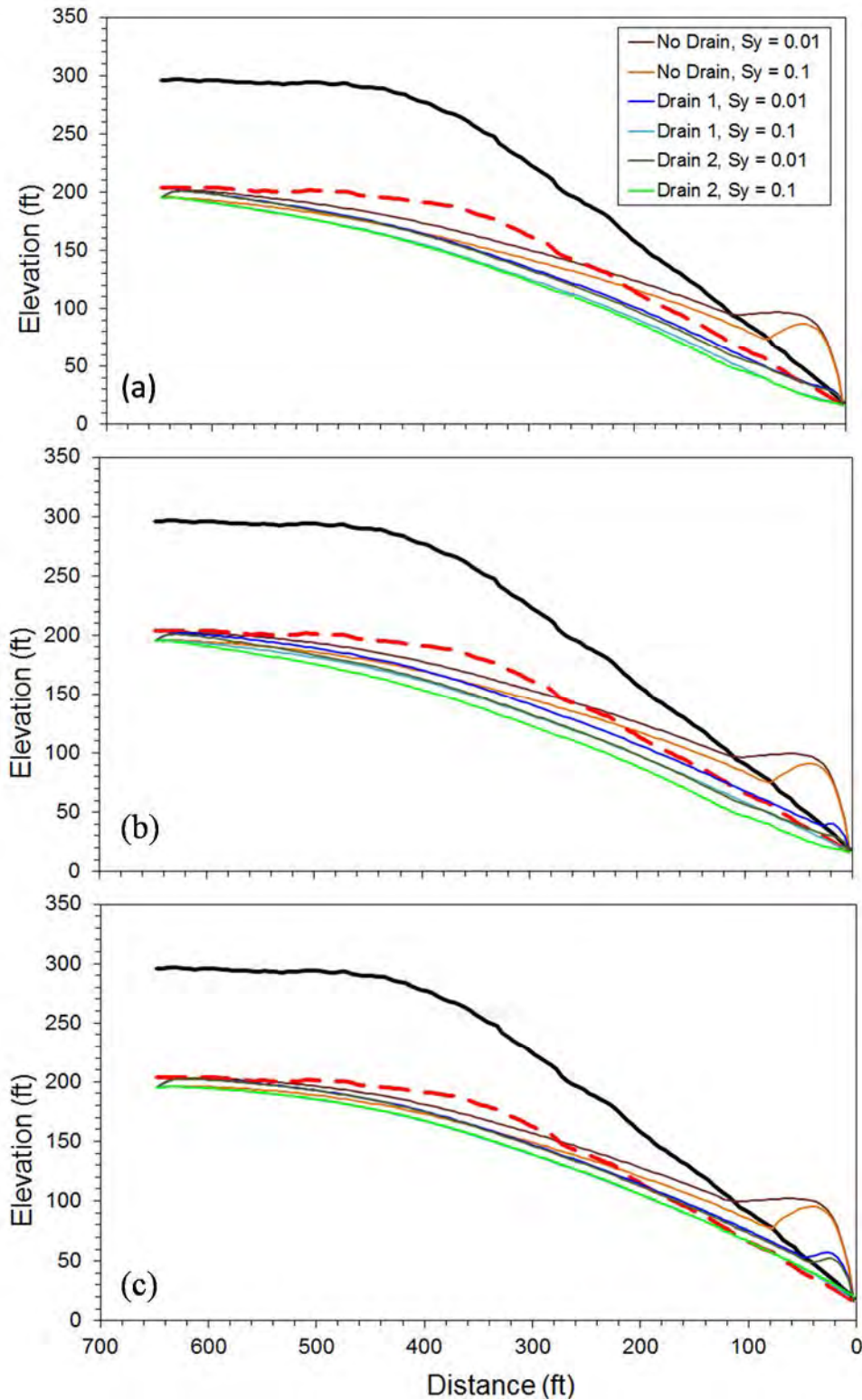


Figure 7.74: Water table elevations for site B along cross section B-B' for $K_x=0.1$ ft/d given anisotropic conditions, (a) VKA = 2 (b) VKA = 5 and (c) VKA=10. The red dashed line is the critical water surface for which FOS = 1.0. The black line is ground surface.

iterative slope stability analyses and groundwater modeling to help ensure stability conditions are met for the entire slope area of interest. However, the slope of site B is fairly uniform and is homogeneous. Therefore, the single cross section along B-B' is assumed representative. In addition, failure potential along the model domain margins is assumed much lower than at the apex of the slope.

Two scenarios of slope failure are modeled using typical water table elevations predicted by MODFLOW. First, the FOS for a no drain scenario given $K_x = 0.1$ ft/d, $S_y = 0.01$ and $VKA \leq 10$ is determined. Water table elevations predicted above ground surface are adjusted to be coincident with (Figure 7.75). It is also assumed that the potential for small rotation failure in the toe area is negligible. FOS is estimated using Morgenstern-Price method with Figure 7.76, indicating the critical rotational failure surface for the whole slope given no drains.

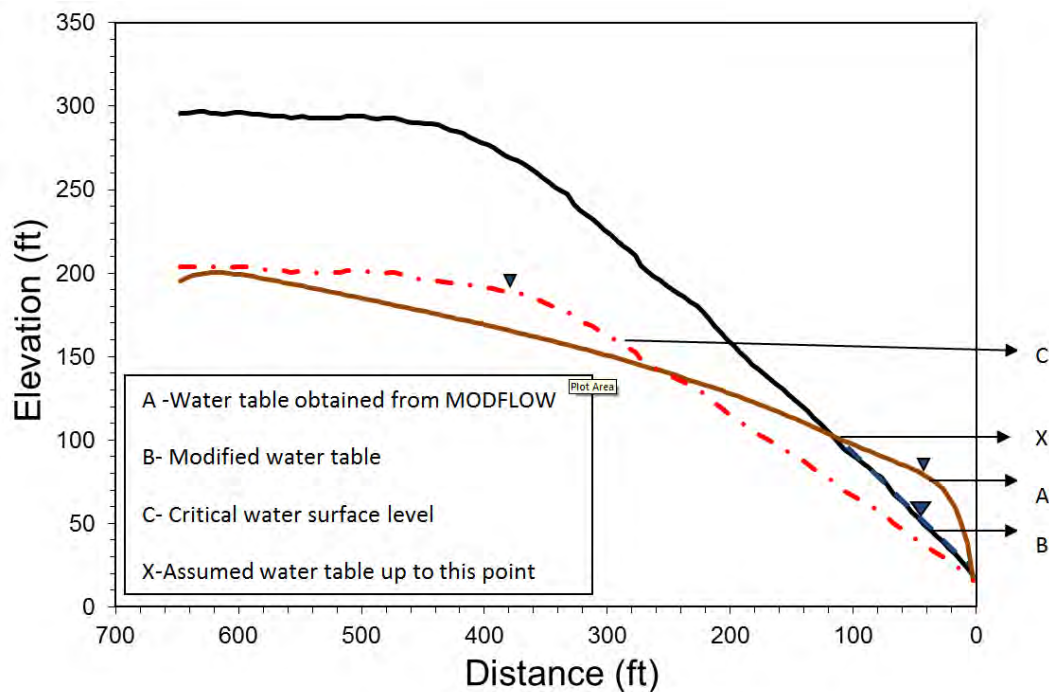


Figure 7.75: An example of how MODFLOW water table surface is adjusted for slope stability analysis. MODFLOW water table surface is typical of $K_x = 0.1$ ft/d, $S_y = 0.01$ and all VKA values given with no horizontal drains.

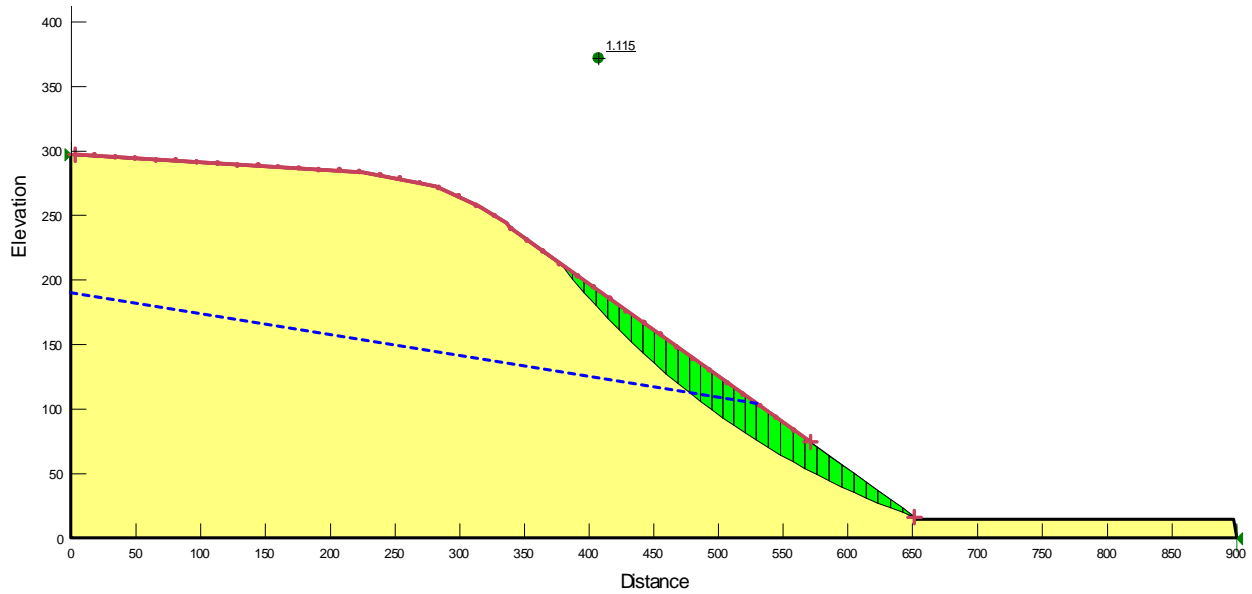


Figure 7.76: Critical rotational failure surface for site B without drains ($K_x = 0.1$ ft/d, $S_y=0.01$ and $VKA \leq 10$)

For isotropic conditions, drain array 1 lowers water table elevations (refer to Figure 7.73a), and the critical rotational failure surface is given in Figure 7.77.

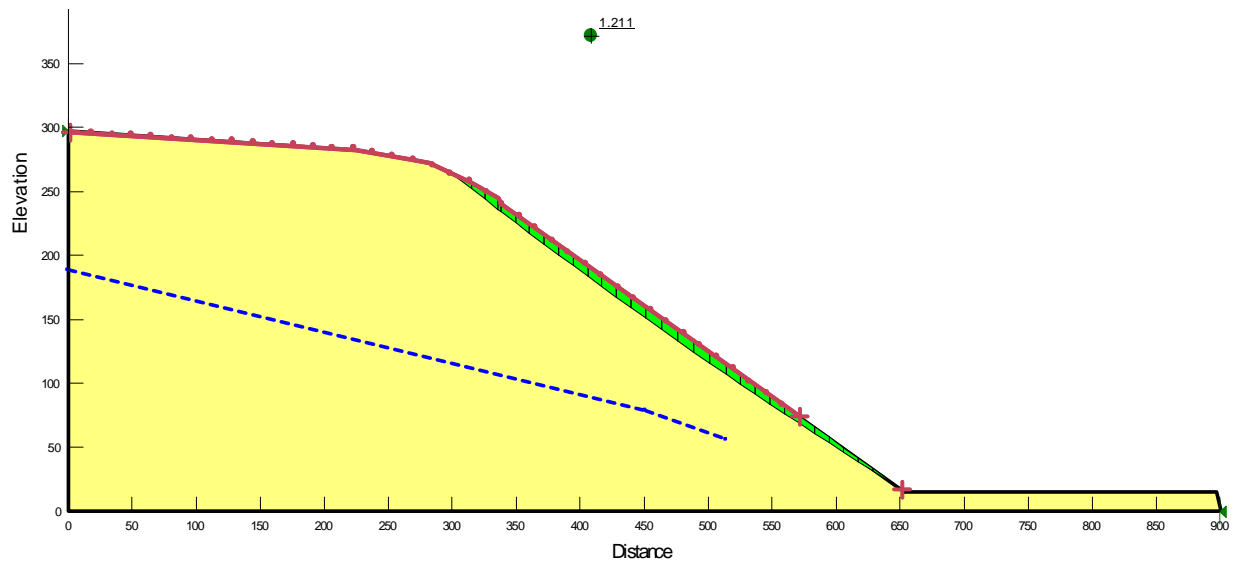


Figure 7.77: Critical rotational failure surface for site B with drain array 1 ($K_x = 0.1$ ft/d, $S_y=0.01$ and $VKA=1$)

Secondly, slope stability analysis was done for different soil types and drain configurations but assuming that the potential for small rotation failure in the toe area is possible. FOS results are provided in Table 7.11. If small rotational failure in the toe region is considered in the FOS calculation, then stabilization of soils comprised of silt, sandy silt, or clayey sand ($K_x = 0.1$ ft/d) and low storage ($S_y = 1\%$), may not be possible given the drain arrays considered. This is true even for isotropic conditions (drain array 2, VKA = 1.16). For anisotropic conditions, FOS values do not deviate much for $VKA \leq 5$, but decrease substantially for $VKA = 10$, such that $FOS < 1.0$ and failure is eminent given any of the drain arrays tested. For larger storage, drain array 1 adequately increases FOS, and reduces the potential for slope failure in the toe region given isotropic conditions. Drain array 2 may be needed for anisotropic conditions up to $VKA = 10$.

Rotational failure in the toe region of more permeable sediments ($K_x \geq 1$ ft/d) is highly likely given no drains are installed. This holds for both low and high storage scenarios. However, drain array 1 is sufficient in reducing the likelihood of failure ($FOS = 1.21$) for all storage values as well as for isotropic and anisotropic conditions.

Table 7.11: FOS values related to small rotational failure in the toe region (site B) for different hydraulic properties and drain scenarios. K_x is in units of ft/d. $VKA = K_x/K_z$. Shaded boxes indicated drain array (with least linear feet) that raises $FOS \geq 1.2$. For more conductive materials ($K_x \geq 1$ ft/d), anisotropy does not significantly impact water levels for $VKA \leq 10$, and so FOS was not calculated for these scenarios (refer to section 7.4.4.5.2).

	K_x	0.1	0.1	1	1	10	10
VKA	S_y	0.01	0.1	0.01	0.1	0.01	0.1
1	No Drain	0.375	0.379	0.428	0.998	0.65	0.998
1	drain 1	1.057	1.211	1.211	1.211	1.211	1.211
1	drain 2	1.163	1.211	1.211	1.211	1.211	1.211
2	No Drain	0.373	0.384	FOS not calculated		FOS not calculated	
2	drain 1	1.106	1.141				
2	drain 2	1.169	1.211				
5	No Drain	0.373	0.384	FOS not calculated		FOS not calculated	
5	drain 1	0.687	1.086				
5	drain 2	1.169	1.211				
10	No Drain	0.373	0.384	FOS not calculated		FOS not calculated	
10	drain 1	0.687	1.086				
10	drain 2	0.529	1.211				

7.6 References Cited

- Chapman, T. G. 1980. Modeling groundwater flow over sloping beds. *Water Resources Research*. •6(6), 1114-1118, 1980.
- Chauhan, H. S., G. O. Schwab, and M. Y. Hamdy, 1968. Analytical and computer solutions of transient water tables of drainage of sloping lands.” *Water Resources Research*, 4, 453–479.
- Childs, E. C., 1971. Drainage of groundwater resting on a sloping bed, *Water Resources Research*, 7(5), 1256–1263.
- Doherty, J. 2005. PEST Model Independent Parameter Estimation. 5th edition. Watermark Numerical Computing. 336 p.
- Donnan, W. W. 1959. Drainage of agricultural lands using interceptor lines, *Journal of Irrigation Drainage*. Division of the American Society of Civil Engineering. 85(IR1): 13-23.
- Fipps, G., and W. Skaggs, 1989. Influence of slope on subsurface drainage of hillsides, *Water Resources Research*, 25(7), 1717–1726.
- Forrester, K. 2001. Subsurface drainage for slope stabilization. ASCE Press. 207 pp.
- Guitjens, J. C., and J. N. Luthin, 1965. Viscous model study of drain spacing on sloping land and comparison with mathematical solution. *Water Resources. Research.*,1(4), 523-530.
- Hooghoudt, S.B. 1940. General consideration of the problem of field drainage by parallel drains, ditches, watercourses, and channels. Publ. No.7 in the series Contribution to the knowledge of some physical parameters of the soil (titles translated from Dutch). Bodemkundig Instituut, Groningen, The Netherlands.
- Keller, J., and A. R. Robinson. 1959. Laboratory research on interceptor drains, *Journal of Irrigation Drainage*. Division of the American Society of Civil Engineering 85(IR3), 25-40,
- Lesaffre, B., 1987. Analytical formulae for traverse drainage of sloping lands with constant rainfall, *Irrigation Drainage Systems*, 1, 105–121.
- Luthin, J. N., and J. C. Guitjens, 1967. Transient solutions for drainage of sloping lands, *Journal of Irrigation and Drainage Engineering*, 43–51.
- Merva, G.E., 1984. The velocity permeameter for rapid determination of hydraulic conductivity. Memo report, 5 pp.
- Moody, W. T., 1967. Nonlinear differential equation of drain spacing, *Journal Irrigation and Drainage Division*, ASCE, 92(2), 1-9.
- Polubarinova-Kochina, P. Y. 1962. *Theory of Groundwater Movement*. translated from Russian by J. M. R. de Wiest, 613 pp., Princeton Univ. Press, Princeton, N.J., 1962.

- Rahardjo, H., K. J. Hritzuk, E. C. Leong, and R. B. Rezaur, 2003. Effectiveness of horizontal drains for slope stability, *Engineering Geology*, 69, 295-308.
- Ram, S., and H.S. Chauhan, 1987a. Drainage of sloping lands with constant replenishment. *Journal of Irrigation and Drainage Engineering*. 113(2): 213-223.
- Ram, S., and H. S. Chauhan. 1987b, Analytical and experimental solutions for drainage of sloping lands with time-varying recharge, *Water Resources Research.*, 23(6), 1090–1096, doi:10.1029/WR023i006p01090.
- Schmid, P., and Luthin, J. 1964. The drainage of sloping lands. *Journal of Geophysical Research.*, 69(8), 1525-1529.
- Shukla, K. N., H. S. Chauhan, and V. K. Srivastava, 1990. Finite difference solution of Boussinesq unsteady-state equation for highly sloping lands, *Journal of Irrigation and Drainage Engineering*, 116(1), 107–113.
- Towner, G. D. 1975. Drainage of groundwater resting on a sloping bed with uniform rainfall, *Water Resources Research*, 11(1), 144–147.
- U.S. Department of the Interior, 1978. *Drainage Manual*, Water Resources Technical Publication, Washington, D.C., 286p.
- Van Beers, W.F.J. 1979. Some nomographs for the calculation of drain spacings. Bulletin 8. International Institute for Land Reclamation and Improvement. ISBN: 90-70260-59 X
- Wesseling, J. 1973. Subsurface flow into drains. *Drainage Principles and Applications Vol. II: Theories of Field Drainage and Watershed Runoff*. 2-56. Publ. 16. ILRI, Wageningen, The Netherlands.
- Willardson, L.S., 1982. Drainage coefficients. ASAE paper No. 80-2576, ASAE, St. Joseph, MI 49085, USA.
- Youngs, E.G., 1971. Seepage through unconfined aquifers with lower boundaries of any shape, *Water Resources Research.*, 7, 624-631.
- Youngs, E.G., and M. A. Al-Najim. 1978. Flow through unconfined aquifers containing interceptor drains, *Journal of Hydrology*. 37, 339-348.

Chapter 8

Network-Scale Flow and Drainage Network Design in Fractured Rock

8.1 Introduction

The preceding chapters describe in detail how the hydrology of watersheds influence drainage network design, and how a hydrological modeling framework can be utilized to evaluate the potential performance of drainage networks in lowering pore pressures to improve slope stability. These discussions have focused on soil and unconsolidated sediment where flow occurs through the interconnected pore space of the medium. Many watersheds are underlain by fractured rock of igneous, metamorphic and sedimentary origin, that are either directly involved in slope instability or host aquifers that can adversely influence the stability of overlying soils. In these cases, drainage networks installed within the overlying soil are likely not to be effective to sufficiently lower pore pressures in or reduce recharge from the underlying fractured rock mass. The installation of a drainage network within the fractured bedrock must then be considered.

Fractured rock presents a very specific challenge to the design of hillslope drainage networks. This is because fractured rock typically has little or negligible porosity and permeability in the rock matrix itself, and connected networks of discontinuous fractures impart secondary porosity and permeability that dominate through-flow of groundwater. Unlike porous media where flow occurs at the pore-scale, flow in fractured rock systems occurs through complex patterns of interconnected, conductive fractures (Long et al., 1982; Smith and Schwartz, 1984; Renshaw, 1999; de Dreuzy et al., 2001; Berkowitz, 2002; Neuman, 2005; Reeves et al., 2008a,b; Klimczak et al., 2010; Reeves et al., 2010). Hence, the design of horizontal hillslope drainage networks must take into account the characteristics of the fracture networks to maximize the probability for drains to intersect flowing fractures that, in turn, will sufficiently reduce pore pressures.

This chapter exclusively focuses on flow through fractured rock in the context of hillslope drainage network design, and is divided into two major parts: network structure and flow, and hillslope network design considerations for fractured rock. The first part emphasizes flow properties of discontinuous fracture networks, and presents methods to determine the equivalent hydraulic conductivity of fractured rock. These equivalent hydraulic conductivity values for fractured rock can be directly input into the hydrologic modeling framework presented in this manual. The second part is dedicated to providing design guidance for the installation of drainage networks in fractured rock, using specific fracture network concepts to enhance the probability of success for achieving hillslope drainage and stability. Multiple illustrations and a case study are presented to reinforce the material presented.

8.2 Network Structure and Flow

A central theme of this Chapter is to impart an understanding of how flow through fractured rock is controlled by fracture attributes. The Fractured Rock Characterization in Chapter 4 (section 4.5) discussed in detail how fractured rock masses can be analyzed according to statistics of fracture orientation, spacing, length, transmissivity and values of fracture density. This section contains detailed explanations on how these attributes are related to flow through a fractured rock mass. We begin by defining network structure, and then discuss how this structure can be used to compute network-scale flow and equivalent hydraulic conductivity tensors. Simulations of flow in two-dimensional discrete fracture networks (DFN) with physically realistic parameters are used to illustrate specific concepts.

8.2.1 Network Structure

The structure of natural fracture networks is the end result of the complex interplay between stress fields and their anisotropy, mechanical properties of the rock, mechanical fracture interaction and distribution of initial flows in a rock mass. The necessary reliance on probabilistic descriptions of fracture attributes reflects our inability to accurately construct fracture networks from mapping or subsurface studies alone. The limited accessibility to the network leaves an incomplete understanding of the patterns of fracturing within a rock mass that can often be improved through visual inspection of representative networks generated according to site-specific statistics (Reeves et al., 2012).

A total of three different network types are generated from two fracture sets with power law distribution of lengths with exponent values in the range $1 \leq a \leq 3$, moderate fracture density, orientations of $\pm 45^\circ$ with variability described by a Fisher distribution with $K=20$ and a log-normal transmissivity distribution with $\log(\tau) = 1$ (Figures 8.1—8.3). Once a network is generated, the *hydraulic backbone* is identified by eliminating dead-end segments and isolated clusters. This is accomplished in our model using both geometric and flow techniques. The hydraulic backbone represents the interconnected subset of a fracture network that is responsible for conducting all flow and transport across a domain. Hence, analysis of backbone characteristics can provide insight into these processes.

The generated networks in this study do not explore the full parameter space for fractured media. However, the wide range of fracture length exponents provide sufficient variability and produce three distinct types of hydraulic backbones. Networks generated with $a = 1$ produce backbone structures dominated by long fractures (Figure 8.1), and networks with $a = 3$ produce backbone structures dominated by short fractures (Figure 8.2). Backbones with a mixture of short and long fractures are produced for networks generated with $a = 2$ (Figure 8.3). Another feature of these networks is that density of the network increases from $\rho_{2D} = 1.0 \text{ m/m}^2$ to $\rho_{2D} = 2.0 \text{ m/m}^2$ as the value of a increases from 1 to 3. This increase in density is necessary to maintain a percolating backbone that promotes fluid flow from one side of the domain to the other. For example, the density values assigned to $a = 1$ and $a = 2$ ($\rho_{2D} = 1.0 \text{ m/m}^2$ and $\rho_{2D} = 1.5 \text{ m/m}^2$, respectively) result in a non-percolating networks if used with $a = 3$. Conversely, networks generated with $a = 1$ and $\rho_{2D} = 2.0 \text{ m/m}^2$ (assigned to $a = 3$) produce unrealistically dense networks. The relationship between network density, power-law exponent and backbone percolation will be further discussed shortly.

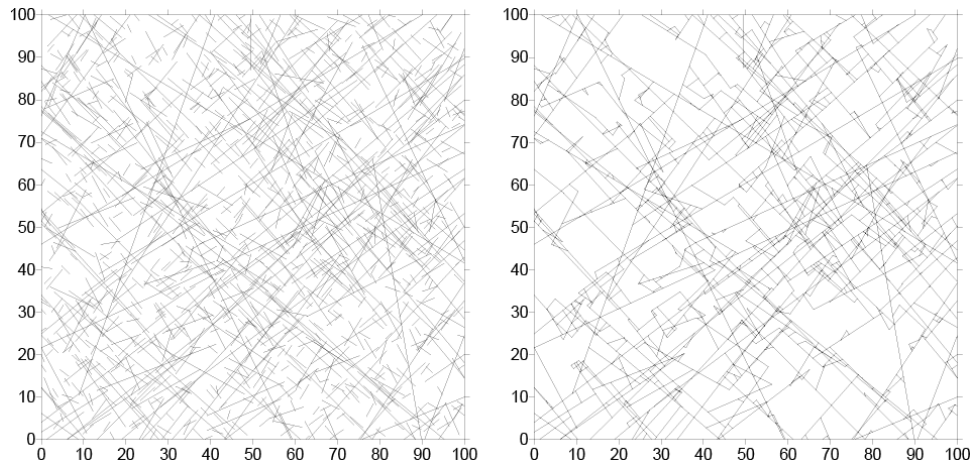


Figure 8.1: Discrete fracture network realization (left) and hydraulic backbone (right) generated from two fracture sets with power distribution of lengths with exponent $\alpha=1$, $\lambda_D=1.0 \text{ m/m}^2$, $l_{min}=2.0 \text{ m}$ and orientations at $\pm 45^\circ$, with variability described by $K=20$. Note that the hydraulic backbone is dominated by long fractures. (Reprinted with permission from Reeves, D.M. et al., Radioactive Waste, 2012, InTech Publishing.)

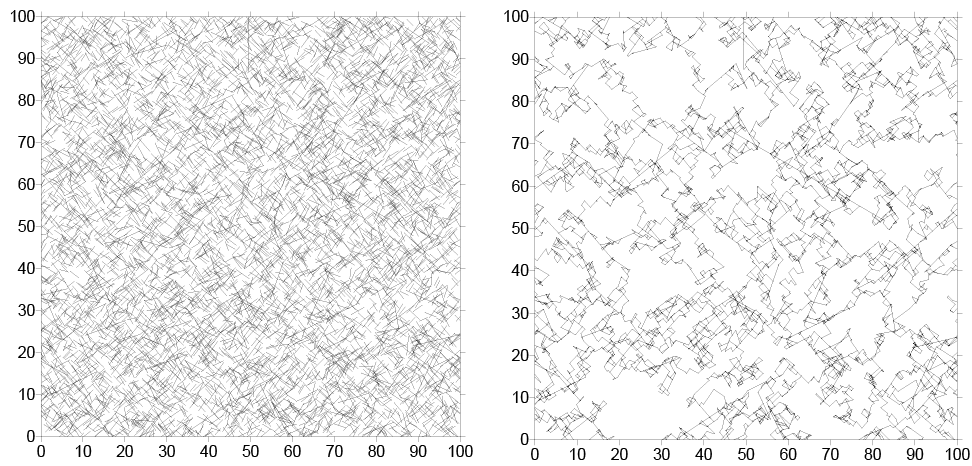


Figure 8.2: Discrete fracture network realization (left) and hydraulic backbone (right) generated from two fracture sets with power distribution of lengths with exponent $\alpha=3$, $\lambda_D=2.0 \text{ m/m}^2$, $l_{min}=2.0 \text{ m}$ and orientations at $\pm 45^\circ$, with variability described by $K=20$. Note that the hydraulic backbone is dominated by short fractures. (Reprinted with permission from Reeves, D.M. et al., Radioactive Waste, 2012, InTech Publishing.)

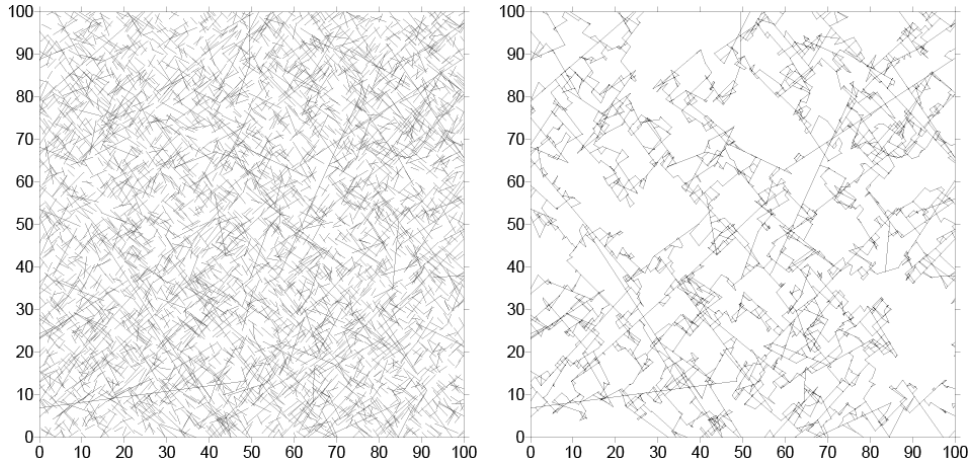


Figure 8.3: Discrete fracture network realization (left) and hydraulic backbone (right) generated from two fracture sets with power distribution of lengths with exponent $\alpha=2$, $\rho_{2D}=1.5 \text{ m/m}^2$, $l_{min}=2.0 \text{ m}$ and orientations at $\pm 45^\circ$, with variability described by $K=20$. Note that the hydraulic backbone is a mix of short and long fractures. (Reprinted with permission from Reeves, D.M. et al., Radioactive Waste, 2012, InTech Publishing.)

To our knowledge, trends between fracture length, density and the total amount of fluid flow a network conducts have not been studied. There has been some work, however, that relates these same fracture parameters to contaminant transport behavior (Reeves et al., 2008a,b,c; Zhang et al., 2010). This lack of knowledge on fluid flow can, in part, be explained by the fact that each natural fracture network exhibits unique combinations of fracture attributes, making it difficult to compare total flow through networks with differing values of mean transmissivity and density. Nonetheless, understanding how these properties influence overall network scale flow is helpful in identifying network types that may or may not be suitable for installation of drainage networks.

We conducted a numerical investigation to understand how total network flow may be related to backbone structure, i.e., primarily fracture trace length and density. A total of 50 network realizations were generated and solved for flow for each of the network types shown in Figures 8.1—8.3 (Table 8.1). Computation of flow in two-dimensional discrete fracture networks involves solving for hydraulic head at all internal nodes (intersection point of two or more fractures) inside the domain according to Darcy's law (Priest, 1993; de Dreuzy and Ehrl, 2003; Klimczak et al., 2010; Parashar and Reeves, 2012). Linear boundary conditions are applied to the networks to induce flow from top to bottom, and fluid flow through the backbone is solved iteratively at each node via a biconjugate gradient method. This process is repeated for each statistically equivalent realization of a given network type.

Table 8.1. Discrete fracture network parameters and results for 50 realizations.

α	$2D$ [m/m ²]	Total Fractures	Backbone $2D$ [m/m ²]	$Q_{=0}$ [m ³ /s]	$Q_{=1}$ [m ³ /s]
1	1.0	1116	0.72	2.86×10^{-3}	2.21×10^{-2}
2	1.5	3898	0.70	1.74×10^{-3}	4.60×10^{-3}
3	2.0	6757	0.83	1.38×10^{-3}	4.22×10^{-3}

Each network type was solved for flow with two different distributions of transmissivity. The first distribution of transmissivity assigns all fractures the same value of T to facilitate direct comparisons on the influence of fracture trace length on overall network flow, Q [m³/s]. The second distribution of transmissivity assigns a log-normal distribution with $\log(\tau) = 1$ to individual fractures, which provides a good representation of variability found in natural fracture networks. Flow through these networks is denoted by $Q_{=0}$ and $Q_{=1}$, respectively in Table 8.1.

Analysis of the DFN data yields several insights. As previously discussed, network percolation requires greater fracture densities as values of α increase. This can be observed in Table 8.1, where values of $2D$ for $\alpha = 1$ and $\alpha = 2$ are 1.0 and 1.5 m/m², respectively, yet produce nearly the same backbone density of 0.70. A value $2D = 2.0$ m/m² for $\alpha = 3$ networks supports this trend, albeit with a slightly higher backbone density of 0.83 m/m². The explanation for this trend is simple: mean fracture length decreases with increases in fracture length exponent values, requiring more fractures to reach a sufficient degree of network connectivity.

The use of a constant T value for all fracture segments along with comparable backbone densities indicates that network-scale flow decreases as values of α increase (Figure 8.4, sigma = 0 case). Implementation of a log-normal T distribution with $\log(\tau) = 1$ increases network scale flow for $\alpha = 1$ networks by approximately an order of magnitude (Figure 8.4, sigma = 1 case). This dramatic increase in network flow results from domain-spanning fractures, which are common in $\alpha = 1$ networks, being assigned T values greater than the mean. Network flow for $\alpha = 2$ and $\alpha = 3$ are very similar. This reflects the higher densities of these networks, where T values lower than the mean serve as ‘bottlenecks’, which have a restrictive influence on total flow.

Variability in network flow for the constant- T simulations was evaluated to study overall network connectivity and backbone structure for individual realizations. Networks with $\alpha = 2$ showed the greatest variability with up to 90% differences in flow from the mean listed in Table 8.1. This indicates that these networks exhibit the greatest variability in backbone structure and connectivity, and this is most likely attributed to the influence of both short and long fractures in producing complex backbone structures (Figure 8.3). Networks with $\alpha = 3$ have up to 45% differences in flow from the mean listed in Table 8.2. These networks are dominated by short fractures (Figure 8.2), and differences in flow are attributed to the degree of connectivity between individual realizations. Networks with $\alpha = 1$ exhibited the lowest degree of variability with only up to 20% differences in flow from the mean listed in Table 8.1. Networks with $\alpha = 1$ are dominated by very long, often domain-spanning fractures (Figure 8.1) that lead to similar degrees of connectivity for individual realizations. Variability in network flow for the log-

normal T distribution show similar trends where $\alpha = 1$ networks have the lowest variability (up to a factor of 2 from the mean) and $\alpha = 2$ and $\alpha = 3$ networks have higher variability (up to a factor of 3 from the mean).

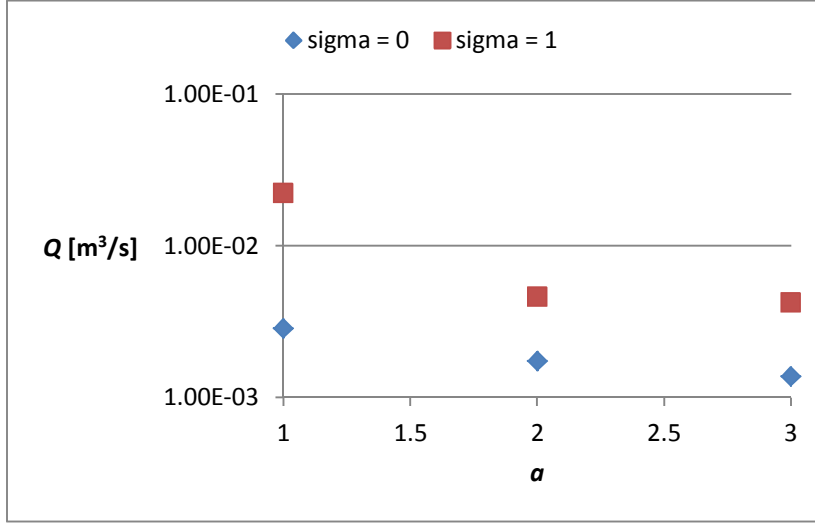


Figure 8.4. Network simulations with comparable backbone densities indicate that total network-scale flow decreases with increasing values of α . This trend linearly decreases when all fracture segments have the same values of T ($\sigma = 0$). Application of a realistically parameterized log-normal distribution with $\log(\tau) = 1$ ($\sigma = 1$) further increases network flow for all cases, with the largest increase in flow for the $\alpha = 1$ networks.

8.2.2 Hydraulic Conductivity Tensor

Fractured media is highly anisotropic and heterogenous, and the tensorial form of hydraulic conductivity K , or more properly denoted \mathbf{K} in its tensor form, is highly useful for modeling the quantity and directional nature of flow in fracture networks. In this section, we explain what a \mathbf{K} tensor is, how it is mathematically defined, and methods for computing the full \mathbf{K} tensor for fractured rock systems. Once computed, this tensor can be properly diagonalized to compute scalar values of K_x , K_y and K_z for use in numerical models.

The discussion of flow through porous media thus far has thus focused on a simple form of Darcy's Law:

$$Q = -KA \frac{dh}{dl} \quad (8.1)$$

which describes the flow of groundwater through a homogenous and isotropic subsurface aquifer, where total discharge Q [L^3/t] is a function of a scalar value of hydraulic conductivity K [L/t], area cross-sectional to flow A [L^2], and a linear horizontal hydraulic gradient dh/dl . Equation (1) can be further simplified to:

$$\frac{Q}{A} = q = -K \frac{dh}{dl} \quad (8.2)$$

where specific discharge q [L/t] (also referred to as Darcy flux) describes groundwater discharge per cross-sectional area. In multiple dimensions, (2) can be expanded to:

$$\mathbf{q} = -\mathbf{K} \nabla h \quad (8.3)$$

where specific discharge \mathbf{q} is a vector along the principal scaling directions of a Cartesian coordinate system (i.e, x -, y -, z -), \mathbf{K} is a second rank tensor, and ∇h is the gradient operator acting on a head field

where head values are allowed to vary in three-dimensions: $\nabla h = \mathbf{i} \frac{\partial h}{\partial x} + \mathbf{j} \frac{\partial h}{\partial y} + \mathbf{k} \frac{\partial h}{\partial z}$. The multi-

dimensional form of Darcy's Law (3) states that the specific discharge vector \mathbf{q} is the sum of its three Cartesian coordinate components:

$$\mathbf{q} = q_x \mathbf{i} + q_y \mathbf{j} + q_z \mathbf{k} \quad (8.4)$$

which can be alternatively written as: $\mathbf{q} = q_1 \mathbf{i} + q_2 \mathbf{j} + q_3 \mathbf{k}$, where Einstein notation is used to denote x , y , z components as indices 1, 2 and 3; and \mathbf{i} , \mathbf{j} , and \mathbf{k} are unit normal vectors along x , y , and z . Thus, in Einstein notation (3) can be expressed as:

$$q_i = K_{ij} J_j, \quad i=1,3 \quad (8.5)$$

where $\mathbf{J} = -\nabla h$ and $\nabla h = \mathbf{i} \frac{\partial h}{\partial x_1} + \mathbf{j} \frac{\partial h}{\partial x_2} + \mathbf{k} \frac{\partial h}{\partial x_3}$. Expanding (5) to a set of linear algebraic equations:

$$\begin{aligned} q_1 &= K_{11} J_1 + K_{12} J_2 + K_{13} J_3 \\ q_2 &= K_{21} J_1 + K_{22} J_2 + K_{23} J_3 \\ q_3 &= K_{31} J_1 + K_{32} J_2 + K_{33} J_3 \end{aligned} \quad (8.6)$$

we can further understand the nature of hydraulic conductivity as a second rank tensor where:

$$\begin{bmatrix} q_1 \\ q_2 \\ q_3 \end{bmatrix} = \begin{bmatrix} K_{11} & K_{12} & K_{13} \\ K_{21} & K_{22} & K_{23} \\ K_{31} & K_{32} & K_{33} \end{bmatrix} \begin{bmatrix} J_1 \\ J_2 \\ J_3 \end{bmatrix} \quad (8.7)$$

Thus, \mathbf{K} is a symmetric, second rank tensor consisting of 9 components to properly scale discharge \mathbf{q} to the directional permeability of the medium and hydraulic gradient \mathbf{J} .

The tensor form of \mathbf{K} in (7) can be diagonalized by eigenvector/eigenvalue transformation:

$$\begin{bmatrix} q_1 \\ q_2 \\ q_3 \end{bmatrix} = \begin{bmatrix} K_{11} & 0 & 0 \\ 0 & K_{22} & 0 \\ 0 & 0 & K_{33} \end{bmatrix} \begin{bmatrix} J_1 \\ J_2 \\ J_3 \end{bmatrix} \quad (8.8)$$

where

$$\begin{aligned} q_1 &= K_{11}J_1 = -K_{xx} \frac{\partial h}{\partial x} = -K_x \frac{\partial h}{\partial x} \\ q_2 &= K_{22}J_2 = -K_{yy} \frac{\partial h}{\partial y} = -K_y \frac{\partial h}{\partial y} \\ q_3 &= K_{33}J_3 = -K_{zz} \frac{\partial h}{\partial z} = -K_z \frac{\partial h}{\partial z}. \end{aligned} \quad (8.9)$$

In this case, K_x , K_y and K_z are commonly referred to as the hydraulic conductivity values in the x-, y- and z-directions, respectively, and the off-diagonal components are equal to 0. These scalar K values can be input into MODFLOW or other ground water models for flow simulations.

Development of methods for computing equivalent \mathbf{K} tensors for fractured rock with discontinuous fractures has been the subject of numerous investigations (e.g., Snow, 1969; Long et al., 1982; Lee et al., 1985; Oda, 1985; Zhang et al., 1996; Min et al., 2004; Klimczak et al., 2010). These studies typically refer permeability (denoted as \mathbf{k}) rather than hydraulic conductivity (denoted as \mathbf{K}) tensors. It is important to note that the relationship of hydraulic conductivity \mathbf{K} [L/t] to permeability \mathbf{k} [L²] is described by:

$$\mathbf{K} = \frac{g}{\mu} \mathbf{k} \quad (8.10)$$

where μ is fluid viscosity, g is the gravitational constant and ρ is fluid density. For example, at 20°C this relationship is: \mathbf{K} [m/s] = $9.7337 \times 10^4 \mathbf{k}$ [m²]. As a general rule hydraulic conductivity values are 5 orders of magnitude greater than permeability when transitioning between units of m/s and m².

There are two primary methods in which the \mathbf{K} tensors can be computed for fractured rock: (1) an analytical expression known as the 'Oda tensor' approach and (2) numerical approach involving the computation of network-scale flow using discrete fracture network (DFN) simulations with specifically applied boundary conditions. Both of these approaches are discussed below.

The Oda tensor approach is based on the following analytical expressions (Oda, 1985):

$$K_{ij} = \frac{g}{\mu} (P_{kk} \delta_{ij} - P_{ij}) \quad (8.11)$$

$$P_{ij} = \frac{p}{4} \int_0^\infty \int_0^\infty \int_\Omega r^2 t^3 n_i n_j E(\mathbf{n}, r, t) d\Omega dr dt \quad (8.12)$$

where P_{ij} is the permeability tensor, p is 3D fracture density (3D), r is fracture radius (half-length), t is fracture aperture, \mathbf{n} is a unit normal vector to the fracture plane (defines orientation) over area Ω , $P_{kk} = P_{11} + P_{22} + P_{33}$, which define principal components of permeability similar to (8), and $E(\mathbf{n}, r, t)$ represents a joint distribution of fracture orientation, fracture radius (half-length) and aperture. These distributions are assumed independent. Values of ω describes fracture connectivity where ω is equal to 1/12 if the network is well connected and ω is less than 1/12 if not well connected. Equations (11) and (12)

compute K based on fracture attributes; however, probability distributions of orientation, length and hydraulic conductivity are ill-defined if sufficient connectivity is not established. There is no way other than the generation of site-specific equivalent discrete fracture networks to precisely define the level of connectivity that is present in a rock mass, and well-connected networks are the exception rather than the rule. Hence, the dominant problem with the Oda tensor approach is reducing the complexity of network connectivity to a single, difficult to define parameter. The prior analysis of network structures for different network types in Section 2.1 illustrates the complexity of network structure and connectivity. More specifically, backbone densities are highly variable and are typically not proportional to total network density measured in the field. We therefore cannot recommend the use of the Oda tensor to compute network K and only include this method for completeness.

The numerical approach to define equivalent network K tensors involves solving flow in discrete fracture networks under specified boundary conditions. The generation of fracture networks requires analysis of site-specific fracture properties to assign probability distributions of orientation, length, aperture/hydraulic conductivity and values of fracture density (refer to Chapter 4 for fracture characterization). With the exception of fracture density and distribution of spacing, these are the same parameters that are required for the Oda tensor. Rather than determining K directly from these statistics using the Oda Tensor approach, the numerical approach stochastically generates discrete fracture networks, computes the hydraulic backbone by eliminating dead-end segments and isolated clusters, and solves for flow. In 2D planar representations of fracture networks, determination of the K tensor requires two different boundary conditions to compute each component of the K tensor (Figure 8.5). This same method can be used to compute the full 3D tensor by first generating a 3D fracture network and projecting the fracture network onto corresponding x - y , y - z and x - z planes and solving for flow in 2D. Each of these planes requires two sets of boundary conditions as illustrated in Figure 8.5. This process is further illustrated in a case study below. Alternatively, 3D discrete fracture network simulators can be used to compute each of the tensor components given specified boundary conditions. Like its 2D counterpart, the use of 3D DFN simulators also requires various configurations of boundary conditions for computation of individual components of the K tensor.

The application of a tensor to model flow in fractured rock depends on two criteria. The first criterion is that representative elementary volume (REV) conditions are met (e.g., Bear, 1972; Long et al., 1982; Klimczak et al., 2010). The REV approach assumes that hydraulic conductivity oscillates heterogeneously within a volume of fractured rock until a specific volume scale is reached where K becomes more or less constant (homogeneous) (Figure 8.6). Thus, the REV represents a volume scale at which variability of fracture attributes, including network connectivity and range of K for individual fractures, has been sufficiently sampled and perturbations caused by scale effects are effectively averaged. Fractured media is extremely complex and REVs do not exist for some networks at any scale, particularly for sparse networks with low power-law length exponent values ($\alpha < 2$) (Klimczak et al., 2010). In general, the denser a network the more quickly an REV can be established. This is because dense networks tend to have shorter fractures and are well connected, effectively homogenizing the network over shorter volume scales.

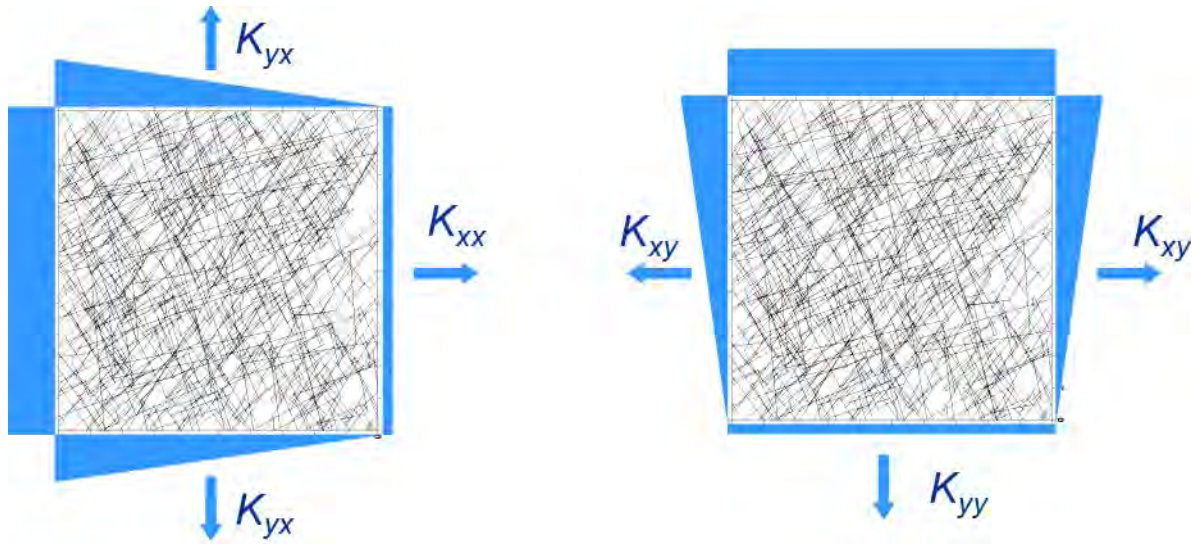


Figure 8.5: Illustration depicting the application of two sets of linear boundary conditions used to solve for individual components of the K tensor in the x - y plane.

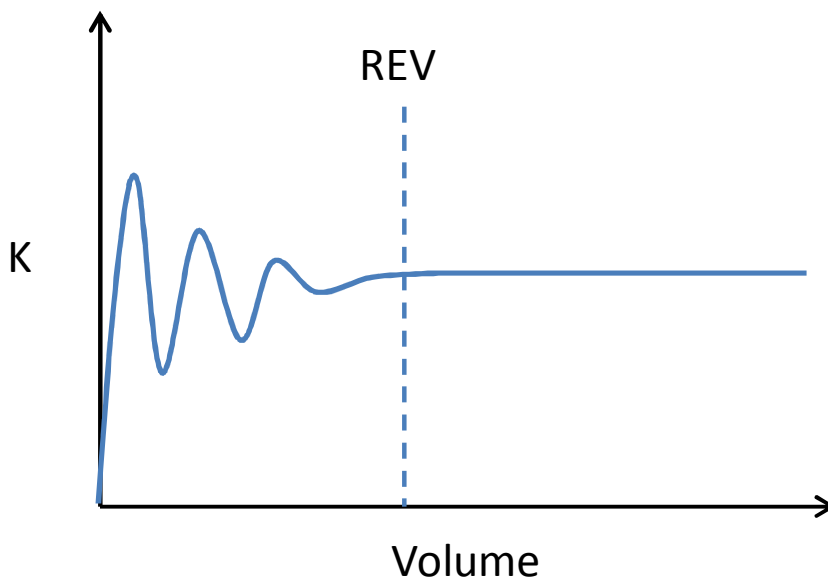


Figure 8.6: Illustration of the representative elementary volume (REV) concept where (in this case) hydraulic conductivity becomes homogenous (constant) after a volume scale is reached. Note that not all fractured media exhibits REV in K .

The second criterion for the application of a \mathbf{K} tensor is that it must be symmetric with orthogonal principal components. The symmetry of the tensor is more difficult to compute as it involves the rotation of a generated, site-specific DFN by small increments and solving for flow under the same boundary conditions as presented in Figure 8.5. Under these conditions, a symmetric tensor in 2D will

form an ellipse with orthogonal major and minor ellipses (Figure 8.7). In 3D, the \mathbf{K} tensor will form an ellipsoid. The REV and tensor symmetry concepts will be further illustrated in the following example using site-specific fracture data.

Case Study Example: Lower Carbonate Aquifer in Southern Nevada

The LCA3 is a hydrostratigraphic unit located on the Nevada National Security Site (NNSS) in the vicinity of the Rainier Mesa Corrective Action Unit (Area 12). The LCA3 label denotes a deep or Lower Carbonate Aquifer of Paleozoic age rock that underlies a large portion of the NNSS; the '3' indicates that this unit is a thrust wedge of the LCA higher in the stratigraphic sequence than the non-thrusted LCA. The LCA3 is densely-fractured and has very low matrix hydraulic conductivity (on the order of 10^{-12} m/s). Thus, the hydraulic conductivity of the LCA3 is fracture dominated.

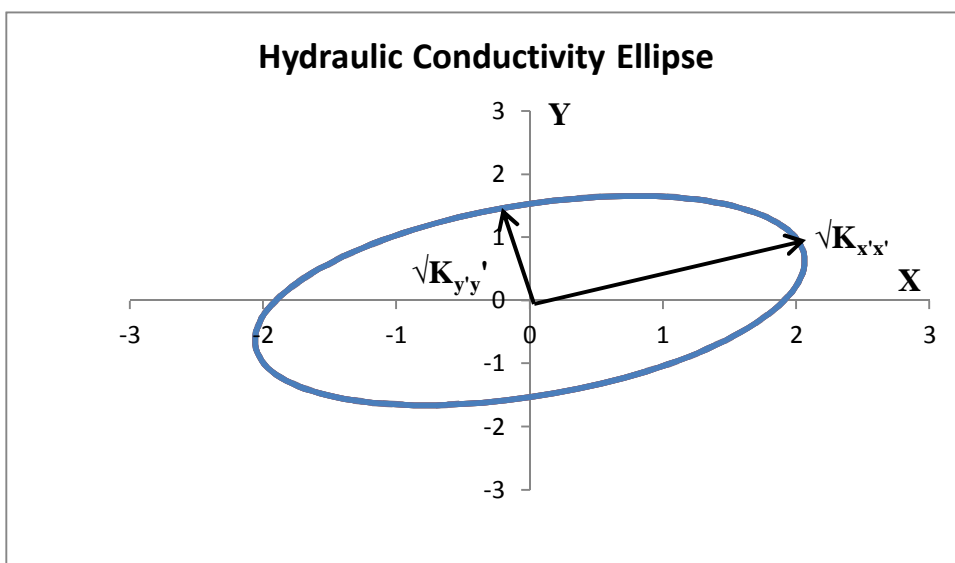


Figure 8.7: Theoretical hydraulic conductivity ellipse in the x-y plane where the principal directions of hydraulic conductivity, $K_{x'x'}$ and $K_{y'y'}$, are oriented 30 degrees from the x-axis. The major and minor axes of the ellipse are represented by $\sqrt{K_{x'x'}}$ and $\sqrt{K_{y'y'}}$ where $K_{x'x'}$ and $K_{y'y'}$ are equal to 5 and 2 m/d, respectively. If this data represented a field site the model grid should be rotated 30 degrees about the x-axis to be consistent with the principal directions of hydraulic conductivity.

Single well hydraulic tests performed on wells ER-12-3 and ER-12-4 yield saturated K values that range between 10^{-6} and 10^{-8} m/s, respectively (SNJV, 2006a,b). Both of these wells each have over 100 meters of screened interval open to the LCA3, and hence, these values represent an average or 'effective' K at these two locations where only a single value of K is applied to the entire system. While hydraulic tests over large screened intervals are very useful in determining ranges of effective K values for densely fractured rock, directional anisotropy cannot be determined from these tests alone, unless multiple monitoring wells are used. In this case, the NNSS has very deep (~800 m) vadose (unsaturated) zones and the cost of drilling precludes the installation of any, let alone multiple, monitoring wells for

purposes of hydraulic testing. It is important to note that fractured rock exhibits very complicated network geometry and connectivity, and the installation of multiple monitoring wells is no guarantee for effective determination of fractured rock anisotropy.

Fractured rock anisotropy is a result of the structure of discontinuous fracture networks (i.e., number of fracture sets of their orientation, length and density), which can lead to the condition $K_x \neq K_y \neq K_z$. To support simulations of flow and radionuclide transport predictions, it was deemed critical to define the anisotropy of the LCA3. This involved computation of the **K** tensor according to collected fracture data. Available fracture data from the LCA3 consists of (Boyle, 2003):

- Dolomite Hill core hole (aperture and frequency/spacing)
- Right rib U12e south drift (orientation, length, and frequency/spacing)
- Outcrops near U12e tunnel south portal (orientation, length and frequency/spacing)

The Dolomite Hill core hole is a 365 m deep core hole within the LCA3 that is located approximately 300 m southeast of the U12e tunnel south portal, the location of the other two data sets. The right rib of the U12e south drift consists of a 17 m long subsurface exposure of the LCA3 along a tunnel drift. Two transects of approximately 20 m and 15 m, oriented E-W and N-S, were used to measure fracture attributes at outcrops of the LCA3 near the U12e tunnel south portal (Figure 8.8).



Figure 8.8: Outcrops near U12e tunnel south portal where transects 1 (left) and 2 (right) were used to collect fracture data. Transect 1 is 20 m in length and is orientated approximately N-S; Transect 2 is 15 m in length and is oriented approximately E-W. Data along these two transects was collected from fractures with lengths greater than 0.45 m (1.5 ft).

Characterization of the LCA3 involved analysis of fracture data to assign distributional properties of fracture orientation, length and aperture and values of frequency/spacing. Poles-to-fracture orientations (strike and dip) were first projected to a southern hemisphere stereonet. Contour plots of

pole density revealed two steeply-dipping fracture sets with orientations of 227°, 81° and 292°, 71°, and prior probabilities of 0.64 and 0.36, respectively (Figure 8.9, left).

The fracture aperture data set is exclusively from the Dolomite Hill core hole at depths greater than 173 m (450 ft) below land surface. This cutoff depth was selected due to an abrupt transition to smaller aperture values that are considered more representative of apertures in the LCA3 at depth. The cutoff depth of 173 m below land surface may approximate the extent of surface weathering at the top of the LCA3 (Boyle, 2003). Aperture data from the underground drift and two surface outcrops were not used in this analysis as the lack of confining stress artificially dilates fracture apertures. An empirical relationship: $K_h = 0.558K_m$ is used to adjust mechanical aperture K_m to hydraulic aperture K_h (Kwicklis, 1998) prior to distributional analysis. Hydraulic aperture values from the Dolomite Hill core hole best fit a lognormal distribution with \log_{10} mean and standard deviation of aperture of -3.75 and 0.39 m prior to log transformation (Figure 8.9, right). The average fracture aperture is 187 microns which is a very reasonable value for fracture aperture (typically in the range of 50 to 350 microns). These values are used to assign transmissivity to the fractures via the cubic law (eqn 4.34).

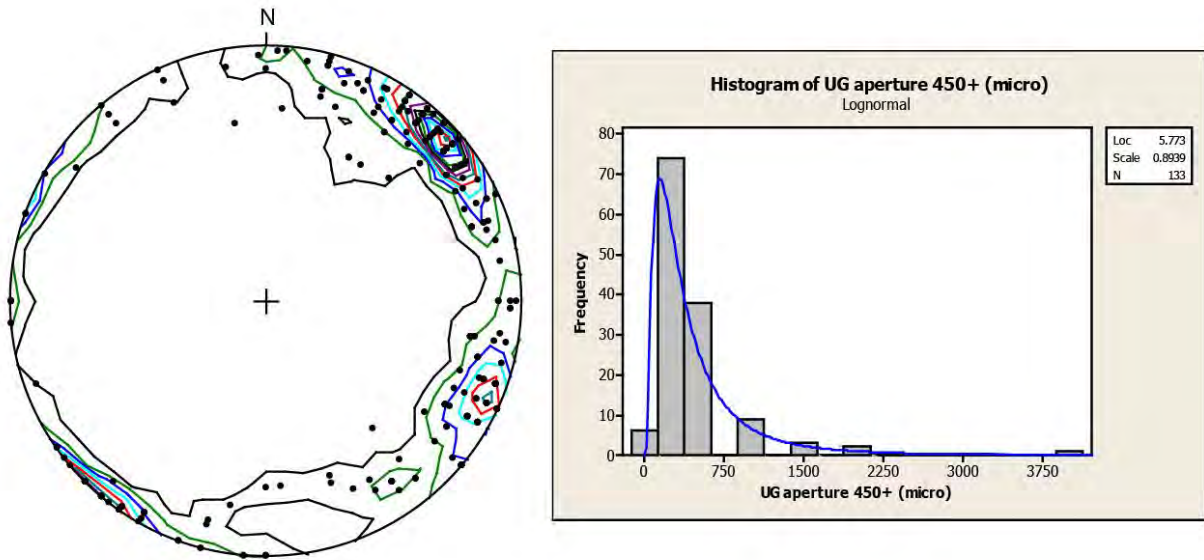


Figure 8.9: Stereonet plot (left) showing lower hemisphere projection of fracture poles (n=176) along with pole density contours. The orientation data indicate two steeply dipping fracture sets with strike and dip orientations of 227°, 81° and 292°, 71°, and prior probabilities of 0.64 and 0.36, respectively. Histogram of fracture aperture (right) indicates a satisfactory fit to a lognormal distribution with \log_{10} mean and standard deviation of aperture of -3.75 and 0.39 m prior to log transformation. Average fracture aperture is 178 microns. Note that the best fit lognormal distribution values listed in the figure represent the equivalent of the parameters given for a log base e distribution.

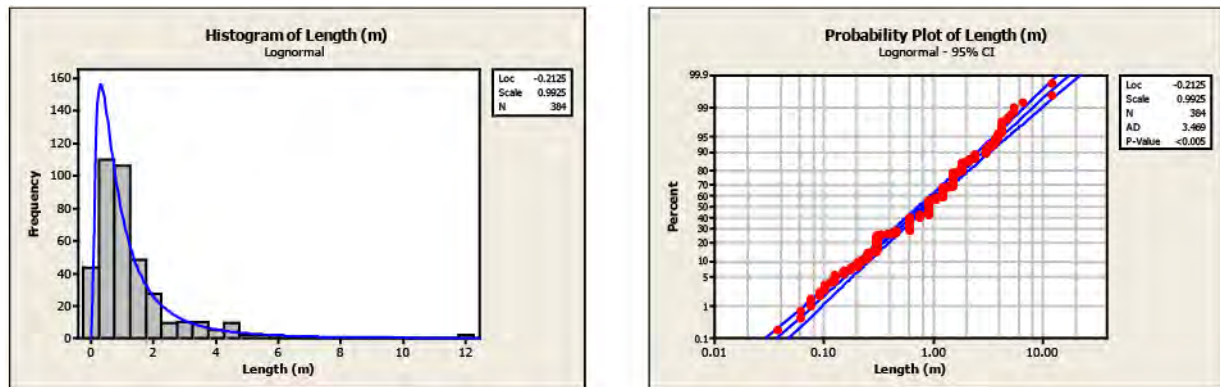


Figure 8.10: Histogram (left) and probability plot of fracture lengths (right) indicate a good fit to a lognormal distribution with \log_{10} mean and standard deviation of fracture length of -0.09 and 0.43 m prior to log transformation. Average fracture length is 0.8 m. Similar to Figure 8.6, best fit lognormal distribution values listed in the figure represent the equivalent of the parameters given for a log base e distribution.

Analysis of fracture lengths collected from the surface and subsurface exposures for fractures with lengths greater than 0.45 m (1.5 ft) indicate that fracture length best fits a lognormal distribution (Figure 8.10). The use of a lognormal distribution in this analysis is somewhat contrary to the previous discussion of power law fracture length distributions in section 4.5.2, and likely arises for two reasons. First, the surface and subsurface exposures are limited in scale and this may cause larger fracture lengths to be truncated in the data set. Second, the LCA3 is very densely fractured, which can cause a truncation in fracture length and produce a lognormal distribution. Analysis of the distribution of fracture length for power-law tails yielded a weak power-law trend with power-law exponent of $\alpha = 2.5$ (not shown). Networks with power-law exponents of $\alpha = 2.5$ or greater are dominated by very short fractures (Figure 8.3), and the utility of power-law distributions in describing a continuum of lengths is somewhat lost. Given the dominance of short fractures (average length is 0.8 m) and goodness of fit of the data, a lognormal distribution of fracture length with \log_{10} mean and standard deviation of fracture length of 0.09 and 0.43 m prior to log transformation is used to describe fracture length.

Fracture spacings from data sets collected from the Dolomite Hill core hole and right rib underground drift are oriented sub-optimally relative to the fracture set orientations. For this reason, 1D fracture frequency and density is computed exclusively from the two transects on the surface exposures. These transect lines produce an average fracture frequency value of 5.5 fractures per meter. The inverse of this calculation produces average fracture spacing which is 0.18 m. We consider networks with spacings under 1 m to be densely fractured, so a 0.18 m fracture spacing corresponds to a very dense network.

The fracture analyses outlined above are then used to reproduce three-dimensional DFN networks consist with site-specific data. These networks are not shown due to challenges in visualizing 3D networks with high fracture density. The process of generating the DFNs involves the generation of individual fractures according to: (1) fracture location via a random point process, (2) orientation via a Fisher distribution consistent with prior probabilities for each set, (3) fracture length via a lognormal distribution and (4) fracture transmissivity via a lognormal distribution of apertures and the cubic law. This process is repeated until the fracture density criterion of 0.18 m is satisfied. The 3D DFNs are then projected onto planes aligned with the Cartesian coordinate system for computation of the **K** tensor (Figure 8.11), i.e., the x-y, x-z and y-z planes. Two sets of these boundary conditions, consistent with Figure 8.5, are used to establish orthogonal flow directions for computation of the diagonal and off-diagonal components of the **K** tensor for each plane:

$$\mathbf{K}_{xy_plane} = \begin{bmatrix} K_{xx} & K_{xy} \\ K_{yx} & K_{yy} \end{bmatrix}; \mathbf{K}_{xz_plane} = \begin{bmatrix} K_{xx} & K_{xz} \\ K_{zx} & K_{zz} \end{bmatrix}; \mathbf{K}_{yz_plane} = \begin{bmatrix} K_{yy} & K_{yz} \\ K_{zy} & K_{zz} \end{bmatrix}. \quad (8.13)$$

Fifty statistically-equivalent fracture network realizations are used to generate these tensor values for the LCA3. The **K** tensor [m/s] for the LCA3 is then computed through arithmetic averaging to determine the mean value for each component:

$$\mathbf{K}_{LCA3} = \begin{bmatrix} K_{xx} & K_{xy} & K_{xz} \\ K_{yx} & K_{yy} & K_{yz} \\ K_{zx} & K_{zy} & K_{zz} \end{bmatrix} = \begin{bmatrix} 6.6 \times 10^{-7} & 6.1 \times 10^{-7} & 6.0 \times 10^{-8} \\ 3.8 \times 10^{-7} & 9.7 \times 10^{-7} & 3.0 \times 10^{-8} \\ 9.6 \times 10^{-8} & 4.7 \times 10^{-8} & 8.8 \times 10^{-8} \end{bmatrix}.$$

The principal components of the **K** tensor are then computed by taken the eigenvalues of the tensor matrix:

$$\mathbf{K}_{LCA3} = \begin{bmatrix} K_{xx} = K_x & & \\ & K_{yy} = K_y & \\ & & K_{zz} = K_z \end{bmatrix} = \begin{bmatrix} 3.2 \times 10^{-7} & & \\ & 1.3 \times 10^{-6} & \\ & & 7.6 \times 10^{-8} \end{bmatrix}.$$

The LCA3 **K** tensor honors network structure and resultant anisotropy and overall ranges of hydraulic conductivity measured from hydraulic tests. Values of the **K** tensor for K_{xx} , K_{yy} and K_{zz} are 3.2×10^{-7} , 1.3×10^{-6} , and 7.6×10^{-8} m/s, respectively. The overall or effective K of the system, computed by taking the geometric mean of the tensor components, is:

$K_{effective} = \exp\left[(\log K_{xx} + \log K_{yy} + \log K_{zz})/3\right] = 3.2 \times 10^{-7}$ m/s . Recall that "effective" estimates of K for the LCA3 range from 10^{-6} to 10^{-8} m/s based on single well hydraulic tests at ER12-3 and ER12-4 over large screened intervals, and the effective K value is in the middle of this range. Higher values of K_{xx} and K_{yy} reflect the higher degree of connectivity in the horizontal plane than the vertical plane.

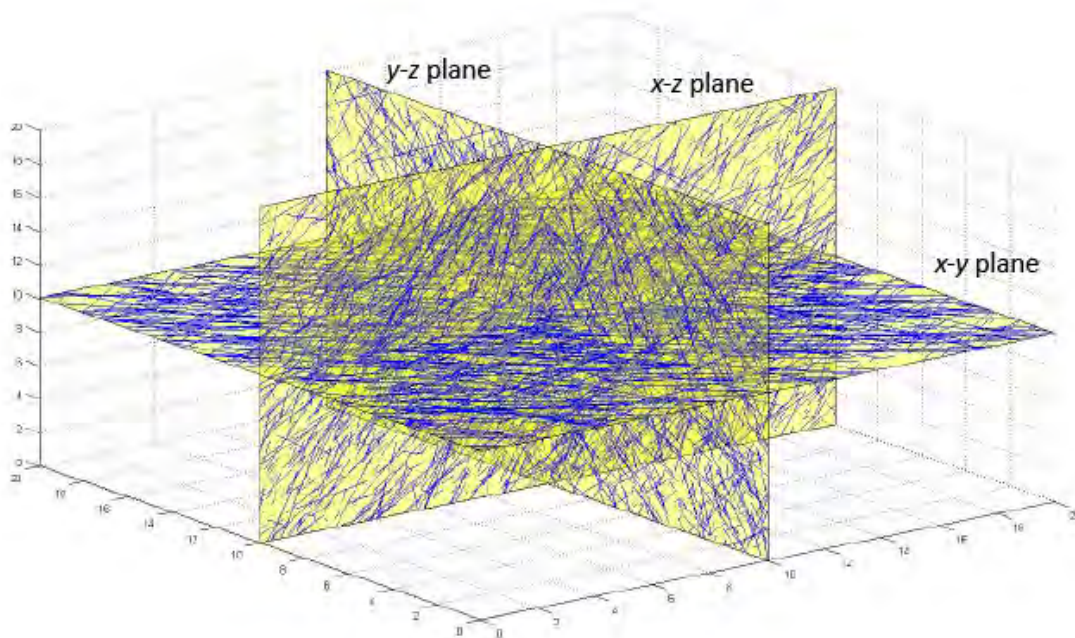


Figure 8.11: Generated three-dimensional fracture network from site-specific LCA3 fracture data projected onto x-y, x-z and y-z planes. Components of the K tensor are then computed for each fracture plane by applying the two sets of boundary conditions shown in Figure 8.5.

8.3 Hillslope Drainage Network Design for Fractured Rock

The information contained in this manual is intended to assist in the design of hillslope drainage networks in fractured rock. The first step in designing a hillslope drainage network in fractured rock is to collect site-specific fracture data. This field data can then be analyzed to determine distributional properties of orientation, length, aperture and hydraulic conductivity/transmissivity and values of fracture density. Generation of discrete fracture networks from this data provides valuable insight into the structure and flow characteristics of the underlying fracture networks. These networks can also be used to compute equivalent hydraulic conductivity tensors that serve as a basis for evaluating the efficiency of hillslope drainage networks in lowering pore pressures using the MODFLOW framework in this manual.

One limitation of the equivalent-hydraulic-conductivity tensor approach, as applied to the MODFLOW grid, is that the use of a tensor assumes that the network at the scale of the MODFLOW grid cell is well-connected. The well-connected assumption, in part, can be satisfied through an analysis to determine the scale at which the Representative Elementary Volume (REV) is valid. However, rock fracture networks exhibit high degrees of heterogeneity in both geometric and hydraulic properties, and certain fracture characteristics, namely fracture length, spacing, and variance of transmissivity, can lead to

networks with irregular connectivity and highly focused flow. REV conditions for these cases may not be satisfied and the tensor approach cannot be utilized.

In this Section, an additional analysis focusing on the intersection of hillslope drainage networks with dominant flow fractures is performed. Intersecting "dominant" fractures is absolutely critical to successfully lowering fluid pore pressures and achieving hillslope stabilization. This analysis is directly performed on models of discrete fracture networks generated from both synthetic and site-specific data. The results of this analysis are valid regardless of REV assumptions, since the analysis itself is performed directly on the discrete fracture networks and no up-scaling is introduced.

8.3.1 Differentiating Fracture Types

Discrete fracture networks are analyzed for intersection with three fracture types: all fractures, hydraulic backbone fractures, and dominant fractures. "All fractures" refer to all fractures present in a rock mass, whereas "hydraulic backbone" fractures refer only to the interconnected fractures of the hydraulic backbone. This concept can be readily visualized in Figures 8.1 through 8.3 in this section. "Dominant" fractures, as defined in this subsection, refer to fractures of the hydraulic backbone that conduct flow exceeding a specified value:

$$\text{Dominant Fracture Flow} \geq \frac{\text{Global DFN Flow}}{\text{Number of Boundary Fractures}/2} \quad (8.14)$$

where flow through a dominant fracture must equal or exceed the total flow through a DFN realization normalized by the number of boundary fractures. Boundary fractures intersect the outside of the DFN model boundary and are responsible for all flow in and out of the model domain. Half of the boundary fractures are used because global DFN flow represents the net flow through a network, and on average approximately half of the boundary fractures conduct flow into the network and approximately half of the boundary fractures conduct flow out from the network.

The use of a robust mathematical definition of dominant fractures in (14) is necessary for comparing networks with different degrees of heterogeneity in transmissivity, defined by the log variance of transmissivity, $\log(\sigma_T)$ (Figure 8.12). In the following intersection analysis, "successful" hillslope drainage attributed to lowering of pore pressures depends on the intersection of dominant fractures with horizontal hillslope drains.

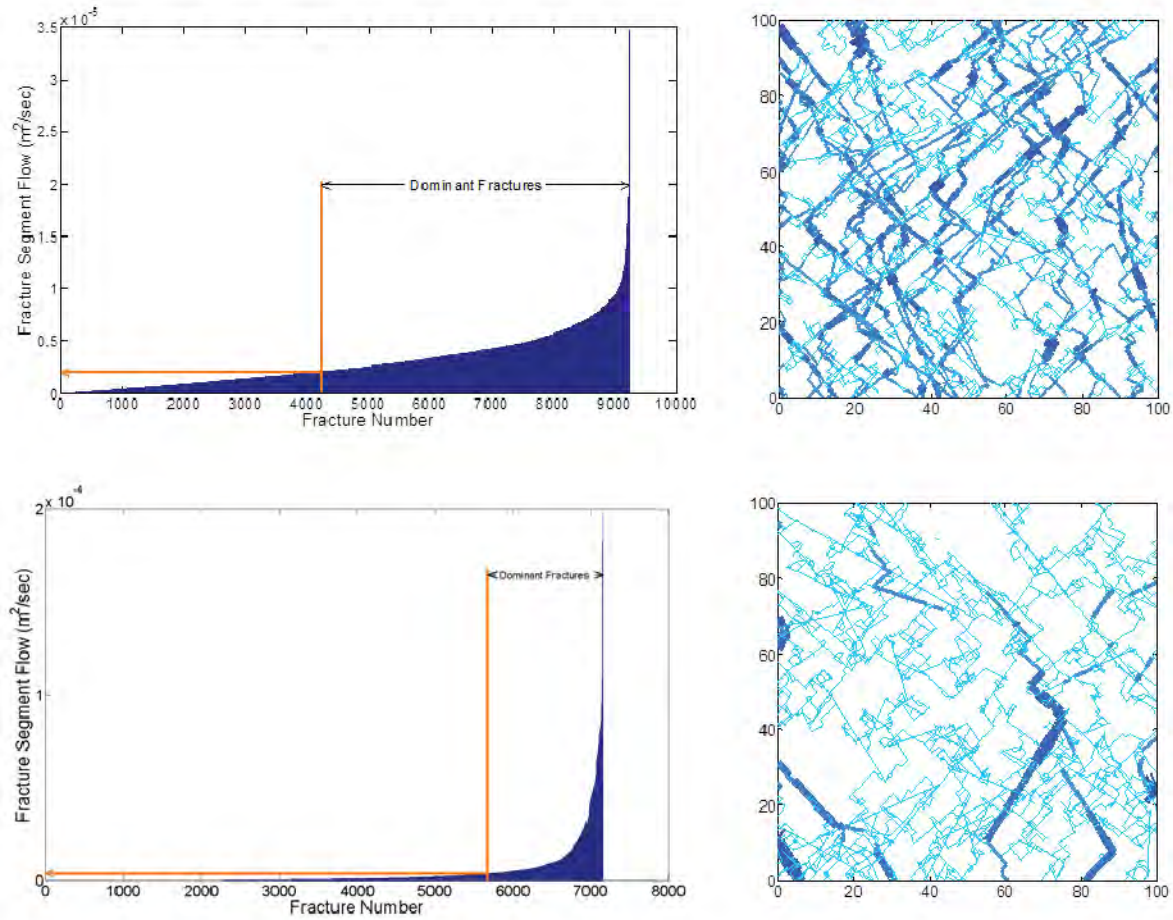


Figure 8.12: Ranked plots of flow through individual fracture segments of the fracture backbone along with the identification of dominant fractures (left). Flow through individual fracture segments of the hydraulic backbone with line thickness proportional to segment flow (right). The plots are made from networks with identical geometric network properties ($\alpha=2.0$, $\theta=\pm 45^\circ$, $K=20$, $\sigma_D=1.5 \text{ m/m}^2$) with $\log(\sigma_K) = 0$ (top) and $\log(\sigma_K) = 1$ (bottom). Note that networks with homogeneous distributions of K ($\log(\sigma_K) = 0$) contain many dominant fractures (top), whereas networks with heterogeneous distributions of K ($\log(\sigma_K) = 1$) exhibit focused flow through a small subset of fractures of the hydraulic backbone (bottom).

It is important to understand that fracture networks are highly heterogeneous and that standard deviations of transmissivity on the order of $\log(\sigma_T) = 1$ are typical for natural networks. Note that $\log(\sigma_K) = 1$ represents fracture networks with transmissivity values encompassing 5-6 orders of magnitude! Consistent with field observations, the discrete fracture network simulations show that a subset of all the fractures belong to the hydraulic backbone and conduct flow, and only a very small subset of the hydraulic backbone fractures conduct the majority of flow across a network for $\log(\sigma_K) = 1$. This prevalent feature of fracture networks emphasizes the need for the directional fracture intersection analyses described below.

8.3.2 Fracture Intersection Analysis

Intersection of horizontal hillslope drainage networks is determined by projecting domain spanning scanlines across the networks and recording intersections of all three fracture types: all fractures, backbone fractures and dominant fractures. The number of intersections is then normalized by the scanline length to provide an average distance of intersection for each the three fracture types. Fracture networks are spatially discontinuous features with non-random orientations, and the scanline orientation is rotated from 0 to 360 degrees in 5 degree increments to fully capture the directional dependence on intersection distances. This process is repeated for 100 DFN flow realizations and ensemble (the average of all realizations) trends are computed. This analysis assumes that these scanlines represent the sampling of a fractured medium with a horizontal drain of varying orientation. Distances of scanline intersection with dominant fractures represent horizontal drain lengths necessary for successful drainage of a rock mass. These distances may or may not have directionally dependence as illustrated in the following examples.

A systematic analysis using both synthetic and site-specific fracture data is conducted to understand the influence on fracture orientation, length, density and transmissivity on ensemble intersection trends. Differences in intersection trends between single fracture network realizations and ensemble-averaged trends are both qualitatively and quantitatively defined. All fractured rock masses are unique and will need to undergo this analysis to enhance the probability of success in lowering pore pressures; however, the following sections provide detailed information on how fracture network properties influence hillslope drainage network design.

8.3.2.1 Influence of Fracture Length and Transmissivity

Discrete fracture networks are generated according to synthetic parameter sets to allow for systematic study of specific fracture attributes on intersection distances. Since network connectivity and global flow are highly dependent on distributions of fracture length and transmissivity, the influence of these parameters on intersection distances is explored first. Six sets of discrete fracture networks consisting of $a=1$, $a=2$ and $a=3$, with standard deviation of transmissivity described by $\log(\sigma_T)=0$ (homogeneous) and $\log(\sigma_T)=1$ (heterogeneous). These networks all consist of two fracture sets with orientations of $\pm 45^\circ$ and deviations in orientation described by $K \leq 20$.

Radial plots of distance r as a function of angle describe the distance of intersection for all fractures, backbone fractures and dominant fractures (Figure 8.13). The top half of Figure 8.13 from left to right describe the influence of these fracture trends with increasing values of α given $\log(\sigma_k)=0$. For the most part, trends of intersection for all fracture types are similar in distance, with the exception that the intersection distance of the all fracture and hydraulic backbone groups are very similar for the $\alpha=1$ networks. This indicates that even though the $\alpha=1$ networks have a larger fracture spacing in these examples, many of these fractures are connected to the hydraulic backbone, because the $\alpha=1$ length distributions favors longer, domain-spanning fractures.

The effect of deviations in transmissivity about the mean value is readily observed during visual inspection of the top ($\log(\sigma_k)=0$) and bottom ($\log(\sigma_k)=1$) plots. Heterogeneity in transmissivity greatly extends intersection distances for the dominant fractures from approximately 3-4 meters to 6-10 meters along the Cartesian coordinate axes. This reflects the trends shown in Figure 8.12 where increasing heterogeneity effectively concentrates flow through a smaller subset of fractures increases the spacing of dominant fractures. Larger intersection distances with increases in $\log(\sigma_k)$ indicate that the number of total fractures intersected by a horizontal drain on average needs to effectively double (approximately 3 to 6) to ensure that a dominant fracture is intersected.

As a final comment, the square shape of average intersection distances signifies a directional dependence on hillslope drain length. If the radial distance to dominant fractures were equal, then the overall shape of these intersection trends would be described by a circle of constant radius as shown later. Rather, the square shape indicates that the distance to intersection with all types ranges from a minimum along the Cartesian coordinate axes to a factor of $\sqrt{2}$ at the diagonals. This pattern reflects the mean fracture set orientations of $\pm 45^\circ$, where the minimum distance represents the angles of maximum intersection by the two fracture sets ($0^\circ, 90^\circ, 180^\circ, 270^\circ$), and the maximum distance represents the diagonals, where intersection of the scanline is reliant on only one fracture set as the other fracture set is parallel to the scanline.

8.3.2.2 Influence of Fracture Set Orientation and Density

Previous intersection analyses have focused on networks containing two fracture sets orientated at $\pm 45^\circ$. In this section, networks with $\alpha=2$ and $\sigma_D=1.5 \text{ m/m}^2$ are utilized to study the influence of fracture set orientation and density assigned to individual fracture sets on resultant intersection distances.

Intersection trends with fracture set orientation of $\pm 45^\circ$ are square with the largest distances to fracture intersections coinciding with mean fracture orientation (Figure 8.13). Changing mean fracture set orientation from $\pm 45^\circ$ to $\pm 90^\circ$ effectively rotates the square shape to a diamond where the largest intersection distances of fracture intersection coincide with mean fracture orientation (Figure 8.14 left). Changing values of K used to describe variability in fracture orientation about the mean was observed to only slightly alter overall intersection trends (not shown). The use of a random fracture orientation results in circular intersection trends absent of directional dependence (Figure 8.14 center). In this case,

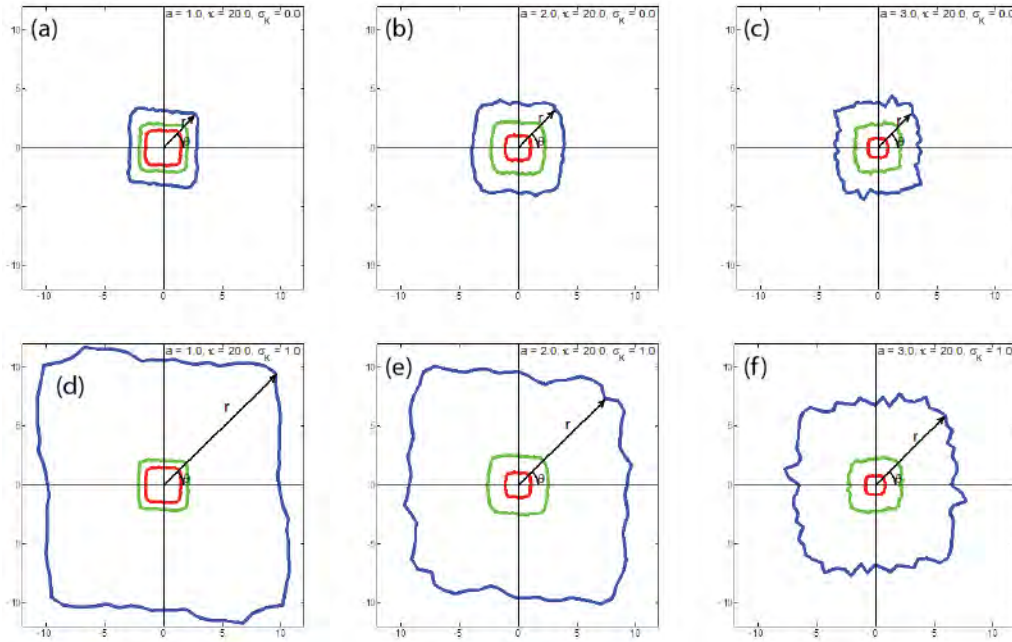


Figure 8.13: Directional distances of scanline intersection with all fractures (red), backbone fractures (green) and dominant fractures (blue) for $a=1$ (a,d), $a=2$ (b,e) and $a=3$ (c,f). All networks contain 2 fracture sets with orientations of $\pm 45^\circ$ with each set having equal density. Plot axes all have the same scale for consistent visual comparison. Values of r denote radial distance of average fracture intersection distance (meters) to each fracture type according to angle θ . Note how intersection distances for all fractures and hydraulic backbone fractures are more or less consistent for values of a , and that intersection distances for dominant fractures are highly dependent on values of $\log(\sigma_K)=0$ (top, a-c) and $\log(\sigma_K)=1$ (bottom, d-f).

the design of a hillslope drainage network would not need to preferentially scale drain length as a function of a . Trends of intersection plots, whether square, circular or diamond in shape, all exhibit symmetry related to fracture orientation. This is specifically caused by the use of two fracture sets with orthogonal orientations (or random in the case of Figure 8.14 center) and assigning an equal number of fractures to each set. These fracture network parameters were intentionally held constant to investigate the influence of fracture length and transmissivity. However, prior probability, defined as the ratio of fractures applied to each fracture set, is commonly unequal for natural fracture networks.

The effect of unequal distribution of fractures among each fracture set is evaluated by assigning 20% and 80% of fractures to the -45° and 45° sets, respectively (Figure 8.14 right). This effectively yields a fracture spacing that is 4 times lower along the 45° fracture set than the -45° fracture set. This type of unequal fracture distribution results in strongly skewed and asymmetric plots with the smallest intersection distances along -45° (due to intersecting the 45° set with higher density), and largest intersection distances along 45° (due to intersecting -45° set with a more sparse density).

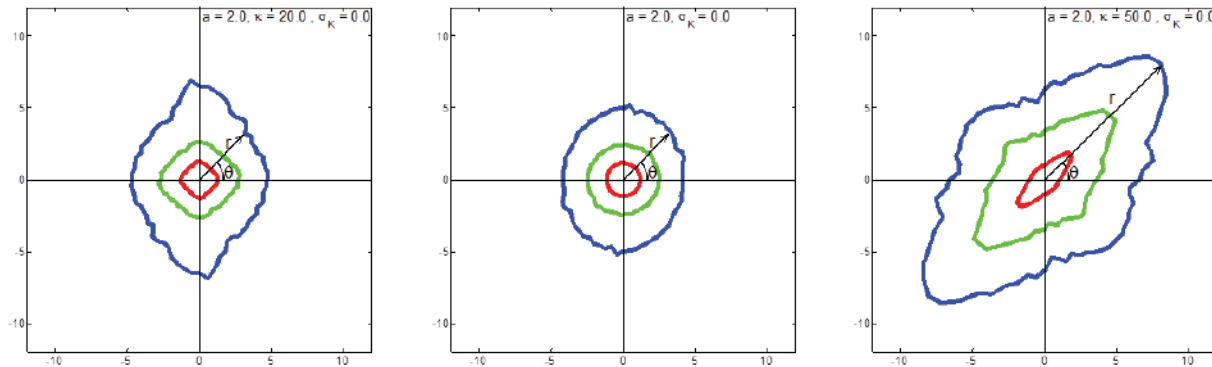


Figure 8.14: Influences of orientation and density on ensemble intersection trends with all fractures (red), backbone fractures (green) and dominant fractures (blue) for networks containing two fracture sets with $a=2$ and $\rho_D=1.5 \text{ m/m}^2$. The previous intersection analyses contained networks with two fracture sets orientated at $\pm 45^\circ$. For these networks, intersection patterns were square and the largest distances to fracture intersections coincide with mean fracture orientation. The use of two fracture sets orientated at $\pm 90^\circ$ (left) effectively rotates the square shape to a diamond where the greatest intersection distances coincide with mean fracture orientation. Use of random fracture orientation (center) results in circular intersection plots absent of directional dependence. Unequal weights assigned to each fracture set can greatly skew directional intersection trends (right), where 20% and 80% of fractures are assigned to the set with orientation -45° and 45° , respectively.

8.3.2.3 Deviations between Individual Realizations and the Ensemble

Thus far, the analysis has focused on ensemble-averaged trends from a total of 100 individual fracture network realizations. Spatial configuration and structure of fracture networks are highly uncertain, and this is reflected in the fracture generation methodology itself. To study deviations of individual realizations with the ensemble trends, individual realizations (light gray) are plotted against the ensemble (dark blue) in Figure 8.15 for networks with $a=1$, $\theta=\pm 45^\circ$, $K=20$, and $\log(\rho_K)=1$. This is the same network shown with ensemble trends in Figure 8.13d.

Variability of intersection distances to dominant fractures for 100 individual realizations about the ensemble is large, with the majority of realizations clustered around the ensemble mean and a small subset of individual realizations showing extreme variability (Figure 8.15a,b). For example, some scanlines for specific network realizations intersect only 1-2 dominant fractures, which generate intersection distances in excess of 40-50 meters. No dominant fractures were intersected along a given angle for a very small subset of realizations.

To restrict variability to a quantitative limit, 95%-confidence intervals are computed from the 100 intersection distance trends (Figure 8.15c,d). The most important confidence interval for the purpose of

hillslope drainage network design is the 95th percentile, as this metric defines the distance necessary to intersect at least one dominant fracture for 95% of the simulations. This is the distance that will be used later on to guide directional length of hillslope drains for the site-specific networks.

It is apparent from examination that the 95th percentile is not fully formed and its shape is inconsistent with the square shape exhibited by the 5th percentile and ensemble mean (Figure 8.15c). The shape of the 95th percentile should be approximately square with a larger length scale than the mean. The 95th percentile trend in Figure 8.15c is a result of undersampling from 100 realizations, and it is anticipated that nearly 10,000 realizations would need to be run before the 95th percentile trend would be stabilized. However, this high number of realizations is not computationally feasible for this analysis.

Instead, a modified 95th percentile is determined by first averaging the distance defined by the 95th percentile over all . The ensemble intersection distance trend is normalized by its average, and the normalized ensemble trend is then multiplied by the 95th percentile average. This process generates the modified 95th percentile curve (red) in Figure 8.15d that is remarkably similar to the trend of a perfect square (dotted pink). This check validates that the constructed 95th percentile trend correctly reproduces the square shape observed in the 5th percentile and ensemble-mean plots.

8.3.2.4 Site-Specific Fracture Networks

The directional-intersection analysis method is applied to two sets of site-specific fracture data in this subsection. The first field site is the Lower Carbonate Aquifer (LCA3) located on the Nevada National Security Site (NNSS), and the second is the Climax Fractured Granite Stock also located on the NNSS. The statistical analysis of fracture data is presented in the case study within Section 8.2.2. To briefly summarize, the LCA3 fracture networks are very dense ($\rho_D=6.9 \text{ m/m}^2$), with two sets of non-orthogonal fractures with strikes of $\phi_1=227^\circ$ and $\phi_2=292^\circ$ and prior probabilities equal to 0.64 and 0.36, respectively. This translates to networks with two non-orthogonal fracture sets separated by 65° and an unequal distribution of fractures between the sets, where one set contains approximately two-thirds of the fractures. These factors result in skewed intersection distance trends (Figure 8.16).

The Climax stock is an intrusive, densely-fractured ($\rho_D=4.3 \text{ m/m}^2$) granite body on the NNSS that was characterized and analyzed for flow and transport properties by Reeves et al. (2010). This rock mass was subjected to multiple fracturing events under various stress-field configurations, which reflects the multiple groups of fracture orientation (Table 8.2). All fracture sets were assigned fracture lengths according to a power-law distribution with exponent $a=1.6$, and transmissivity according to a lognormal distribution with $\log(\tau)=1.0$.

Networks for the Climax stock were generated in 3D according to stochastic methods presented in the manual, and then mapped to horizontal 2D planes. Despite the presence of so many fracture sets, the resultant intersection distances for all fracture types are nearly circular (Figure 8.17).

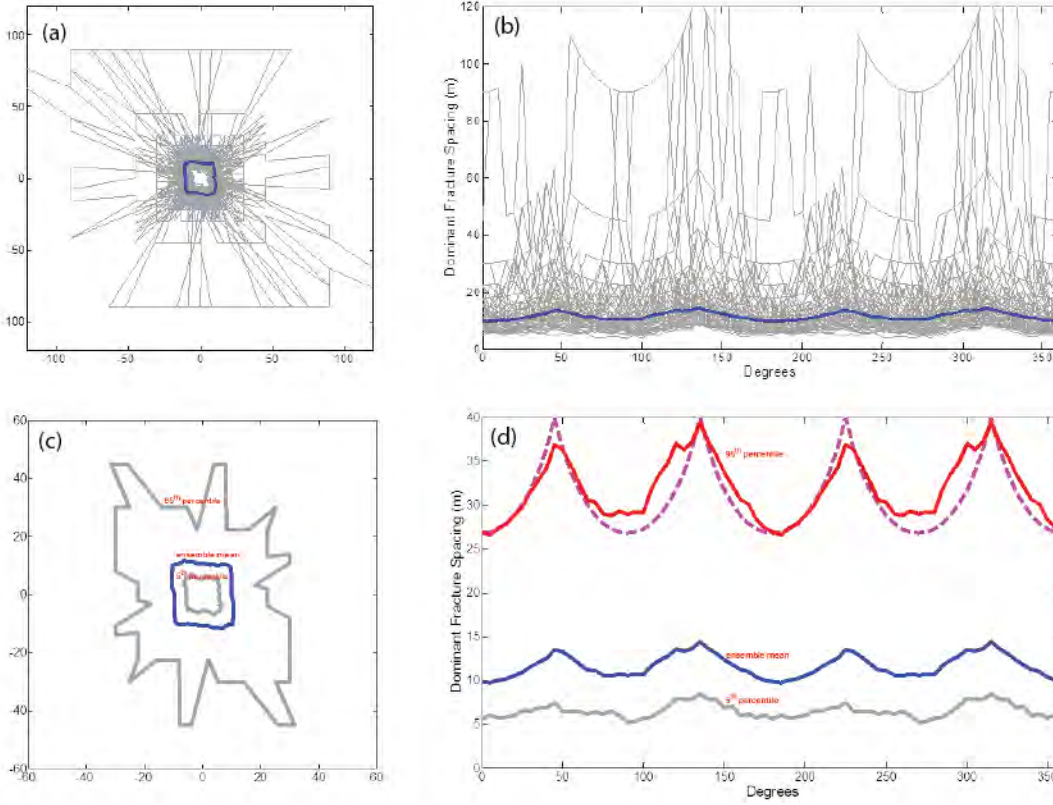


Figure 8.15: Variability of intersection distances to dominant fractures for 100 individual realizations about the ensemble-averaged trends for $\alpha=1$, $K=20$, $\theta=\pm 45^\circ$, and $\log(\kappa)=1$. This is the same network simulations shown in Figure 8.13d. These plots show a high degree of variability about the mean (a,b). To provide quantitative estimates of the uncertainty about the ensemble average, 95% confidence intervals are computed from the individual realizations (bottom). These plots indicate that the 5th percentile and mean trends are well-developed and follow a square trend, yet the 95th percentile is irregular due to incomplete sampling of the fracture network parameter space. The modified 95th percentile shown in (d) was developed by taking the mean of the irregular 95th percentile over all θ , and rescaling the mean trend. This method worked well in preserving the amplitude and frequency of the 95th percentile, as shown by the good match to the theoretical trend for a perfect square (dotted line).

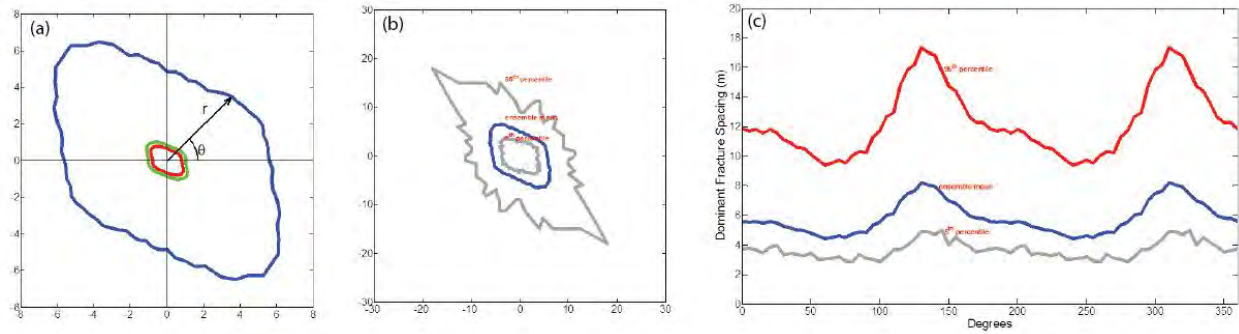


Figure 8.16: Intersection distances for the LCA3 for all fracture types (left) and trends of distance to dominant fractures for ensemble mean with 95% confidence intervals (center, right). Note how the non-orthogonal fracture sets and non-equal number of fractures in each set leads to a skewed trends.

Table 8.2. Fracture properties for each of the six identified fracture sets from Reeves et al. (2010).

	Set 1	Set 2	Set 3	Set 4	Set 5	Set 6
Prior Probability	0.04	0.15	0.12	0.16	0.15	0.38
Mean Strike (°)	125	317	360	321	289	48
Mean Dip (°)	19	25	85	83	82	80
Dispersion (K)	65	37	33	24	23	18

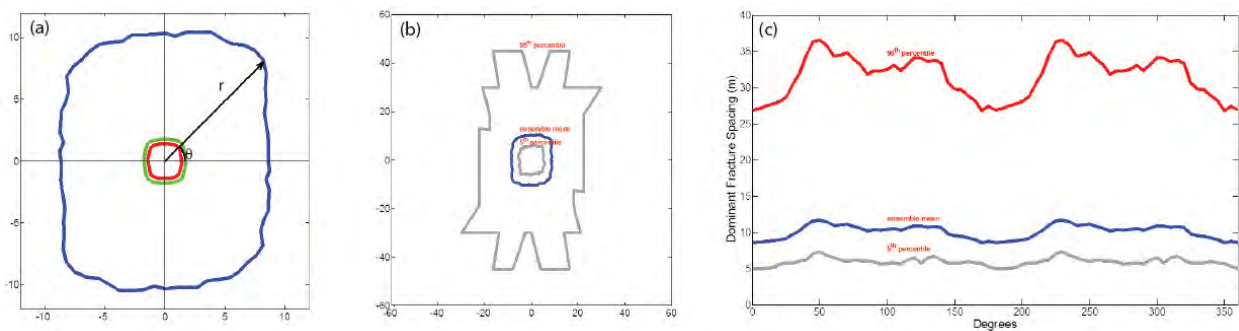


Figure 8.17: Intersection distances for the Climax granite stock for all fracture types (a) and trends of distance to dominant fractures for ensemble mean with 95% confidence intervals (b,c). Note that the presence of multiple fracture sets with of several unique orientations creates intersection trends that are nearly circular.

8.3.3 Summary

Monte Carlo analyses of global flow for networks with $\alpha=1$, $\alpha=2$, and $\alpha=3$ with comparable background densities indicate that total network flow decreases as values of α increase. This trend is further amplified under the influence of heterogeneous distributions of fracture transmissivity. Networks with $\alpha=2$ exhibit the greatest variability in flow about the mean, following by $\alpha=3$ and $\alpha=1$ networks. Surprisingly, the long, domain-spanning fractures in $\alpha=1$ networks result in the least amount of flow variability about the mean. The large degree of flow variability for $\alpha=2$ networks likely reflects variability in backbone structure and connectivity caused by combinations of both short and long fractures.

An analysis of the distance of intersection with three defined fracture types was conducted. The analysis systematically identified the influences of fracture length, transmissivity, orientation and density on directional intersection trends. The overall shape of the intersection distances is highly sensitive to mean fracture orientation, where minimum and maximum distances to two sets of orthogonal fractures coincide with the directions most perpendicular and parallel to the mean fracture set orientations, respectively. All examples, regardless of fracture network attributes, indicate that many fractures need to be intersected on average before a dominant fracture is crossed. The spatially discontinuous nature of fracture networks and large variability in transmissivity indicates that a high degree of variability exists between individual realizations and ensemble averages. For example, the sampling scanline for a very small subset of individual fracture network realizations did not intersect a dominant fracture. To account for this variability, it is suggested that the horizontal drain length is scaled according to the distance defined by the 95th percentile. This concept is illustrated by Figure 8.18, where the length of individual drains is scaled to the directional dependence of the 95th percentile trend for the LCA3 and Climax granite stock fracture statistics.

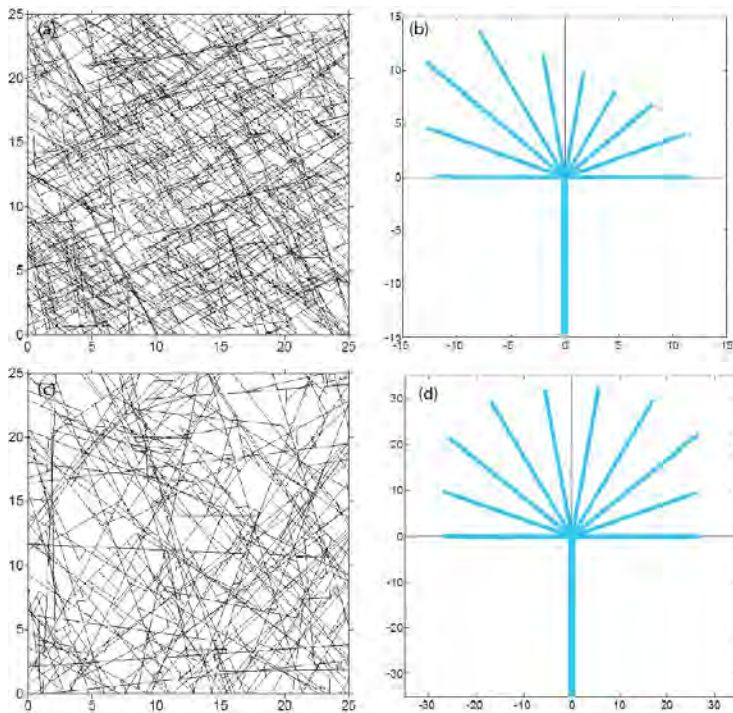


Figure 8.18: Discrete fracture network realization and resultant hillslope drainage network for LCA3 (a,b) and Climax (c,d). Drain length as a function of θ is based on the 95th percentile trend. Note that the drainage network is more symmetric for Climax than for the LCA3, and that hillslope drain lengths are three times larger for the Climax site (~30m) than for LCA3 site (~10 m).

A result of this analysis not yet discussed is the possibility that some sparsely fractured networks may require drain lengths (or drain densities) that are not economically feasible for successful dewatering. As an example, average drain length for the Climax site is approximately 30 meters. This calls into question the practice of installing horizontal hillslope drains prior to a rigorous analysis of fracture network statistics. It is highly recommended that the intersection analysis contained in this section be conducted prior to the design and installation of drainage networks in fractured media.

8.4 References

- Bear, J. 1972. Dynamics of Fluids in Porous Media, Dover, New York.
- Bonnet, E.O.; Bour, O.; Odling, N.; Davy, P.; Main, I.; Cowie, P. and B. Berkowitz, 2001. Scaling of fracture systems in geologic media, *Rev. Geophys.*, Vol. 39, No. 3, 347--383.
- Bour, O. and P. Davy, 1997. Connectivity of random fault networks following a power law fault length distribution, *Water Resour. Res.*, Vol. 33, 1567--1583.
- Bour, O. and P. Davy, 1999. Clustering and size distributions of fault patterns: Theory and measurements, *Geophys. Res. Lett.*, Vol. 26, No. 13, 2001--2004.
- Boyle, G.N. 2003. Summary report on fracture data for dolomite collected at Rainier Mesa, Area 12, Nevada Test Site, unpublished report.
- Darcel, C.; Davy, P.; Bour, O and de J.R. Dreuzy, 2003. Connectivity properties of two-dimensional fracture networks with stochastic fractal correlation, *Water Resour. Res.*, Vol. 39, No. 10, doi:10.1029/2002WR001628.
- de Dreuzy, J.R. and J. Erhel, 2003. Efficient algorithms for the determination of the connected fracture network and the solution to the steady-state flow equation in fracture networks, *Comput. Geosci.*, Vol. 29, No. 1, 107--111.
- de Dreuzy, J.R.; Davy, P. O. and Bour, 2001. Hydraulic properties of two-dimensional random fracture networks following a power-law length distribution: 1. Effective connectivity, *Water Resour. Res.*, Vol. 37, No. 8, 2065--2078.
- Klimczak, C.; Schultz R.A.; Parashar, R. and D.M. Reeves, 2010, Cubic law with correlated aperture to length and implications for network scale fluid flow, *Hydrol. J.*, doi:10.1017/s10040-009-0572-0.
- Kwicklis, E.M.; Thamir, F.; Healy, R.W. and D. Hampson, 1998. Numerical simulations of air- and water-flow experiments in a block of variably saturated, fractured tuff from Yucca Mountain, Nevada, U.S. Geological Survey, Water-Resources Investigations Report 97-4274.
- Lee, C.-H.; Deng, B.-W. and J.-L. Chang, 1985. A continuum approach for estimating permeability in naturally fractured rock, *Eng. Geol.*, Vol. 39, 71--85.

- Long, J.C.S.; Remer; J.S. Wilson, C.R. and P.A. Witherspoon, 1982. Porous media equivalents for networks of discontinuous fractures, *Water Resour. Res.*, Vol. 18, No. 3, 645--658.
- Min, K.-B.; Jing, L. and O. Stephansson, 2004. Determining the equivalent permeability tensor for fractured rock masses using a stochastic REV approach: Method and application to the field data from Sellafield, UK, *Hydrogeol. J.*, Vol. 12, 247--510.
- Munier, R. 2004. Statistical analysis of fracture data adopted for modeling discrete fracture networks -- Version 2., Rep. R. 04-66, Swedish Nuclear Fuel and Waste Management Company SKB, Stockholm, Sweden.
- Oda, M. 1985. Permeability tensor for discontinuous rock masses, *Geotechnique*, Vol. 35, No. 4, 483--495.
- Parashar, R. and D.M. Reeves, 2012 On iterative solution techniques for flow in large two-dimensional discrete fracture networks, *J. Comput. Appl. Math.*, Vol. 236, No. 18, 4712--4724, doi:10.1016/j.cam.2012.02.038
- Priest, S.D. 1993. *Discontinuity Analysis of Rock Engineering*, Chapman and Hall, London.
- Reeves, D.M.; Benson, D.A. and M.M. Meerschaert, 2008a. Transport of conservative solutes in simulated fracture networks: 1. Synthetic data generation, *Water Resour. Res.*, Vol. 44, No. W05401, doi:10.1029/2007WR006069.
- Reeves, D.M.; Benson, D.A.; Meerschaert, M.M. and H.-P. Scheffler, 2008b. Transport of conservative solutions in simulated fracture networks: 2. Ensemble solute transport and the correspondence to operator-stable limit distributions, *Water Resour. Res.*, Vol. 44, No. W05410, doi:10.1029/2008WR006858.
- Reeves, D.M.; Benson, D.A. and M.M. Meerschaert, 2008c. Influence of fracture statistics on advective transport and implications for geologic repositories, *Water Resour. Res.*, Vol 44, No. o8405, doi:10.1029/2007WR006092.
- Reeves, D.M.; Pohlmann, K.; Pohll, G.; Ye, M. and J. Chapman, 2010. Incorporation of conceptual and parametric uncertainty into radionuclide flux estimates from a fractured granite rock mass, *Stoch. Environ. Res. Risk Assess.*, doi:10.1007/s00477-010-0385-0.
- Reeves, D.M.; Parashar, P.; and Y. Zhang, 2012. Hydrogeologic characterization of fractured rock masses intended for disposal of radioactive waste, In: *Radioactive Waste*, Ed. R.A. Rahman, InTech Publishing, ISBN 978-953-0551-0.
- Renshaw, C.E. 1999. Connectivity of joint networks with power law length distributions, *Water Resour. Res.*, Vol. 35, No. 9, 2661--2670.
- Smith, P.A. and F.W. Schwartz, 1984. An analysis of the influence of fracture geometry on mass transport in fractured media, *Water Resour. Res.*, Vol. 20, No. 9, 335--348.

- Snow, D.T. 1965. A parallel plate model of fractured permeability media, Ph.D. Dissertation, University of California, Berkeley.
- Snow, D.T. 1969. Anisotropic permeability of fractured media, *Water Resour. Res.*, Vol. 5, No. 6, 1273--1289.
- SNJV. 2006a. Analysis of ER-12-3 FY2005 Hydrologic Testing, Nevada Test Site, Nye County, Nevada, U.S. Department of Energy, S-N/99205--080.
- SNJV. 2006b. Analysis of FY 2005/2006 Hydrologic Testing and Sampling Results for Well ER-12-4, Nevada Test Site, Nye County, Nevada, U.S. Department of Energy, S-N/99205-083.
- Zhang, X.; Sanderson, D.J.; Harkness, R.M. and N.C. Last, 1996. Evaluation of the 2-D permeability tensor for fractured rock masses, *Int. J. Rock Mech. Min. Sci. and Geomech. Abstr.*, Vol. 33, No. 1, 17--37.
- Zhang, Y.; Baeumer, B. and D.M. Reeves, 2010. A tempered multiscaling stable model to simulate transport in regional-scale fractured media, *Geophys. Res. Lett.*, Vol. 37, No. L11405, doi:10.1029/210GL043609.

Chapter 9

Summary

9.1 Concluding Remarks

Every drainage problem is unique, in which experience and expert opinion cannot be superseded. However, a framework for drain design can aid practitioners with quantitative analysis to reduce ad-hoc decision making. The proposed methodology requires a conceptual model of the site for proper assessment of data collection, water balance and site complexity. A description of important parameters for hydrologic and geotechnical assessment is provided along with a variety of techniques to estimate these parameters, as well as the spatial and temporal scale of collection.

An iterative approach is given for determining the minimum drain construction to lower water levels enough to keep the factor of safety (FOS) greater than 1.2 (refer to Figure 7.1). Simple systems may only require an analytic approach to computing maximum water levels. Techniques are supplied for steady state conditions given a flat surface (Hooghoudt, 1940), a sloped surface less than 10° (U.S. Department of the Interior, 1978) and a discussion is provided on the influence of recharge and hydraulic conductivity on drainage design (Lesaffre, 1987). Analytic equations for transient solutions for a flat surface (U.S. Department of the Interior, 1978) are given for different drain depths with respect to the impermeable barrier as well as for sloping surface with a declining water table over time (Skukla et al., 1999). Past research has found that flow to ditches; water table elevation and the rate of water table decline were independent of slope for slopes less than 15-30% (Luthin and Guitjens, 1967; Fipps and Skaggs, 1989). For these relatively shallower slopes, flat-surfaced assumptions can be maintained with little error. In all cases drainage design based on analytic (and graphical) approaches is focused only on drain spacing or the location of the first interceptor drain in a sloped system. However, analytic results can be used to assess impact of system response to lowering the overall water table prior to a rapid rise caused by a large storm event. This emphasis is concordant with Rahardjo et al. (2003) who found that horizontal drain placement should stress the overall lowering of the water table, not the direct capture of infiltration. Therefore, analysis does not focus on emergency drain placement. Analytic equations can also guide practitioners on the rapidity of water table drawdown given a specified drain spacing and depth, and provide a first-cut on drain efficiency.

Irregular drain networks, heterogeneous or anisotropic aquifer conditions, complex slope geometry as well as fractured rock network may mandate a numeric modeling approach. To create an effective and verifiable numeric model necessitates a full understanding of the assumptions applied, can require significant amounts of data, and be expensive to build. However, numeric models can more fully incorporate data into a unified conceptual rendering of the site so that personnel can make more informed decisions on managing the system. An idealized cross section (chapter 7.2) shows that shallow drains are relatively ineffective at lowering water levels, while drains are most effective when placed at

the lowest elevation possible. If installed a significant distance into the hillside at the lowest possible elevation, drains will capture the majority of groundwater and have the largest effect on lowering the water table. Drains located in the upper region of a slope are found to have no real significance if additional deeper drains are in the lower part of a slope. The water table will eventually be reduced to the lowest drain level and any drains above the lowest-most drain will no longer be effective. The only exception to this rule might be for site conditions that have the ability to setup significant perched water table conditions.

To aid the practitioner, idealized sites for translational (chapter 7.4.3) and rotational (chapter 7.4.4) failure are modeled over a range of hydraulic properties. Water level sensitivity to hydraulic parameters, drain efficiency, storm design and recharge characteristics are also presented.

For translational failure, examples are given for model development given no data collection (i.e. no model calibration), and for a situation where data has been collected (calibration procedure provided). Stability analysis finds that thin geologic sections susceptible to slope failure are most sensitive to increased water levels in the upper regions of the slope, and less sensitive to groundwater seepage in the toe region. Slopes comprised of silt, sandy silt, clayey sand or till with low storage cannot be stabilized with horizontal drains alone. Slopes containing fine material, but higher storage potential can be stabilized with long drains extending to the upper reaches of the slope. While groundwater seepage in the toe region is not important to FOS calculations, seepage can be mitigated by increasing drain density and adding short length toe drains. Modeling results find that FOS is sensitive to anisotropy, with fine soils not stabilized for $K_x = 10K_z$ (i.e. $VKA = 10$). For silty and fine sands ($K_x = 1$ ft/d) with low storage and isotropic or mildly anisotropic ($VKA = 2$) conditions, short length drains in the toe region of medium spacing are sufficient to raise $FOS > 1.2$. Drains should be lengthened to the upper slopes and drain density increased for medium anisotropy (i.e. $VKA = 5$), and no drain array will work for large anisotropy ($VK=10$). Silty and fine sands with higher storage will not require any horizontal drains. Likewise, well sorted sands and glacial outwash should not need horizontal drains to improve stability. Increasing anisotropy in both cases, however, may necessitate drains reaching to the upper slope.

Rotational failure analysis considered for two scenarios: failure along the entire slope and failure in the toe region only. Groundwater seepage prevails in the toe region during large storm events with simple fan arrays placed in the toe region capable of lowering water levels enough to mitigate seepage. Whole surface failure for the conditions modeled is unlikely, but rotational failure in the toe region is very high for lower conductive materials such as silt, sandy silt, clayey sand or till. It may not be possible to stabilize toe-slides for fine materials with low storage since no drain configuration tested was able to achieve $FOS > 1.2$. However, increasing drain density in the toe region comes close for anisotropy ≤ 5 , with the potential for mitigated risk decreasing substantially for $VKA \geq 10$. For higher storage conditions in low conducting soils and isotropic conditions a low density arrangement of toe-drains will suffice. Density of drains should be increased for more anisotropic soils. More conductive soils only require low density toe-drains to mitigate failure.

Chapter 8 on flow in fractured rock and network design represents a special problem for slope stability. Fractured rock typically has little or negligible porosity and permeability in the rock matrix itself. Instead, connected networks of discontinuous fractures impart secondary porosity and permeability. The primary focus of the discussion on fractured systems is two-fold. First, methods are presented to determine the equivalent hydraulic conductivity of fractured rock. These equivalent hydraulic conductivity values can be directly input into the hydrologic modeling framework presented in Chapter 7. Secondly, the stochastic approach, and associated implications of drainage network systems in fractured rocks are presented with case studies located on the Nevada National Security Site. It is highly recommended that drain installation only be done following a rigorous analysis of fracture network statistics and intersection analysis to avoid costly and perhaps not economically feasible, solutions to drainage design.

The purpose of the manual is to provide a single comprehensive reference for geotechnical engineers and hydrogeologist on designing horizontal drainage systems to improve slope stability. Guidelines are provided for translational and rotational failure and consider fractured systems. Basics of hydrogeologic and geotechnical terminology, site characterization and conceptualization, groundwater modeling techniques and template projects help to guide the user with respect to identifying important parameters to drainage design. Type of failure, along with hydraulic properties of hydraulic conductivity, specific yield and anisotropy are found important to effectiveness of drain design. It is hoped that with greater understanding of drainage systems in sloped surfaces, that results become more predictable and performance of drainage networks is improved while simultaneously lowering expenditures for slope stabilization.

Appendix A

Definition of Symbols Used

Geotechnical Symbols

Units Definition: L = Length; M = Mass; T = Time; F = Force (ML/T²)

Symbol	units	definition
	degress	inclination of the base to the horizontal
b	L	width of each slice in FOS calculation
	degress	inclination of slope from the horizontal
c'	F/L ²	cohesion
Δ	degress	inclination angle for normal force acting on side of slice
E_1, E_2	F	normal force acting on the sides
δ	degress	friction angle
FOS	dimensionless	factor of safety
γ	F/L ³	unit weight of dry soil
γ_{sat}	F/L ³	unit weight of saturated soil
γ_w	F/L ³	unit weight of water
h	L	height of slice measured on the center line
l	L	length of base of slice
mz	L	depth of water table above failure plane
N	F	normal force acting on base
N'	F	effective normal force
r	L	radius of circular arc defining failure surface
σ'	F/L ²	effective normal stress
T	F	shear force
τ	F/L ²	shear strength that must be mobilized to maintain a condition of limiting equilibrium
τ_f	F/L ²	available shear strength
τ_m	F/L ²	mobilized shear strength to maintain equilibrium
u	F/L ²	pore water pressure
W	F	weight of soil slice
x_1, x_2	F	shear force on the sides
z	L	depth of failure plane for translational slip

Hydrologic Symbols

Units Definition: L = Length; M = Mass; T = Time; F = Force (ML/T²)

Symbol	units	definition
A	L^2	cross sectional area perpendicular to flow
a	dimensionless	power coefficient for fracture length describing tail of distribution
A_c	L^2	cross sectional area of sample in permeameter
A_t	L^2	inside area of tube in falling head permeameter
	$1/M/LT^2$	compressibility of the aquifer's skeleton
$*$	radians	angle of the transect relative to the mean fracture orientation
B	L	thickness of geologic unit
B'	L	thickness of envelope material around a drain
b	L	thickness of individual geologic layer given multiple layers
	$1/M/LT^2$	compressibility of water
C	dimensionless	dimensionless shape factor
C'	dimensionless	constant based on l_{min} and a
C^*	dimensionless	variable that relates to how the stress singularity at the fault tip is removed
C_d	L^2/T	drain conductance
C_b	L^2/T	general head boundary conductance
C_u	dimensionless	uniformity coefficient
CN	dimensionless	curve number
D	L	true fracture spacing
D'	L	apparent fracture spacing
D^{\wedge}	L	depth of impermeable layer below drain
D^*	L	depth of impermeable layer below water table surface
D_{max}	L	maximum shearing displacement located at the fault midpoint
d	L	pore size diameter
d_d	L	equivalent depth accounts for convergent flow toward drain
d_{10}	L	grain size that is 10% finer by weight
d_{60}	L	grain size that is 60% finer by weight
E	F/L^2	Young's modulus
F_a	L	depth of precipitation that infiltrates
$f(t)$	L/T	infiltration rate as a function of time

f_c	L	constant infiltration rate
f_0	L	initial infiltration rate
$f(x)$	dimensionless	Fisher distribution for fracture orientation
g	L/T^2	gravitational acceleration
and	L	lower and upper fracture length cutoff values
h	L	head
h_b	L	user defined general head boundary
h_d	L	user defined drain elevation
h_o	L	observed head
h_p	L	model predicted head
h_0	L	initial water level in permeameter test
H_a	L	average height of water table above drains
H_m	L	height of water table midway between drains
l_a	L	amount of rainfall that occurs before runoff
l_m	L	minimum depth to water table between drains
l_{min}	L	power length cutoff
K	L/T	hydraulic conductivity in isotropic medium ($K_x = K_y = K_z$)
K_c	$F(L^{0.5}/L^2)$	fracture toughness
K_d	L/T	hydraulic conductivity of drain and its envelop material
K_i	L^2	intrinsic permeability
K_x	L/T	horizontal hydraulic conductivity in the x-direction
K_y	L/T	horizontal hydraulic conductivity in the y-direction
K_z	L/T	horizontal hydraulic conductivity in the z-direction
K_1	L/T	horizontal hydraulic conductivity above drain
K_2	L/T	horizontal hydraulic conductivity below drain
k	$1/T$	decay constant for infiltration rate
	dimensionless	dispersion coefficient
L	L	length in the direction of flow
L_e	L	Length of screened portion of well
L_d	L	drain spacing for flat land surface
L_d^*	L	drain spacing for sloped land surface
L_f	L	horizontal fault trace length
M	M	mass of the control volume
	$F T/L^2$	dynamic viscosity
N	dimensionless	ratio of geologic offset to short-term slip

n	dimensionless	porosity
p^*	M/LT^2	pressure
P	L	depth of precipitation
P_e	L	depth of excess precipitation for runoff
Q	L^3/T	flow rate
Q_b	L^3/T	general head boundary flow rate
Q_d	L^3/T	drain flow rate
q_x, q_y, q_z	L/T	flow per unit cross sectional area in the x, y and z directions
R	L/T	recharge rate
R_e	L	effective radial distance of at which head is dissipated in a slug test
r	L	radial distance from pumping well to a monitoring well
r_c	L	radius of well in slug test
r_d	L	radius of drain and envelope material around the drain
r_w	L	effective radius of well and gravel pack around the well
ρ_w	M/L^3	water density
$rmse$	L	root mean squared error
S	dimensionless	storativity
S'	L	maximum potential storage in basin
S^*	L/L	slope of land surface
S_b	L/L	slope of impermeable layer
S_s	$1/L$	specific storage
S_y	dimensionless	specific yield
s	L	drawdown, also shown as Δh
τ_d	F/L^2	shear driving stress
τ_y	$?$	yield strength of the rock at the fault tip
$1D_r \quad 2D$	$1/L$	ratio of total number of fractures to transect length
T	L^2/T	transmissivity
t	T	time
t_0	T	initial time
v	L/T	velocity of water
V_T	L^3	total volume of soil
V_v	L^3	volume of voids in soil
VKA	dimensionless	ratio of K_x to K_z
	$?$	Poisson's ratio of the rock mass

w	L	width of geologic strata
$W(u)$	dimensionless	well integral
z	L	elevation of water level

Appendix B

MODFLOW Tutorial Using Groundwater Vistas Graphical User Interface

A step-by-step guide to create a model describing translational failure is provided as a tutorial for a beginning groundwater modeler. The site used as an example is described in chapter 7 (section 7.5.3) with reiteration here for ease of manual use. Groundwater Vistas (GWV) is the graphical user interface used to create input and output files necessary for MODFLOW implementation, as well as the display and analysis of modeled water levels. Groundwater modeling begins with a conceptual model, includes setting up the model domain, finite difference grid, adding boundary conditions and stresses and integrating with geotechnical analysis. The tutorial on what menus to access for importing/exporting data, visualization and analysis are presented in detail with screen captures, and formatting requirements for GWV upload and download. Modeling is done with and without calibration, and includes an introduction to sensitivity analysis as well as auto-calibration.

B-1 Site Description

Translational failure (site D) is modeled using the topography shown in Figure B.1 . Slopes are relatively constant from the peak to the base of the slope at approximately 28% (16°). The system contains two geologic layers. Layer 2 is a permeable layer that is 20 ft thick and overlies layer 1 overlying a low permeability unit. The lower unit is assumed impermeable.

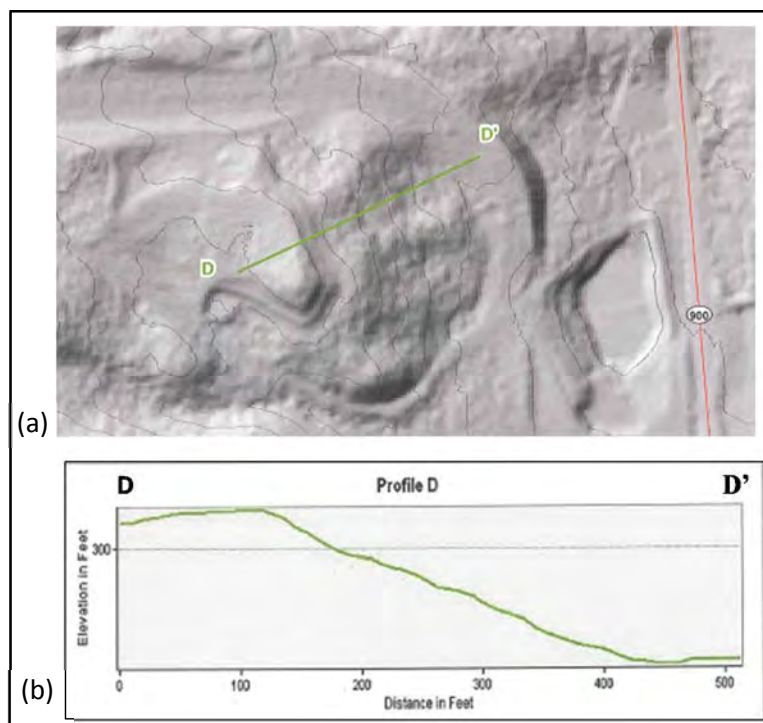
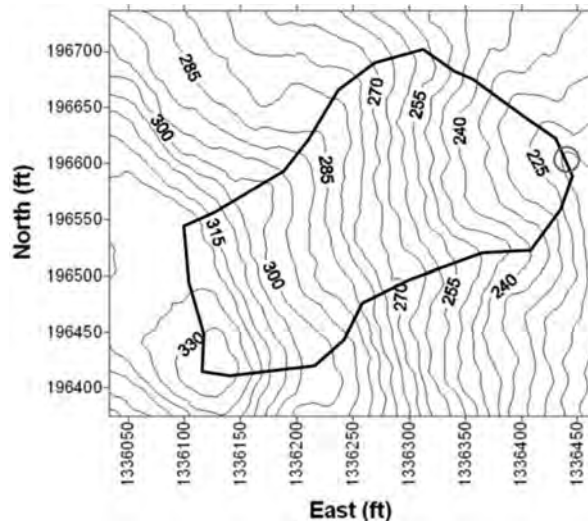


Figure B.1 Site D topography for translational failure (a) hill shade, (b) cross sectional profile of land surface from D-D'.

B-2 Model Domain and Conceptual Model

The model domain encompasses the entire watershed to eliminate the need to designate water flux across boundary conditions (Figure B.2). Water entering the system is assumed to only occur from precipitation, with all water flowing toward the watershed outlet at the lowest elevation. Figure B.3 shows the MODFLOW grid placement in plan-view and a cross section of the model along d-d'. Cell size is 5 ft by 5 ft and a single homogenous unit is modeled at 20 ft thick. The model grid is orientated 27° so that modeled rows run parallel to the slope



(

Figure B.2 Site topographic map showing land surface elevation at 5 ft intervals. Gray circle represents watershed outlet, while thick black line delineates the watershed.

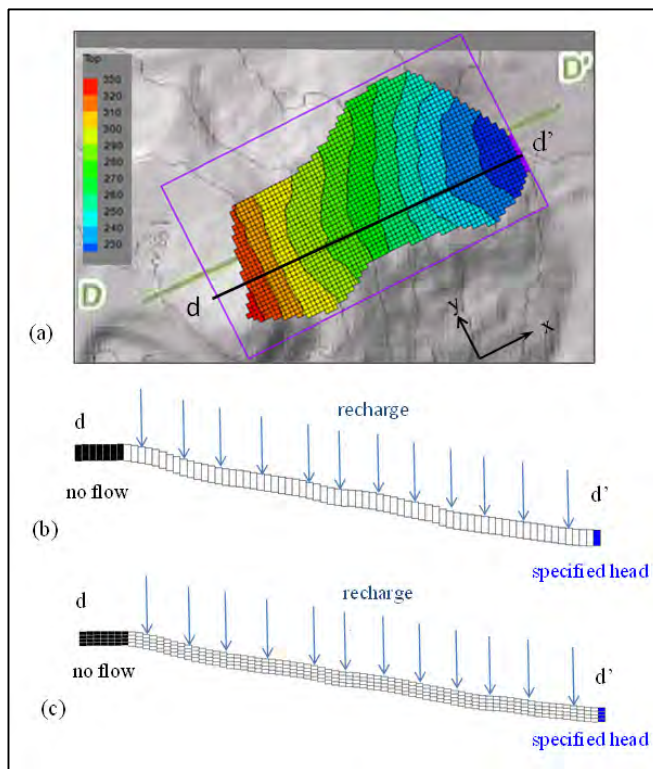


Figure B.3: Model grid for translational failure site. (a) plan view showing modeled grid (purple box), active cells in color scale of assigned land surface elevations, rotated x-y axis and cross section d-d'. cell dimension is 5 ft by 5 ft. (b) Cross section d-d' depicting single layer model (thickness of layer is 20 ft) as well as no flow cells and specified head cells. (c) Four-layer model used to test anisotropy (VKA) on drain design where $VKA = K_x/K_z$. Recharge is applied evenly across modeled domain.

B-3 Steady State Model (Isotropic Conditions)

To build a steady state model one will need to define: grid location and cell size, model domain, land surface elevations, bottom elevations, initial heads, hydraulic conductivity, as well as boundary conditions (e.g. recharge, specified heads).

B-3.1 Model Grid and Domain

Open GWV.

To begin a new model, press File->New

A menu will pop up to initialize the model grid. Fill out the boxes as shown below. The grid is rotated 27 degrees so that model rows are parallel to flow. Grid spacing is set at 5 feet in the x and y directions and the origin of the grid is established to line up with the coordinate system of LIDAR elevation data collected at the site: X = 1336130, Y = 196375.

Horizontal Model Grid	
Number of Rows	43
Number of Columns	75
Uniform X Spacing	5
Uniform Y Spacing	5

Vertical Model Grid	
Number of Layers	1
Model Bottom Elevation	0
Model Top Elevation	100
<input type="checkbox"/> Layers are flat	Layer Elevations

Default Parameter Values							
K	Kx	100	Ky	100	Kz	100	No. Zones
Storage	S	0.01	Sy	0.01	Porosity	0.01	1
Leakance		0.01					1
Recharge	Rate	0	Conc.	0			1
ET	Rate	0	Extinction	0			10
Dispersivity	Long.	0	Transverse	0	Vertical	0	10
Sorption	Kd	0	Density	157			10
Initial Conc.		0					10

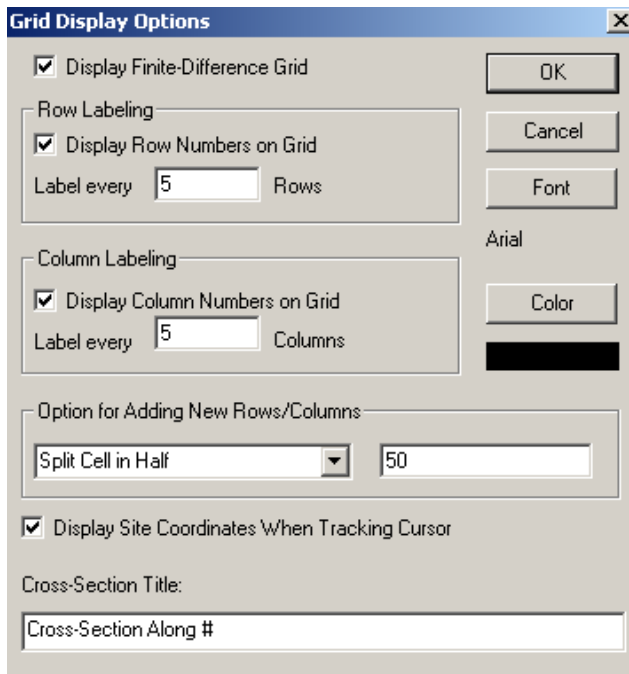
Stress Periods			
Maximum Stress Periods	1	Start with Stress Period	1
Read Every	1	Stress Periods	

World Coordinates of Model Origin			
X	1336130	Y	196375
Rotation	27		

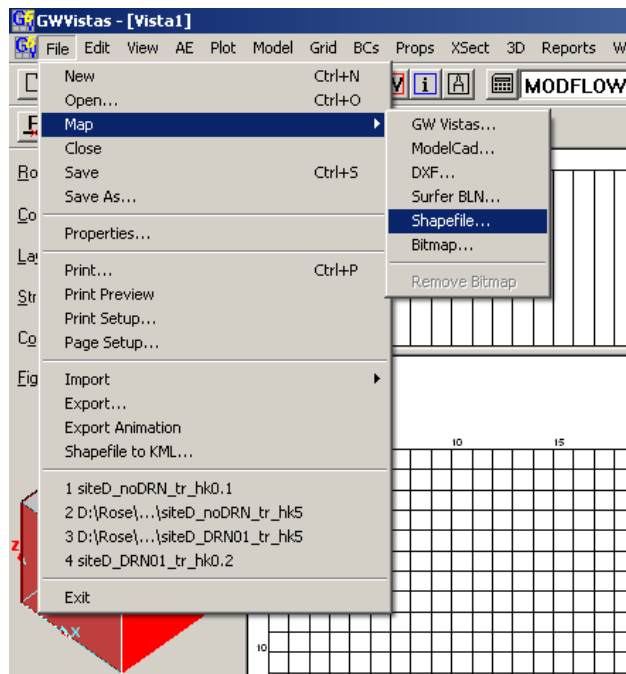
MODFLOW... EVS... TMR... OK Cancel

Go to Grid->Options...

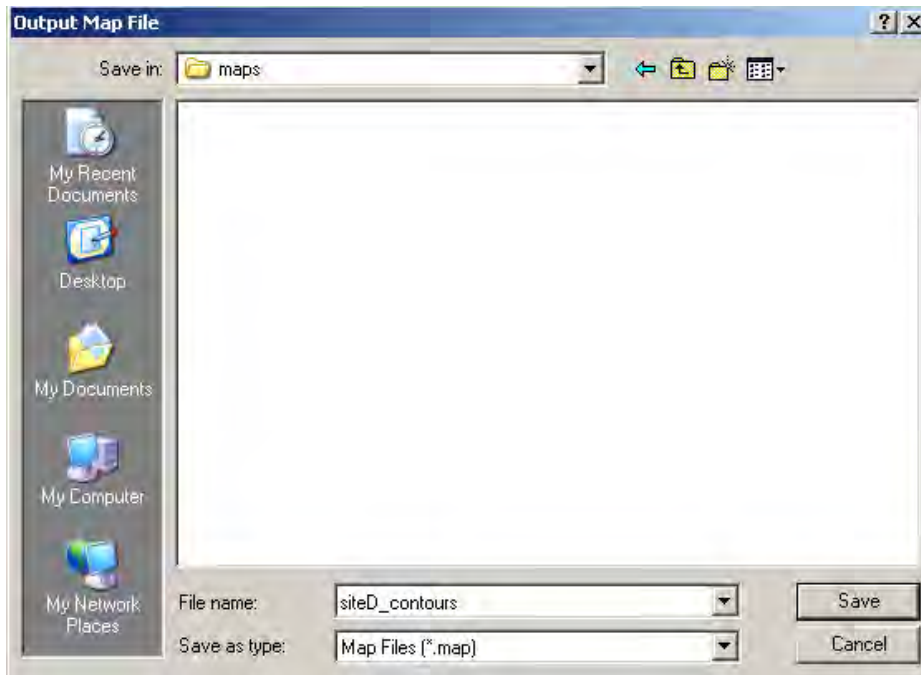
In the Grid Display Options dialogue check the box 'display Site Coordinates When Tracking Cursor.'






To import shapefiles defining regional contours of the land surface at the site, go to File->Map->Shapefile. Navigate to import_files\shapefiles\siteD_contours.shp. Hit the 'open' key.



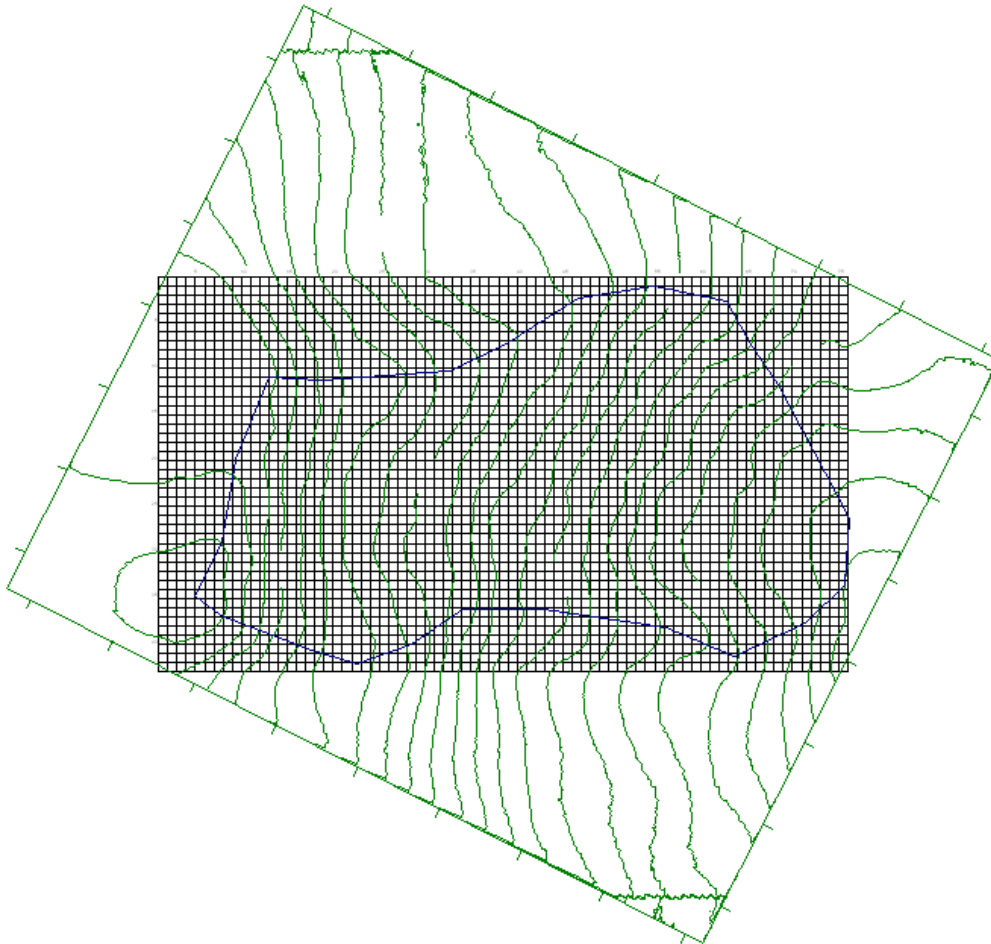
GWV will then ask you to provide a location for the corresponding map file it will produce from the shaptefile. Navigate to to import_files\maps\ and call the file siteD_contours.map and hit 'Save'. Save the color of the contour shapefile to any color you want using the drop-down menu. For this example, green is chosen. Press 'OK'.



If necessary, you may need to hit 'zoom to full grid' button  to scale the grid back to the full screen. Or you can hit  to zoom in or  to zoom out. To change the thickness of the shapefile lines, you can go to Plot->Map Overlays...and use the drop-down to thicken the lines. Lines are thickened to 0.75. This shapefile is imported to provide you some reference of the grid's location in the landscape.

To import the model domain shapefile (built using land surface contours to isolate contributing watershed area (refer to Figure B.2), repeat the same procedure as for contours. Navigate to import_files\shapefiles\siteD_domain_polys.shp and create a map file under import_files\maps\siteD_domain.map. Choose the color 'blue' and thicken the lines to 0.75.

The shapefiles and grid should look as follows.

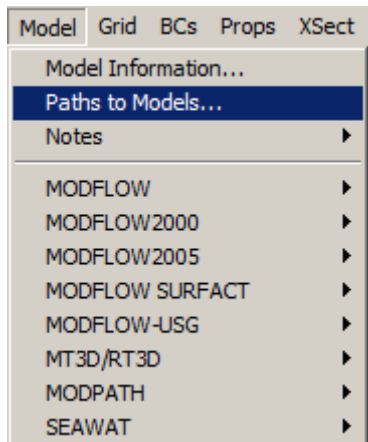


Save your GWV file to sited\noCALIB\SS\ and call the file SS_noDRN.GWV

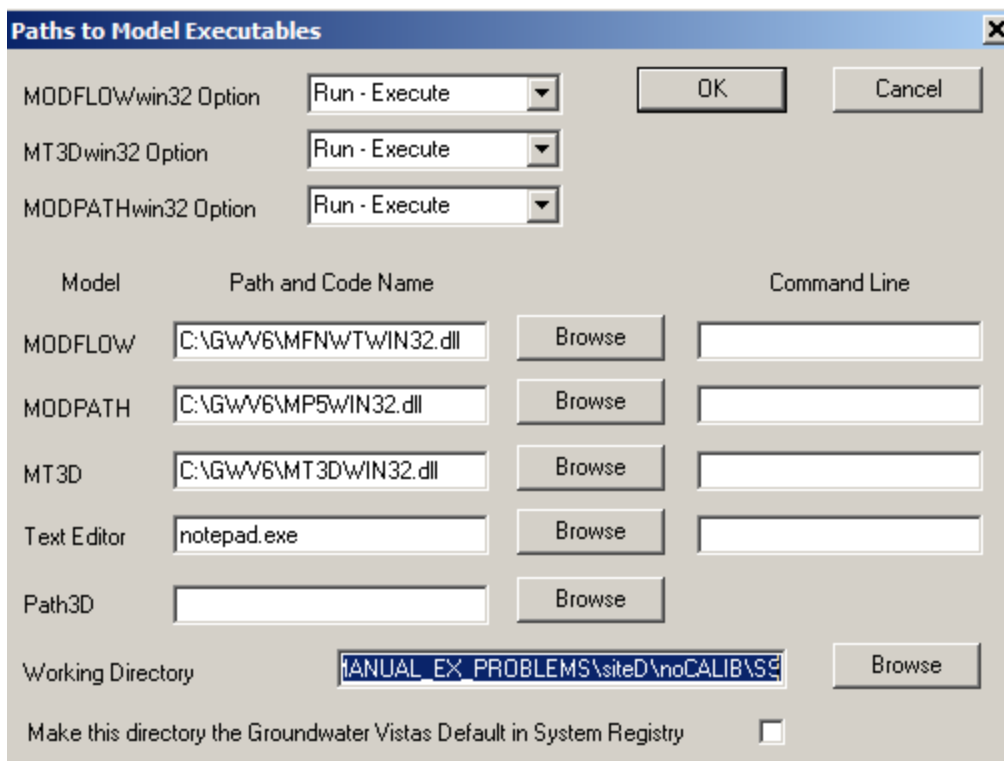
A prompt will ask to change all root file names. Click 'Yes' and repeat the name SS_noDRN under MODFLOW Root File name. Press 'OK'.


A dialog box titled "Change Model Root File Names" with a close button (X) in the top right corner. It contains three text input fields with labels to their left: "MODFLOW Root File Name" with the text "SS_noDRN", "MODPATH Root File Name" with the text "gvmp56", and "MT3D Root File Name" with the text "gvmt56". At the bottom right, there are two buttons: "OK" and "Cancel".

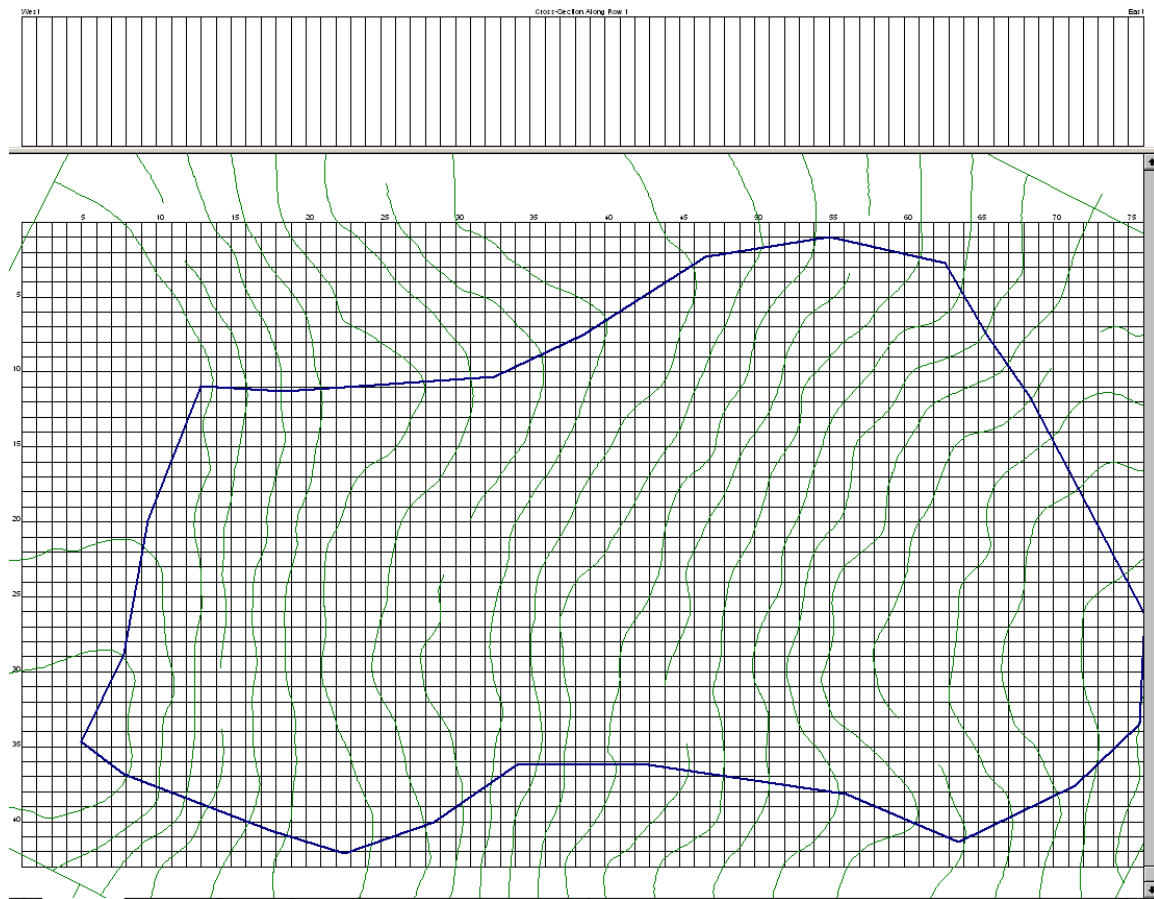
To set up MODFLOW, first it is necessary to set up a path to the directory you want files written. Go to Models->Paths to Models...



And in the Working Directory browse to the location sited\noCALIB\SS\ . Highlight the GWV file SS_noDRN and click "Open", then click "OK".

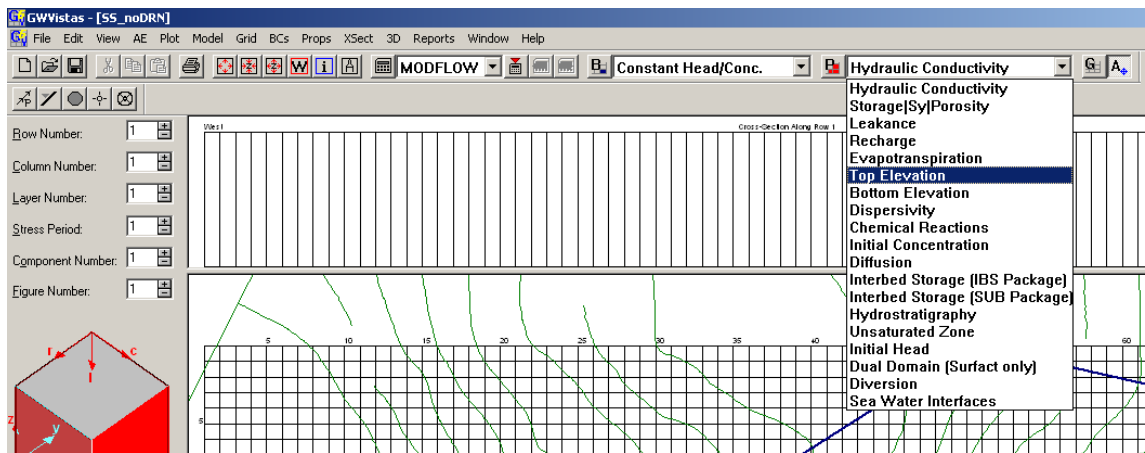


Zoom to full grid 

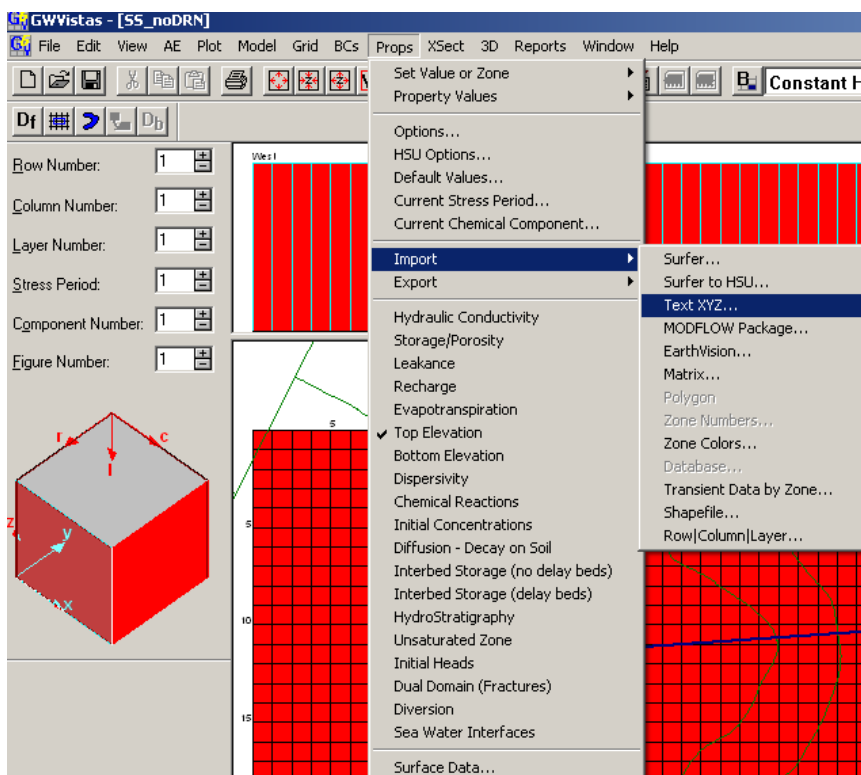


B-3.2 Top and Bottom Elevations

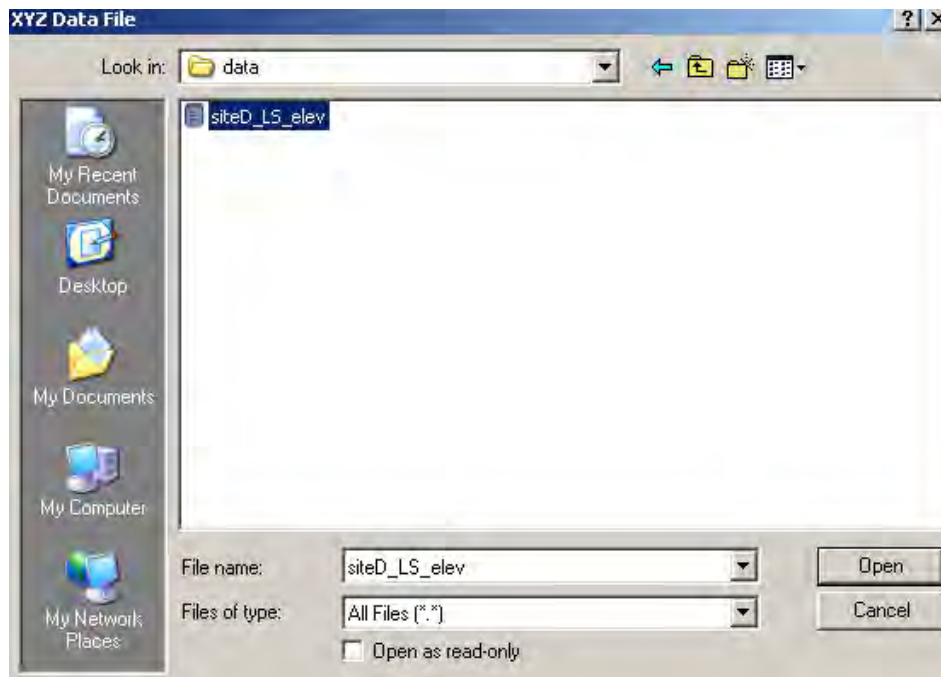
To import land surface elevations, LIDAR for the modeled domain is imported as an XYZ data file and interpolated. Make sure the properties dialogue is on 'Top Elevation'. This can be done by going to Props -> Top Elevation, or by using the drop-down menu as shown below and highlighting Top Elevation. Your grid will become a solid red color, with a default top elevation currently set at 100 feet.



Once the dialogue says 'Top Elevation', go to Props->Import->Text XYZ.



Browse to sited\import_files\data\sited_LIDAR.dat



The format of the text file looks as follows,

siteD_LIDAR.dat - Notepad		
File Edit Format View Help		
X	Y	siteD_elev
1336047.0	196735.2	287.41510009766
1336061.0	196734.2	285.19729614258
1336075.0	196733.2	283.73901367188
1336089.0	196732.2	282.68859863281
1336103.0	196731.2	279.9635925293
1336117.0	196730.2	278.5671081543
1336132.0	196736.2	276.31030273438
1336146.0	196735.2	273.3037109375
1336160.0	196734.2	271.44311523438
1336174.0	196733.2	269.86849975586
1336188.0	196732.2	268.41799926758
1336202.0	196731.2	268.06768798828
1336216.0	196730.2	269.10238647461
1336231.0	196736.2	266.29141235352
1336245.0	196735.2	263.78820800781
1336259.0	196734.2	261.34298706055
1336034.0	196706.2	295.06100463867
1336035.0	196678.2	299.70080566406

With column 1 = X, column 2 = Y and column 3 = land surface elevation. GWV allows flexibility in text file format, with the user telling GWV what each column of data represents. For this example, fill out the import XYZ dialogue as follows. Feel free to view the text file using the button on the right side of the dialogue box and make sure the box 'File contains site coordinates' is checked.

Import an XYZ File for Property Zones

File Information

File:

Column Containing X Coordinate:

Column Containing Y Coordinate:

Column Containing Elevation of Point:

Column Containing Property Value:

No. of Lines to Skip at Top of File:

File contains site coordinates: ☒

Coordinates are row and column format: ☐

Note: The file must be a text file. Numbers are delimited with a comma, space, or tab. When importing row and column format, column is X and row is Y above.

Interpolation

Minimum Nearest Neighbors in Search:

Maximum Nearest Neighbors in Search:

Search Radius:

Automatically Reset Database: ☐

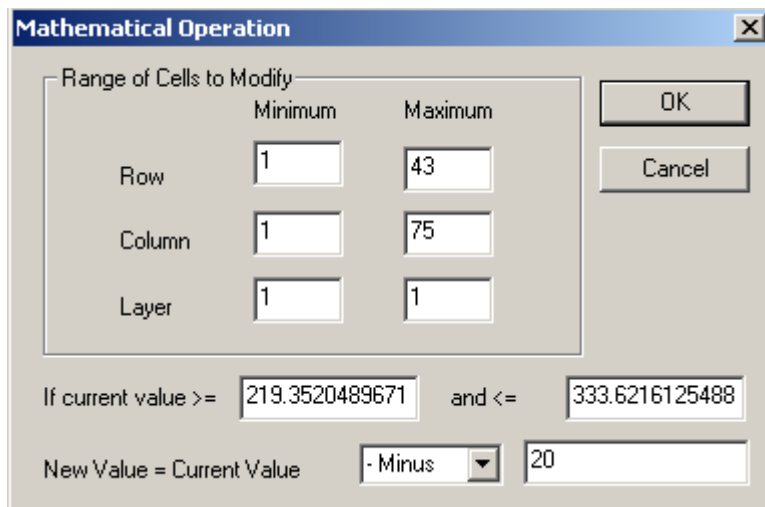
Append Data to Database: ☐

Property Type:

In the bottom left hand corner of the screen the Matrix Top should now show interpolated elevations.

Next it is necessary to assign bottom elevations. This is done by switching the property box to Bottom Elevation

Re-import the top elevations as just done. Cell thickness is 0 ft thick. Go to Props->Property Values->Matrix Editor and hit the “Math” button and fill out the dialogue as shown below to force the bottom elevation to 20 ft below the land surface elevation, and hit “OK”.

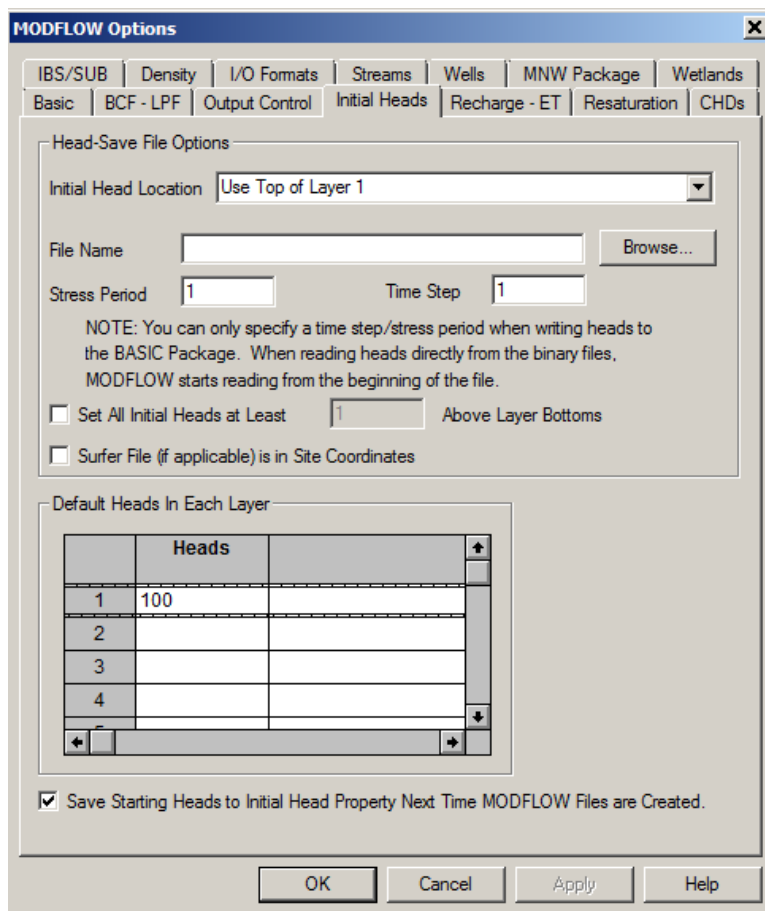


The "Mathematical Operation" dialog box is shown. It has a title bar with a close button. Inside, there's a section "Range of Cells to Modify" with three rows: "Row", "Column", and "Layer". Each row has "Minimum" and "Maximum" input fields. The "Row" row has "1" and "43". The "Column" row has "1" and "75". The "Layer" row has "1" and "1". To the right of these fields are "OK" and "Cancel" buttons. Below the "Range of Cells to Modify" section, there's a line "If current value >= [219.3520489671] and <= [333.6216125488]". Below that, there's a line "New Value = Current Value [- Minus] [20]".

If a thicker/thinner geologic unit is desired, then change the value subtracted.

B-3.3 Initial Heads

For steady state simulations the initial heads are not important, but should be above the bottom of the cell to avoid numeric instabilities caused by cells going dry. Therefore, a starting head is equal to land surface (or top of layer 1) is a good initial guess. Go to Model->MODFLOW->Package Options... and in the initial heads tab, use the drop-down menu to set initial head location to “Use Top of Layer 1” and unclick the “Surfer File. Click “Save Starting Heads to Initial Heads Property Next Time MODFLOW files are created”.



The "MODFLOW Options" dialog box is shown. It has a title bar with a close button. Below the title bar is a tabbed interface with tabs: "IBS/SUB", "Density", "I/O Formats", "Streams", "Wells", "MNW Package", "Wetlands", "Basic", "BCF - LPF", "Output Control", "Initial Heads", "Recharge - ET", "Resaturation", and "CHDs". The "Initial Heads" tab is selected. Inside the "Initial Heads" tab, there's a section "Head-Save File Options" with a "Initial Head Location" dropdown menu set to "Use Top of Layer 1". Below this is a "File Name" input field and a "Browse..." button. There are "Stress Period" and "Time Step" input fields, both set to "1". A note says: "NOTE: You can only specify a time step/stress period when writing heads to the BASIC Package. When reading heads directly from the binary files, MODFLOW starts reading from the beginning of the file." Below the note are two checkboxes: "Set All Initial Heads at Least [1] Above Layer Bottoms" and "Surfer File (if applicable) is in Site Coordinates". Below this is a section "Default Heads In Each Layer" with a table. The table has two columns: "Layer" and "Heads". The "Layer" column has values 1, 2, 3, 4. The "Heads" column has values 100, , , . Below the table are "OK", "Cancel", "Apply", and "Help" buttons. At the bottom, there's a checkbox "Save Starting Heads to Initial Head Property Next Time MODFLOW Files are Created." which is checked.

Now switch to the Basic tab and make sure “Steady State Simulation” is checked and change length units from “Undefined” to “feet”.

MODFLOW Options

IBS/SUB | Density | I/O Formats | Streams | Wells | MNW Package | Wetlands

Basic | BCF - LPF | Output Control | Initial Heads | Recharge - ET | Resaturation | CHDs

Data Set Titles

MODFLOW Data Set Created by Groundwater Vistas

☒ Steady-State Simulation Number of Stress Periods: 1

Use Stress Period Number: 1 For Steady-state Simulation

☐ Simulate a subset of stress periods from: 1 to 1

☒ Save Starting Heads Head Value for No-Flow Cells: 999

☒ Print Comments in Dataset

☐ Continue MODFLOW Simulation Even if Convergence Not Achieved

☐ Convert Dry Cells to No-Flow Cells ☐ Also Convert Dry Cells in Steady-State

☐ Use Diffusion Zones for IBOUND Active Cells

Days Time Units

Feet Length Units

MODFLOW-SURFACT DATUM: 0

☐ Write Input Files in Free Format

Number of Significant Digits to Write: 8

OK Cancel Apply Help

B-3.4 Hydraulic Parameters

Go to Props->Options... and make sure that Hydraulic Conductivity and recharge are not checked under “Use Matrices”. If they are checked, then uncheck.

Switch the properties box to Hydraulic Conductivity

Hydraulic Conductivity

Go to Props->Property Value->Database...

Change the number of zones to 1 and hit “Update”. Place a value of 1 ft/d in the K_x , K_y and K_z box. And hit “Apply”. If a different hydraulic conductivity is desired, then use a different value than 1 ft/d.

Zone Database Information

Zone Database

Hydraulic Conductivity Property Zone Values

Stress Period Number: 1 (Recharge/ET Only)

Number of Zones:

	Kx	Ky	Kz		Color
1	1	1	1	0	
2					
3					
4					
5					
6					
7					

OK Cancel Apply Help

For steady state simulations it is not necessary to parameterize storage terms. For a one layer model, its not necessary to parameterize leakance. These terms will be defined in later examples.

B-3.5 Boundary Conditions

It is now time to define boundary conditions. For this example, boundary cells of no-flow, constant heads and recharge are specified.

First no-flow cells will be defined. Go to BC->No-Flow

Or toggle the BC window to Noflow

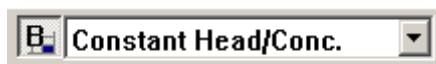
BCs Props XSect 3D Rep

- Insert
- Delete
- Modify
- Copy...
- Options...
- Import
- Export...
- Repair BC Cells
- Constant Head/Conc.
- Well
- River
- Drain
- General Head Boundary
- Stream
- ☒ No-Flow
- Wall
- Lake
- HSSM
- Wetlands
- Flow and Head Bdy

Go to BC->Import->Shapefile... and navigate the browser to
sited\import_files\shapefiles\siteD_domain_polys.shp

Click 'No' to the next two questions. Cells outside the domain are assigned as no-flow cells.

Constant heads (CHD), also known as specified heads, are assigned to the low elevation cells on the right hand side of the modeled domain. They are set at 1 foot below land surface. Switch the BC box from Noflow to Constant Head.



A text file is created defining CHD values.

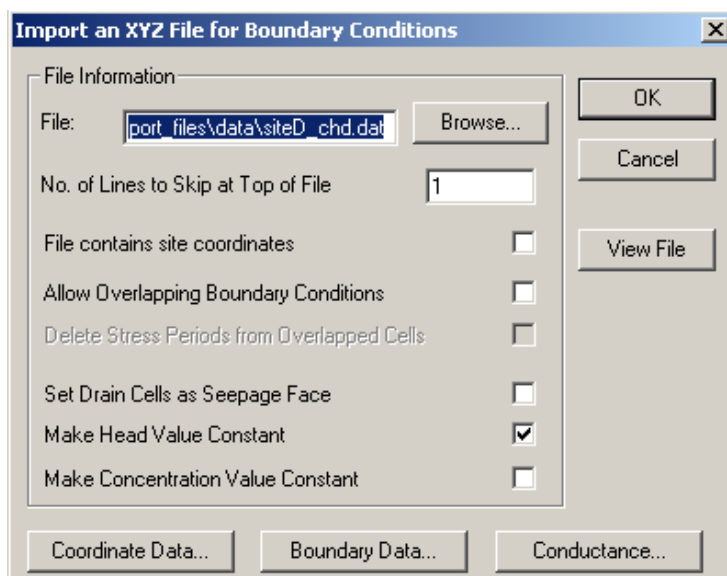
siteD_chd.dat - Notepad			
File	Edit	Format	View Help
row	col	lay	chd_ft
26	75	1	222.12
27	75	1	221.86
28	75	1	221.49
29	75	1	221.13
30	75	1	220.76
31	75	1	220.40
32	75	1	220.04
33	75	1	219.67
34	75	1	219.40

As with land surface elevations, the format of the text file is flexible and defined using the import box.

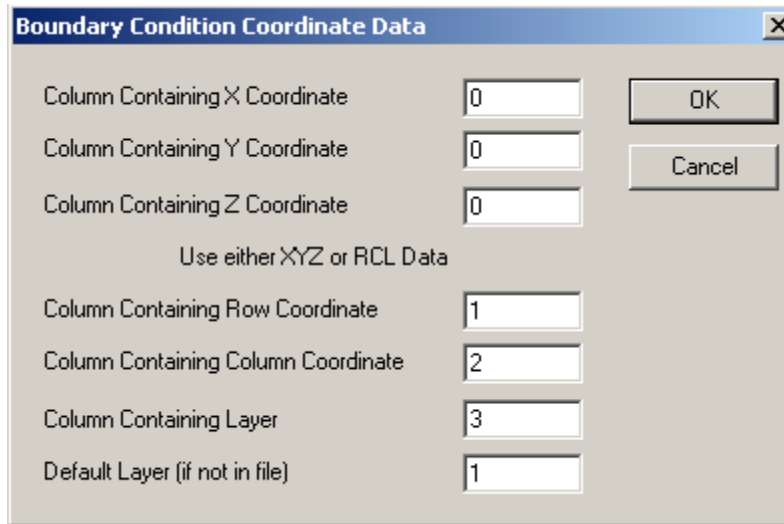
To import CHD values go to BC->Import->Text File...

Browse to
sited\Import_files\data\siteD_chd.dat

The number of lines to skip = 1 and
head is made a constant value.



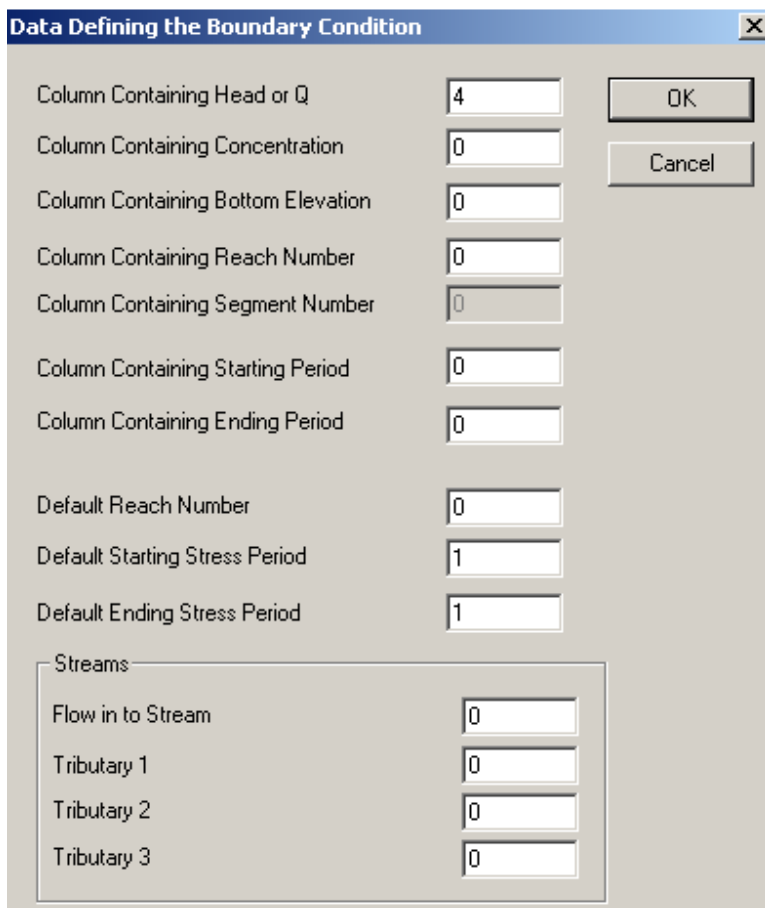
Click on the Coordinate Data... button and fill in as follows.



Boundary Condition Coordinate Data

Column Containing X Coordinate	<input type="text" value="0"/>	<input type="button" value="OK"/> <input type="button" value="Cancel"/>
Column Containing Y Coordinate	<input type="text" value="0"/>	
Column Containing Z Coordinate	<input type="text" value="0"/>	
Use either XYZ or RCL Data		
Column Containing Row Coordinate	<input type="text" value="1"/>	
Column Containing Column Coordinate	<input type="text" value="2"/>	
Column Containing Layer	<input type="text" value="3"/>	
Default Layer (if not in file)	<input type="text" value="1"/>	

Under the Boundary Data... assign the 'Column Containing Head or Q' to 4,



Data Defining the Boundary Condition

Column Containing Head or Q	<input type="text" value="4"/>	<input type="button" value="OK"/> <input type="button" value="Cancel"/>
Column Containing Concentration	<input type="text" value="0"/>	
Column Containing Bottom Elevation	<input type="text" value="0"/>	
Column Containing Reach Number	<input type="text" value="0"/>	
Column Containing Segment Number	<input type="text" value="0"/>	
Column Containing Starting Period	<input type="text" value="0"/>	
Column Containing Ending Period	<input type="text" value="0"/>	
Default Reach Number	<input type="text" value="0"/>	
Default Starting Stress Period	<input type="text" value="1"/>	
Default Ending Stress Period	<input type="text" value="1"/>	
Streams		
Flow in to Stream	<input type="text" value="0"/>	
Tributary 1	<input type="text" value="0"/>	
Tributary 2	<input type="text" value="0"/>	
Tributary 3	<input type="text" value="0"/>	

Hit "OK" twice. To modify head values use BC->modify->simplified editing. Review the GWV manual for other ways to import or create constant heads.

The last boundary condition to define is recharge. For this example, open the excel file under design_storms\percentage recharge.xls

Listed in Table 5.5 are recharge values, percentage recharge and storm maximum recharge rates based on curve numbers (CN) and total precipitation for a 24-hour period.. For this example, the following information is used

Inches of rain in a 24 hour period = 11

Curve Number = 80

Rainfall distribution = IA

Therefore the assumed percentage of recharge is 18%.

Using an example of average total annual precipitation of 35 inches and 18% recharge is 6.3 inches/year or 0.0014 ft/d. This is the estimated steady state recharge.

In the properties dialogue highlight recharge



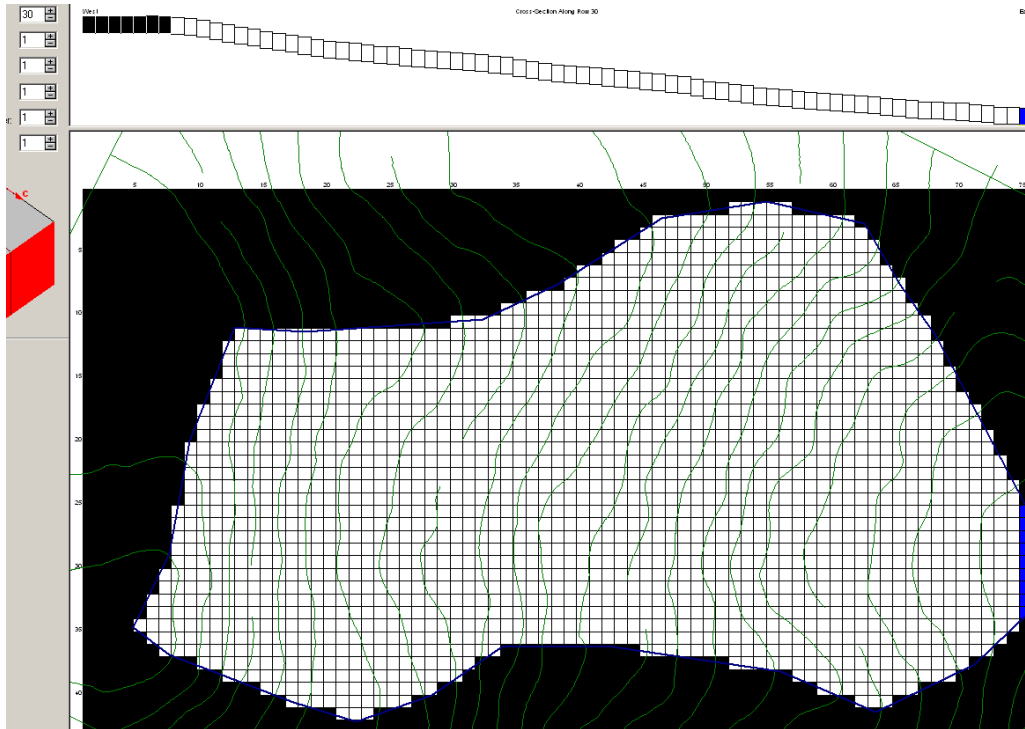
Go to Props->Property Values->Database...

Change the number of zones from 10 to 1 and hit "Update". In zone 1 type 0.0014 and hit "Apply". Then "OK".

A screenshot of the 'Zone Database Information' dialog box. The 'Zone Database' tab is selected. Under 'Recharge Property Zone Values', the 'Stress Period Number' is set to 1 (Recharge/ET Only). The 'Number of Zones' is set to 1, with an 'Update' button next to it. Below this is a table with 7 rows and 6 columns: 'Recharge', 'Conc', 'Ponding_Depth', an empty column, and 'Color'. The first row is populated with '0.0014', '0', '0', and '0'. The other rows are empty. At the bottom are 'OK', 'Cancel', 'Apply', and 'Help' buttons.

	Recharge	Conc	Ponding_Depth		Color
1	0.0014	0	0	0	
2					
3					
4					
5					
6					
7					

The model screen should look similar to the image below.



B-3.6 MODFLOW-NWT

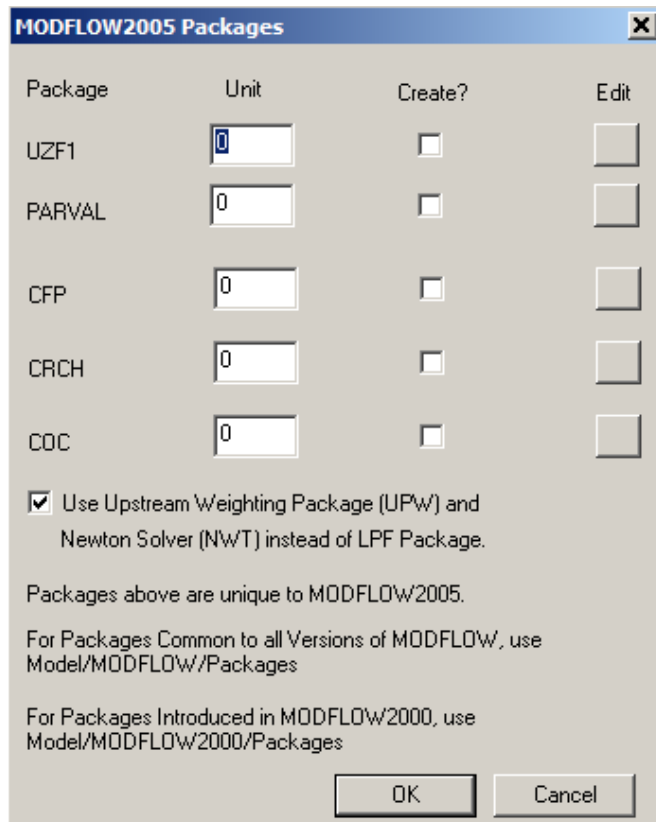
Since unconfined solutions are highly non-linear the new MODFLOW-NWT solver should be used.

Under Models->MODFLOW... change the Model Version from MODFLOW2000 to MODFLOW2005 and click "OK".

Package	Value	Check	UNIT Location	Edit
Basic	1			
BCF	0			
Output Control	22			
Solver	19		PCG2	15
Well	0		0	
River	0		0	
Drain	0		0	
General Head	0		0	
Stream	0		0	14
Recharge	18		50	
ET	0		0	
Wall	0			16
CHD	0			20
MNV	0		0	

☐ Create Map File
☐ Create Path3D Files
☐ MT3D Flow Output
☒ Automatically Reset Package Units

Under Models->MODFLOW2005->Packages... check the box “Use Upstream Weighting Package (UPW) and Newton Solver (NWT) Instead of LPF. Click “OK”.



Go to Models->MODFLOW2005->Options...

Toggle to the NWT General tab, change “MODERATE” to “COMPLEX”, and check “Use Residual Control (BACKFLAG)” and check “Correct Heads Surrounded by Dewatered Cells (IBOTAV)”. Change the FLUXTOL from 100 to 1, and MAXITEROUT from 100 to 3000, as shown below. Then click “OK”.

MODFLOW2005 Options

LPF Options | UZF | CFP | NWT General | **NWT Methods**

Automate Solver Options (OPTIONS) COMPLEX

Head Change Criterion for Outer Iterations (HEADTOL) 1e-005

Flux Change Criterion for Inner Iterations (FLUXTOL) 1

Maximum Outer Iterations (MAXITEROUT) 3000

Print Flag for Convergence Information (IPRNWT) 0

Nonlinear Solution Method (NONMETH) 1 Newton Raphson

Linear Solution Method (LINMETH) 2 - XMD solver

Learning Rate Reduction Factor (DBDTHETA) 0.4

Learning Rate Increment (DBDKAPPA) 0

Memory Term Factor (DBDGAMMA) 0.001

Momentum Term (MOMFACT) 0.001

Maximum Backtracking Iterations (MAXBACKITER) 10

Residual Change Tolerance (BACKTOL) 1.05

Time Step Reduction Factor (BACKREDUCE) 0.9

Proportion of Cell Thickness for Smoothing (THICKFACT) 0.0001

☒ Use Residual Control (BACKFLAG)


☒ Correct Heads Surrounded by Dewatered Cells (IBOTAV)

OK Cancel Apply Help

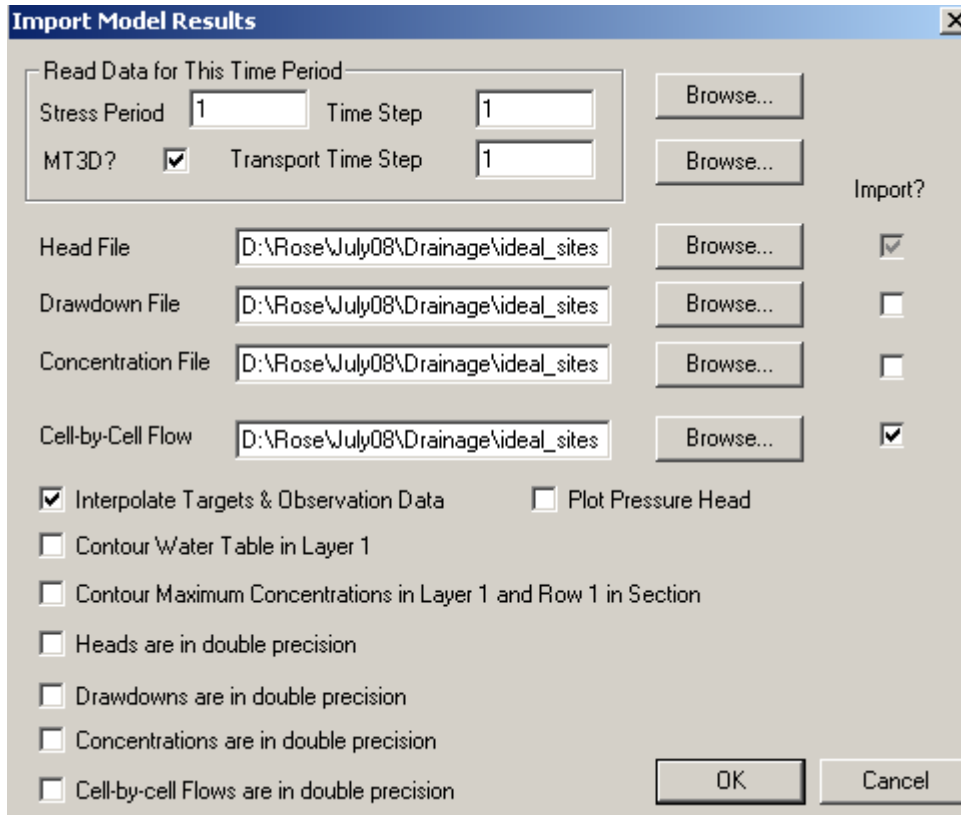
To turn off the plotting of contour and domain shapefiles go to Plot->What to Display... and click on "Maps...". On the drop-down options set to "Do Not Draw". Click "OK". Before exiting the graphics dialogue click "Display Color Flood of head".

Save the model prior to execution.

B-3.7 Model Execution

To run MODFLOW hit the  button. Click “yes” to create Data files first?” and “Yes” to “Display Error File” if desired.

The model will run very quickly and will ask to process results. Click “Yes”. The path to the head file is defined by the path established earlier and automatically imported. The CCF budget file is not automatically imported. It is necessary to click this box to view the flow budget. Go ahead and click the Cell-by-Cell Flow



The dialog box titled "Import Model Results" contains the following elements:

- Read Data for This Time Period:**
 - Stress Period: 1
 - Time Step: 1
 - MT3D?: ☒
 - Transport Time Step: 1
 - Four "Browse..." buttons for file selection.
- Import? Section:**
 - Head File: D:\Rose\July08\Drainage\ideal_sites (Browse... button, ☒)
 - Drawdown File: D:\Rose\July08\Drainage\ideal_sites (Browse... button, ☐)
 - Concentration File: D:\Rose\July08\Drainage\ideal_sites (Browse... button, ☐)
 - Cell-by-Cell Flow: D:\Rose\July08\Drainage\ideal_sites (Browse... button, ☒)
- Options Section:**
 - ☒ Interpolate Targets & Observation Data
 - ☐ Plot Pressure Head
 - ☐ Contour Water Table in Layer 1
 - ☐ Contour Maximum Concentrations in Layer 1 and Row 1 in Section
 - ☐ Heads are in double precision
 - ☐ Drawdowns are in double precision
 - ☐ Concentrations are in double precision
 - ☐ Cell-by-cell Flows are in double precision
- Buttons:** OK, Cancel

The default contour fonts are very small and can be adjusted to preference of the user by going to Plot->Contour->Parameters (Plan View)... Change the minimum Level to 215, the Interval to 5. Change Label every N to 1 and Percision to 0. Font can be made to 18 point and the color and thickness of the contour label line information set to black and 1/3 point. Click “Do not change levels”

Hit “OK”.

Contour Information [X]

Resolution

X Nodes: 100 [+] [-] Y Nodes: 100 [+] [-]

☐ Display Grid

OK

Cancel

Contour Information

Calculated Z Range: 219.489995 - 312.197474

Minimum Level: 215

Maximum Level: 312.2256233

Interval: 5

☐ Use Custom Contour Levels ☒ Do not change levels

Number of Levels: 0

Custom Levels...

Contour Label Information

Label Every N: 1 [+] [-] Format: FIXED

Precision: 0 [+] [-] Distance between: 38 [+] [-]

Font... Arial

Contour Label Line Information

Color... [Black] Thickness: 3/4 point

Contour Line Information

Color... [Black] Thickness: 3/4 point

Make sure head contours are displayed by going to Plot->What to Display... and making sure 'Display Contours of Head' and "Display Color Flood of Head" are checked. Other variables can be mapped by using the drop down menus.

Select Graphics to Display [X]

☒ Display Base Maps ☒ Display Bitmap ☐ Clip Map to Grid Maps...
☒ Display Finite-Difference Grid ☐ Outline Active Area ☐ Draw Each Cell
☒ Display Boundary Conditions ☐ Use BC Symbols ☐ Write Node Numbers
☒ Display No-Flow Boundary Conditions
☐ Display Property Zone Boundaries Width (pixels)
☐ Post Residuals for Calibration ☐ Plot Residual Circles ☐ Plot Pilot Point Circles
☒ Display Contours of Head ▼
☒ Display Color Flood of Head ▼
☐ Display Velocity Vectors
☒ Display Particle Traces ☐ Use Endpoint Analysis
☐ Display Legend
☒ Plot Dry Cells ☒ Plot Flooded Cells (Head > Top Layer 1 +
☒ Display Analytic Wells ☒ Display Particle Starting Locations
☒ Display Analytic Lines ☒ Display Analytic Polygons
☒ Display Analytic Circles ☒ Display Analytic Polylines

Target Types


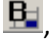

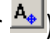
☒ Head Targets ☒ Head Difference Targets ☒ Concentration Targets
☒ Flux Targets ☒ Drawdown Targets ☒ Constraints
☒ Kx Pilot Points ☒ Kz Pilot Points ☒ Prior Information
☒ Ss Pilot Points ☒ Recharge Pilot Points ☒ Porosity Pilot Points

☒ Interpolate Results When Tracking Cursor

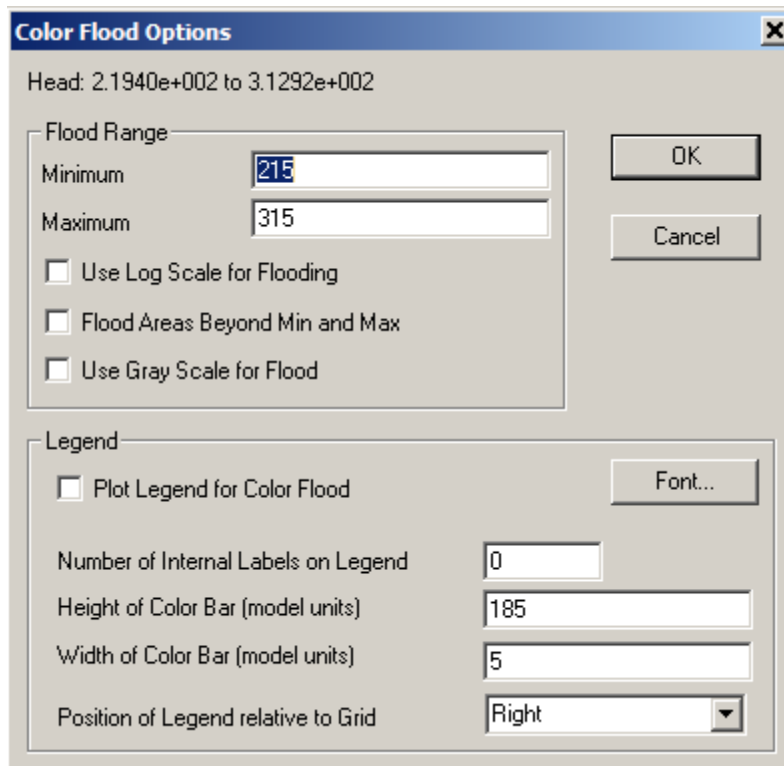
OK
Cancel

Font Options

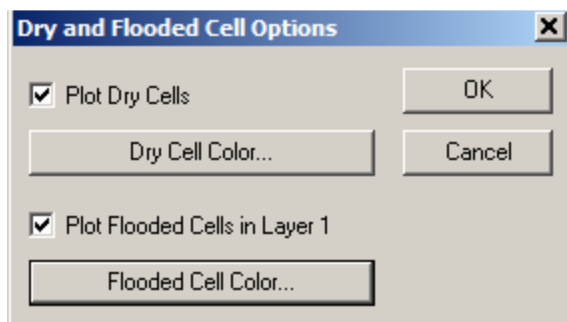
☒ Normal ☐ Scaled ☐ Fixed
 Scale Factor

If you cannot see the color contours, then it is necessary to change from Property view  to any other view (e.g. ,  or )

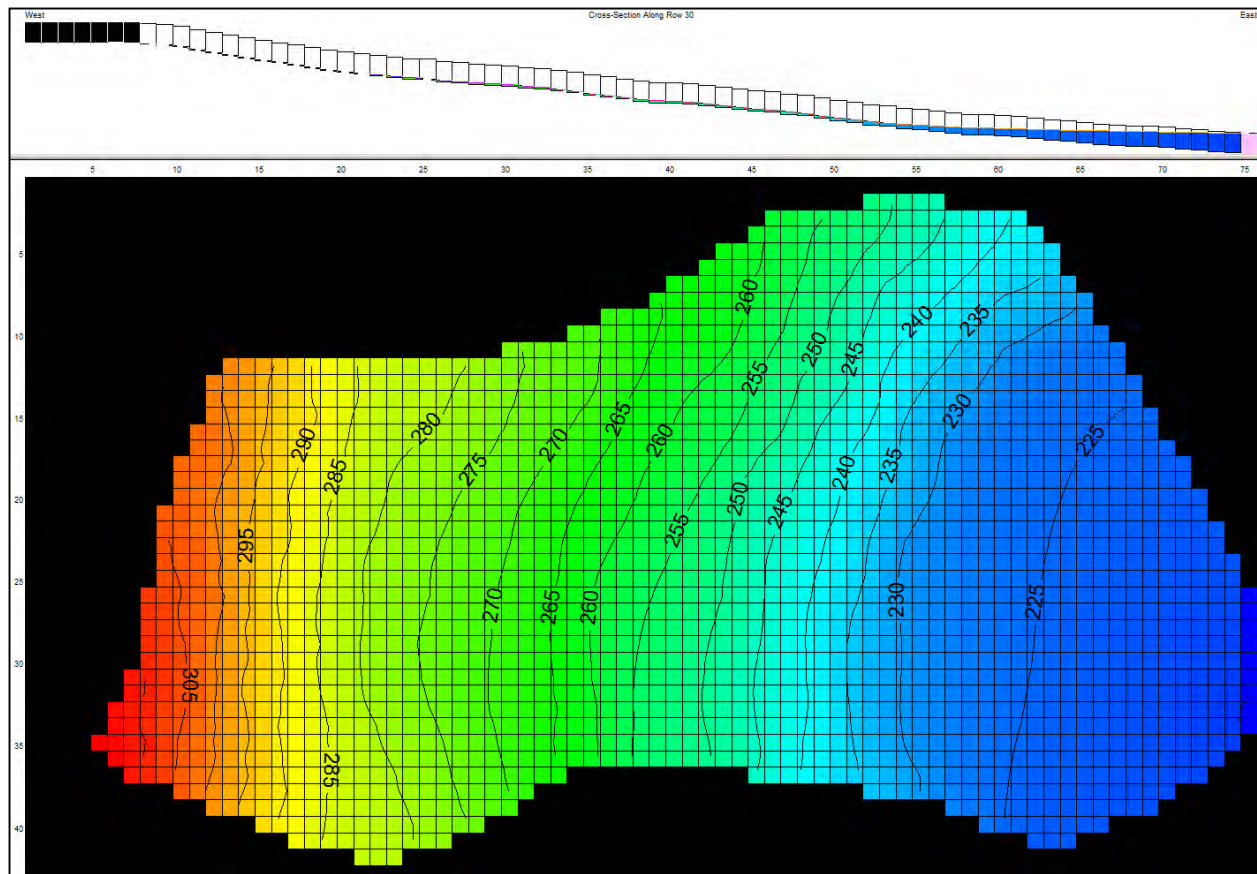
Color flood is defined under Plot->Color Flood->Color Flood Options... The minimum value is set at 215 and the maximum is set at 315.



Flooded cells are plotted automatically, unless one unclicks the box under to Plot->What to Display... To establish the color of flooded cells, go to Plot->Dry/Flooded Cells... and pick Flooded Cell color. The color pink is chosen since it's a color not used in the color scale for heads and easy to visualize.



Screen output should look similar to the image below, with the cross sectional view for row 30. Contours are at 5 ft intervals. One can toggle across rows and columns and layers (if more than one layer) by using the options to the left of the display.



Save the model.

B-3.8 Steady State Calibration

Often the steady state model is used to calibrate hydraulic conductivity to best match observed water level data. Low precipitation months (e.g. end of summer) are most representative of the steady state scenario and data collected during these time periods should be used if available.

Save the model created above in the following location,

siteD\CALIB\SS_noDRN\SS_noDRN_Calib.gww

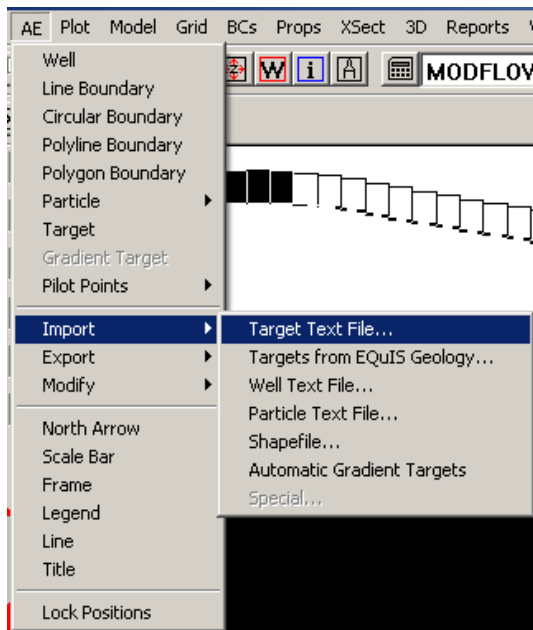
Rename the MODFLOW Root Names SS_noDRN_Calib.

Reassign the working directory by going to Model->Paths to Models... and browsing to siteD\CALIB\SS_noDRN\ and press "OK".

The text file defining observed targets looks like the following

SS_noDRN_obs.dat - Notepad			
File Edit Format View Help			
Name	X	Y	obsWL_ft
ss01	1336153.15	196445.14	303.00
ss02	1336233.73	196579.28	264.00
ss03	1336365.47	196580.44	234.00

To import observed data go to AE->Import->Target Text File... and navigate to siteD\import_files\data\SS_noDRN_obs.dat, click “OK”.



An “Options for Importing Targets” dialogue opens with an option to view the file if desired. Fill in the dialogue as shown below.

Options for Importing Targets

☒ Targets are in Site Coordinates OK

☐ File Contains Transient Targets Cancel

☐ Transient Targets Contain Transient Weights View File

☐ Read one Target Value for transient targets

Time Value for Target

Target Type to Import

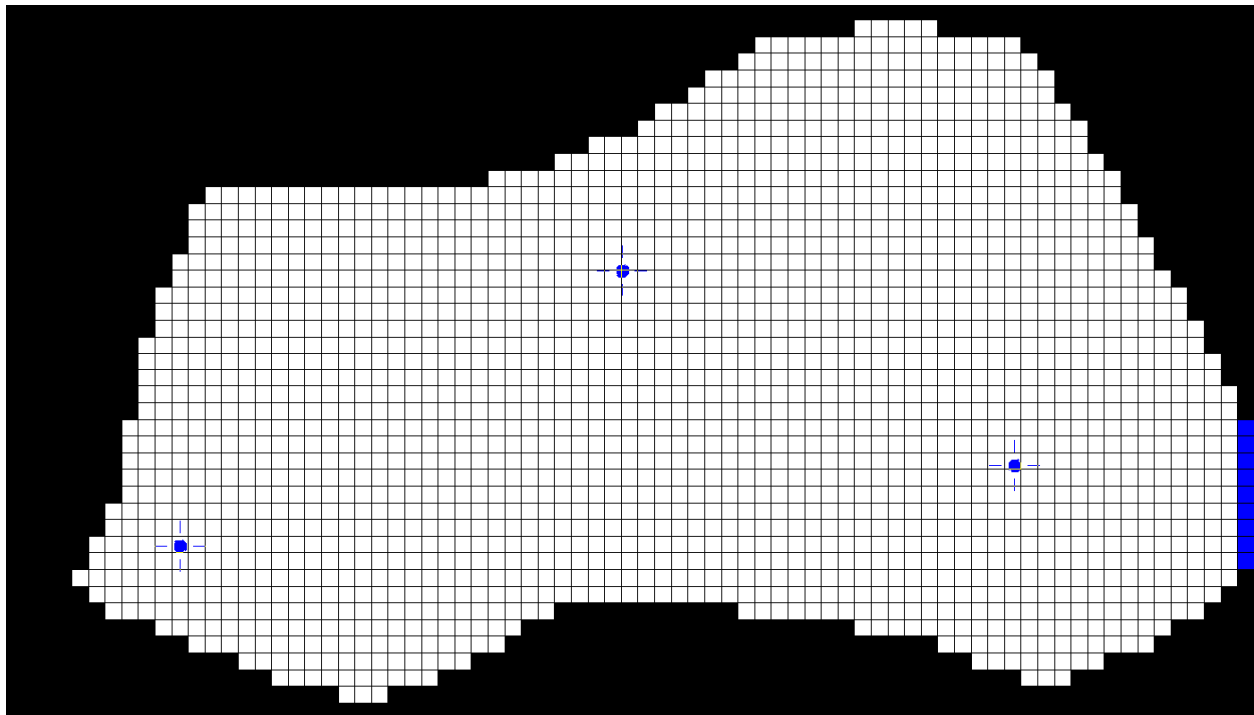
☐ Target Value is a Head Difference

Number of Lines to Skip

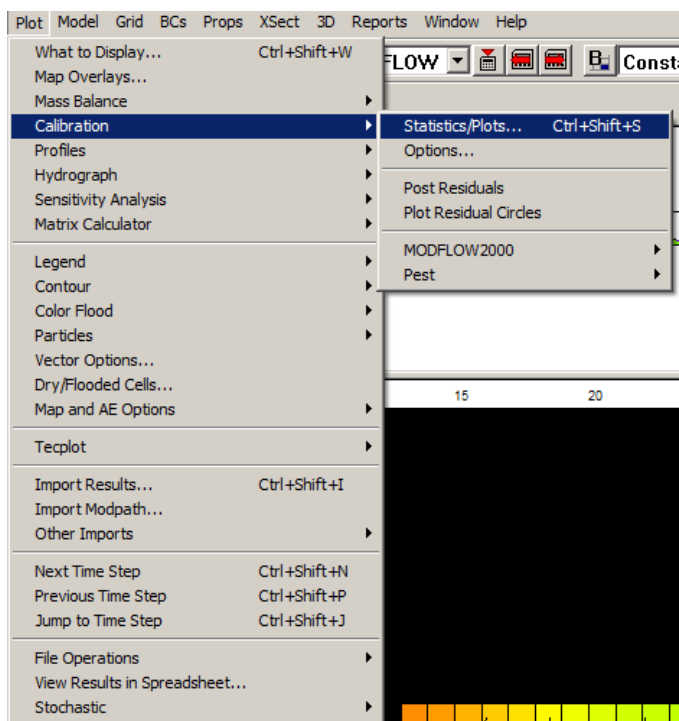
	Column in File		Column in File
Name	<input type="text" value="1"/>	No. Trans. Data Pts.	<input type="text" value="0"/>
X Coordinate	<input type="text" value="2"/>	Column	<input type="text" value="0"/>
Y Coordinate	<input type="text" value="3"/>	Row	<input type="text" value="0"/>
Screen Elev.	<input type="text" value="0"/>	Layer	<input type="text" value="0"/>
Target Value	<input type="text" value="4"/>	Weight	<input type="text" value="0"/>
Group Number	<input type="text" value="0"/>	Lower Layer	<input type="text" value="0"/>
Component	<input type="text" value="0"/>	Minimum Bound	<input type="text" value="0"/>
		Maximum Bound	<input type="text" value="0"/>

The default size of targets is 100, which is too large for this domain. To scale the target symbol, go to AE->Modify->Targets->Display Options... and change the size of target to 15.

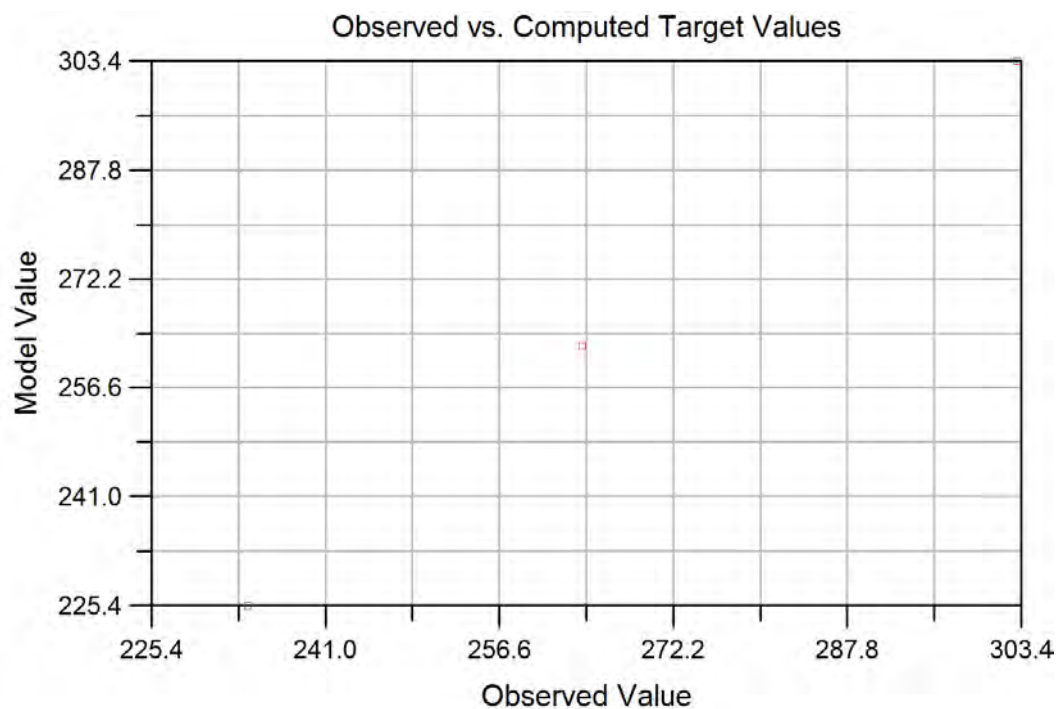
The location of the observation sites, or targets, is shown below,



Assuming K_x and K_y are still at 1 ft/d, rerun the model in its current directory and import results. To see how well the model reproduces observed water levels go to Plot->Calibration->Statistics/Plots.



In the dialogue box press “Plot Observed vs. Simulated”. And the chart given below will appear showing modeled water levels predicted lower than two of the three observed values. The ‘Statistics...’ button on the same dialogue box will produce the statistics shown with a rmse = 5.06 ft, and a scaled rmse of 7.3%.



Target Statistics		
Target	Residual	Name
234.00	8.65	ss03
264.00	1.41	ss02
303.00	-0.40	ss01
<div> <div>Residual Mean = 3.22</div> <div>Residual Standard Dev. = 3.91</div> <div>Absolute Residual Mean = 3.48</div> <div>Residual Sum of Squares = 7.69e+001</div> <div>RMS Error = 5.06</div> <div>Minimum Residual = -0.40</div> <div>Maximum Residual = 8.65</div> <div>Range of Observations = 69.00</div> <div>Scaled Res. Std. Dev. = 0.057</div> <div>Scaled Abs. Mean = 0.050</div> <div>Scaled RMS = 0.073</div> <div>Number of Observations = 3</div> </div> <div>Close</div>		

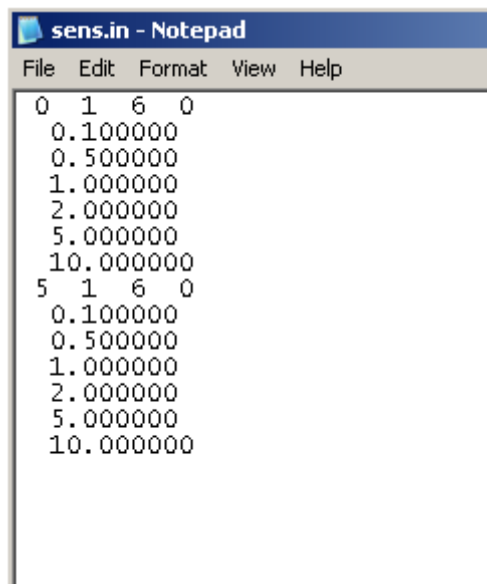
Often a sensitivity analysis is performed before calibration to determine which parameters are most influential on model output. For our example, recharge rate and hydraulic conductivity are tested.

Go to, Model->Autosensitivity->Options...

It is now necessary to produce a script that GWV will use to run different model realizations. First, the parameter $K_x=K_y$ is the default parameter to modify. Leave this as is. Change the Number of Simulations to 6. Then Press the “Multipliers...” button to see the default multipliers used to modify the current K values. Modify these multipliers to 0.1, 0.5, 1, 2, 5, 10. Press the button “New Script”, with a default name of “sens.in”. Press “Open” and then press “OK”.

Now switch the “Parameter to Modify” to Recharge via the drop-down menu. Keep the number of simulations at 6 and the same multipliers as used for hydraulic conductivity. Press “Add to Script”. Press “OK”.

Press the button “Edit Script”. The script should look like the following. If it does not, then edit to be similar.



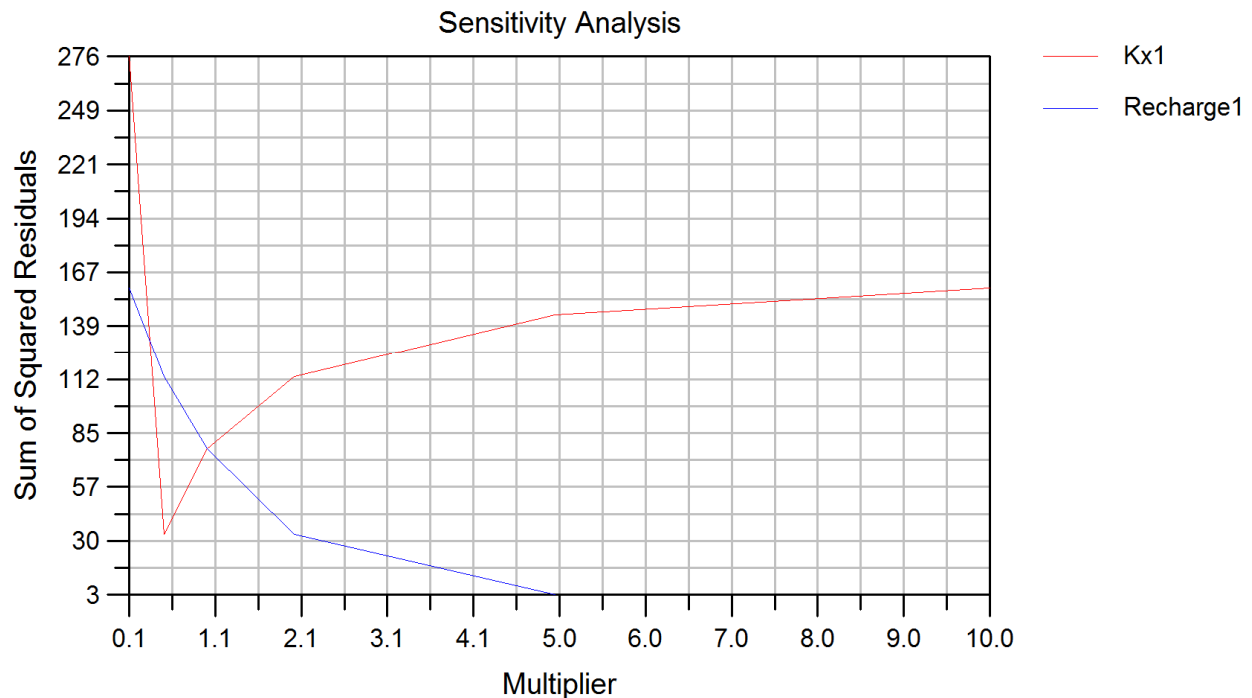
```
sens.in - Notepad
File Edit Format View Help
0 1 6 0
0.100000
0.500000
1.000000
2.000000
5.000000
10.000000
5 1 6 0
0.100000
0.500000
1.000000
2.000000
5.000000
10.000000
```

Click the “Run from Script” box and browse the Script File Name to the sens.in was just created. The default Output file name is sens.in.out. Leave as is.

Press “OK” to exit the dialogue and go to Model->Autosensitivity->Run Analysis. The model runs very quickly and should only take a few moments to run all 12 simulations.

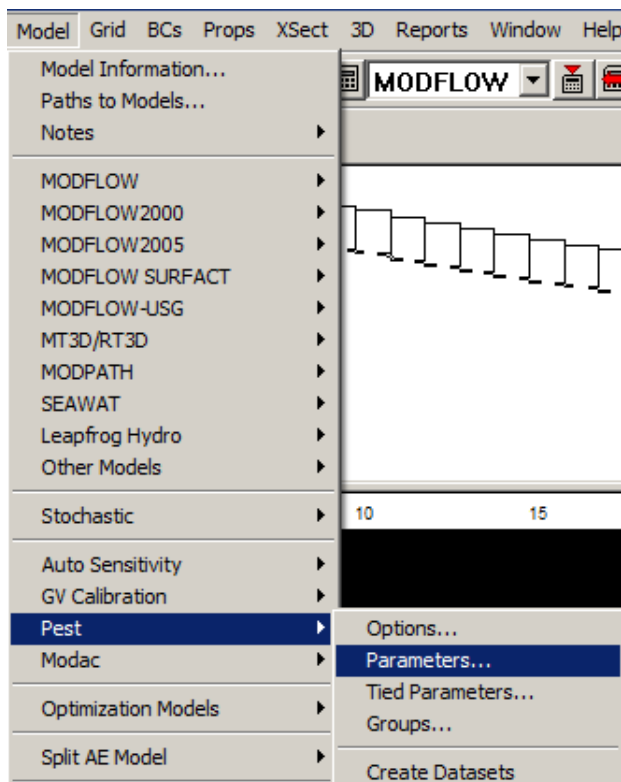
To see results go to Plot->Sensitivity->sum of squared residuals

The graph should look similar to that shown below. Interestingly, modeled water levels are relatively sensitive to hydraulic conductivity for values less than 5 times the K value of 1 ft/d, or 5 ft/d, above which sensitivity decreases. The minimum rmse value occurs when $K_x = 0.5$ ft/d. Recharge is relatively insensitive to a multiplier greater than 5.0 (0.007 ft/d) with sensitivity increasing exponentially for smaller recharge rates.



If uncertainty in parameter values is limited to hydraulic conductivity, then calibration is limited to adjusting hydraulic conductivity and assuming recharge is properly parameterized. This can be done by manually adjusting K_x , or using automated inverse models provided by GWV. PEST is provided with GWV and is considered one of the most robust parameter estimation tools for many groundwater problems. For this example, we will use PEST to help us calibrate K_x to best match water levels.

Go to, Model->PEST-> Parameters



And fill out the dialogue as follows, letting the range in Kx vary between 0.001 and 100 ft/d. The search is run in log-space, since hydraulic conductivity can vary over several orders of magnitude.

PEST Parameters

	Type	Use	Zone	Minimum	Maximum	Transform	Limit
1	Kx	<input checked="" type="checkbox"/>	1	1.00000e-003	100.00	Log	Factor
2	None	<input type="checkbox"/>	1	5.00000e-004	5.00000e-002	Log	Factor
3	None	<input type="checkbox"/>	1	3.50000e-005	35000.00	Log	Factor
4	None	<input type="checkbox"/>	1	3.50000e-002	350.00	Log	Factor
5	None	<input type="checkbox"/>	1	5.00000e-004	5.00000e-002	Log	Factor
6	None	<input type="checkbox"/>	0	1.00000e-004	1000.00	None	Relative
7	None	<input type="checkbox"/>	0	1.00000e-004	1000.00	None	Relative
8	None	<input type="checkbox"/>	0	1.00000e-004	1000.00	None	Relative
9	None	<input type="checkbox"/>	0	1.00000e-004	1000.00	None	Relative
10	None	<input type="checkbox"/>	0	1.00000e-004	1000.00	None	Relative
11	None	<input type="checkbox"/>	0	1.00000e-004	1000.00	None	Relative
12	None	<input type="checkbox"/>	0	1.00000e-004	1000.00	None	Relative
13	None	<input type="checkbox"/>	0	1.00000e-004	1000.00	None	Relative
14	None	<input type="checkbox"/>	0	1.00000e-004	1000.00	None	Relative

Copy to Clipboard Paste All Log/Factor Parameter Setup Clear All Parameters

OK Cancel

Hit "OK"

Now it is time to create the PEST input files and check that all files are properly created. To do this, go to, Model->PEST->Create Data Sets, view the Error/Warning file to ensure no errors were created.

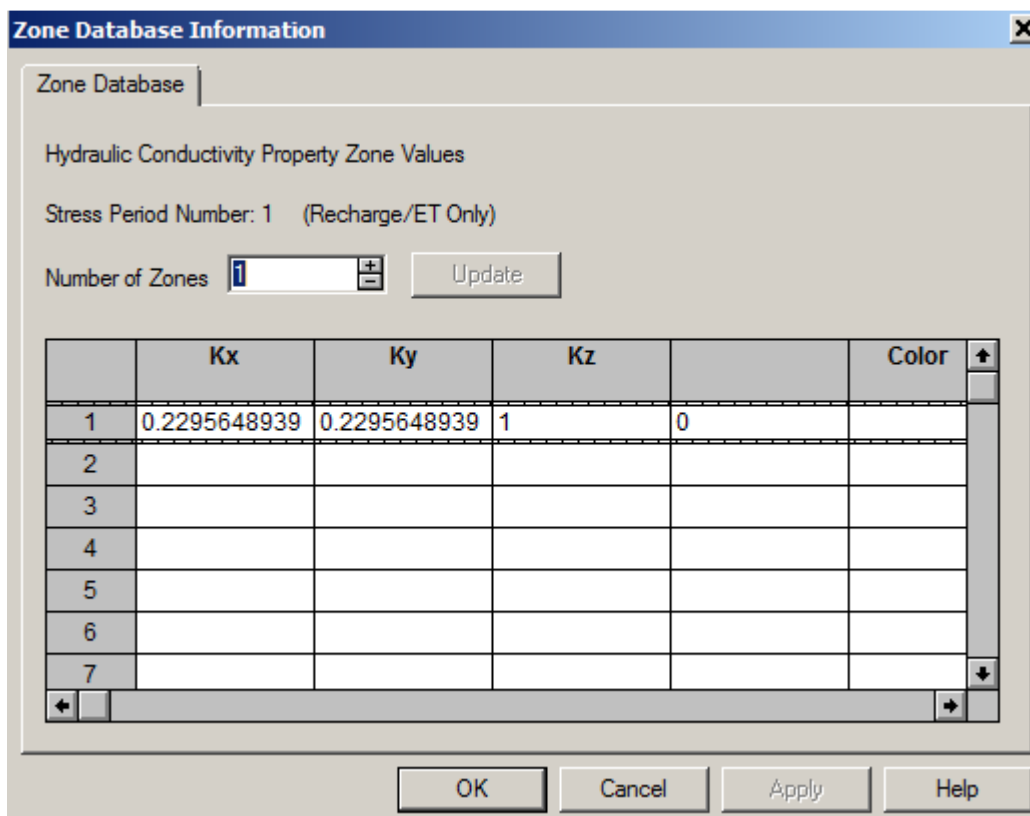
Then Model->PEST->run PESTCheck, and finally, Model->PEST->run PEST.


When PEST is complete, the optimized value for hydraulic conductivity can be uploaded into GWV by going to, Model->PEST->Update Parameters.

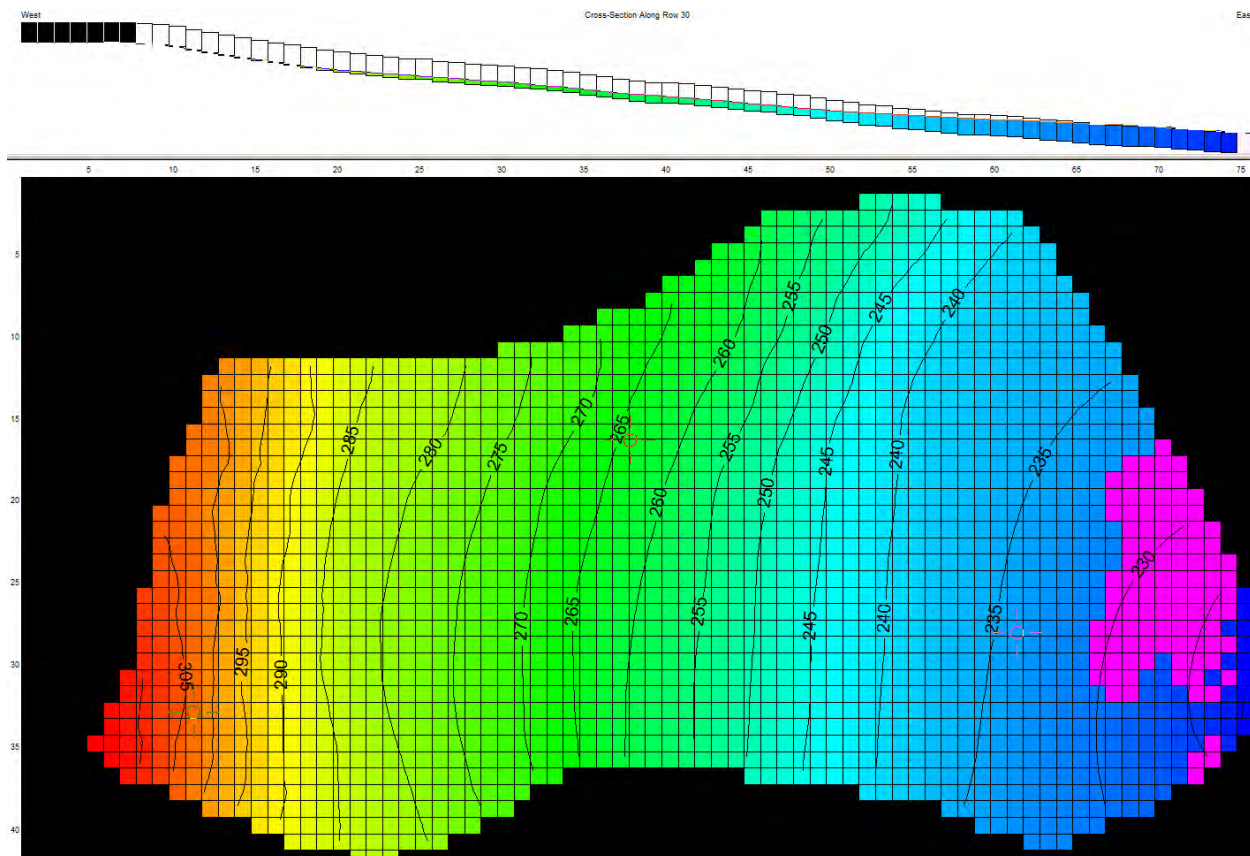
This is checked by having Hydraulic Conductivity toggled,



And going to Props->Property Values->Database and seeing that $K_x = 0.22956$ ft/d.

A screenshot of the 'Zone Database Information' dialog box. The dialog has a title bar with a close button. Inside, there's a tab labeled 'Zone Database'. Below the tab, it says 'Hydraulic Conductivity Property Zone Values'. There's a label 'Stress Period Number: 1 (Recharge/ET Only)'. Below that, there's a label 'Number of Zones' followed by a text box containing '1' and a small '+'/- button. To the right of the text box is an 'Update' button. Below this is a table with 6 columns: 'Kx', 'Ky', 'Kz', an empty column, and 'Color'. The first row of the table has values: '1', '0.2295648939', '0.2295648939', '1', and '0'. The other rows are empty. At the bottom of the dialog are four buttons: 'OK', 'Cancel', 'Apply', and 'Help'.

Rerun the model by clicking on the . The Plot->Calibration->Statistics/Plots->View Statistics, shows that the scaled rmse is reduced to 0.5%. The steady state calibrated K_x will serve as an initial guess in the transient calibration. Modeled heads are given below, with some groundwater seepage in the toe region (pink overlay).



B-4 Transient Conditions (Isotropic Conditions, Pre-Drain)

Save the model created above in the following location,

sited\CALIB\Tr_noDRN\Tr_noDRN_Calib.gww

Rename the MODFLOW Root Names Tr_noDRN_Calib.

Reassign the working directory by going to Model->Paths to Models... and browsing to `sited\CALIB\Tr_noDRNsited\` and press "OK".

B-4.1 Stress Period Set Up

The model must be converted from steady state to transient with the appropriate time steps and length of stress periods provided. The first stress period represents steady state conditions, and the remaining are transient. The length of the steady state stress period does not matter, while each transient stress period is 0.25 days (or 6 hours).

Go to, MODEL->MODFLOW->Options and in the Basics Tab unclick the steady state simulation box and change the number of stress periods to 705 and hit “OK”.

MODFLOW Options

IBS/SUB Density I/O Formats Streams Wells MNW Package Wetlands

Basic BCF - LPF Output Control Initial Heads Recharge - ET Resaturation CHDs

Data Set Titles

MODFLOW Data Set Created by Groundwater Vistas

☐ Steady-State Simulation Number of Stress Periods 705

Use Stress Period Number 1 For Steady-state Simulation

☐ Simulate a subset of stress periods from 1 to 1

☒ Save Starting Heads Head Value for No-Flow Cells 999

☒ Print Comments in Dataset

☒ Continue MODFLOW Simulation Even if Convergence Not Achieved

☐ Convert Dry Cells to No-Flow Cells ☐ Also Convert Dry Cells in Steady-State

☐ Use Diffusion Zones for IBOUND Active Cells

Days Time Units

Feet Length Units

MODFLOW-SURFACT DATUM 0

☐ Write Input Files in Free Format

Number of Significant Digits to Write 8

OK Cancel Apply Help

GWV will ask to copy recharge, hit Yes, and ET, hit Yes (this will be overwritten later). GWV will then ask to set up the new stress periods. Hit Yes.

From the Stress Period Data dialogue box, hit import, and browse to siteD/import_files/data/sp_705.dat. If you cannot see this file, then make sure that text files are viewed, not just cvs files. The stress period data dialogue box should look like the one shown below. The format of the stress period input file must be as follows: stress period length, number of time steps and time step multiplier.

Stress Period Data [X]

	Period Length	No. Time Steps	Time Step Multiplier
1	1	1	1
2	0.25	1	1
3	0.25	1	1
4	0.25	1	1
5	0.25	1	1

OK
Cancel
Import...

GWV will ask if you want to check that the type of stress periods is properly set. Click Yes. The first stress period should be steady state, or set to zero. All other stress periods are transient and should be set to 1.


Stress Period Type (0=SS, 1=TR) [X]

	Type
1	0
2	1
3	1
4	1

OK
Cancel

B-4.2 Observation Wells

The same observation wells used in the steady state simulation are used in the transient simulation. But observation data must be imported for the transient simulation. This will be done for each individual well. Observation data needs to be in the following format: time of observation (e.g. days in simulation) and observation well water level. Observation well 1 is located in the upper portion of the slope.

Double click on this well, with  toggled. Unclick the box that says "Target is steady state". And then click on the Import... button.

Target Information

Target Type: Head

Target Name: ss01

Steady-State Data

☐ Target is Steady-State

Target Value: 303

Weight: 1

Group No.: 1

Species No.: 1

Minimum Bound: 0

Maximum Bound: 0

Residual = -0.58

Spatial Parameters

X: 1336153.15 Y: 196445.14

Layer: 1

☐ Head Target is Difference with Layer 0

Censoring Option: 0 - No Censoring

Transient Data... Graph... Import...

Browse to siteD/import_files/data/wl01.dat. Make sure that all text files, not just cvs files can be viewed. Click on the Transient Data... button and 55 data points should be imported.

Transient Calibration Target Information

Transient

Number of Observation Times: 55 Update

	Time	Target Value	Weight	
1	3.75	305.1741462	1	
2	6.25	305.7152078	1	
3	8.75	305.0728613	1	
4	11.25	304.0939404	1	
5	13.75	307.8174281	1	
6	16.25	308.4653405	1	
7	18.75	306.8868275	1	

OK Cancel Apply Help

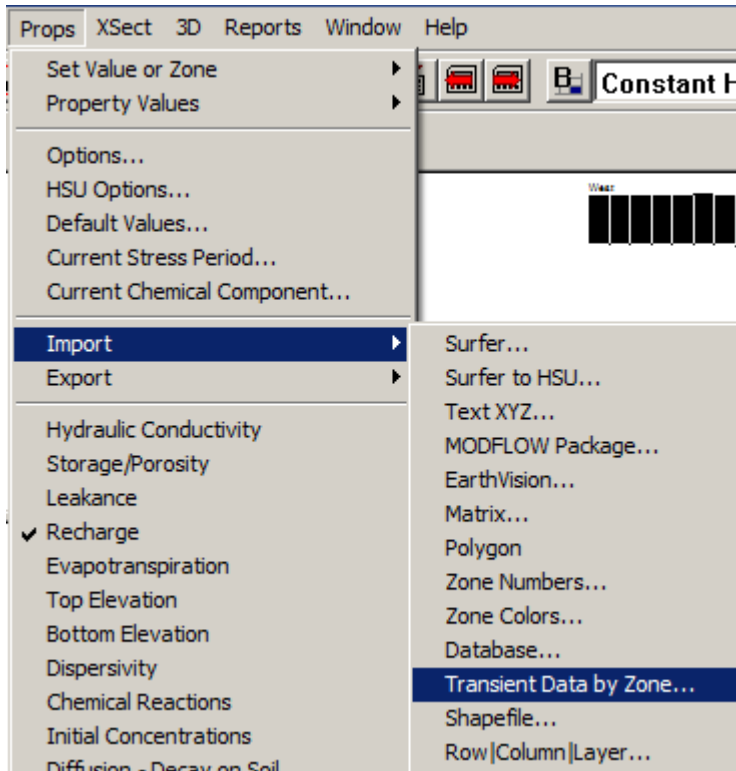
Repeat for well 2 (middle of the basin, wl02.dat) and well 3 (toe of the basin, wl03.dat).

B-4.3 Recharge

Six hour precipitation and calculated recharge values are provided in Figure 7.58. To import recharge values, make sure recharge property is toggled.



Then open Props->Import->Transient Data by Zone...



Browse to siteD/import_files/data/rch_cn90.txt. If you cannot see the file, then double check that all files (*.*) are visible. The recharge data file must have the following format: stress period number and recharge rate.

rch_cn80 - Notepad				
File	Edit	Format	View	Help
1	0.0014			
2	0			
3	0.028957529			
4	0.018212282			
5	0.008800338			
6	0			
7	0.078258039			
8	0.046022596			
9	0.00608462			
10	0.025107382			
11	0			
12	0.003690745			
13	0.001828993			
14	0.001818203			
15	0.001807508			
16	0.008880364			
17	0.001745274			
18	0.063790434			
19	0.012234751			
20	0.006559779			
21	0			
22	0.030489114			
23	0.011216637			
24	0.00109343			
25	0			
26	0			
27	0			
28	0			

GWV will ask if the File Contains Data for Multiple Zones. Click No. Then GWV will ask if the recharge pertains to zone 1. Click OK.

B-4.4 Storage Parameters

Unlike the steady state simulation, transient simulations require storage parameters to be defined.

Toggle the properties box to Storage|Sy|Porosity



Then go to, Props->Property Values->Database. Change the number of zones to 1 and hit 'Update'.

Water Table elevations are not sensitive to specific storage, S_s , and this parameter is set to a commonly used value of 10^{-4} . Porosity values are only defined for transport simulations and so do not need to be specified. Specific yield, S_y , is an important parameter and with no knowledge, S_y is set to 0.1 (or 10%) for the initial run. Calibration of S_y will occur by adjusting S_y to help match observed water levels. Hit OK.

Zone Database Information

Zone Database

Storage Property Zone Values





Stress Period Number: 1 (Recharge/ET Only)

Number of Zones:

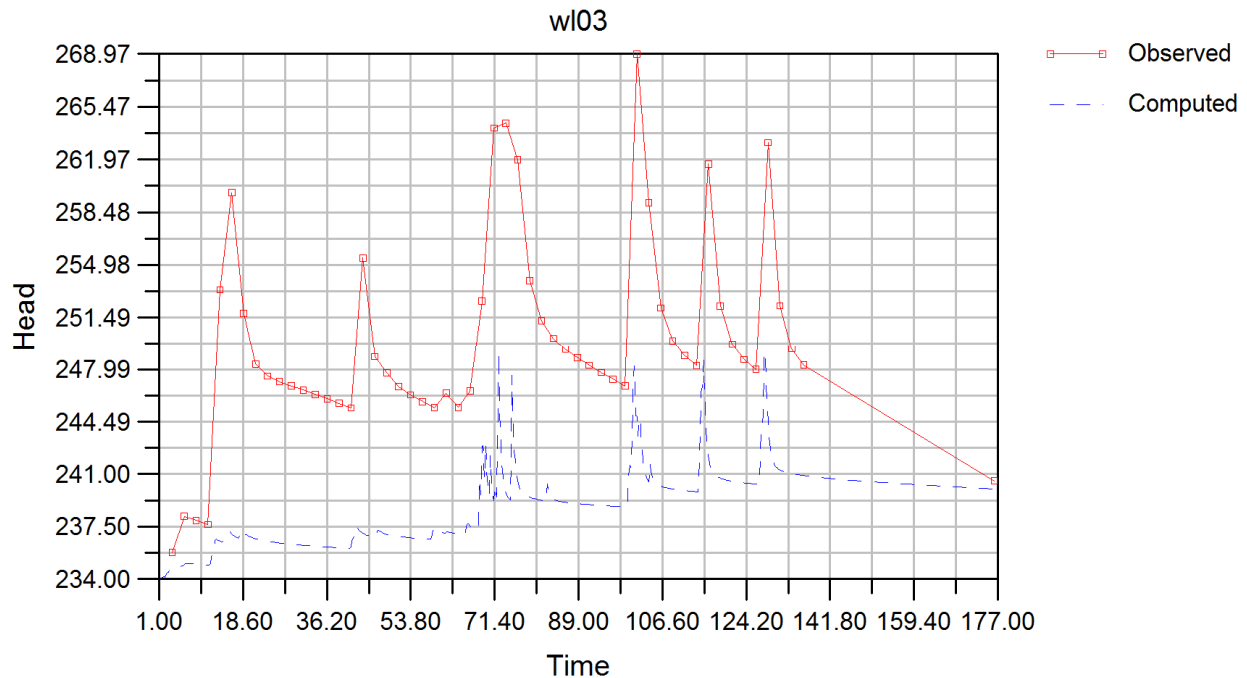
	Ss	Sy	Porosity	Porosity2	Color	
1	0.0001	0.1	0.01	0		
2						
3						
4						
5						
6						
7						

OK Cancel Apply Help

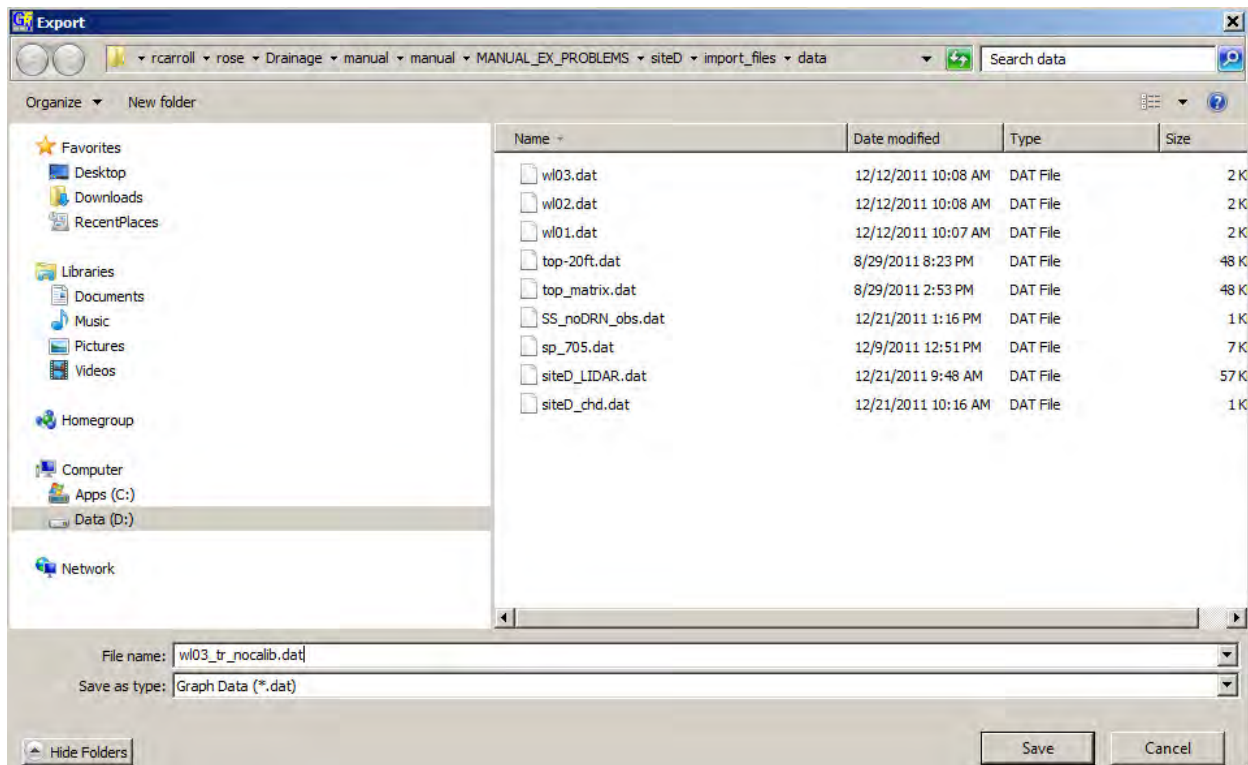
B-4.5 Model Execution.

To run MODFLOW hit the  button. Click “yes” to create Data files first?” and “Yes” to “Display Error File” if desired. The model will take much longer to run than the steady state version as 705 stress period must be solved. Once the simulation is done, GWV will ask if you want to process the results. Click Yes, then hit OK. The water levels visualized will automatically be for the last stress period. If you want to bring in a different stress period, then adjust the dialogue box to reflect the stress period desired. This can also be done by clicking on  and switching the stress period from 705 to the desired stress period. The  will bring in the previous stress period water levels, while  will bring in the water levels for the next stress period.

There are several ways to compare water levels. One can go to Plot->Hydrograph->Target and then specify the well that is desired to view. Or one can double click on the observation well and then click “graph”. For water levels in well 3,

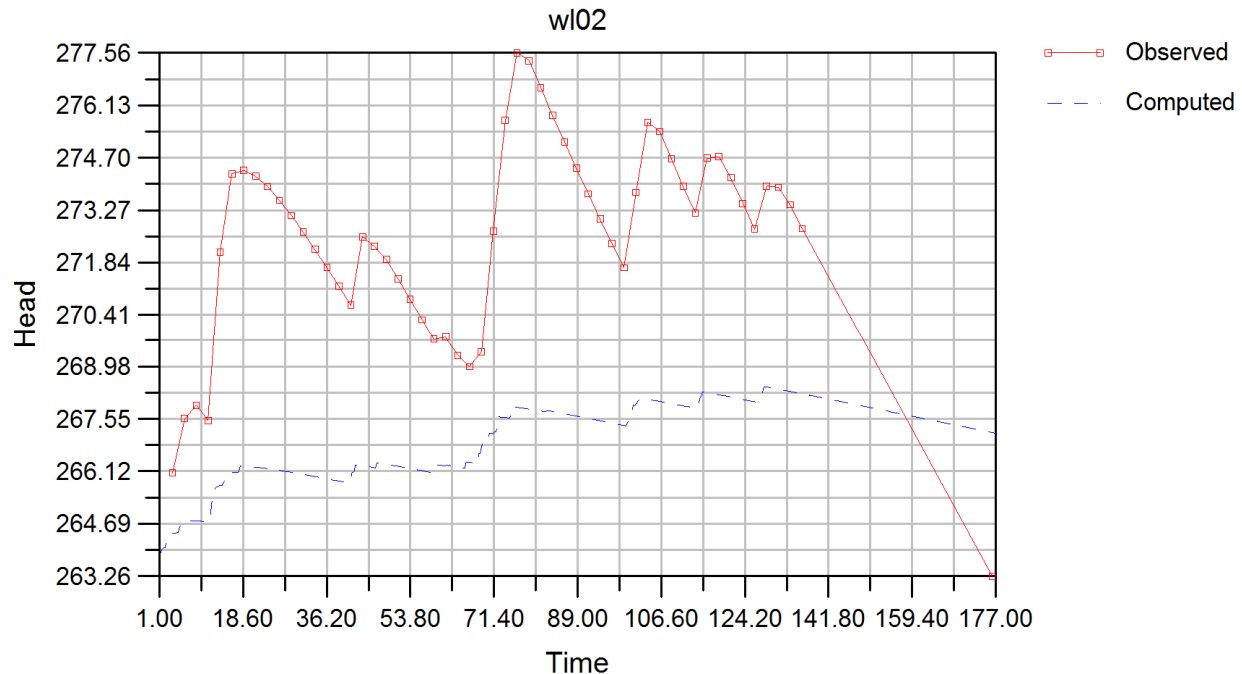


Data can be exported as a data file by right clicking on the graph and exporting,



Results show that the computed water level for well 3 is too low compared to observed values.

For well 2, water levels show a muted response to recharge, indicating that S_y is too high.



B-4.6 Transient Calibration

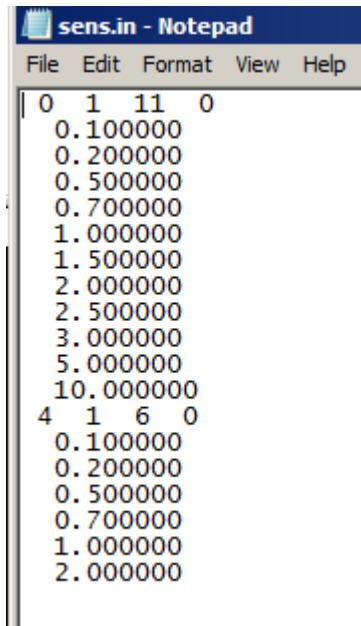
Prior to calibration, it is often informative to run a sensitivity analysis. Since the sensitivity analysis is done using multipliers, K is set back to a value of 1 ft/d and S_y is kept at 0.1. The sensitivity script is set up similar to the one used in the steady state simulation.

Go to, Model->Autosensitivity->Options...and unclick 'run from script file (if its still checked from the steady state simulation).

It is now necessary to produce a script that GWV will use to run different model realizations. First, the parameter $K_x=K_y$ is the default parameter to modify. Leave this as is. Change the Number of Simulations to 11. Then Press the "Multipliers..." button to see the default multipliers used to modify the current K values. Modify these multipliers to 0.1, 0.2, 0.5, 1, 1.5, 2, 2.5, 3, 5, 10. Press OK. Press the button "New Script", with a default name of "sens.in" in the directory CALIB\TR_noDRN\.. Press "Open" and then press "OK".

Now switch the "Parameter to Modify" to Specific Yield via the drop-down menu. Change the number of simulations at 6 and then click the Multipliers... button. Change the multipliers to 0.1, 0.2, 0.5, 0.7, 1, 2. The largest S_y tested is therefore 0.2. Press "Add to Script". Press "OK".

Press the button "Edit Script". The script should look like the following. If it does not, then edit to be similar.



```
sens.in - Notepad
File Edit Format View Help
0 1 11 0
0.100000
0.200000
0.500000
0.700000
1.000000
1.500000
2.000000
2.500000
3.000000
5.000000
10.000000
4 1 6 0
0.100000
0.200000
0.500000
0.700000
1.000000
2.000000
```

Click the “Run from Script” box and browse the Script File Name to the sens.in was just created. The default Output file name is sens.in.out. Leave as is.

Press “OK” to exit the dialogue and go to Model->Autosensitivity->Run Analysis.

Once all 17 simulations are done, GWV will ask to plot results and open the file sens.in.out and plot the sum of squared residuals. Another way to see results is to go to, Plot->Sensitivity->sum of squared residuals.

The scale for SSR is not good in comparing K_x and S_y . To improve, right click on the graph and then hit “properties”. On the Y-Axis tab, change the type from arithmetic scale to logarithmic scale and change the minimum Y to 1000, as well as click the box for Automatic Minimum and Automatic Maximum. Change the number format to POWER

Graph Information [X]

Graph | X-Axis | Y-Axis | Line Types | Line Styles

Axis Type

☐ Arithmetic Scale

☒ Logarithmic Scale

Subdivisions

Major 10

Minor 10

Minimum Y 1000

Maximum Y 1e+013

☒ Automatic Minimum

☒ Automatic Maximum

Axis Numbers

Format POWER

Precision 0

Color: Black

Font... Arial

Axis Label

Text Sum of Squared Residuals

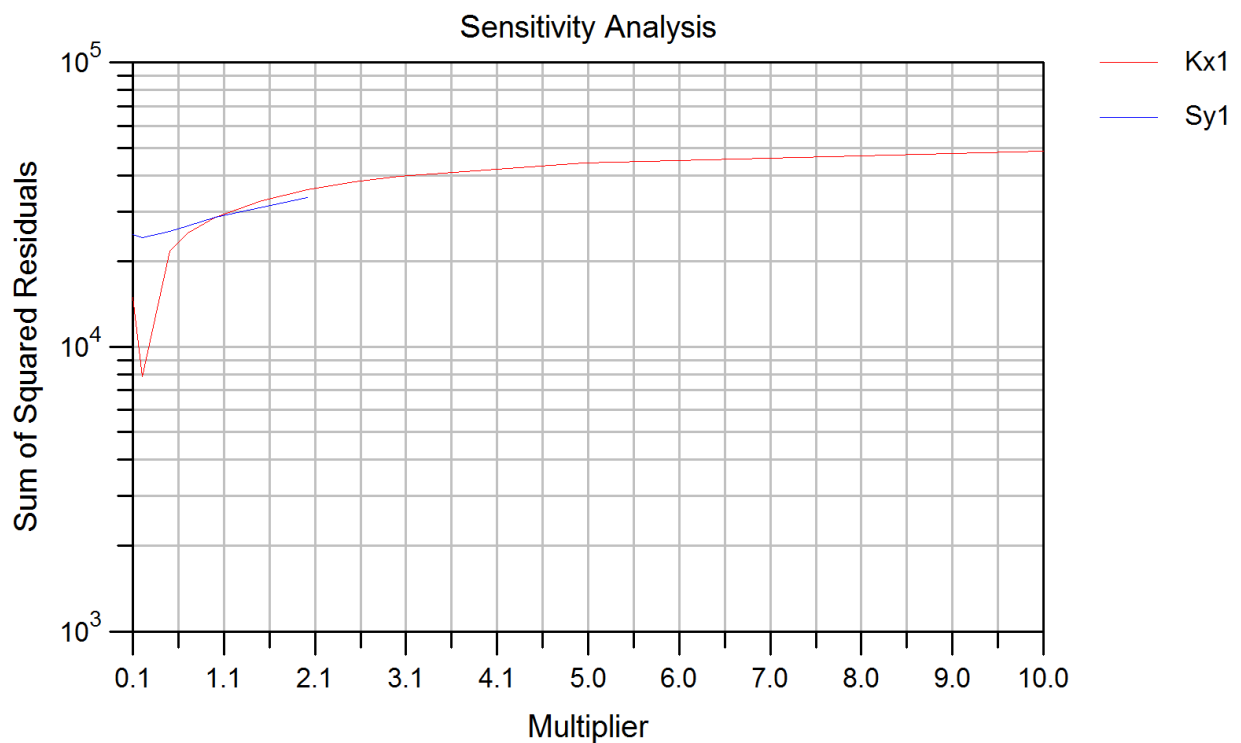
Color: Black

☐ Append Units

Font... Arial

OK Cancel Apply Help

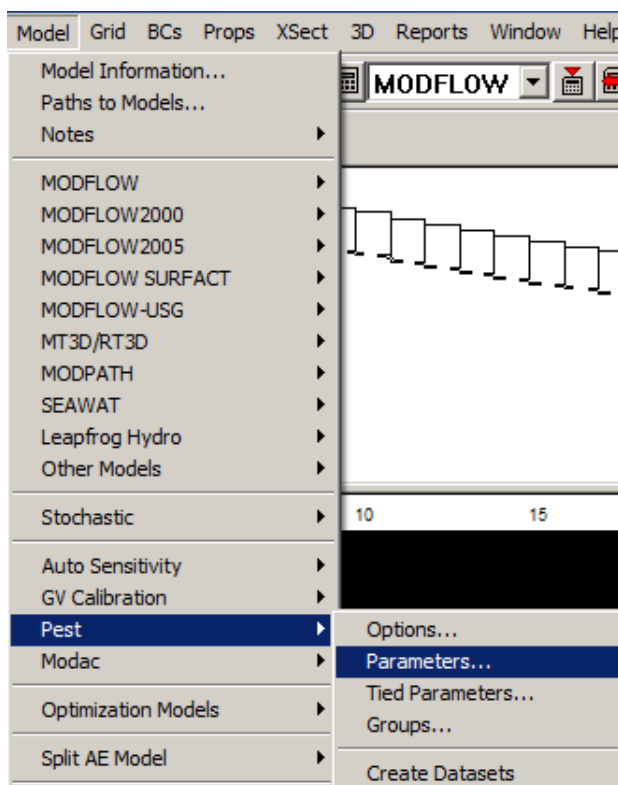
Results for the transient sensitivity are shown graphically below.



Sensitivity shows that K_x minimizes the SSR at 0.2 ft/d, while S_y also minimizes SSR at 0.2. Water levels are relatively insensitive to a multiplier of 2 for K_x ($K_x \geq 2$ ft/d), and sensitivity to S_y is less than for K_x . This is seen with only small changes in SSR with change in multiplier.

Auto-calibration is done using PEST and is similar to that done with the steady state scenario, but no calibration will include S_y . The initial guess of K_x will be set at the steady state value of 0.22956 ft/d. Go to Props->Property Values->Database and change 1 ft/d to the steady state value. From the sensitivity analysis, $S_y = 0.2$ produced the less error. Change the S_y value from 0.1 to 0.02. The better the initial guess, the quicker PEST will converge on the calibrated values.

Go to, Model->PEST-> Parameters



Keep the search range for K_x the same as for the steady state simulation. However, add S_y and allow S_y to vary between 0.001 and 0.35. The dialogue box should look similar to the one shown below.

PEST Parameters [X]

	Type	Use	Zone	Minimum	Maximum	Transform	Limit
1	Kx	<input checked="" type="checkbox"/>	1	1.00000e-003	100.00	Log	Factor
2	Sy	<input checked="" type="checkbox"/>	1	0.001	0.35	None	Factor
3	None	<input type="checkbox"/>	1	3.50000e-005	35000.00	Log	Factor
4	None	<input type="checkbox"/>	1	3.50000e-002	350.00	Log	Factor
5	None	<input type="checkbox"/>	1	5.00000e-004	5.00000e-002	Log	Factor
6	None	<input type="checkbox"/>	0	1.00000e-004	1000.00	None	Relative
7	None	<input type="checkbox"/>	0	1.00000e-004	1000.00	None	Relative
8	None	<input type="checkbox"/>	0	1.00000e-004	1000.00	None	Relative
9	None	<input type="checkbox"/>	0	1.00000e-004	1000.00	None	Relative
10	None	<input type="checkbox"/>	0	1.00000e-004	1000.00	None	Relative
11	None	<input type="checkbox"/>	0	1.00000e-004	1000.00	None	Relative
12	None	<input type="checkbox"/>	0	1.00000e-004	1000.00	None	Relative
13	None	<input type="checkbox"/>	0	1.00000e-004	1000.00	None	Relative
14	None	<input type="checkbox"/>	0	1.00000e-004	1000.00	None	Relative

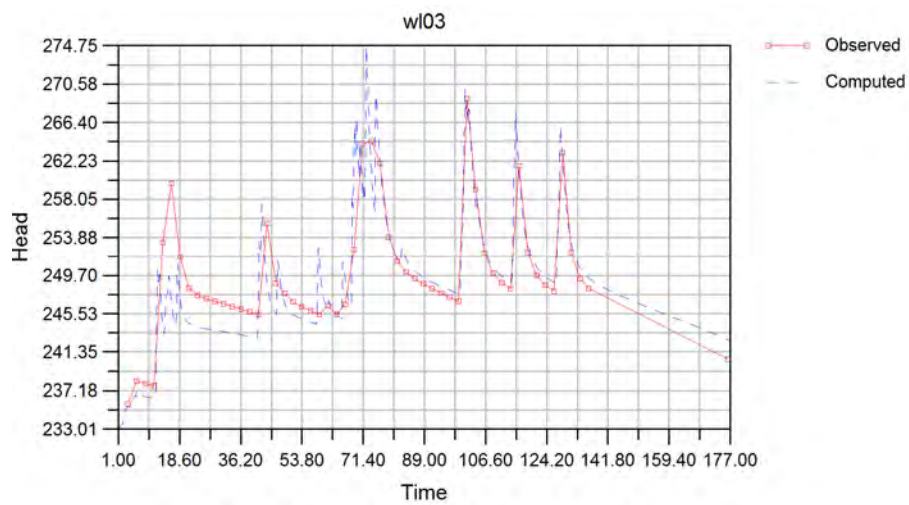
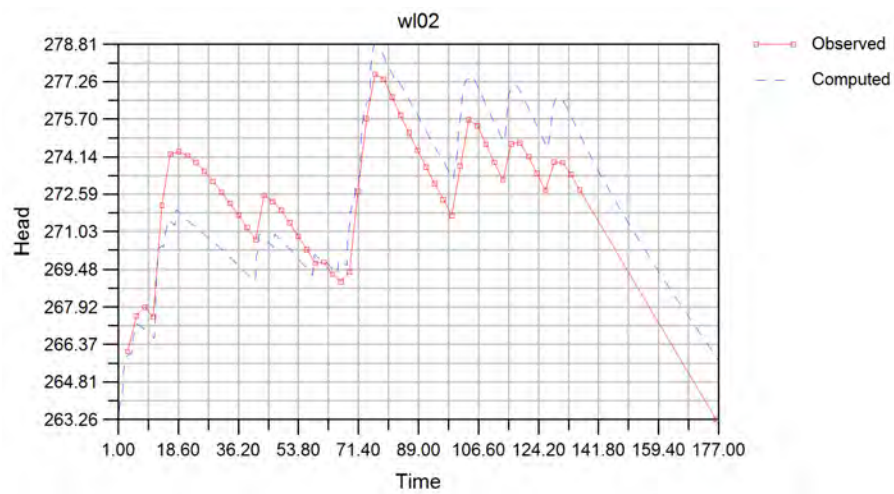
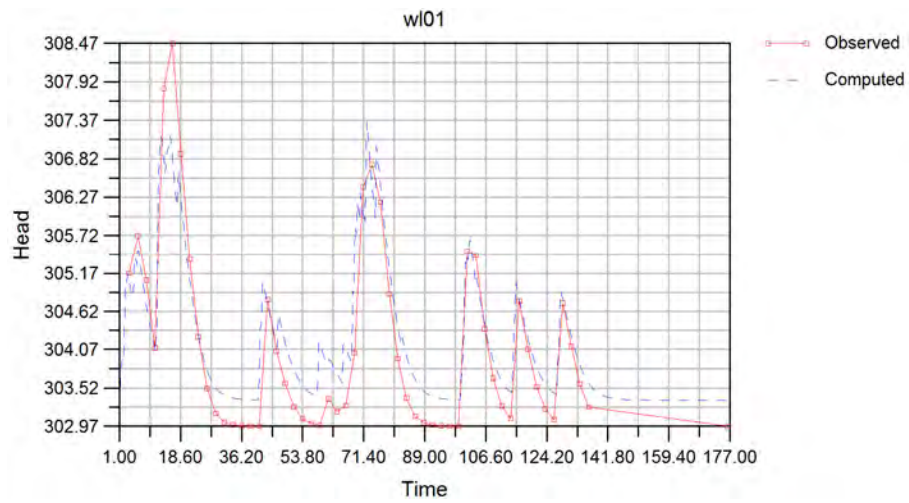
Hit "OK"

Now it is time to create the PEST input files and check that all files are properly created. To do this, go to, Model->PEST->Create Data Sets, view the Error/Warning file to ensure no errors were created.

Then Model->PEST->run PESTCheck, and finally, Model->PEST->run PEST. This may take a little while and is a good opportunity to get a cup of coffee.

When PEST is complete, the optimized value for hydraulic conductivity can be uploaded into GWV by going to, Model->PEST->Update Parameters. Calibrated parameters: Kx =0.2547 ft/d, Sy =0.02404. Rerun MODFLOW with the updated parameters. Calibrated results provide a rmse = 2.26 ft and a scaled rmse = 3.1%.

Plots of calibrated water level for each of the three observation wells are given below. Modeled results do not perfectly match observed data, but system response to recharge events is well mimicked.



Save the model.

B-5 Design Storm (Isotropic Conditions)

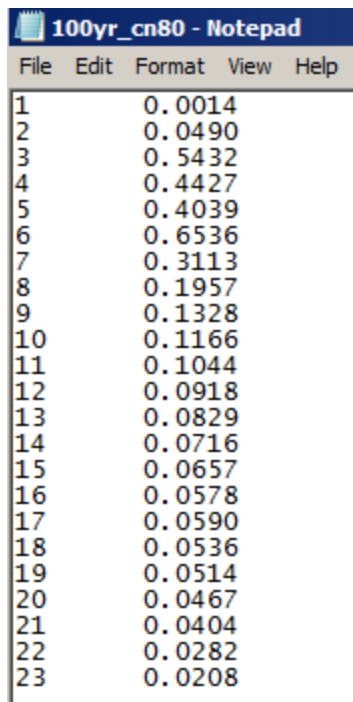
Save the model created above in the following location,

siteD\Design_Storm\Design_Storm_noDRN.gwv

Rename the MODFLOW Root Names Design_Storm_noDRN.

Reassign the working directory by going to Model->Paths to Models... and browsing to siteD\Design_Storm\ and press "OK".

The design storm is the 100 year, 24-hour event. Calculated recharge is formatted as stress period, recharge (ft/d) as given below in data file 100yr_cn80.dat with 23 stress periods.



File	Edit	Format	View	Help
1	0.0014			
2	0.0490			
3	0.5432			
4	0.4427			
5	0.4039			
6	0.6536			
7	0.3113			
8	0.1957			
9	0.1328			
10	0.1166			
11	0.1044			
12	0.0918			
13	0.0829			
14	0.0716			
15	0.0657			
16	0.0578			
17	0.0590			
18	0.0536			
19	0.0514			
20	0.0467			
21	0.0404			
22	0.0282			
23	0.0208			

Go to Model->MODFLOW->Package Options... and on the 'Basics Tab, change the number of stress periods to 23 and click Yes, and OK. Disregard the last message.

MODFLOW Options [X]

IBS/SUB | Density | I/O Formats | Streams | Wells | MNW Package | Wetlands
 Basic | BCF - LPF | Output Control | Initial Heads | Recharge - ET | Resaturation | CHDs

Data Set Titles
 MODFLOW Data Set Created by Groundwater Vistas

☐ Steady-State Simulation Number of Stress Periods
 Use Stress Period Number For Steady-state Simulation
☐ Simulate a subset of stress periods from to
☒ Save Starting Heads Head Value for No-Flow Cells
☒ Print Comments in Dataset
☐ Continue MODFLOW Simulation Even if Convergence Not Achieved
☐ Convert Dry Cells to No-Flow Cells ☐ Also Convert Dry Cells in Steady-State
☐ Use Diffusion Zones for IBOUND Active Cells

Days [v] Time Units
 Feet [v] Length Units

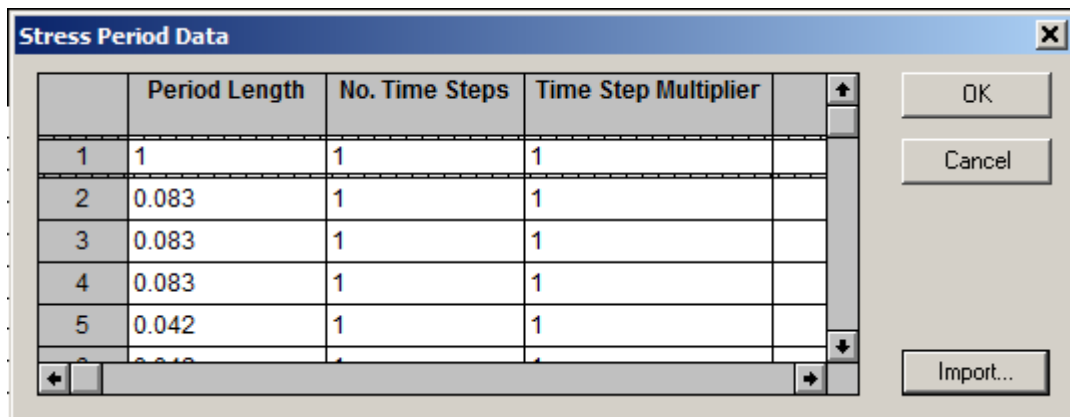
MODFLOW-SURFACT DATUM

☐ Write Input Files in Free Format
 Number of Significant Digits to Write

OK Cancel Apply Help

Next the stress periods need to be redefined for the 100 year event. Go to Model->MODFLOW->Stress Period Setup...

Hit the Import... button, and browse to siteD/import_files/data/sp_100yr.dat. The Stress Period Data dialogue box should look like the following.

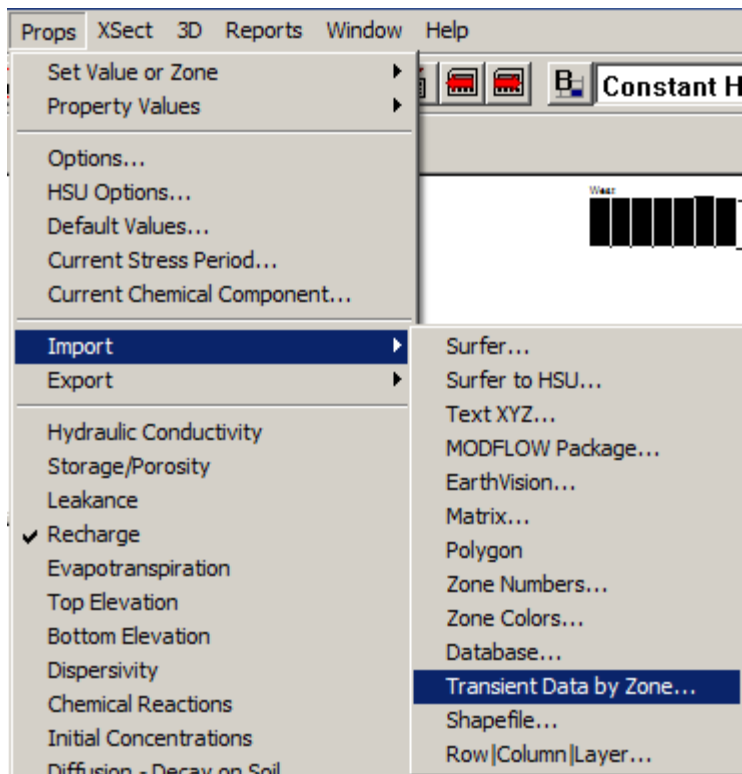


Hit OK to exit.

Toggle the properties box to recharge

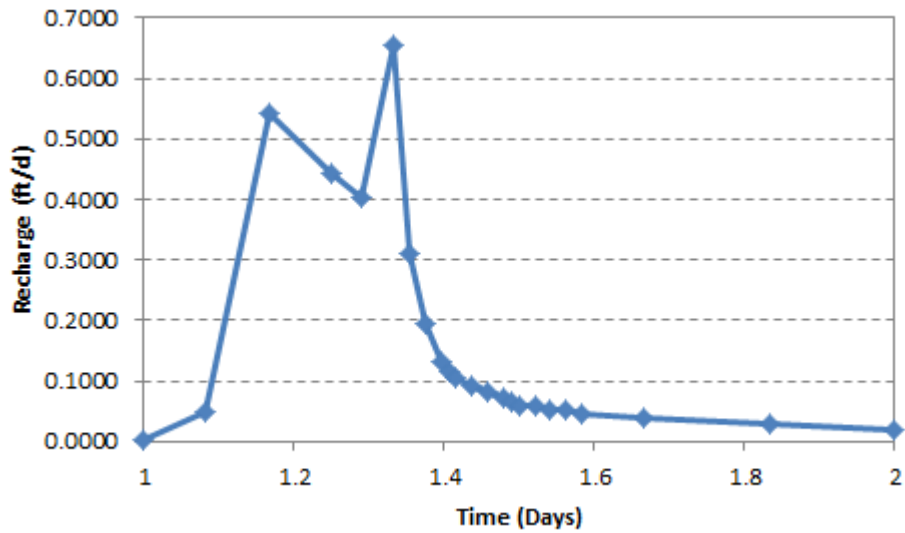


Then open Props->Import->Transient Data by Zone...



Browse to sited/import_files/data/100yr_cn80.txt. If you cannot see the file, then double check that all files (*.*) are visible. Hit "No" and "OK".

A graph of the recharge rates are provided below.



To use the same observation wells, it is necessary to remove the observed data pertaining to the transient run just completed. Double click on any one of the observation wells, then click on the “Transient Data...” button. Change the number of observation times to 1 and hit update. Change the time listed for the observation to 1. The steady state stress period occurs on the first day.

Transient Calibration Target Information


Transient

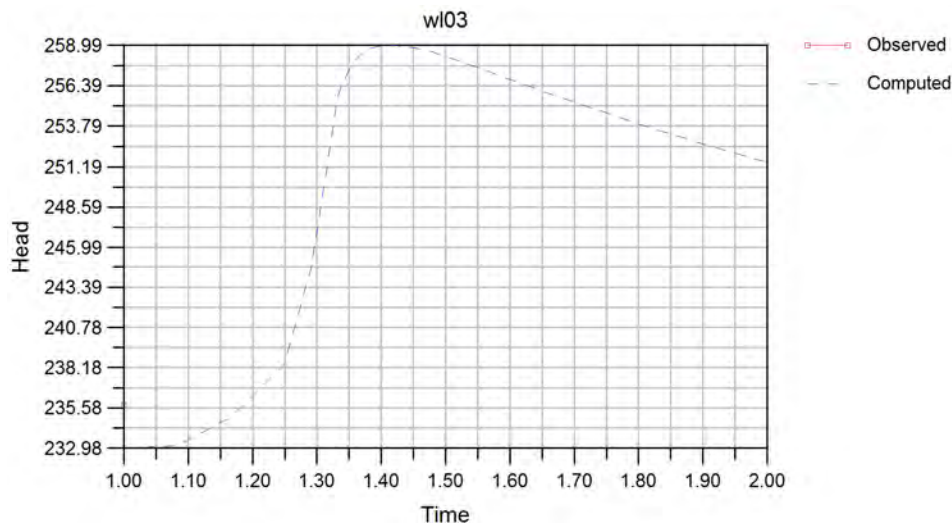
Number of Observation Times:


	Time	Target Value	Weight
1	1	235.7654853	1
2			
3			
4			
5			
6			
7			

OK Cancel Apply Help

Repeat this for the other two observation wells. The observation, or target value, is not important, other than 1 value is needed to see model results without changing the target to a monitoring well (with no data).

Save the model. Then hit  and hit Yes to building the new files. After model execution, import stress period 23. Review of water levels in each of the observation wells shows that the highest water levels occur on stress period 23 for the upper basin, and stress period 11 for the slope toe.



Hit  and import stress period 11.

Import Model Results

Read Data for This Time Period

Stress Period Time Step Browse...

MT3D? ☒ Transport Time Step Browse...

Head File Browse... Import? ☒

Drawdown File Browse... ☐

Concentration File Browse... ☐

Cell-by-Cell Flow Browse... ☐

☒ Interpolate Targets & Observation Data ☐ Plot Pressure Head

☐ Contour Water Table in Layer 1

☐ Contour Maximum Concentrations in Layer 1 and Row 1 in Section

☐ Heads are in double precision

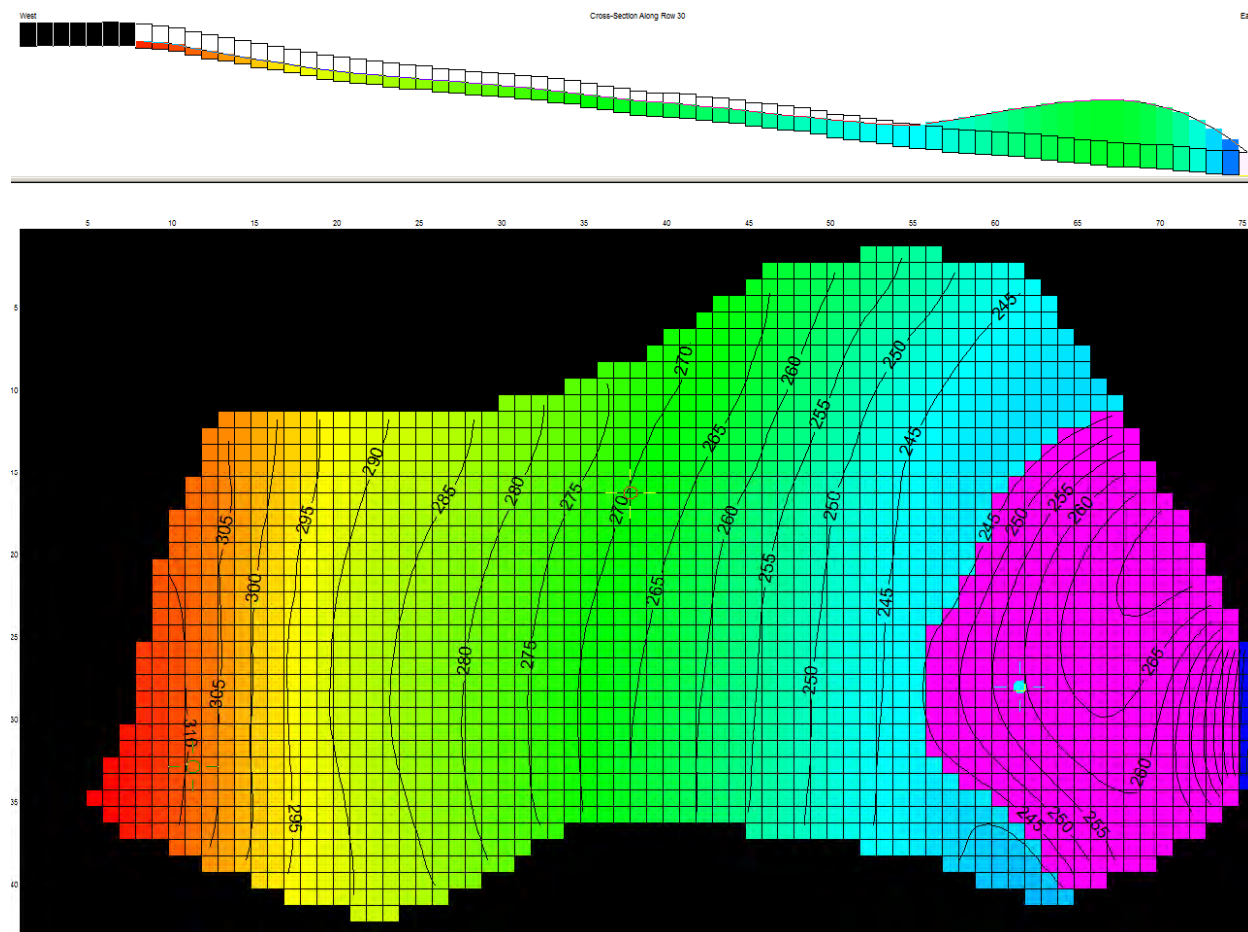
☐ Drawdowns are in double precision

☐ Concentrations are in double precision

☐ Cell-by-cell Flows are in double precision

OK Cancel

Modeled heads should look similar to the figure below,



To see modeled heads in a spread sheet go to Plot->View Results in Spread Sheet.... Results can be copied and pasted to a spread sheet application of choice (e.g. Excel, etc).

Matrix Editor

	1	2	3	4	5	6	7	8	9	10	11	12	13
17	999.00	999.00	999.00	999.00	999.00	999.00	999.00	999.00	999.00	999.00	308.21	307.35	305.80
18	999.00	999.00	999.00	999.00	999.00	999.00	999.00	999.00	999.00	308.87	308.30	307.22	305.55
19	999.00	999.00	999.00	999.00	999.00	999.00	999.00	999.00	999.00	308.92	308.23	306.92	304.92
20	999.00	999.00	999.00	999.00	999.00	999.00	999.00	999.00	999.00	309.08	308.07	306.51	304.58
21	999.00	999.00	999.00	999.00	999.00	999.00	999.00	999.00	310.25	309.53	308.18	306.29	304.07
22	999.00	999.00	999.00	999.00	999.00	999.00	999.00	999.00	310.55	309.85	308.42	306.45	304.10
23	999.00	999.00	999.00	999.00	999.00	999.00	999.00	999.00	310.91	310.22	308.95	306.65	304.05
24	999.00	999.00	999.00	999.00	999.00	999.00	999.00	999.00	311.16	310.43	309.15	306.90	304.11
25	999.00	999.00	999.00	999.00	999.00	999.00	999.00	999.00	311.48	310.64	309.19	306.90	304.13
26	999.00	999.00	999.00	999.00	999.00	999.00	999.00	312.96	312.03	310.81	309.25	307.28	304.29
27	999.00	999.00	999.00	999.00	999.00	999.00	999.00	313.27	312.29	310.81	309.11	307.04	304.33
28	999.00	999.00	999.00	999.00	999.00	999.00	999.00	313.55	312.52	310.95	309.06	306.76	303.95
29	999.00	999.00	999.00	999.00	999.00	999.00	999.00	314.02	312.92	311.26	309.05	306.54	303.72
30	999.00	999.00	999.00	999.00	999.00	999.00	999.00	314.55	313.41	311.55	308.99	306.44	303.81
31	999.00	999.00	999.00	999.00	999.00	999.00	316.35	315.28	313.73	311.68	309.23	306.47	303.71
32	999.00	999.00	999.00	999.00	999.00	999.00	316.44	315.36	313.75	311.66	309.38	306.39	303.57
33	999.00	999.00	999.00	999.00	999.00	317.49	316.59	315.26	313.39	311.46	309.13	306.28	303.69
34	999.00	999.00	999.00	999.00	999.00	317.63	316.66	315.13	313.16	311.13	308.70	305.94	303.69

Current Selection: Change Block... Replace... Math... Go to Row 1 Column 1

Layer: 1 Format Fixed Width 6 Precision 2 Copy Currently Editing: Head OK

☐ Use Color Ramp ☐ Use Log Values for Color Ramp Paste Cancel

Row 28 is highlighted. This is the row used for slope stability analysis. Values of 999.0 are dummy values used by MODFLOW to signify a no-flow cell. Heads are not predicted.

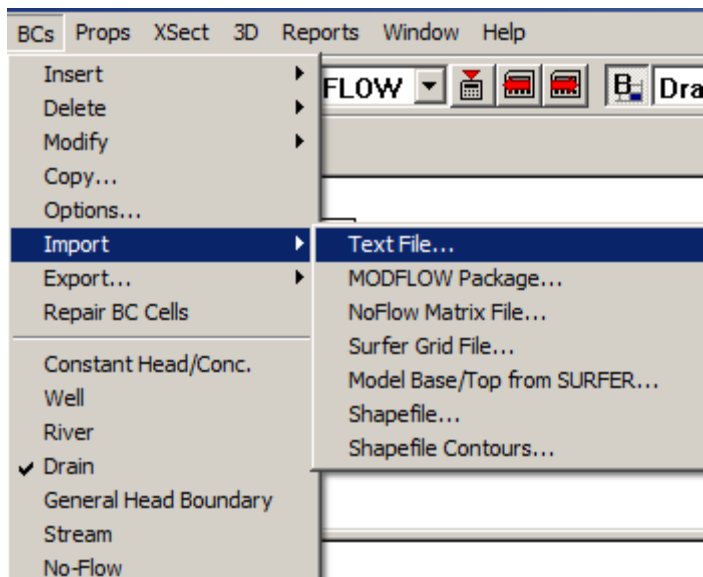
Save the model

Now to install drains. Save the model with a new name but in the same directory, Design_Storm_DRN01. Hit Yes, and change the MODFLOW Root File Name to Design_Storm_DRN01. Hit OK.

Toggle the boundary condition to Drain.



Then go to BCs->Import->Text File...



And navigate to siteD/import_files/data/drn01_siteD.dat. The data file looks like the following,

drn01_siteD.dat - Notepad									
File Edit Format View Help									
Drain array contains 4 short drains with wide spacing.									
id	row	col	layer	length	distance	top_cell	bot_cell	drain_Elev	
4	35	66	1	1.44	50.76	232.09	212.09	225.19	
4	34	66	1	0.81	49.32	231.46	211.46	225.06	
4	34	67	1	6.47	48.51	229.82	209.82	224.99	
4	34	68	1	0.61	42.04	229.01	209.01	224.43	
4	33	68	1	5.86	41.43	228.56	208.56	224.37	
4	33	69	1	2.02	35.57	228.17	208.17	223.86	
4	32	69	1	4.45	33.55	227.78	207.78	223.69	
4	32	70	1	3.43	29.1	227.04	207.04	223.30	
4	31	70	1	3.04	25.67	226.8	206.8	223.00	
4	31	71	1	4.84	22.63	225.63	205.63	222.73	
4	30	71	1	1.63	17.79	225.5	205.5	222.31	
4	30	72	1	6.25	16.16	224.07	204.07	222.16	
4	29	72	1	0.22	9.91	224.06	204.06	221.62	
4	28	73	1	0.17	0.00	223.00	203.00	221.00	

The number of lines to skip = 2 and the box allowing overlapping boundary conditions needs to be checked.

Import an XYZ File for Boundary Conditions

File Information

File:

No. of Lines to Skip at Top of File

File contains site coordinates ☐

Allow Overlapping Boundary Conditions ☒

Delete Stress Periods from Overlapped Cells ☐

Set Drain Cells as Seepage Face ☐

Make Head Value Constant ☒

Make Concentration Value Constant ☐

Now press the Coordinate Data... button and fill out as follows,

Boundary Condition Coordinate Data

Column Containing X Coordinate

Column Containing Y Coordinate

Column Containing Z Coordinate

Use either XYZ or RCL Data

Column Containing Row Coordinate

Column Containing Column Coordinate

Column Containing Layer

Default Layer (if not in file)

Hit OK. Now hit the Boundary Data button and fill out as follows,

Data Defining the Boundary Condition

Column Containing Head or Q

9

Column Containing Concentration

0

Column Containing Bottom Elevation

0

Column Containing Reach Number

1

Column Containing Segment Number

0

Column Containing Starting Period

0

Column Containing Ending Period

0

Default Reach Number

0

Default Starting Stress Period

1

Default Ending Stress Period

23

Streams

Flow in to Stream

0

Tributary 1

0

Tributary 2

0

Tributary 3

0

OK

Cancel

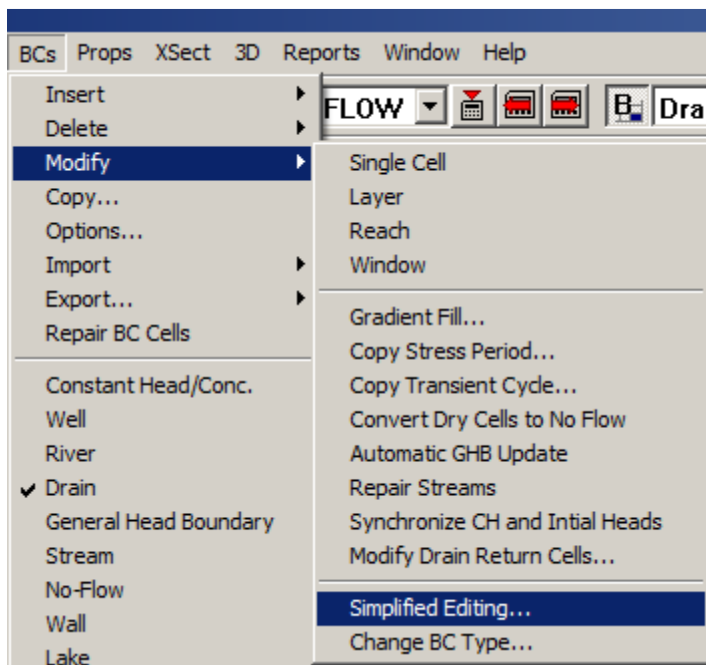
Then hit OK. Now hit the Conductance... button and fill out the dialogue box as follows, where Hydraulic Conductivity of the drains is set to the calibrated value. Length is given in column 5. Hit OK when done and hit OK once more to import the drain data.

	Column in File	Default Value
Conductance	<input type="text" value="0"/>	<input type="text" value="1"/>
Width of Boundary	<input type="text" value="0"/>	<input type="text" value="1"/>
Length of Boundary	<input type="text" value="5"/>	<input type="text" value="1"/>
Hydraulic Conductivity	<input type="text" value="0"/>	<input type="text" value="0.2475"/>
Thickness of Boundary	<input type="text" value="0"/>	<input type="text" value="1"/>
Slope	<input type="text" value="0"/>	
Roughness	<input type="text" value="0"/>	

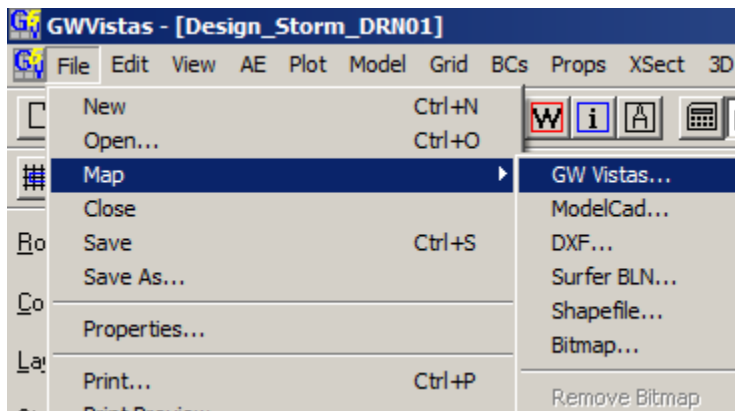
OK Cancel

60 boundary cells should be imported.

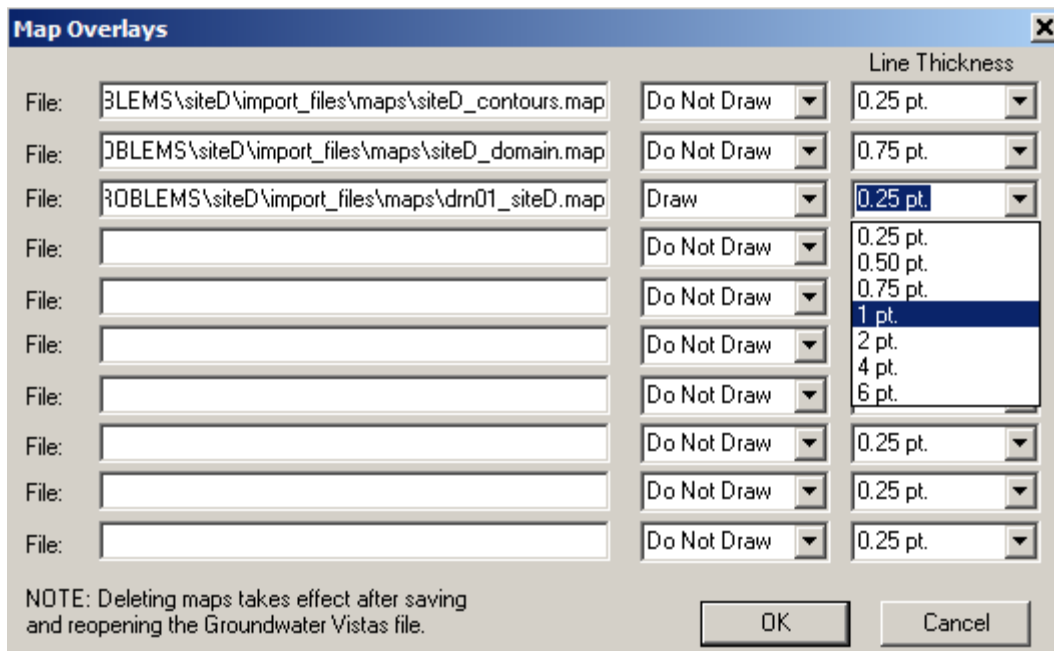
To change boundary condition parameters, such as hydraulic conductivity of the drain cells, it is best to go to BCs->Modify-> Simplified Editing....




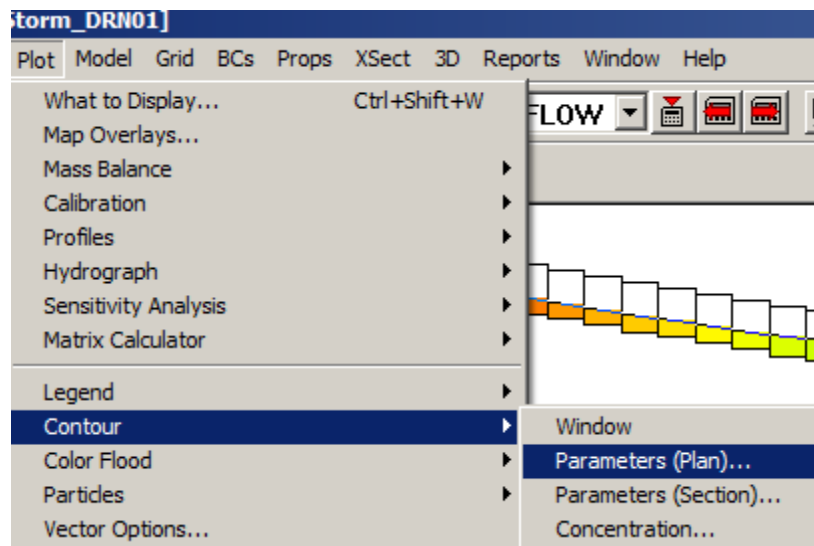
To import either a shapefile, or a GWV map file of drain array 1, go to File->Map->and choose format for import. For purposes of this example, choose GW Vistas....



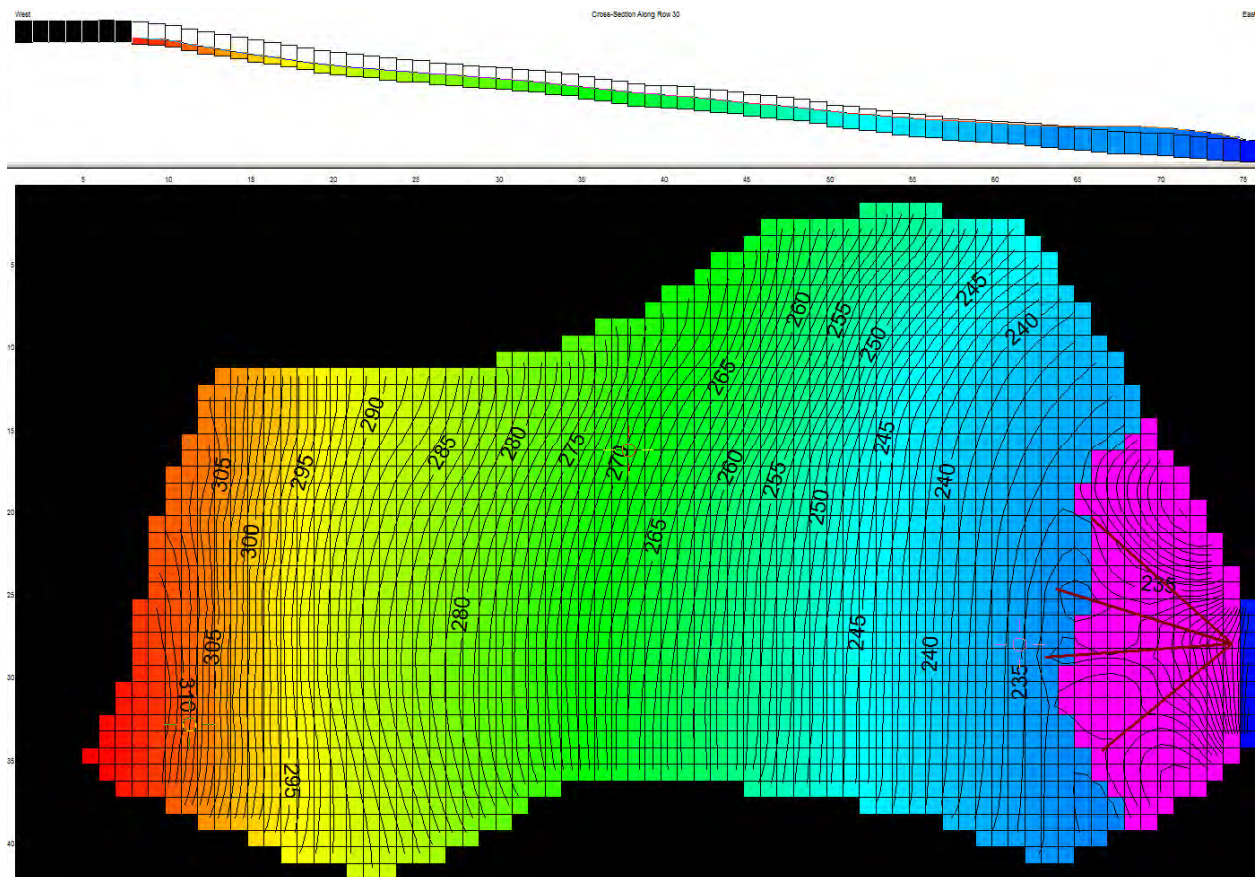
And browse to siteD/import_files/maps/drn01_siteD.map. To change the thickness of the drain lines, go to Plot->Map Overlays... and change line thickness to 1 pt.



Now its time to execute the model. Save the model and then hit  and import stress period 11. Recontour water levels to 2 ft intervals by going to Plot->Contour->Parameters (Plan)...



And changing the contour interval from 5 ft to 1 ft, and label every 5th contour To remove GWV shading of drain cells, go to Plot->What to Display... and unclick Display Boundary Conditions. Your model should look similar to the image below.



Save this model.

Included in the sited\Input_data\ file directory are shapefiles, map files and text files for drain arrays 1 through 13 for experimentation.

B-6 Modeling Anisotropy

B-6.1 Adding Model Layers

In order to model anisotropy it is necessary to have more than one model layer. For this site, four layers are modeled, each layer 5 ft thick. To add layers to the model, take the Isotropic transient model with no drains (siteD\CALIB\TR_noDRN\Tr_noDRN_Calib.GWV) and copy to a new directory sited\CALIB\4L\Tr_4L_noDRN_Calib.gwv.

Hit Yes, and rename the MODFLOW root file names to, Tr_4L_noDRN_Calib and hit OK.

Go to Model->Paths to Model and browse the working directory to the location the GWV file was just saved.

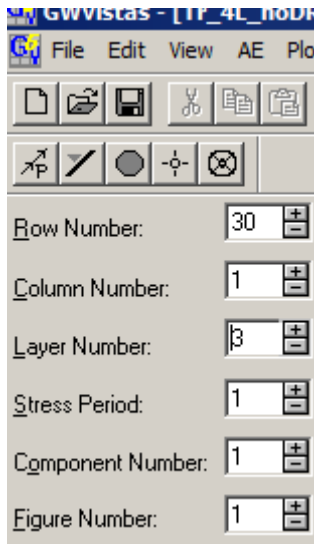
Model	Path and Code Name	Command Line
MODFLOW	C:\GWV6\MFN\WTWIN32.dll	
MODPATH	C:\GWV6\MP5\WIN32.dll	
MT3D	C:\GWV6\MT3D\WIN32.dll	
Text Editor	notepad.exe	
Path3D		

Working Directory: I:\MANUAL_EX_PROBLEMS\sited\CALIB\4L

Make this directory the Groundwater Vistas Default in System Registry ☐

To add layers to the model, go to Grid->Insert->Layer Above. The default is the new layer is 50% of the current layer (layer 1). Hit OK.

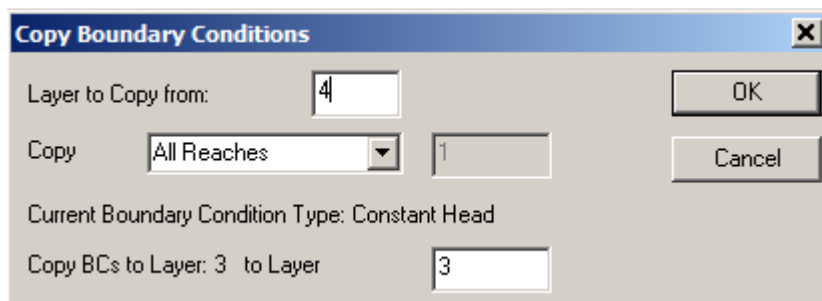
Do this one more time. There are now three layers. Toggle the left hand Layer number to layer 3,



And repeat adding one more layer. By adding layers above, the no-flow cells were copied to the new layers, but the constant head cells were not. To copy CHD cells make sure that the boundary condition is toggled to Constant Head,



And the left hand layer number is still set to 3. Go to BCs->Copy... and copy the BC from layer 4 to layer 3. Hit OK.



Toggle to layer 2 and repeat, then toggle to layer 1 and repeat.

Now it is necessary to define leakance. Toggle the properties box to Leakance,



Go to Props->Property Values->Database... and change the number of zones from 10 to 1 and hit Update. Type in a value of 10 for leakance, and hit OK to exit.

Zone Database Information

Zone Database

Leakance Property Zone Values

Stress Period Number: 1 (Recharge/ET Only)

Number of Zones: 1

	Leakance				Color
1	10	0	0	0	
2					
3					
4					
5					
6					
7					

No go to Model->MODFLOW->Model Options... and go to the BCF-LPF tab. Change Leakance Zones represents Leakance, and switch to Vertical Anisotropy. Vertical anisotropy is the ratio of horizontal hydraulic conductivity to vertical hydraulic conductivity, or VKA. By setting VKA = 10, the vertical hydraulic conductivity is one order of magnitude less than horizontal hydraulic conductivity. Also make all layers unconfined. Make sure that the storage coefficient is set to specific storage.

MODFLOW Options

IBS/SUB | Density | I/O Formats | Streams | Wells | MNW Package | Wetlands

Basic | BCF - LPF | Output Control | Initial Heads | Recharge - ET | Resaturation | CHDs

Definition of the Leakance Coefficient and Top Elevation

☒ Compute Leakance (VCONT) ☐ Use Top Elevation Zones

Leakance Zones Represent: Vertical Anisotropy

Layer Types

Layer	Layer Type (LAYCON)	BCF3/4 Averaging
1	1 - Unconfined (Layer 1)	Harmonic
2	3 - Unconfined (T Varies)	Harmonic
3	3 - Unconfined (T Varies)	Harmonic
4	3 - Unconfined (T Varies)	Harmonic
5	0 - Confined	Harmonic

☐ Use Variable Anisotropy (Ruskauff and Kladas, 1996)

☐ Compute Aquitard Leakance Like ModelCad

☒ Storage Coefficient Represents Specific Storage (Ss)


☒ Multiply K Times Layer Thickness for Confined Layers

☐ Write Vertical Anisotropy to LPF File Instead of Kz

When the single layer model was re-discretized into four layers, the observation wells were automatically kept in the bottom-most layer (this is because layers were added above). GWV observation points (i.e. targets) can only exist in one layer. Water table elevations will be plotted in layer 1 when imported, therefore observation wells need to be moved from layer 4 to layer 1. To do this, double click on an observation well, and change the layer number from 4 to 1.

Repeat for the other two wells. Then save the model.

New observation data is imported to each of the wells. Data files are found in the sited\import_data\data\anisotropic_wl01.dat for the upslope well wl01, anisotropic_wl02.dat for the mid-slope well wl02 and anisotropic_wl03.dat for wl03 located in the slopes toe. To import, double click on the well, then click on Import and browse to data file location and hit OK. Do for all three observation wells.

Hit the  button. Click “yes” to create Data files first?” and “Yes” to “Display Error File” if desired. The model will take much longer to run than the single layer model due to the additional model layers.

When the run is executed, make sure to click Contour Water Table in Layer 1. This is because model layers will go dry and this contouring will allow one to use the spread sheet application in GWV to obtain a single 2D representation of the water table surface without having to export all water levels for all four layers.

Import Model Results

Read Data for This Time Period

Stress Period Time Step Browse...

MT3D? ☒ Transport Time Step Browse...

Head File Browse... Import? ☒

Drawdown File Browse... ☐

Concentration File Browse... ☐

Cell-by-Cell Flow Browse... ☐

☒ Interpolate Targets & Observation Data ☐ Plot Pressure Head

☒ Contour Water Table in Layer 1

☐ Contour Maximum Concentrations in Layer 1 and Row 1 in Section

☐ Heads are in double precision

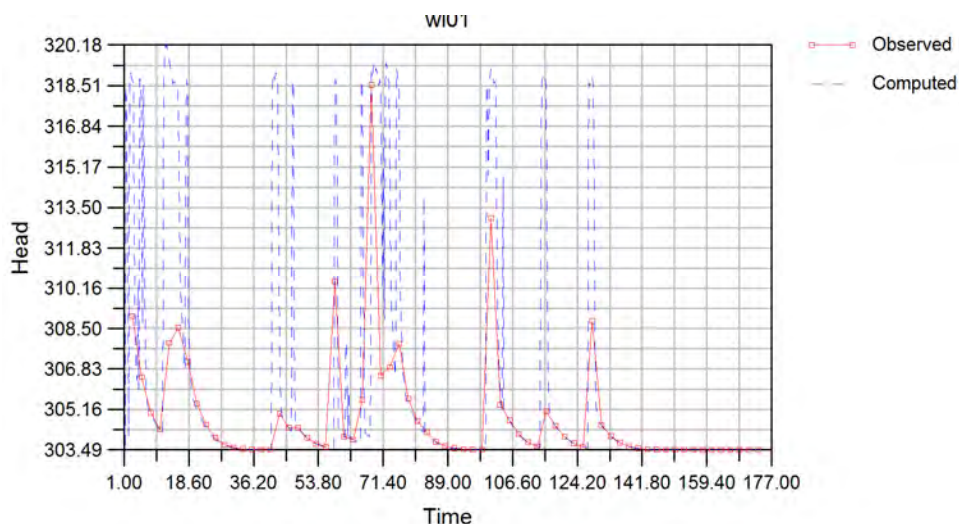
☐ Drawdowns are in double precision

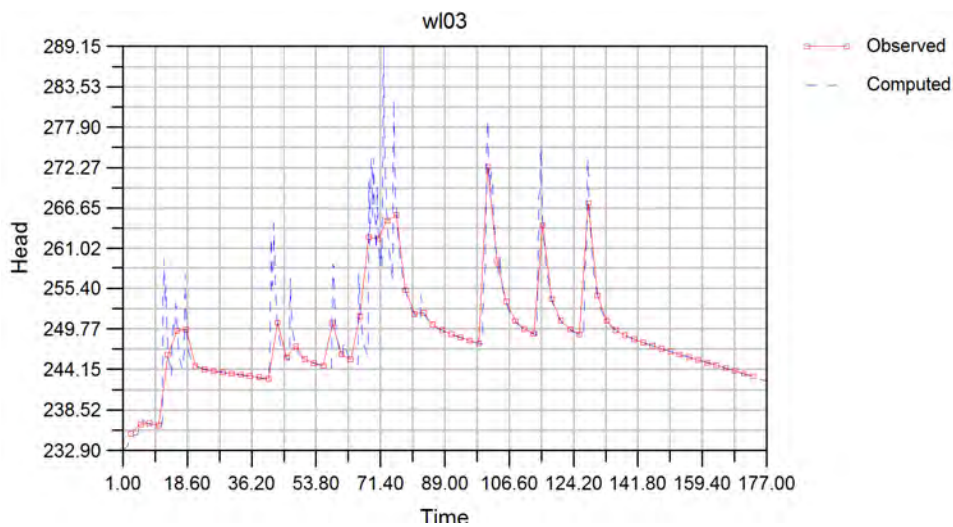
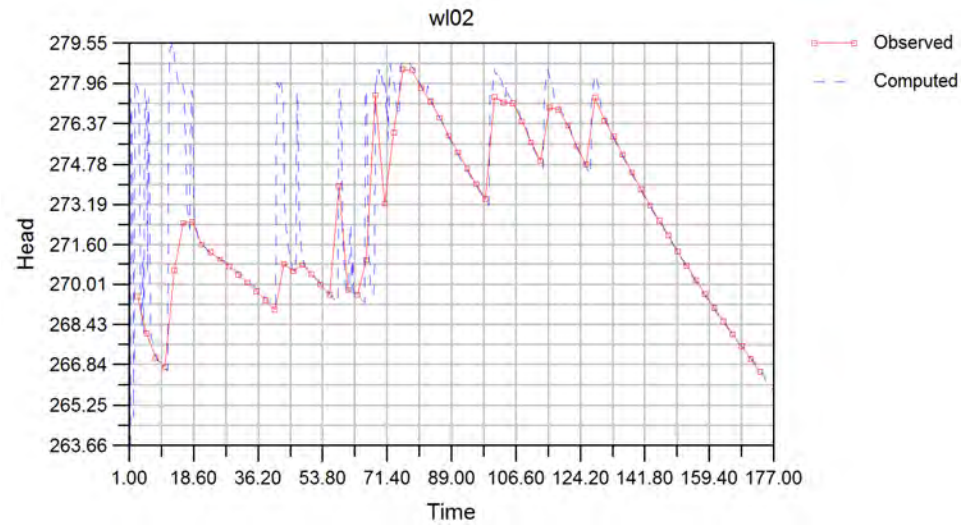
☐ Concentrations are in double precision

☐ Cell-by-cell Flows are in double precision

OK Cancel

Using calibrated K_x and S_y parameters from the isotropic simulation water levels are modeled





B-6.2 Calibration of VKA

Calibration of VKA is done manually. VKA = 1, 2, 4, 6, 8, 10 and 20 are run independently. To accomplish this, change the Leakance value from 10 to 1 in the Zone Database by toggling the property to Leakance,



Then going to Props->Property Values->Database...

Zone Database Information

Zone Database

Leakance Property Zone Values

Stress Period Number: 1 (Recharge/ET Only)

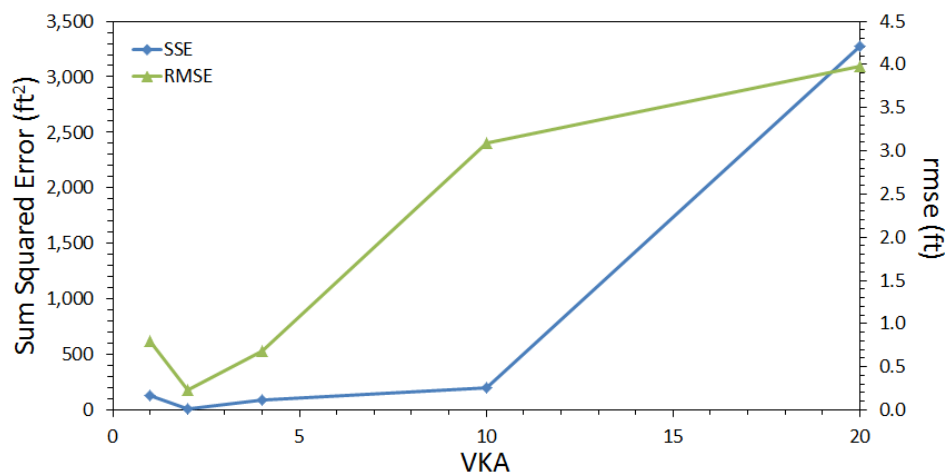
Number of Zones:

	Leakance				Color	
1	1	0	0	0		
2						
3						
4						
5						
6						
7						

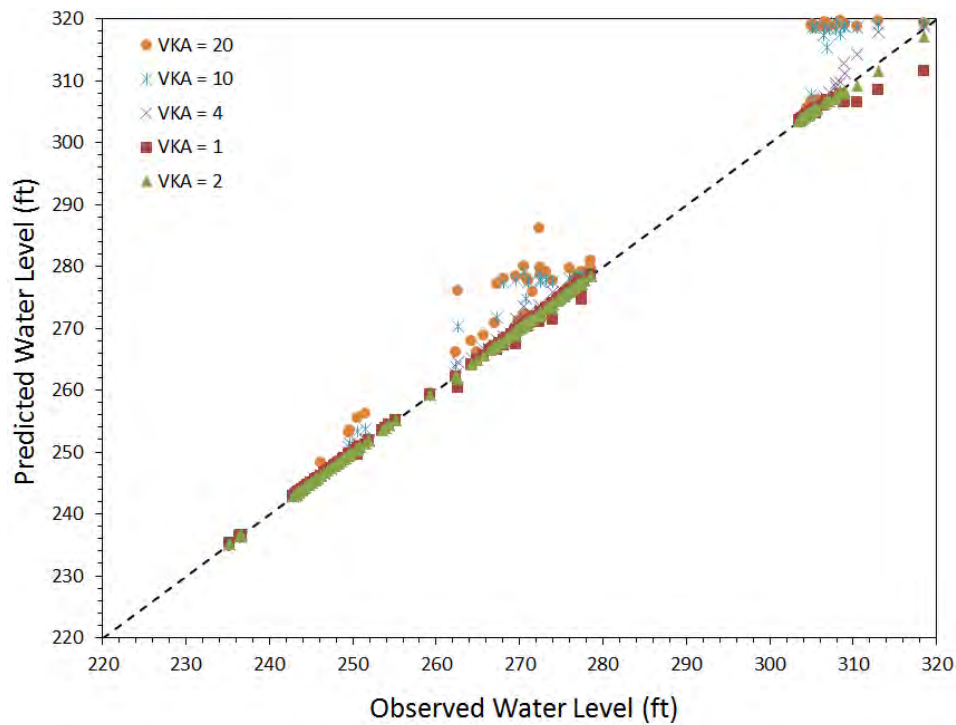
Then hit OK and then after each model simulation, go to Plot->Calibration->Statistics...

Statistics on the sum squared error (SSE) and rmse are obtained by hitting the "Statistics..." button. Results are tabulated and graphed below,

VKA	SSE	rmse (ft)	rmse (%)
1	131	0.8	1
2	10.8	0.23	0.3
4	94.8	0.68	0.8
10	197	3.09	3.5
20	3280	3.98	7.8



Data pertaining to the one-to-one regression are obtained by hitting the “Plot Observed vs. Simulated” button. Data can be exported from the plot by right-clicking and assigning to a *.dat file. Regression results are compared below.



Regression statistics and one-to-one plots show that VKA = 2 produces the best comparison to observed behavior. Variability is most evident at higher elevations in the basin, with increased VKA causing over prediction. VKA = 1 produces nearly equal results to VKA = 2, except at the highest well (wl01), where a VKA of 1.0 (isotropic) slightly under predicts observed behavior.

Appendix C

Groundwater Modeling Example - Site SR 101 MP 69.8

C-1 Site Description

Demonstration site SR 101 MP 69.8 is located in western WA State with Figure C-1 pinpointing the location via Google Earth. The surveyed map for the site is provided in Figure C-2, with 1 ft topographic contours provided. Unfortunately, the site was not surveyed to the top of the hydrologic divide and so uncertainty does exist with respect to possible water flux across the model domain. The highway crosses

the site about 2/3 from the top of the surveyed site and a creek defines the lower portion of the site.



Figure C-1: Location of study site with respect to the state of Washington.

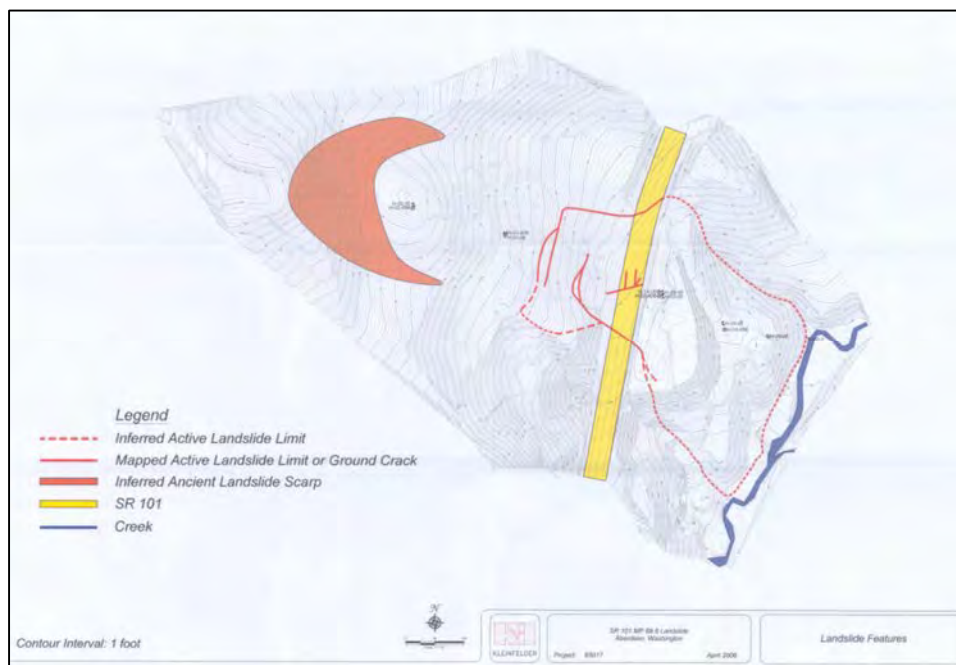


Figure C-2: Site map with 1 ft elevation contours surveyed. SR 101 is mapped across the site as well as inferred ancient and active landslide locations. The creek defines the lower boundary of the site.

Figure C-3 provides a cross section of the site with well locations provided. Geologically, the system consists mostly of disturbed claystone situated above intact claystone. Thickness of the geologic unit is approximately 100 ft. The ancient landslide slip surface is located at the contact of the disturbed and intact claystone and marked with a dashed red line. At the slope toe is a passive zone. This is assigned a separate hydraulic conductivity compared to the disturbed zone.

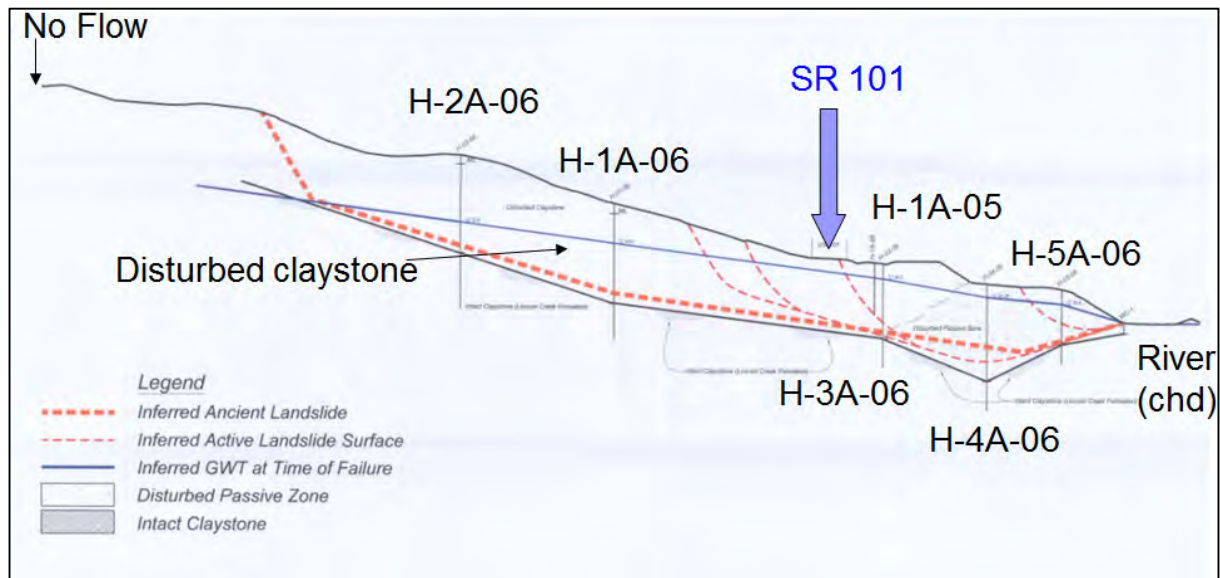


Figure C-3: Cross section of site SR 101 MP 69.8. A no-flow and CHD boundary are assigned to the edges of the site and the intact claystone is assumed impermeable. SR 101 is indicated as are several monitoring wells located at the site.

C-2 Model Domain and Grid

The model domain and grid are shown in Figure C-4. Cell dimension is 10 ft x 10 ft and wells are shown in plan-view.

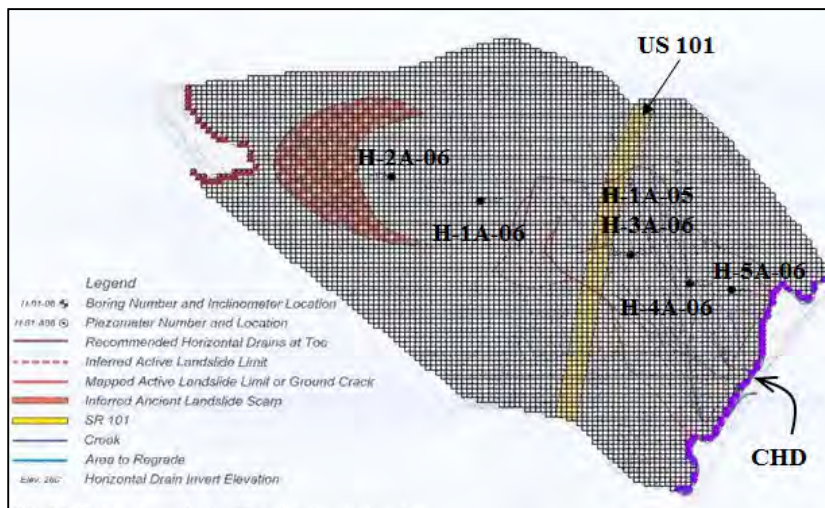


Figure C-4: Model grid with well locations and CHD marked.

C-3 Modeling Strategy

The modeling sequence for MP 69.8 is shown in Figure C-5. A slightly more advanced iterative approach to calibration is done for pre- and post - drain scenarios.

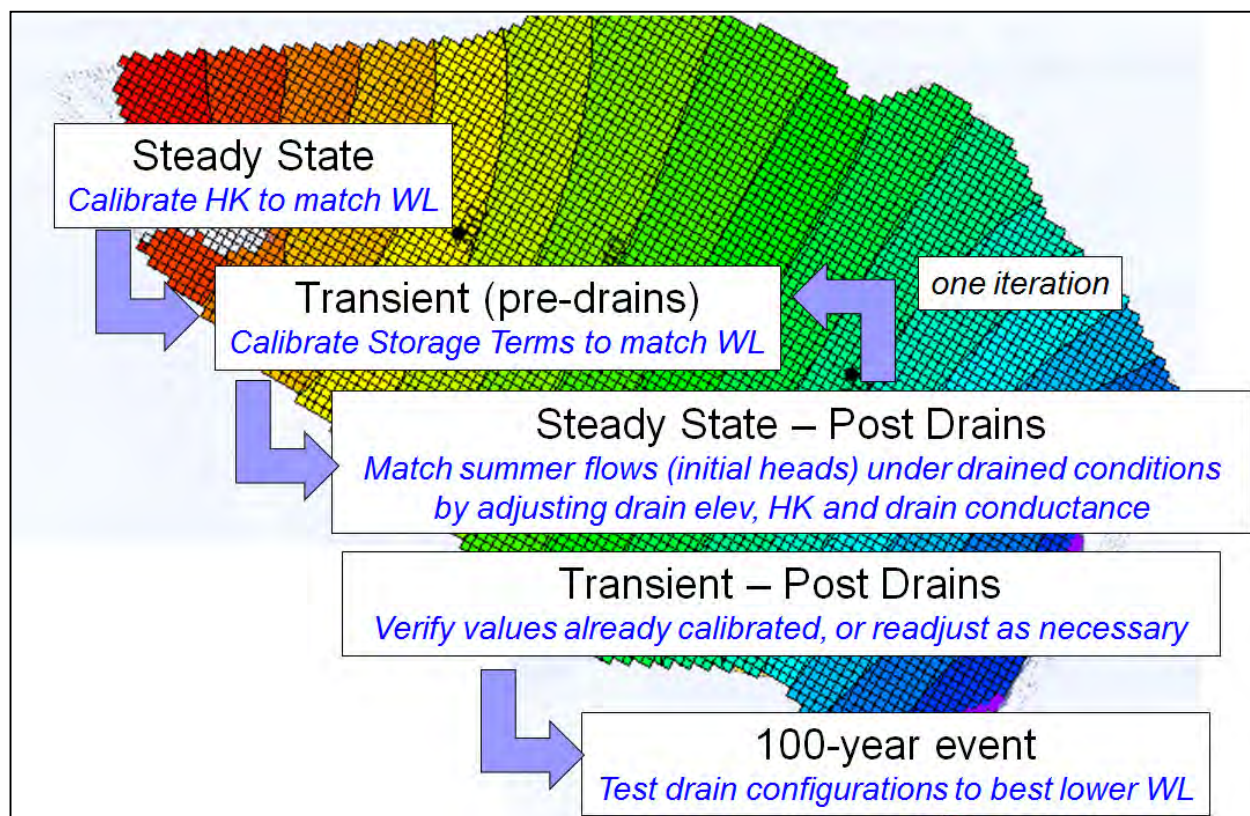


Figure C-5: Modeling sequence used for MP 69.8.

C-3.1 Steady State Conditions

Steady state conditions for pre-drain water conditions in four wells is done by adjusting the hydraulic conductivity in the disturbed claystone to 0.46 ft/d and in the passive zone in the slope toe to 0.6 ft/d. Steady state recharge is estimated at 0.00924 ft/d, to represent the average computed recharge between years 2005-2007. A regression of observed and predicted steady state water levels is given in Figure C-6, with an $rmse = 0.33$ ft.

C-3.2 Transient Conditions

Transient simulations are defined as pre-drain, and post drain. Figure C-7 shows water levels in various drains along with a timeline of when emergency drains were installed in upper slopes of the site during

the winter of 2006, as well as when non-emergency drains were installed in the slope's toe region (summer of 2006).

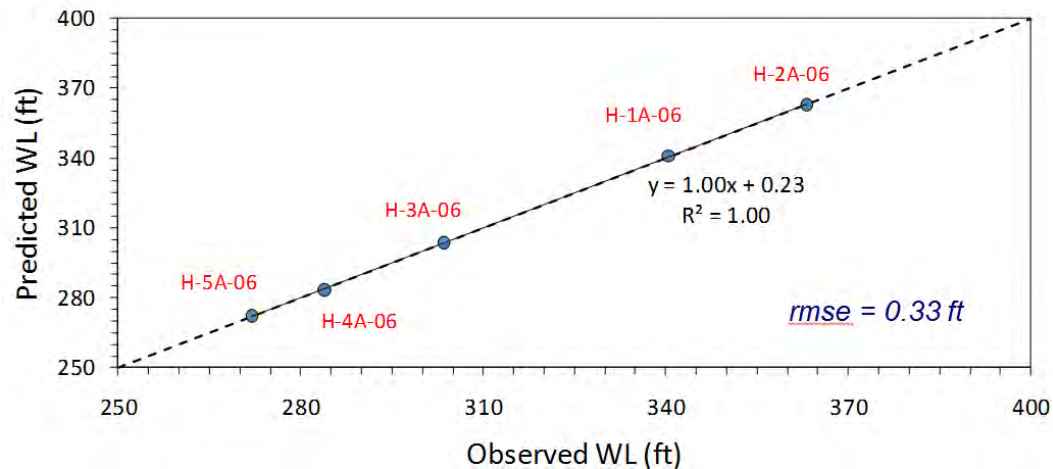


Figure C-6: Pre-drain steady state water levels.

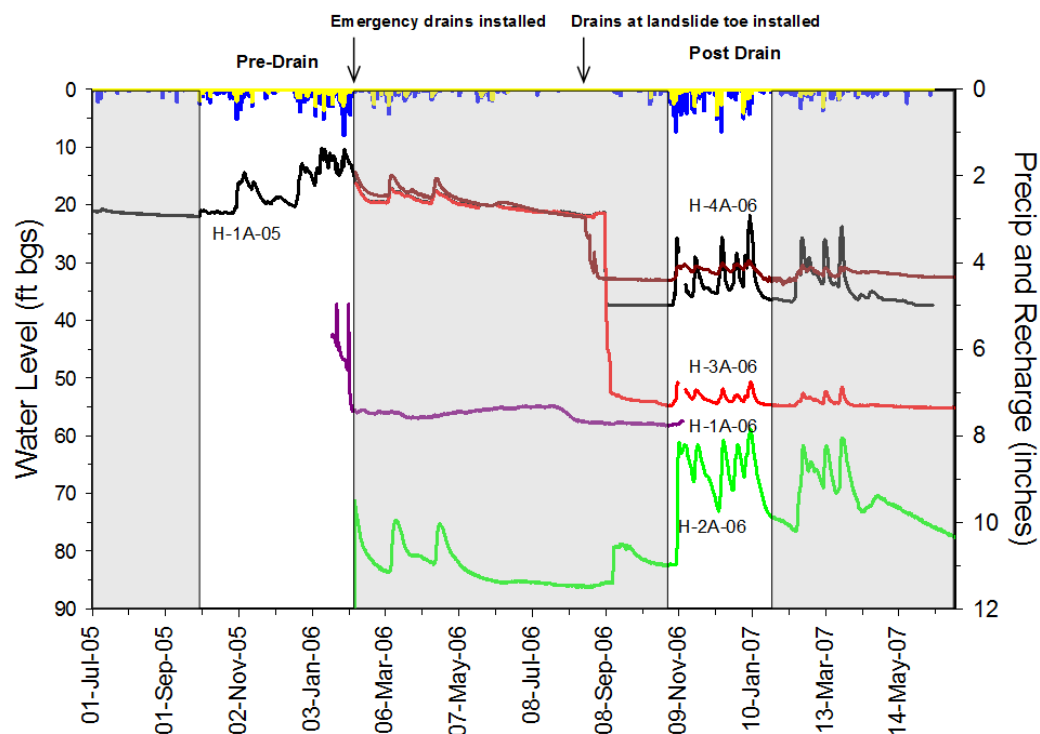


Figure C-7: Water levels for various monitoring wells located in site MP69.8. Modeled time periods are indicated as “pre-drain” and “post drain”. The post drain period represents both emergency and toe drains.

The pre-drain scenario was used to calibrate the storage terms S_s and S_y to 0.003311/ft and 0.045, respectively to best match 2005 water levels in H-1A-05. Figure C-8 shows observed and predicted water levels.

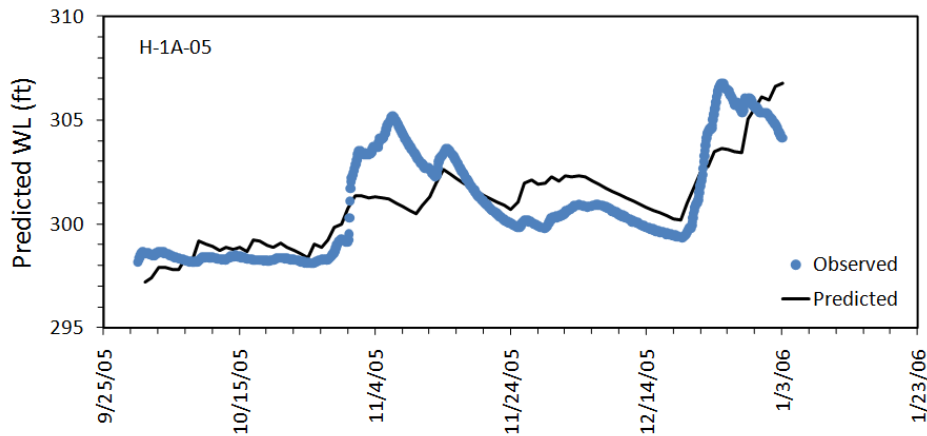


Figure C-8: Observed and predicted water levels for well H-1A-05 for the pre-drain scenario.

Drain layout with wells marked is given in Figure C-9. Modeled water table elevations are provided for the first stress period that is run to steady state in order to get water levels a function of drain layout. Emergency drains are located in the upper portion of the basin (above and just below the highway), while the landslide toe drains originate at the bottom of the slope. Drain specifications were provided by the geotechnical report; however, many of the elevations of drain are only approximate.

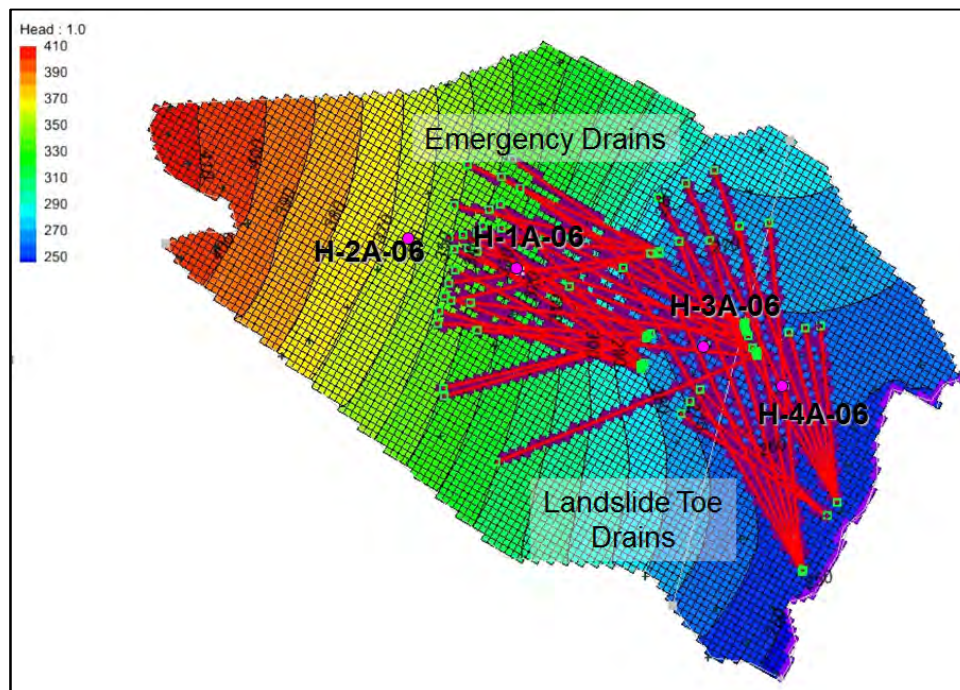


Figure C-9: 2010 post drain scenario showing steady state water levels at the start of the simulation. Well locations are indicated.

Steady state conditions are assumed in the summer of 2010, prior to significant rainfall on the site. Uncertainty in drain elevations and lack of knowledge of drain conductance allowed the adjustment of these parameters to help match summer water levels. The former was adjusted to lower the rmse in predicted water levels while C_d was adjusted to best match observed drain flow ($C_d = 9.0 \text{ ft}^2/\text{d}$). MODFLOW simulated drain flow is unable to capture lags in system since unsaturated flow is not accounted for and recharge is assumed to occur immediately with precipitation. In addition, drains do not always flow with stored water, while MODFLOW tracks all water entering the drain as drain flow at the moment it enters the drain system, not necessarily what exits the drain pipe at the tip of the cluster. However, trends in drain flow are captured as is overall water balance aspects. In addition, calibrated hydraulic conductivity was used as an initial guess in the new simulation. Results indicate little change in K values.

Predicted water levels are provided in Figure C-10 and show that greater response in water levels is predicted than observed. This is believed a result of not including unsaturated flow in the model, which may mitigate water levels as water percolates through the vadose zone during small rain events. Therefore model results are likely a “worst” case scenario of water level response for relatively thick geologic strata, but may be more indicative of water levels for thinner geologic layers (i.e. 20 ft as demonstrated in Chapter 7). Model results oscillate about observed values and are considered adequate for modeling purposes.

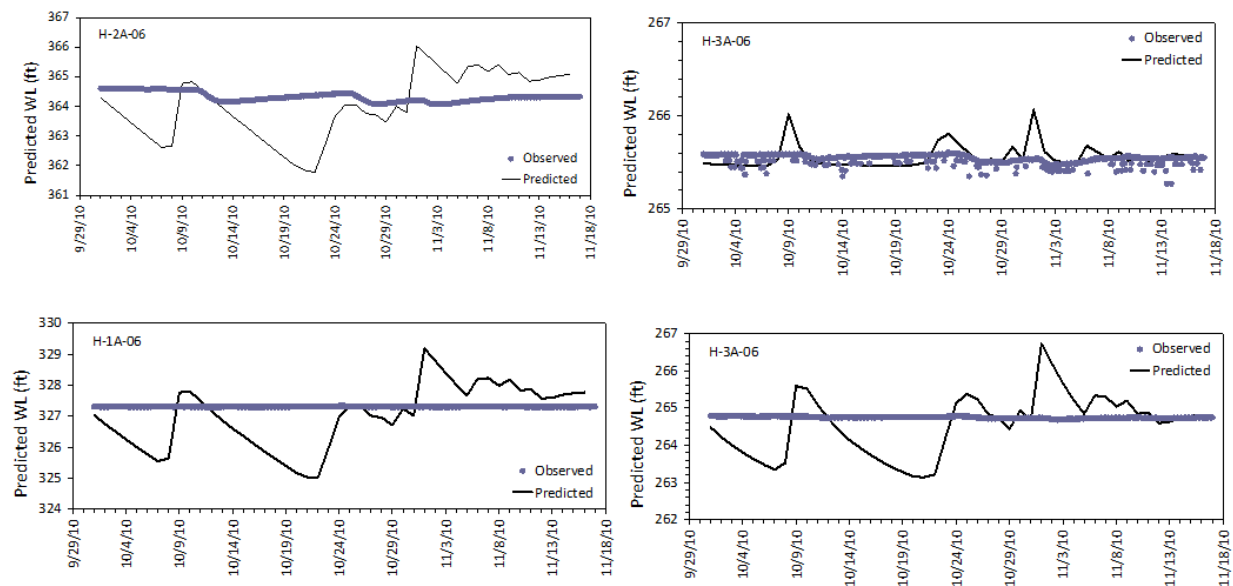


Figure C-10: Transient water levels for post drain scenario 2010.

C-4 Design Storm

The design storm is based on the 100-year 24-hour total precipitation of 6.5 inches based on NOAA atlas 2 (1973, <http://www.wrcc.dri.edu/pcpnfreq.html>). The groundwater model is initiated with steady state conditions prior to the storm using the drain layout shown in Figure C-9. The rise in water levels is compared to steady state conditions. The model is run for a total of two weeks to monitor how water levels recede after the 24-hour storm event. Modeled water levels for each of the monitoring wells is given in Figure C-11.

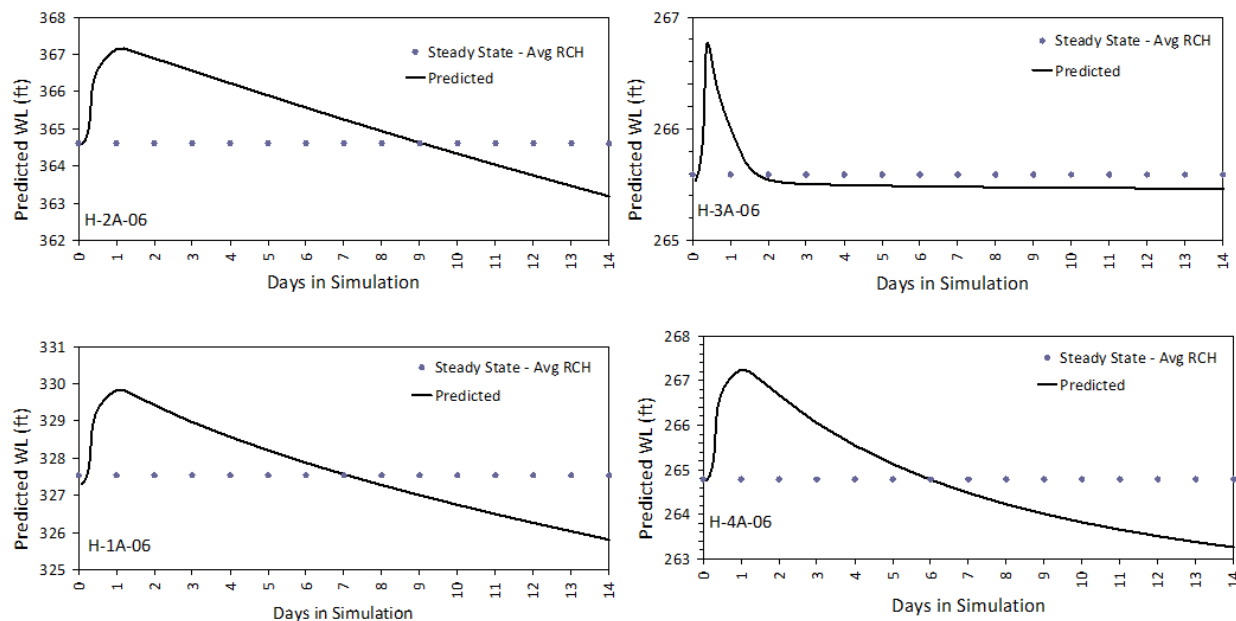


Figure C-11: Predicted water levels at the four monitoring wells for the 100-year design storm. Rising water levels are compared to steady state conditions computed with steady state recharge. Water levels drop below steady state water levels after 10 days with no recharge.

The question that arises in terms of design is which drains are doing the most to maintain water levels at steady state conditions at the end of the 1-day storm event? Figure C-12a shows contours of water level increase over steady state water levels on day 1 of the storm. It is evident that only one drain array is able to keep water levels close to steady state conditions during the storm event. This drain array is located in the toe region. Other drains are ineffectual due to installation elevations that are too high.

A hypothetical simulation is conducted with all drains lowered by 10 ft. Figure C-12b shows contours of water level increase over steady state water levels on day 1 of the storm. Lowering drain elevations improves the effectiveness of the upper slope's emergency drains in lowering water levels, but most of the gain in maintaining steady state water levels is acquired in the toe region of the slope. The experiment is repeated given a lowering of all drains by 20 ft. Figure C-12c shows that effectiveness of

drains continues to improve, with more notable changes in the upper slope. In conclusion, toe drains are most efficient in reducing water levels, with effectiveness of drains highly dependent on the elevation of these drains.

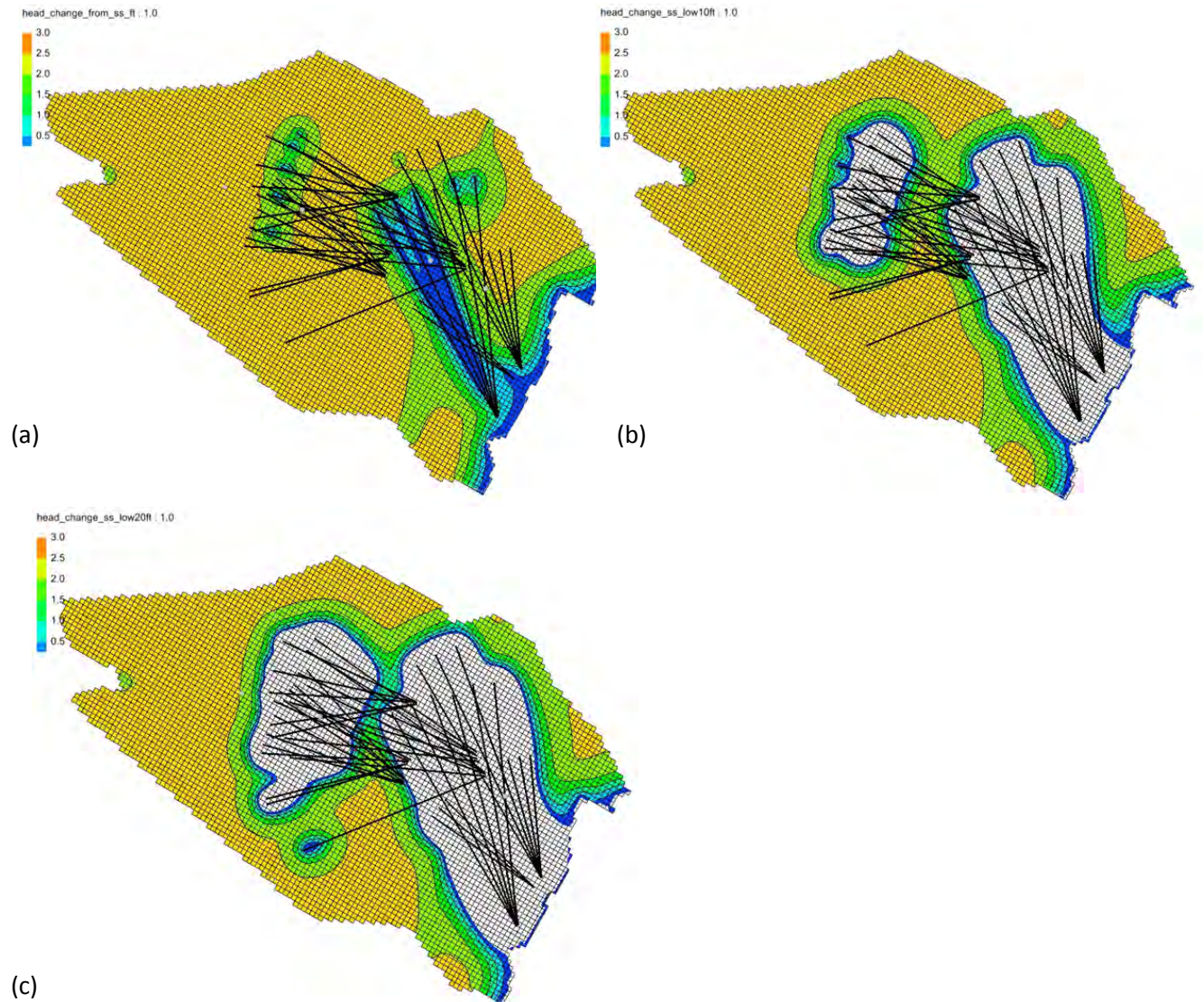


Figure C-12: The maximum change in water level from steady state conditions (a) for estimated drain elevations, (b) drain elevations lowered 10 ft, (c) drain elevations lowered 20 ft.

C-5 Geotechnical Analysis and Drain Arrays

Figure C-13 shows a cross section down the central axis of the basin as provided in Figure C-3. Using the Bishop simplified method two rotational failures are found for which FOS < 1.0. A small rotational failure is predicted to occur below US 101 in the toe of the slope, and a larger rotational failure that extends upslope above the highway. The critical water surface, for which failures are expected to occur

is shown as a dashed red line while the range in observed water levels in well H-1A-05 shows that at this location water levels are close to critical.

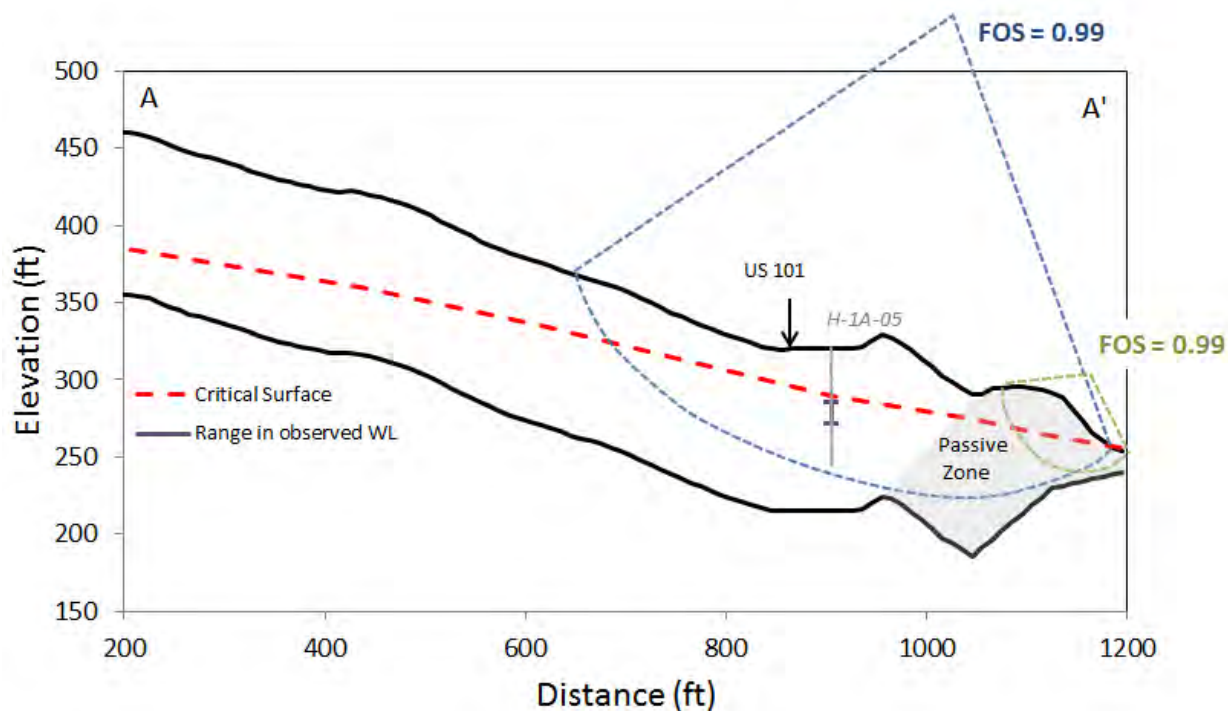


Figure C-13: Estimated critical water surface and associated failures for which FOS < 1.

Figure C-14 shows the water table profile estimated using the numeric model and the design storm event given no horizontal drains. Water levels rise above the critical failure surface and failure will occur above and below the highway. Figure C-15 shows several predicted water level profiles for the design storm given different drain configuration. The blue-line represents water levels if only emergency drains are installed in the upper slope. These drains are unable to sufficiently lower the water table surface below the critical water level in a majority of the slope and failure is likely. Water table profiles for all drains and only slope toe drains are nearly identical. This signifies that landslide toe drains are responsible for most (all) of the water level reduction and the upslope emergency drains are made obsolete after the toe drains are installed.

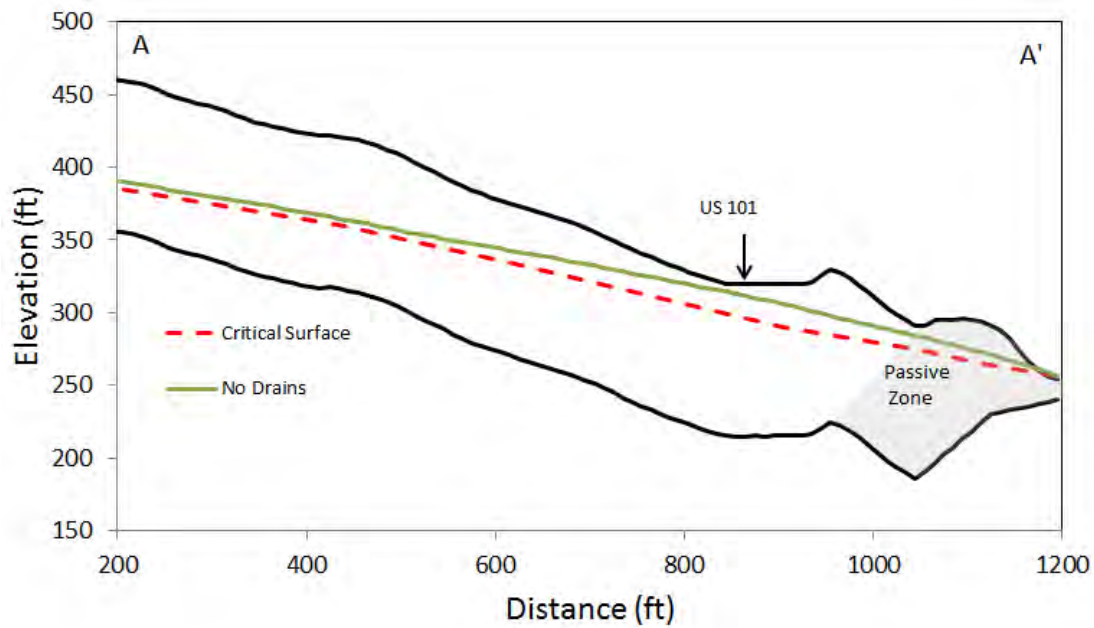


Figure C-13: Water levels predicted during the design storm given no horizontal drains and compared to the critical water surface.

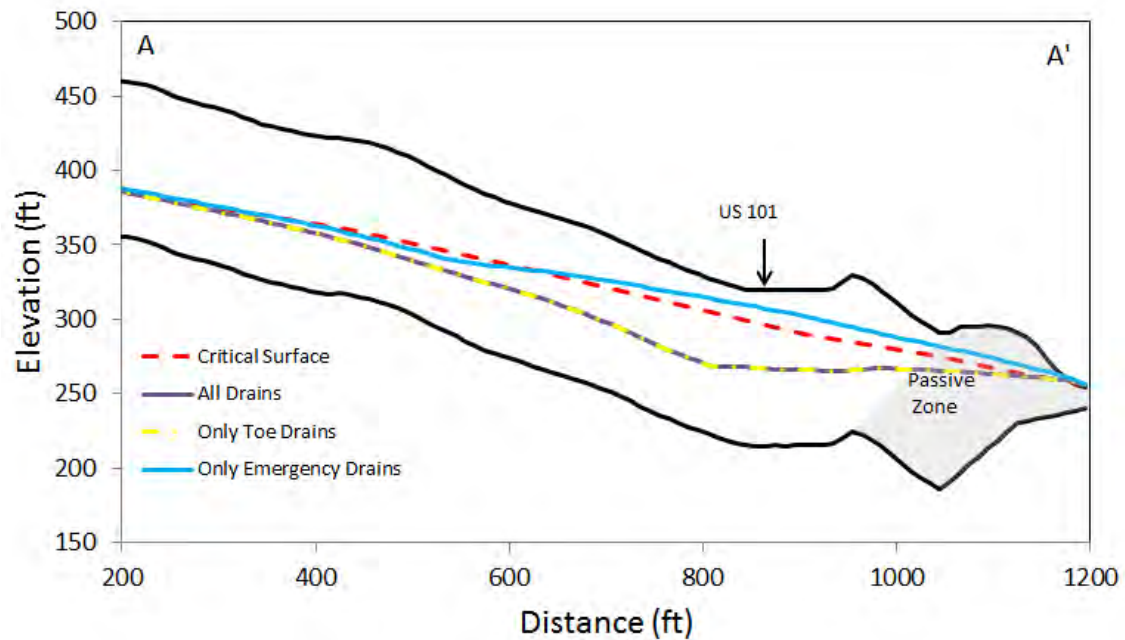


Figure C-14: Water levels predicted during the design storm given the emergency and toe drains are installed (purple line), only the toe drains are installed (dashed yellow line), and only the emergency drains are installed (blue line)

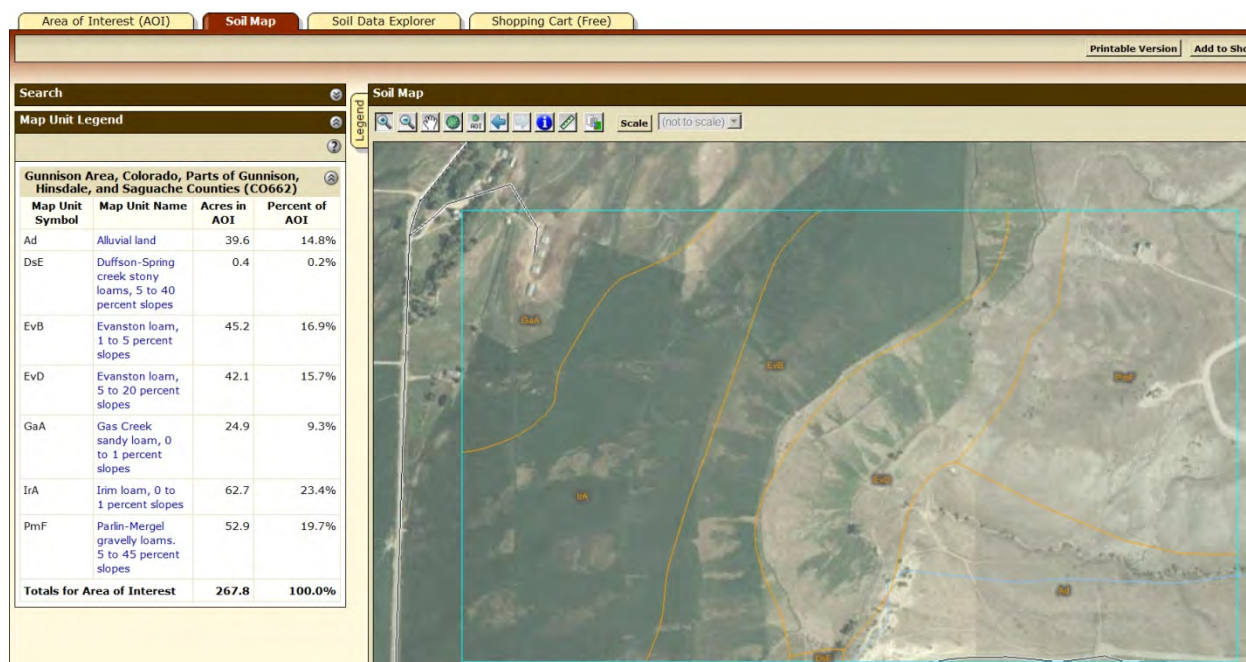
Appendix D

Major Soils and Associated Hydrologic Soil Groups in the United States

Two mechanisms are provided for obtaining the hydrologic soil group. First, the National Resources Conservation Service (NRCS) interactive website can help isolate major soil groups for a region of interest as well as provide hydrologic soil group information. NRCS tabulated values for major soils across the United States are provided (NRCS, 1986).

D-1 NRCS Interactive Website

A comprehensive list of soil surveys by state can be found on the National Resources Conservation Service (NRCS) website (<http://websoilsurvey.nrcs.usda.gov/>). Follow the directions for creating and setting an area of interest (AOI) for which one can then access soil information and associated reports. Once an AOI is defined, soils are listed in the tab “Soil Map” with an example given below.



Navigate to the tab “Soil Data Explorer” and find a sub-tab called “Soil Properties and Quantities”. On the left, is a drop-down menu on “Soil Quantities and Features”. Hydrologic Soil Group is included as a heading. A screen shot of the site is given below.

Area of Interest (AOI)

Soil Map

Soil Data Explorer

Shopping Cart (Free)

View Soil Information By Use: All Uses

Intro to Soils

Suitabilities and Limitations for Use

Soil Properties and Qualities

Search

Properties and Qualities Ratings

Open AllClose All?

Soil Chemical Properties?

Soil Erosion Factors?

Soil Physical Properties?

Soil Qualities and Features?

AASHTO Group Classification (Surface)

Depth to a Selected Soil Restrictive Layer

Depth to Any Soil Restrictive Layer

Drainage Class

Frost Action

Frost-Free Days

Hydrologic Soil Group

View DescriptionView Rating

View Options?

Map☒

Table☒

Description of Rating☒


Rating Options☒

☐ Detailed Description

Soil Map

Legend

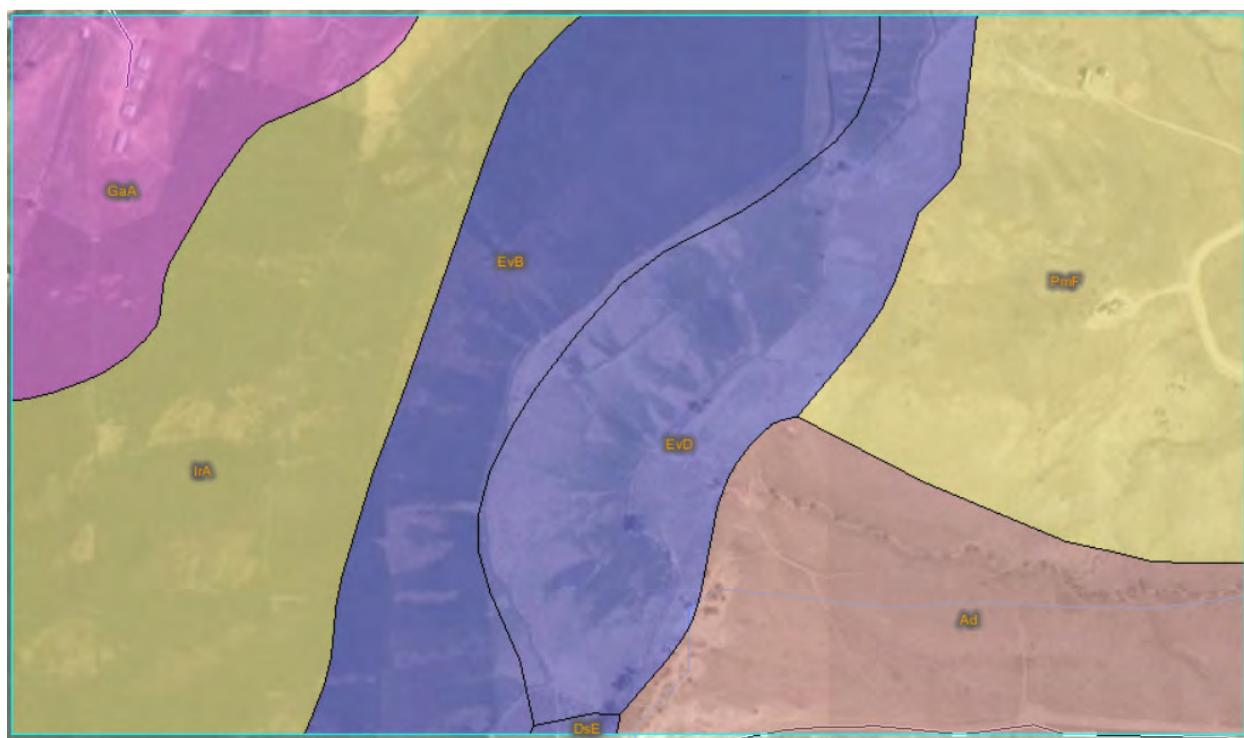
Scale



Hit the button “View Rating”. This results in tabulated summary of hydrologic soil group,

Tables — Hydrologic Soil Group — Summary By Map Unit				
Summary by Map Unit — Gunnison Area, Colorado, Parts of Gunnison, Hinsdale, and Saguache Counties (C0662)				
Map unit symbol	Map unit name	Rating	Acres in AOI	Percent of AOI
Ad	Alluvial land	A	39.6	14.8%
DsE	Duffson-Spring creek stony loams, 5 to 40 percent slopes	B	0.4	0.2%
EvB	Evanston loam, 1 to 5 percent slopes	B	45.2	16.9%
EvD	Evanston loam, 5 to 20 percent slopes	B	42.1	15.7%
GaA	Gas Creek sandy loam, 0 to 1 percent slopes	D	24.9	9.3%
IrA	Irim loam, 0 to 1 percent slopes	C	62.7	23.4%
PmF	Parlin-Mergel gravelly loams. 5 to 45 percent slopes	C	52.9	19.7%
Totals for Area of Interest			267.8	100.0%

Along with a color coded map of the AOI.



D-2 Tabulated Hydrologic Soil Groups for the United States

AABAB.....	D	ACTI.....	D	AGUILITA.....	B	ALBUS.....	B
AABERG.....	D	ACTON.....	B	AGUIRRE.....	D	ALCALDE.....	D
AARON.....	C	ACUFF.....	B	AGUSTIN.....	B	ALCAN.....	D
AARUP.....	D	ACUNA.....	C	AHART.....	B	ALCESTER.....	B
AASTAD.....	B	ACY.....	C	AHCHEW.....	D	ALCOA.....	B
AAZDAHL.....	B	ADA.....	C	AHL.....	C	ALCONA.....	B
ABAC.....	D	ADABOI.....	C	AHLSTROM.....	D	ALCOT.....	A
ABAJO.....	C	ADAIR.....	C	AHMEEK.....	C	ALCOVA.....	B
ABALAN.....	D	ADAMANT.....	B	AHOLT.....	D	ALCOVY.....	C
ABALOBADIAH.....	B	ADAMS.....	A	AHPAH.....	C	ALDA, Saline.....	B/D
ABARCA.....	B	ADAMSLAKE.....	B	AHREN.....	B	ALDA.....	C
ABBAYE.....	B	ADAMSON.....	B	AHRNKLIN.....	C	ALDAPE.....	D
ABBEYLAKE.....	A	ADAMSVILLE.....	B	AHRS.....	B	ALDAX.....	D
ABBIE.....	B	ADATON.....	D	AHSAHKA.....	C	ALDEN.....	D
ABBOTT.....	D	ADAVEN.....	C	AHTANUM.....	C/D	ALDENLAKE.....	B
ABBOTTSPRING.....	B	ADCO.....	D	AHWAHNEE.....	B	ALDER.....	C
ABBOTTSTOWN.....	C	ADDER.....	A/D	AIBONITO.....	D	ALDERDALE.....	C
ABEGG.....	B	ADDERTON.....	B	AIDO.....	D	ALDERFLATS.....	D
ABELA.....	B	ADDICKS.....	D	AIKEN.....	B	ALDERMAND.....	B
ABELL.....	B	ADDIELOU.....	B	AIKMAN.....	D	ALDERON.....	B
ABENAKI.....	B	ADE.....	A	AILEY.....	B	ALDERWOOD.....	C
ABERDEEN.....	C	ADEK.....	B	AIMELIUK.....	B	ALDI.....	D
ABERONE.....	B	ADEL.....	B	AINAKEA.....	B	ALDINE.....	D
ABERSITO.....	C	ADEL, Wet.....	D	AINSLEY.....	B	ALDING.....	D
ABERT.....	B	ADELAIDE.....	D	AINSWORTH.....	B	ALDINO.....	C
ABES.....	D	ADELANTO.....	B	AIRMONT.....	C	ALDO.....	A
ABGESE.....	B	ADELINO.....	B	AIRPORT, Wet.....	C	ALDRICH.....	C
ABILENE.....	C	ADELINO, Saline-Alkali.....	C	AIRPORT.....	D	ALEDO.....	C
ABIN.....	B	ADELMANN.....	C	AITS.....	B	ALEGROS.....	C
ABIQUA.....	B	ADELPHIA.....	B/D	AJAX.....	D	ALEKNAGIK.....	C
ABIQUA, Flooded.....	C	ADEN.....	C	AJO.....	C	ALEMEDA.....	C
ABIQUIU.....	C	ADENA.....	C	AJOLITO.....	D	ALESNA.....	C
ABITA.....	C	ADGER.....	D	AKAD.....	C	ALEX.....	B
ABO.....	C	ADIEUX.....	B	AKAKA.....	A	ALEX, Wet Substratum.....	C
ABOR.....	D	ADILIS.....	B	AKAN.....	B/D	ALEXANDER.....	C
ABORIGINE.....	D	ADINOT.....	D	AKASKA.....	B	ALEXANDRIA.....	C
ABOTEN.....	D	ADIOS.....	D	AKBASH.....	B	ALFLACK.....	C
ABRA.....	B	ADIRONDAK.....	D	AKELA.....	D	ALFORD.....	B
ABRACON.....	B	ADJIDAUMO.....	D	AKELEY.....	A	ALGARROBO.....	A
ABRAM.....	D	ADJUNTAS.....	C	AKERCAN.....	B	ALGIERS.....	C/D
ABRAZO, Gravelly.....	C	ADKINS.....	B	AKERITE.....	B	ALGOA.....	C
ABRAZO.....	D	ADLER.....	C	AKERS.....	B	ALGOMA.....	D
ABREU.....	B	ADMAN.....	D	AKERUE.....	D	ALIBATES.....	B
ABRIGO.....	B	ADOBE.....	D	AKHONI.....	D	ALIBI.....	C
ABSAQUIL.....	B	ADOLPH.....	B/D	AKINA.....	B	ALICEL.....	B
ABSAROKEE.....	C	ADOS.....	C	AKINVILLE.....	B	ALICIA.....	B
ABSAROOK Cool.....	B	ADRIAN.....	A/D	AKLER.....	D	ALIDA.....	B
ABSAROOK.....	C	ADVOKAY.....	D	AKSARBEN.....	B	ALIKCHI.....	B
ABSAY.....	D	ADWELL.....	C	ALABASTER.....	D	ALINE.....	A
ABSCO.....	A	ADY.....	B	ALADDIN.....	B	ALIRE.....	B
ABSCOTA.....	A	ADYEVILLE.....	C	ALADSHI.....	B	ALIVAR.....	B
ABSHER.....	D	AECET.....	C	ALAE.....	A	ALKABO.....	C
ABSTON.....	C	AENEAS.....	B	ALAELOA.....	B	ALKIRIDGE.....	C
ACACIO.....	B	AETNA.....	C	ALAGA.....	A	ALLAGASH.....	B
ACADEMY.....	C	AFFEY.....	C	ALAKAI.....	D	ALLAMORE.....	D
ACADIA.....	D	AFLEY.....	B	PARANAT.....	C	ALLANTON.....	B/D
ACADIANA.....	D	AFLEY, Extremely Stony.....	C	ALAMA.....	B	ALLARD.....	B
ACAMPO.....	C	AFTAD.....	B	ALAMADITAS.....	C	ALLDOWN.....	C
ACANA.....	D	AFTADEN.....	D	ALAMANCE.....	B	ALLEN.....	B
ACANOD.....	C	AFTON.....	C/D	ALAMBIQUE.....	B	ALLENDAL.....	C
ACASCO.....	D	AGA.....	C	ALAMEDAWELL.....	B	ALLENS PARK.....	B
ACCELERATOR.....	B	AGAN.....	D	ALAMO.....	D	ALLENS PARK, Stony.....	C
ACCOLA.....	B	AGAR.....	B	ALAMOGORDO.....	B	ALLENTINE.....	D
ACEITUNAS.....	B	AGASSIZ.....	D	ALAMUCHEE.....	B	ALLENWOOD.....	B
ACEL.....	C	AGATE.....	D	ALANGO.....	D	ALLHANDS.....	D
ACHELAKE.....	B	AGATHA.....	B	ALANOS.....	B	ALLINGHAM.....	B
ACHIMIN.....	C	AGAWAM.....	B	ALANOS, Cool.....	D	ALLIS.....	D
ACKELTON.....	B	AGEE.....	B	ALAPAHA.....	B/D	ALLIVAR.....	B
ACKER.....	B	AGENCY.....	B	ALAPAI.....	A	ALLKER.....	B
ACKERMAN.....	A/D	AGENCY, Stony.....	C	ALAZAN.....	C	ALLOUEZ.....	B
ACKETT.....	D	AGERDELLY.....	D	ALBAN.....	B	ALLOWAY.....	B
ACKLEY.....	B	AGFAYAN.....	D	ALBANO.....	D	ALLUVIAL LAND.....	A
ACKMEN.....	B	AGNAL.....	D	ALBANY.....	C	ALLWIT.....	D
ACKMEN, Wet.....	C	AGNESS.....	B	ALBATON.....	D	ALMAC.....	B
ACKMORE, Poorly Drained.....	B	AGNEW.....	C	ALBEE.....	D	ALMAVILLE.....	D
ACKNA.....	B	AGNOS.....	D	ALBEMARLE.....	B	ALMIRANTE.....	B
ACKWATER.....	D	AGON.....	C	ALBERS.....	D	ALMO.....	D
ACME.....	C	AGORT.....	C	ALBERTI.....	C	ALMOND.....	C
ACO.....	B	AGRA.....	D	ALBERTON.....	B	ALMONT.....	D
ACOMA.....	C	AGUA.....	B	ALBERTVILLE.....	C	ALMORA.....	B
ACORD.....	C	AGUA DULCE.....	B	ALBICALIS.....	D	ALNITE.....	D
ACOVE.....	C	AGUA FRIA.....	C	ALBINAS.....	B	ALNULT.....	B
ACREE.....	C	AGUADILLA.....	A	ALBION.....	B	ALOGIA.....	C
ACRELANE.....	C	AGUALT.....	B	ALBRIGHTS.....	C	ALOHA.....	C
ACTEM.....	D	AGUEDA.....	B	ALBURZ.....	B/C	ALOMAX.....	D
		AGUILARES.....	B				

ALONA	B	AMITY	D	ANOKA	B	ARGALT	D
ALONEMILL	B	AMMON	B	ANONES	C	ARGEE	C
ALONSO	B	AMNICON	D	ANOWELL	D	ARGENTA	C
ALONZEVILLE	B	AMODAC	C	ANSGAR	B/D	ARGONNE	B
ALOVAR	C	AMOLE	C	ANSPING	B	ARGORA	B
ALPENA	A	AMOR	B	ANT FLAT	D	ARGOVAR	D
ALPHA	B	AMORUS	D	ANTARES	A	ARGYLE	B
ALPIN	A	AMOS	C	ANTARES	C	ARIDIC USTIFLUVENTS	B
ALPINEPEAK	C	AMOSTOWN	C	ANTELOPE SPRINGS	D	ARIEL	C
ALPON	B	AMPAD	C	ANTERO	D	ARIMO	B
ALPOWA	B	AMPHION	C	ANTHOLOP	D	ARISTINE	C
ALRED	B	AMSDEN	B	ANTIGO	B	ARIVACA	C
ALROS	C	AMSTERDAM	B	ANTILON	C	ARIVACA, Very Cobbly	D
ALS	A	AMTOFT	D	ANTIOCH	D	ARIZER	B
ALSASH	B	AMUZET	A	ANTOINE	C	ARKABUTLA	C
ALSCO	B	AMUZET, Gravelly	B	ANTOKEN	B	ARKAQUA	C
ALSEA	B	AMWELL	C	ANTON	D	ARKONA	B
ALSPAUGH	C	AMY	D	ANTONITO	C	ARKPORT	B
ALSTAD	C	ANACAPA	B	ANTOSA	B	ARKRIGHT	B
ALSTONY	B	ANACOCO	D	ANTWERP	C	ARKSON	B
ALSTOWN	B	ANACONDA	B	ANUNDE	B	ARKTON	C
ALSUP	C	ANAHEIM	C	ANVIL	C	ARLAND	B
ALTA	B	ANAHUAC	D	APALACHEE	D	ARLE	C
ALTAMONT	D	ANALULU	B	APALO	B	ARLEN	B
ALTAPEAK	B	ANAMAC	B	APELDORN	D	ARLINGTON, Thick Solum	B
ALTAR	B	ANAMITE	D	APEX	B	ARLINGTON	C
ALTASLOUGH	C	ANAN	D	APISON	B	ARLOVAL	A
ALTAVISTA	C	ANAPRA	B	APMAT	B	ARLYNDA	D
ALTDORF	D	ANASAZI	C	APMAY	B	ARMENDARIIS	C
ALTHOUSE	B	ANATOLIAN	C	APOLLO	B	ARMENIA	D
ALTICREST	C	ANATONE	D	APOPKA	A	ARMESA	B
ALTITA	C	ANAUD	D	APPAM	B	ARMESPAN	B
ALTMAR	B	ANAUVERDE	B	APPANOOSE	D	ARMINGTON	D
ALTO	C	ANAWALT	D	APPERSON	C	ARMISTEAD	C
ALTOGA	C	ANCENY	B	APPEDELLIA	C	ARMITAGE	C
ALTON	D	ANCHO	B	APPLEGATE	B	ARMO	B
ALTUDA	A	ANCHO, Saline	C	APPLERIVER	B	ARMOINE	D
ALTURAS	C	ANCHOR POINT	D	APPLESEED	D	ARMPUP	C
ALTUS	B	ANCHORAGE	A	APPLESHALL	D	ARNESS	D
ALTVAN	B	ANCHUSTEQUI	D	APPLING	B	ARNEY	B
ALUF	A	ANCHUTZ	B	APPOMATTOX	B	ARNHEIM	D
ALUM	B	ANCLOTE	B/D	APPOQUINMINK	D	ARNO	D
ALUSA	D	ANCO	C	APRON	B	ARNOLD	A
ALVADA	B/D	ANDERGEORGE	B	APT	B	ARNTZ	C
ALVARADO	B	ANDERLY	C	APTAKISIC	C	AROL	D
ALVIN	B	ANDERSON	B	APTOS	B	AROSA	C
ALVISO	D	ANDERSON, Hard Substratum	C	AQUANDIC HUMAQUEPTS	C	ARP	C
ALVODEST	D	ANDOK	B	AQUARIUS	C	ARRADA	D
ALVOR	D	ANDOVER	D	AQUATNA	D	ARRASTRE	B
ALWILDA	B	ANDRADA	D	AQUILLA	A	ARRIBA	C
ALZADA	D	ANDREGG	B	AQUIMA	B	ARRINGTON	B
ALZOLA	C	ANDRES	C	AQUINAS	C	ARRIOLA	D
AMABILIS	C	ANDREWS	C	ARADA	B	ARRITOLA	D
AMADON	D	ANDRUSIA	A	ARADARAN	C	ARROD	D
AMADOR	D	ANDRY	C	ARAGON	C	ARROLIME	C
AMAGON	D	ANDYS	B	ARAMBURU	C	ARRON	D
AMAL	B	ANED	D	ARAPAHOE	B/D	ARROWHEAD	C
AMALIA	B	ANELA	B	ARARAT	B	ARROYADA	D
AMALU	D	ANGELICA	B/D	ARAT	D	ARROYO SECO	B
AMANA	B	ANGELINA	D	ARAVAIPA	C	ARSITE	D
AMANDA	C	ANGELPEAK	B	ARAWAK	B	ARTA	C
AMARILLO	B	ANGELUS	B	ARBELA	C	ARTIL	A
AMASA	B	ANGIE	D	ARBOLES	C	ARTNOC	B
AMBER	B	ANGLE	A	ARBOR	B	ARTRAY	D
AMBIA	D	ANGLEN	C	ARBUCKLE	C	ARUJO	B
AMBOAT	D	ANGOLA	C	ARBUS	B	ARUNDEL	C
AMBOY	C	ANGORA	B	ARBUTUS	A	ARVA	D
AMBRANT	B	ANGUS	B	ARCADIAN	D	ARVADA	C
AMBRAW	B/D	ANHALT	D	ARCATA	B	ARVANA	C
AMBROSIA	A	ANIAK	D	ARCHABAL	B	ARVILLA	B
AMCEC	B	ANIGON	B	ARCHBOLD	A	ARWITE	B
AMELAR	B	ANIMAS	C	ARCHER	C	ARZO	C
AMELIA	C	ANNABERG	D	ARCHIN, Cool	C	ASAAYI	D
AMENE	D	ANNAHOOTZ	A	ARCHIN	D	ASABEAN	B
AMENIA	B	ANNALAKE	B	ARCO	B/C	ASBILL	D
AMENSON	D	ANNAROSE	B	ARD	C	ASCAR	C
AMERICANOS	B	ANNAW	B	ARDENING	B	ASHART	D
AMERICUS	A	ANNEMAINE	C	ARDENMONT	B	ASHBURN	B
AMERIMINE	B	ANNISQUAM	C	ARDEP	C	ASHCAMP	C
AMERY	B	ANNISTON	B	ARDILLA	C	ASHCROFT	B
AMES	C/D	ANNLAKE	B/D	ARDTOO	B	ASHDALE	B
AMESHA	B	ANNONA	D	ARECIBO	A	ASHDOS	C
AMHERST	D	ANNROMA	D	ARENA	C/D	ASHERTON	B
AMIRET	B	ANNUM	B	ARENALES	A	ASHFORD	D
AMISTAD	D	ANOCON	C	ARENOSA	A	ASHFORK	D

ASHIPPUN.....	C	AVERY.....	C	BALDKNOB.....	D	BART.....	B
ASHKUM.....	B/D	AVIS.....	A	BALDMOUNTAIN.....	B	BARTHOLF.....	B
ASHLEY.....	B	AVISTON.....	B	BALDRIDGE.....	B	BARTINE.....	C
ASHLO.....	B	AVOCA.....	B	BALDWIN.....	D	BARTMUS.....	D
ASHMED.....	B	AVON.....	C	BALE.....	B	BARTO.....	D
ASHMUN.....	D	AVONDA.....	B	BALE, Wet.....	D	BARTOME.....	D
ASHNOLA.....	B	AVONVILLE.....	B	BALHUD LOAM.....	B	BARTON.....	B
ASHOLLOW.....	B	AVTABLE.....	D	BALLAHACK.....	D	BARTONFLAT.....	B
ASHONE.....	C	AWBRIG.....	B	BALLARD.....	B	BARTONHILL.....	B
ASHPORT.....	B	AWET.....	B	BALLINGER.....	D	BARZEE.....	D
ASHTRE.....	C	AXFORD.....	B	BALLTOWN.....	D	BASCAL.....	B
ASHUE.....	B	AXIS.....	D	BALLVAR.....	B	BASCOM.....	B
ASHUELOT.....	D	AXTELL.....	D	BALM.....	D	BASCOVY.....	D
ASHVILLE.....	D	AYCOCK.....	B	BALMAN.....	C	BASH.....	C
ASHWOOD.....	C	AYDELOTTE.....	B	BALMLAKE.....	B	BASHER.....	B
ASHWORTH.....	B	AYERSVILLE.....	D	BALON.....	B	BASILE.....	D
ASKECKSY.....	A/D	AYLMER.....	A	BALSORA.....	B	BASIN.....	C
ASLINGER.....	C	AYMATE.....	C	BALTIMORE.....	B	BASINGER.....	B/D
ASOLT.....	D	AYOCK.....	B	BAMA.....	B	BASINPEAK.....	B
ASOTIN.....	C	AYOUB.....	C	BAMBER.....	B	BASKET.....	B
ASPARAS.....	B	AYR.....	C	BAMFIELD.....	C	BASNOB.....	A
ASPEN.....	B	AYRMOUNT.....	B	BANADERU.....	D	BASSEL.....	B
ASPENLAKE.....	C	AZAAR.....	C	BANAT.....	B	BASSFIELD.....	B
ASPERMONT.....	B	AZABACHE.....	D	BANBURY.....	D	BASTIAN.....	C
ASPERSON.....	C	AZELTINE.....	B	BANCAS.....	B	BASTON.....	C
ASSATEAGUE.....	A	AZTALAN.....	C	BANCKER.....	D	BASTROP.....	B
ASSININS.....	B	AZTEC.....	B	BANDANA.....	B	BASTSIL.....	B
ASTATULA.....	A	AZTEC, High Rainfall.....	C	BANDON.....	C	BATA.....	B
ASTOR.....	B/D	AZURE.....	D	BANE.....	A	BATEMAN.....	B
ASTOR, Flooded.....	D	AZWELL.....	C	BANGTAIL.....	C	BATES.....	B
ASTRAG.....	A	BAAHISH.....	B	BANIDA.....	D	BATESVILLE.....	C
ATASCO.....	C	BABBINGTON.....	B	BANKER.....	D	BATHEL.....	C
ATATE.....	B	BABCO.....	C	BANKHEAD.....	C	BATTEAU.....	C
ATCHISON.....	B	BABELTHUAP.....	B	BANLIC.....	B	BATTLE CREEK.....	C
ATCO.....	B	BABERWIT.....	C	BANNEL.....	B	BATTLEBUTTE.....	D
ATESH.....	C	BABOON.....	C	BANNER.....	C	BATTLEFIELD.....	A/D
ATLANTIS.....	C	BABOQUIVARI.....	B	BANNING.....	C	BATTLEGROUND.....	B
ATLAS.....	D	BABOQUIVARI, Sandy.....	C	BANQUITO.....	B	BATTYDOE.....	B
ATLATL.....	C	Substratum.....	C	BANTRY.....	A/D	BATZA.....	D
ATLEE.....	C	BACBUSTER.....	C	BARANA.....	B	BAUDETTE.....	B
ATMORE.....	B/D	BACH.....	B/D	BARANOF.....	C	BAUGO.....	C
ATOKA.....	C	BACHELOR.....	B	BARASCO.....	C	BAUMAN.....	C
ATOM.....	B	BACHO.....	D	BARATARI.....	A/D	BAUX.....	B
ATRAVESADA.....	D	BACHUS.....	C	BARBARELA.....	B	BAUXSON.....	B
ATRYPA.....	D	BACID.....	B	BARBAROSA.....	D	BAVARIA.....	C
ATSION.....	C/D	BACKBAY.....	D	BARBARY.....	D	BAVDARK.....	B
ATSION, Tide Flooded.....	D	BACKCANYON.....	D	BARBERMILL.....	C	BAXTERVILLE.....	B
ATTELLA.....	D	BACKROAD.....	B	BARBERT.....	D	BAYAMON.....	B
ATTEWAN, Wet.....	D	BACLIFF.....	D	BARBOUR.....	B	BAYFIELD.....	D
ATTICA.....	B	BACONA.....	B	BARBOURVILLE.....	B	BAYHOOK.....	B
ATTOYAC.....	B	BADAXE.....	B	BARCE.....	B	BAYHORSE.....	D
ATWELL.....	D	BADEN.....	C/D	BARCELONA.....	C	BAYLIS.....	B
ATWOOD.....	B	BADGER.....	C	BARCLAY.....	C	BAYLOR.....	A
AU GRES.....	C	BADGERCAMP.....	D	BARCUS.....	A	BAYMEADE.....	A
AUA.....	B	BADGERMONT.....	C	BARDEN.....	C	BAYOU.....	D
AUBARQUE.....	D	BADITO.....	C	BARDWELL.....	B	BAYOUDAN.....	D
AUBERRY.....	B	BADRIVER.....	D	BARFAN.....	D	BAYS.....	C
AUCHARD.....	C	BADUS.....	C/D	BARFUSS.....	B	BAYSHORE, Moderately Wet.....	B
AUDUBON.....	C	BADWATER.....	B	BARGAMIN.....	B	BAYSHORE.....	D
AUFCO.....	D	BAGGER.....	B	BARGE.....	C	BAYTOWN.....	B
AUGANAUSH.....	C	BAGGOTT.....	D	BARGER.....	C	BAYUCOS.....	D
AUGGIE.....	B	BAGGS.....	B	BARHISKEY.....	A	BAYVIEW.....	D
AUGUSTA.....	C	BAGLEY.....	B	BARIO.....	B	BAYWOOD.....	A
AUGUSTINE.....	B	BAGMONT.....	B	BARISHMAN.....	C	BAZETTE.....	C
AUGWOOD.....	B	BAGNESS.....	B	BARKEY.....	B	BEACH.....	D
AURA.....	B	BAHIA.....	A	BARKSHANTY.....	B	BEAD.....	C
AURAND.....	C	BAHIAHONDA.....	B	BARLING.....	C	BEAL.....	C
AURORA.....	C	BAHNER.....	D	BARLOW.....	B	BEALAND.....	B
AUSABLE.....	D	BAILE.....	D	BARNABE.....	D	BEALES.....	B
AUSTIN.....	C	BAILING.....	C	BARNELLCREEK.....	B	BEAMTON.....	C
AUSTINVILLE.....	B	BAINES.....	D	BARNESTON.....	A	BEANBLOSSUM.....	B
AUSTONIO.....	B	BAINTER.....	B	BARNHARDT.....	B	BEANFLAT.....	C
AUSTWELL.....	D	BAINVILLE.....	C	BARNMOT.....	D	BEANO.....	D
AUT.....	C	BAIRD HOLLOW.....	D	BARNSDALL.....	B	BEAR BASIN.....	B
AUTOMBA.....	B	BAKERSFIELD, Drained.....	B	BARNWELL.....	C	BEAR CREEK.....	C
AUTRYVILLE.....	A	BAKERSFIELD, Saline-Sodic.....	C	BARODA.....	D	BEARCAMP.....	B
AUXVASSE.....	D	BAKERSVILLE.....	D	BAROID.....	D	BEARDALL.....	C
AUZQUI.....	B	BAKSCRATCH.....	D	BARPEAK.....	B	BEARDSLEY.....	C
AVA.....	C	BALAKE.....	B	BARRADA.....	D	BEARDSTOWN.....	C
AVAL.....	D	BALATON.....	B	BARRE.....	D	BEARGULCH.....	B
AVANT.....	B	BALCHER.....	C	BARRETT.....	D	BEARHEAD.....	B
AVAR.....	D	BALD.....	C	BARRON.....	B	BEARPEN.....	C
AVAWATZ.....	A	BALDEAGLE.....	B	BARRYMORE.....	C	BEARRUN.....	C
AVENAL.....	B	BALDER.....	D	BARSA.....	C	BEARTOOTH.....	B
AVERLANDE.....	D	BALDHILL.....	B	BARSHAAD.....	D	BEARTRAP.....	B

BEARVILLE.....	C	BELTAVA.....	B	BEW.....	C	BISHOP.....	C
BEARWALLOW.....	C	BELTON.....	C	BEWEARZE.....	B	BISON.....	B
BEASLEY.....	C	BELTSVILLE.....	C	BEWLEYVILLE.....	B	BISPING.....	B
BEASON.....	C	BELUGA.....	C/D	BEXAR.....	D	BISSETT.....	D
BEATRICE.....	D	BELVOIR.....	C	BEZO.....	D	BISSONNET.....	D
BEAUCOUP.....	B/D	BELZAR.....	C	BIAGGI.....	B	BIT.....	C
BEAUFORD.....	D	BEMIDJI.....	B	BICKERDYKE.....	D	BITCREEK.....	B
BEAUGHTON.....	D	BEMIS.....	C	BICKETT.....	D	BITCREEK LOAM.....	B
BEAUREGARD.....	C	BEMISHAVE.....	C	BICKFORD.....	D	BITNER.....	C
BEAUSITE.....	C	BEN LOMOND.....	B	BICKLETON.....	B	BITTER.....	B
BEAUVAIS.....	B	BENADUM.....	C/D	BICONDOA.....	C/D	BITTERCREEK.....	C
BEAVERCREEK.....	B	BENCHLEY.....	D	BIDDLE.....	C/D	BITTERROOT.....	C
BEAVERDAM.....	C	BEND.....	B	BIDONIA.....	D	BIVANS.....	D
BEAVERDUMP.....	B	BENDAHL.....	B	BIDRIM.....	D	BIWABIK.....	A
BEAVERFLAT.....	B	BENDAVIS.....	C	BIEDELL.....	D	BIXBY.....	B
BEAVERTAIL.....	D	BENDER.....	B	BIEDSAW.....	D	BJORKLAND.....	B/D
BEBEEVAR.....	B	BENDERLY.....	A	BIFFLE.....	B	BLACK CANYON.....	C/D
BECA.....	C	BENDOH.....	B	BIG TIMBER.....	D	BLACKBURN.....	B
BECHTEL.....	B	BENEMES.....	A	BIGA.....	C	BLACKCREEK.....	C
BECHYN.....	D	BENEVOLA.....	C	BIGBEAVER.....	C	BLACKDOG.....	B
BECKER.....	B	BENEWAH.....	D	BIGBEE.....	A	BLACKFOOT.....	B/C
BECKHAM.....	B	BENFIELD.....	C	BIGBOW.....	B	BLACKHAMMER.....	B
BECKMAN.....	D	BENITO.....	D	BIGBROWN.....	C	BLACKHOOF.....	D
BECKS.....	C	BENKA.....	B	BIGCREEK.....	B	BLACKHORSE.....	D
BECKSTRAND.....	C	BENKELMAN.....	B	BIGDRAW.....	C	BLACKLAKE.....	D
BECKVILLE.....	B	BENKLIN.....	C	BIGDUTCH.....	B	BLACKLEG.....	D
BECKWITH.....	D	BENMAN.....	C	BIGELOW.....	B	BLACKMORE.....	B
BECCRAFT.....	B	BENNDALE.....	B	BIGFOOT.....	C	BLACKMOUNT.....	B
BEDEN.....	D	BENNING.....	B	BIGFROG.....	D	BLACKNEST.....	B
BEDFORD.....	C	BENRIDGE.....	B	BIGGSVILLE.....	B	BLACKOAR.....	B/D
BEDKE.....	B	BENSLEY.....	B	BIGHAT.....	D	BLACKPIPE.....	C
BEDNER.....	C	BENSON.....	D	BIGHILL.....	B	BLACKRIVER.....	B
BEDSTEAD.....	C	BENSTOT.....	C	BIGLAKE.....	A	BLACKSAN.....	B
BEDWYR.....	D	BENTAXLE.....	D	BIGLICK.....	D	BLACKSPAR.....	D
BEDZEE.....	D	BENTEEN.....	C	BIGLOST.....	B	BLACKSPOT.....	D
BEECH.....	C	BENTILLA.....	C	BIGLOST, Wet.....	C	BLACKTOP.....	D
BEECH GROVE.....	C	BENTONSPORT.....	B	BIGPAW.....	B	BLACKWATER.....	D
BEECHER.....	C	BENZ.....	D	BIGPOOL.....	C	BLACKWOOD.....	B
BEECHWOOD.....	C	BEOR.....	D	BIGRIVER.....	B	BLAG.....	D
BEELEM.....	D	BEOWAWE.....	B	BIGSAG.....	D	BLAGO.....	D
BEENO.....	C	BEQUINN.....	B	BIGSHEEP.....	B	BLAINEGATE.....	D
BEERBO.....	D	BERDA.....	C	BIGWIN.....	C	BLAIR.....	C
BEERSHEBA.....	B	BERDUGO.....	C	BJORJA.....	C	BLAKABIN.....	C
BEESKOVE.....	B	BEREA.....	C	BIKEN.....	D	BLAKENEY.....	D
BEEWON.....	D	BERGQUIST.....	B	BIKEYAH.....	C	BLALOCK.....	D
BEEZEE.....	B	BERGSTROM.....	B	BILGER.....	D	BLAMER.....	C
BEHEMOTOSH.....	C	BERGSVIK.....	D	BILGRAY.....	C	BLANCA.....	B
BEHRING.....	D	BERLAND.....	D	BILHAUL.....	D	BLANCHE.....	B
BEIGLE.....	B	BERLIN.....	C	BILHIL.....	C	BLANCHESTER.....	B/D
BEIRMAN.....	D	BERMUDIAN.....	B	BILLMAN.....	C	BLANCOVERDE.....	C
BEJUCOS.....	B	BERN.....	B	BILLYBOY.....	B	BLAND.....	C
BELAIN.....	C	BERNALDO.....	B	BILLYCREEK.....	C	BLANEY.....	B
BELATE.....	B	BERNARD.....	D	BILLYHAW.....	D	BLANKET.....	C
BELCHER.....	D	BERNICE.....	A	BILLYRIDGE.....	B	BLANKOUT.....	A
BELDEN.....	C	BERNOW.....	B	BILMOD.....	B	BLANTON.....	B
BELDING.....	B	BERON.....	D	BILSON.....	B	BLAPPERT.....	D
BELFON.....	B	BERRAY.....	B	BILTMORE.....	A	BLAQUIRRE.....	C
BELGARRA.....	C	BERRYHILL.....	D	BIMINI.....	C	BLASE.....	C
BELGRADE.....	B	BERRYMAN.....	C	BIMMER.....	D	BLASHKE.....	A
BELINDA.....	D	BERTHAHILL.....	B	BINDLE.....	B	BLAYDEN.....	D
BELK.....	D	BERTHOUD.....	B	BINFORD.....	B	BLAZEFORK.....	D
BELKNAP.....	C	BERTOLOTTI.....	B	BINGER.....	B	BLEAKHILL.....	C
BELLA.....	D	BERTRAND.....	B	BINGHAMPTON.....	B	BLEAKWOOD.....	C
BELLAMY.....	C	BERVILLE.....	B/D	BINGHAMVILLE.....	D	BLEIBLERVILLE.....	D
BELLAVISTA.....	C	BERWOLF.....	B	BINNSVILLE.....	D	BLEUMONT.....	C
BELLE.....	B	BERZATIC.....	D	BINS.....	B	BLEVINS.....	B
BELLECHESTER.....	A	BESHERM.....	C	BINTON, Reclaimed.....	B	BLEVINTON.....	B
BELLEHELEN.....	D	BESNER.....	B	BINTON.....	C	BLEWETT.....	D
BELLENMINE.....	D	BESS.....	C	BINVAR.....	C	BLIGHTON.....	D
BELLEVILLE.....	B/D	BESSIE.....	D	BIPLANE.....	D	BLIMO.....	B
BELLEVILLE, Ponged.....	D	BESSLEN.....	D	BIPPUS.....	B	BLIND.....	B
BELLEVUE.....	B	BESTPITCH.....	D	BIRCHBAY.....	C	BLINDSPRING.....	A
BELLICUM.....	B	BESTROM.....	C	BIRCHFIELD.....	D	BLINN.....	C
BELLINGHAM.....	C/D	BETHALTO.....	B	BIRCHLAKE.....	C	BLINT.....	B
BELLOTA.....	D	BETHANY.....	C	BIRDSALL.....	D	BLISSHILL.....	C
BELLPASS.....	D	BETHUNE.....	C	BIRDSBEAK.....	D	BLITZEN.....	C
BELLPINE.....	C	BETIS.....	A	BIRDSVIEW.....	A	BLIZZARD.....	D
BELLSLAKE.....	D	BETRA.....	C	BIRKBECK.....	B	BLOCKER.....	D
BELLTOWER.....	B	BETTERAVIA.....	C	BIRMINGHAM.....	B	BLOCKHOUSE.....	D
BELLWOOD.....	D	BEULAH.....	B	BISBEE.....	A	BLOCKTOWN.....	C/D
BELMILL.....	B	BEVERIDGE.....	D	BISCAYNE.....	D	BLOOMFIELD.....	A
BELPRE.....	C	BEVERLY.....	A	BISCAYNE.....	B/D	BLOOMING.....	B
BELRICK.....	B	BEVIER.....	C	BISCHOFF.....	B	BLOOMINGDALE.....	D
BELROSE.....	B	BEVIL.....	D	BISCUIT.....	B/D	BLOOR.....	D
BELSAC.....	B	BEVINGTON.....	B	BISGANI.....	B	BLOSSBERG.....	C

BLUCHER.....	C	BONA.....	B	BOTETOURT.....	C	BRASHEAR.....	C
BLUE EARTH.....	D	BONAIR.....	D	BOTHOMPEEK.....	D	BRASSFIELD.....	B
BLUE LAKE.....	A	BONANZA.....	B	BOTHWELL.....	B	BRASSTOWN.....	B
BLUEAGLE.....	B	BONAPARTE.....	A	BOTLEG.....	C	BRATTON.....	B
BLUEBIRD.....	C	BONDMAN.....	D	BOTT.....	B	BRAUN.....	C
BLUECANYON.....	D	BONDOE.....	B	BOTTINEAU.....	B	BRAVO.....	B
BLUECREEK.....	D	BONDUEL.....	C	BOTTLE.....	C	BRAWLEY.....	D
BLUEDOME.....	C	BONE.....	D	BOTTLE ROCK.....	C	BRAY.....	D
BLUEGULCH.....	B	BONFIELD.....	B	BOULDER POINT.....	B	BRAYS.....	C
BLUEHILL.....	C	BONFRI.....	A	BOULDIN.....	B	BRAZILTON.....	D
BLUEMASS.....	D	BONG.....	C	BOULOGNE.....	B/D	BRAZITO, Thick Surface.....	B
BLUENOSE.....	B	BONHAM.....	D	BOUNCER.....	D	BRAZITO, Saline-Alkali.....	C
BLUERIM.....	C	BONIDU.....	C	BOUNDARY.....	B	BREADLOAF.....	D
BLUESKY.....	D	BONIFAY.....	A	BOURBON.....	B	BRECKEN.....	B
BLUESLIDE.....	D	BONJEA.....	D	BOURNE.....	C	BRECKENRIDGE.....	B/D
BLUESTOCKING.....	C	BONJON.....	B	BOUSIC.....	D	BRECKSVILLE.....	C
BLUESTONE.....	D	BONN.....	B	BOWBAC.....	B	BREEDS.....	B
BLUEWATER.....	D	BONNASH.....	D	BOWERS.....	C	BREHM.....	C
BLUEWING.....	B	BONNEAU.....	A	BOWERY.....	B	BREIEN.....	B
BLUEYE.....	C	BONNEFEMME.....	C	BOWES.....	B	BREMER, Sandy Substratum.....	B
BLUFF.....	D	BONNERDALE.....	B	BOWIE.....	B	BREMER.....	D
BLUFFCREEK.....	B	BONNET.....	B	BOWLAK.....	C	BREMOND.....	C
BLUFFTON.....	C/D	BONNEVILLE.....	A	BOWLUS.....	B	BREMS.....	A
BLUFORD.....	C	BONNICK.....	A	BOWMAN.....	C	BRENDA.....	C
BLUHOL.....	D	BONOLDEN.....	B	BOWMANVILLE.....	B/D	BRENNHAM.....	C
BLULA.....	A	BONSAI.....	D	BOWNS.....	C	BRENNAN.....	B
BLUM.....	C	BONSALL.....	D	BOWSTRING.....	A/D	BRENNER.....	D
BLY.....	B	BONWIER.....	C	BOX.....	A	BRENNYVILLE.....	C
BLYBURG.....	B	BONWIER.....	D	BOXELDER.....	C	BRENT, Dry.....	A
BLYTHE.....	D	BOOFUSS.....	C/D	BOXFORD.....	C	BRENT.....	D
BOARDBURN.....	B	BOOKOUT.....	C	BOXIRON.....	D	BRENTWOOD.....	B
BOARDFLOWER.....	C	BOOKWOOD.....	B	BOXJOE.....	A	BREQUITO.....	B
BOARDMAN.....	D	BOOMSTICK.....	D	BOXSPRING.....	D	BRESSA.....	C
BOARDTREE.....	C	BOOMTOWN.....	D	BOXVILLE.....	C	BREVATOR.....	C
BOASH.....	D	BOONDOCK.....	D	BOXWELL.....	B	BRESCO.....	B
BOAZ.....	C	BOONE.....	A	BOY.....	B	BREW.....	C
BOBERT.....	B/C	BOONESBORO.....	B	BOYD.....	D	BREWER.....	C
BOBILLO.....	B	BOONTLING.....	C	BOYERLAKE.....	C	BREWLESS.....	C
BOBKITTY.....	C	BOONVILLE.....	D	BOYKIN.....	C	BREWTON.....	C
BOBS.....	D	BOOTEN.....	B	BOYLESTON.....	B	BREZNIAK.....	D
BOBSGARDEN.....	B	BOOTLAKE.....	B	BOYLESTON, Gravelly Subsoil.....	C	BRIABBIT.....	B
BOBTAIL.....	C	BOOTS.....	A/D	BOYSEN.....	D	BRICKHAVEN.....	C
BOBTOWN.....	B	BOPLAIN.....	A	BOZE.....	B	BRICKMILL.....	C
BOCK.....	B	BOQUILLAS.....	C	BOZEMAN.....	B	BRICKTON.....	C
BOCOX.....	D	BORACHO.....	D	BRABAS.....	D	BRICKYARD.....	D
BODECKER.....	B	BORAH.....	A	BRABBLE.....	C	BRICO.....	C
BODIFORD.....	D	BORCO.....	A	BRACKETT.....	C	BRIDGE CREEK.....	C
BODORUMPE.....	C	BORDA.....	D	BRACOS.....	B	BRIDGER.....	C
BOEL.....	A	BORDENGULCH.....	B	BRADBOLDT.....	B	BRIDGESON.....	C/D
BOEL, Overwash.....	C	BORDERLINE.....	B	BRADCO.....	C	BRIERY.....	C
BOERNE.....	B	BOREA.....	D	BRADDALE.....	B	BRIFOX.....	C
BOESEL, Protected.....	B	BOREALIS.....	D	BRADEN.....	B	BRIGGS.....	A
BOESEL.....	C	BOREHAM.....	B/C	BRADENTON.....	D	BRIGHTON.....	B/D
BOGA.....	B	BORFIN.....	C	BRADER.....	D	BRIGHTWOOD.....	B
BOGACHIEL.....	A	BORGEAU.....	B	BRADFIELD.....	C	BRILEY.....	B
BOGAN.....	C	BORGES.....	D	BRADGATE.....	B	BRILL.....	B
BOGGIANO.....	B	BORGSTROM.....	B	BRADSON.....	B	BRILLIANT.....	B
BOGGS.....	C	BORIANA.....	D	BRADWAY, Thawed.....	C	BRIMHALL.....	B
BOGGY.....	C	BORID.....	D	BRADWAY.....	D	BRIMLEY.....	C
BOGUE.....	D	BORKY.....	B	BRADY.....	B	BRIMSON.....	C
BOGUSCREEK.....	B	BORLAND.....	D	BRADYVILLE.....	C	BRINGMEE.....	B
BOHICA.....	B	BORNSTEDT.....	C	BRAGG.....	C	BRINKERHOFF.....	D
BOHICKET.....	D	BORO.....	D	BRAGTON.....	D	BRINKLOW.....	B
BOHNA.....	B	BOROSAPRISTS.....	D	BRAILS FORD.....	C	BRINNUM.....	C/D
BOHNLY.....	D	BORPARK.....	B	BRAM.....	C	BRIONES.....	B
BOHNSACK.....	B	BORREGO.....	D	BRAMAN.....	B	BRISBANE.....	B
BOILER.....	C	BORREGUERO.....	B	BRAMARD.....	B	BRISCOT.....	C/D
BOISE.....	B	BORSKI.....	B	BRAMLETT.....	D	BRISKY.....	D
BOISTFORT.....	B	BORUNDA.....	C	BRANCHVILLE.....	A	BRISTOL.....	A
BOLACK.....	D	BOSA.....	D	BRANCROFT.....	C	BRISTOW.....	D
BOLD.....	B	BOSCO.....	B	BRAND.....	D	BRITTON.....	D
BOLENT.....	A	BOSKET.....	B	BRANDENBERRY.....	B	BRITWATER.....	B
BOLES.....	C	BOSLAND.....	C	BRANDENBURG.....	A	BROADHEAD.....	D
BOLES Loam Substratum.....	D	BOSLER.....	C	BRANDEN.....	B	BROADHURST.....	D
BOLEY.....	D	BOSO.....	D	BRANDON.....	B	BROADKILL.....	D
BOLFAR.....	B/C	BOSONOAK.....	C	BRANDT.....	B	BROADLAND.....	C
BOLICKER.....	B	BOSQUE.....	B	BRANDYPEAK.....	B	BROADUS.....	B
BOLIO.....	D	BOSQUEJO, Overwash.....	C	BRANDYWINE.....	A	BROADWATER.....	A
BOLLIBOKKA.....	D	BOSQUEJO.....	D	BRANFORD.....	B	BROADWAY.....	B
BOLLING.....	C	BOSSBURG.....	C/D	BRANNAN.....	B	BROADWELL.....	B
BOLTON.....	B	BOSTON.....	C	BRANSCOMB.....	B	BROBETT.....	C
BOLTZ.....	C	BOSTRUM.....	D	BRANSON.....	B	BROCKATONORTON.....	D
BOLUDO.....	D	BOSTWICK.....	B	BRANSTAD.....	B	BROCKET.....	C
BOMAR.....	C	BOSVILLE.....	D	BRANTLEY.....	C	BROCKGULCH.....	B
BOMBAY.....	B	BOSWELL.....	D	BRANYON.....	D	BROCKLISS.....	B

BROCKMAN.....	C	BUCKHILL.....	B	BURNEY.....	B	CALD.....	C
BROCKO.....	B	BUCKHOUSE.....	B	BURNSCREEK.....	B	CALDER.....	D
BROCKPORT.....	D	BUCKING.....	A	BURNSIDE.....	B	CALDERWOOD.....	D
BROCKROAD.....	C	BUCKINGHAM.....	C	BURNSVILLE.....	B	CALDWELL.....	B/C
BROCKSBURG.....	B	BUCKLAKE.....	D	BURNSWICK.....	B	CALEAST.....	C
BROCKWAY.....	B	BUCKLE.....	B	BURNT LAKE.....	A	CALEDONIA.....	B
BROCKWELL.....	B	BUCKLICK.....	B	BURNTCREEK.....	D	CALENDAR.....	C
BRODALE.....	C	BUCKMAN.....	D	BURNTHILL.....	B	CALERA.....	C
BRODEER.....	B	BUCKMEN.....	B	BURNTRIVER.....	B	CALFRANCH.....	B
BRODY.....	C	BUCKNDOE.....	B	BURPEAK.....	B	CALHI.....	B
BRODYK.....	B	BUCKNEY.....	B	BURR.....	D	CALICOTT.....	A
BROE.....	B	BUCKROCK.....	D	BURRANT.....	B	CALICREEK.....	B
BROGAN.....	B	BUCKSHOT.....	B	BURRFOOT.....	B	CALKINS.....	C
BROGDON.....	B	BUCKSKIN.....	C	BURROWSVILLE.....	C	CALLA.....	B
BROKENFINGER.....	B	BUCKTON.....	B	BURSLEY.....	D	CALLABO.....	C
BROKENHORN.....	D	BUCKWILDER.....	D	BURSON.....	C	CALLADITO.....	A
BROKIT.....	C	BUCYRUS.....	C	BURSTEADT.....	B	CALLAN.....	C
BROLAND.....	D	BUDE.....	C	BURWELL.....	C	CALLEGUAS.....	D
BROMAGLIN.....	B	BUENA VISTA.....	B	BURWILL.....	C	CALLISBURG.....	C
BROMER.....	C	BUFALO.....	B	BUSACCA.....	C	CALLISON.....	C
BROMIDE.....	B	BUFFCREEK.....	B	BUSHMAN.....	B	CALNAT.....	C
BROMO.....	B	BUFFMEYER.....	B	BUSHNELL.....	C	CALNEVA.....	C
BRONELL.....	B	BUFFSTAT, Channery.....	B	BUSHONG.....	C	CALODO.....	C
BRONSON.....	B	BUFFSTAT.....	C	BUSHVILLE.....	C	CALOOSA.....	C
BRONTE.....	C	BUFORD.....	B	BUSSY.....	C	CALPEAK.....	D
BROOKE.....	D	BUGCREEK.....	D	BUSTER.....	B	CALROY.....	B
BROOKLINE.....	B	BUGLEY.....	C/D	BUSTERBACK.....	B	CALVERTON.....	C
BROOKSHIRE.....	C	BUHL.....	D	BUSTI.....	C	CALVISTA.....	D
BROOKSVILLE.....	D	BUHLER.....	D	BUSYWILD.....	B	CALWOODS.....	D
BROOME.....	B	BUHRIG.....	B	BUTANO.....	C	CALZACORTA.....	D
BROPHY.....	A/D	BUICK.....	C	BUTCHERKNIFE.....	C	CAMAC.....	C
BROSE.....	D	BUKO.....	B	BUTLER.....	D	CAMAGUEY.....	D
BROSELEY.....	B	BUKO, Wet.....	C	BUTLERTOWN.....	C	CAMARGO.....	B
BROUGHTON.....	D	BUKREEK.....	B	BUTTECREEK.....	B	CAMARILLO.....	B/C
BROUILLETT.....	C	BULADEAN.....	B	BUTTERMILK.....	B	CAMASCREEK.....	D
BROWARD.....	C	BULGRAN.....	D	BUTTERS.....	B	CAMATTA.....	D
BROWER.....	B	BULL RUN.....	B	BUTTONCREEK.....	B	CAMBARGE.....	B
BROWNBear.....	B	BULL RUN, Hardpan.....	B	BUXIN.....	D	CAMBERN.....	C
BROWNEDELL.....	D	BULLARDS.....	C	BUZZTAIL.....	D	CAMILLUS.....	B
BROWNELL.....	B	BULLFLAT.....	B	BYBEE.....	C	CAMMASPATCH.....	D
BROWNFIELD.....	A	BULLFOR.....	C	BYGLAND.....	C	CAMOCKA.....	A/D
BROWNSBURG.....	B	BULLGULCH.....	C	BYINGTON.....	C	CAMPAIR.....	C
BROWNSCOMBE.....	C	BULLIS.....	D	BYLER.....	C	CAMPANA.....	B
BROWNSCREEK.....	B	BULLOCK.....	C	BYRAM.....	C	CAMPANILE.....	C
BROWNSDALE.....	C	BULLTOWN.....	B	BYWELL.....	D	CAMPBELL.....	B/C
BROWNSTONE.....	B	BULLVARO.....	B	CABINET.....	B	CAMPBELLTON.....	C
BROWNSTOWN.....	B	BULLVILLE.....	B	CABLON.....	B	CAMPCREEK.....	C
BROWNSVILLE.....	C	BULLWINKLE.....	D	CABO ROJO.....	C	CAMPFOUR.....	B
BROWNTON.....	C/D	BULLY.....	B	CABOOL.....	B	CAMPPIA.....	B
BROXON.....	B	BULOW.....	A	CABOOSE.....	B	CAMPONE.....	C
BRUBECK.....	D	BUMBOB.....	C	CABRILLO.....	C	CAMPRA.....	B
BRUCE.....	B/D	BUNANCH.....	C	CABSTON.....	B	CAMPSPASS.....	B
BRUELLA.....	B	BUNCELVOIR.....	D	CACHEBUTTE.....	B	CAMPSPASS, Deep.....	C
BRUELLA, Hard Substratum.....	C	BUNCETON.....	C	CACHECAN.....	C	CAMPTOWN.....	D
BRUFFY.....	C	BUNCHPOINT.....	C	CACHECREEK.....	B	CAMPUS.....	B
BRUHEL.....	B	BUNCOMBE.....	A	CACIQUE.....	D	CAMPWOOD.....	D
BRUJA.....	B	BUNDORA.....	B	CACTUSFLAT.....	C	CAMRODEN.....	C
BRULE.....	C	BUNDORF.....	D	CADDO.....	D	CANA.....	C
BRUNEEL.....	D	BUNDY.....	C	CADELAKE.....	D	CANADIAN.....	B
BRUNELDA.....	D	BUNDYMAN.....	C	CADELL.....	D	CANAL.....	C
BRUNSWICK.....	B	BUNGALOW.....	D	CADEVILLE.....	D	CANALOU.....	B
BRUSHCREEK.....	C	BUNKER.....	B	CADILLAC.....	A	CANASERAGA.....	C
BRUSHER.....	B	BUNKERHILL.....	D	CADIZ.....	B	CANCENNE.....	C
BRUSHTON.....	B	BUNKUM.....	C	CADMUS.....	B	CANDELERO.....	C
BRUSHY.....	B	BUNKY.....	C	CADOMA.....	C	CANDERLY.....	B
BRUSSELS.....	C	BUNNELL.....	B	CADOTTE.....	B	CANDLESTICK.....	C
BRYARLY.....	D	BUNSELMEIER.....	B	CAESAR.....	A	CANE.....	C
BRYDE.....	C	BUNTING.....	A	CAFETAL.....	B	CANEADEA.....	D
BRYDEN.....	C	BUNTINGVILLE.....	C	CAFFEY.....	C	CANEK.....	B
BRYSTAL.....	B	BUNTLINE.....	D	CAGAS.....	C	CANELO.....	D
BRYWAY.....	C	BUNYAN.....	B	CAGEY.....	C	CANEST.....	D
BTREE.....	C	BURCHAM.....	B	CAHABA.....	B	CANEYHEAD.....	C
BUB.....	D	BURCO.....	D	CAHONA.....	B	CANEZ.....	B
BUCAN.....	D	BUREN.....	C	CAID.....	B	CANISTEO.....	D
BUCCANEER.....	D	BURFORD.....	C	CAINHOY.....	A	CANIWE.....	B
BUCHER.....	D	BURGET.....	D	CAIRN.....	B	CANLON.....	D
BUCHENAU.....	B	BURGRAFF.....	B	CAJALCO.....	C	CANMER.....	B
BUCKBAY.....	C	BURKEMONT.....	C	CAJON.....	B	CANNELL.....	B
BUCKBERT.....	B	BURKETOWN.....	C	CALABAR.....	D	CANNING.....	B
BUCKBOARD.....	B	BURKEVILLE.....	D	CALABASAS.....	B	CANNON.....	B
BUCKCREEK.....	C	BURLESON.....	D	CALAMINE.....	D	CANONEROS.....	D
BUCKEAR.....	D	BURLINGTON.....	A	CALAMITY.....	D	CANOSIA.....	C
BUCKETLAKE.....	B	BURMAN.....	A	CALAMUS.....	A	CANOVA.....	B/D
BUCKEYE.....	C	BURNBOROUGH.....	B	CALAWAH.....	B	CANQUYA.....	D
BUCKHALL.....	B	BURNEL.....	C	CALCIO.....	A	CANTALA.....	B

CANTEEN	B	CARRIZALES	A	CEBONE	C	CHARDOTON	C
CANTINA	C	CARROLLTON	C	CEBOYA	C	CHARDOTON, Hardpan	D
CANTLIN	A	CARRWASH	A	CEDAR BUTTE	D	CHARETTE	C
CANTON BEND	C	CARSITAS	B	CEDARAN	D	CHARGO	D
CANTRIL	B	CARSTAIRS	A	CEDARBLUFF	C	CHARITON	C
CANTUA	B	CART	B	CEDARCREEK	C	CHARITY	D
CANTUCHE	D	CARTAGENA	D	CEDARFALLS	A	CHARLEBOIS	B/C
CANWALL	C	CARTER	D	CEDARGROVE	B	CHARLESTON	C
CANYADA	D	CARTERET	D	CEDARLAKE	D	CHARLOS	B/D
CANYONCREEK	B	CARTERSVILLE	D	CEDARPASS	B	CHARLOTTE	B/D
CANYOUNG	B	CARTHAGE	B	CEDARROCK	D	CHARNOCK, Moderately Wet	B
CAPA	D	CARTWRIGHT	B	CEDARTOWN	A	CHARNOCK	C
CAPAC	C	CARVER	A	CEDONIA	B	CHARTERS	B
CAPE	D	CARVIX	D	CEDRIC	D	CHARWELL	D
CAPE FEAR	D	CARWALKER	C	CEDVAR	B	CHATBURN	B
CAPEBLANCO	B	CARWAY	D	CEEDEE	B	CHATCOLET	B
CAPEHORN	D	CARWILE	D	CEEJAY	D	CHATHAM	B
CAPERS	D	CARYTOWN	D	CEEK	C	CHATT	C
CAPERTON	D	CASABONNE	B	CELACY	C	CHATTERDOWN	B
CAPHEALY	B	CASAMERO	D	CELAVAR	B	CHATTERTON	A
CAPISTRANO	B	CASCILLA	B	CELAVAR, Loamy Surface	C	CHATTICUP	D
CAPITAN	D	CASE	B	CELESTE	D	CHATUGE	D
CAPLEN	D	CASEY	D	CELETON	D	CHAUMONT	D
CAPLES	C/D	CASEYLAKE	B	CELINA	C	CHAUNCEY	C
CAPOOSE	C	CASEYVILLE	B/C	CELIO	C	CHAUTAUQUA	C
CAPPS	B	CASHEL	C	CELT	C	CHAVIES	B
CAPSHAW	C	CASHIERS	B	CENCOVE	B	CHAWANAKEE	C
CAPSUS	D	CASHNER	C	CENIZA	B	CHAZNER	C
CAPTIVA	B/D	CASITO	D	CENTENARY	A	CHAZOS	C
CAPTOM	B	CASLO	C/D	CENTENNIAL	C	CHAZY	C
CARACARA	C	CASPIANA	B	CENTER	C	CHEAHA	D
CARACOLES	D	CASSAL	B	CENTER CREEK	A	CHECKER	C
CARADAN	D	CASSIA	B/C	CENTERBURG	C	CHEDATNA	B
CARALAMPI	C	CASSIDAY	C	CENTERVILLE, Gravelly Substra-	B	CHEDESKI	B
CARAMON	C	CASSOLARY	C	tum	B	CHEDESEY	C
CARBENGLE	B	CASSOPOLIS	B	CENTERVILLE	D	CHEEKTOWAGA	D
CARBERRY	B	CASTAIC	C	CENTISSIMA	B	CHEESEMAM	B
CARBIKA	D	CASTAN	A	CENTRALIA	B	CHEESEMAM, Loamy Surface	C
CARBINE	D	CASTANA	B	CENTRALPEAK	C	CHEETHAM	B
CARBONDALE	A/D	CASTANEDA	C	CERBAT	D	CHEHALEM	C
CARBONTON	C	CASTEE	B	CERP	B	CHEHULPUM	D
CARDENAS	D	CASTELL	C	CERROCOSO	B	CHEKIKI	D
CARDIFF	B	CASTELLEIA	B	CESARIO	C	CHELINA	B
CARDINAL	B	CASTEPHEN	C	CESSNA	D	CHELMO	D
CARDINGTON	C	CASTILE	B	CESTNIK	C	CHEMAWA	B
CARDON	D	CASTLE	D	CETRACK	B	CHEME	D
CARDSOUND	D	CASTLEPEAK	A	CETREPAS	D	CHENA	A
CAREFREE	D	CASTLEROCK	B	CEWAT	C	CHENAULT	B
CARETT	B	CASTLEROCK	D	CHABENEAU	B	CHENEGA	A
CAREY LAKE	B	CASTLEWOOD	C/D	CHACON	D	CHENOA	B
CARFALL	B	CASTO	C	CHACUACO	C	CHENOWETH	B
CARGENT	B	CASTROVILLE	B	CHAD	C	CHEOAH	B
CARGILL	C	CASVARE	D	CHAFFEE	D	CHEOSA	D
CARIB	D	CASWELL	B	CHAGRIN	B	CHEQUEST	C
CARIBEL	B	CATALINA	B	CHAIN	C	CHEROKEE	D
CARIBOU	B	CATALPA	B	CHAINLINK	D	CHERRY CREEK	B
CARIBOURIDGE	B	CATANO	A	CHAIRES	D	CHERRYHILL	B
CARIOCA	B	CATARACT	B	CHALKCREEK	B	CHESANING	B
CARIS, High Rainfall	B	CATAULA	B	CHALKFORD	C	CHESBROOK	D
CARIS	C	CATELLI	B	CHALKHILL	B	CHESNIMNUS	B
CARLAIN	B	CATH	C	CHALKVILLE	D	CHESTATEE	B
CARLIN	D	CATHARPIN	C	CHALLENGER	B	CHESTERTON	D
CARLITO	D	CATHEEN	B	CHALLENGER, Alkali	D	CHESTOA	B
CARLOS	A/D	CATHERINE	C	CHALLIS	C	CHESTONIA	D
CARLOTTA	B	CATHLAMET	B	CHALMERS	B/D	CHETASLINA	B
CARLSBAD	C	CATILLA	B	CHAMA	C	CHETCO	D
CARLSBORG	A	CATLA	D	CHAMATE	B	CHETEK	B
CARLSON	B	CATNIP	D	CHAMBEAM	B	CHETOMBA	B/D
CARLSTROM	C	CATPOINT	A	CHAMBERLAIN	B	CHEVAL	C
CARLTON	C	CATT CREEK	A	CHAMITA	C	CHEW	B
CARMAN	B	CATTO	D	CHAMOKANE	C	CHEWACK	B
CARMEL	C	CAULEY	B	CHAMPLAIN	A	CHEWAUCAN	C
CARMI	B	CAUSEWA	C	CHANAC	B	CHEWELAH	C
CARMINE	C	CAVANAGH	C	CHANCELLOR	C	CHEYENNE	B
CARMODY	C	CAVENDISH	B	CHANNAHON	D	CHIA	D
CARNEGIE	C	CAVERNS	B	CHANTIER	D	CHIC	B
CARNERO	C	CAVINISS	B	CHANYBUCK	D	CHICANE	C
CAROLINE	C	CAVO	D	CHAPANOKE	C	CHICHAGOF	D
CAROLLO	D	CAX	B	CHAPARRAL	B	CHICHANTNA	D
CARON	A/D	CAYAGUA	C	CHAPEL	D	CHICKAMAN	B
CARPENTERVILLE	D	CAYO	B	CHAPETT	B	CHICKASAW	C
CARRACAS	D	CAYUGA	C	CHAPPELL	A	CHICKASHA	B
CARRCREEK	B	CAYUSE	B	CHAPPUIS	C	CHICO	B
CARRI	B	CAZADERO	C	CHARBONO	B	CHICOLETE	C
CARRICK	C	CEBOLIA	C	CHARCO	C	CHICONE	D

CHICOTE	D	CHUMMY	D	CLIMAX	D	COLDSPRING	B
CHIDAGO	A	CHUNILNA	D	CLINE	D	COLEMAN	C
CHIEFLAND	B	CHUNKMONK	C	CLINEFALLS	A	COLEMANTOWN	C/D
CHIGLEY	C	CHUPE	A	CLINETOP	D	COLEPOINT	B
CHILAO	C	CHURCH	D	CLINGMAN	D	COLERIDGE	C
CHILCOTT	C	CHURCH SPRINGS	B	CLINKENBEARD	D	COLFAX	C
CHILDS	B	CHURCHVILLE	D	CLIPPER	C/D	COLFER	A
CHILGREN	C	CHURUBUSCO	D	CLIQUE	C	COLHILL	B
CHILHOWEE	B	CHUTE	A	CLITHERALL	B	COLIBRO	B
CHILICOTAL	B	CHUTUM	B	CLODINE	D	COLINAS	B
CHILLICOTHE	B	CIALES	D	CLOQUALLUM	C	COLLEGECREEK	B
CHILLIGAN	B	CIBEQUE	B	CLOQUET	B	COLLETT	C/D
CHILLUM	B	CID	C	CLOSKEY	C	COLLIER	A
CHILLYBU	D	CIDERMILL	B	CLOTHO	C/D	COLLINGTON	B
CHILOQUIN	D	CIDRAL	C	CLOUD PEAK	B	COLLINS	C
CHILSON	D	CIENEGA	B	CLOUDCROFT	D	COLLISTER	B
CHIMAY	D	CIENO	D	CLOUDLAND	C	COLMA	B
CHIME	C	CIERVO	C	CLOUDLESS	C	COLNEVEE	B
CHIMINET	D	CIFIC	C	CLOUGH	D	COLOMEX	B
CHIMNEY	A	CINCO	A	CLOVELLY	D	COLONVILLE	C
CHIMNEYROCK	B	CINDERHURST	D	CLOVER SPRINGS	B	COLORADO	B
CHINA	D	CINNAMON BAY	B	CLOVERCREEK	C	COLOROCK	D
CHINABUTTE	D	CINTRONA	B	CLOWERS	B	COLOROW	B
CHINAHAT	B	CIRCLE	B	CLOWERS	B/C	COLPIEN	B
CHINCAP	B	CIRCLEBACK	A	CLOWFIN	B	COLSAVAGE	C
CHINCOTEAGUE	D	CIRCLEBAR	C	CLOYD	D	COLUMBINE	A
CHINDE	C	CIRCLEVALLEY	B	CLUBCAF	D	COLUMBUS	C
CHINHILL	B	CIRCULAR	D	CLUNIE	D	COLUSA	C
CHINIAK	A	CISCO	B	CLUNTON	D	COLVARD	B
CHINKLE	D	CISPUS	B	COACHELLA	B/C	COLVILLE	C/D
CHINLINI	B	CITICO	B	COAHUILA	B	COLY	B
CHINO	B/C	CITRONELLE	D	COALDALE	D	COLYELL	C
CHINVAR	C	CITYPOINT	A/D	COALDRAW	D	COLYER	D
CHINWHISKER	A	CLACKAMAS	D	COALGATE	D	COMAR	C
CHIPENDALE	D	CLAMP	D	COAMO	C	COMBE	B
CHIPENHILL	D	CLANA	A	COARSEGOLD	C	COMBEST	B
CHIPLEY	C	CLANALPINE	C	COARSEWOOD	B	COMBS	B
CHIPOLA	A	CLAPHAM	C	COATSBURG	D	COMER	B
CHIPPENY	D	CLARA	B/D	COBATUS	C	COMETCRIK	D
CHIRENO	D	CLARA	D	COBB	B	COMFORT	D
CHISMORE	D	CLARENA	B	COBBLANK	D	COMFREY	D
CHISOLM	A	CLARENCE	D	COBEN	D	COMITAS	A
CHISPA	B	CLARENDON	C	COBERLY	B	COMO	A
CHISTNA	B	CLARESON	C	COBERLY, Low Rainfall	C	COMPASS	B
CHISTOCHINA	B	CLAREVILLE	C	COBEY	B	COMSTOCK	C
CHITA	B	CLARITA	D	COBLENTZ	C	COMUS	B
CHITINA	B	CLARK	B	COBLYNN	B	CONA	C
CHITTUM	C	CLARKIA	C	COBOC	C	CONABY	B/D
CHITWOOD	D	CLARKRANGE	C	COBRE	C	CONALB	B
CHIVATO	C	CLARKSDALE	C	COBSTONE	B	CONANT	C
CHIVATO, Elevation>8000	D	CLARKSTONE	B	COCHINA	D	CONATA	D
CHIWAUKUM	B	CLAUNCH	B	COCHRAN	C	CONBOY	D
CHIWAWA	B	CLAVERACK	C	COCKSCOMB	C	CONCEPCION	D
CHO	C	CLAYBANKS	C/D	COCOA	A	CONCHAS	C
CHOATES	C	CLAYCREEK	B	COCODRIE	C	CONCHOVAR	C
CHOCOLOCOCO	B	CLAYHAM	C	COCOLALLA	C/D	CONCORD	D
CHOCK	D	CLAYHOLE	B	COCONINO	B	CONCORDIA	D
CHOCKTOOT	B	CLAYSVILLE	C	COD	B	CONDA	D
CHOCORUA	D	CLAYTON	B	CODORUS	C	CONDIDO	D
CHOICE	D	CLE ELUM	C	CODQUIN	D	CONDIT	D
CHOKE	B	CLEARCREEK	D	CODYLAKE	B	CONDON	C
CHOOP	D	CLEARFORK	D	COE	A	CONECUH	D
CHORALMONT	A	CLEARLINE	B	COESSE	C/D	CONETOE	A
CHOSKA	B	CLEARRIVER	B	COFF	C	CONEWARD	A
CHOTEAU	C	CLEARVIEW	B	COFFEE	B	CONGAREE	B
CHOWAN	D	CLEAVMOR	D	COFFEEN	B	CONGLE	B
CHRIS	C	CLEGHORN	C	COFFEEPOT	B	CONICAL	B
CHRISHALL	B	CLEMENTINE	B/C	COFFTON	B	CONLEN	B
CHRISMAN	D	CLEMVILLE	B	COGHILL	C	CONLEY	C
CHRISTIANA	C	CLENAGE	C	COGLIN	C	CONNAH	D
CHRISTIANBURG	C	CLENDENEN	D	COHAGEN	C	CONNERIDGE	C
CHRISTINE	D	CLEONE	B	COHAGEN, Cool	D	CONNET	D
CHRISTOFF	C	CLEORA	B	COHAS	C	CONOSTA	C
CHRISTY	C	CLERGERN	B	COHOE	B	CONOTTON	B
CHROME	C	CLERMONT	D	COILE	D	CONOVER	C
CHRYSLER	C	CLEVELAND	C	COILS	C	CONOWINGO	C
CHUBBFLAT	C	CLEVESCOVE	B	COIT	D	CONPEAK	D
CHUCKANUT	B	CLEYMOR	B	COKATO	B	CONQUISTA	D
CHUCKRIDGE	D	CLICK	A	COKEDALE	C/D	CONRAD	A/D
CHUCKRIVER	D	CLIFF	B	COKER	D	CONSEJO	C
CHUFFA	B	CLIFFDELL	B	COKEVILLE	B	CONSER	D
CHUGCREEK	C	CLIFFFIELD	B	COLBE	D	CONSTABLE	A
CHUGTER	B	CLIFFORD	C	COLBERT	C	CONSTANCE	D
CHUICHU	D	CLIFFSIDE	B	COLBURN	D	CONSTANCIA	D
CHUIT	B	CLIFTY	B	COLDENT	C	CONSUMO	B

CONTACT	A	COSPERVILLE	C	CREDO	B	CUCAMUNGO	D
CONTEE	D	COST	D	CREEDMOOR	C	CUCCHARAS	C
CONTENTION	D	COSTAVAR	D	CREEL	C	CUCHILLAS	C
CONTIDE	B	COTEAU	C	CREFORK	C	CUDEI	B
CONTO	B	COTHA	C	CREOLE	D	CUDJOE	D
CONVENT	C	COTITO	B	CRESAL	B	CUERBIO	B
COOERS	B	COTO	B	CRESKEN	B	CUERO	B
COOKCAN	D	COTT	B	CRESPIN	C	CUESTA	C
COOLBRITH	C	COTTER	B	CRESS	A	CUEVA	D
COOLVILLE	C	COTTON	C	CRESSLER	D	CUEVITAS	D
COOMBS	B	COTTONBEND	B	CREST	C	CUEVOLAND	B
COONSKIN	C	COTTONEVA	C	CRESTMEADE	D	CUJOB	D
COOPER	B	COTTONTOMAS	B	CRESTVALE	C	CULBERTSON	B
COOPMONT	B	COTTONWOOD	C	CRESTWAY	B	CULDECOLE	B
COOSAW	B	COTTREE	B	CREVA	D	CULDESAC	B
COOSCANYON	B	COTTRELL	C	CREVISCREEK	C	CULITAS	C
COOT	B	COTULLA	D	CREX	B	CULLIUS	D
COOTER	C	COUGARBAY	D	CRIMS	D	CULLOWHEE	B/D
COPALIS	C	COUGHANOUR	C	CRINKER	C	CULP	C
COPANO	D	COULTERVILLE	D	CRISFIELD	B	CULPEPER	C
COPASTON	D	COUNTRYMAN	C	CRISPIN	C	CULTUS	B
COPEAK	C	COUNTS	D	CRITCHELL	B	CULVING	C
COPELAND	B/D	COUPEE	B	CRITTENDEN	B	CULVOP	B
COPELAND, Depressional	D	COUPEVILLE	C/D	CROCAMP	B	CUMBERLAND	B
COPENHAGEN	D	COURSEY	C	CROCAN	D	CUMBRES	C
COPITA	B	COURT	B	CROCKETT	D	CUMLEY	C
COPPER RIVER	D	COURTNEY	D	CROFLAND	C	CUMMINGS	D
COPPERBASIN	D	COURTOIS	B	CROFTSHAW	B	CUMMISKEY	B
COPPERCAN	D	COURVASH	B	CROGHAN	B	CUNDICK	D
COPPERCREEK	B	COUSE	C	CROKE	B	CUNIFF	D
COPPEREID	D	COVEDALE	B	CRONESE	A	CUNIFF	C
COPPERFIELD	B	COVEGAP	B	CRONKHITE	C	CUNNINGHAM	C
COPPLER	A	COVELAND	C/D	CRONKS	C	CUPCO	C
COPUS	C	COVERTFALLS	C	CROOKED	D	CUPEL	D
COQUAT	D	COVILLE	B	CROOKSFORD	B	CUPINE	C
CORA	D	COVING	C	CROOKSTON	B	CUPOLA	B
CORAL	C	COVINGTON	D	CROOM	C	CUPPER	B
CORAZONES	A	COWAN	A	CROPLEY	D	CUPPLES	C
CORBIN	B	COWBONE	D	CROQUIB	D	CUPPY	D
CORBLV	A	COWCREEK	B	CROSIER	C	CUPVAR	D
CORCEGA	C	COWCREEK, Protected	C	CROSSCREEK	B	CURABITH	A
CORDALE	B	COWDEN	D	CROSSEN	B	CURANT	B
CORDELL	D	COWEEMAN	D	CROSSETT	C	CURDLI	B
CORDES	B	COWHORN	B	CROSSNORE	B	CURRAN	C
CORDOVA	C/D	COWSPRING	B	CROSSPLAIN	C	CURRENT SPRING	C
CORDY	B	COWTRACK	A	CROSSTELL	D	CURRIER	A
CORIFF	B/D	COX	D	CROSSVILLE	B	CURRITUCK	D
CORINTH	C	COXIT	B	CROSWOOD	A	CURRY	C
CORKSTONE	D	COXLAKE	D	CROT	D	CURTIN	D
CORLENA	A	COXRANCH	C	CROW	C	CURTIS CREEK	D
CORLETT	A	COXVILLE	D	CROW CREEK	B	CURTIS SIDING	A
CORLEY	B/D	COXWELL	C	CROW HILL	C	CURTISTOWN	B
CORLISS	A	COY	D	CROWELL	A	CURTISVILLE	D
CORNELIA	A	COYANOSA	D	CROWERS	B	CUSHENBURY	B
CORNELIUS	C	COYATA	C	CROWFORK	A	CUSHING	B
CORNHILL	B	COYNE	B	CROWHEART	C	CUSHMAN	B
CORNICK	D	COYOTE	A	CROWLEY	D	CUSHOOL	B
CORNVILLE	B	COZETICA	A	CROWRIVER	B/D	CUSICK	D
CORNWALL	C	COZY	C	CROWSHAW	B	CUSTCO	B
COROLLA	D	CRABCREEK	B	CROZIER	C	CUSTER	C/D
CORONA	B	CRABTREE	C	CRUBAS	D	CUTCOMB	D
CORONACA	B	CRACKER	D	CRUCES	D	CUTHAND	B
COROZAL	C	CRACKERCREEK	B	CRUCKTON	B	CUTHBERT	D
COROZO	A	CRACKLER	B	CRUICKSHANK	C	CUTSHIN	B
CORRALCREEK	C	CRADLEBAUGH	D	CRUMARINE	B	CUTTOR	D
CORRALITOS, Silty Substratum	B	CRAFTON	C	CRUMLEY	B	CUTZ	D
CORRALITOS, Clayey Substratum	C	CRAGGEY, Organic Surface	A	CRUNKER	B	CUYAMA	B
CORRALRIDGE	B	CRAGGEY	D	CRUNKVAR	A	CUYAMUNGUE	A
CORRIGAN	D	CRAIG	B	CRUSTOWN	C	CUYON	A
CORSAIR	A	CRAIGEN	B	CRUTCH	C	CYAN	B
CORSICA	C/D	CRAMER	C	CRUTCHFIELD	B	CYCLONE	B/D
CORTA	D	CRAMONT	C	CRUZE	C	CYCLOPIC	C
CORTADA	B	CRANECREEK	C	CRYLUHA	C	CYGNET	B
CORTARO	D	CRANFILL	B	CRYSTAL LAKE	B	CYMRIC	D
CORTELYOU	D	CRANMLER	B	CRYSTALCREEK	B	CYNTHIANA	D
CORTINA	A	CRANSTON	B	CRYSTALEX	B	CYPRESS	D
CORUM	C	CRASH	B	CRYSTALGYP	C	CYRIL	B
CORVUSO	C/D	CRATER LAKE	B	CRYUMBREPTS	B	CYVAR	D
CORWITH	B	CRATERMO	C	CUATE	C	CZAR	B
CORY	C	CRAVEN	C	CUBA	B	DAB	B
CORZUNI	B	CRAWFISH	D	CUBCREEK	C	DABNEY	A
COSAD	C	CRAWFORD	D	CUBDEN	C	DABOB	C
COSH	C	CRAWLEY	D	CUBERANT	B	DACKEY	C
COSLAW	D	CRAWLEYVILLE	B	CUBHILL	C	DACRON	B
COSMOS	C/D	CREASEY	C/D	CUBLAKE	A	DADE	A

DADINA.....	D	DAXTY.....	C	DELEON.....	C	DESKAMP.....	B
DAGUAO.....	C	DAYBROOK.....	C	DELEPLAIN.....	D	DESKER.....	A
DAGUEY.....	C	DAYCREEK.....	A	DELETTE.....	C	DESMET.....	B
DAHAR.....	C	DAYSCHOOL.....	B	DELHEW.....	B	DESOLATION.....	B
DAHL.....	D	DAYTONA.....	B	DELICIAS.....	B	DESONS.....	C
DAILEY.....	B	DAYVILLE.....	C	DELISH.....	C	DESTER.....	C
DAINT.....	B	DAZE.....	D	DELKS.....	C/D	DETERSON.....	C
DAISY.....	B	DEACON.....	B	DELL.....	C	DETOUR.....	B
DAISYBAY.....	A	DEADFALL.....	C	DELLO.....	D	DETRITAL.....	B
DALBY.....	D	DEADFOOT.....	B	DELLS.....	C	DETROIT.....	C
DALCO.....	D	DEADHORSE.....	C	DELLWOOD.....	A	DEUCE.....	D
DALECREEK.....	B	DEADLINE.....	B	DELMITA.....	C	DEUCHARS.....	C
DALEROSE.....	D	DEADWOOD.....	B	DELMO.....	B	DEV.....	A
DALESBURG.....	B	DEADYON.....	D	DELNORTE.....	C	DEVARGAS.....	B
DALEVILLE.....	D	DEAM.....	C	DELOSS.....	B/D	DEVILFENCE.....	D
DALHART.....	B	DEANBURG.....	B	DELP.....	A	DEVILS.....	D
DALIG.....	B	DEANRAN.....	D	DELPHI.....	B	DEVILSCREEK.....	C
DALKENA.....	C	DEARYTON.....	C	DELPLAIN.....	D	DEVINE.....	C
DALLAM.....	B	DEATMAN.....	C	DELRAY.....	D	DEVISADERO.....	C
DALLARDSVILLE.....	C	DEAVER.....	C	DELRIDGE.....	B	DEVNOT.....	D
DALTON.....	C	DEBENGER.....	B	DELRIO.....	B	DEVOE.....	D
DALUPE.....	B	DEBEQUE.....	B	DELTAJO.....	C	DEVOIGNES.....	D
DALVORD.....	D	DEBOOK.....	B	DELUGE.....	C	DEVRIES.....	C
DAMASCUS.....	B/D	DEBORAH.....	D	DELVALLE.....	B	DEWBERRY.....	B
DAMEWOOD.....	C	DEBS.....	B	DELVAR.....	C	DEWEY.....	B
DAMON.....	D	DEBUTE.....	C	DELWAY.....	D	DEWEYVILLE.....	D
DAMORE.....	C	DECAN.....	C	DELWIN.....	A	DEWITT.....	C
DANABROOK.....	B	DECANTEL.....	D	DELYNDIA.....	A	DEWMINE.....	D
DANAVORE.....	B	DECATHON.....	C	DEMAYO.....	D	DEWRUST.....	C
DANCY.....	B/D	DECATUR.....	B	DEMENT.....	B	DEWVILLE.....	B
DANDAN.....	C	DECEPTION.....	B	DEMILL.....	B	DEXTER.....	B
DANDREA.....	C	DECHEL.....	D	DEMING.....	B	DEZELLEM.....	B
DANGULCH.....	D	DECKERVILLE.....	C/D	DEMKY.....	D	DIAFLATS.....	B
DANHUNT.....	B	DECORDOVA.....	B	DEMOGUL.....	B	DIAGULCH.....	B
DANIA.....	B/D	DEGRAM.....	C	DEMONA.....	C	DIAMOND.....	D
DANIELSON.....	C/D	DECY.....	B	DEMONTREVILLE.....	B	DIAMONDHIL.....	C
DANIELVIL.....	B	DEDAS.....	D	DEMOPOLIS.....	C	DIAMONKIT.....	C
DANJER.....	D	DEDMOUNT.....	C	DEMOPOLIS, cobbly.....	D	DIANEV.....	D
DANKO.....	D	DEDMOUNT, Lacustrine Substra- tum.....	D	DEMORY.....	D	DIANOLA.....	D
DANKWORTH.....	A	DEDRICK.....	D	DEMOSSE.....	D	DIATEE.....	B
DANSKIN.....	B	DEE.....	D	DEMOX.....	B	DIAWELL.....	D
DANT.....	D	DEECREE.....	B	DEMPSEY.....	B	DIBOLL.....	D
DANUBE.....	B/D	DEEFAN.....	D	DEMPSTER.....	B	DICECREEK.....	C
DAPOIN.....	C	DEEMER.....	B	DENAUD.....	B/D	DICK.....	A
DARAS.....	B	DEEPCUT.....	D	DENBAR.....	C	DICKERSON.....	D
DARBONNE.....	B	DEEPEEK.....	D	DENBY.....	C	DICKEYPEAK.....	C
DARBY.....	C	DEEPWATER.....	B	DENCO.....	C	DICKLE.....	D
DARCO.....	A	DEEPWOOD.....	B	DENKA.....	D	DICKSON.....	C
DARDANELLE.....	B	DEER PARK.....	A	DENIO.....	B	DIEBERT.....	B
DARDEN.....	A	DEERCUT.....	C	DENNIS.....	C	DIEHLSTADT.....	C
DARDOOW.....	B	DEERFIELD.....	B	DENNISVILLE.....	B	DIERSSSEN.....	D
DARE.....	D	DEERHEART.....	C	DENOMIE.....	C	DIGBY.....	B
DARFUR.....	B/D	DEERHORN.....	C	DENROCK.....	D	DIGHTON.....	B
DARKCANYON.....	C	DEERRUN.....	C	DENT.....	B	DIGIORGIO.....	B
DARL.....	C	DEERWOOD.....	B/D	DENTDRAW.....	D	DILLARD.....	C
DARLAND.....	B	DEFENBAUGH.....	B	DENTON.....	D	DILLCOURT.....	B
DARLEY.....	C	DEFIANCE.....	D	DENURE.....	A	DILLEY.....	C
DARLINGTON.....	A	DEGATER.....	D	DENVACA.....	D	DILLINGHAM.....	A
DARLOW.....	C	DEGNER.....	B	DEPALT.....	D	DILLWYN.....	A
DAROW.....	C	DEGOLA.....	B	DEPCOR.....	B	DILMAN.....	C
DARR.....	B	DEGRAND.....	B	DEPEYSTER.....	C	DILTON.....	D
DARRAH.....	C	DEGREY.....	D	DEPNER.....	B	DILWORTH.....	D
DARROCH.....	C	DEHAVEN.....	B	DEPOE.....	D	DIMAL.....	C
DARROUZETT.....	D	DEHILL.....	B	DEPORT.....	D	DIME.....	B
DARSIL.....	C	DEHLINGER.....	B	DERAPTER.....	B	DIMEBOX.....	D
DART.....	A	DEIGHT.....	B	DERB.....	C	DIMO.....	B
DARTMOUTH.....	B	DEINACHE.....	A/D	DERBY.....	A	DINA.....	C
DARVEY.....	B	DEKALB, Stony.....	A	DERECHO.....	B	DINCO.....	B
DARWASH.....	B	DEKALB.....	B	DERMALA.....	B	DINES.....	B
DASHER.....	D	DEKAPEN.....	C	DEROIN.....	B	DINEVO.....	B
DASHIKI.....	A	DEKKAS.....	A	DEROUX.....	C	DINGLE.....	C
DASSEL.....	B/D	DEKOOM.....	B	DERR.....	C	DINGLISHNA.....	D
DATINO.....	B	DEKOVEN.....	D	DERRINGER.....	C	DINGMAN.....	C
DATOM.....	D	DELA.....	B	DERRYNANE.....	C	DINKEY.....	A
DATWYLER.....	C	DELACIT.....	D	DERWELL.....	B	DINZER.....	B
DAVEGGIO.....	B	DELAMAR.....	B	DES MOINES, Dry.....	B	DIOBSUD.....	C
DAVIDELL.....	B	DELAMETER.....	A	DES MOINES, Cobbly.....	C	DIPCREEK.....	D
DAVIDSON.....	B	DELAND.....	A	DESAN.....	A	DIPMAN.....	D
DAVILLA.....	D	DELANO.....	B	DESATOYA.....	C	DIPSEA.....	B
DAWHOO.....	B/D	DELANO, Sandy.....	C	DESCALABRADO.....	D	DIQUE.....	B
DAWN.....	B	DELAWARE.....	B	DESCHUTES.....	B	DIREGO.....	D
DAWNY.....	B	DELCOMB.....	D	DESERTLAKE.....	D	DIRTYHEAD.....	C
DAWSIL.....	A/D	DELENA.....	D	DESFIRES.....	B	DISAGE.....	D
DAWTONIA.....	B	DELENBAW.....	D	DESHA.....	D	DISAPPOINT.....	D
				DESHASER.....	B	DISCO.....	B

DISCOVERY	D	DOROTHEA	C	DUCKHILL	D	EAGLESPRING	B
DISHNER	D	DOROVAN	D	DUCKSTON	A/D	EAGLETON	D
DISHNO	C	DORRANCE	A	DUELM	A	EAGLEVIEW	A
DISHPAN	C	DORS	B	DUETTE	A	EAGLEVILLE	D
DISTELL	C	DORSET	B	DUFFAU	B	EAGLEWING	B
DISWOOD	D	DORVAL	A/D	DUFFERN	B	EAGLEYE	D
DITCHCAMP	C	DOSA	D	DUFFYMONT	C	EAGREEK	B
DITHOD	B	DOSAMIGOS	D	DUFFYMONT, Dry	C	EAKIN	B
DITNEY	C	DOSEWALLIPS	D	DUFUR	B	EALY	B
DIVIDE	C	DOSIE	C	DUGGINS	D	EAPA	B
DIVISION	D	DOSLOMAS	C	DUGUESCLIN	D	EARLE	D
DIVOT	C	DOSS	D	DUGWAY	C	EARLMONT	C/D
DIXALETA	D	DOSSMAN	B	DUKES	A	EARP	B
DIXBORO	B	DOTLAKE	D	DULA	D	EASBY	C
DIXIEJETT	B	DOTSERO	B	DULAC	C	EASLEY	C
DIXON	B	DOTSLOT	D	DULANDY	B	EASPUR	B
DIXONVILLE	C	DOTY	B	DULCE	D	EAST LAKE	A
DOANE	B	DOUBLEDIA	D	DULEYLAKE	C	EASTABLE	B
DOBALT	B	DOUBLEO	D	DULLAXE	B	EASTCHOP	A
DOBBINS	C	DOUCETTE	B	DULLES	D	EASTHAM	D
DOBEL	D	DOUDLE	B	DUMAS	B	EASTPARK	D
DOBENT	C/D	DOUGAL	D	DUMFRIES	B	EASTPINE	B
DOBIE	B	DOUGAN	C	DUMONT	D	EASTWOOD	D
DOBSON	D	DOUGCITY	B	DUMPS, Tailings	B	EASYCHAIR	B
DOCAS	B	DOUGCLIFF	D	DUNBAR	D	EATONCREEK	D
DOCENA	C	DOUGHBOY	B	DUNBRIDGE	B	EAUCLAIRE	A
DOCKLAKE	B	DOUGHERTY	A	DUNC	C	EAGALLIE	D
DOCPAR	B	DOUGHSPON	C	DUNCANNON	B	EBADLOW	B
DODD	D	DOUGHTY	B	DUNFORD	C	EBAL	B
DODES	B	DOUGLAS	B	DUNGAN	B	EBBERT	C/D
DODGE	B	DOUHIDE	D	DUNGENESS	B	EBBING	C
DODGECREEK	B	DOURO	B	DUNKIRK	B	EBBS	B
DODGEVILLE	C	DOUTHIT	B	DUNKLEBER	D	EBIC	D
DODSON	C	DOWAGIAC	B	DUNLATOP	B	EBODA	B
DODY	C/D	DOWDE	B	DUNMORE	B	EBODA, Stony	C
DOE	B	DOWELLTON	D	DUNNBOT	B	EBRO	D
DOEL	C	DOWNER	B	DUNSMUIR	B	ECHAW	A
DOGIECREEK	B	DOWNEY	B	DUNSMUIR, Nongravelly	C	ECHETA	C
DOGLAKE	A	DOWNEYGULCH	C	DUNTON	C	ECKERT	D
DOGMOUNTAIN	C	DOWNSOUTH	B	DUPLIN	C	ECKHART	B
DOGTOOTH	D	DOWNSVILLE	B	DUPO	C	ECKLUND	B
DOGUE	C	DOWPER	B	DUPREE	D	ECKMAN	B
DOKER	C	DOYLESTOWN	D	DURADOS	A	ECKRANT	D
DOLBEE, Sandy Substratum	B	DOYN	D	DURALDE	C	ECKVOLL	B
DOLBEE	C	DRAGSTON	C	DURAND	B	ECLETO	D
DOLEKEI	B	DRAKE	B	DURANGO	B	ECLIPSE	B
DOLEN	B	DRAKESFLAT	B	DURANT	D	ECOLA	C
DOLES	C	DRAKESPEAK	B	DURAZO	A	ECON	B
DOLLAR	C	DRAMMEN	A	DURBIN	D	ECONFINA	A
DOLLARD	C	DRANBURN	B	DURELLE	B	ECUR	B
DOLLARHIDE	D	DRASCO	C	DURKEE	C	EDA	A
DOLLYCLARK	C	DRAX	B/C	DURRSTEIN	D	EDALFRED	A
DOLMAN	C	DREKA	D	DURSTON	C	EDALGO	C
DOLUS	C	DRESDEN	B	DUSEN	B	EDDINGS	B
DOME	B	DREWING	D	DUSKPOINT	A	EDDS	B
DOMENGINE	C	DREWSEY	B	DUSLER	C	EDDY	C
DOMERIE	B	DREWSGAP	C	DUSON	C	EDEMAYS	C
DOMEZ	B	DREXEL	B	DUSTON	A	EDENBOWER	D
DOMINGUEZ	C	DRIFTWOOD	C/D	DUSTY	B	EDENTON	C
DOMINSON	A	DRIGGS	B	DUTCHATT	B	EDENVALLEY	B
DOMKEY	B	DRINO	C	DUTCHCANYON	B	EDGAR	B
DOMO	B	DRIVER	C	DUTCHENRY	C	EDGEHILL	C
DOMPIER	C	DROEM	C	DUTCHFLAT	C	EDGELEY	C
DONA ANA	C	DROVAL	D	DUTCHJOHN	B	EDGEMERE	D
DONAHUE	C	DRUM	B	DUTEK	A	EDGEWATER	C
DONALD	C	DRURY	B	DUTTON	C	EDGEWICK	C
DONALDSON	C	DRY LAKE	C	DUVAL	B	EDGINGTON	C/D
DONEGAN	C	DRYADINE	C	DUZEL	C	EDINBURG	C/D
DONERAIL	C	DRYBED	B	DWARF	D	EDISTO	C
DONICA	B	DRYBUCK	B	DWORSHAK	B	EDJOBE	C
DONKEHILL	D	DRYBURG	B	DYE	D	EDMINSTER	D
DONLONTON	C	DRYCK	A	DYERHILL	B	EDMORE	D
DONNEL	B	DRYDEN	B	DYLAN	D	EDMUNDSTON	B
DONNELSVILLE	B	DRYFALLS	B	DYNAL	A	EDOM	C
DONNING	D	DRYHOLLOW	B	EACHUS	B	EDROY	C
DONNYBROOK	D	DRYN	C	EAD	C	EDSON	C
DOOH	B	DUART	C	EAGAR	B	EDWARDS	B/D
DOOLIN	D	DUBACH	B	EAGLECAP	B	EDWARDSVILLE	B/D
DOONE	B	DUBAY	B	EAGLECONE	B	EDWIN	B
DORA	B/D	DUBBS	B	EAGLECREEK	B	EELCOVE	D
DORERTON	B	DUBBS, Flooded	C	EAGLELAKE	B	EELWEIR	C
DORITTY	B	DUBINA	C	EAGLEPOINT	D	EENREED	B
DORNA	B	DUBLON	B	EAGLEROCK	C	EEP	C
DORNA, Thin	C	DUCKABUSH	B	EAGLESNEST	C	EFFIE	C
DOROSHIN	D	DUCKCLUB	C	EAGLESON	C	EFFINGTON	C

EGAM	C	ELMER	C	EREMIS	B	EXETER	B
EGAN	B	ELMINA	C	ERICSON	B	EXTEND	C
EGANROC	C	ELMONT	B	ERIG	B	EXUM	C
EGGLAKE	C/D	ELMRIDGE	C	ERIN	B	EXWAY	B
EGGLESON	B	ELMVILLE	B	ERMABELL	A	EYAK	C
EGHELM	C	ELMWOOD	C	ERMATINGER	B/D	EYERBOW	C
EGLIN	A	ELNORA	C	ERNBET	C	EYLAU	C
EGLIRIM	C	ELOCHOMAN	B	ERNO	B	EYOTA	A
EGUAJE	B	ELOCIN	D	ERRAMOUSPE	C	EZEL	B
EGYPT	D	ELON	B	ERVIDE	C	EZELL	C
EGYPTCREEK	C	ELOSO	D	ESAU	A	FABIUS	B
EICKS	C	ELPAM	D	ESCAMBIA	C	FACEVILLE	B
EIGHTLAR	C	ELPASO	B/D	ESCANABA	A	FACEY	B
EIGHTMILE	D	ELRED	B/D	ESCANO	C	FACTORY	B
EILERTSEN	B	ELRIN	B	ESCARLO	B	FADDIN	D
EINE	D	ELROSE	B	ESCONDIDO/ Thick Solum	B	FADOLL	B
EITZEN	B	ELSIE	B	ESCONDIDO	C	FAGAN	C
EKAH	C	ELSINBORO	B	ESEL	B	FAGASA	C
EKAL	D	ELTOPIA	C	ESHA	B	FAGES	D
EKIM	C	ELTSAC	D	ESHAMY	B	FAHNESTOCK	B
EKOMS	B	ELVERS	B/D	ESKA	B	FAIM	B
EKRUB	D	ELVIRA	B/D	ESMERALDA	B	FAIRANGEL	B
EL PECO	C	ELWELL	C	ESMOD	D	FAIRBERG	C
ELAM	A	ELWHA	C	ESPARTO	B	FAIRBIRCH	C
ELAM, Hard Substratum	B	ELWOP	B	ESPELIE	B/D	FAIRBURN	D
ELANDCO	B	ELY	B	ESPERANZA	C	FAIRCHILD	C
ELBA	C	ELYSIAN	B	ESPII	D	FAIRFAX	B
ELBAVILLE	B	EMACHAYA	D	ESPINAL	A	FAIRHAVEN	B
ELBERT	D	EMAGERT	B	ESPINOSA	B	FAIRLESS	B
ELBON	B	EMBAL	B	ESPINT	D	FAIRLIE	D
ELBOW	C	EMBERTON	C	ESPY	D	FAIRLO	B
ELBOWLAKE	B	EMELINE	D	ESRO	D	FAIRMOUNT	D
ELBUCK	B	EMERALDA	D	ESSEN	C	FAIRPLAY	D
ELBUTTE	D	EMERSON	B	ESTACION	B	FAIRSMITH	B
ELCANEJO	B	EMERY	B	ESTATE	C	FAIRYDELL	C
ELCAPITAN	B	EMIGHA	B	ESTELLE	B	FAIRYLAWN	D
ELD	B	EMIGHA, Alkaline	C	ESTELLINE	B	FAJADA	C
ELDADO	B	EMILY	B	ESTER, Thawed	C	FAJARDO	C
ELDER HOLLOW	D	EMMA	C	ESTER	D	FALAYA	D
ELDERON, Stony	A	EMMERT	A	ESTERO	D	FALBA	D
ELDERON	B	EMOT	B	ESTESLAKE	D	FALERIA	B
ELDRIDGE	C	EMPIRE	B	ESTO	B	FALFA	C
ELEMENTS	B	EMYD	B	ETACH	C	FALFURRIAS	A
ELENORE	D	ENBAR	C	ETHEL	C	FALK	C
ELEROY	B	ENBAR, Stony	C	ETHELMAN	B	FALKIRK	B
ELEVASIL	B	ENBAR, Wet	D	ETHETE	B	FALKNER	C
ELEVATOR	C	ENCANTADO	A	ETHETE, Saline	C	FALLBROOK	B
ELFCREEK	C	ENCHANTED	B	ETIL	A	FALLCREEK	C
ELFLINT	B	ENCICADO	D	ETOILE	C	FALLERT	B
ELGEE	A	ENCINA	B	ETOWAH	B	FALLON	B
ELGIN	C	ENCROW	D	ETOWN	B	FALLSINGTON	B/D
ELIAS	C	ENDERSBY	B	ETTER	B	FALSEN	A
ELIZABETH	B	ENERGY	B	ETTRICK	B/D	FANAL	C
ELK HOLLOW	B	ENFIELD	B	EUCHRAND	D	FANCHER	C
ELKADER	B	ENGADINE	B/D	EUCHRE	C	FANDOW	D
ELKHEIGHT	C	ENGLE	B	EUCLID	C	FANNO	C
ELKHEIGHTS	B	ENKO	A	EUDY	C	FANSHAW	B
ELKHORN	B	ENKO, Overblown	B	EUER	B	FANTZ, High Rainfall	B
ELKINSVILLE	B	ENLOE	D	EUFAULA	A	FANTZ	C
ELKINTON	B	ENNING	D	EUHARLEE	C	FANU	B
ELKMOUND	D	ENOCHVILLE	C/D	EULONIA	C	FARBER	B
ELKPRAIRIE	B	ENOLA	B	EUNOLA	C	FARDRAW	B
ELKRIDGE	B	ENOREE	D	EUREKA	D	FARDRAW, Dark Surface	C
ELKTON	C/D	ENOS	C	EUSBIO	C	FARISITA	D
ELKWALOW	D	ENOSBURG	C	EUSTIS	A	FARLOW	C
ELLA	B	ENSENADA	B	EUTAW	D	FARMERSTOWN	C
ELLEN	B	ENSTROM	B	EUTROBORALFS	B	FARMINGTON	C
ELLENA	C	ENTENTE	B	EVA	B	FARMTON	D
ELLETT	D	ENTERO	D	EVADALE	D	FARNHAMTON	C
ELLICOTT	A	ENTERPRISE	B	EVANGELINE	C	FARNUF	C
ELLIJAY	B	ENVILLE	C	EVANOT	B	FARQUAR	B
ELLINGTON	B	ENVOL	D	EVANSHAM	D	FARRAGUT	C
ELLINOR	C	ENZIAN	D	EVANT	D	FARRENBURG	B
ELLIOTT	C	EODY	D	EVART	D	FARRINGTON	B
ELLIS	D	EOJ	C	EVELETH	C	FARROT	C
ELLISTON	C	EOLA	D	EVENDALE	C	FARRY	B
ELLISVILLE	B	EPHRATA, Cool	A	EVERETT	B	FARSIDE	B
ELLOREE	D	EPHRATA	B	EVERGLADES	B/D	FARSON	C
ELLSBURG	C/D	EPITAPH	D	EVERGREEN	D	FARVA	C
ELLUM	C	EPLEY	C	EVERMAN	C	FARVANT	D
ELLWOOD	C	EPOI	B	EVERRY	B	FARVIEW	D
ELLZEY	B/D	EPSOM	B/D	EVICK	A	FARWAY	B
ELM LAKE	A/D	EPVIP	D	EWAN	D	FASHING	D
ELMDALE	B	ERAM	C	EXCLOSE	B	FASKIN	B
ELMENWOOD	D	ERD	D	EXEL	C	FATIMA	B

FATTIG.....	C	FIRCREEK.....	C	FLYCREEK.....	C	FRAILEY.....	B
FAUNCE.....	A	FIREBALL.....	B	FLYNN.....	B	FRAILTON.....	D
FAUNSDALE.....	D	FIREBAUGH.....	B	FLYVALLEY.....	C	FRANCIS.....	A
FAVORETTA.....	D	FIRESTEEL.....	B	FOAD.....	C	FRANCISQUITO.....	C
FAVRET.....	C	FIRESTONE.....	C	FOARD.....	D	FRANCITAS.....	D
FAWCETT.....	B	FIRETOWER.....	B	FOGGYFLAT.....	B	FRANCONIA.....	B
FAWIN.....	B	FIRMAGE.....	C	FOGLAKE.....	C	FRANEAU.....	D
FAWNSPRING.....	C	FIROKE.....	B	FOLAVAR, Elevation 6000-7400.....	A	FRANKCREEK.....	B
FAYETTEVILLE.....	B	FIRTH.....	B/C	FOLAVAR.....	B	FRANKENMUTH.....	C
FE.....	D	FISHAVEN.....	C	FOLDAHL.....	B	FRANKENSTEIN.....	C
FEAGINRANCH.....	D	FISHBERRY.....	D	FOLEY.....	D	FRANKFORT.....	C
FEARS.....	B	FISHERHILL.....	B	FOLLET.....	D	FRANKKIRK.....	C
FEATHER.....	B	FISHERMAN.....	D	FOMSENG.....	C	FRANKLIN.....	B
FEATHERSTONE.....	D	FISHHOOK.....	D	FONDA.....	D	FRANKTOWN.....	D
FEDJI.....	A	FISHLAKE.....	D	FONDILLAS.....	D	FRAVAL, Gravelly.....	B
FEDORA.....	B/D	FISHPOT.....	C	FONNER.....	B	FRAVAL.....	C
FELDA.....	D	FISHROCK.....	B	FONS.....	B	FRAZERTON.....	B
FELDHAUSER.....	B	FISHWAY.....	B	FONTAFLOA.....	A	FRED.....	C
FELDTMAN.....	A	FISK.....	B	FONTAINE.....	B	FREDA.....	D
FELICIANA.....	B	FITZHUGH.....	B	FONTANA.....	B	FREDENSBORG.....	C
FELICITY.....	A	FITZWIL.....	B	FOOLHEN, Stony, Cool.....	B	FREDERICKTOWN.....	B
FELIPE.....	D	FIVEBLOCK.....	C	FOOLHEN.....	D	FREDONYER.....	C
FELIX.....	D	FIVEMILE.....	B	FOOTHILL.....	C	FREDRIKSDAL.....	D
FELKER.....	C	FIVEMILE, Saline.....	C	FOPIANO.....	D	FREE.....	B/D
FELLA.....	B/D	FIVES.....	B	FORAKER.....	D	FREEBURG.....	C
FELOR.....	B	FIVESPRINGS.....	C	FORBAR.....	D	FREECE.....	D
FELT.....	B	FLACKVILLE.....	C	FORBES.....	C	FREEHOLD.....	B
FELTA.....	C	FLAGG.....	B	FORBESVILLE.....	C	FREELAND.....	C
FELTNER.....	D	FLAGSTAFF.....	D	FORBING.....	D	FREELS.....	B
FENELON.....	C	FLAMBEAU.....	B	FORDBUTTE.....	B	FREEMAN.....	C
FEPS.....	D	FLAMEN.....	B	FORDCREEK.....	B	FREEMANVILLE.....	B
FERA.....	C	FLAMING.....	A	FORDICE.....	B	FREEON.....	B
FERBALL.....	C	FLANAGAN.....	B	FORDNEY.....	A/C	FEER.....	C
FERD.....	C	FLANDREAU.....	B	FORDSTERROR.....	C	FREESOIL.....	B
FERDELFORD.....	C	FLANE.....	C	FORDTOWN.....	B	FREET.....	C
FEREBEE.....	D	FLANK.....	D	FORDTRAN.....	C	FREETSTONE.....	C
FERGIE.....	C	FLANLY.....	C	FORELAND.....	D	FREETPEAK.....	B
FERGUS.....	B	FLANNERY.....	B	FORELEFT.....	B	FREEWATER.....	B
FERGUSON.....	B	FLARM.....	C	FORESTBURG.....	A	FREEZENER.....	B
FERN.....	B	FLAT HORN.....	B	FORESTCITY.....	B/D	FREEZEOUT.....	B
FERN CLIFF.....	B	FLATCREEK.....	D	FORESTDALE.....	D	FRELSBURG.....	D
FERNCREEK.....	D	FLATHEAD.....	B	FORESTER.....	C	FREMKE.....	C
FERNDALE.....	B	FLATIRONS.....	C	FORESTON.....	C	FRENCH.....	C
FERNHAVEN.....	B	FLATONIA.....	D	FORK.....	C	FRENCHJOHN.....	C
FERNOW.....	B	FLATSTONE.....	C	FORKHORN.....	B	FRENCHMAN.....	B
FERNPOINT.....	B	FLATTOP.....	D	FORLORN.....	B	FRENCHMILL.....	B
FERNWOOD.....	B	FLATWOODS.....	C	FORMADER.....	C	FRENCHHOLLOW, Moist.....	C
FERRELO.....	B	FLAXTON.....	B	FORMDALE.....	B	FRENCHHOLLOW.....	D
FERROBURRO.....	D	FLEAK.....	C	FORNOR.....	B	FRESHWATER.....	D
FERTEG.....	C	FLEAK, cool.....	D	FORSEER.....	B	FRESNO, Thick Solum.....	C
FESSLER.....	B	FLEENER.....	B	FORSOREN.....	C	FRESNO, Saline Alkali.....	D
FESTINA.....	B	FLEER.....	D	FORSOREN.....	C	FREWA.....	B
FETCH.....	D	FLEISCHMANN.....	D	FORT MEADE.....	A	FREWSBURG.....	C
FETERITA.....	D	FLEMING.....	C	FORT MOTT.....	A	FREYA.....	A/D
FETT.....	D	FLEMINGTON.....	D	FORT ROCK.....	A	FRIANA.....	D
FETZER.....	C	FLETCHER.....	B	FORTBENTON.....	C	FRIEBERG.....	B/D
FEZ.....	C	FLEWSIE.....	B	FORTBOIS.....	A	FRICABA.....	B
FEZIP.....	D	FLINK.....	B	FORTESCUE.....	C/D	FRIEDLANDER.....	C
FIANDER.....	C/D	FLINTCREEK.....	D	FORTAN.....	B	FRIENDLY.....	D
FIAT.....	C	FLO.....	A	FORTSAGE.....	B	FRIENDS.....	C
FIBRE.....	B/D	FLOER.....	D	FORTUNA.....	D	FRIES.....	D
FICO.....	B	FLOKE.....	C	FORTYONE.....	B	FRINDLE.....	C
FIDALGO.....	C	FLOMATON.....	A	FOSS.....	B	FRINES.....	C
FIDDLETOWN.....	B	FLOMOT.....	B	FOSSILON.....	D	FRINT.....	C
FIDDYMENT.....	D	FLOODWOOD.....	B	FOSTERBURG.....	D	FRIO.....	B
FIDISIX.....	B	FLORAHOME.....	A	FOSTORIA.....	B	FRIONA.....	C
FIELDCREEK.....	B	FLORALA.....	C	FOUNTAIN.....	D	FRIOTON.....	C
FIELDING.....	B	FLORAS.....	C	FOUNTAINVILLE.....	C	FRIPP.....	A
FIELDON.....	B/D	FLORAVILLE.....	D	FOUR STAR.....	B/C	FRISITE.....	B
FIFESRIDGE.....	B	FLORENCE.....	C	FOURCHE.....	B	FRITSLAND.....	B
FIFIELD.....	C	FLORESVILLE.....	C	FOURCORNERS.....	D	FRIZZELL.....	C
FIG.....	B	FLORIDANA.....	B/D	FOURLOG.....	D	FRODO.....	D
FIGARO.....	C	FLORIN.....	C	FOURME.....	B	FROHMAN.....	C
FIKEL.....	C	FLORIS.....	B	FOURSIXES.....	C	FROLIC.....	B
FILBERT.....	D	FLOTAG.....	B	FOURWHEEL.....	D	FRONDORF.....	B
FILION.....	D	FLOTT.....	B	FOXCAN.....	D	FRONTENAC.....	B
FILIRAN.....	D	FLOUTIER.....	B	FOXCREAK.....	C/D	FRONTIER.....	C
FINAL.....	D	FLOYD.....	B	FOXHOME.....	B	FRONTON.....	D
FINCHFORD.....	A	FLUE.....	C	FOXLAKE.....	C	FROZARD.....	C
FINDOUT.....	D	FLUE, Gravelly.....	D	FOXMOUNT.....	C	FRUITA.....	B
FINLAND.....	C	FLUETSCH.....	B	FOXVILLE.....	D	FRUITFIELD.....	A
FINN.....	D	FLUKER.....	C	FOXVIRE.....	B	FRUITLAND.....	B/C
FINNEY.....	B	FLUMECREEK.....	B	FOXWORTH.....	A	FRUITVALE.....	C
FINOL.....	C	FLUMEVILLE.....	D	FRADDLE.....	B	FRYINGPAN.....	D
FINROD.....	C	FLUVAQUENTS.....	D	FRAGUNI.....	B	FRYMIRE.....	C

FRYREAR.....	B	GARFAN.....	D	GHOLSON.....	B	GOATROCK.....	B
FT. DRUM.....	C	GARHILL.....	D	GHORMLEY.....	C	GOATROCKS.....	B
FUEGO.....	C	GARIPER.....	D	GIANELLA.....	B	GOBAR.....	B
FUEGOSTA.....	D	GARLAND.....	B	GIARCH.....	D	GOBBLER.....	B
FUGAWEE.....	B	GARLIC.....	A	GIBBONSCREEK.....	C	GOBERNADOR.....	D
FULCHER.....	C	GARLIN.....	D	GIBNEY.....	C	GODDE.....	D
FULCRUM.....	C	GARLOCK.....	C	GIBALTAR.....	C	GODECKE.....	C
FULDA.....	D	GARMON.....	C	GIBSONVILLE.....	D	GODECKE, Clay Substratum.....	D
FULLER.....	D	GARMORE.....	B	GIBWELL.....	C	GODWIN.....	D
FULMER.....	C/D	GARNE.....	B	GICHIGAMI.....	C	GOEMMER.....	C
FULSHEAR.....	C	GARNEL.....	D	GIDEON.....	C	GOESSEL.....	D
FULTS.....	D	GARNER.....	D	GIDWIN.....	D	GOFFPEAK.....	B
FUNMAR.....	C	GARNES.....	B	GIELOW.....	C	GOGOMAIN.....	B/D
FUNTER.....	D	GARO.....	D	GIESE.....	D	GOL.....	C
FURLONG.....	A	GARR.....	D	GIGGER.....	D	GOLD CREEK.....	D
FURNISS.....	D	GARRETT.....	B	GILBERT.....	C	GOLDAHO.....	D
FURSHUR.....	D	GARROCHALES.....	D	GILBOA.....	B	GOLDBEACH.....	C
FURY.....	C/D	GARSID.....	C	GILEAD.....	C	GOLDCORD.....	D
FUSULINA.....	D	GARTON.....	C	GILES.....	B	GOLDEAGEL.....	C
FUSUVAR.....	D	GARVIN.....	D	GILFORD.....	D	GOLDEN.....	D
GABBS.....	C	GARWOOD.....	D	GILLAND.....	C	GOLDFINCH.....	C
GABEL.....	C	GASPER.....	B	GILLENDER.....	D	GOLDHEAD.....	B/D
GABINO.....	D	GASQUET.....	B	GILLIAM.....	C	GOLDHILL, Loamy Substratum.....	C
GABRIEL.....	C	GASSAWAY.....	D	GILLIGAN.....	B	GOLDHILL.....	D
GACIBA.....	D	GASSVILLE.....	C	GILLS.....	C	GOLDIVIDE.....	B
GADDES.....	C	GASTON.....	C	GILLSBURG.....	D	GOLDLAKE.....	B
GADONA.....	B	GASTROW.....	C	GILMAN.....	D	GOLDMAN.....	C
GADWELL.....	C	GASUP.....	D	GILMORE.....	D	GOLDMIRE.....	C
GAGEBY.....	B	GAT.....	B	GILROY.....	C	GOLDSBORO.....	B
GAGETOWN.....	B	GATCHEL.....	B	GILT EDGE.....	D	GOLDSMITH.....	B
GAHEE.....	B	GATERIDGE.....	C	GILWOOD.....	B	GOLDSTON.....	C
GAIA.....	B	GATESON.....	C	GIMLETT.....	B	GOLDSTREAM, Thawed.....	B
GAIBSON.....	D	GATEWALL.....	B	GINAT.....	D	GOLDSTREAM.....	D
GAILA.....	B	GATLIN.....	B	GINEX.....	D	GOLDVALE.....	C
GAINESVILLE.....	A	GATTON.....	B	GINGER.....	D	GOLDVEIN.....	C
GAKONA.....	B	GAULD.....	B/D	GINI.....	B	GOLDYKE.....	D
GALATA.....	D	GAULDY.....	B	GINSBURG.....	B	GOLETA.....	B
GALBRETH.....	D	GAUSE.....	C	GIRARD.....	D	GOLIAD.....	C
GALCHUTT.....	C	GAVEL.....	B	GIRARDOT.....	D	GOLIME.....	C
GALESTINA.....	C	GAVERS.....	C	GIST.....	D	GOLLAHER.....	D
GALEY.....	B	GAVILAN.....	C	GITABYTE.....	C	GOLONDRINA.....	B
GALIENTE.....	C	GAVINS.....	C	GITAKUP.....	C	GOLTRY.....	A
GALILEE.....	C	GAY.....	B/D	GITAM.....	D	GOLVA.....	B
GALLEGOS.....	B	GAYHART.....	C	GIVEOUT.....	C	GOMERY.....	B
GALLEN.....	B	GAYLORD.....	C	GIVIN.....	C	GOMEZ.....	B
GALLIA.....	B	GAYVILLE.....	D	GLADDICE.....	C	GOMINE.....	D
GALLIME.....	B	GAZELLE.....	D	GLADEVILLE.....	D	GONZALES.....	D
GALLIMORE.....	B	GAZWELL.....	D	GLANCE.....	C	GOODINGTON.....	D
GALLION.....	B	GEARHART.....	A	GLASGOW.....	B	GOODLAND.....	B
GALLIPOLIS.....	C	GED.....	D	GLASSNER.....	D	GOODLOW.....	B
GALLUP.....	B	GEE.....	B/D	GLAWE.....	B/D	GOODNESS.....	B
GALTSMILL.....	B	GEEBURG.....	C	GLAZE.....	B	GOODPASTER.....	D
GALVESTON.....	A	GEEMORE.....	C	GLEN.....	B	GOODRICH.....	B
GALVEZ.....	C	GEERTSEN.....	B	GLENBLAIR.....	C	GOODSON.....	C
GALVIN.....	D	GEISEL.....	B	GLENCARB.....	C	GOODVIEW.....	D
GALZUNI.....	C	GEISERCREEK.....	B	GLENCOE.....	C/D	GOODWILL.....	B
GAMBOA.....	B	GELSINGER.....	C	GLENDENNING.....	C	GOODWIN.....	B
GAMBOGY.....	B	GEM.....	C	GLENDERSON.....	B	GOOLAWAY.....	C
GAMELAKE.....	B	GEM, Stony.....	D	GLENDIVE.....	C	GOOSE CREEK.....	C
GAMM.....	D	GEMELO.....	B	GLENDON.....	B	GOOSEBURY.....	B
GANADO.....	D	GEMSON.....	B	GLENEDEN.....	D	GOOSENAWT.....	B
GANAFLAN.....	C	GENATS.....	D	GLENEYRE.....	D	GOOVAL.....	D
GANHONA.....	C	GENEVA.....	B	GLENHAM.....	B	GORDONPOINT.....	B
GANIS.....	D	GENTILLY.....	D	GLENMEN.....	B	GORE.....	D
GANO.....	B/D	ENTRY.....	D	GLENMORA.....	C	GOREEN.....	D
GANSNER.....	C	GEOCONDA.....	C	GLENOMA.....	B	GORESVILLE.....	B
GANY.....	B	GEORGE CANYON.....	B	GLENPOOL.....	A	GORGONIO.....	B
GAP.....	B	GEORGE CREEK.....	B	GLENRIO.....	D	GORHAM.....	B/D
GAPBUTTE.....	B	GERBANA.....	D	GLENROSS.....	D	GORIN.....	C
GAPCOT.....	D	GERBER.....	D	GLENSTED.....	D	GORMAN.....	C
GAPHILL.....	B	GERLACH.....	D	GLENTON.....	C	GORUS.....	B
GAPO.....	C/D	GERLANE.....	B	GLENTOSH.....	A	GOSHAWK.....	B
GARCENO.....	C	GERMANO.....	B	GLENVIEW.....	B	GOSIL.....	A
GARCIA.....	C	GERMANTOWN.....	B	GLENWOOD.....	B	GOSINTA.....	C
GARCITAS.....	C	GERMER.....	B	GLENYON.....	B	GOSNEY.....	C
GARDELLA.....	D	GERRARD.....	B	GLIDE.....	B	GOSPER.....	B
GARDENCAN.....	B	GERSTLE.....	B	GLOHM.....	C	GOTCHELL.....	D
GARDENCREEK.....	D	GESSNER.....	B/D	GLOIN.....	C	GOTEBO.....	B
GARDENISLE.....	B	GESTRIN.....	B	GLORIA.....	D	GOUGEVILLE.....	A/D
GARDENS.....	D	GETA.....	B	GLYNN.....	C	GOULDER.....	B
GARDENVALE.....	B	GETCHELL.....	C	GLYPHS.....	B	GOULDSBORO.....	D
GARDINER.....	A	GETRAIL.....	B	GNAWBONE.....	B	GOURDIN.....	C
GARDNER'S FORK.....	B	GETZVILLE.....	D	GNOJEK.....	D	GOURLEY.....	C
GARECK.....	B	GEWTER.....	B	GOATBUTTE.....	B	GOUVERNEUR.....	D
GAREY.....	B	GEYSEN.....	C	GOATJOE.....	A	GOVE.....	B

GOVEY.....	C	GREENVILLE.....	B	GUBE.....	C	HALFWAY.....	D
GOWDY.....	B	GREENVINE.....	D	GUDGEL.....	C	HALII.....	B
GOWEN.....	B	GREENWAY.....	B	GUDGREY.....	B	HALIIMAILE.....	B
GOWKER.....	C	GREENWICH.....	B	GUERIN.....	D	HALLCREEK.....	A
GOWTON.....	B	GREGGO.....	D	GUERO.....	C	HALLECK.....	B
GOZEM.....	D	GREGORY.....	D	GUERRERO.....	A	HALLENTON.....	D
GRACOT.....	A	GREGSON.....	C	GUEST.....	C	HALLETTSVILLE.....	D
GRADCO.....	C	GRELL.....	D	GUEYDAN.....	D	HALLIHAN.....	B
GRADON.....	C	GREMMERS.....	D	GUFFIN.....	D	HALLISON.....	C
GRAFF.....	D	GRENET.....	A	GUGUAK.....	D	HALLORAN.....	C
GRALIC.....	B	GRENNAN.....	B	GUIJARRAL.....	B	HALLSBLUFF.....	D
GRAN.....	D	GRENOBLE.....	D	GUISER.....	B	HALSO.....	D
GRANATH.....	B	GRESHAM.....	C	GULCH.....	B	HALVERSON.....	B
GRANBUL.....	D	GRETDIVID.....	B	GULF.....	B/D	HALVERT.....	D
GRAND.....	C	GRETOR.....	C	GULKANA.....	B	HAMACER.....	A
GRANDAD.....	B	GRETTUM.....	A	GULLIED LAND.....	D	HAMAKUAPOKO.....	B
GRANDBEND.....	B	GREWINGK.....	C	GULLION.....	C	HAMBLEN.....	C
GRANDFIELD.....	B	GREYBEAR.....	C	GULLROCK.....	B/D	HAMBONE.....	B
GRANDJEAN.....	D	GREYBO.....	B	GULNARE.....	D	HAMBROOK.....	B
GRANDMESA.....	C	GREYBROOK.....	B	GUMBOOT.....	C/D	HAMBURG.....	B
GRANDMORE.....	B	GREYCLIFF.....	C	GUNCLUB.....	C/D	HAMBURN.....	B
GRANDPON.....	B	GREYLOCK.....	B	GUNDY.....	C	HAMBY.....	C
GRANDVIEW.....	B/C	GREYS.....	B	GUNNEL.....	D	HAMDEN.....	B
GRANDWASH.....	D	GREYSTOKE.....	B	GUNNINGS.....	B	HAMEL.....	B/D
GRANER.....	B	GRIBBLE.....	D	GUNNUK.....	C	HAMILTON.....	B
GRANFLAT.....	A	GRIDELL.....	D	GUNSONE.....	D	HAMLET.....	B
GRANGE.....	C	GRIDLEY.....	C	GUNSTOCK.....	C	HAMMACK.....	B
GRANGEMONT.....	C	GRIER.....	D	GUNTER.....	B	HAMMAHAMMA.....	C
GRANGEVILLE.....	C	GRIFFITH.....	D	GURDANE.....	C	HAMMERSLEY.....	C
GRANIPEAK.....	B	GRIFFON.....	D	GURDON.....	C	HAMMOND.....	C
GRANITEPASS.....	B	GRIMM.....	B	GURLEY.....	C	HAMPLAIN.....	B
GRANMOUNT.....	C	GRINDALL.....	D	GURNEY.....	B	HAMPSHIRE.....	C
GRANSHAW.....	B	GRINDSTONE.....	C	GUSTIN.....	D	HAMPSON.....	C
GRANTCENTER.....	B	GRINK.....	D	GUSTSPRING.....	B	HAMRE.....	C/D
GRANTFORK.....	D	GRISDALE.....	B	GUTPORT.....	D	HAMRUB.....	B
GRANTHAM.....	D	GRISMAR.....	A	GUVO.....	D	HANA.....	A
GRANTSBURG.....	C	GRISWOLD.....	B	GUYAN.....	C	HANAGITA.....	D
GRANTSDALE.....	B	GRITNEY.....	C	GUYANDOTTE.....	B	HANAKER.....	C
GRANTURK.....	D	GRIVER.....	B/D	GWENA.....	D	HANAMAULU.....	B
GRANVILLE.....	B	GRIZZLE.....	D	GWINNER.....	C	HANCEVILLE.....	B
GRANYON.....	B	GRIZZLY.....	B	GWINNETT.....	B	HAND.....	B
GRANZAN.....	B	GRIZZLYBLUFF.....	B	GYBERG.....	C	HANDKE.....	A
GRAPELAND.....	A	GROESBECK.....	B	GYPLA.....	C	HANDOFF.....	B
GRASMERE.....	B	GROMES.....	B	HAAR.....	D	HANDBORO.....	D
GRASSHOPPER.....	B	GROOM.....	C	HAARVAR.....	D	HANEY.....	B
GRASSTON.....	B	GROSS.....	C	HACCKE.....	C	HANGAARD.....	A/D
GRASSVAL.....	D	GROSSCHAT.....	D	HACHITA.....	C	HANGDO.....	B
GRASSVALLEY.....	D	GROTON.....	A	HACKBERRY.....	B	HANGROCK.....	D
GRASSYCAN.....	D	GROTTO.....	A	HACKERS.....	B	HANGTOWN.....	B
GRASSYCONE.....	A	GROUNDHOUSE.....	B	HACKNEY.....	D	HANIPOE.....	C
GRASSYKNOB.....	B	GROUSECREEK.....	B	HACREEK.....	B	HANIS.....	C
GRASSYLAKE.....	C	GROUSEHAVEN.....	D	HADAR.....	B	HANKS.....	B
GRASSYTRAIL.....	B	GROUSEVILLE.....	C	HADENCREEK.....	C	HANKSVILLE.....	C
GRAUFELS.....	C	GROUSLOUS.....	D	HADLEY.....	B	HANLON.....	B
GRAVELTON.....	B/D	GROVE.....	A	HADSELVILLE.....	D	HANN.....	B
GRAVES.....	D	GROVENA.....	B	HAFLINGER.....	A	HANNA.....	B
GRAVEYA.....	B	GROVETON.....	B	HAGATA.....	D	HANNAHATCHEE.....	B
GRAVEYARD.....	B	GROWDEN, Shaly Substratum.....	B	HAGEN.....	B	HANNAWA.....	D
GRAYBERT.....	B	GROWDEN.....	C	HAGENSVILLE.....	C	HANNEGAN.....	D
GRAYFORD.....	B	GROWLER.....	B	HAGER.....	B	HANNON.....	D
GRAYLOCK.....	B	GROWLER, Sandy Substratum.....	C	HAGERMAN.....	B	HANS.....	B
GRAYMONT.....	B	GROWSET.....	D	HAGGA.....	C	HANTHO.....	B
GRAYPOINT.....	B	GRUBBS.....	D	HAGGARD.....	D	HAOZOUS.....	B
GRAYROCK.....	C	GRUBE.....	B	HAGSTADT.....	C	HAPJACK.....	D
GRAYSILL.....	C	GRUBROB.....	B	HAGUE.....	A	HAPNEY.....	D
GRAYSTONE.....	B	GRUBSTAKE.....	B	HAIG.....	C/D	HAPPEL.....	B
GRAYWOLF.....	B	GRUENE.....	D	HAIGHT.....	C	HAPPUS.....	A
GRAZANE.....	C	GRULLA.....	D	HAIGHTS.....	B	HAPPYHOME.....	C
GRAZER.....	C	GRUMBLEN.....	D	HAIGLER.....	B	HAPUR.....	D
GREANEY.....	C	GRUNDELEIN.....	B	HAIKU.....	C	HARAHILL.....	C
GREDGE.....	D	GRUVER.....	C	HAILESBORO.....	C	HARBESON.....	D
GREEN BLUFF.....	B	GRYTAL.....	B	HAINES.....	C	HARBOR.....	C
GREEN CANYON.....	B	GSCHWEND.....	B	HAIRE.....	D	HARBORD.....	B
GREENBRIAR.....	B	GUADALUPE.....	B	HAKKER.....	C	HARCO.....	B
GREENCREEK.....	B	GUAM.....	D	HAL.....	B	HARCOT.....	B/D
GREENDALE.....	B	GUAMANI.....	B	HALACAN.....	D	HARDEMAN.....	B
GREENE.....	C	GUANABANO.....	B	HALAWA.....	B	HARDESTY.....	B
GREENFIELD.....	C	GUANAJIBO.....	C	HALBERT.....	C	HARDHART.....	B
GREENGULCH.....	C	GUANICA.....	D	HALDER.....	D	HARDISTER.....	B
GREENHORN.....	D	GUANO.....	D	HALE.....	C/D	HARDOL.....	B
GREENLEE.....	B	GUARDLAKE.....	A	HALEY.....	B	HARDSCRABBLE.....	D
GREENMAN.....	C	GUAYABO.....	A	HALF MOON.....	B	HARDTRIGGER.....	B
GREENOUGH.....	B	GUAYABOTA.....	D	HALFADAY.....	A	HARDWICK.....	C
GREENSCOMBE.....	B	GUAYAMA.....	D	HALFCIRCLE.....	B	HARDY.....	C
GREENTIMBER.....	C	GUAYNAKA.....	D	HALFOSS.....	B	HARDZEM.....	C

HARECREEK.....	B	HAWICK.....	A	HENCO.....	B/D	HIGHLAND.....	C
HARGILL.....	B	HAWKEYE.....	A	HENDAP.....	D	HIGHPOINT.....	D
HARGREAVE.....	B	HAWKSNEST.....	C/D	HENDERSON.....	B	HIGHSPLINT.....	B
HARJO.....	D	HAWKSPRINGS.....	B	HENDON.....	C	HIGHTOWER.....	C
HARKEN.....	C	HAWKSTONE.....	B	HENDRICKS.....	B	HIGHUP.....	C
HARL.....	B	HAWLEY.....	B	HENDY.....	C	HIGHVALLEY.....	B
HARLAKE.....	D	HAWTHORNE.....	B	HENKIN.....	B	HIHIMANU.....	B
HARLESTON.....	C	HAXBY.....	C	HENKLE, Extremely Cobby.....	B	HILAIRE.....	B
HARM.....	D	HAYCRIK.....	C	HENKLE.....	C	HILDEBRECHT.....	C
HARMILLER.....	B	HAYES.....	B	HENLEY.....	C	HILDRETH.....	D
HARNEY.....	B	HAYESTON.....	B	HENLINE.....	D	HILEA.....	D
HARPER.....	D	HAYESVILLE.....	B	HENMEL.....	C	HILES.....	B
HARPERSVILLE.....	D	HAYESVILLE, Stony.....	C	HENNEWAY.....	B	HILGRAVE.....	B
HARPEETH.....	B	HAYFORD.....	C	HENNINGS.....	B	HILINE.....	D
HARPOLE.....	A	HAYLAND.....	C	HENRIETTA.....	B/D	HILKEN.....	C
HARPOLE.....	B	HAYNAP.....	A	HENRY.....	D	HILLBRICK.....	D
HARPS.....	C	HAYNER.....	C	HENRYSFORK.....	C	HILLCITY.....	B
HARPT.....	B	HAYNESS.....	D	HENRYSLAKE.....	D	HILLCO.....	B
HARRAH.....	B	HAYRACK.....	C	HEPPSIE.....	D	HILLCREEK.....	B
HARREL.....	B	HAYRIVER.....	B	HERAKLE.....	D	HILLEMANN.....	C
HARRIMAN.....	C	HAYSPUR.....	D	HERBEL.....	A	HILLIARD.....	B
HARRINGTON.....	C	HAYSTACK.....	B	HERBERT.....	B	HILLIARD, Moderately Well Drained.....	C
HARRIS.....	D	HAYSTORE.....	C	HERBMAN.....	A	HILLSDALE.....	B
HARRISBURG.....	D	HAYSUM.....	B	HERBOLD.....	C	HILLTISH.....	B
HARRISON.....	B	HAYTI.....	D	HERCULES.....	C	HILLTO.....	C
HARROD.....	B	HAYWIRE.....	C	HERDCAMP.....	D	HILLTOPPE.....	C
HARSLow.....	C	HAZELAIR.....	D	HERITO.....	C	HILLVIEW.....	B/D
HARSTINE.....	C	HAZELCAMP.....	B	HERJUN.....	B	HILLWOOD.....	B
HART.....	C	HAZEN.....	B	HERLONG.....	D	HILMAR.....	B/D
HARTER.....	C	HAZLEHURST.....	C	HERMANTOWN.....	C	HILO.....	A
HARTFORD.....	A	HAZTON.....	D	HERMERING.....	B	HILTABIDEL.....	D
HARTLAND.....	B	HEADLEY.....	B	HERMISHALE.....	C	HINDES.....	C
HARTLESS.....	B	HEADQUARTERS.....	B	HERNANDEZ.....	B	HINDMAN.....	B
HARTNIT.....	C	HEAKE.....	D	HERNDON.....	B	HINESBURG.....	C
HARTOP.....	B	HEALDTON.....	D	HERO.....	B	HINGHAM.....	B
HARTSELLS.....	B	HEALING.....	B	HEROD.....	D	HINKER.....	C
HARTSHORN.....	B	HEAPO.....	C	HERRICK.....	B	HINKLE.....	D
HARTWELL.....	D	HEARNE.....	D	HERSEY.....	B	HINMAN.....	C
HARTWICK.....	A	HEATH.....	D	HERSH.....	B	HINSDALE.....	D
HARTZ.....	B	HEATHCOAT.....	D	HERTY.....	D	HINTERLAND.....	D
HARVESTER.....	B	HEATLY.....	A	HESHOTAUTHLA.....	D	HINTON.....	B
HARVEY.....	C	HEATON.....	A	HESPER.....	B	HIRAMSBURG.....	C
HASKILL.....	B	HEBBRONVILLE.....	B	HESS.....	B	HIRSCHDALE.....	C
HASLIE.....	A/D	HEBER.....	A	HESSSELBERG.....	D	HISEGA.....	C
HASSE.....	D	HEBO.....	D	HESSING.....	B	HISNA.....	D
HASSELL.....	C	HECETA.....	D	HESSLAN.....	C	HISTOSOLS.....	D
HASSLER.....	C	HECHTMAN.....	D	HETLAND.....	C	HITCHCOCK.....	B
HASSMAN.....	D	HECKER.....	B	HETTINGER.....	C/D	HITLO.....	A
HASTEE.....	B	HECKISON.....	D	HEUSSER.....	C	HITT.....	B
HAT.....	C	HECKLY.....	C	HEUVELTON.....	C	HIWOOD.....	A
HATBORO.....	D	HEDGE.....	D	HEVERLO.....	B	HOADLY.....	C
HATCH.....	D	HEDSTROM.....	B	HEWITT.....	B	HOBAN.....	B
HATCHERY.....	C	HEDVILLE.....	D	HEWOLF.....	B	HOBBS.....	B
HATCHET.....	B	HEELAND.....	D	HEXT.....	B	HOBBY.....	C
HATCHIE.....	C	HEELY.....	B	HEYDER.....	B	HOBE.....	A
HATERMUS.....	D	HEESER.....	B	HEYDLAUFF.....	D	HOBIT.....	C
HATERTON.....	C	HEFED.....	B	HEYTOU.....	B	HOBONNY.....	D
HATFIELD.....	C	HEFLIN.....	B	HEYTO, Stony, Cool.....	C	HOBSON.....	C
HATHAWAY.....	B	HEGGE.....	D	HIARC.....	C	HOBUCKEN.....	D
HATKNOLL.....	B	HEGLAR.....	B	HIATHA.....	D	HOCAR.....	D
HATLIFF.....	C	HEIDEL.....	B	HIBAR.....	C	HOCKINSON.....	B/D
HATMAKER.....	C	HEIGHTS.....	B/D	HIBBARD.....	C	HOCKINSO, Moderately Wet.....	C
HATRANCH.....	D	HEIL.....	D	HIBBING.....	C	HOCKLEY.....	C
HATSPRING.....	C	HEINSAW.....	C	HIBLER.....	C	HOCKLE, Graded.....	D
HATTON.....	C	HEINZ.....	B	HIBRITEN.....	B	HODEDO.....	C
HATU.....	D	HEISLER.....	B	HIBSAW.....	B	HODENPYL.....	B
HATUR.....	C	HEISSPITZ.....	D	HICKEY.....	B	HODGSON.....	C
HATWAI.....	C	HEITT.....	C	HICKIWAN.....	D	HOEHNE.....	A
HAUBSTADT.....	C	HEIZER.....	D	HICKS.....	B	HOFFMAN.....	B
HAUG.....	B/D	HELEMANO.....	B	HICKSVILLE.....	C	HOFFMANVILLE.....	C
HAUGAN.....	B	HELLGATE.....	B	HICORIA.....	B/D	HOFSTAD.....	D
HAUGEN.....	B	HELLMAN.....	C	HICOTA.....	B	HOGADERO.....	B
HAULINGS.....	D	HELLWIG.....	C/D	HIDATSA.....	B	HOGAN.....	C
HAUZ.....	C	HELM.....	D	HIDEAWAY.....	D	HOGCREEK.....	C
HAVA.....	C	HELMER.....	C	HIDEWOOD.....	B/D	HOGENSBOG.....	D
HAVANA.....	B	HELMET.....	C	HIDVALLE.....	B	HOGHEAVEN.....	B
HAVELOCK.....	B/D	HELMICK.....	D	HIGGINS.....	D	HOGMALAT.....	D
HAVEN.....	B	HELVETIA.....	C	HIGGINSVILLE.....	C	HOGGRANCH.....	B
HAVENSNECK.....	B	HELY.....	C	HIGH GAP.....	C	HOGGRIS.....	B
HAVERDAD.....	C	HEMAN.....	D	HIGHBANK.....	C	HOGGRIS, Extremely Cobby.....	D
HAVERHILL.....	D	HEMCROSS.....	B	HIGHCAMP.....	B	HOH.....	B
HAVERMOM.....	B	HEMINGFORD.....	B	HIGHCREEK.....	B	HOHMANN.....	C
HAVERSID.....	B	HEMPHILL.....	D	HIGHHORN.....	B	HOKO.....	C
HAVERTEL.....	B	HEMPSTEAD.....	B	HIGHLAND.....	B	HOLBORN.....	C
HAVILAND.....	B						

HOLCOMB	D	HOREB	C	HUGUSTON	D	IDWAY	B
HOLDEN	B	HORNBECK	D	HUICHICA	C/D	IFFGULCH	D
HOLDERMAN	C	HORNELL	D	HUILEPASS	B	IFTEEN	B
HOLDERTON	B	HORNELLSVILLE	D	HULDA	D	IGERT	C
HOLDINGFORD	C	HORNER	A	HULDERMAN	D	IGNORD	C
HOLINROCK	C	HORNER, Graavelly Substratum	B	HULETT	D	IGUALDAD	D
HOLKAT	B	HORNEYBUCK	C	HULLIGAN	B/D	IHLEN	B
HOLLACE	D	HORNICK	C	HULLS	C	IJAM	D
HOLLANDLAKE	B	HORNING	A	HULLSGULCH	B	IKE	D
HOLLISTER	D	HORNITOS	D	HULLT	B	IKIT	D
HOLLOMEX	B	HORNSBORO	D	HULUA	D	IKSGIZA	D
HOLLOW	C	HORNSBY	C	HUMACAO	B	ILACHETOMEL	D
HOLLOWTREE	C	HORNSVILLE	C	HUMATAS	C	ILDECARB	B
HOLLY	B/D	HORROCKS	C	HUMBARGER	B	ILILI	D
HOLLYBROOK	C	HORSECAMP	D	HUMBARSPRINGS	B	ILLABOT	C
HOLLYWOOD	D	HORSEHEAD	A	HUMBUG	B	ILLAHEE	B
HOLMAN	A	HORSEPRAIRIE	B	HUME	C	ILLER	B
HOLMDEL	C	HORSLEY	D	HUMMINGTON	C	ILLIANO	D
HOLMQUIST	D	HORTONVILLE, Limestone	D	HUMSKEL	C	ILLITO	D
HOLMZIE	C	Substratum	B	HUNCHBACK	D	ILTON	C
HOLOHAN	B	HORTONVILLE	C	HUNDRAW	D	ILWACO	B
HOLOMUA	B	HOSFORD	D	HUNGRY	C	IMBLER	B
HOLSINE	B	HOSKAY	C	HUNGRYGULCH	B	IMLAY	D
HOLSTEIN	B	HOSLEY	D	HUNSINGER	B	IMMANUEL	C
HOLSTON	B	HOSMER	C	HUNTDAL	B	IMMIANT	C
HOLT	B	HOSPAH	D	HUNTERS	B	IMMOKALEE	D
HOLTER	B	HOSSICK	B	HUNTERSCOVE	C	IMNAHA	C
HOLTVILLE	D	HOSTA, Loamy Surface	C	HUNTIMER	C	INCELL	D
HOMA	C	HOSTA	D	HUNTLEY	D	INCHELIUM	B
HOMELAKE	B	HOSTAGE	B	HUNTMOUNT	B	INCY	A
HOMELAND	C	HOT LAKE	C	HUNTROCK	B	INDART	C
HOMEN	B	HOTAW	B	HUNTSBURG	D	INDEX	A
HOMESTEAD	B	HOTCREEK	D	HUOT	B	INDIAHOMA	D
HOMEWOOD	C	HOTEL	C	HURDS	B	INDIANOLA	A
HOMME, Moderately Wet	B	HOTSPOT	D	HURLBUT	C	INDIANPASS	B
HOMME	C	HOTSPRINGS	B	HURLOCK	B/D	INDIANTOWN	D
HOMOSASSA	D	HOTTIS	D	HURRYBACK	B	INDLETON	B
HONAUNAU	C	HOUCTOWN	B	HUSE	D	INEL	D
HONDEE	B	HOUGHTON	D	HUSKA	D	INEZ	D
HONEYCREEK	B	HOUK	C	HUSSA	B/C	INFERNO	C
HONEYDEW	C	HOULA	B	HUSSELL	B	INGALLS	B
HONEYVILLE	C	HOULKA	D	HUSSEY	B	INGENIO	B
HONGA	D	HOURLASS	C	HUSTONTOWN	C	INGERSOLL	B
HONLAK	C	HOUSE ROCK	D	HUSUM	B	INGLEDOVE	B
HONOBIA	C	HOUSTENADER	D	HUTCHINSON	C	INGLESIDE	B
HONOKAA	A	HOUSTON	D	HUTSON	B	INKOM	C/D
HONOLUA	B	HOUSTON BLACK	D	HUTT	D	INKOSR	D
HONOMANU	A	HOVDE	D	HUXLEY	C	INLOW	C
HONONEGAH	A	HOVEN	D	HUYSINK	B	INMACHUK	D
HONOUULIULI	D	HOVERT	D	HYALL	C	INPENDENCE	B
HONTAS	B	HOWARD	A	HYANNIS	B	INSAK	D
HONTOON	B/D	HOWARDSVILLE	A	HYAS	B	INSIDERT	D
HONUAULU	A	HOWCREE	C	HYATTS	C	INSKIP	C
HOOD	B	HOWE	C	HYATTSTOWN	D	INVERNESS	B
HOOD CANAL	C	HOWELL	C	HYATTVILLE	C	INVERSHIEL	C
HOODVIEW	B	HOWMEADOWS	D	HYDABURG	D	IO	B
HOOGDAL	C	HOWSON	C	HYDE	B/D	IOGOON	B
HOOKSAN	A	HOXIE	D	HYDELAND	B/D	IOLEAU	C
HOOKTON	C	HOYLETON	C	HYDRO	C	ION	B
HOOLEHUA	B	HOYLETON, Mines Sinks	D	HYE	B	IONA	B
HOOLY	C	HOZHO	D	HYLOC	D	IONIA	B
HOOP	B	HOZOMEEN	B	HYNES	B	IOTA	D
HOOPAL	D	HUACHUCA	D	HYPRAIRIE	C	IOTLA	B
HOOPPOLE	B/D	HUALAPAI	C	HYSHAM	D	IPANO	C
HOOSAN	B	HUB	B	HYSHOT	D	IPAVA	B
HOOSEGOW	B	HUBBELL	B	HYZEN	D	IPISH	C
HOOSIERVILLE	C	HUBERLY	D	IAO	B	IPSOOT	A
HOOSKANADEN	D	HUBERT	B	IARGO	C	IRAAN	B
HOOTEN	D	HUBLERSBURG	B	IBERIA	D	IRAK	B
HOOTENTOWN	B	HUCKLEBERRY, High Rainfall	B	IBEX	B	IRASBURG	C
HOOTER	C	HUCKLEBERRY	C	IBOLA	C	IRENE	B
HOOVERS	D	HUCKRIDGE	B	ICACOS	D	IRIS	B
HOOVERTON	C	HUDDLE	B	ICARIA	D	IRMA	B
HOPBURN	B	HUDNUT	B	ICEBERG	D	IROCK	C
HOPCO	C	HUDSPETH	C	ICESLEW, Cool	C	IRON BLOSSOM	C
HOPDRAW	A	HUECO	C	ICESLEW	D	IRONA	D
HOPKINS	B	HUEL	A	ICHBOD	D	IRONBRIDGE	D
HOPLAND	B	HUEY	D	ICHETUCKNEE	D	IRONCITY	B
HOPLEY	B	HUFFLING	D	IDABEL	B	IRONDALE	C
HOPPERS	C	HUFFMAN	B	IDAHOME	B	IRONDYKE	B
HOPPS	D	HUFFTON	B	IDAMONT	B	IRONGATE	B
HOPPSWELL	B	HUFMAN	D	IDEE	C	IRONGOLD	D
HOQUIAM	B	HUGGINS	C	IDLEWILD	C/D	IRONRUN	B
HORCADO	A	HUGHES	B	IDMON	B	IRONSPPRINGS	B
HOREB, Gravelly Substratum	B	HUGHESVILLE	C	IDMONTON	C	IROQUOIS	B/D

IRRAWADDY	C	JARDAL	C	JOLAN	C	KAIMU	A
IRRIGON	C	JARDIN	D	JOLIET	D	KAINALIU	A
IRVINE	D	JAREALES	D	JOLLIES	B	KAINTUCK	B
IRVINGTON	C	JARITA	C	JONATHAN	B	KAIPOIOI	B
ISAAC	C	JAROSO	B	JONCA	C	KAITO	B
ISCHUA	B	JARRE	B	JONDA	B	KAIWIKI	A
ISELLA	B	JARRON	D	JONES	B	KALAE	B
ISHI PISHI	C	JASCO	D	JONESBORO	B	KALALOE	B
ISHMAEL	A	JASSEEK	C	JONESVILLE	C	KALAMA	C
ISIDOR	D	JAUCAS	C	JONLAKE	D	KALAMAZOO	B
ISKNAT	D	JAURIGA	B	JONNIC	C	KALAMBACH	B
ISLAMORADA	D	JAWBONE	D	JONPOL	C	KALAPA	B
ISLAND	B	JAY	C	JOPPA	B	KALAUPAPA	D
ISLANDLAKE	A	JAYAR	C	JORDY	B	KALEETAN	B
ISLANDPARK	B	JAYEL	D	JORGE	B	KALEETAN, Till Substratum	C
ISLES	A/D	JAYHAWKER	D	JORGENSEN	B	KALIFONSKY	D
ISLOTE	B	JAYNES	D	JORN	C	KALIGA	B/D
ISMAY	B	JAYPE	C	JORNAHAM	B	KALIHU	D
ISTOKPOGA	B/D	JAYPEAK	B	JORSTED	C	KALLIO	C
ITANO	C	JAYWI	B	JOSHUA	C	KALMARVILLE	B/D
ITASCA	B	JEAGER	B	JOSIE	B	KALO	C
ITAT	B	JEALOUSY	C	JOSLIN	B	KALOKO	D
ITHACA	C	JEAN LAKE	B	JOSSET	C	KALONA	C
ITMANN	C	JEANERETTE	D	JOTAVA	C	KALSIN	C
ITSWOOT	B	JEBE	B	JOURDANTON	B	KAMAKOA	B
IUKA	C	JEBO	A	JOVEATCH	D	KAMAOLE	B
IULUS	B	JEBO	B	JOVINE	B	KAMAY	D
IVA	C	JEDBURG	C	JOWEC	D	KAMELA	C
IVAN	B	JEDDO	C/D	JOYCE	B	KAMIE	B
IVANELL	C	JEFFERS	B/D	JUANA DIAZ	B	KAMM	B
IVANHOE	D	JEFFLAKE	C	JUANDEFUCA	B	KAMPVILLE	C
IVANPATCH	B	JEKLEY	C	JUBILEE	B/D	KANACKEY	D
IVER	B	JELICO	C	JUBIN	A	KANAKA	B
IVERSEN	C	JEMERSON	B	JUDA	B	KANARANZI	B
IVES	D	JENA	B	JUDD	C	KANASKAT	B
IVIE	A	JENERA	B	JUDGETOWN	B	KANCAN	B
IVORY	C	JENEVA	B	JUDICE	D	KANDALY	A
IWAIT	B	JENKINS	A	JUG	B	KANDIK	B
IWELA	B	JENKINSON	D	JUGHANDLE	B	KANDIYOHI	C/D
IWICA	C	JENKS	C	JUGSON	C	KANEBREAK	C
IXIAN	C	JENOR	C	JUGTOWN	C	KANELOA	B
IZAGORA	C	JERAG	D	JULIN	D	KANEOHE	B
IZEE	C	JERKTAIL	C	JUMBLE	B	KANEPUU	B
JABU	B/C	JEROME	D	JUMBO	B	KANER	A
JACAGUAS	B	JERUSALEM	A	JUMPCREEK	C	KANESPRINGS	D
JACANA	D	JESBEL	D	JUMPER	C	KANG	C
JACEE	C	JESKE	C	JUMPMORE	C	KANGAS	A
JACINTO	B	JESSIETOWN	B	JUMPOFF	C	KANIKSU	B
JACK CREEK	A	JESSUP	C	JUNALUSKA	B	KANKAKEE	B
JACKLAND	D	JESTER	A	JUNCAL	C	KANORADO	C
JACKMAN	B	JETCOP	D	JUNCOS	D	KANOTIN	A/D
JACKPORT	D	JETMINE	D	JUNEBEE	B	KANTISHNA	D
JACKPOT	C	JETSTER	C	JUNGO	B	KANUTCHAN	D
JACKSBACK	C	JEVETS	C	JUNIPERO	B	KANZA	D
JACKSBORO	D	JEVNE	C	JUNIUS	C	KAPAA	B
JACKSON	B	JIGSAW	B	JUNQUITOS	C	KAPAPALA	B
JACOBSEN	D	JILSON	D	JUNTURA	D	KAPAPALA, Bedrock Substratum	C
JACOBY	C	JIM	C	JURVANNAH	C	KAPLAN	D
JACONITA	A	JIMBEE	D	JUSTIN	B	KAPPES	B
JACQUITH	C	JIMBLUFF	B	KAALUALU	A	KAPUHIKANI	D
JACRATZ	D	JIMCOMLATE	B	KAB	D	KARAMIN	A
JADIS	B	JIMCREEK	C	KABEAR	B	KARANKAWA	D
JADPOR	B	JIMEK	C	KABOOM	D	KARBANA	C
JAFI	C	JIMENEZ	C	KACHEMAK	B	KARHEEN	D
JAGERSON	C	JIMGREEN	D	KACHESS	B	KARLAN	C
JAGON	D	JIMLAKE	B	KACKLEY	C	KARLO	D
JAGUEYES	B	JIMSAGE	B	KADLETZ	C	KARLOFF	B
JAHAHNT	D	JIMTOWN	C	KADOKA	B	KARLSBERG	C
JAHO	D	JIVAS	B	KAENA	D	KARLSRUHE	A
JALMAR	A	JOBOS	C	KAFFUR	D	KARLSTAD	A
JAM	B	JOBPEAK	D	KAFING	B	KARLUK	D
JAMES CANYON	B/D	JOEBALDY	B	KAHALUU	B	KARMA	B
JAMESTON	C/D	JOEBAS	D	KAHANA	B	KARNES	B
JAMESTOWN	C	JOEMRE	B	KAHANUI	C	KARNEY	D
JANELEW	C	JOENEY	B	KAHLOTUS	B	KAROC	B
JANESBURG	D	JOEVAR	B	KAHMAH	B	KARPP	D
JANILE, Bouldery	C	JOHNS	C	KAHN	B	KARS	A
JANISE, Overblown, Drained	B	JOHNSBURG	C/D	KAHNEETA	C	KARS/ Loamy Substratum	B
JANKOSH	C	JOHNSBUTTE	C	KAHOLA	B	KARSHNER	D
JANNEY	C/D	JOHNSTON	D	KAHOOLAWA	B	KARTA	C
JANSITE	B	JOHNSTOWN	B	KAHUA	C	KASEBERG	D
JANUDE	C	JOHNTOM	D	KAI	C	KASHWITNA	B
JARAB	D	JOICE	D	KAIDERS	B	KASIANA	D
JARBIDGE	D	JOINER	A	KAIKLI	D	KASKELA	D
JARBOE	D	JOKODOWSKI	D	KAILUA	A	KASOTA	C

KASPAL	C	KENOTRAIL	C	KINCO	A	KLAWATTI	C
KASSON	C	KENRAY	A	KINDANINA	D	KLAYENT	C
KATAMA	B	KENRIDGE	C	KINDER	C	KLICKIMA	D
KATELANA	B	KENSAL	B	KINDIG	B	KLICKO	B
KATEMCY	C	KENSINGTON	C	KINDY	C	KLIENPETER	B
KATHER	C	KENSPUR	B	KINESAVA	C	KLINE, Cobby	B
KATKA	B	KENTLAND	A/D	KINGCO	D	KLINE, Protected	C
KATLON	C	KENTUCK	B/D	KINGDON	B	KLINGER	B
KATPA	B	KENUSKY	D	KINGFISHER	B	KLIPSTEIN	B
KATSEANES	D	KEO	B	KINGILE	C	KLISKON	C
KATULA	C	KEOKUK	B	KINGINGHAM	C	KLONDIKE	D
KATY	D	KEOSAUQUA	B	KINGMAN	B	KLOOQUEH	B
KATYBLAY	B	KEOTA	B	KINGMONT	B	KLOOTCH	C
KAUDER	D	KEOWNS	B/D	KINGS	D	KLOSSNER	D
KAUKAUNA	C	KEPHART	B	KINGSBURY	D	KLOTEN	D
KAUPO	A	KERBER	B	KINGSDOWN	B	KLUG	B
KAUPPI	B	KERBY	B/C	KINGSFERRY	B/D	KLUMP	B
KAVON	B	KERHAYDEN	B	KINGSLAND	A/D	KLUNA DEEP	B
KAWAH	A	KERMIT	A	KINGSLEY	B	KNAPPA	B
KAWAIIAE	C	KERNAN	C	KINGSPOINT	B	KNAPPTON	B
Kaweeta	B	KERR	B	KINGSRIVER	B/D	KNEELAND	C
KAWKAWLIN	C	KERRDAM, Moderate Perm	B	KINGSTON	B	KNEFF	C
KAYMINE	C	KERRDAM	C	KINGTUT	D	KNEP	C
KAYO	B	KERRFIELD	C	KINKEAD	C	KNICKERBOCKER	A
KEALIA	D	KERRICK	B	KINKEL, Gravelly	B	KNIFEHILL	C
KEANSBURG	D	KERRVILLE	C	KINKEL	C	KNIFFIN	C
KEARL	C	KERSHAW	A	KINKORA	D	KNIGHT	B/D
KEARNSAR	B	KERSTON	A/D	KINLEY	B	KNIK	B
KEATING	C	KERT	C	KINMAN	C	KNIKLIK	B
KEAUALALO	B	KESHENA	B	KINNAR	B	KNIPPA	C
KEAUKAHA	D	KESSON	D	KINNICK	B	NOB HILL	B
KEAWAKAPU	B	KETCHLY	B	KINNICK	C	KNOBBY	D
KEBA	B	KETLAND	C	KINOCKITY	D	KNOLLE	B
KEBLER	B	KETTLEBELLY	B	KINSMAN	C	KNOSS	D
KECKSROAD	C	KETTLEMAN, Gravelly	B	KINSTON	B/D	KNOWLES	B
KEDA	B	KETTLEMAN	C	KINTA	D	KNOWLTON	C
KEECHI	C	KETTNER	C	KINTON	C	KNOX	B
KEEFA	B	KEUTERVILLE	B	KINUSTA	D	KNOXDALE	B
KEEI	D	KEVANTON	C	KINZEL	B	KNULL	B
KEEKEE	B	KEVILAR	B	KINZUA	B	KOBARTER	C
KEEL	C	KEWACH	C	KIOMATIA	A	KOCH	C/D
KEELDAR	B	KEWAKE	A	KIOTE	B	KODAK	B
KEELE	B	KEYLARGO	D	KIOUS	D	KODAK, Nonflooded	C
KEENE	C	KEYNER	B	KIPER	D	KODIAK	B
KEENER	B	KEYOLE	B	KIPLING	D	KODRA	C
KEESE	D	KEYPORT	C	KIPSON	D	KOEHLER	C
KEETER	C	KEYSTONE	A	KIRBYVILLE	B	KOELE	B
KEEWATIN	C	KEYVACA	D	KIRKENDALL	C	KOERLING	C
KEG	B	KEYWEST	D	KIRKLAND	D	KOETHER	D
KEGEL	C/D	KEZAR	B	KIRKSEY	C	KOFFGO	C
KEGLER	C	KIAN	C	KIRKVILLE	C	KOGISH	D
KEGONSA	B	KIAWAH	B/D	KIRLEY	C	KOHALA	B
KEHAR	D	KIBESILLAH	C	KIRVIN	C	KOHATK	D
KEHENA	C	KICHATNA	A	KIRVIN, Graded	D	KOKEE	B
KEHOE	B	KICKERVILLE	B	KISATCHIE	D	KOKERNOT	C
KEIFFER	C	KICKINGHORSE	B	KISCOVE	D	KOKO	B
KEISER	B	KIDAMI	B	KISHWALK	D	KOKORUDA	B
KEITHVILLE	C	KIDWELL	B	KISHWAUKEE	B	KOKOSING	C
KEKAKE	D	KIESEL	C	KISRING	C/D	KOLAR	D
KELL	B	KIETZKE	D	KISSICK	C	KOLBERG	C
KELLER	C	KILAUEA	B	KISTIRN	B	KOLEKOLE	C
KELLERBUTTE	B	KILDOR	C	KITCARSON	B	KOLIN	C
KELLISON	D	KILGORE	C	KITCHEN CREEK	B	KOLLUTUK	D
KELLOGG	A	KILLARNEY	C	KITI	D	KOLOA	C
KELLOGGS	C	KILLBUCK	C/D	KITKUN	D	KOLOB	C
KELLY	D	KILLET	B	KITSAP	C	KOLOMOKI	B
KELSEY	B	KILLEY	C	KITSILI	B	KOMONDOR	B
KELSO	C	KILLINGTON	D	KITTERLL	D	KOMRO	A
KELSTRUP	B	KILLMASTER	C	KITTERMAN	C	KONA	D
KELTYS	B	KILMANAGH	C	KITTITAS	C/D	KONAWA	B
KELVIN	C	KILMER	C	KITTLESON	B	KONERT	C/D
KEMAH	D	KILMERQUE	C	KITTSOON	C	KONNAROCK	C
KEMAN	B	KILOA	A	KIYI	C	KONNER	C/D
KEMMERER	D	KILOHANA	A	KIZHUYAK, Modeately Wet	B	KONOCI, Stony	B
KEMOO	B	KILOWAN	C	KIZHUYAK	D	KONOCI	C
KEMP	C	KILTABAR	C	KLABER	C/D	KONSIL	B
KENAI	C	KILWINNING	D	KLACKING	A	KONZA	D
KENDRICK	A	KIM	C	KLADNICK	A	KOOCH	C
KENEFICK	B	KIMBLE	B	KLADNICK, Stony	B	KOOLAU	C
KENESAW	B	KIMBLES	D	KLAWOWYA	C	KOONICH	A
KENILWORTH	C	KIMMELL	C	KLAMATH	D	KOOSKIA	C
KENMOOR	B	KIMPTON	C	KLANELNEECHENA	D	KOOTENAI	B
KENNEY	A	KIMROSE	D	KLAPOT	B	KOPIE	D
KENNY LAKE	B	KINA	D	KLASI	D	KOPPERL	B
KENO	D	KINCHELOE	D	KLAUS	C	KOPPEL	A

KORNMAN	C	LA GRANDE	C	LAMINE	D	LASVAR	C
KOROBAGO	C	LA POSTA	B	LAMINGTON	D	LATAH	D
KORONIS	B	LA ROSE	B	LAMKIN	B	LATAHCO	D
KORTTY	B	LABELLE	D	LAMOILLE	D	LATANIER	D
KOSETH	B	LABETTE	C	LAMOTTE	B	LATCH	A
KOSMOS	D	LABKEY	B	LAMPASAS	D	LATES	C
KOSSE	B	LABLUE	D	LANARK	B	LATEX	C
KOSSUTH	B/D	LABORCITA	B	LANCASTER	B	LATHER	D
KOST	A	LABOU	D	LANCE	B	LATIERRA	B
KOTO	D	LABRE	B	LAND	B/C	LATIGO	B
KOTZMAN	B	LABSHAFT	D	LANDAVASO	B	LATIMER	D
KOUNTER	D	LABU	D	LANDCO	C	LATINA	D
KOURY	B	LABYRINTH	A	LANDINGHAM	B	LATUM	D
KOYNIK	D	LACERDA	D	LANDMAN	B	LATONIA	B
KOYOKEE	C	LACEYCREEK	B	LANDO	C	LATOUCHE	D
KOYUKTOLIK	D	LACKSCREEK	C	LANDUSKY	A	LATOUR	B
KRACKLE	B	LACLEDE	B	LANEVILLE	B	LATOURELL	B
KRADE	B	LACONNER	D	LANEXA	D	LATRASS	D
KRAKON	D	LACOOCHEE	D	LANEY	B	LATTAS	D
KRAKOW	B	LACOSTE	C	LANFAIR	B	LAUBY	B
KRAM	D	LACOTA	B/D	LANGDON	A	LAUDERDALE	D
KRANSKI	B	LACRESCENT	B	LANGELLAINE	D	LAUDERHILL	B/D
KRANZBURG	B	LACROL	D	LANGER	A	LAUER	C/D
KRAUSE	B	LADERLY	C	LANGLADE	B	LAUGENOUR	C
KREAMER	C	LADNER	C	LANGLESS	C	LAURAMIE	B
KREBS	B	LADO	B	LANGLOIS	D	LAUREL	D
KREFT	C	LADRON	B	LANGOLA	C	LAURELWOOD	B
KREM	A	LADUE	B	LANGSPRING	B	LAUREN	B
KRENKA	B	LADYBIRD	B	LANGSTON	B	LAVALLEE	B
KRESSON	C	LADYCOMB	D	LANGWELL	D	LAVEAGA	C
KREYENHAGEN	B	LADYSMITH	D	LANIER	A	LAVELLGA	B
KREZA	D	LAFAYETTE	B	LANIP	B	LAVERDER	B
KRIER	D	LAFE	D	LANKBUSH	B	LAVENTANA	C
KRIEST	B	LAFOLETTE	B	LANOAK	B	LAVEY	D
KROME	A	LAGITOS	C	LANONA	B	LAVINA	D
KRON	D	LAGLORIA	B	LANSDOWNE	C	LAVODNAS	C
KROTO	B	LAGO	C	LANTERN	B	LAWAI	B
KRUBATE	B	LAGONOT	C	LANTIS	B	LAWEN	B
KRUEGER	C	LAGRANGE	D	LANTON, Low Rainfall	C	LAWNDALE	B
KRUM	D	LAGROSS	A	LANTON	D	LAWNES	D
KRUTAR	B	LAGUNITA	C	LANTONIA	B	LAWNWOOD	B/D
KUBE	B	LAHAINA	B	LANTRY	B	LAWRENCE	C
KUBLER	C	LAHOGUESS	B	LANTZ	D	LAWRENCEVILLE	C
KUBLI	D	LAHOOD	B	LANYON	C/D	LAWSON	C
KUCKUP	A	LAHRITY	C	LAOLAO	B	LAWVER	B
KUDLAC	C	LAHTIDA	C	LAONA	B	LAX	C
KUKAIAU	A	LAINAND	B	LAPARITA	C	LAXTON	C
KUKAIAU, Bedrock Substratum	B	LAIRDSVILLE	D	LAPHAM	A	LAYCOCK	B
KUKVEY	A	LAKASH	B	LAPLATA	C	LAYTON	B
KULA	B	LAKASKIA	D	LAPOINTE	C	LAZAN	D
KULLIT	B	LAKE	A	LAPON	D	LAZBUDDIE	D
KULSHAN	C	LAKE, Clayey Surface	C	LAPPANS	A	LE BAR	B
KUNAYOSH	A	LAKE CHARLES	D	LAPWAI	B	LEA	C
KUNCIEDER	A	LAKEBEDDER	B	LARA	C	LEADER	B
KUNIA	B	LAKEFIELD	B	LARCHMOUNT	B	LEADORE	B
KUNUWEIA	C	LAKELAND	A	LARCHPOINT	C	LEADPOINT	C
KUPREANOF	B	LAKEPARK	B/D	LARES	C	LEADVALE	C
KUPREANOF, Moderately Wet	C	LAKESHORE	B	LARIAT	B	LEAF	D
KUREB	A	LAKESHORE	D	LARIC	D	LEAFLAKE	B
KURK	C	LAKESOL	B	LARIIM	D	LEAGUE	D
KURO	D	LAKETON	C	LARIMER	B	LEAGUEVILLE	B/D
KURSTAN	B	LAKEWOOD	A	LARIOSCAMP	D	LEAKEY	D
KURTEN	D	LAKIN	A	LARMINE	D	LEAKSVILLE	D
KURTH	C	LAKOMA	D	LAROQUE	B	LEANDER	B
KURTZ	C	LAKOTA	D	LAROSE	D	LEANNA	D
KUSAL	C	LAKRIDGE	C	LAROSS	B	LEATHAM	C
KUSDY	C	LALAAU	A	LARPENTEUR	B	LEATHERBARK	C
KUSHNEAHIN	D	LALINDA	B	LARRY	C/D	LEATHERS	B
KUSKOKWIM	D	LALOS	B	LARTON	A	LEATHERWOOD	B
KUSLINA	D	LAM	D	LARUE	A	LEAVENWORTH	C
KUSLINAD	D	LAMA	C	LARUSH	B	LEBAM	B
KUSSHI	B	LAMADRE	B	LARVIE	D	LEBEAU	D
KUTLER	C	LAMANGA	C	LARWOOD	C	LEBEC	B
KUVASZ	C	LAMAR	B	LAS FLORES	D	LEBRON	D
KUY	A	LAMARSH	C	LAS LUCAS	B	LECKMAN	B
KVICHAK	B	LAMARTINE	C	LAS VEGAS	D	LECOMA	B
KWAKINA	B	LAMATH	D	LASAC	A	LECRAG	D
KWATAHEIN	B	LAMAWA	B	LASALLE	D	LEDFOORD	B
KWEO	A	LAMBERJACK	B	LASAUSES	D	LEDGER	D
KYBURZ	B	LAMBMAN	C	LASERE	C	LEDOW	B
KYDAKA	D	LAMBRANCH	D	LASH	B	LEDRU	D
KYGER	B	LAMBUTTE	B	LASKA	C	LEDWITH	B/D
KYLE	D	LAMEDEER	B	LASSEL	B	LEECREEK	D
KZIN	D	LAMESA	D	LASSITER	B	LEEDSVILLE	B
LA FARGE	B	LAMESHUR	A	LASTANCE	B	LEEFIELD	C

LEELANAU	A	LIBERAL	D	LITRO	D	LONELY	C
LEEMONT	D	LIBERTY	B	LITTLE HORN	C	LONEMAN	B
LEEMORRIS	C	LIBRARY	D	LITTLEAXE	B	LONEOAK	C
LEEN	B/D	LIBUSE	C	LITTLEBALD	B	LONEPINE	B
LEEPER	D	LICK	B	LITTLEFAWN	C	LONERANCH	B
LEERAY	D	LICKCREEK	B	LITTLEFIR	C	LONESOME	B
LEERCO	D	LICKING	B	LITTLEHAT	B	LONEWOOD	B
LEESVILLE	B	LICKSKILLET	C	LITTLEJOHN	C	LONGBAR	B
LEGALL	B	LIDA	B	LITTLEMO	B	Longbell	A
LEGAULT	A	LIDAN	C	LITTLEMUD	C	Longbilly	D
LEGGETT	C	LIDDELL	B/D	LITTLED	B	Longbranch	C
LEIDIG	B	LIDDEVILLE	B	LITTLESALMON	A	Longhike	C
LEILEHUA	B	LIDOS	B	LITTLESAND	B	Longhope, Ponded	D
LEISY	B	LIEBER	B	LITTSAN	C	Longjohn	B
LEITER	C	LIEBERMAN	B	LIVAN	A	Longlois	B
LEMAH	A	LIESNOI	D	LIVCO	D	Longmare	C
LEMBOS	C	LIGAI	C	LIVENGOD	B	Longmarsh	D
LEMCAGE	B	LIGHTNING	D	LIVERMORE	B	Longmont	C
LEMCO	C	LIGNUM	C	LIVIA	D	Longort	B
LEMETA	D	LIGNUMVITAE	D	LIVONA	B	Longpen	B
LEMHI	D	LIGOCKI	C	LIZARDHEAD	B	Longpine	D
LEMING	C	LIGURTA	B	LIZARDLAKE	D	Longs	B
LEMM	B	LIHUE	B	LIZE	B	Longshoal	D
LEMMON	C	LILAH	A	LIZZIE	B	Longsidning	B
LEMOLO	D	LILBERT	B	LIZZYSPRINGS	C	Longval	B
LEMONEX	C	LILBOURN	B	LLANOS	C	Longview	C
LEMOORE	C	LILLE	B	LOARC	B	Longigan, Cobly Substratum	C
LEMOYNE	B	LILLINGS	B	LOBAT	B	Lonjon	B
LEMPIRA	B	LILLINGTON	B	LOBEISNER	B	Lonniebee	B
LEMROI	D	LILLIS	D	LOBERT	B	Lonoke	B
LENA	A/D	LILLIWAUP	B	LOBO	D	Lonon	B
LENACREEK	B	LILLYLANDS	C	LOBURN	D	LONTI	D
LENAPAH	D	LILSHEEP	B	LOCEY	C	Loonlake	B
LENAPE	D	LILSNAKE	C	LOCHLOOSA	C	Loony	C
LENAWEE	D	LILTEN	B	LOCHSA	B	LOPENO	A
LENBERG	C	LILYLAKE	D	LOCKDOWN	D	LOPER	B
LENGBY	B	LIM	C	LOCKE	B	LOPEZ	D
LENNEP	C	LIMBERJIM	B	LOCKERBY	D	LOPWASH	B
LENOIR	D	LIMECREEK	B	LOCKHART	B	LORACK	B
LENORAH	C	LIMINGA	A	LOCKNEY	D	LORADALE	C
LENZLO	B	LIMKING	B	LOCKPORT	D	LORAY	A
LENZWHEEL	B	LIMON	D	LOCKSPRINGS	C	LOREAUVILLE	C
LEOLA	B	LIMONES	B	LOCKTON	B	LORENZO	B
LEONARD	D	LIMPY	D	LOCO	C	LORHUNT	D
LEONARDO	B	LINCO	B	LOCOBILL	B	LORING	C
LEONARDTOWN	D	LINDALE	C	LOCUST	C	LORMAN	D
LEOPOLD	C	LINDELL	C	LODALLEY	D	LORRAINE	B
LEPNER	C	LINDEN	B	LODE	B	LOS ALAMOS	C
LEQUIEU	D	LINDER	B	LODICO	D	LOS OSOS	C
LEQUIRE	D	LINDQUIST	A	LOEB	C	LOS TANOS	C
LEROUX	C	LINDSTROM	B	LOEMSTONE	C	LOSANTVILLE	C
LEROY	B	LINDY	C	LOFFTUS	C	LOSEGATE	C
LESBUT	A	LINGANORE	B	LOFTON	D	LOSLOBOS	B
LESIER	B	LINGUA	D	LOGDELL	B	LOSMARIOS	C
LESON	D	LINHART	A	LOGGERT	B	LOSTBASIN	C
LESPATE	C	LININGER	B	LOGHILL	B	LOSTCOVE	B
LESWILL	B	LINKLETTER	C	LOGHILL, Very Deep	C	LOSTCREEK	B
LETAVARIA	D	LINKSTERLY	B	LOGHILL, Thick Solum	D	LOSTHORSE	D
LETHENT	C	LINLITHGO	B	LOGSDEN	B	LOSTINE	B
LETNEY	A	LINNE	C	LOGSPRINGS	C	LOSTPOINT	D
LETON	D	LINNEUS	B	LOHSMAN	D	LOSTSPRING	B
LETORT	B	LINO	A	LOIRE	B	LOSTVALLEY	D
LETRI	B/D	LINPEAK	B	LOKEN	C	LOSTWELLS	B/C
LETTIA	B	LINSLAW	D	LOKERN	C	LOTEx	D
LEVAC	D	LINTON	B	LOKOSSE	B/D	LOTHAIR	C
LEVASSEUR	A	LINVELDT	B	LOLALITA	B	LOTT	C
LEVELTON	C/D	LIONHEAD	B	LOLEKAA	B	LOTUS	C
LEVENGOD	B	LIONWOOD	B	LOLETA	C	LOU	B
LEVENMILE	B	LIPKE	D	LOLITE	D	LOUDON	C
LEVERETT	C	LIPPITT	C	LOLON	B	LOUDONVILLE	C
LEVNIK	D	LIRIOS	B	LOLOPEAK	A	LOUELLA	B
LEVY	D	LISBON	B	LOMAKI	B	LOUGHBORO	C
LEVYVILLE	B	LISBON, Silty Clay Loam Substratum	C	LOMALTA	D	LOUIECREEK	B
LEWDLAC	D	LISCUM	D	LOMART	B	LOUIN	D
LEWELLEN	B	LISK	B	LOMAX	B	LOUISA	B
LEWHAND	D	LITAG	B	LOMBARD	C	LOURIS	B
LEWIS	D	LITCHY	C	LOMETA	C	LOUSCOT	C
LEWISBURG	C	LITEN	A	LOMILL	D	LOVEDALE	B
LEWISVILLE	B	LITEN, Till Substratum	B	LOMIRA	B	LOVEJOY	C
LEWKALB	B	LITHEE	C	LOMOND	B	LOVELACE	B
LEWNOT	C	LITHGOW	C	LOMPICO	C	LOVELADY	B
LEXINGTON	B	LITHIC HAPLUSTALFS, L,M,M	D	LONCAN	B	LOVELAND	D
LEXTON	B	LITIMBER	B	LONDO	C	LOVELL	D
LEYBA	D	LITTLE	D	LONEBEAR	B	LOVELOCK	D
LIART	D			LONECONE	B	LOVENESS	B

LOVETT.....	B	LYNXCREEK.....	B	MALLOPASS.....	B	MARIMEL.....	B/D
LOVLINE.....	C	LYONMAN.....	B	MALMESA.....	D	MARINA.....	B
LOWASSIE.....	D	LYRA.....	D	MALMESBURY.....	C	MARINE.....	C
LOWDER.....	C	LYSTAIR.....	B	MALMO.....	D	MARION.....	D
LOWE.....	B/D	LYTELL.....	B	MALO.....	B	MARIOSIA.....	D
LOWERBLUFF.....	D	LYTLE.....	B	MALONEY.....	C	MARISCAL.....	D
LOWERCREEK.....	A	LYX.....	B	MALOTERRE.....	D	MARJANE.....	C
LOWLEIN.....	B	MABANK.....	D	MALSTROM.....	B	MARKER.....	B
LOWNDES.....	A	MABEN.....	C	MALTESE.....	D	MARKES.....	D
LOWRY.....	B	MABI.....	D	MAMALA.....	D	MARKESAN.....	B
LOWS.....	B/D	MACAREENO.....	C	MANADA.....	C	MARKEY.....	D
LOWVILLE.....	B	MACE.....	B	MANAHAWKIN.....	D	MARKLAKE.....	C
LOX.....	C	MACEDONIA.....	B	MANANA.....	C	MARKLEPASS.....	D
LOYAL.....	C	MACHETE.....	C	MANARD.....	C	MARKSBUTTE.....	B/D
LOYALTON.....	D	MACHIAS.....	B	MANARY.....	C	MARKTON.....	C
LOYPLACE.....	D	MACHONE.....	B	MANASHTASH.....	C	MARLA.....	D
LOYSVILLE.....	D	MACHUELO.....	D	MANASSAS.....	B	MARLEY.....	C
LOZANO.....	B	MACIVER.....	B	MANATEE.....	B/D	MARLTON.....	C
LOZEAU.....	C	MACKERRICHER.....	A	MANAWA.....	C	MARMARTH.....	C
LUANA.....	B	MACKINAC.....	B	MANBURN.....	D	MARNA.....	C/D
LUBBOCK.....	B	MACKLYN.....	C	MANCHESTER.....	A	MAROTZ.....	C
LUBKIN.....	B	MACKSBURG.....	B	MANCO.....	C	MARPA.....	C
LUBRECHT.....	C	MACLAREN.....	B	MANCOS.....	C	MARPLEEN.....	D
LUCE.....	C	MACOMB.....	B	MANDARIN, Flooded.....	B/D	MARQUAND.....	C
LUCEDALE.....	B	MACON.....	B	MANDARIN.....	C	MARQUETTE.....	A
LUCILE.....	B/C	MACREEING.....	B	MANDERSON.....	C	MARQUEZ.....	C
LUCKENBACH.....	C	MACYFLET.....	D	MANGUM.....	D	MARR.....	B
LUCKETTS.....	C	MADAWASKA.....	B	MANHATTAN.....	A	MARRIOTT.....	B
LUCKIAMUTE.....	D	MADDEN.....	C	MANI.....	C	MARSDEN.....	B
LUCKYFUSE.....	B	MADELIA.....	B/D	MANIKAN.....	B	MARSH.....	B
LUCKYRICH.....	B	MADERBAK.....	C	MANILA.....	D	MARSHDALE.....	C/D
LUCY.....	A	MADGE.....	B	MANITA.....	C	MARSHFIELD.....	B/D
LUDINGTON.....	B	MADILL.....	B	MANITOWISH.....	B	MARSHILL.....	B
LUFKIN.....	D	MADONNA.....	C	MANKOMEN.....	D	MARSING.....	B
LUGERT.....	B	MADRAK.....	C	MANN.....	B/D	MARSITE.....	D
LUGOFF.....	B	MADUREZ.....	B	MANNINGTON.....	D	MART.....	B
LUKE.....	C	MAES.....	B	MANNIXLEE.....	D	MARTEE.....	D
LUKIN.....	C	MAGDALENA.....	D	MANSIC.....	B	MARTEL.....	D
LULA.....	B	MAGENS.....	B	MANSKER.....	B	MARTELLA.....	C
LULUDE, High Rainfall.....	B	MAGGIE.....	D	MANSON.....	B	MARTILLO.....	D
LULUDE, Short FFS.....	C	MAGGIN.....	C	MANTECA.....	C	MARTIN PENA.....	D
LUMAN.....	B	MAGIC.....	D	MANTON.....	B	MARTINEZ.....	D
LUMBEE.....	B/D	MAGNET.....	C	MANU.....	C	MARTINSBURG.....	B
LUMMI.....	C/D	MAGNETIC.....	C	MANVEL.....	C	MARTINSON.....	C
LUMMUS.....	C	MAGOTHA.....	D	MANZANITA, Gravelly.....	B	MARTINTON.....	C
LUNCH.....	C	MAGROC.....	C	MANZANITA.....	C	MARTIS.....	B
LUNDER.....	D	MAGUAYO.....	C	MANZANST.....	D	MARTY.....	B
LUNDGREN.....	A	MAHAFFEY.....	C	MAPLE HOLLOW.....	C	MARUMSCO.....	C
LUNDLAKE.....	B/D	MAHAN.....	C	MAPLECREEK.....	C	MARVELL.....	B
LUNSFORD.....	D	MAHANA.....	B	MAPLECREST.....	B	MARVYN.....	B
LUNT.....	C	MAHASKA.....	B	MAPLEHILL.....	C	MARYSTOWN.....	C
LUPCHO.....	B	MAHKONCE.....	C	MAPLEHURST.....	C	MARYSVILLE.....	B
LUPE.....	B	MAHO BAY.....	D	MAPLEWOOD.....	C	MASARYK.....	A
LUPINE.....	B	MAHOGAN.....	C	MARA.....	B	MASCARENAS.....	C
LUPINTO.....	C	MAHOOSUC.....	A	MARACK.....	C	MASCHETAH.....	B
LUPOYOMA.....	B	MAHTOWA.....	C/D	MARAGUEZ.....	B	MASCOTTE.....	B/D
LUPPINO.....	D	MAIDENPEAK.....	A	MARANA.....	B	MASCOUTAH.....	B/D
LUPTON.....	D	MAILE.....	A	MARBIE.....	C	MASEEYA.....	B
LURAY.....	C/D	MAILTRAIL.....	C	MARBLECREEK.....	B	MASET.....	B
LURNICK.....	C	MAJIK.....	B	MARBLEHEAD.....	C	MASHAM.....	D
LUSETTI.....	B	MAJUBA.....	C	MARBLEMOUNT.....	B	MASHEL.....	B
LUSK.....	C	MAJURO.....	A	MARBLEMOUNT, Channery.....	C	MASHULAVILLE.....	B/D
LUTA.....	D	MAKAH.....	B	MARBLETOWN.....	B	MASKELL.....	B
LUTAK.....	B	MAKALAPA.....	D	MARCADO.....	D	MASON.....	B
LUTHER.....	B	MAKAPILI.....	B	MARCEL.....	C	MASONFORT.....	D
LUTIE.....	B	MAKAWAO.....	B	MARCELINAS.....	D	MASONTOWN.....	D
LUTZCAN.....	D	MAKAWELI.....	B	MARCELLON.....	C	MASSACK.....	B/C
LUTZKE.....	B	MAKENA.....	B	MARCETTA.....	D	MASSADONA.....	C
LUVAR.....	B	MAKI.....	C	MARCLAY.....	B	MASSADONA.....	D
LYBRAND.....	C	MAKIKI.....	B	MARCOLA.....	C	MASSANETTA.....	B
LYCURGUS.....	B	MAKLAK.....	A	MARCONI.....	C	MASSBACH.....	B
LYDICK.....	B	MAL.....	C	MARCOU.....	B	MASSIE.....	D
LYERLY.....	D	MALA.....	B	MARCUS.....	B/D	MASTERSON.....	B
LYFORD.....	C	MALACHY.....	B	MAREMMA.....	B	MASTLY.....	B
LYKAL.....	C	MALAMA.....	A	MARENGO.....	C/D	MATA.....	C
LYKENS.....	C	MALARDI.....	B	MARESUA.....	B	MATAGORDA.....	D
LYKORLY.....	C	MALARGO.....	B	MARGERUM.....	B	MATAMOROS.....	C
LYMANSON.....	B	MALAYA.....	D	MARGIE.....	C	MATANUSKA.....	B
LYNCH.....	D	MALBIS.....	B	MARGO.....	B	MATANZAS.....	B
LYNDEN.....	B	MALCOLM.....	B	MARIANA.....	C	MATAWAN.....	C
LYNN HAVEN.....	B/D	MALDEN.....	A	MARIAVILLE.....	D	MATCHER.....	A
LYNNBOW.....	D	MALEZA.....	B	MARICAO.....	B	MATECUMBE.....	D
LYNNE.....	B/D	MALHEUR.....	C	MARIEL.....	D	MATFIELD.....	C
LYNNVILLE.....	C	MALIBU.....	D	MARIETTA.....	C	MATHERS.....	B
LYNNWOOD.....	A	MALJAMAR.....	B	MARILLA.....	C	MATHERTON.....	B

MATHERTON, Clay Substratum ..	C	MCCUE	C	MECOSTA	A	METANOB	B
MATHIAS	B	MCCULIGAN	D	MEDFRA	D	METCALF	D
MATHISTON	C	MCCULLAN	B	MEDICI	A	METH	C
MATHON	B	MCCUMBER	B	MEDICINE	B	METIGOSHE	B
MATILO	B	MCCUNE	D	MEDLAKE	A	METOLIUS	B
MATMON	D	MCCURDY	C	MEDLAVAL	D	METONGA	B
MATOON	D	MCCUTCHEN	D	MEDLEY	B	METRE	D
MATTOY	C	MCDANIELAKE	B	MEDO	A/D	METSER	C
MATQUAW, Dry	B	MCDERMOTT	B	MEDOC	C	MEXICO	D
MATQUAW	C	MCDOLE	B	MEDRICK	B	MEXISPRING	D
MATTAMUSKEET	D	MCDONALDSVILLE	C/D	MEEGERNOT	B	MEXTANK	B
MATTAN	D	MCDOUGH	B	MEENON	C	MEYSTRE	B
MATTAPEX	C	MCDUFF	C	MEGONOT	C	MEZZER	B
MATTERHORN	A	MCELMO	D	MEGUIN	B	MICANOPY	C
MATTEX	C	MCEWEN	B	MEHURIN	C	MICAVILLE	B
MATTIX	B	MCFAIN	D	MEIKLE	C	MICCO	B/D
MATUNUCK	D	MCFARLAND	B	MEISS	D	MICCOSUKEE	C
MAU	C	MCFAY	C	MEKINOCK	D	MICKEY	D
MAUDE	B	MCGAFFEY	B	MELAKWA	C	MICROSPEECH	D
MAUKEY	C	MCGARVEY	C	MELBOURNE	B	MICROY	C
MAUMEE	D	MCGEHEE	C	MELBY	B	MIDAS	C
MAUNABO	D	MCGILVER	D	MELD	C	MIDCO	A
MAUPIN	C	MCGINN	B	MELDER	B	MIDDLEBOX	B
MAURY	B	MCGINNIS	C	MELFA	D	MIDDLEBROOK	C
MAVCO	C	MCGIRK	C	MELGA	D	MIDDLEBURG	B
MAVERICK	C	MCGIRK, Low Rainfall	D	MELHOMES	B	MIDDLEBURY	B
MAVIE	B/D	MCGOWAN	B	MELHORN	B	MIDDLEHILL	C
MAVREESO	B	MCGRATH	B	MELLING	D	MIDDLEWOOD	B
MAWAE	A	MCGRAVEY	B	MELLOTT	B	MIDELIGHT	B
MAWER	B	MCGUFFEY	B	MELLOWMOON	B	MIDESSA	B
MAXEY	C	MCGUIRE	B	MELOCHE	D	MIDFORK	B
MAXTON	B	MCHANDY	D	MELOZA	C	MIDO	B
MAY	B	MCINTOSH	C	MELROSE	C	MIDPEAK	B
MAYBELL	A	MCIVOR	D	MELRUDE	C/D	MIDVALE	C
MAYBESO	D	MCKAMIE	D	MELTON	D	MIERHILL	C
MAYBID	D	MCKAY	C	MELVINA	C	MIERUF	B
MAYDOL	B	MCKEE	C	MEMALOOSE	C	MIFFLIN	B
MAYES	D	MCKEETH	B	MEMMOTT	B	MIGERN	B
MAYFLOWER	C	MCKENNA	C/D	MENA	C	MIGUEL	D
MAYGAL	D	MCKENTON	D	MENAN	B	MIJAY	C
MAYGER	C	MCKINLEY	B	MENARD	B	MIKADO	C
MAYHEW	D	MCKINNEY	C	MENBAR	C	MIKIM, Wet Substratum	C
MAYMEAD	B	MCKNIGHT	B	MENDEBOURE	C	MIKIM, Saline-Alkali, Wet	D
MAYNARD LAKE	A	MCLAIN	C	MENDELTNA	D	MILAN	B
MAYO	B	MCLANGOR	D	MENDENHALL	D	MILBY	B
MAYQUEEN	B	MCLAURIN	B	MENDI	B	MILCAN	C
MAYS SPRINGS	B	MCLEAN	D	MENDNA	D	MILDRED	D
MAYSWELL	D	MCLENNAN	C	MENDON	B	MILES	B
MAYTAG	D	MCLEOD	B	MENDOTA	B	MILITARY	B
MAYTOWN	C	MCLOUGHLIN	B	MENFRO	B	MILKWEED	C
MAYVILLE	B	MCMANUS	D	MENINIK	C	MILL	D
MAZARN	C	MCMEE	C	MENO	C	MILLADORE	C
MAZASKA	C/D	MCMILLAN	A	MENOKEN	C	MILLAN	B
MAZDALE	B	MCMILLE	B	MENOMIN	B	MILLBORO	D
MAZIE	D	MCMURDIE	B	MENTO	C	MILLBURNE	B
MAZUMA	C	MCMURRAY	C/D	MENTONE	C	MILLDAM	C
MCADOO	B	MCNAB	C	MENTZ	D	MILLECOQUINS	C
MCAFFEE	C	MCNARY	B	MENZEL	B	MILLERDITCH	C
MCCALLEN	B	MCNEELY	B	MEQUITHY	B	MILLERFLAT	B
MCCALLISTER	B	MCNULTY	A	MEQUON	C	MILLERPOINT	B
MCCARTHUR	B	MCNYE	B	MER ROUGE	B	MILLERSBURG	B
MCBAIN	B	MCPAN	C	MERCER	C	MILLERTON	D
MCBEGGAM	C	MCQUEEN	C	MERCEY	C	MILLERVILLE	A/D
MCCAFFERY	A	MCRABE	B	MEREDITH	B	MILLHEIM	C
MCCALEB	B	MCRABEN	B	MERIMOD	B	MILLHI	D
MCCALLY	D	MCTAGGART	B	MERINO	D	MILLICH	D
MCCAMMON	C	MCVAR	A	MERIT	B	MILLIGAN	C
MCCANN	B	MCVICKERS	C	MERKLEY	B	MILLING	D
MCCASH	B	MCWATT	B	MERMENAU	D	MILLOX, Nonsaline	C
MCCAY	B	MEAD	B	MERNA	B	MILLOX, Saline-Sodic	D
MCCLANAHAN	D	MEADOWBANK	B	MEROS	A	MILLPAW	C
MCCLAVER	C	MEADOWLAKE	C	MERRILL	C	MILLPAW, Sandy Subsoil	D
MCCLELLAN	B	MEADOWPASS	C	MERRILLAN	C	MILLPOCKET	D
MCCLOUD	C	MEADOWPEAK	C	MERRIMAC	A	MILLPOND	B
MCCLUNG	B	MEADOWPORT	C	MERRYVILLE	D	MILLPOND	C
MCCLORE	C	MEADOWS	D	MERSON	C	MILLPOT	B
MCCOIN	D	MEADOWVILLE	B	MERTON	B	MILLRACE	B
MCCOLL	D	MEANS	D	MERWIN	A/D	MILLROCK	A
MCCOMAS	C	MEARES	C	MESABA	C	MILLSAP	D
MCCONAUGHY	B	MEATON	C	MESCAL	C	MILLSDALE	C/D
MCCORNICK	C	MECAN	B	MESCALERO	C	MILLSITE	B
MCCOY	C	MECHANICSBURG	C	MESEI	D	MILLSITE, Stony	C
MCCREE	B	MECKLENBURG	C	MESSER	C	MILLSTADT, Drained	C
MCCRORY	D	MECKLING	B	MET	B	MILLSTONE	B
MCCROSKET	B	MECLO	D	METALLAK	B	MILLSTREAM	B

MILLWARD	B	MODYON	C	MOONSTONE	C	MOUNTZION	B
MILLWOOD	D	MOE	B	MOONVILLE	B	MOUZON	D
MILNER	B	MOENKOPIC	B	MOORETOWN	C/D	MOVIEFLAT	C
MILTON	C	MOENTRIA	D	MOORHEAD	C	MOVILLE	C
MILVAR	C	MOFFSPRING	C	MOOSE RIVER, Moderately Wet	C	MOWAKO	B
MINA	B	MOGG	D	MOOSE RIVER	D	MOWATA	D
MINALOOSA	B	MOGLIA	C	MOOSECREEK	B	MOWBRAY	B
MINCHUMINA	D	MOGOLLON	B	MOOSED	C	MOWICH	D
MINCO	B	MOGOTE	C	MOOSED, Sandy	D	MOYERS	C
MINDEN	B	MOHAT	B	MOOSEFLAT	D	MOYINA	D
MINEOLA	A	MOHLER	B	MOOSEHEAD	B	MT. AIRY	A
MINERAL, Dry	B	MOHOCKEN	C	MOOSELAKE	A/D	MT. HOOD	B
MINERAL	C	MOHON	C	MOOSHAUNEE	C	MT. OLIVE	C
MINERAL MOUNTAIN	D	MOIESE	B	MOPANA	D	MT. VERNON	C
MINERSVILLE	B	MOINES	C	MOPANG	B	MT. ZION	C
MINERVA	B	MOINGONA	B	MOPPET	B	MTSTERLING	B
MINESINGER	C	MOJO	C	MOQUAH	B	MUCKALEE	D
MINGO	C	MOKAAC	A	MORADO	C	MUDBUZ	B
MINGPOINT	B	MOKENA	C	MORALES	C	MUDCO	D
MINKLER	D	MOKIAK	C	MORANCH	B	MUDCREE	C
MINKWELL	B	MOKINS	D	MORANVILLE	B	MUDLAKE	C
MINLITH	D	MOKULEIA	B	MORBENCH	B	MUDLAVIA	B
MINNEHA	C	MOLALLA	B	MORCLAY	D	MUDPOT	D
MINNEHAHA	B	MOLAND	B	MORCOM	C	MUELLER	B
MINNEISKA	B	MOLAS	D	MORCONICK	B	MUES	C
MINNETONKA	C/D	MOLENA	A	MOREGLADE	B	MUGATU	C
MINNIEPEAK	A	MOLION	D	MOREHEAD	C	MUGGINS	B
MINNIEVILLE	C	MOLLOCO	D	MORET	D	MUGHUT	C
MINNIMAUD	C	MOLLYCY	C	MOREY	D	MUIRKIRK	B
MINNYE	B	MOLOKAI	B	MORGAMINE	C	MUKILTEO	C/D
MINO	C	MOLTKE	B	MORGANFIELD	B	MULA	B
MINOA	C	MOLTONER	C	MORGANHILLS	D	MULAT	D
MINOQUA	B/D	MOLTONER, Silty Clay Loam		MORIAH	B	MULDOON	B
MINONG	D	Substratum	D	MORIAH, Clayey Subsoil	C	MULDROW	D
MINWELLS	C	MONA	B	MORICAL	C	MULE	B
MIPPON	B	MONACAN	C	MORIMOUNT	D	MULETT	D
MIRABAL	B	MONACHE	B	MORITZ	C	MULHALL	B
MIRACLE	B	MONAHANS	B	MORLING	D	MULHOLLAND	B
MIRAGE	C	MONARCH	D	MORMON MESA	D	MULKEY	C
MIRAMAR	B	MONASTERIO	C	MORMOUNT	D	MULLERS	D
MIRASOL	B	MONAVILLE	B	MORNINGSTAR	B	MULLICA	C
MIREROCK	D	MONBUTTE	C	MOROCCO	B	MULLIG	B
MIRES	A	MONCHA	B	MORPH	B/D	MULLINS	D
MIRES, Stony	B	MONCISCO	A	MORPHEY	D	MULLYON	D
MISENHEIMER	C	MONEE	D	MORRISVILLE	C	MULSTAY	C
MISERY	C	MONGLE	C	MORSE	D	MULT	C
MISFIRE	B	MONGO	D	MORTENSON	D	MULTEY	B
MISHAK	C/D	MONIDA	B	MORTIMER	D	MULTORPOR	A
MISHAKAL	C	MONIDA	C	MORVEN	C	MULVEY	C
MISHAWAKA	A	MONITOR	C	MOSBY	C	MUMFORD	D
MISKOAKI	D	MONJEAU	D	MOSEL	C	MUNCIE	C
MISLATNAH	B	MONORIDGE	C	MOSHANNON	B	MUNDALITE	C
MISPILLION	D	MONOX	B	MOSHEIM	D	MUNDELEIN	B
MISSION	D	MONPARK	D	MOSHUP	C	MUNDEN	B
MISSISQUOI	A	MONSE	C	MOSLANDER, Elevation 7000-9000	B	MUNDOS	B
MISSISSINAWA	C	MONSERATE	C			MUNDT	C
MISSLER	B	MONSERATE, Thin Surface	D	MOSLANDER	D	MUNI	D
MISSOULA	D	MONTBORNE	C	MOSMAN	D	MUNSET	D
MISTEGUAY	D	MONTCALM	A	MOSO	B	MUNSON	D
MITCH	C	MONTCAN	B	MOSQUITO	D	MUNUSCONG	B/D
MITCHELLPOINT	B	MONTE CRISTO	D	MOSROC	D	MURAD	B
MITIWANGA	C	MONTEAGLE	B	MOSSBACK	B	MURANCH	C
MITKOF	C	MONTEGRANDE	D	MOSSCREEK	B	MURDO	B
MITRE	C	MONTELLO	C	MOSSYROCK	B	MUREN	B
MITRING	C	MONTEOCHA	D	MOSWELL	D	MURHUT	B
MITTEN	B	MONTEROSA	C	MOTARK	B	MURKEN	C
MIZEL	D	MONTESA	C	MOTEN	C	MUROC	D
MIZPAH	D	MONTEVALLO	D	MOTLEY	B	MURPHILL	D
MOANO	D	MONTEZ	B	MOTT	D	MURPHY	C
MOAPA	C	MONTEZUMA	A	MOTTO	B	MURRAY	B
MOAULA	A	MONTIETH	B	MOULTRIE	D	MURRIETA	D
MOBATE	D	MONTONIA	B	MOUNDHAVEN	A	MURRSTAD	D
MOBEETIE	B	MONTOSO	B	MOUNDPRAIRIE	B/D	MURVILLE	A/D
MOBERG	B	MONTOUR	D	MOUNDVILLE	A	MUSCATUNE	B
MOBL	B	MONTROSS	C	MOUNTADAMS	B	MUSE	C
MOCA	D	MONTVERDE	B/D	MOUNTAINBOY	D	MUSGRAVE	D
MOCAREY	D	MONTWEL	B	MOUNTAINEER	B	MUSGROVE	B
MOCKLEY	C	MONVERO	A	MOUNTAINVILLE	C	MUSHEL	B
MOCKVILLE	B	MONZA	C	MOUNTEMILY	B	MUSKELLUNGE	D
MOCO	B	MONZINGO	B	MOUNTHAT	B	MUSKOGEE	C
MOCTILEME	C	MOOERS	B	MOUNTMCULL	D	MUSOFARE	C
MODALE	C	MOOHOO	B	MOUNTMED	C	MUSQUIZ	C
MODESTY	C	MOOLACK	A	MOUNTOM	D	MUSSENTUCHIT	B
MODJESKA	B	MOONLIGHT	B	MOUNTPLEASANT	B	MUSSENTUCHIT, Dry	C
MODOC	B	MOONSHINE	D	MOUNTPOR	C	MUSSERHILL	C

MUSSEY	B/D	NARU	C	NEMOURS	C	NICELYTOWN	C
MUSTANG	A/D	NASH	B	NENNO	C	NICHOLFLAT	D
MUSTANG	D	NASHMEAD	B	NEOLA	D	NICHOLIA	D
MUSTINKA	C/D	NASHVILLE	B	NEOPIT	B	NICHOLSON	C
MUSTY	C	NASHWAUK	C	NEOTOMA	B	NICHOLVILLE	C
MUTNALA	B	NASKEAG	C	NEOTSU	C	NICKEL	C
MUTT	C	NASON, Gravelly	B	NEPONSET	C	NICKERSON	B
MUTTON	B	NASON	C	NEPTUNE	A	NICKIN	B
MYATT	D	NASS	D	NERELNA	B	NICKLUND	B
MYERS	D	NASSAU	C	NERESON	B	NICKOLNA	B
MYFORD	D	NASSAWANGO	B	NERWOODS	B	NICODEMUS	B
MYOMA	A	NATAANI	B	NESBITT	B	NICOLAS	A
MYOMA, Wet	B	NATAGA	A	NESDA	A	NIDAROS	D
MYRA	C	NATAL	D	NESHOBA	C	NIDIX	B
MYRICK	C	NATALBANY	B	NESIKA	B	NIDO	C
MYRTLE	B	NATAPOC	D	NESIU	A	NIELSVILLE	C/D
MYRTLECREEK	B	NATCHEZ	B	NESKOWIN	C	NIKAL	B
MYSOL	C	NATCHITOCHES	D	NESO	D	NIKFUL	D
MYSTEN	A	NATHALE	C	NESS	D	NIKISHKA	B
NAALEHU	B	NATHROP	C	NESSEL	B	NIKLAVER	D
NAALEHU, Bedrock Substratum	C	NATI	C	NESTLEY	B	NIKWASI	B/D
NABB	C	NATIONAL	B	NETARTS	B	NILE	B
NABESNA	D	NATKIM	B	NETAWAKA	B	NILER	D
NABOR	B	NATOMAS	B	NETOMA	B	NILRAP	B
NACHES	B	NATROY	B	NETRAC	A	NIMERICK	C
NACHUSA	B	NATURITA	B	NETTLETON	C	NIMMO	D
NACIMIENTO	C	NAUKATI	D	NEUBERT	B	NIMROD	B
NACLINA	D	NAUMBURG	C	NEVARC	C	NIMS	C
NACO	C	NAUVOO	B	NEVAT	B	NINCH	B
NACONICHE	D	NAVACA	D	NEVENS	C	NINEPIPE	B
NADA	D	NAVAN	D	NEVILLE	C	NINEVEH	B
NADEAU	B	NAVASAN	A	NEVO	D	NINIGRET	B
NADRA	D	NAVIDAD	B	NEVTAH	C	NINOT	B
NAEGELIN	D	NAVINA	B	NEVU	C	NIOBRARA	D
NAGEEZI	B	NAVO	D	NEWALBIN	B/D	NIOTA	D
NAGLE	B	NAWAKWA	C	NEWALLA	D	NIPE	B
NAHA	B	NAWT	C	NEWANNA	C	NIPINTUCK	D
NAHA	C	NAYE	C	NEWAUKUM	B	NIPISSING	B
NAHUNTA	C	NAYFAN	C	NEWAYGO	B	NIPPENO	D
NAILKEG	B	NAYPED	B	NEWBERN	C	NIPSUM	C
NAIWA	B	NAYRIB	D	NEWCO	D	NIRAC	C
NAKAIBITO	B	NAYTAHWAUSH	B	NEWCOMER	B	NIRE	C
NAKINA	B/D	NAZATON	B	NEWDALE	B	NIRLING	C
NAKNEK	D	NEABSCO	C	NEWDEAL	D	NISENE	B
NAKOCHNA	D	NEAH	B	NEWFLAT	D	NISHNA	C/D
NAKWASINA	D	NEALY	B	NEWFOLDEN	C	NISHNA, Ponded	D
NALAKI	C	NEARL	C	NEWFORK	D	NISHON, Warm	C/D
NALDO	B	NEBGEN	D	NEWFOUND	C	NISHON	D
NALIVAG	B	NEBISH	B	NEWGLARUS	B	NISQUALLY	A
NALL	D	NEBONA	D	NEWGLARUS, Severely Eroded	C	NISULA	B
NAMEOKI	D	NECESSITY	C	NEWHAN	A	NITCHA	B
NAMMOTH	C	NECHE	C	NEWHAVEN	B	NITCHE	B
NAMUR	C	NECHES	C	NEWHORN	B	NITCHLY	B
NANA	D	NECKROCK	B	NEWHOUSE	B	NITER	C
NANAMKIN	A	NECONDA	C	NEWKIRK	D	NITPAC	D
NANIAK	D	NECTAR	C	NEWLANDS	C	NIU	B
NANICH	A	NEDA	C	NEWLANG	A/D	NIULII	C
NANNYTON	B	NEDHILL	B	NEWLIN	B	NIVA	D
NANSEMOND	C	NEEDHILL	B	NEWLONDON	C	NIWANA	B
NANSEPSEP	C	NEEDLE PEAK	C	NEWMARC	C	NIXON	B
NANTAHALA	B	NEEDMORE	C	NEWNAN	C	NIXONTON	B
NANTICOKE	D	NEEL	D	NEWRY	B	NIZHONI	D
NAPIER	B	NEELEY	B	NEWSKAH	B	NOAH	B
NAPOLEON	A/D	NEEN	B/C	NEWSROCK	B	NOBLE	B
NAPOLEON	D	NEEN, Wet	D	NEWSTEAD	C	NOBLETON	C
NAPOLI	C	NEEPER	B	NEWTMAN	D	NOBOCO	B
NAPPANEE	D	NEESES	C	NEWTONIA	B	NOBSCOT	A
NAPTOWNE	B	NEHALEM	B	NEWULM	B	NOBUCK	C
NARANJITO	C	NEHALEM, Flooded	C	NEWVIENNA	B	NOCKAMIXON	C
NARANJO	C	NEHAR	C	NEWVILLE	D	NOCKEN	C
NARBONA	B	NEHASNE	B	NEYGAT	D	NODHILL	B
NARCISSE	B	NEICE	B	NEZ PERCE	C	NODINE	B
NARD	C	NEISSENBERG	C	NEZ PERCE, Friable Substratum	D	NODMAN	B
NARDINE	C	NEKIA	B	NGARDMAU	B	NODUR	D
NARDMONT	B	NEKIA, Stony	C	NGARDOK	B	NOELKE	D
NAREA	A	NEKKEN	B	NGERSUUL	C	NOHILI	D
NAREL	B	NEKOMA	B	NGERUNGOR	D	NOKASIPPI	B/D
NARGAR	B	NELLSRING	D	NIARADA	B	NOKHU	C
NARGON	C	NELSCOTT	C	NIBBS	B	NOLAVA	C
NARK	C	NELSE	B	NIBEN	B	NOLTEN	C
NARLON	D	NELSON	C	NIBLACK	D	NOMARA	C
NARNETT	B	NEMADJI	B	NIBLEY	C	NOMBERVILLE	B
NARRAGUINNEP	D	NEMAH	C/D	NIBSON	D	NOME	D
NARROWS	D	NEMICO	D	NICANOR	D	NOMRAH	B
NARTA	D	NEMOTE	A	NICELY	C	NONAME	D

NONAMELAKE	C	NUSIL	A	OHTOG, Wet	C	ONECO	B
NONAMEWASH	B	NUSMAG	D	OHTWO	C	ONEIL	C
NONDALTON	B	NUTREEAH	C	OIDEM	A	ONEONTA	B
NONOPAHU	D	NUTTER	B	OJATA	C	ONKEYO	D
NONPAREIL	D	NUTVAL	B	OJIBWAY	C	ONOVILLE	C
NOOBAB	C	NUTZAN	C	OJITO	C	ONSLow	B
NOOK	C	NUVALDE	B	OKAN	B	ONSTAD	B
NOOKSACK	C	NYAK	B	OKAY	B	ONTKO	D
NOPAH	C	NYALA	B	OKEE	B	ONTRAIL	B
NORA	B	NYE	B	OKEECHOBEE	B/D	OOKALA	A
NORA VARIANT	B	NYMAN	C	OKEELALA	B	OOKEN	A
NORAD	B	NYMORE	A	OKEELANTA	B/D	OPALOCKA	D
NORAX	B	NYSERVA	B	OKEETEE	D	OPIE	D
NORBERT	D	NYSSATON	B	OKEMAH	C	OPIHIKAO	D
NORBORNE	B	NYSWONGER	D	OKERLAND	B	OPLIN	C
NORDBY	B	NYTHAR	D	OKIOTA	D	OPNISH	C
NORDHOUSE	A	O'BRIEN	B	OKLARED	B	OPOLIS	C
NORENE	C	O'NEILL	B	OKLARK	B	OPPIO, Stony	C
NORFOLK	B	OAHE	B	OKLAWAHA	B/D	OPPIO	D
NORGE	B	OAK GROVE	B	OKO	C	OPTIMA	A
NORGO	D	OAKALLA	B	OKOBOJI	D	OQUIN	C
NORIA	D	OAKBORO	C	OKOLONA	D	OQUOSSOC	D
NORKOOL	B	OAKCITY	C	OKREEK	C	ORA	A
NORMA	C/D	OAKCREEK	B	OKRIST	B	ORAGRAN	D
NORMAL	B	OAKDALE	B	OKTAHA	B	ORAD	C
NORMANDY	B/D	OAKHURST	D	OLALLIE	D	ORAMEL	C
NORMANGEE	D	OAKLAND	C	OLANCHA	B	ORAN	B
NORMANIA	B	OAKLET	C	OLAND	B	ORANGEVALE	B
NORMANNA	C	OAKMETER	C	OLANTA	B	ORCADIA	D
NOROD	C	OAKTON	B	OLASHES	B	ORDNA	D
NORPEL	C	OAKWOOD	B	OLATHE	D	ORDNANCE	C
NORRIS	D	OAKY	D	OLATON	B	ORDWAY	D
NORTE	C	OANAPUKA	B	OLBUT	D	OREANNA	B
NORTH POWDER	C	OATUU	D	OLDBUTTE	C	ORENDA	B
NORTHBEND	C	OBAN	C	OLDMAN	C	OREOKE	B
NORTHCASTLE	C	OBARO	B	OLDS	D	ORHOOD	D
NORTHCove	B	OBIE	D	OLDSMAR	D	ORIF	A
NORTHFIELD	D	OBISPO	D	OLDSPAN	B	ORINOCO	C
NORTHFORK	B	OBNOT	D	OLDTRAIL	B	ORIO	B/D
NORTHMORE	C	OBRAY	C	OLDWOLF	B	ORION	C
NORTHMOUND	B	OBRIEN	C	OLEAN	B	ORITA	B
NORTHPOINT	D	OBSCURITY	B	OLELO	B	ORIZABA	B/C
NORTHROP	C	OBURN	D	OLEMAN	B	ORLA	B
NORTHVILLE	C	OCCIDENTAL	D	OLEMAN	D	ORLANDO	A
NORTHWAY	A/D	OCCUM	B	OLENO	D	ORLIE	B
NORTON	C	OCCUR	C	OLENTANGY	A/D	ORMSBY	C
NORWEST	B	OCEANET	D	OLEO	A	ORNBAUN	B
NORWIDGE	B	OCEANO	A	OLEPHANT	B	ORNEA	B
NORWOOD	B	OCHLOCKONEE	B	OLEQUA	B	ORO FINO	B
NOSAL	C	OCHO	D	OLETE	C	ORONOCO	B
NOSLO	C	OCHOPEE	B/D	OLETHA	D	ORONTO	C
NOSONI	B	OCOE	B/D	OLEX	B	OROSE	C
NOSSER	D	OCONALUTTEE	B	OLF	D	ORPARK	C
NOTCHER	B	OCONEE	C	OLGUN	B	ORR	C
NOTI	D	OCONTO	B	OLI	C	ORSET	B
NOTNED	B	OCQUEOC	A	OLIAGA	B	ORSINO	A
NOTSTEW	D	OCQUEOC, Moderately Wet	B	OLIN	B	ORTEGA	A
NOTTAWA	B	OCUD	B	OLINDA	B	ORTELLCREEK	C
NOTUS	B/C	ODANAH	D	OLIVE	D	ORTHENTS, Maa147-53	C
NOUQUE	D	ODAS	D	OLIVENHAIN	D	ORTING	D
NOVACAN	D	ODEM, Overwash	A	OLIVIER	C	ORTIZ	D
NOVAK	B	ODEM	B	OLLA	B	ORTON	B
NOVARK	B	ODENSON	D	OLLEI	D	ORTONVILLE	B
NOVARY	D	ODERMOTT	B	OLLIERIVAS	D	ORUPA	B
NOVINA	B	ODESSA	D	OLMITO	D	ORWET	A/D
NOWATA	B	ODIN	C	OLMITZ	B	ORWIG	B
NOWEN	B/D	ODONNELL	C	OLMOS	C	OSAGE	D
NOWOY	B	OESTERLE	C	OLOAVA	B	OSBORN	C
NOYES	C/D	OFFENBACHER	C	OLOKUI	D	OSCAR	D
NOYO	C	OFU	B	OLOMOUNT	C	OSCEOLA	B
NOYSON	C	OGDEN	C	OLOMPALI	D	OSCO	B
NUAHS	B	OGDENSBURG	C	OLPE	B	OSDITCH	B
NUBY	D	OGEMAW	C/D	OLYIC	B	OSGOOD	C
NUC	C	OGILVIE	B/D	OLYMPUS	A	OSHAWA	D
NUCKOLLS	B	OGLE	B	OMAHALING	C	OSHONE	D
NUCLA	B	OGLES	B	OMAK	C	OSHOTO	C
NUECES	C	OGLESBY	B	OMENA	D	OSITO	C
NUFFEL	B	OGRAL	B	OMIO	B	OSKA	C
NUFFER	C	OGTNA	B	OMRO	C	OSMUND	B
NUKA	D	OHACO	C	OMSTOTT	C	OSO	C
NUKRUM	D	OHANA	C	OMULGA	C	OSOLL	D
NULEY	B	OHMAN	A	ONASON, Nongravelly	C	OSOLO	A
NUMA	C	OHOP	C	ONASON	D	OSSIAN	B/D
NUPART	D	OHSCOW	B	ONATE	A	OSSIPEE	D
NUPPER	D	OHTOG	B	ONDAWA	B	OSSMER	C

OST	B	PADEN	C	PANMOD	C	PATRICIA	B
OSTIN	A	PADIGAN	D	PANOLA	D	PATRICK	B
OSTRANDER	B	PADINA	B	PANOR	B	PATRICKSBURG	D
OSWALD	D	PADONIA	C	PANORAMA	B	PATROLE	C
OTANYA	B	PADRES	B	PANTANO, Gravelly	C	PATTANI	D
OTEN	C	PADRONES	B	PANTANO	D	PATTEE	B
OTEGO	B	PADUCAH	B	PANTEGO	B/D	PATTENBURG	B
OTERODRY	B	PADWET	B	PANTERA	B	PATTERSON	C
OTHELLO	C/D	PADWOOD	B	PANTEX	C	PATTIWAY	C
OTHELLO, Very Wet	D	PAGARI	B	PANTON	D	PAULDING	D
OTISVILLE	A	PAGELAND	C	PAOLA	A	PAULSON	B
OTOE	D	PAGESPRINGS	D	PAPAA	D	PAUMALU	B
OTOMO	D	PAGINA	C	PAPAC	C	PAUPACK	D
OTOOLE	C	PAHLOW	B	PAPAGUA	C	PAUSANT	B
OTTERHOLT	B	PAHOKEE	B/D	PAPAI	A	PAUWELA	B
OTTERSON	A	PAHRANGE	C	PAPALOTE	C	PAVAIAI	C
OTTMAR	B	PAHROC	D	PAPASPILA	C	PAVELEK	D
OTTMAR, Very Deep	C	PAHRUMP	C	PAPEEK	C	PAVER	B
OTTOKEE	A	PAHSIMEROI	B	PAPINEAU	C	PAVER, Fan	C
OTTOSEN	B	PAHTO	C	PAQUIN	A	PAWCATUCK	D
OTTUMWA	D	PAHUK	A	PARA	B	PAWHUSKA	D
OTWAY	D	PAIA	B	PARADISE	C	PAWLING	B
OTWIN	C	PAIGES	C	PARADISE SPRING	D	PAWTOOT	C
OUACHITA	C	PAILO	B	PARADOX, Clayey	C	PAX	B
OUARD	D	PAINESVILLE	C	PARADOX, Wet	D	PAXVILLE	B/D
OULA	D	PAINT	D	PARAGON	C	PAYNE	C
OUPICO	C	PAINTBRUSH	C	PARAGONAH	D	PAYPOINT	B
OURAY, Cool	A	PAISANO	D	PARAJE	B	PEACHSPRINGS	B
OURAY, Sandy Loam Surface	B	PAJARA	C	PARANAT, Drained, Saline	B	PEAHKE	B
OUSELFAL	D	PAJUELA	B	PARASOL	B	PEARCE	D
OUSLEY	C	PAKA	B	PARCELAS	D	PEARL	B
OUTLAW	D	PAKINI	B	PARCHIN	C	PEARL HARBOR	D
OUTLET	C	PALACID	B	PARDEE	D	PEARLWISE	B
OUTLOOK	C/D	PALACIOS	D	PARDEEVILLE	B	PEARNE	D
OUTPOST	C	PALAFOX	C	PARIATO	D	PEARSONCREEK	B
OVAL	C	PALANUSH	C	PARIDA	B	PEASLEY	D
OVAN	D	PALAPALAI	B	PARISIAN	D	PEASPEAR	D
OVERCUP	D	PALATINE	B	PARKALLEY	B	PEAVINE	B
OVERLAKE	A	PALAU	B	PARKDALE	B	PEAWICK	D
OVERLOOK	B	PALAZZO	B	PARKFIELD	C	PEBBLEPOINT	C
OVERSHUE	B/D	PALERF	C	PARKINSON	B	PECATONICA	B
OVERSIGHT	B	PALINOR	D	PARKS	B	PECKHAM	C
OVIATT	B	PALISADE	B	PARKVIEW	B	PECKISH	D
OVIDCREEK	C	PALISADE, wet	C	PARKVILLE	C	PEDEE	C
OVINA	B	PALIX	B	PARKWOOD	B/D	PEDERNALES	C
OVINGTON	B	PALLS	C/D	PARLE	C/D	PEDIGO	B/D
OWANKA	C	PALM	D	PARMELE	C	PEDLEFORD	C
OWENTOWN	B	PALM BEACH	A	PAROD	D	PEDREGAL	B
OWINZA	D	PALMAR	D	PARREGO	C	PEDRICK	B
OWLCAN	B	PALMAREJO	C	PARRITA	C	PEDRICKTOWN	D
OWLHOLE	D	PALMER CANYON	B	PARSIPPANY	C/D	PEDRO	C
OWLROCK	D	PALMERDALE	B	PARSNIP	D	PEEBLES	C
OWLSRING	C	PALMETTO	B/D	PARSONS	D	PEEDEE	A
OWSEL	B	PALMICH	B	PARTLOW	D	PEEKO	D
OWYHEE	B	PALMONT	A	PARTOV	D	PEEL	C
OXBOW	C	PALO	D	PARTRIDGE	B	PEERLESS	B
OXFORD	D	PALOBIA	B	PARVIS	B	PEETZ	A
OXHEAD	B	PALODURO	B	PASAGSHAK	C	PEGLEG	C
OXLEY	C	PALOMARIN	B	PASCACK, Moderately Well		PEJI	A
OXMAN	B	PALOMAS	B	Drained	B	PEKAY	C
OXY	C	PALOMINO	D	PASCACK, Smowhat Poorly		PELAHATCHIE	C
OYHUT	C	PALOS VERDES	C	Drained	C	PELAN	B
OYLEN	B	PALOS VERDES, Dry	D	PASCO	C/D	PELATO	D
OZAN	D	PALSGROVE	B	PASHUA	C	PELELIU	D
OZETTE	C	PALUXY	B	PASO SECO	D	PELICAN	B
OZIAS	D	PAMISON	B	PASQUETTI	D	PELION	B/D
PAAIKI	B	PAMOA	B	PASQUOTANK	B/D	PELKIE	A
PAALOA	B	PAMSDER	C	PASSAIC	D	PELLEJAS	B
PAAUHAU	A	PANA	B	PASTIK	D	PELLICER	D
PABLO	D	PANAWEA	D	PASTORPEAK	B	PELTON	B
PACER	B	PANAK	B	PATAHA	C	PEMBERTON	B
PACHAPPA	D	PANAMAKER	B	PATBURN	C	PEMI	C
PACHEL	B	PANAMAKER, Flooded	B	PATCHIN	D	PEN ARGYL	B
PACHNEUM	B	PANAMINT	B	PATE	C	PENAGUL	D
PACIFICO	C	PANDO	B	PATEL	C	PENALOSA	C
PACKARD	B	PANDOAH	C	PATELZICK	D	PENASCO	D
PACKMO	B	PANDORA	B/D	PATEMOS	B	PEND OREILLE	B
PACKSADDLE	C	PANDURA	D	PATENT	B	PENDARVIS	C
PACKTRAIL	C	PANE	B	PATEROS	B	PENDEN	B
PACKWOOD	D	PANHANDLE	B	PATHFINDER	A	PENDER	C
PACO	C	PANHILL	B	PATILLAS	B	PENDERGRASS	D
PACTOLUS	A	PANIN	B	PATILO	A	PENDOLA	B
PADDY	D	PANIOGUE	C	PATOS	C	PENELAS	D
PADDYKNOB, Stony	A	PANKY	B	PATOUTVILLE	C	PENEY	D
PADDYKNOB	C	PANKY, Clayey	C	PATOUZA	C	PENGILLY	B/D

PENGRA.....	C	PETTUS.....	C	PINEISLAND.....	C	PLUMCREEK.....	B
PENINSULA.....	B	PETTY.....	B	PINELLAS.....	B/D	PLUMFIELD.....	C
PENLAW.....	C	PETTYJON.....	B	PINENUT.....	D	PLUSH.....	B
PENNARGYL.....	B	PEVELY.....	B	PINEOLA.....	B	PLUTOS.....	B
PENNEKAMP.....	D	PEVETO.....	A	PINERUN.....	B	POACHIE.....	B
PENNELL.....	B	PHALANX.....	B	PINESPRING.....	C	POALL.....	C
PENNEY.....	A	PHANTOM.....	C	PINETOP.....	C	POALL, Cool.....	D
PENNICHUCK.....	B	PHAROAH.....	D	PINETUCKY.....	B	POARCH.....	B
PENNING.....	B	PHEBA.....	C	PINETUCKY, Graded.....	C	POBER.....	B
PENNYCREEK.....	D	PHELAN.....	D	PINEVILLAGE.....	B	POCALLA.....	A
PENTHOUSE.....	C	PERSON.....	B	PINEYNECK.....	B	POCASSET.....	B
PENWELL.....	A	PHIFERSON.....	C	PINEYWOODS.....	D	POCATELLO.....	B
PENWOOD.....	A	PHILBON.....	D	PINEZ.....	B	POCATY.....	D
PENZANCE.....	C	PHILIPPA.....	C	PINGREE.....	D	POCKER.....	C
PEOH.....	C/D	PHILIPSBURG.....	B	PINHOOK.....	B/D	POCOLA.....	D
PEOLA.....	C	PHILLCHER.....	B	PINICON.....	B	POCUM.....	D
PEONE.....	C/D	PHILLIPS.....	C	PINKEL.....	C	PODEN.....	B
PEORIA.....	D	PHILLIPSBURG.....	B	PINKHAM.....	A	PODMOR.....	C
PEOTONE.....	C/D	PHILOMATH.....	D	PINNEBOG.....	A/D	PODUNK.....	B
PEP.....	B	PHILOMONT.....	B	PINNOBIE.....	B	PODUS.....	C
PEPAL.....	B	PHING.....	C	PINNTANK.....	C	POE.....	C
PEPIN.....	B	PHLISS.....	D	PINONES.....	D	POGAL.....	C
PEPOON.....	D	PHLYNSPA.....	B	PINOTY.....	B	POHAKUPU.....	B
PEPPER.....	D	PHOEBE.....	B	PINRIDGE.....	B	POHOCO.....	B
PEPPERBOX.....	B	PHOENIX.....	D	PINSRING.....	C	POINSETT.....	B
PEPTON.....	D	PHYS.....	B	PINTAS.....	B	POINT.....	C
PEQUAYWAN.....	B	PIANKESHAW.....	B	PINTO.....	C	POINT ISABEL.....	C
PEQUEA.....	B	PIANOHILL.....	C	PINWHEEL.....	C	POINTLA.....	C
PERCELL.....	B	PIAR.....	B	PIOCHE.....	D	POISONHOL.....	C
PERCHAS.....	D	PIASA.....	D	PIONEER.....	D	POJO.....	C
PERCHE.....	B	PICACHO.....	C	PIPEFLAT.....	D	POKEGEMA.....	B
PERCHLAKE.....	B	PICANTE.....	D	PIPELINE.....	A	POKER.....	C
PERCILLA.....	D	PICARD.....	B	PIPPIN.....	A	POKEY.....	C
PERCOUN.....	C	PICEANCE.....	C	PIPPOD.....	A	POLALLIE.....	C
PERDIDO.....	B	PICKAWAY.....	B	PIRAPEAK.....	B	POLANDER.....	B
PERECHENEY.....	B	PICKENS.....	D	PIRD.....	B	POLAR.....	B
PERFA.....	D	PICKETPIN.....	B	PIRKEY.....	C	POLAWANA.....	A/D
PERGRIN.....	B	PICKNEY.....	A/D	PIRODEL.....	B	POLECAT.....	B
PERICO.....	B	PICKTON.....	A	PISCASAW.....	B	POLETA.....	C
PERIDA.....	B	PICKWICK.....	B	PISCOE.....	B	POLETAD.....	B
PERIDGE.....	B	PICOSA.....	C	PISGAH.....	C	POLICH.....	C
PERIL.....	D	PICTURE.....	D	PISMO.....	D	POLKING.....	D
PERING.....	C	PIDCOKE.....	D	PISTOL.....	C	POLLARD, High Rainfall.....	B
PERINOS.....	C	PIDINEEN.....	D	PISTOLRIVER.....	B	POLLARD.....	C
PERITSA.....	C	PIE CREEK.....	D	PITCHER.....	B	POLLASKY.....	B
PERKINS.....	D	PIEDAWN.....	B	PITCO.....	D	POLLUX.....	C
PERKS.....	A	PIEDMONT.....	D	PITNEY.....	C	POLO, Moderate Perm.....	B
PERLOR.....	D	PIEGON.....	B	PITTSBURG.....	B	POLO, Moderately Slow Perm.....	C
PERN.....	B	PIERCEPARK.....	B	PITTVILLE.....	B	POLSON.....	B
PERNITAS.....	C	PIERIVER.....	D	PITVAR.....	D	POLUM.....	B
PERQUIMANS.....	D	PIERKING.....	D	PITZER.....	D	POLUMAR.....	B
PERREAU.....	B	PIERPONT.....	C	PIUMPSHA.....	B	POLVADERO.....	C
PERRIN.....	B	PIERRE.....	B	PIVOT.....	A	POMAN.....	C
PERRINE.....	B/D	PIERRON.....	D	PIXLEY.....	D	POMAT, Dry.....	B
PERRY.....	D	PIERSONTE.....	A	PIZENE.....	B	POMAT.....	C
PERRYGULCH.....	D	PIERZ.....	B	PLACEDO.....	D	POMERENE.....	C
PERSANTI.....	C	PIETOWN.....	B	PLACER.....	B	POMERENING.....	A
PERSAYO.....	C	PIEZON.....	B	PLACID.....	B/D	POMME.....	B
PERSIS.....	B	PIGEONROOST.....	B	PLACK.....	D	POMO.....	B
PERSONVILLE.....	B	PIGTAIL.....	D	PLAINBO.....	A	POMONA.....	B/D
PERT.....	D	PIKADEN.....	A	PLAINS.....	A	POMONIO.....	C
PERVINA.....	B	PIKE.....	B	PLAINVIEW.....	C	PONCA.....	B
PESCAO.....	D	PIKEVILLE.....	B	PLAINVIEW.....	A	PONCENA.....	D
PESCAR.....	C	PILABO.....	B	PLANK.....	C	PONCHA.....	A
PESHTIGO.....	C	PILCHUCK.....	A	PLANKINTON.....	D	PONCIANO.....	C
PESKAH.....	B	PILEUP.....	B	PLANTATION.....	B/D	POND CREEK.....	B
PESO.....	C	PILGRIMS.....	B	PLASKETT.....	D	PONDER.....	D
PESOWYO.....	C	PILLERY.....	B	PLATEA.....	C	PONDEROSA.....	B
PETACA.....	D	PILLIKEN.....	B	PLATO.....	C	PONE.....	B/D
PETAL.....	C	PILLOT.....	C	PLATSHER.....	C	PONINA.....	D
PETAN.....	D	PILONI.....	A	PLATTVILLE.....	B	PONTOTOC.....	B
PETCAN.....	C	PILOT PEAK.....	C/D	PLAYMOOR.....	C/D	PONYCREEK.....	A/D
PETERMAN, Sandy Substratum, Alkali.....	C	PILOT ROCK.....	C	PLAZA.....	C	PONZER.....	D
PETERMAN.....	D	PILOTWELL.....	B	PLEASANT.....	C	POOBAA.....	C
PETERS.....	D	PILTZ.....	C	PLEDGER.....	D	POOCHAM.....	B
PETERSON.....	B	PINAL.....	D	PLEINE.....	D	POOKALOO.....	D
PETESCREEK, Stony.....	B	PINBIT.....	B	PLEIOVILLE.....	C	POOKU.....	B
PETESCREEK, Gravelly.....	C	PINCHER.....	C	PLEITO.....	B	POOLEVILLE.....	C
PETRIE.....	C	PINCHOT.....	B	PLEMONS.....	B	POORCAL.....	B
PETROF.....	B	PINE FLAT.....	B	PLEV.....	B	POORHOUSE.....	D
PETROS.....	D	PINEAL.....	D	PLEVNA.....	D	POORMA.....	B
PETSPRING.....	D	PINEDA.....	D	PLINCO.....	B	POORMAN.....	B
PETTIGREW.....	D	PINEGAP.....	B	POLOVER.....	C	POORMAN.....	D
PETTJOHN.....	B	PINEGUEST.....	B	PLUCK.....	C	POOSE.....	D
		PINEHILL.....	B	PLUMBROOK.....	B	POPASH.....	D

POPHERS	C	PRESA	B	PUROB	D	QUITTER	B
POPLE	B/D	PRESHER	B	PURSLEY	B	QUIVER	B/D
POPSON	B	PRESNAL	B	PUSHMATAHA	C	QUIVERA	C
POQUITA	B	PRESTO	B	PUSTOI	B	QUOMUS	B
PORONTO	C	PREUSS	C	PUTCO	B	QUONAL	B
PORRETT	D	PREUSSRANGE	C	PUTNAM	D	QUOPANT	D
PORRONE	B	PRICE	B	PUTNEY	B	QUOSATANA	D
PORTAGEVILLE	D	PRICECREEK	D	PUTT	C	RABBS	B
PORTAL	B	PRICETOWN	B	PUU LAI	D	RACE	B
PORTALES	B	PRIDHAM	D	PUU MOIWI	B	RACING	D
PORTALTO	B	PRIESTLAKE	B	PUU OO	A	RACKER	A
PORTDICK	B	PRILL	D	PUU OPAE	B	RADER	D
PORTER	B	PRIM	D	PUUKALA	D	RADFORD	B
PORTERFIELD	D	PRIMEAUX	C	PUUONE	C	RADIUM	A
PORTERSPRINGS	B	PRIMGHAR	B	PUYE	C	RADLEY	B
PORTGRAHAM	B	PRINCETON	B	PUZZLECREEK	C	RADNOR	C
PORTHILL	D	PRINEVILLE	C	PYBURN	D	RAFTRIVER	C
PORTIA	C	PRINSBURG	B/D	PYEATT	B	RAFTVILLE	B
PORTILLO	B	PRISONER	C	PYLE	B	RAGAMUFFIN	B
PORTINO	C	PRISSEL	A	PYLON	D	RAGGULCH	C
PORTLAND	D	PRITCHARD	C	PYOTE	A	RAGNAR	B
PORTMOUNT	B	PROBERT	B	PYRADY	C	RAGPIE	D
PORTSMOUTH	B/D	PROMONTORY	D	PYRAMID	D	RAHAL	C
PORTVILLE	C	PRONG	C	PYRENEES	C	RAHM	C
PORUM	D	PROPER	A	PYRMONT, Bedrock Substratum	C	RAHWORTH	B
POSEY	B	PROPHETSTOWN	B/D	PYRMONT	D	RAIL	D
POSEYVILLE	C	PROTIVIN	C	PYSHT	C	RAILCITY	A
POSKIN	C	PROUT	C	QENI	C	RAILROAD	C
POSO	B	PROVIDENCE	C	QUADRIA	D	RAINBOLT	C
POSOS	C	PROVIG	C	QUAFENO	C	RAINEY	C
POSSUMTROT	B	PROW	D	QUAGLE	B	RAINIER	C
POST	D	PRUCREE	C	QUAILPRAIRIE	C	RAINO	D
POTAGANNISSING	D	PRUDY	B	QUAILRIDGE	B	RAINS	B/D
POTAMUS	B	PRUE	B	QUAKERTOWN	C	RAINS, Flooded	D
POTATOLAKE	B	PRUITTON	B	QUAKING	B	RAINSBORO	C
POTAWATOMI	C	PRUNIE	D	QUALLA, Dry	B	RAINSVILLE	B
POTCHUB	C	PRYOR	C	QUALLA	C	RAINTUF	B
POTEET	C	PSAMMAQUENTS	D	QUAM	B/D	RAISIO	C
POTELL	B	PSAMMENTS	B	QUANAH	B	RAKANE	C
POTH	C	PSUGA	B	QUANTICO	B	RALDRIDGE	B
POTLATCH	C	PSUYAAH	C	QUARDERER	B	RALORE	D
POTOSI	D	PTARMIGAN	C	QUARLES	D	RALPH	B
POTRATZ	C	PUAPUA	D	QUARTELES	D	RALPHSTON	B
POTRERO	A/D	PUAULU	A	QUARTERBACK	B	RALSEN	D
POTRILLO	B	PUCKUM	D	QUARTERMASTER	C	RAMADERO	B
POTRMOUND	C	PUEBLO	B	QUARTZVILLE	B	RAMAH	B
POTTER	C	PUELZMINE	D	QUATAMA	C	RAMBLA	C
POTTERSVILLE	C	PUERCO	D	QUAY	B	RAMMEL	C
POTTINGER	B	PUGET	C	QUEALMAN	B/C	RAMONA	C
POTTSBURG	C	PUGSLEY, Dry	B	QUEALY	D	RAMOTH	B
POUDRE	D	PUGSLEY	C	QUEBRADA	C	RAMPART	B
POUJADE	B	PUHI	B	QUEENY	D	RAMSDELL	C
POULSBO	D	PUHIMAU	D	QUEETS	B	RANA	D
POUNCEY	D	PUICE	C	QUEMADO	C	RANACKER	D
POVERTY	D	PULA	C	QUENCHEROO	B	RANCE	C
POVERTYFLAT	B	PULANTAT	C	QUENZER	D	RANCHOSECO	D
POVIRT	D	PULASKI	B	QUERC	C	RANCO	D
POWDERHORN	C	PULCAN	C	QUETICO	C	RANDADO	C
POWDERWASH	C	PULEXAS	B	QUEZCAN	C	RANDALL	D
POWEEN	C	PULLMAN	D	QUIBURI	B	RANDCORE	D
POWELL	C	PULLUP	A	QUICKSELL	C	RANDMAN	D
POWER	B	PULPIT	C	QUICKSILVER	D	RANDOLPH	C
POWLEY	D	PULSIPHER	D	QUIDEN	B	RANDS	C
POWLOW	D	PULTNEY	C	QUIENSABE	C	RANDSBURG	D
POWMENT	C	PUMEL, Nongravelly	C	QUIERO	C	RANGEE	D
POWVAL	B	PUMEL	D	QUIETUS	C	RANGER	C
POWWAHKEE	B	PUMPHOUSE	B	QUIGG	D	RANKOR	B
POWWATKA	C	PUMPHOUSE, Clayey Subsoil	C	QUIHI	C	RANRUFF	D
POYGAN	D	PUMPKIN	B	QUILCENE	C	RANSECT	C
POZEGA	C	PUNA	A	QUILLAMOOK	B	RANSLO	D
POZO BLANCO	B	PUNALUU	D	QUILLAYUTE	B	RANSOM	B
PRADE	D	PUNG	C	QUILLIAN	C	RANSTEIN	B
PRAIRIE	A	PUNOHU	A	QUIMA	B	RANTOUL	D
PRAIRIECREEK	C	PUNSIT	C	QUIMERA	C	RAPADO	C
PRAIRIEVILLE	B	PUNTA	B/D	QUINAULT	D	RAPATEE	D
PRAMISS	C	PUNTILLA	B	QUINBINS	C	RAPELJE	B
PRATHER	D	PURCELLVILLE	B	QUINCREEK	C	RAPH	B
PRATLEY	C	PURCHASE	C	QUINCY	B	RAPHO	B
PRATT	A	PURCHES	C	QUINLIVEN	C	RAPIDAN	B
PREAKNESS	B/D	PURDIN	C	QUINN	B/D	RAPPAHANNOCK	D
PREATORSON	B	PURETT	B	QUINNEY	C	RAPSON	B
PREGO	A	PURGATORY	C	QUINTO	D	RAQUETTE	B
PRELO	B	PURGATORY, Cool Dry	D	QUIRK	C	RARICK	C
PREMIER	B	PURNELL	D	QUITERIA	C	RARITAN	C
PRENTISS	C	PURNER	D	QUITMAN	C	RASSER	B

RASSET	B	REDO	A	RENTZEL	C	RINCON	C
RASTER	A	REDPEAK	B	RENTERS	D	RINCONFLAT	B
RASTUS	C	REDPEN	B	RENWASH	B	RINDGE, Drained	C
RATIOPEAK	B	REDPORT	B	RENWICK	B	RINEARSON	B
RATLAKE	D	REDRIDGE	B	REPARADA	D	RINEY	B
RATLEFLAT	B	REDRIM	B	REPKIE	B	RINGLE	B
RATLIFF	B	REDROB	C	REPMIS	C	RINGO	D
RATROOT	D	REDSLIDE	B	REPP	B	RINGWOOD	B
RATSNEST	D	REDSPEAR	D	REPPART	B	RINKER	C
RATSOW	C	REDSPOON	C	RESOOT	C	RINQUIN	C
RATTLER	D	REDSPRINGS	B	RESOTA	A	RIO ARRIBA	D
RATTO	C	REDSPRINGS, Graded	D	RESTON	D	RIO DIABLO	C
RAUB	C	REDSTOE	B	RET, High Elevation	C	RIO FRIO	B
RAUS	C	REDSUN	D	RET	D	RIO GRANDE	B
RAUSTER	C	REDTHAYNE	B	RETAW	D	RIO KING	C
RAUZI	B	REDUN	B	RETEP	B	RIO LAJAS	A
RAVALLI, Bedrock Substratum	B	REDVALE	C	RETSOVER	C	RIO PIEDRAS	B
RAVALLI	D	REDVIEW	C	RETTIB	B	RIOBLANCHO	C
RAVEENWASH	A	REDVINE	C	RETTIB LOAM	B	RIOLINDA	C
RAVEN	A	REDWASH	D	REUTER	C	RIOLOMAS	B
RAVENELL	D	REDWATER	B	REVA	D	RIONUTRIA	C
RAVENNA	C	REED	D	REVEL	C	RIOVISTA	A
RAVENSROOST	B	REEDER	C	REVERE	B/D	RIPGUT	C
RAVIA	C	REEDPOINT	D	REVIT	C	RIPLEY	C
RAWAH	C	REEDSBURG	C	REVLING	B	RIPON	B
RAWLES	B	REEDSCREEK	B	REVROR	D	RIPPLE	B
RAWSON	B	REEDSLAKE	B	REWARD	B	RISBECK	B
RAYBURN	D	REEDWEST	C	REXFORD	C	RISLEY	C
RAYCREEK	B	REEDY	C	REXOR	B	RISUE	D
RAYFORD	C	REEFRIDGE	D	REYAB	B	RISWOLD	B
RAYLAKE	D	REELFOOT	C	REYCREEK	C	RITA	D
RAYNAL	C	REEPO	C	RHEA	B	RITCHEY	D
RAYNOLDSON	B	REESE	C	RHOAMETT	D	RITIDIAN	D
RAYOHILL	C	REESER	C	RHYLOW	B	RITNER	C
RAYPOL	C	REESVILLE	C	RHYMES	A	RITO	B
RAZORBA	B	REEUP	C	RIB	B/D	RITTEL	C
RAZORBACK	D	REFLECTION	B	RIBERA	C	RITTER	B
RAZUN	D	REGAL	B/D	RIBHILL	B	RITZ	C/D
READLYN	B	REGER	B	RIBRIVER	B	RITZCAL	B
REALLIS	B	REGGAD	A	RICCO	D	RIVALIER	B
REAM	B	REGNAPS	C	RICEBORO	B/D	RIVERBY	A
REAP	D	REGRACIC	B	RICELAKE	D	RIVERDALE	A
REARDAN	C	REHBURG	C	RICES	C	RIVERLOST	B
REAVILLE	C	REHFIELD	B	RICETON, Sandy Substratum	A	RIVEROAD	C
REAVIS	B	REHM	C	RICETON	B	RIVERSIDE	A
REBA	C	REHOBETH	D	RICEVILLE	C	RIVERTON	B
REBECCA	B	REICISS	B	RICH	C	RIVERVIEW	B
RECK	D	REILLY	A	RICH, Wet	D	RIVERWASH	A
RECKLOR	C	REINACH	B	RICHARDVILLE	B	RIVIERA, Limestone Substratum	B/D
RED BAY	B	REINECKE	B	RICHFIELD	C		
RED BLUFF	B	REINER	B	RICHFORD	A	RIVIERA	D
RED HILL	B	REINHART	D	RICHSUM	B	RIXON	C
RED HOOK	C	REIS	D	RICHVIEW	C	RIZ	D
RED SPUR	B	REK	C	RICHWOOD	B	RIZNO	A
REDARROW	D	REKIMA	D	RICKETTS, Nonstony	B	ROACHA	C
REDBELL	B	RELAN	B	RICKETTS	C	ROADMASTER	D
REDBIRD	B	RELEEP	B	RICKMAN	C	ROANE	C
REDBOW	C	RELFE	A	RICKMORE	C	ROANHIDE	C
REDBUD	C	RELIZ	D	RICKREALL	D	ROARING	B
REDCAMERON	D	RELYEA	B	RICKS	A	ROATCAP	B
REDCANYON	B	REMBERT	D	RICOT	C	ROBAGO	B
REDCAP	B	REMEDIOS	C	RIDENBAUGH	D	ROBANA	B
REDCHIEF	C	REMLAP	C	RIDGE	B	ROBBS	D
REDCLOUD	B	REMMEL	B	RIDGELAND	B/D	ROBBS CREEK	C
REDCO	D	REMMIT	B	RIDGELAWN, wet	D	ROBCO	C
REDCREEK	C	REMOUNT	A	RIDGELITE	D	ROBER	C
REDDALE	D	REMSEN	D	RIDGEVIEW	C	ROBERTSDALE	C
REDDIES	B	REMUS	B	RIDGEWOOD	D	ROBERTSVILLE	D
REDFIELD	B	REN	C	RIDIT	C	ROBINETTE	B
REDFIELD, Wet	C	RENCALSON	D	RIDLEY	C	ROBINLEE	C
REDFIST	C	REND	B	RIEDEL	C	ROBOLATA	C
REDFLAME	B	RENDOVY	B	RIEDTOWN	C	ROCHELLE	C
REDFLAT	B	RENEGADE	D	RIESEL	C	ROCHEPORT	B
REDHOOK	A	RENFROW	D	RIFT	C	ROCHER	B
REDIG	B	RENHA	C	RIGA	D	ROCHPAH	D
REDLAKE	D	RENICK	D	RIGDON	C	ROCK OUTCROP	D
REDLEVEL	C	RENNER	B	RIGGSVILLE	C	ROCKABIN	C
REDLOCK	B	RENNIE	D	RIGOLETTE	C	ROCKBLUFF	A
REDLODGE	D	RENOX	B	RILEY	B	ROCKCASTLE	D
REDMANSON	B	RENSHIGH	B	RILLA	B	ROCKCUT	B
REDMORE	C	RENSSELAER	C	RILLOSO	A	ROCKDALE	A
REDMOUNT	B	RENTIN	D	RIMINI	A	ROCKDAM	A
REDNIK	B	RENTILL	B	RIMROCK	D	ROCKERS	C
REDNIK, Nonstony	C	RENTON	C/D	RIMTON	D	ROCKFIELD	B
REDNUN	C	RENTSAC	C	RIN	B	ROCKFORD	B

ROCKHILL	D	ROSELLE	C	RUNGE	B	SALERNO	B/D
ROCKHOUSE	A	ROSENBROCK	D	RUNLETT	B	SALGA	C
ROCKLIN	D	ROSENDALE	C	RUPLE	C	SALINAS	D
ROCKMILL	C/D	ROSENWALL	D	RUPLEY	A	SALINE=SODIC	A
ROCKO	B	ROSESPRING	B	RUPRECHT	D	SALISBURY, High Elevation	D
ROCKOA	B	ROSEWOOD	D	RUSBACH	A	SALIX	B
ROCKPENS	B	ROSHE SPRINGS	C/D	RUSHCREEK	B	SALKUM	B
ROCKRUN	B	ROSHOLT	B	RUSHFORD	B	SALLYANN	C
ROCKSAN	C	ROSINE	B	RUSHLAKE	A	SALMON	B
ROCKY FORD	C	ROSLYN	B	RUSHMORE	B/D	SALONIE, Moderately wet	C
ROCKYBAR	B	ROSMAN	B	RUSHRIVER	B/D	SALT CHUCK	A
ROCKYBROOK	B	ROSS	B	RUSHTOWN	A	SALT FLAT	D
RODAD	D	ROSSMOOR	B	RUSHVILLE	D	SALTCREEK	C
RODELL	D	ROSSMOYNE	C	RUSKTOWN	B	SALTERY	D
RODEN	D	ROSSPEAK	B	RUSO	B	SALTILLO	C
RODEO	D	ROSSVILLE	B	RUSSLER	C	SALTINE	C
RODESSA	D	ROSWELL	A	RUSTIGATE	C	SALTON	D
RODIE	B	ROSY	B	RUSTLERPEAK	C	SALUDA	C
RODNEY	D	ROTAMER	B	RUSTY	B	SALVISA	C
RODROF	D	ROTAN	C	RUSTYBUTTE	B	SALZER, Protected	C
ROELLEN	D	ROTHICAN	B	RUTERSVILLE	C	SAMARIA	B
ROEMER	C	ROTHSAY	B	RUTHERFORD	C	SAMBA	D
ROGAN	B	ROVINOM	B	RUTLAND	C	SAMBRITO	B
ROGERSON	D	ROTTULEE	C	RYALLEN	D	SAMINIEGO	C
ROGGER	B	ROTURA	B	RYAN	D	SAMOIST	D
ROGRUBE	B	ROUEN	B	RYARK	B	SAMOR	D
ROHAN	D	ROUGHCREEK	D	RYCO	D	SAMSIL	D
ROHNERVILLE	B	ROUND BUTTE	D	RYDOLPH	C	SAN ANDREAS	B
ROHONDA	C	ROUNABOUT	C	RYEGATE	C	SAN ANTON	B
ROHRBECK	B	ROUNDBARN	B	RYELL	D	SAN ANTONIO	C
ROHRERSVILLE	D	ROUNDHEAD	B/D	RYER	C	SAN BENITO	B
ROJO	C	ROUNDOR	C	RYKER	B	SAN GERMAN	D
ROLETTE	C	ROUNDUP	C	RYORP	C	SAN ISABEL, Stony	A
ROLFE	C/D	ROVAL	D	RYUS	B	SAN ISABEL, Cobbiy	B
ROLIE	D	ROWDEN	C	SAAR	C	SAN MIGUEL	D
ROLLA	C	ROWDY	B	SABANA	D	SAN RAFAEL	B
ROLLAWAY	D	ROWE	D	SABANA SECA	D	SAN SEBASTIAN	B
ROLLINGSTONE	C	ROWEL	D	SABENYO	B	SAN SIMEON	D
ROLLINS	A	ROWENA	C	SABIES	C	SAN YSIDRO	D
ROLO	B	ROWLAND	C	SABINA	C	SANBEE, Thin	A
ROMAN	B	ROWLEY	C	SABINE	A	SANBEE	B
ROMANOSE	D	ROXAL	D	SACATAR	B	SANBORG	D
ROMBERG	C	ROXANA	B	SACH	C	SANBORN	C
ROMBO	D	ROXER	B	SACKETT	B	SANBURN	B
ROME	B	ROXTON	D	SACO	D	SANCAJO	C
ROMEO	D	ROYCE	C	SACTUS	D	SANDBERG	A
ROMGAN	C	ROYERTON	B	SACVILLE	D	SANDBRANCH	B
ROMINE	B	ROYSTONE	B	SADDLEBUNCH	D	SANDBUR	A
ROMINELL	C	ROZARA	D	SADDLEBUTTE	D	SANDCREEK	D
ROMNELL	B/D	ROZELLVILLE	B	SADDLEPEAK	B	SANDERSON	B
ROMONA	D	ROZLEE	C	SADIE	C	SANDHILL	B
ROMOUND	C	RUBBLE LAND	A	SADLER	C	SANDIA	B
ROMSTOCK	B	RUBICITY	B	SADORUS	D	SANDOSE	A
RONAN	D	RUBIO	C/D	SAEMO	B	SANDOVER	A
ROND	C	RUBSON	B	SAFETY	B	SANDOW	C
RONDELL	B	RUBY	B	SAGANING	A/D	SANDRIDGE, Alkali	A
RONEY	C	RUBYCREEK	B	SAGASER	B	SANDSPRING	B
RONNEBY	C	RUBYLAKE, Strongly Saline	C	SAGE	D	SANDUN	B
RONSON	B	RUBYLAKE	D	SAGECREEK	B	SANDUSKY	D
ROOKS	B	RUCHEZ	C	SAGEDALE	C	SANDVIEW	B
ROONEY	D	RUCKER	B	SAGEHEN	D	SANDWASH	C
ROOP	B	RUDDLEY	D	SAGERTON	C	SANDWICK	B
ROOSET	C	RUDEEN	C	SAGEVALLEY	B	SANDY POINT	D
ROOSTERCOMB	C	RUDO	B	SAGLE	C	SANFECO	C
ROOT	B/D	RUDYARD	D	SAGLEY	B	SANFELIPE	B
ROOTEL	C	RUEDLOFF	B	SAGO	D	SANGO	C
ROPER	B/D	RUELLA	B	SAGOUSPE	B/C	SANHEDRIN	B
ROQUES	D	RUESH	B	SAHALIE	B	SANHUD	B
ROSALIE	B	RUGAR	C	SAHAPTIN	D	SANILAC	B
ROSAMOND	C	RUGLES	B	SAHKAHTAY	B	SANJE	B
ROSARIO	C	RUINS, Thick Surface	A	SAHUARITA	B	SANKEY	C
ROSCED	B	RUINS	C	SAID	B	SANKLUNA	B
ROSCHE	C	RUIZ	B	SAILBOAT	B/C	SANLOREN	B
ROSE VALLEY	D	RUMA	A	SAILES	B	SANOSTEE	C
ROSEBERRY, Sandy Substratum	C	RUMBO	C	SAIN	B	SANPITCH	C
ROSEBERRY, Drained	D	RUMFORD	B	SAKAKAWEA	B	SANSARC	D
ROSEBRIAR	D	RUMLEY	B	SAL	D	SANTA	C
ROSEBURG	B	RUMNEY	C	SALADAR	D	SANTA CLARA	C
ROSEDALE	A	RUMPAH	D	SALAL	C	SANTA ISABEL	D
ROSEHU	B/D	RUMPELTEASER	D	SALAMANCA	D	SANTA LUCIA	C
ROSEGLEN	B	RUMPLE	C	SALAMATOF	B	SANTA MARTA	C
ROSEHAVEN	B	RUMSEY	B	SALANDER	B	SANTANELA, Alkali	D
ROSEHILL	D	RUMUNG	C	SALCO	C	SANTAQUIN	A
ROSELAND	B	RUNCLINT	A	SALCREEK	B	SANTAROSA, Flooded	B
ROSELLA	D	RUNE	C	SALEM	B	SANTEE	D

SANTEETLAH	B	SAYNER	A	SEBAGO	D	SHADELEAF	C
SANTIAGO, Moderate Perm	B	SCALEROCK	C	SEBASTIAN	D	SHADEVILLE	B
SANTIAM	C	SCALLEY	B	SEBASTOPOL	C	SHADILTO	D
SANTO	B	SCALPCREEK	B	SEBBO	B	SHADOVAL	D
SANTONI	D	SCAMMAN	D	SECCA	C	SHADY	B
SANTOP	B	SCANDARD	C	SECHLER	B	SHADYGROVE	C
SANTUC	C	SCAPONIA	B	SECO	C	SHADYPASS	A
SANWELL	B	SCAR	B	SECONDCREEK	D	SHAFFTON	B
SANYON	D	SCAREDMAN	B	SECREPASS	D	SHAFTER	D
SAPEHA	B	SCARFACE	B	SECREST	C	SHAG	D
SAPINERO, Cool	B	SCARPER	C	SECRET CREEK	B	SHAGNASTY	C
SAPKIN	C	SCARUL	B	SECTION	B	SHAKAMAK	C
SAPPHO	B	SCATLAKE	D	SED	C	SHAKAN	C
SARA	D	SCATTERSVILLE	D	SEDALE	D	SHAKESPEARE	C
SARAGOSA	B	SCHAFER	C	SEDALIA	C	SHAKOPEE	C
SARAGOTE	C	SCHAFFER	C	SEDGEFIELD	C	SHALAKE	C
SARAHSVILLE	D	SCHALLER	A	SEDGWICK	D	SHALBA	D
SARAZAN	B	SCHALOW	B	SEDONA	D	SHALCLEAV	D
SARBO	B	SCHATTEL	C	SEDROWOOLLEY	C	SHALONA	B
SARCILLO	D	SCHAINER	A	SEEBURG	A	SHALPER	D
SARDINIA	C	SCHERRARD	D	SEEDSKADEE	D	SHAM	D
SARDIS	C	SCHIEFFLIN	D	SEEG	B	SHAMEL	B
SARGEANT	D	SCHILLER	B	SEELEZ	A	SHAMIZO	A
SARILDA	C	SCHISLER	C/D	SEELOVERS	C	SHAMOCK	C
SARITA	A	SCHLOMER	C	SEES	C	SHANDEP	B/D
SARKAR	D	SCHNEBLY	D	SEEWEE	B	SHANE	D
SARNOSA	B	SCHNOORSON, Drained	C	SEFERINO	B	SHANGHAI	B/C
SARTELL	A	SCHNORBUSH	C	SEGNO	C	SHANGLAND	B
SARUCHE	D	SCHODSON	C	SEGUIN	B	SHANKBA	D
SASALAGUAN	C	SCHOER	C	SEGUNDO	B	SHANKLER	A
SASPAMCO	B	SCHOLTEN	C	SEHARNEY	D	SHANKS	C
SASSER	B	SCHOODIC	D	SEHOME	C	SHANLEY	B
SATAGO	D	SCHOOLCRAFT	B	SEIS	C	SHANNONDALE	C
SATANKA	C	SCHOOLER	D	SEJITA	D	SHANTOWN	A
SATATTON	D	SCHOOLEY	D	SEKIL	B	SHANTY	D
SATELLITE	C	SCHOOLHOUSE	D	SEKIU	D	SHAR	C
SATILLA	D	SCHOONER	D	SELBIT	B	SHARATIN	B
SATIN	C	SCHRIEVER	D	SELDEN	C	SHARESNOUT	C
SATSOP	B	SCHROCK	B	SELDOVIA	B	SHARLAND	B
SATSUMA	C	SCHULENBURG	B	SELFRIEDGE	B	SHARON	B
SATT	C	SCHULINE	B	SELIA	C	SHARPS	C
SATURDAY	B	SCHUTZ	B	SELLE	B	SHARPSHOOTER	B
SATURN	B	SCHWACHEIM	D	SELLERS	B/D	SHARPTOWN	C
SAUCEL	D	SCHWALBE	B	SELMAN	B	SHARROTT	D
SAUCIER	C	SCIOTA	C	SELON	B	SHARVANA	C
SAUCITO	D	SCIOTOVILLE	C	SELOW	D	SHASER	B
SAUCON	B	SCIPIO	D	SELT	C	SHASKIT	C
SAUGATUCK	C	SCITICO	C	SELWAY	B	SHASTA	B
SAUGUS	B	SCLOME	C	SEMIAMMOO	C/D	SHASTACOSTA	C
SAUK	B	SCOAP	B	SEMINOLE	D	SHASTINA	B
SAUM	B	SCOBA	B	SEMPER	C	SHATTA	C
SAURIN	C	SCOGGIN	D	SEN	B	SHATTUCK	B
SAUTER	B	SCONSIN	B	SENACHWINE	B	SHAVASH	C
SAUVIE, Protected	B	SCOTAL	D	SENGTOWN	B	SHAVER	B
SAUVIE, Moderately Wet	C	SCOTCH	D	SENLAR	C	SHAWA	C
SAUVIE	D	SCOTCO	B	SENTINEL	B	SHAWANO	A
SAUVOLA	C	SCOTMONT	B	SEQUATCHIE	B	SHAWAVE	B
SAUXHEAD, Very Stony	D	SCOTT LAKE	A	SEQUIM	B	SHAWMOUNT	B
SAUZ	B	SCOTTCAS	B	SEQUITE	D	SHAWTOWN	B
SAVAGETON	D	SCOTTSBURG	C	SEQUOIA	C	SHAYLA	D
SAVANNAH	C	SCOTTSVILLE	C	SERDEN	C	SHEBANG	D
SAVAR	B	SCRANTON	A/D	SEROCO	A	SHEBEON	C
SAVENAC	C	SCRIVER	B	SERPEN	C	SHEDD	C
SAVO	C	SCROGGIN	C	SERPENTANO	B	SHEDDENBROOK	A
SAVOIA	B	SCUFFE	C	SERPOD	C	SHEEK	B
SAVONA	C	SCUPPERNONG	D	SERRANO	D	SHEEPCAN	B
SAW	B	SEABOARD	B	SESAME	C	SHEEPSKIN	B
SAWABASH	B/D	SEABROOK	C	SESPE	C	SHEFFLEIN	B
SAWABE	D	SEAFIELD	B	SESSIONS	B	SHELBYVILLE	B
SAWATCH, Gravelly	B/D	SEAFORTH	B	SESSUM	D	SHELD	B
SAWBUCK, Shale Substratum	C	SEAGATE	A/D	SETILL	C	SHELLBLUFF	B
SAWCREEK	C	SEAGOVILLE	D	SETNUM	C	SHELLCREEK	C
SAWDUST	B	SEAGRAVES	B	SETTERS	C	SHELLDRAKE	A
SAWLIT	C	SEALY	B	SETTERS	D	SHELLROCK	A
SAWPEAK	B	SEAQUEST	B	SETTLEMEYER	B	SHELLWOOD	B
SAWTELL	C	SEAR	B	SEVAL	C	SHELTER	D
SAWTELPEAK	D	SEARCH	B	SEVAR	C	SHELTON	C
SAWTOWN	C	SEARCHLIGHT	B	SEVENOAKS	A	SHENA	D
SAWYER	C	SEARCY	C	SEVERN	B	SHENANDOAH	D
SAX	D	SEARING	B	SEWANEE	B	SHENANGO	C
SAXON	C	SEARVAR	B	SEWELL	C	SHENON	B
SAY	B	SEASIDE	D	SEYMOUR	C	SHEP	B
SAYDAB	C	SEATTLE	C/D	SEZNA	D	SHEPAN	C
SAYERS	A	SEAVERTON	D	SHAAK	C	SHERAR	C
SAYLES	D	SEAWILLOW	B	SHACK	B	SHERBURNE	C

SHERLOCK	B	SHULLSBURG	C	SIRRETTA	C	SLOCUM, Moist	D
SHERM	D	SHUMBEGAY	B	SISKIYOU	B	SLODUC	D
SHERMORE	B	SHUMLA	C	SISLEY	B	SLUICE	C
SHERMOUNT	D	SHURLEY	A	SISSABAGAMA	A	SLUKA	C
SHEROD	C	SHUSHUSKIN	C	SISSETON	B	SLY	B
SHERRY	B/D	SI	C	SITAR	B	SMACKOUT	B
SHERRY, Stony	D	SIBANNAC	D	SITKA	B	SMALLCONE	D
SHERRYL	B	SIBELIA	B	SIWASH	D	SMEDLEY	D
SHERVAL	C	SIBLEY	B	SIWELL	C	SMELTER	C
SHERWIN	D	SIBLEYVILLE	B	SIXES	B	SMESTAD	C
SHERWOOD	B	SIBOLD	C	SIXMILE, Loamy	B	SMIDALE	B
SHEVA	C	SICKLES	B/D	SIXMILE, Stony	C	SMILEYVILLE	D
SHEZA	C	SICKLESTEETS	B	SKAGEN	C	SMINA	C
SHIAWASSEE	C	SIEBERELL	B	SKAGIT	D	SMITH	B
SHIELDS	C	SIEBERT	A	SKAGWAY	C	SMITHBORO	D
SHIFFER	B	SIECHE	B	SKAMANIA	B	SMITHDALE	B
SHILLA	B	SIEGEL	B	SKAMO	C	SMITHLAND	B/D
SHILLING	B	SIERRA	B	SKEEL	B	SMITHNECK	B/C
SHILLY	C	SIERRAVILLE	B	SKEIN	D	SMITHTON	D
SHIMA	C	SIERRAVISTA	B	SKELIDA	B	SMITHVILLE	B
SHIMMON	C	SIESTA	D	SKELLOCK	B	SMITHWICK	D
SHINAKU	D	SIEVERS	C	SKELTER	B	SMOKEY	B
SHINANDO	D	SIGBIRD	D	SKELTON	B	SMOKYHILL	C
SHINBONE	B	SIKESTON	B/D	SKETERVILLE	C	SMOLAN	C
SHINDLER	C	SILAWA	B	SKIBO	B	SMOTHERS	C
SHINER	C	SILCAT	D	SKIDMORE	B	SMOUT	B
SHINGLEMILL	D	SILCOX	B	SKILAK	B	SMYRNA	B/D
SHINGLETOWN	B	SILENT	D	SKIME	A	SNACREEK	C
SHINGLETOWN	C	SILER	B	SKINNER	B	SNAG	B
SHINKEE	C	SILERTON	B	SKINWOOD	B	SNAHOPIH	B
SHINNPEAK	D	SILESCA	C	SKIPANON	B	SNAKE	C
SHIOYA	A	SILETZ	B	SKIPEAK	B	SNAKEJOHN	B
SHIPLEY	C	SILEX	D	SKIPOPA	D	SNAKELUM	B
SHIPPA	D	SILHOUE	B	SKIYOU	B	SNAKER	D
SHIPS	D	SILICO	B	SKOKOMISH	C/D	SNAPEED	C
SHIPSHE	B	SILKIE	D	SKOLY	B	SNAPILL	B
SHIRCLIFF	C	SILSBEE	B	SKOOKER	B	SNAVEE	B
SHIRED	D	SILSTID	A	SKOOKUM	C	SNEFFELS	C
SHIRK	C	SILVA	C	SKOOKUMHOUSE	B	SNELLBY	C
SHIRLEY	B	SILVER CREEK	D	SKOVEN	D	SNELLMAN	B
SHIRLEYBASIN	B	SILVERBELL	C	SKOWHEGAN	B	SNETTISHAM	D
SHIRO	C	SILVERCITY	B	SKRANKA	B	SNIDER	C
SHIRTS	C	SILVERDALE	A	SKULL CREEK	C	SNIDERPEAK	B
SHIRTTAIL	B	SILVERHILL	B	SKULLGULCH	C	SNILEC	B
SHIVA	B	SILVERHORN	C	SKULLWAK	D	SNILLOC	B
SHIVLUM	B	SILVERKING	B	SKUNKFARM	D	SNOOK	D
SHOAT	C	SILVERLAKE	C	SKYBERG	C	SNOPOC	B
SHOBA	D	SILVERN	A	SKYHAVEN	C	SNOQUALMIE	C
SHOBAN	B	SILVERSTRIKE	C	SKYHAWK	C	SNOTOWN	B
SHODDY	D	SILVERTON	C	SKYLIGHT	D	SNOWBRIER	C
SHOEBEND	B	SIMANNI	B	SKYLINE	D	SNOWCREEK	B
SHOEGAME	B	SIMCOE	C	SKYMOR	C	SNOWDANCE, Moderately Wet	C
SHOEMAKER	B	SIMEON	A	SKYROCK	D	SNOWDANCE	D
SHOEPAC	C	SIMESCREEK	C	SKYTOP	B	SNOWDON	C
SHOEPEG	C	SIMITARQ	D	SKYUKA	B	SNOWLAKE	B
SHOHOLA	C	SIMMONT	C	SKYVIEW	C	SNOWPLOW	B
SHOKEN	D	SIMONA	D	SLAB	D	SNOWSHOE	B
SHONGO	C	SIMONIN	B	SLABTOWN	B	SNOWVILLE	D
SHONKIN	D	SIMPARK	D	SLACREEK	B	SOAKPAK	B
SHONTIK	C	SIMPATICO	B	SLACWATER	B/D	SOAPCREEK	C
SHOOFLIN	D	SIMPER	C	SLAPJACK	B	SOBEGA	C
SHOOFLY	D	SIMSFIELD	C	SLATEGOAT	B	SOBSON	C
SHOOKER	C	SINAMOX	B	SLATERY	C	SOCAGEE	D
SHORE	B	SINBAD	D	SLATTER	D	SOCO	B
SHOREEK	C	SINCLAIR	C	SLAUGHTER	C	SODA LAKE	C
SHORT CREEK	C	SINDION	B	SLAUGHTERVILLE	B	SODABAY	B
SHORTBREAD	A	SINGERTON	B	SLAWHA	D	SODACREEK	B
SHORTCUT	C	SINGH	B	SLAYTON	C	SODASPRING	B
SHORTHAIR	D	SINGLETON	D	SLEEPER	B	SODERVILLE	A
SHORTHORN	D	SINGLETREE	C	SLEETH	C	SOELBERG	B
SHOSHONE	C	SINKER	C	SLICKEAR	B	SOEN	C
SHOTGUN	C	SINONA	B	SLICKLOG	B	SOFA	C
SHOWALTER	B	SINTON	B	SLICKPOO	B	SOFTBACK	B
SHOWLOW	D	SINUK	D	SLICKSPOTS	D	SOGI	C
SHREE	B	SION	B	SLIDE	B	SOJOURN	D
SHREWDER	B	SIUOX CREEK	C	SLIDECAMP	C	SOJUR	D
SHREWSBURY	C/D	SIUOXON	B	SLIDECREEK	B	SOKOLOF	A
SHROE	C	SIPAPU	D	SLIDELL	D	SOLARVIEW	D
SHROUTS	D	SIPHONCAN	D	SLIDYMTN	D	SOLDATNA	B
SHROYTON	A	SIPHONLAKE	B	SLIGHTS	C	SOLDIER	C
SHRUBCREEK	B	SIPPLE	B	SLIMBUTTE	B	SOLDIERCREEK	B
SHUBUTA	C	SIPSEY	B	SLIMLAKE	B	SOLDUC	B
SHUE	C	SIRDRAK	A	SLINGER	B	SOLIER	D
SHUKSAN	C	SIREN	C	SLOCAGE	D	SOLIS	C
SHULE	C	SIRREF	D	SLOCUM	C	SOLITE	B/D

SOLITUDE	D	SPIKE	B	STAINKY	B	STIVERSVILLE	B
SOLLEKS	C	SPILCO	B	STAKE	C	STOCKDRIVE	C
SOLLER	D	SPILLER	C	STALEY	B	STOCKEL	D
SOLNESS	C	SPILOCK	D	STALLARD	D	STOCKHOLM	C
SOLO	C	SPILYAY	C	STALLINGS	C	STOCKLAND	B
SOLSBERRY	C	SPINDLETOP	D	STAMFORD	D	STOCKPEN	D
SOLVAY	D	SPIRES	B	STANDISH	C	STOHLMAN	D
SOMA	D	SPIRES	D	STANDISH	D	STOKES	D
SOMBORDORO	D	SPIRO	B	STANDUP	B	STOKLY	B
SOMBREDO	C	SPLANOD	D	STANEY	D	STONEBERGER	D
SONAHNPIL	B	SPLAWN	C	STANFLOW	C	STONEBURG	B
SONNETT	D	SPLENDORA	C	STANHOPE	C	STONEHEAD	C
SONOCAN	C	SPLIT	C	STANISLAUS	C	STONEHILL	C
SONOMA, Stratified Substratum	D	SPLITBUTTE	C	STANISLAUS, Wet	D	STONELAKE	A
SONORA	B	SPLITROCK	B	STANROD	C	STONER	B
SONSELA	B	SPLITTOP	C	STAPALOOP	B	STONEVILLE	B
SONTAG	D	SPLOTTER	D	STARGULCH	B	STONEWALL	C
SONYOK	D	SPOKEL	B	STARHOPE, Low Elevation	C	STONEWELL	A
SOO	C/D	SPONIKER	B	STARHOPE	D	STONO	B/D
SOOLAKE	B	SPONIKER, Warm	C	STARICHKOF	D	STONYBROOK	B
SOONAHBE	B	SPONSOR	B	STARKE	C	STOOKMOOR	C
SOONAKER	C	SPOOL	C	STARKEY	C	STOPATOE	C
SOONER	B	SPOONER	C/D	STARLAKE	D	STORMKING	B
SOOPER	D	SPOONERHILL	A	STARLITE	B	STORNETTA	D
SOOSAP	C	SPORLEY	B	STARR	C	STOTT	C
SOPELA	D	SPOT	A/D	STARVEOUT	B	STOUGH	C
SOPER	C	SPOTSylvania	C	STASER	D	STOVALL	B
SOPERTON	B	SPOTTEDHORSE	C	STASH	B	STOVEPIPE	D
SOPHER	C	SPOTVILLE	B	STATE	B	STOVHO	C
SOQUEL	B	SPRABAT	B	STATELINE	D	STOWELL	D
SORENSEN	B	SPRAUER	C	STATEMEADOW	B	STOY	C
SORF	C	SPRAY	B	STATION	D	STRABER	C
SORTER	D	SPRECKELS	C	STATLER	B	STRADDLEBUG	C
SORUM	D	SPRING	C	STATZ	D	STRAHLE	D
SOSA	C	SPRINGCOVE	C	STAVELY	B	STRAIGHT	C
SOSTIEN	D	SPRINGCREEK	C	STAYTON	D	STRANDLINE	B
SOUDAN	C	SPRINGERTON	B/D	STEADMAN	C	STRANDQUIST	B/D
SOURDOUGH	B	SPRINGFIELD	D	STEAMBOAT	B	STRAWBCEK	B
SOUTHAM	D	SPRINGGULCH	B	STEAMBURG	B	STRAYHOSS	B
SOUTHFORK	D	SPRINGHILL	B	TEARNS	D	STREATOR	B/D
SOUTHGATE	D	SPRINGHOLLOW	C	STECOAH	B	STRELL	D
SOUTHHAVEN	B	SPRINGLAKE	A	STECUM	C	STRELSA	C
SOUTHMOUNT	B	SPRINGSTEEN	C	STEED	B	STREULING	D
SOUTHPAC	B	SPRINGWARM	C	STEEDMAN	C	STRICKER	B
SOUTHPLAINS	D	SPRINGWATER	C	STEEKEE	C	STRICKLAND	C
SOUTHRIDGE	B	SPRINGWOOD	B	STEELE	C	STRINGLEY	B
SOUTHWELLS	A	SPRINKLER	C	STEESE	B	STRINGTOWN	B
SOUTHWEST	C/D	SPRIPAR	D	STEEVER	B	STRINGTOWN, Graded	C
SOUTIN	B	SPROUL	D	STEFF	C	STROLE	C
SOWARD	B	SPRUCEDALE	D	STEGALL	C	STROM	C
SOWCAN	C	SPUD	C	STEILACOOM	C	STROMAL	B
SPADE	B	SPUKWUSH	B	STEIN	C	STRONGHOLD	C
SPADRA	B	SPUR	C	STEINHATCHEE	B/D	STRONGHURST	B
SPAINHOWER	C	SPURGER	B	STEINSBURG	B	STROUPE	B
SPAN	D	SPURLOCK	B	STEIWER	C	STROUT	C
SPANG	B	SQUALICUM	B	STELLA	C	STROZI	C
SPANGLER	C	SQUALLY	B	STEMLEY	C	STRUGGLE	A
SPANPEAK	B	SQUAMSCOTT	C	STENGEL	B/D	STRYKER	C
SPANARA	B	SQUAWCAVE	B	STEPHEN	C	STU	C
SPARGUS	B	SQUAWCREEK	D	STERLING	A	STUBBS	C
SPARKS	C	SQUAWTIP	C	STERLINGTON	B	STUBENVILLE	B
SPARTA	B	SQUAWVAL	C	STERRETT	D	STUCK	C
SPASSKI	D	SQUIRES	C	STETSON	B	STUDEBAKER	B
SPEAKER, High Rainfall	B	SREDNIC	C	STETTER	D	STUKEL, Cobby	B
SPEAKER	C	ST. ANDREWS	C	STEUBEN	B	STUKEL, Sandy	C
SPEAR	C	ST. ANTHONY	B	STEVENSON	B	STUKEL	D
SPEARHEAD	B	ST. AUGUSTINE	B	STEVIE	B	STULTZ	C
SPEARMAN	B	ST. ELMO	A	STEWART	D	STUMOUNT	D
SPEARVILLE	C	ST. HELENS	B	STICES	B	STUMPP	D
SPECTACLE	C	ST. IGNACE	D	STIDHAM	B	STUNTZ	C
SPECTER	C	ST. JOHNS	D	STIEN	B	STURGEON	B
SPEED	C	ST. LUCIE	A	STIGLER	D	STURGES	D
SPEEDWELL	B	ST. MARTIN	D	STILES	C	STURGILL	D
SPEELYAI	D	ST. NICHOLAS	D	STILGAR	B	STURKIE	B
SPEER	B	ST. ONGE	B	STILLWELL	B	STUTTART	D
SPEIGLE	B	ST. PAUL	B	STILSKIN	C	STUTZMAN	C
SPELLACY	B	ST. MARYS	B	STILSON	B	STUTZMAN, Wet	D
SPELVIN	B	STABBART	D	STIMSON	D	STYERS	D
SPERRY	C/D	STABLER	B	STINE	D	STYLITE	C
SPESSARD	A	STACHER	B	STINESVILLE	B	STYX	B
SPEXARTH	C	STACKER	B	STINGAL	B	SUAK	C
SPICERTON	D	STACKYARDS	B	STINGER	B	SUBACO	D
SPICEWOOD	C	STACY	B	STINKCREEK	D	SUBLETTE, Elevation 7000-9000	A
SPICKERT	C	STAFFORD	C	STIPE	C	SUBLETTE	B
SPIDERCREEK	A/D	STAHL	C	STIRUM	D	SUBLIGNA	B

SUBRAN	C	SUTPHEN	D	TAFOYA	C	TASCOSA	B
SUBWELL	B	SUTRO	C	TAFT	C	TASSEL CREEK	A
SUCARNOOCHEE	D	SUTTLE	A	TAFTOWN	B	TASSELMAN	D
SUCCOR	D	SUVER	D	TAFUNA	A	TASSI	D
SUCHES	B	SVERDRUP	B	TAGUM	B	TASSO	B
SUCKERFLAT	B	SWAFFORD	C	TAGUS	B	TATAI	C
SUDLEY	B	SWAGER	C	TAHKENITCH	B	TATERPA	B
SUDPEAK, Nonflooded	C	SWAHLEN	B	TAHOULA	D	TATLUM	D
SUDPEAK, Flooded	D	SWAINTON	B	TAHQUATS	B	TATOCHE	B
SUEPERT	C	SWALECREEK	B	TAINÉ	D	TATTON	D
SUEY	B	SWAMP CREEK	D	TAINTOR	C/D	TAUMSAUK	D
SUFFIELD	C	SWAMPOODLE	C	TAJO	C	TAUNCAL	C
SUFFOLK	B	SWAMPYDRAW	B	TAKOTNA	B	TAVER	D
SUGAKOOL	B	SWAN	D	TAKPOCHAO	D	TAVERNIER	D
SUGAR BEACH	D	SWANBERGER	D	TALAG	D	TAWAH	B
SUGARBOWL	B	SWANLAKE	B	TALANTE	D	TAWCAW	C
SUGARBUSH	B	SWANNER	D	TALAPUS	B	TAYLOR CREEK	C
SUGARCREEK	C	SWANPOND	C	TALCO	D	TAYLORSFLAT	C
SUGARDEE	B	SWANSON	C	TALLA	D	TEAGARD	D
SUGARTOWN	D	SWANTON	C/D	TALLADEGA	C	TEAGO	A
SUGLO	B	SWANTOWN	D	TALLCREEK	B	TEAGULF	C
SUILOTEM	C	SWANWICK	D	TALLEYVILLE	B	TEAKEAN	B
SUISUN	D	SWARTZ	D	TALLOWBOX	C	TEALSON	D
SUKOI	D	SWAYNE	C	TALLULA	B	TEALWHIT	D
SULA	B	SWEAGERT	B	TALMAGE	B	TEAMONT	D
SULLIVAN	B	SWEATBEE	B	TALMAKS	B	TEARNEY	D
SULOAF	B	SWEATBEE, Wet	C	TALMOON	D	TEASDALE	B
SULPHURA	B	SWEATMAN	C	TALMOON, Depressional	D	TEBAY	B
SULPHURA	D	SWEDE	B	TALOKA	D	TEBO	B
SULSAVAR	B	SWEDEGROVE	B/D	TALQUIN	B/D	TECHICK	B
SULTZ	A	SWEDEHEAVEN	B	TALUWIK	B	TECHICKNOT	B
SUMAN	B/D	SWEDESBORO	B	TAMAHA	D	TECKLA	B
SUMATRA	B	SWEDNA	D	TAMALCO	D	TECO	B
SUMAVA	B	SWEETAPPLE	B	TAMALPAIS	D	TECOPA	D
SUMMERFIELD	D	SWEETBRIAR	B	TAMARA	B	TECTAH	B
SUMMERFORD	C	SWEETBUTTE	B	TAMARACK	B	TECUMSEH	B
SUMMERMUTE	B	SWEETGRASS	B	TAMARACKCANYON	C	TECZUNI	C
SUMMERS	B	SWEETWATER	D	TAMARRON	C	TEDDY	C
SUMMERTON	B	SWEITBERG	C	TAMBA	D	TEEBAR	D
SUMMIT	C	SWENSON	D	TAMELY	D	TEEBONE	C
SUMMITVILLE	C	SWIFT CREEK	B	TAMFLAT	D	TEEDOWN	B
SUMPF	D	SWIFTCURRENT	B	TAMFORD	D	TEEGARDEN	C
SUMPLEY	C	SWIFTON	B	TAMIAMI	D	TEEMAT	B
SUMTERVILLE	C	SWIMLEY	C	TAMMANY	B	TEETERS, Protected	C
SUMYA	D	SWIMS	B	TAMMING	D	TEETERS	D
SUNBURG	B	SWINK	D	TAMP	B	TEFTON	C
SUNBURY	B	SWINOMISH	C	TAMRED	C	TEHRAN	A
SUNCITY	D	SWINT	B	TANACROSS	D	TEIGEN	C
SUNCOOK	A	SWIPKIN	B	TANAH	C	TEJA	D
SUND	C	SWISBOB	D	TANAMA	D	TEJABE	D
SUNDANCE	B	SWISS	C	TANANA, Thawed	B	TEJANA	B
SUNDAY	A	SWISSVALE	D	TANANA, Moderately Wet	C	TEKAPO	D
SUNEV	B	SWITCHBACK	C	TANAZZA	D	TEKENINK	B
SUNKEN	D	SWITZERLAND	B	TANDY	D	TEKISON	C
SUNLIGHT	D	SWORMVILLE	C	TANEUM	C	TEKLANIKA	A
SUNNY	C	SWYGERT	C	TANGI	C	TEKOA	B
SUNNYHAY	D	SYBIL	B	TANGLE	C	TELA	B
SUNNYSIDE	B	SYBILLE	B	TANGLENOK	D	TELAQUANA	B
SUNRAY	B	SYBLON	D	TANKERVILLE	C	TELAY	B
SUNRIVER	C	SYCAN	A	TANNAWASHA	B	TELCHEER	B
SUNSTROKE	D	SYCLE	B	TANNER	C	TELECAN	B
SUNSWEET	C	SYCREEK	C	TANNER, Low Rainfall	D	TELEFONO	C
SUNTRANA	D	SYKES	B	TANOAN	B	TELEMON	D
SUP	B	SYLACAUGA	D	TANOB	B	TELESCOPE	A
SUPOSO	C	SYLVA	B/D	TANSEM	B	TELFAR	C
SUPPAH	A	SYLVANIA	C	TANTALUS	A	TELFERNER	D
SUR	C	SYLVANIAM	C	TANTILE	C/D	TELL	B
SURFSIDE	D	SYLVESTER	B	TANWAX	C/D	TELLER	B
SURGEM	C	SYLVIA	C	TANYARD	C	TELLICO	B
SURPLUS	C	SYMCO	C	TAOPI	B	TEMBLOR	D
SURRETT	C	SYNAREP	B	TAPAWINGO	C	TEMDILLE	A
SURVEYORS	B	SYRETT	C	TAPICITOES	D	TEMESCAL	D
SURVYA	C	SYRUPCREEK	B	TAPPAN	B/D	TEMKIK	B
SURYON	B	TABECHEDING	C	TARA	B	TENAH	B
SUSANNA	C/D	TABERNASH	B	TARAL	B	TENAS	C
SUSANNABERG	D	TABLER	D	TARHOLLOW	C	TENDOY	D
SUSANVILLE	D	TABLEROCK	D	TARKIO	D	TENEB	D
SUSIVAR	C	TABOOSE	A	TARLOC	B	TENEX	B
SUSQUEHANNA	D	TABOOSE, Gravelly Substratum	B	TARLTON	C	TENINO	C
SUTA	B	TABOR	D	TARNAV	B	TENMILE	C
SUTHER	C	TACHI	D	TARRETE	D	TENNCO	C
SUTHERLAND, Gravelly	C	TACODA	C	TARRYALL	C	TENNECO	B
SUTHERLAND	D	TACOOSH	B/D	TARRYTOWN	C	TENOT	C
SUTHERLIN	C	TADLOCK	B	TASAJAL	B	TENPIN	D
SUTLEY	B	TAFFOM	B	TASAYA	C	TENRAG	B

TENSAS	D	THREEK	C	TINTON	A	TOMOKA	B/D
TENSED	C	THREEMILE	B	TINTSON	A	TOMOTLEY	B/D
TENSLEEP	B	THREERIV	D	TINYTOWN	B	TOMS	C
TENVORRD	D	THREETREES	B	TIOGA	B	TOMSHERRY	C
TENWALTER	C	THRIFTON	C	TIONESTA	A	TOMTY	D
TENWELL	C	THROCKMORTON	B	TIPLER	B	TONATA	D
TEOCULLI	B	THULEPAH	B	TIPNAT	B	TONEY	D
TEQUESTA	B/D	THUNDER	B	TIPPAH	C	TONIO	B
TERADA	B	THUNDERBAY	D	TIPPECANOE	B	TONKAVAR	A
TERBIES	B	THUNDEREGG	C	TIPPER	C	TONKAWA	A
TERCA	D	THURBER	D	TIPPIPAH	B	TONKIN	B
TERESA	D	THURLONI	C	TIPPO	C	TONKIN, Moderately Wet	C
TERLINGUA	D	THURLOW	B	TIPSAW	C	TONKS	C
TERMO	D	THWOOP	C	TIPTON	B	TONOR	B
TEROMOTE	B	TIAGOS	C	TIPTONVILLE	B	TONOWEK	B
TEROUGE	D	TIAK	B	TIPTOP	B	TONRA	B
TERRA CEIA	B/D	TIBBCREEK	C	TIRO	C	TONSINA	B
TERRABELLA	D	TIBBITTS	B	TIROD	B	TONUCO	D
TERRACECREEK	C	TIBKEY	B	TISBURY	B	TOOLES	B/D
TERRAD	C	TIBURONES	D	TISDALE	C	TOOLESBORO	B
TERRAROSSA	D	TICANOT	B	TISHAR	B	TOONE	B
TERRETON	C	TICELL	D	TISMID	C	TOOTERVILLE	D
TERRO	B	TICESKA	C	TISONIA	D	TOPAWA	B
TERT	D	TICONIC	A	TITCHENAL	B	TOPAWA, Very Gravelly	C
TESSFIVE	D	TIDERISHI	C	TITIACK	B	TOPEMAN	C
TETHEROW	A	TIDEWATER	D	TITUSVILLE	C	TOPETAUL	C
TETILLA	B	TIDINGS	B	TIVOLI	A	TOPIA	D
TETLIN	D	TIEFORT	B	TIVY	C	TOPKNOT	D
TETONIA	B	TIERRANEGRA	B	TOA	B	TOPO	D
TETONVILLE, Gravelly	C	TIESIDE	D	TOADLAKE	B	TOPOCK	D
TETONVILLE	D	TIETON	B	TOADLENA	D	TOPPENISH	C/D
TETOTUM	C	TIEVILLE	D	TOBA	B	TOPPER	B
TEVAL	B	TIFF	C	TOBINSPOIT	B	TOPSEY	C
TEVIS	B	TIFFANY	C	TOBOSA	B	TOQUIMA	C
TEWFEL	C	TIFTON	B	TOBY	B	TORAX	B
TEX	B	TIGER CREEK	B	TOCALOMA	C	TORHUNTA	C
TEXANA	D	TIGIT	B	TOCAN	B	TORNEY	D
TEXASCREEK	B	TIGIWON	B	TOCCOA	B	TORNILLO	B
TEXLA	D	TIGON	D	TOCITO	B	TORNING	B
TEXLINE	B	TILDEN	B	TOCK	C	TORODA	B
TEXROY	B	TILK	A	TOCOI	B/D	TORONTO	C
THADER	C	TILLEDA	B	TODACHEENE	B	TOROX	B
THAGE	C	TILLCUM	B	TODDSTAV	D	TORPEDO LAKE	D
THATCHERFLATS	D	TILLMAN	D	TODDVILLE	B	TORREON	D
THAYNE	B	TILLMONT	B	TODOS	C	TORRES	A
THEBES	B	TILLOU	C	TOECANE	B	TORRY	B/D
THEBO	D	TILMA	C	TOEFOOT	B	TORULL	D
THEECAN	C	TILSIT	C	TOGCHA	B	TOSP	B
THENARROWS	D	TILTON	B	TOGUS	D	TOTAVI	B
THENAS	C	TILVERN	D	TOHATIN	B	TOTEM	B
THENIPEL	B	TIMBALIER	C	TOHOBIT	C	TOTIER	C
THEODOR	D	TIMBERBUTTE	B	TOIMI	C	TOTNESS	D
THERESA	C	TIMBERG	C	TOINE	B	TOTO	B/D
THERMO	D	TIMBERHEAD	B	TOISNOT	B/D	TOTTEN	C/D
THETFORD	A	TIMBERLY	B	TOISNOT, Poned	D	TOTTLES	C
THETIS	B	TIMBLIN	D	TOKAY	B	TOTZ	B
THIBAUT	D	TIMBUCTOO	C	TOKEEN	C	TOUCHET	C
THIEFRIVER	B/D	TIMGULCH	D	TOKIO	B	TOULA	C
THIKE	D	TIMHILL	D	TOKLAT	D	TOURN	C
THIMBLE	C	TIMHUS	B	TOKO	C	TOURNQUIST	B
THIRST	D	TIMKEN	D	TOKOSITNA	B	TOUTLE	B
THIRSTYGULCH	D	TIMMERCREEK	B	TOKUL	C	TOWAVE	B
THISTLEBURN	B	TIMMONS	B	TOLANY	B	TOWERVILLE	B
THISTLEDEW	B	TIMOR	A	TOLER	C	TOWNSEND	C
THOENY	D	TIMPAHUTE	D	TOLFORK	D	TOWNSHIP	B
THOMAS	B/D	TIMPER	D	TOLICHA	D	TOWOSAHGY	B
THOMASFORK	C	TIMPIE	C	TOLIU	B	TOXAWAY	B/D
THOMHILL	B	TIMULA	B	TOLKE	B	TOY	D
THOMS	D	TINA	C	TOLLGATE	B	TOZE	B
THOR	B	TINAJA	B	TOLMAN	C	TRACE	B
THORN	D	TINAJA, Cool	C	TOLNA	B	TRACK	C/D
THORNCREEK	C	TINAMOU	C	TOLONIER	B	TRACKLER	C
THORNDALE	D	TINCAN	D	TOLOVANA	B	TRACOSA	D
THORNOCK	D	TINCUP	A	TOLSONA	D	TRACTUFF	D
THORNTON	D	TINDAHAY	B	TOLUCA	B	TRACYLEE	B
THOUT, Gravelly Surface	B	TINE	B	TOMAHAWK	A	TRADELAKE	C
THOUT	C	TINEMAHA	D	TOMALES	B	TRAEER	B/D
THOW	B	TINEMAN	C	TOMARIZO	D	TRAHAM	C
THRASH	B	TINIAN	C	TOMASAKI	C	TRAHERN	D
THREADGILL	B	TINKER	C	TOMAST	C	TRAIL	B
THREEBEAR	C	TINN	D	TOMBEALL	B	TRAILAMP	D
THREEBUCK	C	TINNIN	A	TOMEK	B	TRAILCREEK	C
THREECHOP	B	TINPAN	D	TOMERA	C	TRAILHEAD	B
THREECREEKS	C	TINT	A	TOMERA, Cemented Substratum	D	TRAINER	B
THREEFORKS	B	TINTERO	B	TOMODO	B	TRAITORS	D

TRALEY	B	TSCHAMMAN	D	TWEBA, Drained	C	UPCREEK	C
TRAMWAY	B	TSCHICOMA	B	TWEEDY	C	UPDEGRAFF	B
TRANSFER	D	TSEBITAI	B	TWELVEMILE	B	UPSATA	B
TRANSQUAKING	D	TSETTA	A	TWENTY DAY	B	UPSEL	A
TRANSYLVANIA	B	TSIRKU	C	TWICK	D	UPSON	C
TRAPPER	B	TUCANNON	C	TWIG	D	UPSTEER	B
TRAPPERCREEK	B	TUCES	D	TWINBUTTES	A	URBANA	C
TRASK	C	TUCKAHOE	B	TWINING	C	URBO	D
TRAUNIK	B	TUCKERDOWNS	B	TWINMOUND	A	URBODEN	B
TRAVER	B	TUCSON	B	TWISSELMAN	C	UREAL	D
TRAVERTINE	C	TUCSON, saline-Alkali	C	TWOBUTTE	B	URGESTEIN	B
TRAVILAH	C	TUCUMCARI	B	TWOCABIN	B	URICH	C/D
TRAZUNI	B	TUFFIT	C	TWOMILE	C/D	URIPNES, Gravelly	C
TREATY	B/D	TUFON	B	TWOTOP	D	URIPNES	D
TREBLOC	D	TUGAS	A	TYBO	D	URLAND	C
TREBOR	C	TUKEY	C	TYDEN	C	URMAFOT	D
TREEBUTTE	D	TUKUHNIAK	C	TYEE	D	URSA	C
TREEKOR, nonstony	C	TUKWILA	C/D	TYENDE	B	URSINE	D
TREEKOR	D	TULANA, Moderately Drained	C	TYGH	C	URWIL	C
TREEN	D	TULANA	B/D	TYLER	D	USAL, Gravelly	B
TREFRY	B	TULARGO	B	TYLERPEAK	B	USAL	C
TREGO	C	TULAROSA	B	TYMOSLING	C	USEFUL	C
TREGONING	C	TULCH	B	TYNDALL	B/C	USINE	A
TREHARNE	C	TULE	C	TYNER	A	USKABWANKA	A
TRELONA, Moist	C	TULEBASIN	D	TYONEK	D	USTARENTS, Loamy	B
TRELONA	D	TULECAN	C	TYRE	A/D	USTIBUCK	D
TREMLES	C	TULIA	B	TYSON	B	USTIDUR	D
TREMENTINA	B	TULIK	B	UANA	B	USTORTHEMETS, Sandy	A
TREMONA	C	TULIP	C	UBANK	D	UTALINE	C
TREMONT	B	TULLAHASSEE	C	UBAR	D	UTE	D
TREMPE	A	TULLOCK, Dry	A	UBEHEBE	C	UTLEY	B
TREMPEALEAU	B	TULLOCK, Warm	B	UCHEE	A	UTUADO	B
TRENHOLM	D	TUMARION	D	UCOPIA	B	UTURIN	C/D
TRENTON	C	TUMBLETON	C	UDAHO	B	UVADA Loamy Surface	C
TREOFF	D	TUNAWEE	C	UDARENTS	B	UVALDE	B
TREON	D	TUNEHILL	D	UDECIIDE, Cobbly	B	UVER	A
TREP	B	TUNELCREEK	B	UDECIIDE	C	UWALA	B
TRESTLE	B	TUNIS	D	UDEL	D	UWELL	C
TRETEN	B	TUNITCHA	B	UDELOPE, Bouldery	B	UZANEVA	D
TREVLAC	B	TUNKCREEK	A	UDELOPE	D	VABBING	B
TREY	A	TUNNEL	B	UDIPSAMMENTS, Flooded	A	VABEM	C
TRIANGLE	D	TUOMI	B	UGAK	D	VADAHO	D
TRIBBEY	C	TUPELO	D	UHL	B	VADER	B
TRICART	B	TUPPER	A	UHLAND	B	VAEDA	D
TRICERA	A	TUPUKNUK	D	UHLORN, Cool	B	VAIDEN	D
TRICON	C	TUQUE	B	UHLORN	C	VAILTON	B
TRID, Nonstony	B	TURBA	D	ULA	C	VALBY	C
TRID	C	TURCOTTE	B	ULANDO	B	VALCO	C
TRIGGER	D	TURIST	D	ULHALF	B	VALCREEK	B
TRIGO	D	TURK	C	ULLOA	B	VALCREST	C
TRIMMER	C	TURKEY	A	ULMET	C	VALDOSTA	A
TRIMONT	B	TURKEYSPRINGS	B	ULRANT	B	VALE	B
TRINIDAD	D	TURKEYTRACK	C	ULRIC	C	VALENA	D
TRIO	D	TURLIN	B	ULTO	B	VALENCIA, Saline, Flooded	C
TRIOMAS	B	TURLOCK	D	ULTRA	D	VALERA	C
TRIPIT	C	TURMOUND	D	ULTRAMONT	B	VALHALLA	A
TRIPLEN	B	TURNBACK	C	ULUPALAKUA	B	VALKARIA	B/D
TRIPLETT	D	TURNBULL	D	ULY	B	VALKARIA, Depressional	D
TRIPOLI	B/D	TURNERCREST	B	UMA	A	VALLAN	D
TRISTAN	B	TURON	A	UMAPINE	C/D	VALLE	B
TRITON	D	TURRAH	C	UMATILLA	B	VALLEONO	B
TRIVAR	B	TURRET	B	UMBARG	B	VALLERS	D
TRIX	C	TURRIA	C	UMIAT	D	VALLETTA	B
TROMP	C	TURZO	C	UMPA	B	VALLEYCITY	D
TRONSON	B	TUSCARAWAS	C	UMPUMP	B	VALMAR	C
TROOK	C	TUSCAWILLA	D	UMTANUM	C	VALMONT	C
TROSKY	B/D	TUSCOSSO	B	UNAKA	B	VALPAC	C
TROUP	A	TUSCUMBIA	D	UNAKWIK	D	VALTON	B
TROUTER	C	TUSIP	B	UNCAS	D	VALTON, Severely Eroded	C
TROUTLAKE	B	TUSLER	A	UNCOMPAGHGRE	D	VALVERDE	B
TROUTMEADOWS	B	TUSLER	B	UNDERWOOD	B	VAMER	B
TROVE	B	TUSSY	D	UNDUSK	B	VAMONT	D
TRUCKEE	B/C	TUSTELL	C	UNGENE	A	VAN HORN	B
TRUEFISSURE	B	TUSUNE	C	UNICOI	C	VANBRUNT, Warm	B
TRUHOY	D	TUTE	B	UNICORN	B	VANBRUNT	C
TRULAE	D	TUTKA	D	UNION	C	VANCE	C
TRUMBULL	D	TUTNI	B	UNIONGROVE	B/D	VANCECREEK	B/D
TRUMP	D	TUTNI, Loamy Substratum	C	UNIONVILLE	B	VANDAMINE	B
TRUSCREEK	B	TUTTLE	C	UNIQUE	B	VANDAMME	B
TRUSSUM	C/D	TUTUILLA	C	UNIUS	D	VANDAMORE	B
TRUXTON	B	TUTWILER	B	UNIVEGA	D	VANDERBILT	B
TSADAKA	B	TUWEEP	B	UNIVERSITY	A	VANDERBILT, Moderately Wet	C
TSALI	C	TUXEKA	B	UNKEE	B	VANDERGRIFT	C
TSANA	B	TUZIGOOT	C	UNLIC	B	VANDERPOOL	B
TSAYA	D	TWEBA, Moderately Wet	B	UNSON	B	VANEPPS	C

VANGOE.....	C	VIBO.....	B	WAAS.....	B	WALLUSKI.....	C
VANGUARD.....	C	VIBORAS.....	D	WABANICA.....	C	WALNETT.....	C
VANLUE.....	C	VICK.....	C	WABASSO.....	D	WALNUT.....	B
VANMETER.....	C	VICKSBURG.....	B	WABEDO.....	C	WALONG.....	B
VANNOY.....	C	VICTORVILLE.....	B	WABUN.....	A/D	WALPOLE.....	C
VANOCKER.....	B	VICTORY.....	C	WACAHOOTA.....	D	WALREES.....	B
VANOSS.....	B	VICU.....	B	WACCASASSA.....	D	WALSEY.....	B
VANPETTEN.....	B	VIDA.....	B	WADDINGTON.....	A	WALTERS.....	B
VANSICKLE.....	D	VIDAURI.....	D	WADDUPS.....	B	WALTHAM.....	D
VANSTEL.....	B	VIDRINE.....	D	WADECREEK.....	C	WALUM.....	B
VANWYPER.....	D	VIEJA.....	D	WADELL.....	B	WALVAN.....	B
VANZANDT.....	C	VIENNA.....	B	WADENILL.....	B	WALVILLE.....	B
VANZILE.....	B	VIEQUES.....	B	WADESPRINGS.....	C	WAMBA.....	C/D
VAQUERO.....	D	VIEWPOINT.....	D	WADLEIGH.....	D	WAMBOLT.....	B
VARELUM.....	B	VIGAR.....	C	WADLEY.....	A	WAMEGO.....	C
VARELUM, Clay Loam Substratum	C	VIGIA.....	D	WADMALAW.....	D	WAMIC.....	B
VARGAS.....	C	VIGILANTE.....	C	WADSWORTH.....	C	WAMPEE.....	C
VARICK.....	D	VIGNOLO.....	C	WAEELDER.....	B	WAMPOO.....	C
VARRO.....	B	VIGO.....	C	WAFLA.....	B	WAMPSVILLE.....	B
VARWASH.....	A	VILLA.....	B	WAGNER.....	D	WANAGAN.....	B
VARYSBURG.....	B	VILLARD.....	D	WAGONBED.....	B	WANDO.....	A
VASA.....	B	VILLEDY.....	D	WAGONBOW.....	D	WANETTA.....	B
VASSETT.....	B	VILLEGREEN.....	C	WAGONBOX.....	D	WANILLA.....	C
VASTINE, Map>16.....	B	VILLMEAGHER.....	C	WAGONHOUND.....	B	WANNACOTT.....	B
VASTINE.....	D	VILLSPRINGS.....	C	WAGONJACKET.....	C	WANOGA, Elevation>4000.....	A
VAUGHAN.....	D	VILLY.....	B/D	WAGONTIRE.....	D	WANOGA.....	B
VAUGHNSVILLE.....	C	VILOT.....	C	WAGONTOWN.....	B	WANOMIE.....	C
VAYAS.....	D	VIMVILLE.....	D	WAGORE.....	B	WANSEY, Drained.....	B
VEAL.....	B	VINCOM.....	C	WAGRAM.....	A	WAPAHANI.....	C
VEATCH.....	C	VINDICATOR.....	D	WAGSTAFF.....	C	WAPAL.....	B
VECONT.....	C	VINEGARROON.....	C	WAHEE.....	D	WAPELLO.....	B
VEEDUM.....	D	VINELAND.....	A	WAHGUYHE.....	D	WAPI.....	D
VEGA ALTA.....	B	VINELAND, Wet.....	B	WAHIAWA.....	B	WAPINITIA.....	A
VEGA BAJA.....	C	VINGO.....	B	WAHKEENA.....	B	WAPITI.....	A
VELASCO.....	D	VINITA.....	C	WAHLSTEN.....	C	WAPPINGER.....	B
VELDA.....	B	VINLAND.....	D	WAHLUKE.....	B	WAPPO.....	D
VELDKAMP.....	B	VINSAD.....	D	WAHOO.....	D	WAPSHILLA.....	B
VELOW.....	B	VINSON.....	B	WAHPETON.....	C	WAPTUS.....	C
VENA.....	C	VINTON.....	A	WAHREKIDAM.....	C	WARDA.....	B
VENAGRO.....	B	VIOLA.....	D	WAHSTAL.....	D	WARDABAY.....	B
VENAPASS.....	D	VIPONT.....	C	WAHTUM.....	D	WARDBORO.....	A
VENATOR, Channery.....	B	VIRDEN.....	B/D	WAHWEAP.....	D	WARDELL.....	C
VENATOR.....	C	VIRGIN RIVER.....	C	WAI HONU.....	B	WARDWELL.....	C
VENETA.....	D	VIRKULA.....	C	WAIALEALE.....	D	WARE.....	B
VENEZIA.....	D	VIRTUE.....	C	WAIWA.....	D	WAREAGLE.....	B
VENICE.....	C	VISE.....	B	WAIHUNA.....	D	WARHORSE.....	D
VENLO.....	A/D	VISTA.....	B	WAIKALOA.....	B	WARM SPRINGS.....	D
VENNOB.....	D	VISTULA.....	A	WAIKANE.....	B	WARMAN.....	A/D
VENSON.....	B	VITERBO.....	B	WAIKAPU.....	B	WARMINSTER.....	C
VENSORA.....	C	VITRINA.....	B	WAIKOMO.....	D	WARNOCK.....	B
VENUM.....	D	VITROFF.....	B	WAILUKU.....	B	WARNUT.....	D
VERBOORT.....	D	VITZTHUM.....	D	WAINEE.....	B	WARRENTON.....	D
VERCLIFF.....	C	VIUM.....	D	WAINOLA.....	B	WARRIOR.....	B
VERDEL.....	D	VIVES.....	B	WAIPAHU.....	C	WARROAD.....	C
VERDIGRE.....	C	VIVI.....	B	WAITS.....	B	WARSING.....	B
VERDUN.....	D	VIVIAN.....	B	WAITSFIELD.....	B	WARWICK.....	A
VERENDRYE.....	B/D	VIXEN.....	B	WAKAMO.....	C	WASA.....	D
VERGENNES.....	C	VIZCAINO.....	D	WAKE.....	D	WASDA.....	B/D
VERHART.....	B	VIZCAPOINT.....	D	WAKEEN.....	B	WASHINGTON.....	C
VERICK.....	C	VIZCAYA.....	D	WAKELEY.....	D	WASHPASS.....	B
VERIDGE.....	B	VLASATY.....	C	WAKEMAN.....	C	WASKISH.....	D
VERJELES.....	D	VODA.....	C	WAKENDA.....	B	WASKOM.....	C
VERLOT.....	C	VODERMAIER.....	B	WAKEPISH.....	B	WASNOT.....	C
VERMILLION.....	D	VOELKER.....	B	WAKETICKEH.....	D	WASSON.....	D
VERNAL.....	B	VOIGHT.....	B	WAKEVILLE.....	B	WATAB.....	C
VERNDALE.....	B	VOLADORA.....	B	WAKITA.....	D	WATAHALA.....	A
VERNIA.....	A	VOLASH.....	B	WAKONDA.....	B	WATAUGA.....	B
VERNONIA.....	B	VOLCO.....	D	WAKONDA, Till Substratum.....	C	WATCHABOB.....	C
VERO.....	D	VOLENTE.....	C	WAKULLA.....	A	WATCHES.....	B
VERSHAL.....	D	VOLINIA.....	B	WALBERT.....	C	WATERFALL.....	D
VERSON.....	C	VOLLMER.....	C	WALCO.....	B	WATERFLAT.....	C
VERSTOVIA.....	D	VOLMONT.....	B	WALCOTT.....	B	WATERFORD.....	B
VERTEL.....	D	VOLNEY.....	B	WALDECK.....	C	WATERGATE.....	B
VERTINE.....	D	VOLSTEAD.....	B	WALDEN.....	D	WATERTOWN.....	B
VERTREES.....	B	VONALF.....	B	WALDO.....	D	WATHENA.....	B
VESEY.....	B	VONASON.....	B	WALDORF.....	C/D	WATKINS.....	B
VESPER.....	D	VONDERGREEN.....	C	WALDROUP.....	D	WATNE.....	B
VESTA.....	B	VOORHIES.....	C	WALKERSVILLE.....	B	WATONGA.....	D
VETAGRANDE.....	B	VOSSET.....	B	WALKINSHAW.....	D	WATONY.....	A
VETEADO.....	C	VOTAW.....	B	WALKON.....	C	WATOOPAH.....	B
VIA.....	B	VOYAGER.....	B	WALKOVER.....	B	WATROUS.....	C
VIAN.....	B	VULCAN.....	C	WALL.....	B	WATSEKA.....	B
VIBLE.....	A	VYCKYL.....	D	WALLKILL.....	B/D	WATSONIA.....	D
				WALLOWA.....	C	WATTON.....	C
				WALLROCK.....	C	WATUSI.....	C

WAUBERG.....	D	WENOTA.....	D	WHITE STORE.....	D	WILLIAMSVILLE.....	C
WAUCHULA.....	B/D	WENZEL.....	B	WHITE SWAN.....	D	WILLIMAN.....	B/D
WAUCHULA, Depressional.....	D	WEOGUFKA.....	C	WHITEARTH.....	C	WILLISTON.....	C
WAUCOBA.....	D	WEOTT.....	D	WHITEBIRD.....	D	WILLOSIPI.....	C
WAUCONDA.....	B	WEPO.....	C	WHITECAP.....	D	WILLOW CREEK.....	B
WAUKENA.....	D	WERELD.....	B	WHITECLOUD.....	B	WILLOWDALE.....	B
WAUKENABO.....	B/D	WERITO.....	C	WHITEDEER.....	B	WILLOWFORK.....	D
WAULD.....	C	WERNOCK.....	B	WHITEFACE.....	D	WILLSPRINGS.....	C
WAURIKA.....	D	WESFIL.....	D	WHITEFIELD.....	D	WILLYNAT.....	B
WAUTOMA.....	B/D	WESIX.....	D	WHITEFORD.....	B	WILMA.....	C
WAVELAND.....	B/D	WESKA.....	D	WHITEHALL.....	B	WILMER.....	C
WAVELAND.....	D	WESLEY.....	B	WHITEHORN.....	D	WILMONT.....	B
WAWAKA.....	B	WESPAC, Sandy Substratum Alkali.....	C	WHITEHORSE.....	B	WILMONTON.....	B
WAWASEE.....	B	WESPAC, Alkali.....	D	WHITEKNOB.....	B	WILPAR.....	C
WAWINA.....	A	WESSEL.....	C	WHITEMARSH.....	C/D	WILPOINT.....	D
WAX.....	C	WESTBEND.....	B	WHITEOAK.....	B	WILSALL.....	D
WAXPOOL.....	D	WESTBORO.....	D	WHITEPEAK.....	D	WILSHIRE.....	A
WAYCUP.....	B	WESTBROOK.....	D	WHITEPINE.....	D	WILSON.....	D
WAYLAND.....	C/D	WESTBUTTE.....	B	WHITERIVER.....	C	WILSONGULCH.....	B
WAYMET.....	B	WESTERVILLE.....	B	WHITEROCK.....	D	WILSONVILLE.....	D
WAYMOR.....	B	WESTFORK.....	D	WHITESBORO.....	C	WILSOR.....	B
WEA.....	A	WESTGATE.....	C	WHITESBURG.....	C	WILSPRING.....	C
WEALTHWOOD.....	A/D	WESTINDIAN.....	C	WHITESIDE.....	B	WILST.....	C
WEASH.....	C	WESTLAKE, Thin Surface.....	C	WHITESON.....	D	WILT.....	B
WEATHERFORD.....	B	WESTLAKE.....	D	WHITETHORN.....	B	WILTON.....	B
WEATHERWAX.....	D	WESTMION.....	D	WHITEWATER.....	D	WIMPEY.....	C
WEAVER.....	C	WESTMORE.....	C	WHITEWOOD, Nonflooded.....	B/D	WINADA.....	C
WEAVERVILLE.....	B	WESTOLA.....	B	WHITEWOOD.....	C/D	WINBERRY.....	C
WEBB.....	C	WESTON.....	D	WHITEWRIGHT.....	C	WINBLOW.....	C
WEBBRIDGE.....	B	WESTOVER.....	B	WHITEYE.....	D	WINCHUCK.....	C
WEBBTOWN.....	C	WESTPHALIA.....	B	WHITING.....	B	WIND RIVER.....	B
WEBFOOT.....	C	WESTPLAIN.....	D	WHITINGER.....	C	WINDCOAT.....	D
WEBILE.....	C	WESTPORT.....	A	WHITLEY.....	B	WINDCOMB.....	D
WECHERCH.....	D	WESTPORT, Thin Surface.....	B	WHITNEY.....	C	WINDEGO.....	B
WEDDERBURN.....	B	WESTSHORE.....	D	WHITSON.....	D	WINDER.....	D
WEDGE.....	A	WESTSIDE.....	C	WHITTEMORE.....	C/D	WINDERE.....	B
WEDGEMONT.....	B	WESTSUM.....	D	WHITVIN.....	D	WINDERNOT.....	B
WEEDING.....	D	WESTVACO.....	C	WHITWELL.....	C	WINDICREEK.....	A
WEEDMARK.....	B	WESTVIEW.....	B	WHORLED.....	C	WINDLASS.....	C
WEEDPATCH.....	C	WESTVILLE.....	B	WICHITA.....	C	WINDMILL.....	B
WEEDZUNIT.....	B	WESTWEGO.....	D	WICKAHONEY.....	D	WINDRY.....	D
WEEKIWACHEE.....	D	WESWIND.....	C	WICKENBURG.....	D	WINDTHORST.....	C
WEEKS.....	C	WESWOOD.....	B	WICKERSHAM.....	B	WINDWHISTLE.....	B
WEENA.....	D	WETA.....	D	WICKETT.....	C	WINDYBUTTE.....	B
WEEPAH.....	C	WETBETH.....	C	WICKIUP.....	C	WINDYHOLLOW.....	C
WEESATCHE.....	B	WETHEY.....	A/C	WICKSBURG.....	B	WINDYPOINT.....	B
WEETOWN.....	B	WETHEY.....	C	WICKWARE.....	C	WINEADE.....	D
WEEZWEE.....	B	WETSAW.....	C	WICUP.....	C	WINEG.....	B
WEGERT.....	A	WETTERDON.....	B	WIDEN.....	C	WINEGAR.....	C
WEGLIKE.....	A	WETZEL.....	D	WIDOWSPRING.....	B	WINEVADA.....	C
WEIDER.....	B	WEWELA.....	B	WIERGATE.....	D	WINFALL.....	B
WEINBACH.....	C	WEWOKA.....	C	WIFFO.....	B	WINFIELD.....	B
WEIR.....	D	WEYANOKE.....	C	WIFTON.....	B	WING.....	D
WEIRMAN.....	D	WEYERS.....	C/D	WIGTON.....	A	WINGATE.....	B
WEISBURG.....	C	WEYMOUTH.....	B	WILAH.....	B	WINGDALE.....	D
WEISSENFELS.....	C	WHAKANA.....	B	WILBANKS.....	D	WINGINA.....	B
WEITAS.....	B	WHALESHEAD.....	B	WILBUR.....	B	WINGINAW.....	D
WEITCHPEC.....	C	WHALEY.....	D	WILCO.....	C	WINGROCK.....	B
WELAKA.....	A	WHATCOM.....	C	WILCOX.....	D	WINGVILLE.....	D
WELCH.....	B	WHATELY.....	D	WILCOXSON.....	C	WINKLEMAN.....	D
WELCHLAND.....	B	WHEATBELT.....	D	WILDALE.....	C	WINKLER.....	B
WELCOME.....	B	WHEATON.....	B	WILDCAT.....	D	WINKLO.....	C
WELDA.....	C	WHEATWOOD.....	B	WILDER.....	A	WINLER.....	D
WELEETKA.....	D	WHEELER.....	B	WILDGEN.....	B	WINLO.....	D
WELLESLEY.....	B	WHEELERPEK.....	D	WILDHILL.....	C	WINN.....	C
WELLIE.....	A	WHEELERVILLE.....	B	WILDHORSE.....	A	WINNEBAGO.....	B
WELLINGTON.....	D	WHEELON, Cool.....	B	WILDMESA.....	C	WINNEMUCCA.....	C
WELLMAN.....	B	WHEELRIDGE.....	A	WILDORS.....	C	WINNETT.....	C
WELLROCK.....	B	WHEELS.....	D	WILDROSE.....	C	WINNETT.....	D
WELLS.....	B	WHERRY.....	D	WILE.....	C	WINNIPEG.....	B
WELLSBENCH.....	B	WHETSOON.....	C	WILHOIT.....	B	WINNSBORO.....	C
WELLSCREAK.....	B	WHETSTONE.....	C	WILKESON.....	B	WINOM.....	D
WELLSHAM.....	C	WHICHMAN.....	B	WILL.....	B/D	WINOOSKI.....	B
WELLSSED.....	C	WHIDBEY.....	C	WILLABY.....	C	WINOPEE.....	B
WELLSFORD.....	D	WHILPHANG.....	D	WILLAKENZIE.....	C	WINRIDGE.....	D
WELOY.....	C	WHIPP.....	D	WILLAMETTE.....	C	WINSAND.....	B
WELSUM.....	D	WHIPPANY.....	C	WILLANCH.....	D	WINSTON.....	B
WELTER.....	D	WHISK.....	D	WILLAPA.....	C	WINT.....	D
WEMPLE.....	B	WHISKEY.....	B	WILLARD.....	B	WINTERCANYON.....	C
WENAS.....	C/D	WHISKEYCREEK.....	C	WILLETTE.....	A/D	WINTERIM.....	C
WENATCHEE.....	C	WHISKLAKE.....	C	WILLHILL.....	C	WINTERMUTE.....	C
WENDANE.....	B/C	WHISPERING.....	C	WILLHO.....	C	WINTERS.....	C
WENDELL.....	A	WHISTLE.....	B	WILLIAMSBURG.....	B	WINTERSBURG.....	B
WENGLER.....	C			WILLIAMSPORT.....	C	WINTerset.....	C
WENONAH.....	B			WILLIAMSTOWN.....	C	WINTLEY.....	B

WINTON	C	WOODVILLE	D	YAD	D	YORK	C
WINTONER	B	WOODWARD	B	YAGGY, Protected	B	YORKSHIRE	C
WINU	C	WOODWEST	D	YAGGY	C	YORKTOWN	D
WINWELL	C	WOOFUS	C	YAHANA	D	YORKTREE	C
WISBEY	B	WOOLLY	B	YAHARA	C	YOSEMITE	B
WISBY	B	WOOLPER	B	YAHMORE	B	YOST	C/D
WISCOW	D	WOOLSEY	B	YAHNE	C	YOTES	B
WISCOY	C	WOOLSTALF	B	YAHOO	D	YOUGA, Sandy Substratum	D
WISE	C	WOOLSTED	B	YAINAX	B	YOUJAY	D
WISEMAN	A	WOOLWICH	B	YAKOBI	D	YOUMAN	C
WISFLAT	D	WOONSOCKET	B	YAKUS	D	YOUNGSTON, Wet	C
WISHARD	C	WORCESTER	C	YAKUTAT	A	YOURAME	B
WISHBONE	B	WORFSTONE	C	YALELAKE	B	YOUTLKUE	B
WISHEYLU	C	WORKMAN	C	YALESVILLE	C	YOVIIPA	D
WISHKAH	C/D	WORLAND	C	YALLANI	B	YPSI	C
WISKAN	C	WORLEY	D	YAMHILL	C	YRIBARREN	D
WISKISPRINGS	D	WORMCREEK	B	YAMSAY	D	YTURBIDE	A
WISNER	B/D	WORMET	B	YANA	B	YTURRIA	A
WISTER	C	WORMSER	C	YANCY	D	YUCCA	B
WISTONA	B	WORSHAM	D	YANKEE	D	YUKON	D
WITCHER	B	WORSWICK	C	YANKEEFORK	B	YUNES	D
WITHAM	D	WORTHENTON	D	YANKTON	B	YURM	D
WITHEE	C	WORTMAN	A	YAP	B	YUTAN	B
WITHERBEE	A/D	WORWOOD	C	YAPOAH	A	YUTRUE	D
WITHERELL	D	WOVOKA	D	YAQUI	B	YUZARRA	B
WITHERS	C	WRANGELL	D	YAQUICAN	D	ZAAR	D
WITTEN	D	WRAYHA	C	YAQUINA	C/D	ZABA	B
WITTENBERG	B	WRAYS	B	YATA	C	ZABOROSKY	B
WIVILLE	B	WREDAH	B	YATAHONEY	C	ZACA	D
WIX	C	WREFORD	D	YATAHONEY, Stony	D	ZACHARY	C
WIXOM	B	WRENCOE	D	YATAMA	B	ZADE	C
WIZARD	C	WRENGART	C	YATES	D	ZADOG	A/D
WOCKLEY	C	WRENMAN	C	YAUCO	C	ZADVAR	D
WOCKUM	B	WRENTAM	C	YAUHANNAH	B	ZAFOD	B
WODA	D	WRIGHTMAN	C	YAUPON	D	ZAGG	C
WODAVAR	D	WRIGHTSBORO	C	YAWHEE	B	ZAIDY	C
WODEN	B	WRIGHTSVILLE	D	YAWKEY	D	ZAKME	D
WODOMONT	D	WRIGHTWOOD	B	YAWKOLA	C	ZALCO	A
WODSKOW	B/C	WUKOKI	B	YAXING	B	ZALEA	B
WOHLY	B	WUKSI	A	YEAGER	A	ZALESKA	D
WOLCO	C	WULFERT	D	YEARIAN	D	ZALLA	A
WOLDALE	C/D	WUNABUNA	C/D	YEARY	C	ZALVIDEA	B
WOLFCREEK	B	WUNJEY	B	YEATON	C	ZAMORA	B
WOLFER	B	WUPATKI	D	YECROSS	A	ZANBUR	B
WOLFESON	C	WURTSMITH	A	YEDLICK	B	ZANE	B
WOLFESON, Wet	D	WUTCHUMNA	D	YEGUAS	C	ZANGO	D
WOLFHEY	C	WYALUSING	D	YELLOW HORSE	D	ZAPA	C
WOLFPKAK	B	WYANDOTTE	D	YELLOWBANK	D	ZAPATA	C
WOLFPEN	A	WYANT	C	YELLOWBAY	B	ZAQUA	D
WOLFTEVER	C	WYARD	B	YELLOWDOG	A	ZARK	C
WOLFVAR	B	WYARNO	B	YELLOWHILLS	B	ZASTER	C
WOLLARD	C	WYATT	C	YELLOWLARK	C	ZAU	C
WOLLENT	D	WYCOLO	C	YELLOWMULE	C	ZAVALA	B
WOLOT	B	WYEAST	D	YELLOWRIVER	B	ZAVCO	C
WOLVERTON	B	WYECREEK	B	YELLOWROCK	B	ZAYANTE	A
WOMACK	C	WYETH	D	YELLOWSTONE	D	ZBART	D
WOODBECK	B	WYEVILLE	C	YELLOWWASH	D	ZEALE	B
WOODBINE	B	WYICK	D	YELM	C	ZEB	B
WOODBURN	C	WYKOFF	B	YELTON	C	ZEE	B
WOODBURY	D	WYLO	D	YENNICK	B	ZEEBAR	B
WOODCANYON	C	WYNHOFF, Moist	B	YENSUS	B	ZEEGEE	D
WOODCHOPPER	B	WYNHOFF	C	YEOPIM	B	ZEEKA	C
WOODCUTTER	D	WYNN	B	YERBA	D	ZEELAND	C
WOODCUTTERS, Stony	B	WYNNVILLE	B	YERINGTON	A	ZEELNOT	D
WOODFORD	D	WYNONA	C	YESUM	B	ZEEMAL	B
WOODHURST	C	WYNOOSE	D	YIGO	B	ZEGRO	C
WOODIN	C	WYNTON	B	YIKES	A	ZEIBRIGHT	B
WOODINGTON	B/D	WYOMINGCREEK	C	YLIQ	C	ZEKIAH	D
WOODINVILLE	C/D	WYOTITE	B	YNOT	B	ZELA	D
WOODLAWN	B	WYRICK	B	YOKRAN	A	ZELDA	D
WOODLEAF	C	WYSOCKING	C/D	YOCUM	C	ZENDA	C
WOODLY	B	WYVA	B	YODAL	B	ZENIFF	B
WOODMANSIE	B	XANA	B	YODER	B	ZENITH	B
WOODMERE	B	XANADU	B	YODY	C	ZENOBI	B
WOODMONT	C	XANKEY	B	YOGAVILLE	D	ZENORIA	C
WOODPASS	B	XAVIER	B	YOHN	B	ZEOMONT	A
WOODROCK	C	XERTA	C	YOKAYO	D	ZEPH	D
WOODS	D	XERXES	D	YOKUT	B	ZEPHYR	D
WOODSFIELD	C	XICA	D	YOLLABOLLY	D	ZEPOL	B
WOODSIDE	B	XINE	C	YOLOGO	D	ZERKEL	B
WOODSLAKE	D	XIPE	D	YOMONT	B	ZERKER	B
WOODSON	D	XMAN	D	YONCALLA	C	ZEUGIRDOR	B
WOODSPOINT	B	XOBOBO	B	YONNA	D	ZIBATE	D
WOODSTOCK	D	YABAMAR	D	YORBA	D	ZIBETOD	D
WOODTEX	D	YACHATS	B	YOREL	B	ZIEGENFUSS	D

ZIEGLER	C
ZIGGY	B
ZILABOY	D
ZILLAH	C/D
ZILWAUKEE	D
ZIMMER	D
ZIMWALA	C
ZING	C
ZIPPEL	B/D
ZIRAM	D
ZITA	B
ZITTAU	C
ZITZIANA	B
ZOAR	C
ZOATE	D
ZODA	C
ZOE	D
ZOLFO	C
ZOMAX	B
ZONO	A
ZORRA	D
ZOZOBRA	B
ZUBER	C
ZUFELT	C
ZULCH	D
ZUMAN, Protected	C/D
ZUMAN	D
ZUMBRO	A
ZUMMO	D
ZUNALEI	B
ZUNDELL	C
ZUNHALL	C
ZUNI, Gravelly	C
ZUNI	D
ZUNIVEN	B
ZUNKER	B
ZWAGG	B
ZWICKER	C
ZWIEFEL	C
ZWINGLE	D
ZYMER	B
ZYNBAR	B
ZYNBAR Till Substratum	C
ZYPLAR	D
ZYZYL	B
ZYZZI	D
ZYZZUG	D

D-3 References Cited

NRCS. 1986. Urban Hydrology for Small Watersheds, TR-55. United States Department of Agriculture Conservation Engineering Division. 164 pp.